

DISSERTATION

PART ONE: THE FORMAL TOTAL SYNTHESIS OF DEHYDROGLIOTOXIN AND THE  
FIRST SYNTHESIS OF AN EPIDISELENODIKETOPIPERAZINE

AND

PART TWO: TOWARDS THE TOTAL SYNTHESIS OF THE TETRAPETALONES

Submitted by

Travis Chandler McMahon

Department of Chemistry

In partial fulfillment of the requirements

For the Degree of Doctor of Philosophy

Colorado State University

Fort Collins, Colorado

Summer 2013

Doctoral Committee:

Advisor: John L. Wood

Alan J. Kennan  
Eric M. Ferreira  
Travis S. Bailey  
Dean C. Crick

Copyright by Travis Chandler McMahon 2013

All Rights Reserved

## ABSTRACT

PART ONE: THE FORMAL TOTAL SYNTHESIS OF DEHYDROGLIOTOXIN AND THE FIRST  
SYNTHESIS OF AN EPIDISELENODIKETOPIPERAZINE  
AND  
PART TWO: TOWARDS THE TOTAL SYNTHESIS OF THE TETRAPETALONES

Tuberculosis (TB), caused by *Mycobacterium tuberculosis* (MTB), affects approximately one third of the global population and is associated with nearly two million deaths annually. Although there are known cures for TB, current treatment plans suffer due to length, usually taking 6–9 months to complete. Additionally, developing countries lack the infrastructure and resources necessary to both efficiently diagnose and treat patients. Of particular concern are an increasing number of strains of TB that are becoming resistant to the current drug regimens, which has been a result of patients beginning, but not completing their treatment. In light of these facts it is clear there is a continuing need to develop simplified and shorter treatments for TB, and with the increasing prevalence of resistant strains, chemically unique targets should be investigated.

As part of a collaborative effort with the Hung group at the Broad Institute, we identified two related epidithiodiketopiperazine (ETP) natural products, gliotoxin and dehydrogliotoxin, as potential candidates for exploration as anti-TB agents. We initially targeted a synthesis of dehydrogliotoxin, as it had also never been tested against MTB, whereas gliotoxin was known to be active. Additionally, as dehydrogliotoxin was the simpler of the two compounds, we believed it could be synthesized more rapidly and also be more amenable to derivatization to form structural analogs. The synthetic studies towards dehydrogliotoxin culminated in a formal total synthesis that featured a key two step amidation–intramolecular ring–closure.

With access to dehydrogliotoxin we were able to test it against MTB and found its activity to be comparable to gliotoxin. We next turned our attention to the synthesis of structural analogs in hopes of identifying a compound that could potentially be used as an anti-TB therapeutic. In that regard, we targeted a compound wherein the disulfide region of the natural product was replaced with a diselenide. As an epidiselenodiketopiperazine (ESeP) had never been synthesized before, we initially explored the installation of this functional group in a model system. These synthetic efforts resulted in the synthesis of an ESeP, both from a simple diketopiperazine and directly from an ETP. Additionally, in these model systems, the ESeP exhibited comparable activity towards MTB as the ETP.

Tetrapetalone A was isolated in 2003 by Hirota and coworkers from a culture filtrate of *Streptomyces* sp. USF-4727. The related compounds tetrapetalones B, C, and D were isolated from the same *Streptomyces* strain in 2004. We became interested in this family of natural products due to their interesting structural features and the synthetic challenge they present. Salient features of the tetrapetalones include a tetracyclic core containing a tetramic acid, a seven-membered ring possessing a trisubstituted double bond, a *p*-quinol, and a five-membered ring with a pendant  $\beta$ -rhodnose.

Several strategies towards the synthesis of the tetrapetalones have been explored. In our initial approach we hoped to form the seven-membered ring of the natural product through nucleophilic attack of the aromatic ring onto a pendant palladium  $\pi$ -allyl species. While exploring this process, we found that the desired seven-membered product was not formed, instead we isolated a product containing a five-membered ring, the result of attack at the wrong position of the palladium  $\pi$ -allyl species. Attempts to bias the substrate towards formation of the desired seven-membered ring through a transannular palladium  $\pi$ -allyl approach proved unfruitful.

Our current route features a Friedel-Crafts acylation to form the seven-membered ring containing the trisubstituted double bond. The precursor for this approach was built up rapidly

from simple starting materials, and the desired Friedel–Crafts reaction proceeds smoothly. Furthermore, we have implemented a C–H oxidation protocol to install a synthetic handle, which can ultimately be converted to an alkyne that we envision can be transformed into the five–membered ring bearing the sugar moiety in order to finish the natural product.

Concurrent to the approaches described above, we have also targeted the related natural product, ansaetherone, which was isolated from the same *Streptomyces* strain as the tetrapetalones and is proposed to be a biosynthetic precursor to the family. The ultimate goal in this approach was to develop a synthesis of ansaetherone and explore methods to convert it to one of the members of the tetrapetalones in a biomimetic fashion. Our proposed synthesis included a key tandem enyne–cross metathesis to form the eleven–membered ring present in the natural product. Although this synthesis is still in its infancy, we have accessed a compound that is a few synthetic steps away from the precursor to explore the key step. We are currently exploring an improved synthesis of this intermediate and ways to elaborate it to the natural product.

## ACKNOWLEDGEMENTS

First and foremost, I would like to thank my advisor John Wood. I have learned so much from you over the last five years and I cannot thank you enough for giving me the opportunity to work in your group. You have been an incredible mentor and I am grateful for the opportunities you have given me to grow and succeed both in the lab and in the chemistry community.

Dr. Vyvyan, I am forever grateful for the opportunity to perform undergraduate research in your lab. You gave me the foundation and the guidance to become the chemist that I am today. I do not imagine being better prepared for graduate school, and I owe that mostly to you. Thank you for introducing me to the chemistry world.

Eric Ferreira, I have learned so much from you, and I am grateful for the opportunity to seek your advice and talk chemistry over the last five years. We started at CSU at the same time, and I am privileged to have been in your first class here. Although I was not a part of your group, I am thankful for the many invitations Oz and I received to your group parties.

To all my lab mates in the Wood group over the years, it was a pleasure to work with all of you. I cannot imagine a better environment to work in everyday. Matt and Brett, thank you for answering all my “stupid” questions as a first year. Graham, thank you for working mechanisms with me on the board. Sarah, thank you for being “group mom” and being there every time I cut myself (also for the awesome Cars Band-Aids). Ke, you are the best. Jenn, thank you for giving me your project and for being a great friend. Genessa, thank you for being a truly amazing person. Matt and Chris, you two made me into a much better chemist; having the two of you to learn from, joke with, and eat sunflower seeds with was great. Naoto, thank you for being a curious, stubborn, and an amazing guy. Taka, I am so glad to have worked in the hood next to you, I know so much about Japanese baseball because of you. You and Rika are great friends to Sam and I, and one day I hope to visit you in Japan. Jenny, you were only here for a short time, but you are my absolute favorite person in the whole world. I am truly grateful to have

gotten to know you and for the many laughs we enjoyed together, even if they were a result of Aaron and I scaring you. Aaron, “you’re a bitch.” But seriously, thank you for helping me stay sane, and being one of my best friends. I don’t know how I’m going to be able to work in the lab without being able to yell over to you. I seriously will probably have to skype with you guys just to get some yelling in. Monica, thank you for putting up with Aaron and I talking about sports all the time, also the yelling. You are an amazing person, and I’m so glad you joined our lab. I will miss game nights. Mike, you are the worst. In all seriousness I like you quite a bit, listen to Aaron, he will teach you how to be a good chemist. Heemal, please finish tetrapetalone. Also, clean your hood! I have high hopes for you; you are such an awesome and smart person. Just remember, “got to be like Travis.” John Enquist, thank you for being an amazing post-doc. I greatly appreciate all the advice you gave me over the last couple years, and I especially thank you for calming me down the last nights before my dissertation was due. Jonas, I left you for last because you are the most important. Working with you on tetrapetalone has been amazing. I want you know how much I appreciate our daily conversations and how much of an honor it was to work with you.

To all my classmates, you guys are awesome. We have had a lot of fun together, and I couldn’t think of a better group to share this entire graduate school experience with. Doug, you have been a great friend and brewing partner. Todd, I am sorry I punched you that one time, but you are an amazing person and an exceptional chemist. Oz, you are one of my very best friends. I am forever grateful for everything you have done for me, and my life is better because I know you.

To my family, I am really bad at expressing my emotions, and I do not say it enough, but I love you. To my Mom and Dad, you are the best parents that anyone could ever hope for. I am only successful at life because the two of you raised me. Shanna, although sometimes you were a brat when we were younger, you are a pretty awesome sister. You are an extremely intelligent and caring person and I am happy to be your brother. Nana, you are the best grandmother

period. I don't think there are too many people out there who just call their grandma to talk about baseball. Thank you for being there for me.

Finally, Samantha. You are my best friend and I love you. I can't begin to tell you how grateful I am for you. Thank you for making me "awesome dinners" and being here for me everyday. I love being with you and look forward to spending the rest of my life with you.

## AUTOBIOGRAPHY

Travis Chandler McMahon was born on October 31<sup>st</sup>, 1985 to Phil and Lyanna McMahon in Tacoma, WA. He is the older brother to Shanna Rose McMahon. Growing up, Travis enjoyed sports, especially baseball, basketball, and tennis, and is an avid Seattle Mariners fan. He graduated from Spanaway Lake High School in 2004 where he was captain of the tennis team and a member of the varsity baseball team. In high school his favorite subjects were math and science, which ultimately led him to pursue a college degree in the sciences. He began college in 2004 at Western Washington University, where he first fell in love with Organic Chemistry. At Western, Travis was able to perform undergraduate research in the labs of Prof. James Vyvyan. Upon graduating from Western in 2008 with a B.S. in chemistry, Travis pursued a graduate degree in synthetic organic chemistry. In 2008 he began his graduate career at Colorado State University, ultimately ended up in the labs of Prof. John L. Wood. Over the next five years Travis flourished at CSU, contributing as an author on five publications from the Wood lab, and ultimately obtaining his Ph.D. in July of 2013. Travis will begin as a postdoctoral research associate in the labs of Prof. Neil Garg at the University of California, Los Angeles in the fall of 2013.

## TABLE OF CONTENTS

ABSTRACT.....	ii
ACKNOWLEDGMENTS .....	v
AUTOBIOGRAPHY.....	viii
TABLE OF CONTENTS.....	ix
LIST OF TABLES.....	xiii
LIST OF FIGURES .....	xiv
LIST OF SCHEMES.....	xxvi
Part One: The formal total synthesis of dehydrogliotoxin and the first synthesis of an epidiselenodiketopiperazine .....	1
Chapter One: Introduction .....	2
1.1 Tuberculosis .....	2
1.2 Gliotoxin and Dehydrogliotoxin .....	4
1.3 Biosynthesis.....	6
Chapter Two: Previous Synthetic Work .....	8
2.1 Methods to Install the Disulfide Bridge .....	8
2.2 Kishi's Synthesis of Gliotoxin .....	11
2.3 Kishi's Synthesis of Dehydrogliotoxin .....	14
Chapter Three: Towards the Synthesis of Dehydrogliotoxin .....	17
3.1 Intermolecular Copper Mediated Aryl-Amidation .....	17
3.2 Intramolecular Copper Mediated Aryl-Amidation .....	23

3.3 Attempts to Incorporate Sulfur .....	27
Chapter Four: Synthesis of Dehydrogliotoxin .....	32
4.1 Revised Route Towards the Synthesis of Dehydrogliotoxin .....	32
4.2 Biological Activity .....	34
Chapter Five: Analog Design and the First Synthesis of an Epidiselenodiketopiperazine .....	36
5.1 Replacing the Disulfide with a Diselenide .....	36
References for Part One .....	47
Part Two: Towards the total synthesis of the tetrapetalones .....	51
Chapter Six: The Tetrapetalones .....	52
6.1 Isolation and Structure Determination .....	52
6.2 Biosynthesis .....	55
Chapter Seven: Previous Synthetic Efforts .....	57
7.1 Porco's Efforts Towards Tetrapetalone A .....	58
7.2 Sarpong's Efforts Towards Tetrapetalone A .....	61
7.3 Hong's Synthetic Studies Towards the Core of Tetrapetalone A .....	63
Chapter Eight: Previous Approaches in the Wood Group .....	66
Chapter Nine: Formation of the Seven-Membered Ring Utilizing the Aromatic Ring as a Nucleophile .....	74

9.1 Cascade Friedel–Crafts Approach.....	74
9.2 Intramolecular $\pi$ -Allyl Approach .....	79
Chapter Ten: A Transannular $\pi$ -Allyl Approach.....	85
10.1 A Transannular $\pi$ -Allyl Approach.....	85
10.2 Implementation of Hartwig’s Borylation Conditions .....	88
10.3 A Nozaki–Hiyama–Kishi Approach to the desired Ten–Membered Ring .....	94
Chapter Eleven: Revisiting the Previous $\pi$ -Allyl Strategy .....	99
11.1 Testing a New Palladium $\pi$ -Allyl Approach .....	100
11.2 Revisiting the Friedel–Crafts Approach .....	102
11.3 A New Strategy Towards Tetrapetalone A Utilizing the Friedel–Crafts Acylation.....	106
11.4 Installation of the Alkyne After the Friedel–Crafts Reaction .....	109
Chapter Twelve: Exploring the Phenolic Oxidation.....	111
12.1 Deprotection Problems .....	111
12.2 Phenolic Oxidation Attempts.....	113
Chapter Thirteen: Elaboration of the Alkyne .....	117
13.1 Attempts to Form a Vinyl Stannane .....	117
13.2 Attempts to Form an Aryl Ketone.....	119
13.3 Attempts to Reduce the Alkyne to an Olefin .....	120
13.4 Conclusions and Future Work .....	121
Chapter Fourteen: Ansaetherone .....	123
14.1 Proposed Conversion of Ansaetherone to the Tetrapetalones.....	123

14.2 A Phenolic Oxidation Pathway to Ansaetherone .....	126
14.3 Turning to a Fries Rearrangement.....	130
14.4 Forming an Oxy–Michael Precursor Through an Aldol Reaction.....	133
References for Part Two.....	136
Appendix One: Experimental .....	140
Appendix Two: Spectra.....	238
Appendix Three: Crystallographic Data and Tables .....	440
List of Abbreviations .....	459

## LIST OF TABLES

Table 3.1. Attempts at using alternate aryl-amidation coupling conditions .....	20
Table 3.2. Attempted aryl-amidation utilizing aryl iodide <b>61</b> .....	21
Table 3.3. Attempted aryl-amidation utilizing aryl iodide <b>62</b> .....	22
Table 3.4. Duterium Incorporation of tricycle <b>84</b> .....	28
Table 3.5. Attempts at reacting tricycle <b>84</b> with a sulfur electrophile .....	29
Table 4.1. Antitubercular activities .....	35
Table 5.1. Attempts at reacting dibromide <b>109</b> with a diselenide dianion equivalent .....	40
Table 5.2. Activation of bithiomethyl ether <b>116</b> .....	43
Table 10.1. Attempted formylation of aryl bromide <b>301</b> .....	96
Table 11.1. Attempted oxidation of ketone <b>339</b> to enone <b>340</b> .....	104
Table 13.1. Attempts to form vinyl stannane <b>390</b> .....	118
Table 13.2. Attempts to form ketone <b>396</b> .....	120

## LIST OF FIGURES

Figure 1.1. Typical drugs used to treat tuberculosis .....	4
Figure 1.2. Initially proposed structure of gliotoxin .....	5
Figure 1.3. X-ray crystal structure of gliotoxin ( <b>9</b> ) .....	5
Figure 1.4. Dehydrogliotoxin ( <b>10</b> ) .....	6
Figure 2.1. Epidithiodiketopiperazine natural products that have recently been synthesized .....	8
Figure 3.1. Mechanism of the copper mediated aryl-amidation .....	23
Figure 3.2. Undesired indole byproduct <b>87</b> .....	29
Figure 4.1. Graphs showing a) antitubercular activity and b) human cell toxicity .....	35
Figure 5.1. Regions of dehydrogliotoxin that could be modified in analog generation .....	36
Figure 5.2. Redox cycling of gliotoxin ( <b>9</b> ) forming harmful reactive oxygen species .....	37
Figure 5.3. Activity of compounds tested against MTB.....	45
Figure 6.1. Initially proposed structure of tetrapetalone A .....	53
Figure 6.2. Tetrapetalones B ( <b>132</b> ), C ( <b>133</b> ), and D ( <b>134</b> ).....	54
Figure 6.3. Structure of Ansaetherone ( <b>135</b> ) .....	55
Figure 7.1. (+)-Q-1047H-A-A ( <b>140</b> ) and (+)-Q-1047H-R-A ( <b>141</b> ).....	57
Figure 12.1. Crystal structure of allylic alcohol <b>367</b> .....	114
Figure A2.1. <sup>1</sup> H-NMR of DKP <b>72</b> .....	239
Figure A2.2. <sup>13</sup> C-NMR of DKP <b>72</b> .....	240
Figure A2.3. FTIR of DKP <b>72</b> .....	240
Figure A2.4. <sup>1</sup> H-NMR of DKP <b>76</b> .....	241
Figure A2.5. <sup>13</sup> C-NMR of DKP <b>76</b> .....	242
Figure A2.6. FTIR of DKP <b>76</b> .....	242
Figure A2.7. <sup>1</sup> H-NMR of protected amino acid <b>82</b> .....	243
Figure A2.8. <sup>13</sup> C-NMR of protected amino acid <b>82</b> .....	244

Figure A2.9. FTIR of protected amino acid <b>82</b> .....	244
Figure A2.10. <sup>1</sup> H-NMR of amino ester <b>79</b> .....	245
Figure A2.11. <sup>13</sup> C-NMR of amino ester <b>79</b> .....	246
Figure A2.12. <sup>1</sup> H-NMR of dipeptide <b>83</b> .....	247
Figure A2.13. <sup>13</sup> C-NMR of dipeptide <b>83</b> .....	248
Figure A2.14. <sup>1</sup> H-NMR of DKP <b>70</b> .....	249
Figure A2.15. <sup>13</sup> C-NMR of DKP <b>70</b> .....	250
Figure A2.16. <sup>1</sup> H-NMR of DKP <b>84</b> .....	251
Figure A2.17. <sup>13</sup> C-NMR of DKP <b>84</b> .....	252
Figure A2.18. FTIR of DKP <b>84</b> .....	252
Figure A2.19. <sup>1</sup> H-NMR of indole <b>87</b> .....	253
Figure A2.20. <sup>1</sup> H-NMR of indole <b>89</b> .....	254
Figure A2.21. <sup>1</sup> H-NMR of DKP <b>90</b> .....	255
Figure A2.22. <sup>1</sup> H-NMR of amide <b>91</b> .....	256
Figure A2.23. <sup>13</sup> C-NMR of amide <b>91</b> .....	257
Figure A2.24. FTIR of amide <b>91</b> .....	257
Figure A2.25. <sup>1</sup> H-NMR of bisselenobenzoate <b>103</b> .....	258
Figure A2.26. <sup>13</sup> C-NMR of bisselenobenzoate <b>103</b> .....	259
Figure A2.27. FTIR of bisselenobenzoate <b>103</b> .....	259
Figure A2.28. <sup>1</sup> H-NMR of bisselenobenzoate <b>104</b> .....	260
Figure A2.29. <sup>13</sup> C-NMR of bisselenobenzoate <b>104</b> .....	261
Figure A2.30. FTIR of biselenobenzoate <b>104</b> .....	261
Figure A2.31. <sup>1</sup> H-NMR of diselenide <b>106</b> .....	262
Figure A2.32. <sup>13</sup> C-NMR of diselenide <b>106</b> .....	263
Figure A2.33. <sup>77</sup> Se-NMR of diselenide <b>106</b> .....	263
Figure A2.34. FTIR of diselenide <b>106</b> .....	264

Figure A2.35. $^1\text{H-NMR}$ of dibromide <b>109</b> .....	265
Figure A2.36. $^{13}\text{C-NMR}$ of dibromide <b>109</b> .....	266
Figure A2.37. $^1\text{H-NMR}$ of bisselenoether <b>120</b> .....	267
Figure A2.38. $^{13}\text{C-NMR}$ of biselenoether <b>120</b> .....	268
Figure A2.39. $^{77}\text{Se-NMR}$ of bisselenoether <b>120</b> .....	268
Figure A2.40. FTIR of biselenoether <b>120</b> .....	269
Figure A2.41. $^1\text{H-NMR}$ of dithioacetal <b>121</b> .....	270
Figure A2.42. $^{13}\text{C-NMR}$ of dithioacetal <b>121</b> .....	271
Figure A2.43. FTIR of dithioacetal <b>121</b> .....	271
Figure A2.44. $^1\text{H-NMR}$ of dithioacetal <b>125</b> .....	272
Figure A2.45. $^1\text{H-NMR}$ of disulfide <b>126</b> .....	273
Figure A2.46. $^1\text{H-NMR}$ of bithiomethyl ether <b>127</b> .....	274
Figure A2.47. $^{13}\text{C-NMR}$ of bithiomethyl ether <b>127</b> .....	275
Figure A2.48. FTIR of bithiomethyl ether <b>127</b> .....	275
Figure A2.49. $^1\text{H-NMR}$ of bromoketone <b>236</b> .....	276
Figure A2.50. $^{13}\text{C-NMR}$ of bromoketone <b>236</b> .....	277
Figure A2.51. FTIR of bromoketone <b>236</b> .....	277
Figure A2.52. $^1\text{H-NMR}$ of aniline <b>237</b> .....	278
Figure A2.53. $^{13}\text{C-NMR}$ of aniline <b>237</b> .....	279
Figure A2.54. FTIR of aniline <b>237</b> .....	279
Figure A2.55. $^1\text{H-NMR}$ of phenol <b>287</b> (higher $R_f$ diastereomer).....	280
Figure A2.56. $^{13}\text{C-NMR}$ of phenol <b>287</b> (higher $R_f$ diastereomer) .....	281
Figure A2.57. FTIR of phenol <b>287</b> (higher $R_f$ diastereomer).....	281
Figure A2.58. $^1\text{H-NMR}$ of phenol <b>287</b> (lower $R_f$ diastereomer) .....	282
Figure A2.59. $^{13}\text{C-NMR}$ of phenol <b>287</b> (lower $R_f$ diastereomer).....	283
Figure A2.60. FTIR of phenol <b>287</b> (lower $R_f$ diastereomer) .....	283

Figure A2.61. $^1\text{H-NMR}$ of ketone <b>234</b> (higher $R_f$ diastereomer).....	284
Figure A2.62. $^{13}\text{C-NMR}$ of ketone <b>234</b> (higher $R_f$ diastereomer) .....	285
Figure A2.63. FTIR of ketone <b>234</b> (higher $R_f$ diastereomer) .....	285
Figure A2.64. $^1\text{H-NMR}$ of ketone <b>234</b> (lower $R_f$ diastereomer) .....	286
Figure A2.65. $^{13}\text{C-NMR}$ of ketone <b>234</b> (lower $R_f$ diastereomer).....	287
Figure A2.66. FTIR of ketone <b>234</b> (lower $R_f$ diastereomer) .....	287
Figure A2.67. $^1\text{H-NMR}$ of enal <b>239</b> .....	288
Figure A2.68. $^{13}\text{C-NMR}$ of enal <b>239</b> .....	289
Figure A2.69. FTIR of enal <b>239</b> .....	289
Figure A2.70. $^1\text{H-NMR}$ of carboxylic acid <b>247</b> .....	290
Figure A2.71. $^{13}\text{C-NMR}$ of carboxylic acid <b>247</b> .....	291
Figure A2.72. FTIR of carboxylic acid <b>247</b> .....	291
Figure A2.73. $^1\text{H-NMR}$ of ketone <b>259</b> .....	292
Figure A2.74. $^{13}\text{C-NMR}$ of ketone <b>259</b> .....	293
Figure A2.75. FTIR of ketone <b>259</b> .....	293
Figure A2.76. $^1\text{H-NMR}$ of allylic carbonate <b>265</b> .....	294
Figure A2.77. $^{13}\text{C-NMR}$ of allylic carbonate <b>265</b> .....	295
Figure A2.78. FTIR of allylic carbonate <b>265</b> .....	295
Figure A2.79. $^1\text{H-NMR}$ of allylic carbonate <b>268</b> .....	296
Figure A2.80. $^{13}\text{C-NMR}$ of allylic carbonate <b>268</b> .....	297
Figure A2.81. FTIR of allylic carbonate <b>268</b> .....	297
Figure A2.82. $^1\text{H-NMR}$ of fused tricycle <b>269</b> .....	298
Figure A2.83. $^{13}\text{C-NMR}$ of fused tricycle <b>269</b> .....	299
Figure A2.84. FTIR of fused tricycle <b>269</b> .....	299
Figure A2.85. $^1\text{H-NMR}$ of allylic carbonate <b>462</b> .....	300
Figure A2.86. $^{13}\text{C-NMR}$ of allylic carbonate <b>462</b> .....	301

Figure A2.87. FTIR of allylic carbonate <b>462</b> .....	301
Figure A2.88. <sup>1</sup> H-NMR of allylic carbonate <b>275</b> .....	302
Figure A2.89. <sup>13</sup> C-NMR of allylic carbonate <b>275</b> .....	303
Figure A2.90. FTIR of allylic carbonate <b>275</b> .....	303
Figure A2.91. <sup>1</sup> H-NMR of tricycle <b>276</b> .....	304
Figure A2.92. <sup>13</sup> C-NMR of tricycle <b>276</b> .....	305
Figure A2.93. FTIR of tricycle <b>276</b> .....	305
Figure A2.94. <sup>1</sup> H-NMR of phenol <b>463</b> .....	306
Figure A2.95. <sup>13</sup> C-NMR of phenol <b>463</b> .....	307
Figure A2.96. FTIR of phenol <b>463</b> .....	307
Figure A2.97. <sup>1</sup> H-NMR of tetramic acid <b>280</b> .....	308
Figure A2.98. <sup>13</sup> C-NMR of tetramic acid <b>280</b> .....	309
Figure A2.99. FTIR of tetramic acid <b>280</b> .....	309
Figure A2.100. <sup>1</sup> H-NMR of diene <b>287</b> .....	310
Figure A2.101. <sup>13</sup> C-NMR of diene <b>287</b> .....	311
Figure A2.102. FTIR of diene <b>287</b> .....	311
Figure A2.103. <sup>1</sup> H-NMR of tetramic acid <b>295</b> .....	312
Figure A2.104. <sup>13</sup> C-NMR of tetramic acid <b>295</b> .....	313
Figure A2.105. FTIR of tetramic acid <b>295</b> .....	313
Figure A2.106. <sup>1</sup> H-NMR of aryl boronic ester <b>296</b> .....	314
Figure A2.107. <sup>13</sup> C-NMR of aryl boronic ester <b>296</b> .....	315
Figure A2.108. FTIR of aryl boronic ester <b>296</b> .....	315
Figure A2.109. <sup>1</sup> H-NMR of styrene <b>297</b> .....	316
Figure A2.110. <sup>1</sup> H-NMR of ketone <b>298</b> .....	317
Figure A2.111. <sup>1</sup> H-NMR of aryl bromide <b>301</b> .....	318
Figure A2.112. <sup>13</sup> C-NMR of aryl bromide <b>301</b> .....	319

Figure A2.113. FTIR of aryl bromide <b>301</b> .....	319
Figure A2.114. <sup>1</sup> H-NMR of enone <b>300</b> .....	320
Figure A2.115. <sup>13</sup> C-NMR of enone <b>300</b> .....	321
Figure A2.116. FTIR of enone <b>300</b> .....	321
Figure A2.117. <sup>1</sup> H-NMR of enal <b>464</b> .....	322
Figure A2.118. <sup>13</sup> C-NMR of enal <b>464</b> .....	323
Figure A2.119. FTIR of enal <b>464</b> .....	323
Figure A2.120. <sup>1</sup> H-NMR of triene <b>303</b> .....	324
Figure A2.121. <sup>13</sup> C-NMR of triene <b>303</b> .....	325
Figure A2.122. <sup>1</sup> H-NMR of allylic alcohol <b>304</b> .....	326
Figure A2.123. <sup>13</sup> C-NMR of allylic alcohol <b>304</b> .....	327
Figure A2.124. FTIR of allylic alcohol <b>304</b> .....	327
Figure A2.125. <sup>1</sup> H-NMR of styrene <b>313</b> .....	328
Figure A2.126. <sup>1</sup> H-NMR of benzaldehyde <b>312</b> .....	329
Figure A2.127. <sup>13</sup> C-NMR of benzaldehyde <b>312</b> .....	330
Figure A2.128. FTIR of benzaldehyde <b>312</b> .....	330
Figure A2.129. <sup>1</sup> H-NMR of vinyl iodide <b>314</b> .....	331
Figure A2.130. <sup>1</sup> H-NMR of alkyne <b>315</b> .....	332
Figure A2.131. <sup>13</sup> C-NMR of alkyne <b>315</b> .....	333
Figure A2.132. FTIR of alkyne <b>315</b> .....	333
Figure A2.133. <sup>1</sup> H-NMR of alkyne <b>358</b> .....	334
Figure A2.134. <sup>13</sup> C-NMR of alkyne <b>358</b> .....	335
Figure A2.135. FTIR of alkyne <b>358</b> .....	335
Figure A2.136. <sup>1</sup> H-NMR of aldehyde <b>325</b> .....	336
Figure A2.137. <sup>13</sup> C-NMR of aldehyde <b>325</b> .....	337
Figure A2.138. FTIR of aldehyde <b>325</b> .....	337

Figure A2.139. $^1\text{H}$ -NMR of vinyl carbonate <b>321</b> .....	338
Figure A2.140. $^{13}\text{C}$ -NMR of vinyl carbonate <b>321</b> .....	339
Figure A2.141. FTIR of vinyl carbonate <b>321</b> .....	339
Figure A2.142. $^1\text{H}$ -NMR of bromide <b>335</b> .....	340
Figure A2.143. $^{13}\text{C}$ -NMR of bromide <b>335</b> .....	341
Figure A2.144. FTIR of bromide <b>335</b> .....	341
Figure A2.145. $^1\text{H}$ -NMR of tosylate <b>336</b> .....	342
Figure A2.146. $^{13}\text{C}$ -NMR of tosylate <b>336</b> .....	343
Figure A2.147. FTIR of tosylate <b>336</b> .....	343
Figure A2.148. $^1\text{H}$ -NMR of carboxylic acid <b>337</b> .....	344
Figure A2.149. $^{13}\text{C}$ -NMR of carboxylic acid <b>337</b> .....	345
Figure A2.150. FTIR of carboxylic acid <b>337</b> .....	345
Figure A2.151. $^1\text{H}$ -NMR of ketone <b>339</b> .....	346
Figure A2.152. $^{13}\text{C}$ -NMR of ketone <b>339</b> .....	347
Figure A2.153. FTIR of ketone <b>339</b> .....	347
Figure A2.154. $^1\text{H}$ -NMR of aldehyde <b>342</b> .....	348
Figure A2.155. $^{13}\text{C}$ -NMR of aldehyde <b>342</b> .....	349
Figure A2.156. FTIR of aldehyde <b>342</b> .....	349
Figure A2.157. $^1\text{H}$ -NMR of carboxylic acid <b>343</b> .....	350
Figure A2.158. $^{13}\text{C}$ -NMR of carboxylic acid <b>343</b> .....	351
Figure A2.159. $^1\text{H}$ -NMR of ketone <b>344</b> .....	352
Figure A2.160. $^1\text{H}$ -NMR of enone <b>345</b> (diastereomer A) .....	353
Figure A2.161. $^{13}\text{C}$ -NMR of enone <b>345</b> (diastereomer A) .....	354
Figure A2.162. $^1\text{H}$ -NMR of enone <b>345</b> (diastereomer B) .....	355
Figure A2.163. $^{13}\text{C}$ -NMR of enone <b>345</b> (diastereomer B) .....	356
Figure A2.164. $^1\text{H}$ -NMR of alcohol <b>346</b> .....	357

Figure A2.165. $^{13}\text{C}$ -NMR of alcohol <b>346</b> .....	358
Figure A2.166. FTIR of alcohol <b>346</b> .....	358
Figure A2.167. $^1\text{H}$ -NMR of tetracycle <b>347</b> .....	359
Figure A2.168. $^{13}\text{C}$ -NMR of tetracycle <b>347</b> .....	360
Figure A2.169. FTIR of tetracycle <b>347</b> .....	360
Figure A2.170. $^1\text{H}$ -NMR of aldehyde <b>355</b> .....	361
Figure A2.171. $^{13}\text{C}$ -NMR of aldehyde <b>355</b> .....	362
Figure A2.172. FTIR of aldehyde <b>355</b> .....	362
Figure A2.173. $^1\text{H}$ -NMR of carboxylic acid <b>356</b> .....	363
Figure A2.174. $^{13}\text{C}$ -NMR of carboxylic acid <b>356</b> .....	364
Figure A2.175. FTIR of carboxylic acid <b>356</b> .....	364
Figure A2.176. $^1\text{H}$ -NMR of aldehyde <b>359</b> .....	365
Figure A2.177. $^{13}\text{C}$ -NMR of aldehyde <b>359</b> .....	366
Figure A2.178. FTIR of aldehyde <b>359</b> .....	366
Figure A2.179. $^1\text{H}$ -NMR of carboxylic acid <b>360</b> .....	367
Figure A2.180. $^{13}\text{C}$ -NMR of carboxylic acid <b>360</b> .....	368
Figure A2.181. FTIR of carboxylic acid <b>360</b> .....	368
Figure A2.182. $^1\text{H}$ -NMR of phenol <b>365</b> .....	369
Figure A2.183. $^{13}\text{C}$ -NMR of phenol <b>365</b> .....	370
Figure A2.184. FTIR of phenol <b>365</b> .....	370
Figure A2.185. $^1\text{H}$ -NMR of triflate <b>366</b> .....	371
Figure A2.186. $^{13}\text{C}$ -NMR of triflate <b>366</b> .....	372
Figure A2.187. $^{19}\text{F}$ -NMR of triflate <b>366</b> .....	372
Figure A2.188. FTIR of triflate <b>366</b> .....	373
Figure A2.189. $^1\text{H}$ -NMR of alkyne <b>351</b> .....	374
Figure A2.190. $^{13}\text{C}$ -NMR of alkyne <b>351</b> .....	375

Figure A2.191. FTIR of alkyne <b>351</b> .....	375
Figure A2.192. <sup>1</sup> H-NMR of allylic alcohol <b>367</b> (diastereomer A) .....	376
Figure A2.193. <sup>13</sup> C-NMR of allylic alcohol <b>367</b> (diastereomer A) .....	377
Figure A2.194. <sup>1</sup> H-NMR of allylic alcohol <b>367</b> (diastereomer B) .....	378
Figure A2.195. <sup>13</sup> C-NMR of allylic alcohol <b>367</b> (diastereomer B) .....	379
Figure A2.196. FTIR of allylic alcohol <b>367</b> (diastereomer B) .....	379
Figure A2.197. <sup>1</sup> H-NMR of aldehyde <b>370</b> .....	380
Figure A2.198. <sup>13</sup> C-NMR of aldehyde <b>370</b> .....	381
Figure A2.199. FTIR of aldehyde <b>370</b> .....	381
Figure A2.200. <sup>1</sup> H-NMR of carboxylic acid <b>371</b> .....	382
Figure A2.201. <sup>13</sup> C-NMR of carboxylic acid <b>371</b> .....	383
Figure A2.202. FTIR of carboxylic acid <b>371</b> .....	383
Figure A2.203. <sup>1</sup> H-NMR of ketone <b>372</b> .....	384
Figure A2.204. <sup>13</sup> C-NMR of ketone <b>372</b> .....	385
Figure A2.205. FTIR of ketone <b>372</b> .....	385
Figure A2.206. <sup>1</sup> H-NMR of enone <b>373</b> .....	386
Figure A2.207. <sup>13</sup> C-NMR of enone <b>373</b> .....	387
Figure A2.208. FTIR of enone <b>373</b> .....	387
Figure A2.209. <sup>1</sup> H-NMR of phenol <b>374</b> .....	388
Figure A2.210. <sup>13</sup> C-NMR of phenol <b>374</b> .....	389
Figure A2.211. FTIR of phenol <b>374</b> .....	389
Figure A2.212. <sup>1</sup> H-NMR of triflate <b>375</b> .....	390
Figure A2.213. <sup>13</sup> C-NMR of triflate <b>375</b> .....	391
Figure A2.214. <sup>19</sup> F-NMR of triflate <b>375</b> .....	391
Figure A2.215. FTIR of triflate <b>375</b> .....	392
Figure A2.216. <sup>1</sup> H-NMR of alkyne <b>376</b> .....	393

Figure A2.217. <sup>13</sup> C-NMR of alkyne <b>376</b> .....	394
Figure A2.218. FTIR of alkyne <b>376</b> .....	394
Figure A2.219. <sup>1</sup> H-NMR of allylic alcohol <b>377</b> .....	395
Figure A2.220. <sup>13</sup> C-NMR of allylic alcohol <b>377</b> .....	396
Figure A2.221. FTIR of allylic alcohol <b>377</b> .....	396
Figure A2.222. <sup>1</sup> H-NMR of phenol <b>368</b> .....	397
Figure A2.223. <sup>13</sup> C-NMR of phenol <b>368</b> .....	398
Figure A2.224. <sup>1</sup> H-NMR of carbonate <b>378</b> .....	399
Figure A2.225. <sup>13</sup> C-NMR of carbonate <b>378</b> .....	400
Figure A2.226. <sup>1</sup> H-NMR of silyl ether <b>465</b> .....	401
Figure A2.227. <sup>13</sup> C-NMR of silyl ether <b>465</b> .....	402
Figure A2.228. FTIR of silyl ether <b>465</b> .....	402
Figure A2.229. <sup>1</sup> H-NMR of alcohol <b>466</b> .....	403
Figure A2.230. <sup>13</sup> C-NMR of alcohol <b>466</b> .....	404
Figure A2.231. FTIR of alcohol <b>466</b> .....	404
Figure A2.232. <sup>1</sup> H-NMR of aldehyde <b>425</b> .....	405
Figure A2.233. <sup>13</sup> C-NMR of aldehyde <b>425</b> .....	406
Figure A2.234. FTIR of aldehyde <b>425</b> .....	406
Figure A2.235. <sup>1</sup> H-NMR of alcohol <b>467</b> .....	407
Figure A2.236. <sup>13</sup> C-NMR of alcohol <b>467</b> .....	408
Figure A2.237. FTIR of alcohol <b>467</b> .....	408
Figure A2.238. <sup>1</sup> H-NMR of phenol <b>429</b> .....	409
Figure A2.239. <sup>13</sup> C-NMR of phenol <b>429</b> .....	410
Figure A2.240. FTIR of phenol <b>429</b> .....	410
Figure A2.241. <sup>1</sup> H-NMR of β-hydroxy ketone <b>437</b> .....	411
Figure A2.242. <sup>13</sup> C-NMR of β-hydroxy ketone <b>437</b> .....	412

Figure A2.243. FTIR of $\beta$ -hydroxy ketone <b>437</b> .....	412
Figure A2.244. $^1\text{H-NMR}$ of diol <b>438</b> .....	413
Figure A2.245. $^{13}\text{C-NMR}$ of diol <b>438</b> .....	414
Figure A2.246. FTIR of diol <b>438</b> .....	414
Figure A2.247. $^1\text{H-NMR}$ of acetal <b>440</b> .....	415
Figure A2.248. $^{13}\text{C-NMR}$ of acetal <b>440</b> .....	416
Figure A2.249. FTIR of acetal <b>440</b> .....	416
Figure A2.250. $^1\text{H-NMR}$ of phenol <b>468</b> .....	417
Figure A2.251. $^{13}\text{C-NMR}$ of phenol <b>468</b> .....	418
Figure A2.252. FTIR of phenol <b>468</b> .....	418
Figure A2.253. $^1\text{H-NMR}$ of phenol <b>441</b> .....	419
Figure A2.254. $^{13}\text{C-NMR}$ of phenol <b>441</b> .....	420
Figure A2.255. $^1\text{H-NMR}$ of spirotetrahydrofuran <b>443</b> .....	421
Figure A2.256. $^{13}\text{C-NMR}$ of spirotetrahydrofuran <b>443</b> .....	422
Figure A2.257. $^1\text{H-NMR}$ of ester <b>448</b> .....	423
Figure A2.258. $^{13}\text{C-NMR}$ of ester <b>448</b> .....	424
Figure A2.259. FTIR of ester <b>448</b> .....	424
Figure A2.260. $^1\text{H-NMR}$ of enone <b>445</b> .....	425
Figure A2.261. $^1\text{H-NMR}$ of ester <b>451</b> .....	426
Figure A2.262. $^{13}\text{C-NMR}$ of ester <b>451</b> .....	427
Figure A2.263. FTIR of ester <b>451</b> .....	427
Figure A2.264. $^1\text{H-NMR}$ of anhydride <b>452</b> .....	428
Figure A2.265. $^{13}\text{C-NMR}$ of anhydride <b>452</b> .....	429
Figure A2.266. FTIR of anhydride <b>452</b> .....	429
Figure A2.267. $^1\text{H-NMR}$ of enone <b>449</b> .....	430
Figure A2.268. $^{13}\text{C-NMR}$ of enone <b>449</b> .....	431

Figure A2.269. FTIR of enone <b>449</b> .....	431
Figure A2.270. <sup>1</sup> H-NMR of ester <b>453</b> .....	432
Figure A2.271. <sup>13</sup> C-NMR of ester <b>453</b> .....	433
Figure A2.272. FTIR of ester <b>453</b> .....	433
Figure A2.273. <sup>1</sup> H-NMR of aldol product <b>456</b> .....	434
Figure A2.274. <sup>13</sup> C-NMR of aldol product <b>456</b> .....	435
Figure A2.275. FTIR of aldol product <b>456</b> .....	435
Figure A2.276. <sup>1</sup> H-NMR of bismesylate <b>457</b> .....	436
Figure A2.277. <sup>13</sup> C-NMR of bismesylate <b>457</b> .....	437
Figure A2.278. FTIR of bismesylate <b>457</b> .....	437
Figure A2.279. <sup>1</sup> H-NMR of enone <b>458</b> .....	438
Figure A2.280. <sup>13</sup> C-NMR of enone <b>458</b> .....	439
Figure A2.281. FTIR of enone <b>458</b> .....	439

## LIST OF SCHEMES

Scheme 1.1. Degradation of gliotoxin ( <b>9</b> ) to dehydrodethiogliotoxin ( <b>8</b> ) .....	5
Scheme 1.2. Proposed biosynthesis of gliotoxin ( <b>9</b> ) .....	7
Scheme 2.1. Methods to install the disulfide bridge into ETPs .....	9
Scheme 2.2. Kishi's use of a dithioacetal as a protecting group .....	10
Scheme 2.3. Alkylation of dithioacetal <b>30</b> .....	11
Scheme 2.4. Resonance structures of dithioacetal <b>30</b> , illustrating its reactivity .....	11
Scheme 2.5. Kishi's retrosynthetic analysis of gliotoxin ( <b>9</b> ) .....	12
Scheme 2.6. Kishi's synthesis of enantiopure dithioacetal <b>38</b> .....	13
Scheme 2.7. Kishi's completion of gliotoxin ( <b>9</b> ) .....	14
Scheme 2.8. Kishi's retrosynthetic analysis of dehydrogliotoxin ( <b>10</b> ) .....	15
Scheme 2.9. Kishi's synthesis of dehydrogliotoxin ( <b>10</b> ) .....	16
Scheme 3.1. Synthesis of aryl–amide coupling precursors <b>39</b> and <b>50</b> .....	18
Scheme 3.2. Attempted aryl–amidation utilizing Kishi's conditions .....	18
Scheme 3.3. Copper–catalyzed aryl–amidation conditions .....	19
Scheme 3.4. Palladium–catalyzed aryl–amidation conditions .....	19
Scheme 3.5. Revised retrosynthetic analysis of dithioacetal <b>69</b> .....	24
Scheme 3.6. Attempted synthesis of coupling precursor <b>77</b> .....	24
Scheme 3.7. Revised retrosynthetic analysis of coupling precursor <b>70</b> .....	25
Scheme 3.8. Alkylation of glycine derivative <b>81</b> .....	26
Scheme 3.9. Synthesis of tricycle <b>84</b> .....	27
Scheme 3.10. Unsuccessful bromination of tricycle <b>84</b> .....	27
Scheme 3.11. Attempted formation of bis–silyl enol ether <b>88</b> .....	30
Scheme 3.12. Oxidation of DKP <b>84</b> .....	30
Scheme 4.1. Modified retrosynthetic analysis of intermediate <b>49</b> .....	32

Scheme 4.2. Synthesis of precursors (a) aniline <b>92</b> and (b) acid <b>93</b> .....	33
Scheme 4.3. Formal total synthesis of dehydrogliotoxin ( <b>10</b> ) .....	34
Scheme 5.1. Retrosynthetic analysis of model diselenide <b>100</b> .....	38
Scheme 5.2. Attempted synthesis of diselenides <b>105</b> and <b>106</b> .....	39
Scheme 5.3. Proposed reaction of dibromide <b>22</b> with a diselenide dianion equivalent .....	39
Scheme 5.4. a) Synthesis of bromide <b>112</b> . b) Attempted reaction of bromide <b>112</b> with the diselenide dianion equivalent derived from Se and superhydride. c) Successful reaction of bromide <b>112</b> with the diselenide dianion equivalent derived from Se and sodium borohydride .	41
Scheme 5.5. Successful synthesis of diselenide <b>106</b> from DKP <b>72</b> .....	41
Scheme 5.6. Proposed synthesis of diselenide <b>114</b> from disulfide <b>115</b> .....	42
Scheme 5.7. Synthesis of diselenide <b>106</b> from disulfide <b>115</b> .....	43
Scheme 5.8. Synthesis of a) bis-selenomethyl ether <b>120</b> and b) dithioacetal <b>121</b> .....	44
Scheme 5.9. Attempted synthesis of diselenide <b>128</b> .....	46
Scheme 6.1. Revised structure of tetrapetalone A ( <b>130</b> ) and conversion to tetrapetalone A-Me <sub>2</sub> ( <b>131</b> ).....	53
Scheme 6.2. Proposed biosynthetic pathway of the tetrapetalones .....	56
Scheme 7.1. Porco's retrosynthetic analysis of tetrapetalone A ( <b>130</b> ) .....	58
Scheme 7.2. Porco's attempted ring-closing metathesis of triene <b>146</b> .....	59
Scheme 7.3. Porco's revised retrosynthetic analysis of intermediate <b>145</b> .....	60
Scheme 7.4. Porco's synthesis of hydroquinone <b>145</b> .....	60
Scheme 7.5. Porco's attempted synthesis of tetracycle <b>157</b> .....	61
Scheme 7.6. Sarpong's retrosynthetic analysis of tetrapetalone A ( <b>130</b> ) .....	61
Scheme 7.7. Sarpong's synthesis of intermediate <b>166</b> .....	62
Scheme 7.8. Sarpong's synthesis of tetracycle <b>173</b> .....	63
Scheme 7.9. Hong's proposed synthesis of the six-seven-five skeleton of tetrapetalone A .....	64
Scheme 7.10. Hong's synthesis of tetracycles <b>183</b> and <b>184</b> .....	64

Scheme 7.11. Hong's synthesis of the barebone skeleton of tetrapetalone A .....	65
Scheme 8.1. Initial retrosynthetic analysis of tetrapetalone A ( <b>130</b> ).....	66
Scheme 8.2. Retrosynthetic analysis of vinyl halide <b>189</b> .....	67
Scheme 8.3. Synthesis of undesired <i>syn</i> diastereomer <b>199</b> .....	67
Scheme 8.4. Unsuccessful attempts of the Stetter reaction to form <b>204</b> .....	68
Scheme 8.5. Revised strategy for Buchwald–Hartwig coupling .....	68
Scheme 8.6. Attempted Buchwald–Hartwig coupling to form <b>212</b> .....	69
Scheme 8.7. Unsuccessful attempts at ring–closing metathesis.....	70
Scheme 8.8. Revised retrosynthetic analysis .....	71
Scheme 8.9. Attempted ring–closing metathesis to form lactone <b>220</b> .....	72
Scheme 8.10. Revised retrosynthetic analysis of intermediate <b>187</b> .....	72
Scheme 8.11. Synthesis of aryl amine <b>230</b> .....	73
Scheme 9.1. Retrosynthetic analysis of tetrapetalone A ( <b>130</b> ).....	75
Scheme 9.2. Attempted synthesis of 1,4–adduct <b>239</b> .....	76
Scheme 9.3. Yamamoto's bulky Lewis acid .....	77
Scheme 9.4. Synthesis of <b>247</b> .....	77
Scheme 9.5. Proposed cascade Friedel–Crafts to form tetracycle <b>253</b> from acid chloride <b>233</b> .	78
Scheme 9.6. Literature precedent showing a) an olefin isomerization before conjugate addition and b) a Friedel–Crafts type acylation forming a seven–membered ring .....	78
Scheme 9.7. Attempts at a cascade Friedel–Crafts pathway .....	79
Scheme 9.8. Successful Friedel–Crafts with anisole.....	79
Scheme 9.9. Proposed $\pi$ -allyl pathway to form the seven–membered ring ( <b>264</b> ).....	80
Scheme 9.10. Attempted palladium $\pi$ -allyl reactions .....	82
Scheme 9.11. Proposed mechanism for the formation of fused tricycle <b>269</b> .....	83
Scheme 9.12. Synthesis of tricycle <b>276</b> .....	84
Scheme 10.1 Retrosynthetic analysis of <b>130</b> utilizing a transannular $\pi$ -allyl reaction .....	86

Scheme 10.2. Proposed transannular palladium $\pi$ -allyl reaction .....	87
Scheme 10.3. Synthesis of unreactive ester <b>287</b> .....	88
Scheme 10.4. Hartwig's iridium-catalyzed borylation .....	89
Scheme 10.5. a) Unsuccessful borylation of <b>234</b> and b) successful borylation of <b>295</b> .....	90
Scheme 10.6. Synthesis of bisketone <b>298</b> .....	91
Scheme 10.7. Revised retrosynthetic analysis of enone <b>300</b> .....	91
Scheme 10.8. Successful synthesis of ring-closing metathesis precursors <b>303</b> and <b>304</b> .....	92
Scheme 10.9. Attempted ring-closing metathesis of enone <b>303</b> .....	93
Scheme 10.10. Attempted ring-closing metathesis of allylic alcohol <b>304</b> .....	94
Scheme 10.11. Revised retrosynthetic analysis of tetrapetalone A ( <b>130</b> ) .....	95
Scheme 10.12. Synthesis of aldehyde <b>312</b> .....	96
Scheme 10.13. Attempted synthesis of NHK precursor <b>311</b> .....	97
Scheme 10.14. Montgomery's synthesis of Aigalomycin utilizing a reductive alkyne-aldehyde coupling .....	97
Scheme 10.15. Attempted nickel-catalyzed alkyne-aldehyde coupling .....	98
Scheme 11.1. Our previous $\pi$ -allyl attempt that led to five-membered product <b>276</b> .....	100
Scheme 11.2. Revised palladium $\pi$ -allyl strategy .....	100
Scheme 11.3. Attempted palladium $\pi$ -allyl reaction on substrate lacking double bond .....	101
Scheme 11.4. Allylic epoxide palladium $\pi$ -allyl approach .....	101
Scheme 11.5. a) Synthesis of epoxide <b>335</b> and <b>336</b> and b) attempts to form allylic epoxide <b>327</b> .....	102
Scheme 11.6. Proposed Friedel-Crafts pathway to ketone <b>339</b> .....	103
Scheme 11.7. Synthesis of ketone <b>339</b> via Friedel-Crafts reaction .....	103
Scheme 11.8. Formation of $\alpha$ -bromo ketone <b>344</b> .....	105
Scheme 11.9. Elimination of $\alpha$ -bromo ketone <b>344</b> to form enone <b>345</b> and elaboration to tetracycle <b>347</b> .....	106

Scheme 11.10. Revised retrosynthetic analysis of tetrapetalone A ( <b>130</b> ) .....	107
Scheme 11.11. Alternate retrosynthetic analysis of tetrapetalone A ( <b>130</b> ) .....	107
Scheme 11.12. Attempted Friedel–Crafts acylation of aryl bromide <b>356</b> .....	108
Scheme 11.13. Attempted Friedel–Crafts acylation of aryl alkyne <b>360</b> .....	109
Scheme 11.14. a) The desired functionalization of enone <b>345</b> and b) Dong’s selective C–H oxidation utilizing ketone as a directing group .....	110
Scheme 11.15. Synthesis of keto alkyne <b>351</b> .....	110
Scheme 12.1. Attempted removal of methyl protecting group .....	111
Scheme 12.2. Synthesis of TIPS protected ketone <b>373</b> .....	112
Scheme 12.3. Synthesis of TIPS protected alkyne <b>376</b> .....	113
Scheme 12.4. Attempted phenolic oxidation to form epoxide <b>369</b> .....	114
Scheme 12.5. Proposed synthesis of cyclic carbonate <b>381</b> .....	115
Scheme 12.6. Sarpong’s synthesis of <b>384</b> .....	116
Scheme 12.7. Attempted synthesis of phenol <b>379</b> .....	116
Scheme 13.1. Proposed synthesis of tetracycle <b>348</b> from vinyl stannane <b>386</b> .....	118
Scheme 13.2. Proposed synthesis of tetracycle <b>395</b> from ketone <b>391</b> .....	119
Scheme 13.3. Proposed synthesis of tetracycle <b>348</b> from styrene <b>397</b> .....	121
Scheme 13.4. Attempted reduction of alkyne <b>389</b> .....	121
Scheme 13.5. Proposed reaction to form a) styrene <b>400</b> through a Stille coupling and b) tetracycle <b>395</b> through a carbonylative Stille coupling followed by conjugate reduction .....	122
Scheme 14.1. Relationship between ansaetherone ( <b>135</b> ) and the tetrapetalones .....	123
Scheme 14.2. Proposed conversion of ansaetherone ( <b>135</b> ) to tetrapetalone B ( <b>132</b> ) .....	124
Scheme 14.3. Proposed synthesis of tetracycle <b>409</b> through a Lewis acidic or basic pathway .....	125
Scheme 14.4. Proposed alternate synthesis of tetrapetalone B from phenol <b>408</b> .....	126
Scheme 14.5. George’s Paternó–Büchi/ elimination route to tetracycle <b>419</b> .....	126

Scheme 14.6. Retrosynthetic analysis of ansaetherone ( <b>135</b> ) .....	127
Scheme 14.7. Attempted phenolic oxidation of <b>429</b> .....	128
Scheme 14.8. Kit's synthesis of dihydropyran <b>433</b> .....	128
Scheme 14.9. Revised retrosynthetic analysis of dihydropyran <b>422</b> .....	129
Scheme 14.10. Attempted synthesis of dihydropyran <b>439</b> .....	129
Scheme 14.11. Attempted synthesis of dihydropyran <b>439</b> .....	130
Scheme 14.12. Revised retrosynthetic analysis of ansaetherone ( <b>135</b> ).....	131
Scheme 14.13. Attempted synthesis of oxy-Michael product <b>444</b> .....	132
Scheme 14.14. Revised retrosynthetic analysis of nitrobenzene <b>444</b> .....	132
Scheme 14.15. Synthesis of aryl ketone <b>449</b> .....	133
Scheme 14.16. Attempts at Fries of photo Fries rearrangements .....	133
Scheme 14.17. Aldol attempts to form aryl ketone <b>449</b> .....	134
Scheme 14.18. Synthesis of enone <b>458</b> .....	135
Scheme 14.19. Proposed future work to obtain nitrobenzene <b>444</b> .....	135

## **Part One**

The formal total synthesis of dehydrogliotoxin and the first synthesis of an epidiselenodiketopiperazine.

# Chapter One

## Introduction

Tuberculosis (TB), caused by *Mycobacterium tuberculosis* (MTB), affects approximately one third of the global population and is associated with nearly two million deaths annually.<sup>1</sup> Although there are known cures for TB, most of the problems associated with TB exist in developing countries that lack the infrastructure and resources to efficiently diagnose and then treat the illness. This establishes a clear and continuing need for economically accessible treatments, and the growing presence of TB strains resistant to current drug regimens serves to accentuate this need. As part of a collaborative effort with the Hung group at the Broad Institute, we have identified two related natural products, gliotoxin and dehydrogliotoxin, as potential candidates for further exploration as anti-TB agents.

### 1.1. Tuberculosis

Tuberculosis is a serious infection that is mostly localized in the lungs, and is spread by inhaling droplets in the air containing the bacteria.<sup>2</sup> Once inhaled the bacteria enters the host cell through phagocytosis by the alveolar macrophages. Although phagocytosis is the normal function of the macrophage, MTB has acquired the ability to survive and replicate within the macrophage. It does this by inhibiting the phagolysosomes, which are responsible for digesting unwanted objects consumed by the macrophage. In most healthy individuals the bacteria is contained by isolating the infected macrophage in what is called a tubercle, preventing the bacteria from spreading. The tubercle can become calcified and the bacteria can lay dormant within for many years. If the immune system is weakened (commonly from another disease

such as HIV) the tubercle can liquefy, releasing the bacteria, which can multiply at very high rates and eventually spread throughout the body and ultimately lead to death.

Approximately one third of the global population is infected with MTB, which leads to nearly two million deaths annually. Of particular concern is the fact that most cases of TB reside in developing countries that lack the resources and infrastructure to efficiently treat the disease. Although TB can typically be cured, the drug regimen required usually lasts 6–9 months and consists of a combination of multiple drugs. It is often the case, especially in underdeveloped countries, that a patient begins treatment, starts to feel better, and stops treatment before the disease is fully cured. It is due to this that multi-drug resistant strains of TB are becoming more and more prevalent, with nearly 500,000 cases (4.6% of the global burden) as of 2008.<sup>1</sup>

The typical treatment of TB consists of a combination of drugs.<sup>3</sup> In most cases the patient is given the so-called 1<sup>st</sup> line drugs, isoniazid (**1**), rifampicin (**2**), and ethambutol (**3**) as well as any number of the so-called 2<sup>nd</sup> line drugs such as the fluoroquinolones (**4**), capreomycin (**5**), amikacin (**6a**), kanamycin (**6b**), and others (Figure 1.1). Multi-drug resistant strains are those that are resistant to isoniazid and rifampicin. Extensively resistant strains are not only resistant to **1** and **2**, but also to the fluoroquinolones and at least one of the other three 2<sup>nd</sup> line drugs.

Given the above information it is clear that there is a continuing need to develop new therapies for TB. Both more simplified and shorter treatment regimens are needed to encourage patients to finish treatments, which will not only lead to the disease being cured, but also to less instances of multi-drug and extensively resistant strains. Due to the presence of these resistant strains, new targets that are chemically distinct from the existing treatments should be targeted.

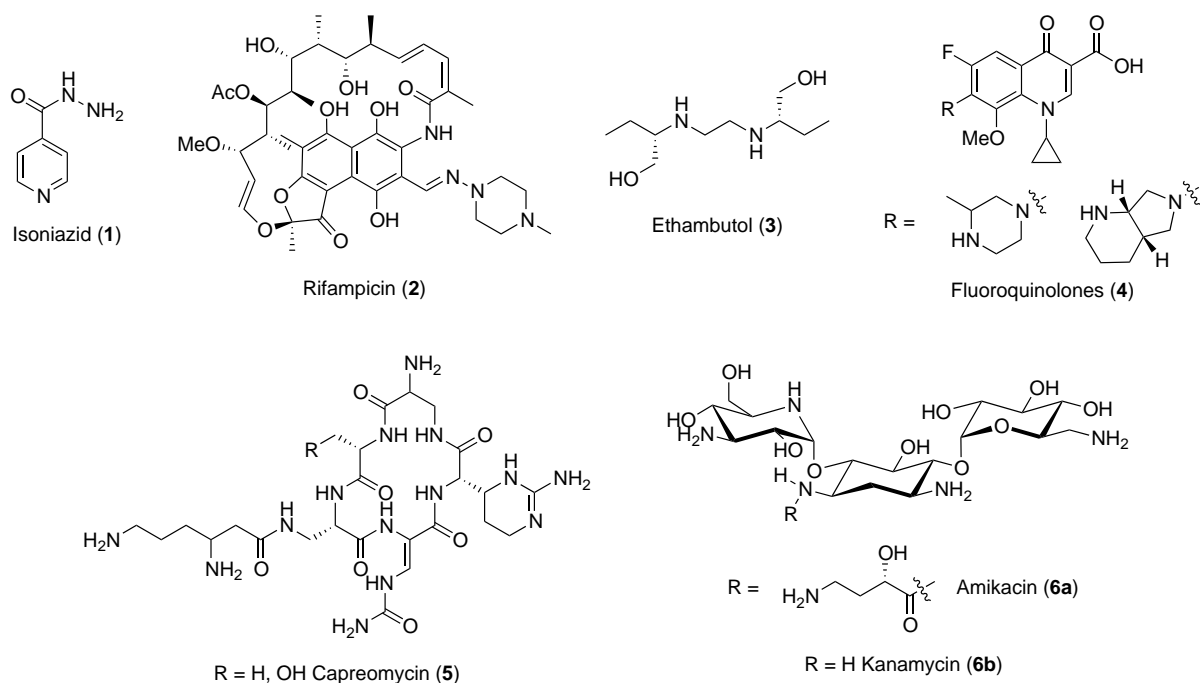


**Figure 1.1.** Typical drugs used to treat tuberculosis.

## 1.2. Gliotoxin and Dehydrogliotoxin

In 1936 Weindling and Emerson reported the isolation of a toxic crystalline solid from the wood fungus *Gliocladium fimbriatum*,<sup>4</sup> which has since been isolated from a variety of microorganisms including *Aspergillus fumigatus*<sup>5</sup> and *Penicillium terlikowsii*.<sup>6</sup> In this initial report the molecular formula was erroneously reported as  $C_{14}H_{16}N_2O_4S_2$ . In 1943 Johnson and coworkers further investigated the physical properties of this compound, now named gliotoxin, and with the help of elemental analysis, revised the molecular formula to  $C_{13}H_{14}N_2O_4S_2$ .<sup>7</sup> The first structure of gliotoxin was proposed 20 years later by Johnson and Buchanan, who after extensive degradation studies, proposed pentacycle **7** as the structure of gliotoxin (Figure 1.2).<sup>8</sup>



In 1966 the related compound, dehydrogliotoxin (**10**), was isolated from *Penicillium terlikowsii* (Figure 1.4).<sup>10</sup> It differs in structure from **9** only by the presence of the aromatic ring in **10** in place of the dihydrobenzene moiety.

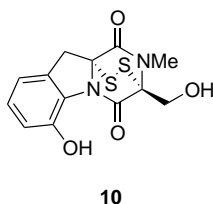
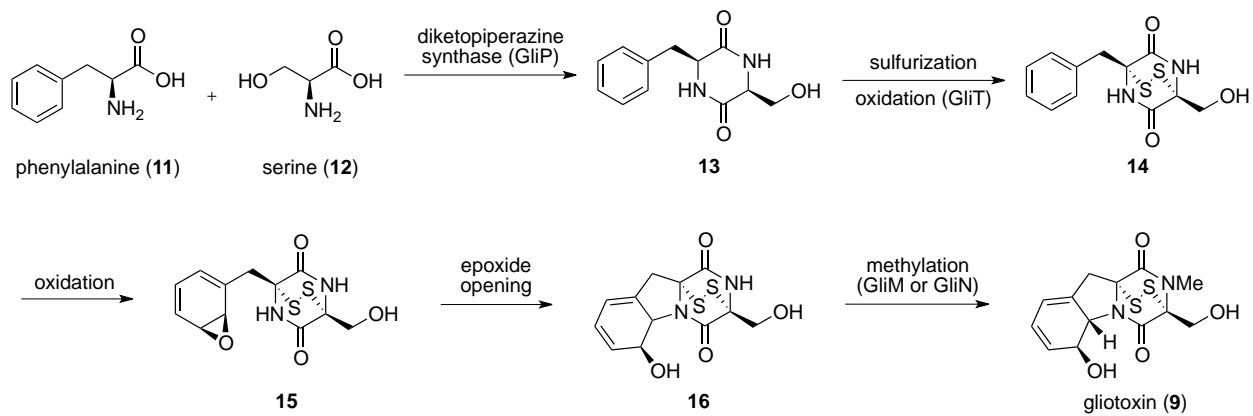


**Figure 1.4.** Dehydrogliotoxin (**10**).

Gliotoxin has been known to inhibit MTB since 1950, where it was found to exhibit minimum inhibitory concentrations (MICs) ranging from 6 to 45 nM.<sup>11</sup> Unfortunately gliotoxin has also been found to be toxic, with an LD<sub>50</sub> of 25 to 65 mg/kg.<sup>7, 11b</sup> When this project was started, dehydrogliotoxin had never been tested against MTB; however, it had been shown to inhibit macrophage phagocytosis in concentrations similar to that of gliotoxin,<sup>12</sup> suggesting that it could also be relevant to MTB. Given these facts we became interested in gliotoxin, dehydrogliotoxin, and analogs of the two as potential anti-TB therapeutics. In the context of analogs, we would hope to identify a compound that both retains activity against MTB, but also exhibits less toxicity compared to **9** and **10**.

### 1.3. Biosynthesis

Biosynthetically, gliotoxin derives from the condensation of phenylalanine (**11**) and serine (**12**), which produces diketopiperazine **13**. It is widely believed that after sulfur incorporation the aromatic ring is oxidized to arene oxide **14**, which undergoes subsequent intramolecular attack by the DKP amide nitrogen. Methylation of the remaining free amide nitrogen completes the biosynthesis of gliotoxin (Scheme 1.2).<sup>13</sup>



**Scheme 1.2.** Proposed biosynthesis of gliotoxin (9).

## Chapter Two

### Previous Synthetic Work

Due to their interesting structural features and considerable biological activity, epidithiodiketopiperazine (ETP) natural products have received considerable attention from the synthetic community. The most well studied class of these ETP natural products is the gliotoxin family, with both dehydrogliotoxin and gliotoxin being synthesized by the Kishi group in 1973 and 1976 respectively.<sup>14</sup> More recently other ETPs have been synthesized including gliocladine C (**17**), acetylaranotin (**18**), chaetocin A (**19**), and 11,11'-dideoxyverticillin A (**20**) (Figure 2.1).<sup>15</sup>

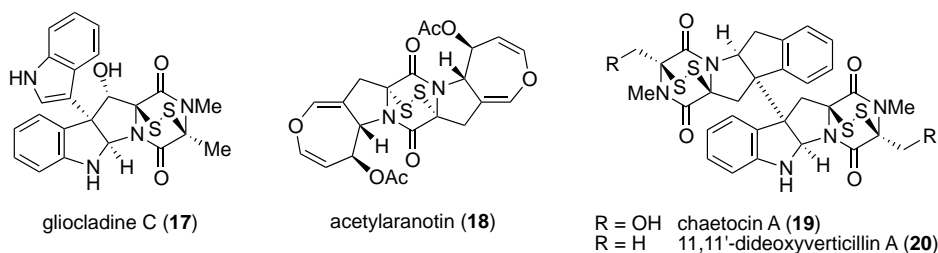


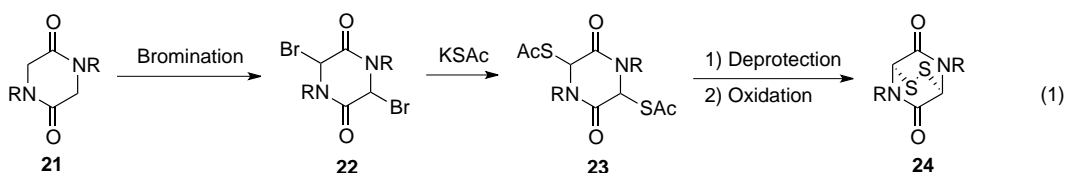
**Figure 2.1.** Epidithiodiketopiperazine natural products that have recently been synthesized.

#### 2.1. Methods to Install the Disulfide Bridge

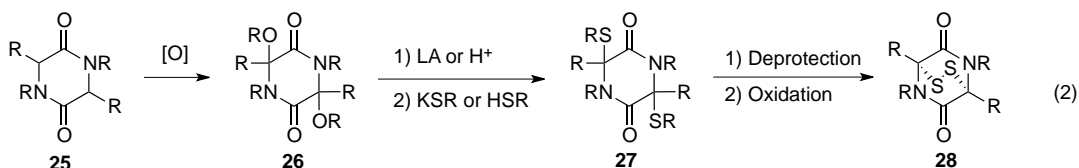
Along with being the structural feature that defines the ETP natural products, the bridging disulfide is also one of the most significant synthetic challenges one faces when attempting to prepare any member of the family. To date, there have been three basic approaches utilized to install this challenging functional group (Scheme 2.1). The first relies on initial radical bromination followed by attack with a sulfur nucleophile such as potassium thioacetate, which presumably proceeds through an acyl iminium species. Removal of the acetates and oxidation gives bridging disulfide **24** (eq. 1).<sup>16</sup> The second method utilizes a non-

radical oxidation to give **26**, which can undergo a Lewis or Brønsted acid catalyzed acyl iminium formation and trapping with a sulfur nucleophile. The protecting group can be removed to reveal bridging disulfide **28** after oxidation (eq. 2).<sup>15c, 17</sup> The last method involves deprotonating DKP **25** with a strong base followed by reacting it with a sulfur electrophile to furnish **27**. Bridging disulfide **28** is obtained after deprotection and oxidation (eq. 3).<sup>18</sup>

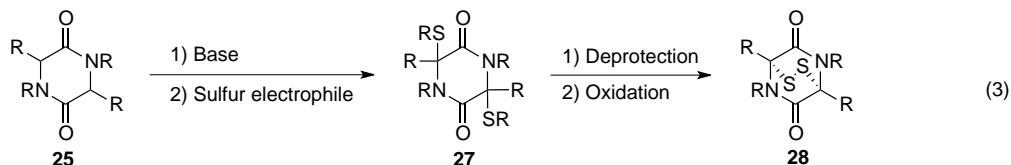
Radical Bromination:



Non-radical Oxidation:



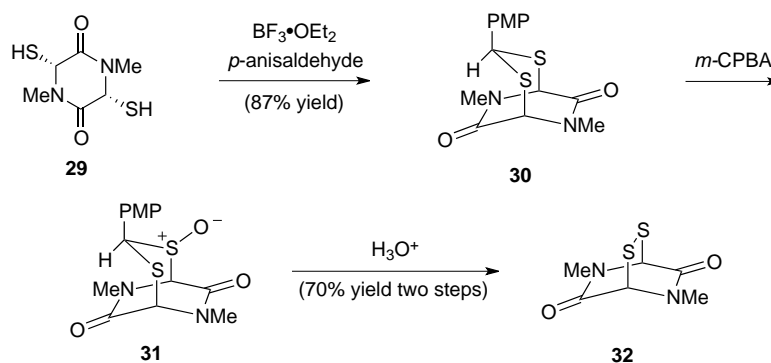
Electrophilic Sulfur:



**Scheme 2.1.** Methods to install the disulfide bridge into ETPs.

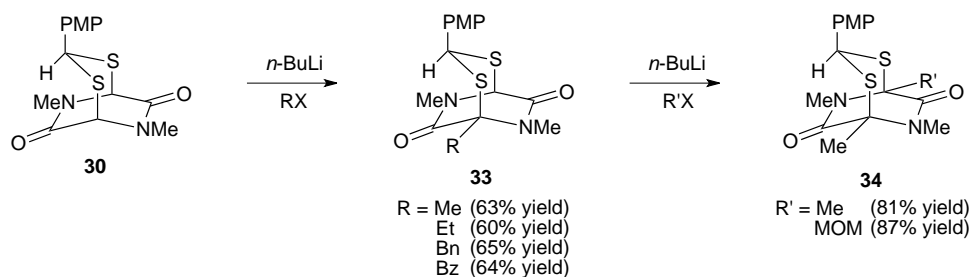
In the context of the total synthesis of gliotoxin, Kishi and coworkers decided that early incorporation of the disulfide and further functionalization of the DKP was more promising than late stage sulfur incorporation. However, studies on simple substrates revealed the disulfide bridge as being sensitive to oxidative, reductive, and basic conditions. To circumvent the instability of the disulfide and still utilize a strategy that incorporated sulfur in the early stages, they chose to pursue a strategy wherein the requisite sulfur atoms were protected as the corresponding dithioacetal. As a proof of concept, simple dithiol **29** was reacted with *p*-anisaldehyde to form dithioacetal **30**. Importantly this dithioacetal was stable to strongly acidic,

strongly basic, reductive, and some oxidative conditions. Cleavage was realized by first oxidizing to the monosulfoxide then adding acid to give disulfide **32** (Scheme 2.2).



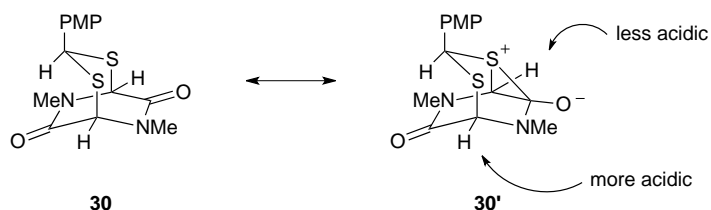
**Scheme 2.2.** Kishi's use of a dithioacetal as a protecting group.

Given their focus on the early installation of sulfur, the Kishi group needed to develop chemistry that would allow for the introduction of numerous other structural components. Specifically they needed to alkylate at the bridgehead carbon. Although formation of an anion at a bridgehead carbon is normally very difficult, the Kishi group hypothesized that deprotonation of the carbon  $\alpha$  to the dithioacetal may be possible due to the extra stabilization from the d-orbital of the neighboring sulfur atom. To test the viability of this alkylation, simple dithioacetal **30** was exposed to *n*-BuLi followed by a variety of electrophiles and the corresponding alkylated products (**33**) were obtained in good yields. Furthermore, they found that by resubjecting the compound where R = methyl to the reaction conditions, they could get a product (**34**), where both sides have been alkylated differentially (Scheme 2.3).



**Scheme 2.3.** Alkylation of dithioacetal **30**.

Interestingly, while performing these alkylations, the Kishi group observed that one regioisomeric product would preferentially be obtained depending on which diastereomer of the dithioacetal was subjected to the reaction. They hypothesized that the observed regioselectivity arose from the fact that one of the sulfurs of the dithioacetal could interact with the nearby amide carbonyl to form resonance structure **30'** (Scheme 2.4). The proton  $\alpha$  to that carbonyl is now much less acidic due to less stabilization from both the sulfur and the carbonyl, leading to preferential deprotonation  $\alpha$  to the other carbonyl, which does not interact with the dithioacetal.

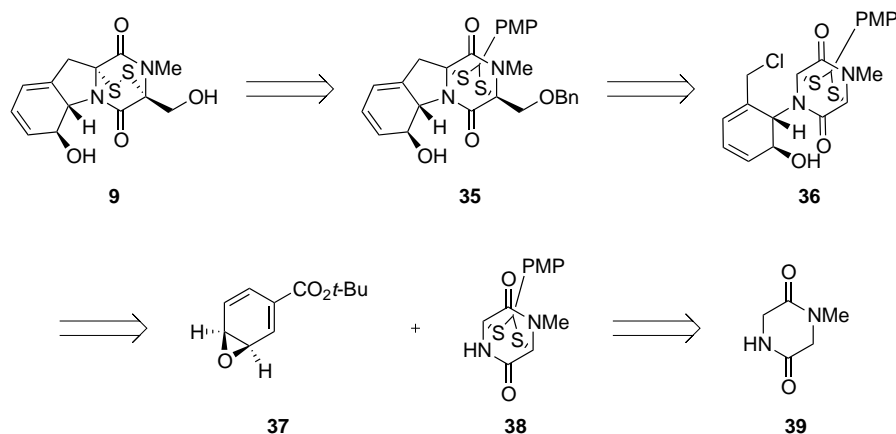


**Scheme 2.4.** Resonance structures of dithioacetal **30**, illustrating its reactivity.

## 2.2. Kishi's Synthesis of Gliotoxin

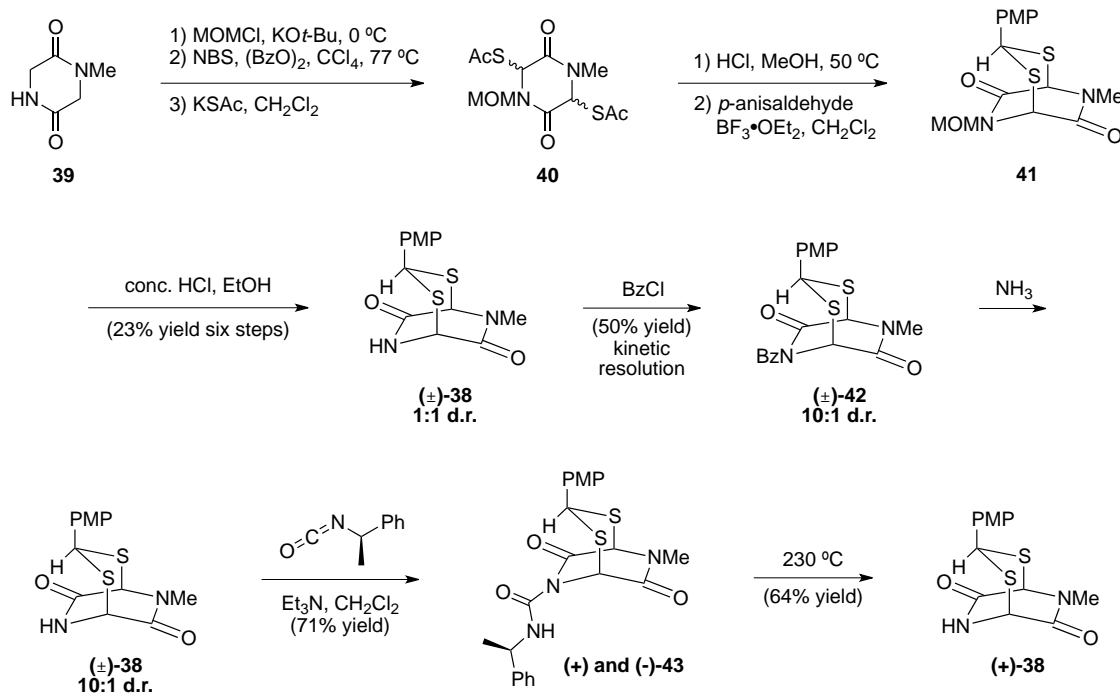
Based on this body of exploratory research, a synthetic plan for gliotoxin became clear and is illustrated below in retrosynthetic fashion (Scheme 2.5). As illustrated, gliotoxin (**9**) would be formed from late stage deprotection of dithioacetal **35**, which itself would arise from

dialkylation of **36** employing the method they developed for bridgehead anion formation. Alkyl chloride **36** would arise from attack of arene oxide **37** with DKP **38**. The latter would derive from **39** after sulfur incorporation and dithioacetal formation.



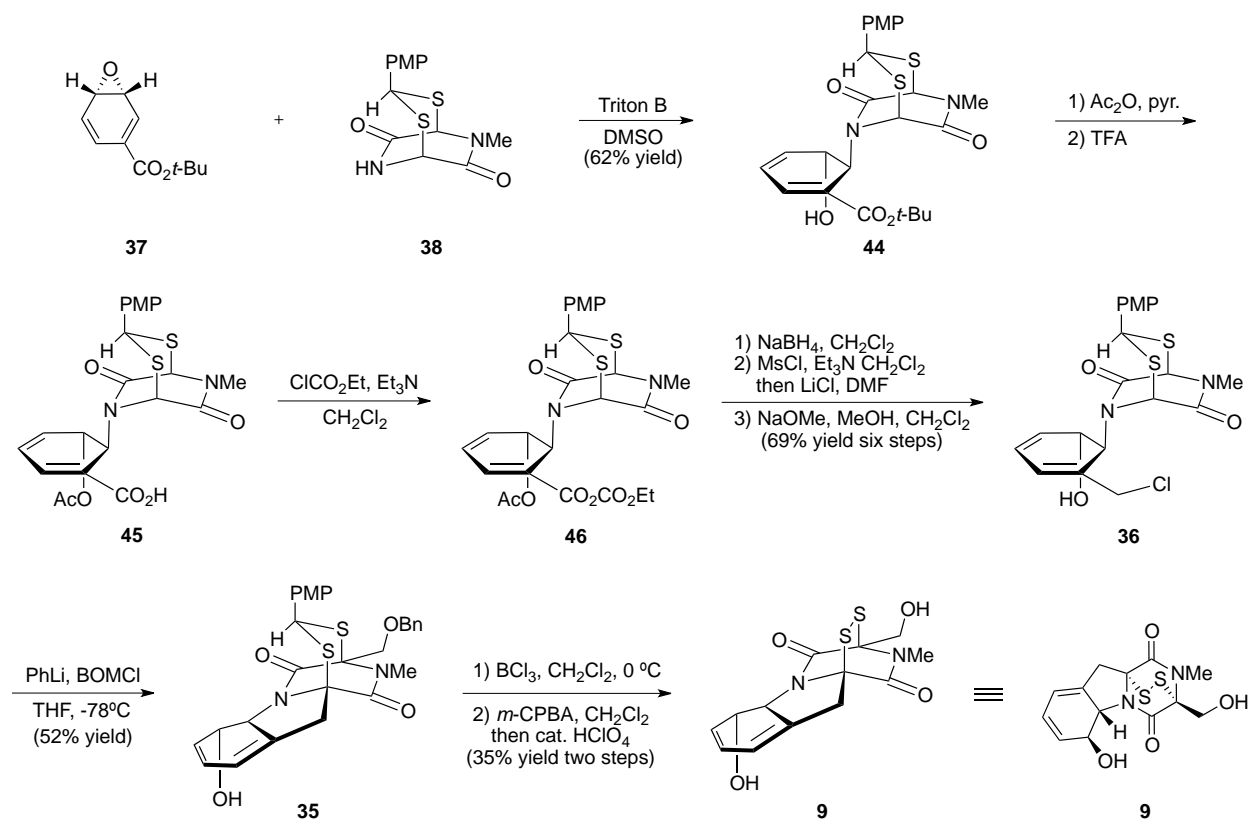
**Scheme 2.5.** Kishi's retrosynthetic analysis of gliotoxin (**9**).

In the forward sense, Kishi commenced by protecting the amide of known DKP **39**. Radical bromination and displacement of the bromides with potassium thioacetate gave dithioacetate **40**. Removal of the acetate protecting groups followed by dithioacetal formation produced intermediate **41**, which was subjected to concentrated HCl in ethanol to furnish racemic DKP **38** as a 1:1 mixture of diastereomers. A subsequent kinetic resolution with benzoyl chloride enhanced the diastereomeric ratio to 10:1. Deprotection of the racemic mixture followed by reaction with a chiral isocyanate furnished urea **43** as a mixture of two diastereomers, which proved to be readily separable via flash chromatography. The urea of the desired enantiomer was then hydrolyzed to produce enantiopure dithioacetal **38** (Scheme 2.6).



**Scheme 2.6.** Kishi's synthesis of enantiopure dithioacetal **38**.

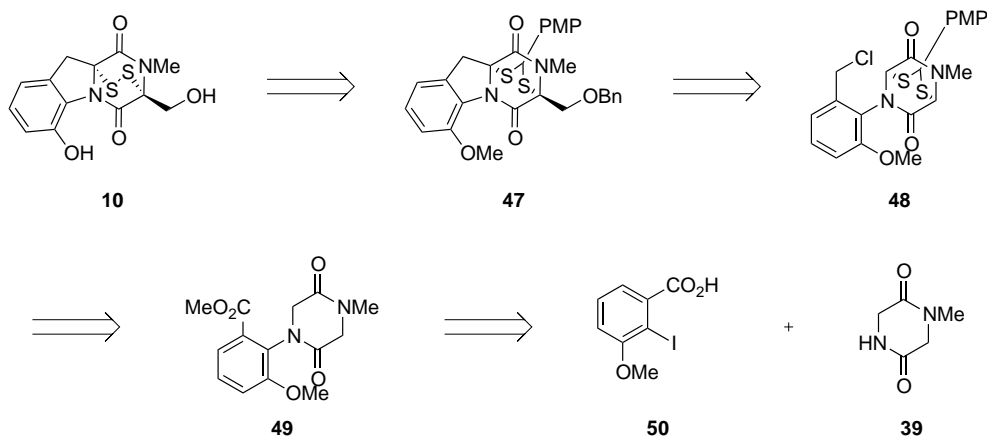
Enantioenriched dithioacetal **38** was reacted with arene oxide **37** in the presence of Triton B to give alcohol **44**. The free alcohol was acetylated and the *t*-butyl ester hydrolyzed to give carboxylic acid **45**, which was converted to mixed anhydride **46**. After reduction with sodium borohydride, the resultant alcohol was converted to the mesylate and displaced with chloride and the acetate removed to give alkyl chloride **36**. Dithioacetal **36** was then alkylated in the presence of 3.2 equivalents of phenyl lithium and BOMCl to give the desired dialkylated product **35**. It is important to note that having the alcohol unprotected was crucial in the alkylation step to prevent dehydration–aromatization of the hydrated benzene moiety. Removal of the benzyl protecting group followed by cleavage of the dithioacetal through initial oxidation to the monosulfoxide then exposure to acid revealed the natural product (**9**) (Scheme 2.7).



**Scheme 2.7.** Kishi's completion of gliotoxin (**9**).

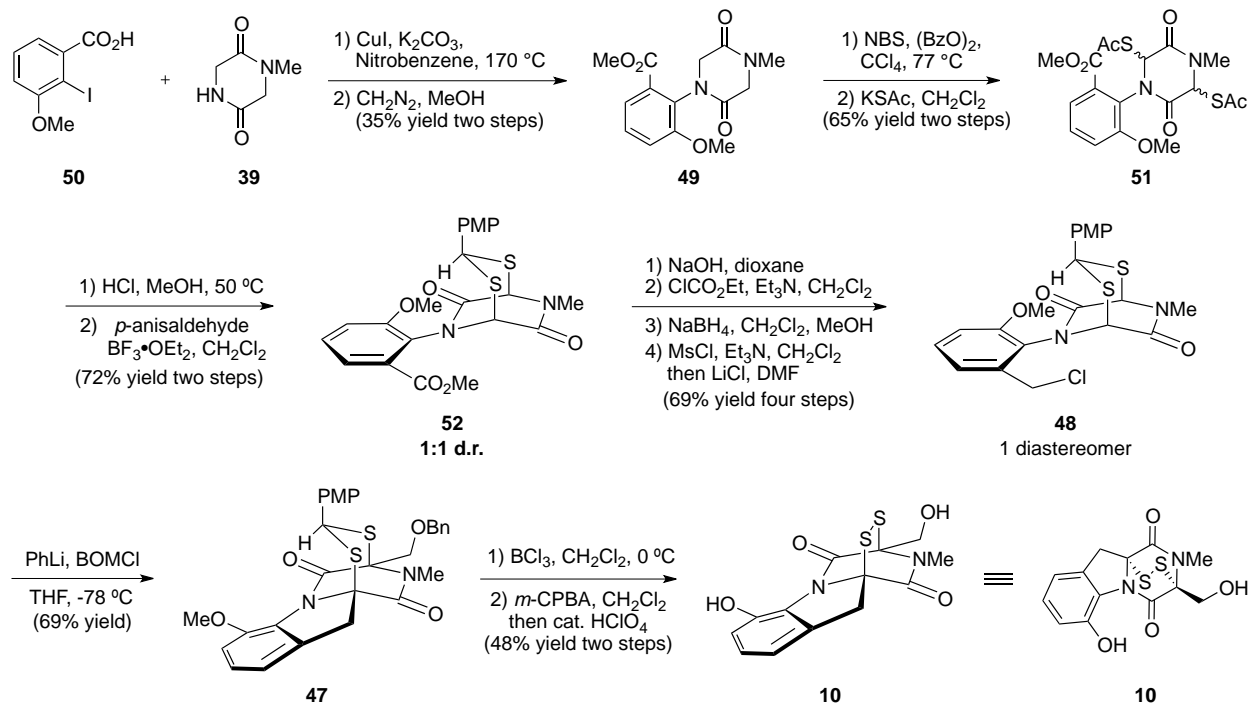
### 2.3. Kishi's Synthesis of Dehydrogliotoxin

Dehydrogliotoxin (**10**) is structurally related to gliotoxin (**9**) and contains many of the same synthetic challenges including the disulfide moiety, however it lacks the cyclohexadienol system. In light of this, the late stages of the synthesis were envisioned to be similar as for **9**, however construction of the core would require a different approach (Scheme 2.8). Dehydrogliotoxin would once again be produced from dialkylation and deprotection of a dithioacetal (**48**), which in this case would be derived from ester **49**, the product of an Ullman-type coupling of DKP **39** and aryl iodide **50**.



**Scheme 2.8.** Kishi's retrosynthetic analysis of dehydrogliotoxin (**10**).

To initiate the synthesis of dehydrogliotoxin (**10**), aryl iodide **50** was coupled with DKP **39** and the resultant carboxylic acid esterified with diazomethane to give aryl DKP **49**. In a sequence analogous to that of gliotoxin, sulfur was incorporated and protected as the dithioacetal and the ester was converted to the alkyl chloride to give **48** over eight steps. A single diastereomer of **48** was obtained through fractional crystallization. Exposure of dithioacetal **48** to phenyl lithium and BOMCl furnished bisalkylated product **47**, which was converted to the natural product (**10**) after deprotection (Scheme 2.9).



**Scheme 2.9.** Kishi's synthesis of dehydrogliotoxin (**10**).

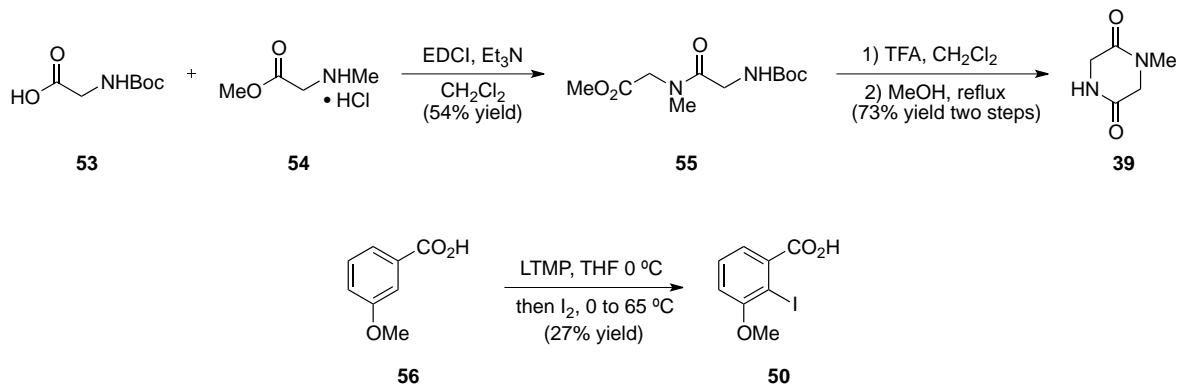
## Chapter Three

### Towards the Synthesis of Dehydrogliotoxin

Although we were interested in both gliotoxin (**9**) and dehydrogliotoxin (**10**), we choose to begin our synthetic efforts by focusing on the synthesis of dehydrogliotoxin (**10**). In addition to being the simpler of the two targets, the fact that **10** had never been tested against MTB helped guide our decision. As well as offering quicker access to a potentially interesting anti-MTB agent, we believed that **10** might more readily lend itself to derivatization to form structural analogs. Given that the primary objective of our efforts was analog generation, rather than develop a completely new synthetic approach, we initially decided to reproduce the elegant chemistry developed by Kishi and coworkers.

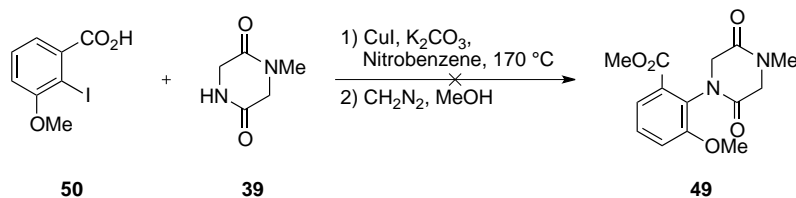
#### 3.1 Intermolecular Copper Mediated Aryl-Amidation

The first task at hand was preparing the precursors for Kishi's copper-mediated Ullman-type coupling. The necessary coupling partners **39**<sup>19</sup> and **50**<sup>20</sup> were synthesized as outlined in Scheme 3.1. Dipeptide **55** was synthesized by an EDCI mediated peptide coupling of acid **53** and amine **54**. The Boc protecting group was removed with TFA and DKP **39** formed by refluxing in methanol. The requisite aryl iodide (**50**) was synthesized in one step from benzoic acid **56** by ortho-lithiation followed by quenching with iodine.



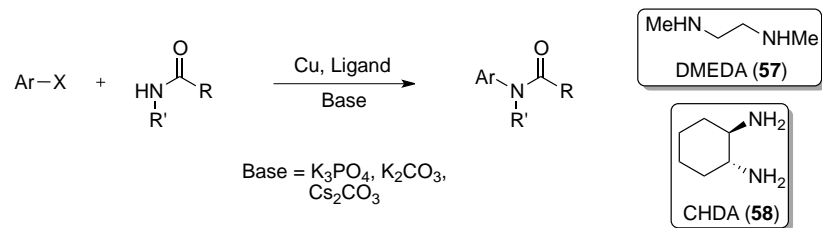
**Scheme 3.1.** Synthesis of aryl-amide coupling precursors **39** and **50**.

With the two coupling partners in hand, we were ready to explore the aryl–amidation under Kishi’s conditions. Unfortunately, under these conditions we were unable to obtain the desired coupled product **49** (Scheme 3.2).

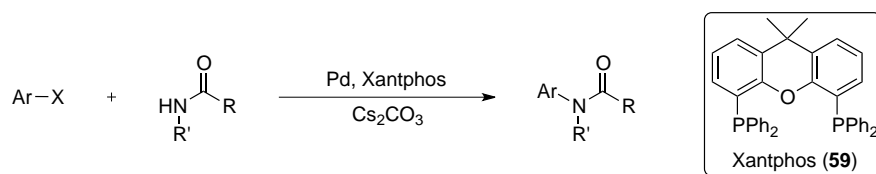


**Scheme 3.2.** Attempted aryl–amidation utilizing Kishi’s conditions.

Buchwald and coworkers have studied these aryl–amidation reactions in greater depth in the time since Kishi reported his synthesis.<sup>21</sup> They have found by combining a diamine ligand such as dimethylethylenediamine (**57**) or cyclohexyldiamine (**58**) with the copper catalyst, this reaction can proceed at lower temperatures than classical Ullman–type conditions (Scheme 3.3). Another benefit is the use of the copper in catalytic quantities as opposed to the stoichiometric amounts utilized by Kishi. The aryl–amidation reaction has also been shown to proceed with a palladium catalyst in the presence of a diphosphine ligand such as Xantphos (**59**) (Scheme 3.4).



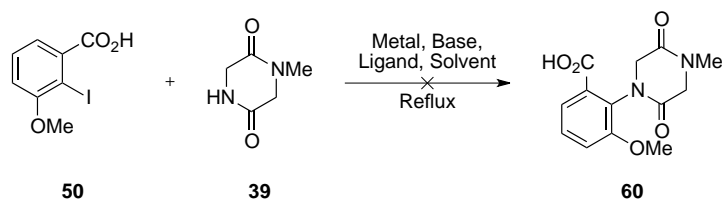
**Scheme 3.3.** Copper-catalyzed aryl-amidation conditions.



**Scheme 3.4.** Palladium-catalyzed aryl-amidation conditions.

These results prompted us to try alternate coupling conditions in our system (Table 3.1). Standard conditions using catalytic copper iodide in the presence of potassium phosphate and diamine ligand **57** were attempted first without success (entry 2). Buchwald has suggested that the use of a weaker base is advantageous in particularly tough couplings, which led us to try potassium carbonate as the base (entries 3 and 4). The coupling was also attempted with standard palladium conditions (entry 5); however all of these conditions were met with no success.

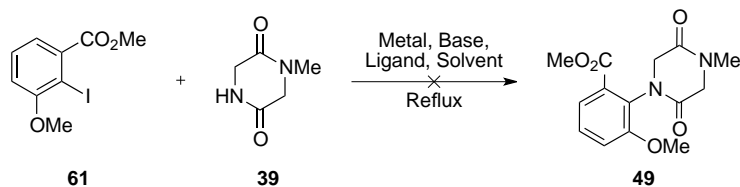
**Table 3.1.** Attempts at using alternate aryl-amidation coupling conditions.



Entry	Metal	Base	Ligand	Solvent	
1	CuI	K <sub>2</sub> CO <sub>3</sub>	none	Nitrobenzene	 MeHN-CH <sub>2</sub> -CH <sub>2</sub> -NHMe DMEDA (57)
2	CuI	K <sub>3</sub> PO <sub>4</sub>	DMEDA	Toluene	
3	CuI	K <sub>2</sub> CO <sub>3</sub>	DMEDA	Toluene	 PPh <sub>2</sub> PPh <sub>2</sub> Xantphos (59)
4	CuCl	K <sub>2</sub> CO <sub>3</sub>	DMEDA	Toluene	
5	Pd <sub>2</sub> (dba) <sub>3</sub>	Cs <sub>2</sub> CO <sub>3</sub>	Xantphos	Toluene	

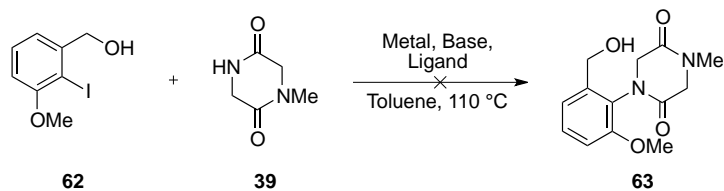
Reversal of the order of the coupling reaction and ester formation was also attempted (Table 3.2). Use of either copper iodide or copper chloride in toluene with potassium carbonate gave no desired product (entries 1 and 2). A switch to dioxane as a solvent also was attempted without success (entries 3 and 4). Lastly, standard palladium-catalyzed conditions proved unproductive (entry 5).

**Table 3.2.** Attempted aryl-amidations utilizing aryl iodide **61**.



Entry	Metal	Base	Ligand	Solvent	
1	CuI	K <sub>2</sub> CO <sub>3</sub>	DMEDA	Toluene	<p>DMEDA (<b>57</b>)</p>
2	CuCl	K <sub>2</sub> CO <sub>3</sub>	DMEDA	Toluene	
3	CuI	K <sub>3</sub> PO <sub>4</sub>	DMEDA	Dioxane	<p>Xantphos (<b>59</b>)</p>
4	CuI	K <sub>2</sub> CO <sub>3</sub>	DMEDA	Dioxane	
5	Pd <sub>2</sub> (dba) <sub>3</sub>	Cs <sub>2</sub> CO <sub>3</sub>	Xantphos	Toluene	

At this point we were attracted to the idea of using benzylic alcohol **62**<sup>22</sup> for the synthesis of dehydrogliotoxin, due to the fact it is already in the oxidation state required for the subsequent steps. The coupling between aryl iodide **62** and DKP **39** was the most extensively studied (Table 3.3). We first looked at standard conditions utilizing the three most common bases for this reaction: potassium carbonate, potassium phosphate, and cesium carbonate (entries 1 – 3). After these proved unsuccessful, diamine ligand **58** was screened (entries 4 and 5). Replacing the copper source with copper chloride also gave no desired product (entries 6 and 7). Lastly the reaction did not proceed under the standard palladium–catalyzed conditions either (entry 8).

**Table 3.3.** Attempted aryl-amidation utilizing aryl iodide **62**.

Entry	Metal	Base	Ligand
1	CuI	K <sub>2</sub> CO <sub>3</sub>	DMEDA
2	CuI	K <sub>3</sub> PO <sub>4</sub>	DMEDA
3	CuI	Cs <sub>2</sub> CO <sub>3</sub>	DMEDA
4	CuI	K <sub>3</sub> PO <sub>4</sub>	CHDA
5	CuI	Cs <sub>2</sub> CO <sub>3</sub>	CHDA
6	CuCl	K <sub>2</sub> CO <sub>3</sub>	DMEDA
7	CuCl	K <sub>3</sub> PO <sub>4</sub>	DMEDA
8	Pd <sub>2</sub> (dba) <sub>3</sub>	Cs <sub>2</sub> CO <sub>3</sub>	Xantphos

DMEDA (**57**)

CHDA (**58**)

Xantphos (**59**)

To test whether this type of coupling could be carried out with DKP **39**, several control experiments were conducted. Gratifyingly couplings with DKP **39** and simple aryl iodides such as iodobenzene and *o*-iodoanisole were successful under both copper- and palladium-catalyzed conditions. Furthermore, couplings with benzylic alcohols, methyl esters, and methyl ethers attached to the aryl halide with various substitution patterns are known in the literature; however there are very few examples of couplings where there are two substituents *ortho* to the halide.<sup>21a-c, 23</sup> Such couplings are difficult presumably because formation of the aryl-amide bond is very slow, or cannot happen at all, due to sterics. Looking at the mechanism, the first step is deprotonation and formation of copper amidate **65**. Next is the formation of the aryl-amide bond, most likely through an oxidative addition/ reductive elimination sequence. However, if the formation of the aryl-amide bond is especially slow, and the rate of deprotonation of the amide is particularly fast, then the unreactive cuprate complex **68** is formed, which effectively shuts down the catalytic cycle (Figure 3.1).<sup>21c, 24</sup>

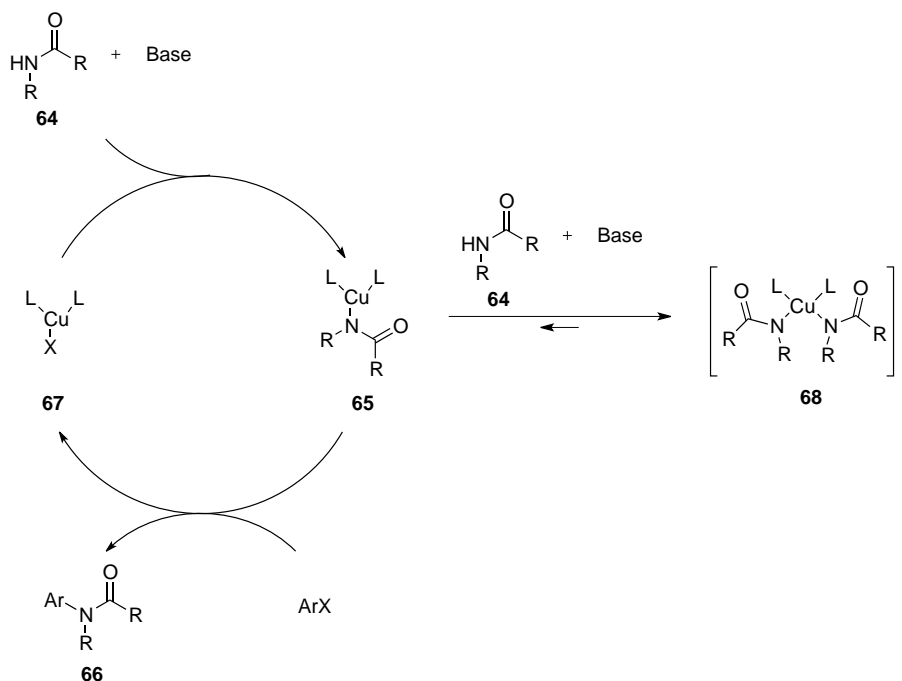
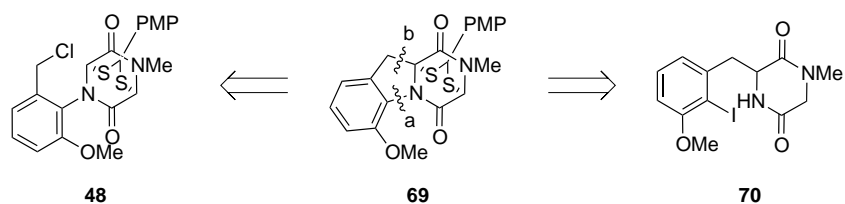


**Figure 3.1.** Mechanism of the copper mediated aryl-amidation.

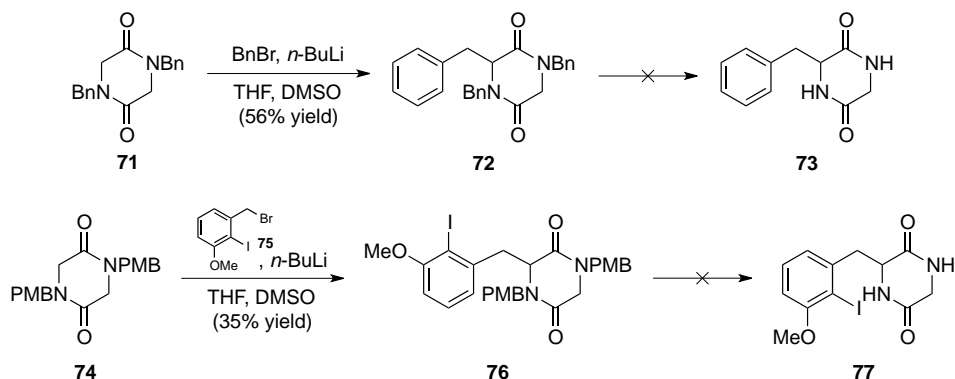
### 3.2 Intramolecular Copper Mediated Aryl-Amidation

Having explored several unsuccessful options for intermolecular aryl-amidation, we considered a new intramolecular approach (Scheme 3.5). Initially our strategy had been to first form bond **a** by an intermolecular aryl–amidation then bond **b** by an intramolecular alkylation. It is conceivable the same intermediate (**69**) could be generated by first forming bond **b** by some sort of alkylation then forming bond **a** through an intramolecular aryl–amidation. We hoped that by making this an intramolecular process, we could overcome the difficult coupling step as the two coupling partners are in close proximity to each other, and generally intramolecular processes are more favorable than the corresponding intermolecular reaction.



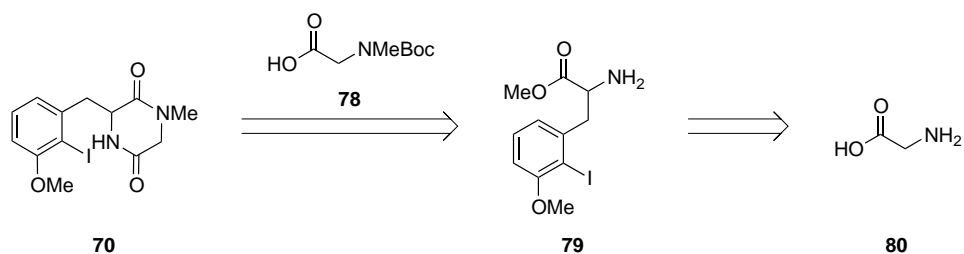
**Scheme 3.5.** Revised retrosynthetic analysis of dithioacetal **69**.

In accordance with this new strategy, coupling precursor **70** needed to be constructed. Both *p*-methoxybenzyl and benzyl protected DKPs were obtained according to known procedures.<sup>25</sup> In order to access an appropriate aryl–amidation precursor the alkylations of **71** and **74** were examined (Scheme 3.6). Benzyl protected DKP **71** could be benzylated with benzyl bromide to give **72**, a product that lacks the necessary iodide, but still shows that the important C-C bond could be formed. Unfortunately, the benzyl protecting groups could not be removed from this compound. Hoping that the *p*-methoxybenzyl protecting group would be removed more readily, DKP **74** was also tested in this route. This time utilizing the benzyl bromide<sup>22</sup> needed for the synthesis of dehydrogliotoxin, alkylated product **76** was formed. Unfortunately, the protecting groups once again could not be removed and coupling precursor **77** could not be formed.



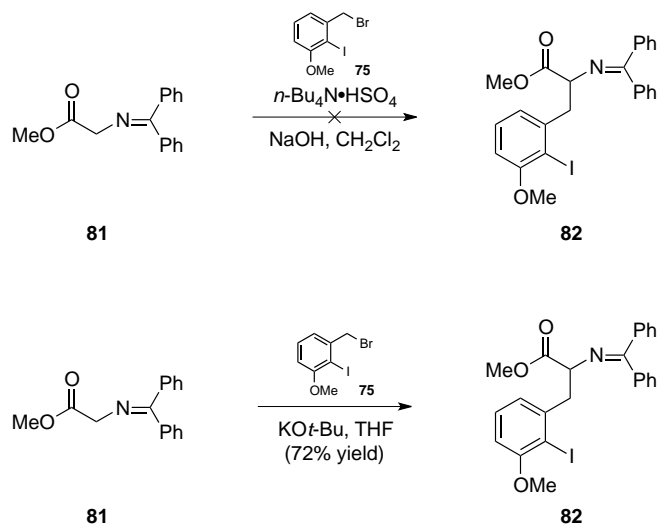
**Scheme 3.6.** Attempted synthesis of coupling precursor **77**.

Although we could screen other differentially protected DKPs for this alkylation/deprotection sequence, we believed a different approach was warranted. Specifically the diketopiperazine ring would be constructed from an amino acid that already contained the essential aryl iodide. To that end, coupling precursor **70** would come from DKP formation between Boc-sarcosine (**78**) and unnatural amino acid **79**, which itself would ultimately arise from alkylation of glycine (**80**) (Scheme 3.7).



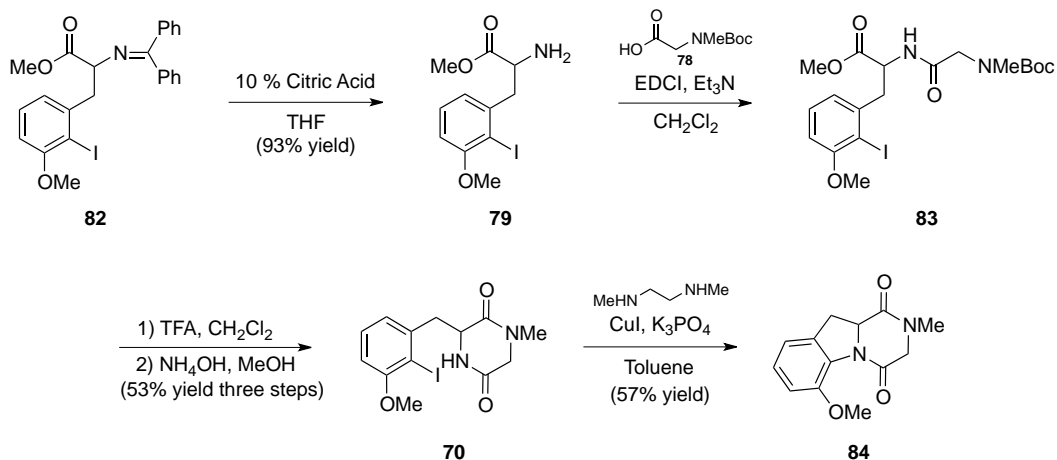
**Scheme 3.7.** Revised retrosynthetic analysis of coupling precursor **70**.

In order to access unnatural amino acid **79**, known glycine derivative **81** was prepared.<sup>26</sup> This doubly protected amino acid is known to undergo alkylation with a variety of electrophiles including benzyl halides. Typically these alkylations are performed under phase-transfer conditions; however in our case that proved futile. Conversely, turning to anhydrous conditions utilizing potassium *tert*-butoxide as a base in THF provided alkylated product **82** in good yield.<sup>27</sup>



**Scheme 3.8.** Alkylation of glycine derivative **81**.

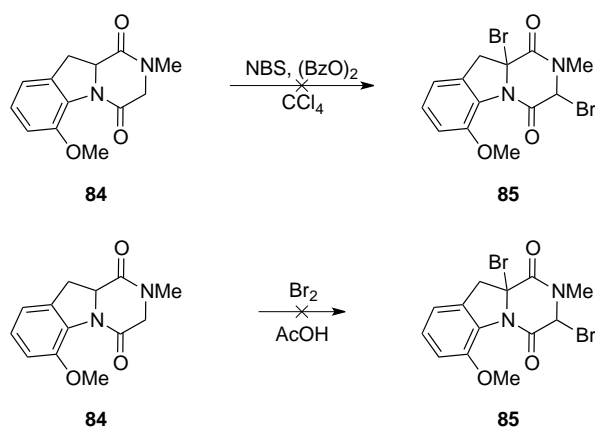
With the alkylation complete, the benzophenone imine was hydrolyzed to give amine **79**. Peptide coupling with Boc-sarcosine (**78**) gave dipeptide **83**, which could be deprotected and the ring closed to give coupling precursor **70**. Gratifyingly, exposing **70** to standard copper-catalyzed coupling conditions delivered tricycle **84** in good yield (Scheme 3.9). By performing this coupling in an intramolecular fashion we were able to overcome the reactivity issue and readily form the requisite C–N bond.



**Scheme 3.9.** Synthesis of tricycle **84**.

### 3.3 Attempts to Incorporate Sulfur

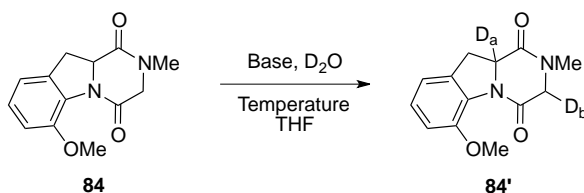
Having successfully synthesized tricycle **84**, we next sought a method for installing the requisite disulfide. In analogy to Kishi's synthesis, we initially attempted to brominate **84**; however none of the desired product was obtained. Bromination under acidic conditions also proved futile (Scheme 3.10).



**Scheme 3.10.** Unsuccessful bromination of tricycle **84**.

As outlined in section 2.1, bromination is initially employed in only one of the three methods that have led to successful incorporation of sulfur into the DKP framework. Given the above results, we next looked at forming an enolate and trapping with a sulfur electrophile. To test the viability of this strategy, we first ran a deuterium quenching study of DKP **84** (Table 3.4). Using LHMDS as a base at  $-10\text{ }^{\circ}\text{C}$  lead to a complex mixture of products (entry 1). Switching to LDA at  $-78\text{ }^{\circ}\text{C}$  gave deuterium incorporation solely at the less hindered position,  $\text{D}_b$  (entry 2). Warming the solution to  $0\text{ }^{\circ}\text{C}$  with LDA as a base not only gave full deuterium incorporation at  $\text{D}_b$ , but also gave approximately 50% incorporation at the more hindered position,  $\text{D}_a$  (entry 3). The same observation was seen using NaH at  $0\text{ }^{\circ}\text{C}$  (entry 4).

**Table 3.4.** Deuterium incorporation of tricyclic **84**.

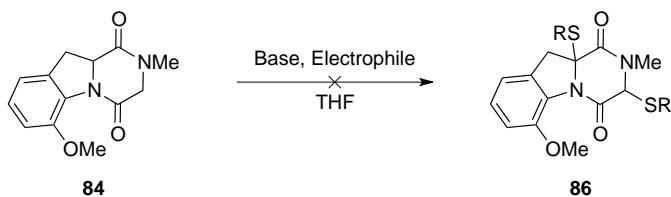


Entry	Base	Temperature ( $^{\circ}\text{C}$ )	Incorporation (%)	
			$\text{D}_a$	$\text{D}_b$
1	LHMDS	-10	Decomp.	
2	LDA	-78	0	~100
3	LDA	0	~50	~100
4	NaH	0	~50	~100

Having demonstrated the feasibility of enolate formation, we next examined the reactivity toward various sulfur electrophiles (Table 3.5). Our very first attempt employed the classical conditions of sodium amide and elemental sulfur; however no product was observed (entry 1). We next surveyed a variety of bases using disulfides as the sulfur electrophile (entries 2 – 5, 7). Concerned that the reactivity of the electrophile might be the issue, we turned to a more active sulfur electrophile. Unfortunately these efforts were also unsuccessful (entries 6 and 8).

Although in most of these reactions we observed starting material or decomposition, we did observe indole **87** as a byproduct in some cases (Figure 3.2).

**Table 3.5.** Attempts at reacting tricycle **84** with a sulfur electrophile.



Entry	Base	Electrophile
1	NaNH <sub>2</sub>	S <sub>8</sub>
2	LHMDS	BzSSBz
3	LHMDS	BnSSBn
4	KHMDS	BnSSBn
5	LDA	BnSSBn
6	LDA	BnSCl
7	NaH	BnSSBn
8	NaH	BnSCl

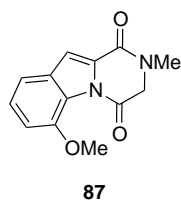
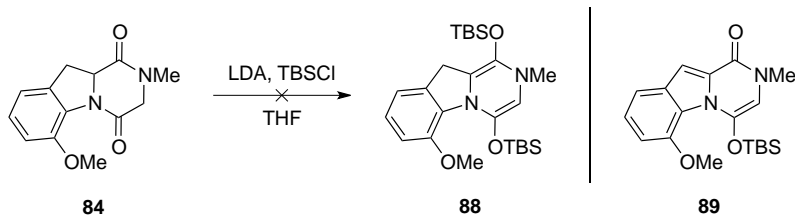


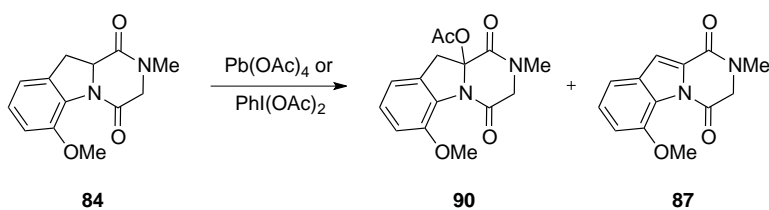
**Figure 3.2.** Undesired indole byproduct **87**.

After unsuccessfully attempting to trap an enolate directly with a sulfur electrophile, we explored the use of a silyl enol ether as a nucleophile. However, in our attempts to form bis-silyl enol ether **88**, we observed no desired product, instead only undesired indole **89** and starting material (Scheme 3.11).



**Scheme 3.11.** Attempted formation of bis-silyl enol ether **88**.

From here it seemed that trapping an enolate or silyl enol ether with an electrophilic sulfur reagent was not a viable option, however, there remained a potentially viable approach that had not been investigated. This involved oxidizing the DKP with a non-radical oxidant to form a hemi-aminal, which would serve as a precursor to an acyl-iminium intermediate which would, in turn, react with a sulfur nucleophile. Unfortunately, exposing DKP **84** with either  $\text{Pb}(\text{OAc})_4$  or  $\text{PhI}(\text{OAc})_2$ , while giving a small amount of monoacetate **90**, gave undesired indole **87** as the major product (Scheme 3.12).



**Scheme 3.12.** Oxidation of DKP **84**.

At this point three distinct pathways to incorporate sulfur had been explored unsuccessfully. It is not too surprising in hindsight that there were complications involving the formation of undesired indole side products given the propensity with which the dihydroindole can oxidize to form an aromatic system. Although this route ultimately failed due to the complications in sulfur incorporation, it did provide a valuable solution to the difficult

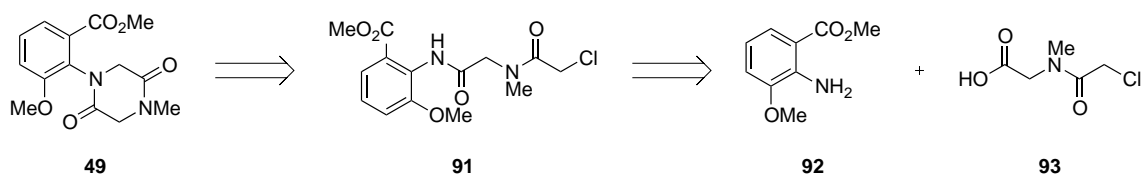
intermolecular aryl–amidation step. Nevertheless, at this point a new route needed to be investigated towards the synthesis of dehydrogliotoxin (**10**).

## Chapter Four

### Synthesis of Dehydrogliotoxin

#### 4.1 Revised Route Towards the Synthesis of Dehydrogliotoxin

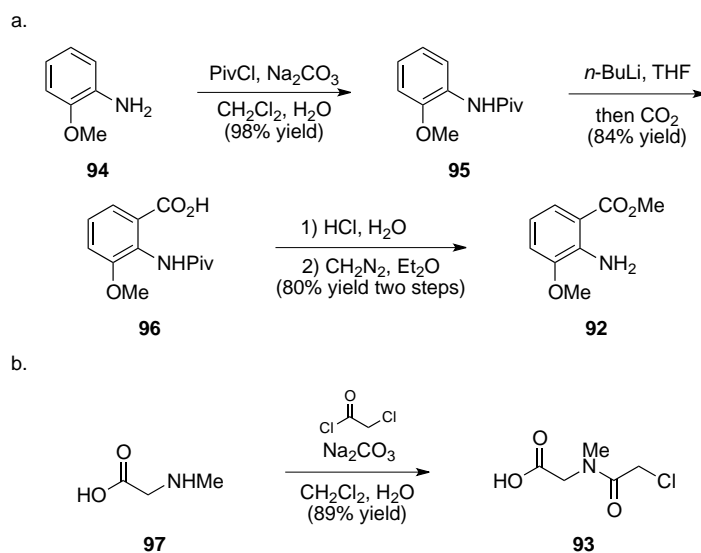
Having encountered problems in routes toward the synthesis of dehydrogliotoxin (**10**) that involved both inter- and intramolecular Ullman-type couplings, we sought a synthetic strategy that avoided this reaction altogether. Because our ultimate goal was to access **10** in the most expedient fashion, we again decided to focus on variations of Kishi's approach and began to consider an alternate strategy utilizing intermediate **49**, the product of the problematic arylamidation. Specifically we envisioned a strategy where the recalcitrant C–N bond was preassembled and would serve as a template for construction of the DKP (Scheme 4.1). In the event, key intermediate **49** would arise from intramolecular ring closure of alkyl chloride **91**, the bis-amide derived from coupling of aniline **92** and acid **93**. Along with generating the necessary intermediate **49**, an additional potential benefit of this approach is the absence of the metal-mediated cross coupling that would prohibit the preparation of analogs bearing aryl halides.



**Scheme 4.1.** Modified retrosynthetic analysis of intermediate **49**.

Although simple esterification of the commercially available benzoic acid corresponding to aniline **92** would provide the first of the two coupling partners required for our approach, the extravagant cost of this acid prompted us to consider a more economical starting material. We

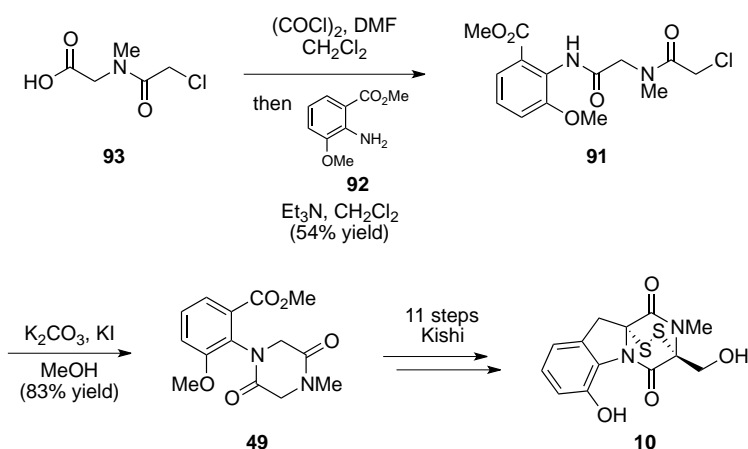
were pleased to find that large quantities of aniline **92** could be accessed in high yield in four steps from inexpensive *o*-anisidine (**94**).<sup>28</sup> This involved conversion of **94** to the pivaloyl amide followed by *ortho*-lithiation with *n*-butyl lithium forming an aryl anion that would be quenched with carbon dioxide to give benzoic acid **96**. Removal of the pivaloyl directing group followed by esterification with diazomethane gave aniline **92**. Carboxylic acid **93** was synthesized following the procedure of Ciufolini wherein sarcosine (**97**) was acylated with chloroacetyl chloride (Scheme 4.2).<sup>29</sup>



**Scheme 4.2.** Synthesis of precursors (a) aniline **92** and (b) acid **93**.

With straightforward methods to both desired coupling partners in hand, we explored their conversion to key intermediate **49**. Gratifyingly, the two partners could be joined by first converting acid **93** to the acid chloride and adding aniline **92** to give bis-amide **91**. The ring-closure was accomplished upon heating in methanol in the presence of potassium carbonate and potassium iodide to give key intermediate **49**, thus effecting a formal total synthesis of dehydrogliotoxin (**10**). Given that our purpose was to synthesize the natural product and not just

achieve a formal synthesis, we carried the material through the remaining eleven steps according to Kishi's procedure and obtained dehydrogliotoxin (**10**) (Scheme 4.3).<sup>14b, 14d</sup>



**Scheme 4.3.** Formal total synthesis of dehydrogliotoxin (**10**).

## 4.2 Biological Activity

With a synthesis of dehydrogliotoxin complete, we next were interested in its biological activity. Four compounds were sent to our collaborator Dr. Deborah Hung at the Broad Institute. Graphs showing the antitubercular activity and human cell toxicity are shown in Figure 4.1, and the  $\text{IC}_{50}$  values of the antitubercular activity are given in Table 4.1. It was found that synthetic dehydrogliotoxin (**10**) showed significant activity against MTB with an  $\text{IC}_{50}$  of  $0.13 \mu\text{M}$ ,<sup>30</sup> comparing favorably to gliotoxin (**9**) our collaborators purchased which exhibited an  $\text{IC}_{50}$  of  $0.09 \mu\text{M}$ . Not surprisingly, **10** also proved significantly toxic as seen in Figure 4.1.b.<sup>31</sup> Compound **84**, which contains the carbon skeleton of dehydrogliotoxin, however lacks the bridging disulfide, was not active against MTB and also was the least toxic. Benzyl chloride **48** showed both activity against MTB and human toxicity, however this is most likely due to indiscriminate toxicity of the benzylic chloride. Lastly dithioacetal **98**, which contains the entire dehydrogliotoxin core, however has the disulfide tied up in a dithioacetal, exhibited no antitubercular activity,

supporting the theory that the disulfide is the most important site of the molecule for its observed activity.

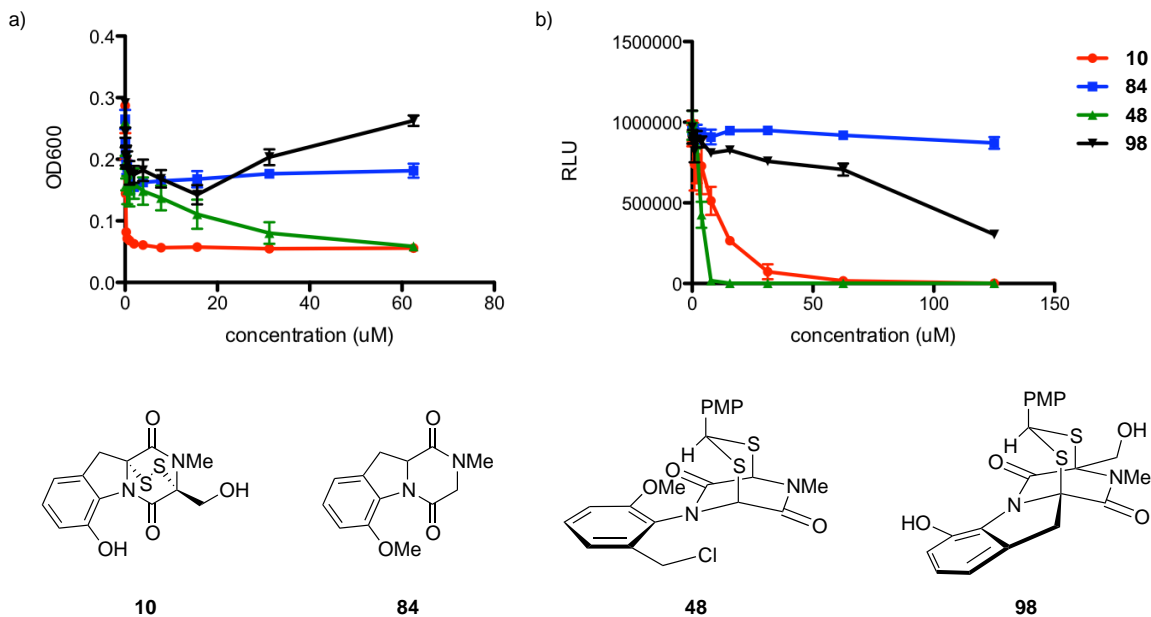


**Figure 4.1.** Graphs showing a) antitubercular activity and b) human cell toxicity.

**Table 4.1.** Antitubercular activities.

compound	IC <sub>50</sub> (µM)
gliotoxin ( <b>9</b> )	0.09
dehydrogliotoxin ( <b>10</b> )	0.13
<b>84</b>	>62.5
<b>48</b>	7.9
<b>98</b>	>62.5

## Chapter Five

### Analog Design and the First Synthesis of an Epidiselenodiketopiperazine

With a synthesis of dehydrogliotoxin (**10**) complete, we next turned our attention to the generation of analogs. When examining dehydrogliotoxin we identified three major regions to target in analog synthesis: the hydrophobic (blue), the hydrophilic (red), and the disulfide (yellow) (Figure 5.1). We initially choose to study the disulfide region.

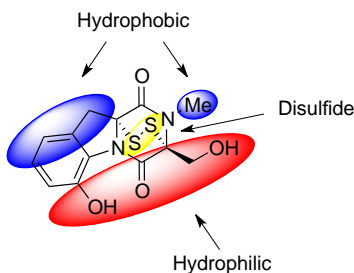


**Figure 5.1.** Regions of dehydrogliotoxin that could be modified in analog generation.

#### 5.1 Replacing the Disulfide with a Diselenide

Although the mode of action of the ETPs is not known, it is believed that the disulfide plays an important role in both their activity and their toxicity.<sup>13b, 32</sup> In fact it has been shown that removal of the disulfide or conversion to a dithioether eliminates antiviral activity in ETPs.<sup>16</sup> Because our eventual goal is accessing potential drug targets, we are interested in finding analogs that both retain anti-TB activity, and importantly, exhibit lessened human cell toxicity. Toxicity is thought to arise in one of two ways: by forming covalent disulfide bonds with cysteine residues in proteins in an unselective fashion or through a redox cycle that forms harmful reactive oxygen species (ROS). A schematic showing this redox process is outline in Figure 5.2 and is the process we hope to attenuate.<sup>13b</sup>

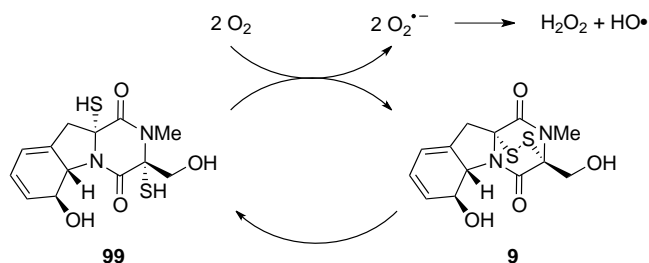
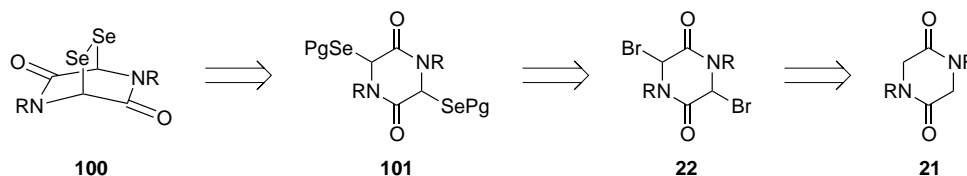


**Figure 5.2.** Redox cycling of gliotoxin (**9**) forming harmful reactive oxygen species.

To this end we became interested in replacing the disulfide with a diselenide and thus form an epidiselenodiketopiperazine (ESeP). We believed the diselenide would be a good bioisostere of the disulfide due to the proximity of the two atoms on the periodic table. Selenium is the larger of the two (atomic radius of 1.17 Å vs. 1.04 Å), however that difference is minor (only 0.13 Å). As a result of the size difference, the Se–Se bond length (2.30 Å) is larger than the S–S bond (2.00 Å). Although there are differences in size of the two, the dimension of the unit cell of crystalline hexagonal cysteine<sup>33</sup> and selenocystine<sup>34</sup> are almost identical, suggesting that at least in that system the two are isomorphous.<sup>35</sup> The disulfide and diselenide also have some differences. The difference that we are most interested in exploiting is the redox properties of the two. Although the redox properties of ETPs and ESePs have not been investigated, the redox potentials of model peptides containing disulfides ( $E_0 = -180$  mV), diselenides ( $E_0 = -381$  mV), and mixed selenosulfides ( $E_0 = -326$  mV) have been determined using dithiothreitol (DTT,  $E_0 = -323$  mV, pH = 7.0) as a reference.<sup>36</sup> As can be seen from this data, the disulfide is a much better oxidant than the diselenide, which would have implications in the redox cycling event described in Figure 5.2. Because it is a better oxidant, more of the open dithiol form would be generated, which in turn would lead to a greater production of reactive oxygen species. It has been suggested that ROS can play important roles in both cell proliferation and cell death, and the difference between the two pathways is dependent on the concentration of these ROS.<sup>37</sup> Furthermore, the redox potential in proliferating cells has been

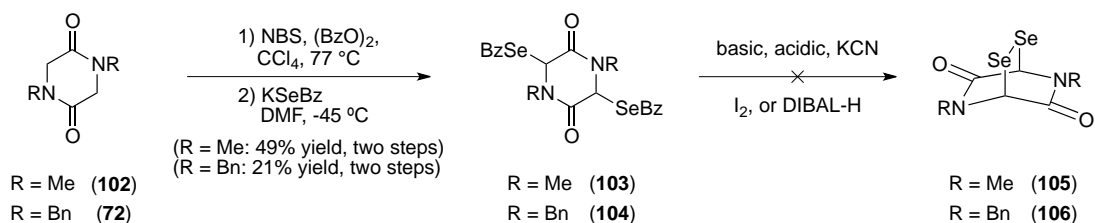
reported to be  $-240$  mV, while necrotic cells ( $-150$  mV) and apoptotic cells ( $-170$  mV) exhibited much more oxidizing environments. Thus, it appears that switching to a diselenide, which would favor the closed diselenide form due to its more negative reduction potential, would help reduce the presence of ROS in normal cells, which would hopefully lead to lessen toxicity.

In the literature there are very few examples of bridging diselenides,<sup>38</sup> and no examples containing the [2.2.2] scaffold we required. Without bias we set off to develop a method to form the desired ESeP. To explore this chemistry we first targeted simple ESeP **100** as a model system. Our initial strategy was to mimic the method we had previously utilized to incorporate sulfur. In that regard, diselenide **100** would come from protecting group removal and oxidation of bis-protected selenide **101**. Selenium incorporation would arise from a nucleophilic selenium reagent reacting with dibromide **22**, which would be derived from simple DKP **21**.



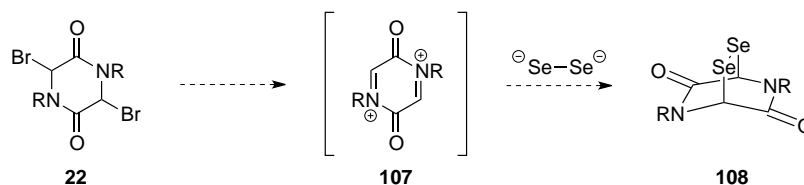
**Scheme 5.1.** Retrosynthetic analysis of model diselenide **100**.

To investigate this sequence we looked at DKPs protected with either a methyl (**102**) or benzyl (**72**) group (Scheme 5.2). The bromination was carried out as before and when reacted with potassium selenobenzoate, gave diselenides **103** and **104** respectively. Unfortunately, the benzoate protecting groups could not be removed in either case under a variety of different conditions including: basic, acidic, transesterification (KCN), oxidative ( $I_2$ ), or reductive (DIBAL-H). Other differentially protected selenium nucleophiles were not fruitful, mostly due to difficulties in their synthesis.



**Scheme 5.2.** Attempted synthesis of diselenides **105** and **106**.

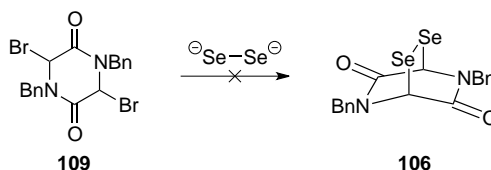
It seemed that reacting a dibromide with a selenium nucleophile was a viable way to incorporate selenium, however, because we had problems finding a protecting group that could be removed from selenium after incorporation, we sought a method that would incorporate the diselenide directly with no protecting groups. Specifically we were interested in reacting a diselenide dianion equivalent with an acyl iminium (**107**) derived from dibromide **22** (Scheme 5.3).



**Scheme 5.3.** Proposed reaction of dibromide **22** with a diselenide dianion equivalent.

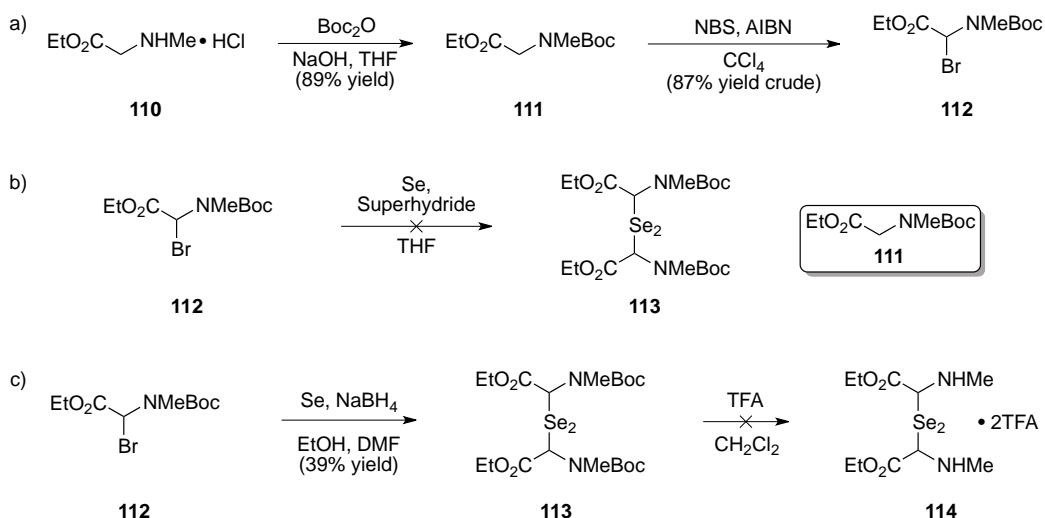
There are a variety of methods known to generate a diselenide dianion equivalent. Initially we tried the classical conditions of combining elemental selenium with either lithium or sodium metal to form M<sub>2</sub>Se<sub>2</sub>, however no desired product was observed (entries 1 and 2, Table 5.1). We next looked at other reductants that have been used in this reaction. Unfortunately, attempted reductions utilizing superhydride (entry 2), hydrazine (entry 3), or samarium iodide (entry 4) did not lead to any desired product.

**Table 5.1.** Attempts at reacting dibromide **109** with a diselenide dianion equivalent.



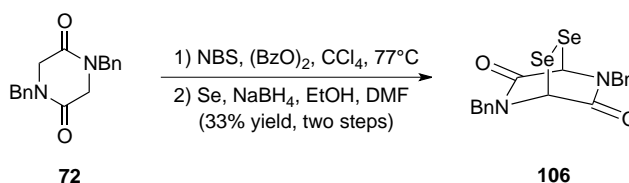
entry	conditions
1	Li + Se
2	Na + Se
3	superhydride + Se
4	N <sub>2</sub> H <sub>4</sub> • H <sub>2</sub> O + Se
5	Sml <sub>2</sub> + Se

At this point we were wondering if having the diketopiperazine ring already in place was a problem. We thought the diselenide could be installed between two linear amino acids, and the DKP could then be formed with the diselenide already in place. To investigate this we synthesized bromide **112** from sarcosine derivative **111** through Boc protection and bromination under radical conditions (Scheme 5.4.a). Our first attempt utilized elemental selenium and superhydride to form the diselenide dianion equivalent. Under these conditions we observed none of the desired product, instead obtaining amino acid **111**, presumably from reduction with superhydride of an *in situ* generated iminium (Scheme 5.4.b). However, we were able to find success by utilizing conditions developed by Krief and Derock to generate a diselenide dianion equivalent with elemental selenium, sodium borohydride, DMF, and ethanol, giving diselenide **113** in moderate yield.<sup>39</sup> In a single attempt to form the DKP ring with the diselenide already in place, **113** was exposed to TFA, which only led to decomposition (Scheme 5.4.c).



**Scheme 5.4.** a) Synthesis of bromide **112**. b) Attempted reaction of bromide **112** with the diselenide dianion equivalent derived from Se and superhydride. c) Successful reaction of bromide **112** with the diselenide dianion equivalent derived from Se and sodium borohydride.

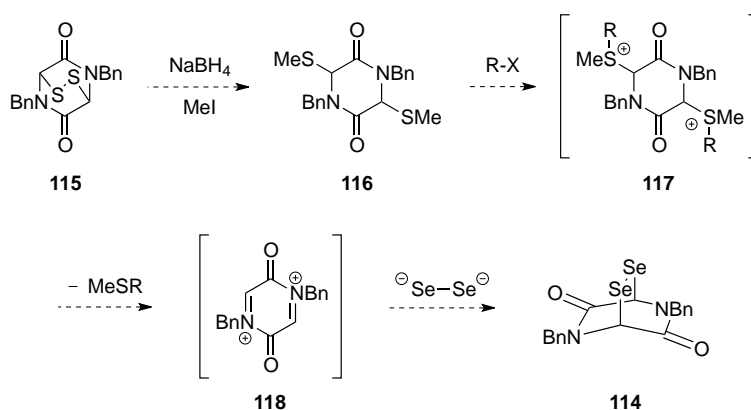
Having finally found success forming a diselenide, albeit in a linear system, we decided to reinvestigate the system with the DKP already in place. Gratifyingly, by first converting DKP **72** to the dibromide, diselenide **106** could be formed utilizing the conditions developed by Krief and Derock (Scheme 5.5). This constituted the first synthesis of an epidiselenodiketopiperazine (ESeP).



**Scheme 5.5.** Successful synthesis of diselenide **106** from DKP **72**.

While we were pleased to have successfully synthesized diselenide **106**, we ultimately wanted to incorporate the diselenide into more complex structures such as dehydroglitoxin. Therefore it would be advantageous to develop a route to convert an ETP to an ESeP directly. We decided to investigate this in the same model system as before. Therefore, disulfide **115**

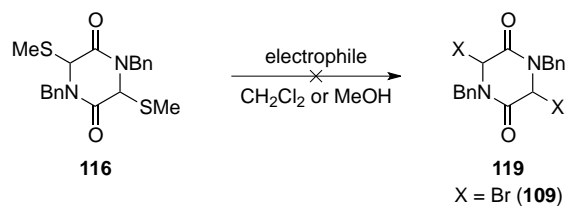
would be converted to bis–thiomethyl ether **116** upon reduction with sodium borohydride and capture of the resultant thiolates with iodomethane. The sulfur of bis–thiomethyl ether **116** would be activated with an electrophile, forming acyl iminium ion **118**, which would be reacted with the diselenide dianion equivalent to form diselenide **114** (Scheme 5.6).



**Scheme 5.6.** Proposed synthesis of diselenide **114** from disulfide **115**.

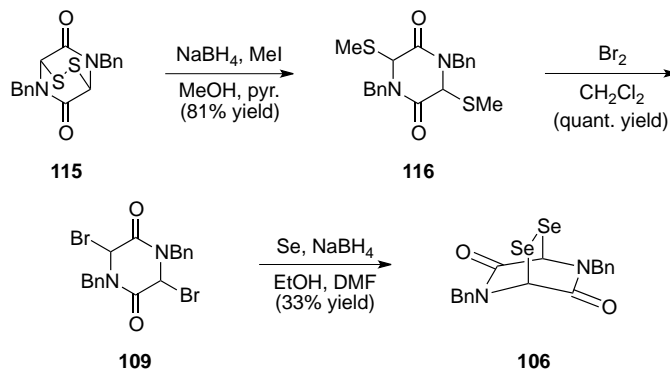
Bis–thiomethyl ether **116** was synthesized via a known procedure<sup>40</sup> and reacted with a variety of electrophiles in hopes of activating the sulfide and promoting acyl iminium ion formation (Table 5.2). Hoping to form dimethyl sulfide as a leaving group, a variety of methylating conditions were attempted with no success (entries 1–3). Switching to halogenating reagents NBS or NCS also lead to no desired product (entries 4 and 5). Eventually we discovered that simply utilizing bromine as the electrophile resulted in the conversion of bis–thiomethyl ether **116** to dibromide **109** quantitatively (entry 6).

**Table 5.2.** Activation of bithiomethyl ether **116**.



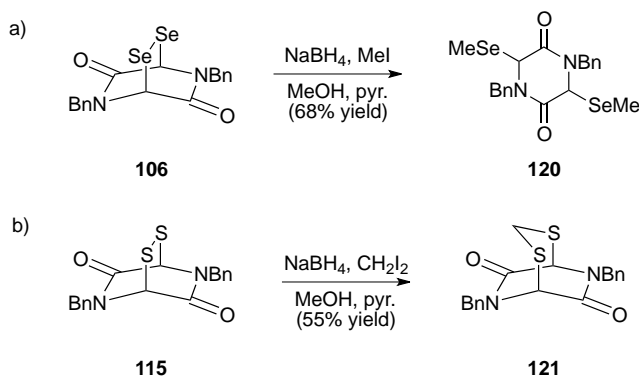
entry	electrophile	result
1	MeI	—
2	MeI, AgBF <sub>4</sub>	—
3	Me <sub>3</sub> OBF <sub>4</sub>	—
4	NBS	—
5	NCS	—
6	Br <sub>2</sub>	dibromide <b>109</b> (quant. yield)

With a method to convert bis-thiomethyl ether **115** to dibromide **109** in place, we had realized all of the steps in a sequence for converting disulfide **115** to diselenide **106** (Scheme 5.7). Overall, this sequence involved conversion of ETP **115** to bis-thiomethyl ether **116** with sodium borohydride and iodomethane. Reaction of **116** with bromine gave dibromide **109**, which could be reacted under the same conditions as before to provide ESeP **106** in three steps from ETP **115**.



**Scheme 5.7.** Synthesis of diselenide **106** from disulfide **115**.

With the first synthesis of an epidiselenodiketopiperazine accomplished and a method to access this ESeP directly from an ETP, we were excited to look at its biological activity against MTB. Along with the ETP and ESeP, we were interested in the bis-thiomethyl ether and bis-selenomethyl ether counterparts due to previous reports that replacing the disulfide with the bis-thiomethyl ether resulted in loss of activity. Bis-selenomethyl ether **120** was therefore synthesized by adding sodium borohydride followed by iodomethane to ESeP **106** (Scheme 5.8.a). We were also interested in removing the redox active disulfide, while keeping the bicyclic scaffold intact. In that regard, we synthesized compound **121**, which contained a one-carbon linker between the two sulfur atoms, from disulfide **115** (Scheme 5.8.b).



**Scheme 5.8.** Synthesis of a) bis-selenomethyl ether **120** and b) dithioacetal **121**.

With the compounds of interest in hand we sent them to our collaborators for testing (Figure 5.3). Disulfide **115**, which mimics the epidithiodiketopiperazine natural products, exhibited an  $\text{IC}_{50}$  of 2.3  $\mu\text{M}$ . This was impressive in itself as **115** is a simplified model of the ETP natural products. To our delight diselenide **106** exhibited an  $\text{IC}_{50}$  of 2.7  $\mu\text{M}$ , which is comparable to the disulfide and suggests that the diselenide could be a potential target for further investigation as a drug lead. As expected alkylated disulfides **116** and **121** showed no activity against MTB;<sup>16</sup> however bis-selenoether **120**, although not as potent, was active with an  $\text{IC}_{50}$  of 16.2  $\mu\text{M}$ . Interestingly dithioacetate **122** was also active against MTB with an  $\text{IC}_{50}$  of 2.5  $\mu\text{M}$ ,

however this is most likely a prodrug effect where the acetate is being cleaved *in situ* and the disulfide is forming in the assay.

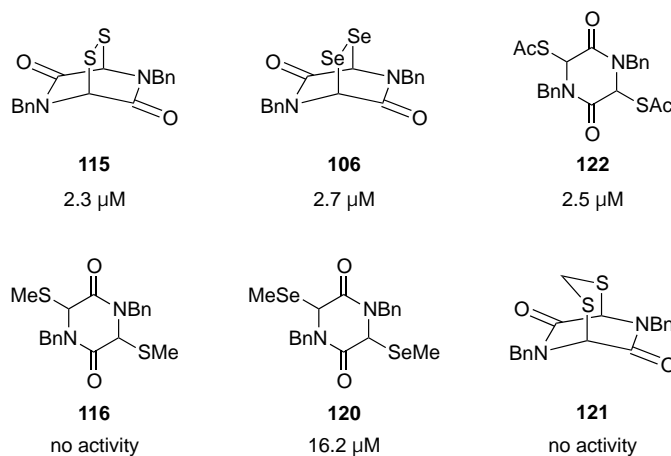
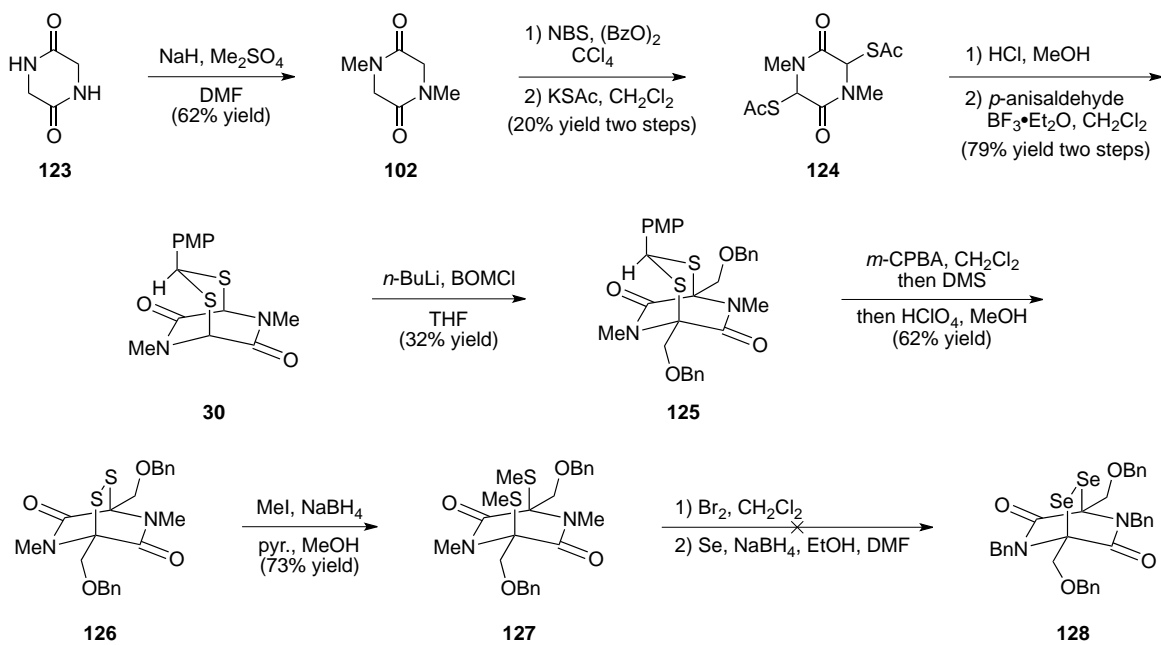


**Figure 5.3.** Activity of compounds tested against MTB.

Having successfully found a method to convert an ETP to an ESeP and after demonstrating that an ESeP has comparable activity to an ETP in a model system, we next looked at translating to a more complex system with the eventual goal of trying this sequence on dehydroglucosin (Scheme 5.9). Specifically we wanted to see if having substitution on the carbon bearing the disulfide would be tolerated in the sequence. To test this disulfide **126** was formed in seven steps. Commercially available DKP **123** was protected and subjected to the bromination/ nucleophilic sulfur displacement to give bis-thioacetate **124**. Removal of the acetate protecting groups and formation of the dithioacetal produced **30**. Addition of *n*-BuLi in the presence of BOMCl gave bis-alkylated product **125**, which was deprotected to give disulfide **126**. Conversion to bis-thiomethyl ether **127** proceeded uneventfully. Unfortunately, the conversion of bis-thiomethyl ether **127** to diselenide **128** did not proceed. This reaction was only attempted once and warrants further investigation; however at this time I turned my attention to the tetrapetalone project.



**Scheme 5.9.** Attempted synthesis of diselenide **128**.

## References for Part One

1. Wright, A. Z., M. *Anti-Tuberculosis Drug Resistance in the World*. World Health Organization, Ed.; Geneva, **2008**; Vol. Report No. 4.
2. Alberts, B.; Johnson, A.; Lewis, J.; Raff, M.; Roberts, K.; Walter, P. *Molecular Biology of the Cell*. Fourth Edition ed.; Garland Science, Ed.; New York, NY, **2002**.
3. Sacchettini, J. C.; Rubin, E. J.; Freundlich, J. S. *Nat. Rev. Micro.* **2008**, *6*, 41-52.
4. Weindling, R.; Emerson, O. H. *Phytopathology* **1936**, *26*, 1068-1070.
5. Glister, G. A.; Williams, T. I. *Nature* **1944**, *153*, 1068.
6. Johnson, J. R.; Kidwai, A. R.; Warner, J. S. *J. Am. Chem. Soc.* **1953**, *75*, 2110-2112.
7. Johnson, J. R.; Bruce, W. F.; Dutcher, J. D. *J. Am. Chem. Soc.* **1943**, *65*, 2005-2009.
8. Johnson, J. R.; Buchanan, J. B. *J. Am. Chem. Soc.* **1953**, *75*, 2103-2109.
9. Bell, M. R.; Johnson, J. R.; Wildi, B. S.; Woodward, R. B. *J. Am. Chem. Soc.* **1958**, *80*, 1001.
10. Lowe, G.; Taylor, A.; Vining, L. C. *J. Chem. Soc. C* **1966**, 1799.
11. (a) Tompsett, R.; McDermott, W.; Kidd, J. G. *J. Immunol.* **1950**, *65*, 59-63; (b) Porter, J. N.; De Mello, G. C. *Handbook of Toxicology*. W. B. Saunders Company, Ed.; Philadelphia, **1957**; Vol. 2; (c) Rightsel, W. A.; Schneider, H. G.; Sloan, B. J.; Graf, P. R.; Miller, F. A.; Bartz, Q. R.; Ehrlich, J.; Dixon, G. J. *Nature* **1964**, *204*, 1333; (d) Miller, P. A.; Milstrey, K. P.; Trown, P. W. *Science* **1968**, *159*, 431.
12. Müllbacher, A.; Waring, P.; Tiwari-Palni, U.; Eichner, R. D. *Mol. Immunol.* **1986**, *23*, 231.
13. (a) Kirby, G. W.; Robins, D. J. *The Biosynthesis of Gliotoxin and Related Epipolythiodioxopiperazines*. In *The Biosynthesis of Mycotoxins*. Academic Press, Ed.; San

Francisco, CA, **1980**; (b) Gardiner, D. M.; Waring, P.; Howlett, B. J. *Microbiology* **2005**, *151*, 1021-1032.

14. (a) Kishi, Y.; Fukuyama, T.; Nakatsuka, S. *J. Am. Chem. Soc.* **1973**, *95*, 6490; (b) Kishi, Y.; Fukuyama, T.; Nakatsuka, S. *J. Am. Chem. Soc.* **1973**, *95*, 6492; (c) Fukuyama, T.; Kishi, Y. *J. Am. Chem. Soc.* **1976**, *98*, 6723; (d) Fukuyama, T.; Nakatsuka, S.-I.; Kishi, Y. *Tetrahedron* **1981**, *37*, 2045.

15. (a) Overman, L. E.; Sato, T. *Org. Lett.* **2007**, *9*, 5267-5270; (b) Peng, J.; Clive, D. L. *J. J. Org. Chem.* **2008**, *74*, 513-519; (c) Kim, J.; Ashenhurst, J. A.; Movassaghi, M. *Science* **2009**, *324*, 238-241; (d) Gross, U.; Nieger, M.; Bräse, S. *Chem.-Eur. J.* **2010**, *16*, 11624-11631; (e) Iwasa, E.; Hamashima, Y.; Fujishiro, S.; Higuchi, E.; Ito, A.; Yoshida, M.; Sodeoka, M. *J. Am. Chem. Soc.* **2010**, *132*, 4078-4079; (f) Kim, J.; Movassaghi, M. *J. Am. Chem. Soc.* **2010**, *132*, 14376-14378; (g) Codelli, J. A.; Puchlopek, A. L. A.; Reisman, S. E. *J. Am. Chem. Soc.* **2011**, *134*, 1930-1933; (h) DeLorbe, J. E.; Jabri, S. Y.; Mennen, S. M.; Overman, L. E.; Zhang, F.-L. *J. Am. Chem. Soc.* **2011**, *133*, 6549-6552.

16. Trown, P. W. *Biochem. Biophys. Res. Commun.* **1968**, *33*, 402.

17. Öhler, E.; Tatarurh, F.; Schmidt, U. *Chem. Ber.* **1973**, *106*, 396-398.

18. (a) Hino, T.; Sato, T. *Tetrahedron Lett.* **1971**, *12*, 3127-3129; (b) Öhler, E.; Poisel, H.; Tataruch, F.; Schmidt, U. *Chem. Ber.* **1972**, *105*, 635-641.

19. Levene, P. A.; Bass, L. W.; Steiger, R. E. *J. Biol. Chem.* **1929**, *81*, 697.

20. (a) Stanley, W. M.; McMahon, E.; Adams, R. *J. Am. Chem. Soc.* **1933**, *55*, 706; (b) Nguyen, T.-H.; Chau, N. T. T.; Castanet, A.-S.; Nguyen, K. P. P.; Mortier, J. *J. Org. Chem.* **2007**, *72*, 3419.

21. (a) Yin, J.; Buchwald, S. L. *Org. Lett.* **2000**, *2*, 1101; (b) Klapars, A.; Antilla, J. C.; Huang, X.; Buchwald, S. L. *J. Am. Chem. Soc.* **2001**, *123*, 7727; (c) Klapars, A.; Huang, X.; Buchwald, S. L. *J. Am. Chem. Soc.* **2002**, *124*, 7421; (d) Strieter, E. R.; Bhayana, B.; Buchwald, S. L. *J. Am. Chem. Soc.* **2008**, *131*, 78.

22. Piers, E.; Harrison, C. L.; Zetina-Rocha, C. *Org. Lett.* **2001**, *3*, 3245.
23. (a) Ley, S. V.; Thomas, A. W. *Angew. Chem. Int. Ed.* **2003**, *42*, 5400-5449; (b) Evano, G.; Blanchard, N.; Toumi, M. *Chem. Rev.* **2008**, *108*, 3054-3131.
24. Strieter, E. R.; Bhayana, B.; Buchwald, S. L. *J. Am. Chem. Soc.* **2008**, *131*, 78-88.
25. Williams, R. M.; Armstrong, R. W.; Maruyama, L. K.; Dung, J. S.; Anderson, O. P. *J. Am. Chem. Soc.* **1985**, *107*, 3246.
26. (a) O'Donnell, M. J.; Boniece, J. M.; Earp, S. E. *Tetrahedron Lett.* **1978**, *19*, 2641-2644; (b) Danner, P.; Bauer, M.; Phukan, P.; Maier, Martin E. *Eur. J. Org. Chem.* **2005**, *2005*, 317-325.
27. Pintér, Á.; Haberhauer, G. *Eur. J. Org. Chem.* **2008**, *2008*, 2375-2387.
28. Macdonald, S. J. F.; McKenzie, T. C.; Hassen, W. D. *J. Chem. Soc., Chem. Commun.* **1987**, 1528.
29. Ciufolini, M. A.; Valognes, D.; Xi, N. *Tetrahedron Lett.* **1999**, *40*, 3693.
30. To assess antitubercular activity, **10**, **84**, **48**, and **98** were inoculated into a 96 well plate containing MTB at a final OD of 0.025. Cells were allowed to incubate for three days at which point bacterial growth was assessed by reading OD600.
31. For mammalian cell toxicity, J774 macrophages were plated at 50,000 cells per cell well in 96 well plates, and **10**, **84**, **48**, and **98** were added. Cells were incubated for three days at which point macrophages viability was assessed using Cel Titer Glo reagent.
32. Jiang, C.-S.; Guo, Y.-W. *Mini-Rev. Med. Chem.* **2011**, *11*, 728-745.
33. Oughton, B. M.; Harrison, P. M. *Acta. Cryst.* **1959**, *12*, 396-404.
34. Walkter, R.; Roy, J. *Organic Selenium Compounds: Their Chemistry and Biology*. Wiley, Ed.; New York, NY, **1973**.
35. Quaderer, R. J. Selenocysteine-Mediated Native Chemical Ligation. Swiss Federal Institute of Technology (ETH) Zurich, Zurich, 2002.

36. Besse, D.; Siedler, F.; Diercks, T.; Kessler, H.; Moroder, L. *Angew. Chem. Int. Ed.* **1997**, *36*, 883-885.
37. Sarsour, E. H.; Kumar, M. G.; Chaudhuri, L.; Kalen, A. L.; Goswami, P. C. *Antioxid. Redox Signal.* **2009**, *11*, 2985-3011.
38. (a) Tonkikh, N.; Duddeck, H.; Petrova, M.; Neilands, O.; Strakovs, A. *Eur. J. Org. Chem.* **1999**, *1999*, 1585; (b) Sureshkumar, D.; Ganesh, V.; Chandrasekaran, S. *J. Org. Chem.* **2007**, *72*, 5313.
39. Krief, A.; Derock, M. *Synlett* **2005**, *2005*, 1012,1014.
40. Cook, K. M.; Hilton, S. T.; Mecinoviá, J.; Motherwell, W. B.; Figg, W. D.; Schofield, C. *J. J. Biol. Chem.* **2009**, *284*, 26831.

## **Part Two**

Towards the total synthesis of the tetrapetalones.

## Chapter Six

### The Tetrapetalones

Tetrapetalone A was isolated in 2003 by Hirota and coworkers from a culture filtrate of *Streptomyces* sp. USF-4727.<sup>1</sup> In 2004 the structurally related tetrapetalones B, C, and D were isolated from the same *Streptomyces* strain.<sup>2</sup> The tetrapetalones have shown inhibitory activity against soybean lipoxygenase (SBL), which is similar to human lipoxygenase and cyclooxygenase, which have relevance in a variety of human diseases. We became interested in the tetrapetalones due to their interesting structural features and the synthetic challenge they present.

#### 6.1 Isolation and Structure Determination

During their quest to discover new lipoxygenase inhibitors, Hirota and coworkers, while screening soil *Streptomyces* sp. strains using a well-known SBL assay, discovered the novel soybean lipoxygenase inhibitor tetrapetalone A from a culture filtrate of *Streptomyces* sp. USF-4727 in 2003.<sup>1a</sup> This particular soil sample was taken from Yada, Shizuoka City, Japan. Tetrapetalone A was isolated as a pale yellow amorphous powder with a melting point of 190 °C and a molecular formula of C<sub>26</sub>H<sub>33</sub>NO<sub>7</sub>. Through extensive NMR studies including <sup>1</sup>H, <sup>13</sup>C, DEPT, <sup>1</sup>H–<sup>1</sup>H COSY, HMQC, HMBC and 2D–INADEQUATE experiments they proposed structure **129** as the structure of tetrapetalone A (Figure 6.1). The relative stereochemistry of **129** was determined through analogy of the sugar moiety to β-rhodinose and through NOESY correlations. The absolute stereochemistry of **129** was determined by analysis employing the modified Mosher's method to the oxygens attached to C(4') and C(9). The latter analysis

following hydrolysis of the appended deoxy sugar. The stereochemistry at C(4) and C(15) were not reported in the initial publication.

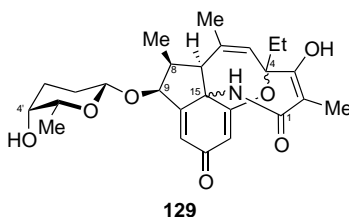
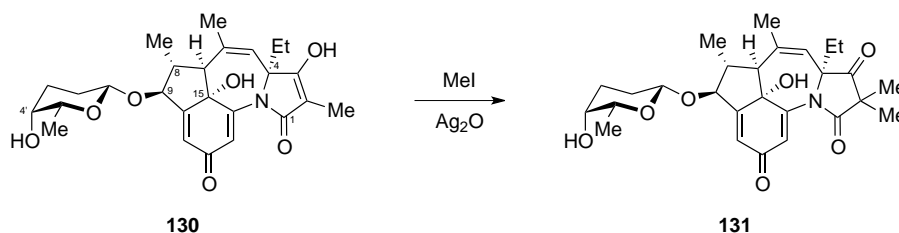


**Figure 6.1.** Initially proposed structure of tetrapetalone A.

In 2003, in an attempt to confirm the position and type of nitrogen atom in tetrapetalone A, Hirota and coworkers performed a  $^1\text{H}$ - $^{15}\text{N}$  HMBC experiment and found the data was inconsistent with their initially proposed structure. Specifically they noted a long range coupling between the nitrogen and the proton on the ethyl group, which is not possible in structure **129**. Therefore they revised the structure of tetrapetalone A to be **130**.<sup>1b</sup> Additionally they were able to assign the absolute stereochemistry of **130** from the data already reported and extensive NOESY studies of **130** and methylated derivative **131** (Scheme 6.1). This included the previously unassigned C(4) and C(15) and revise the stereochemistry of C(8).



**Scheme 6.1.** Revised structure of tetrapetalone A (**130**) and conversion to tetrapetalone A-Me<sub>2</sub> (**131**).

In 2004, after further investigations of the culture filtrate of *Streptomyces* sp. USF-4727, Hirota and coworkers isolated three more novel lipoxygenase inhibitors, tetrapetalones B (**132**),

C (**133**), and D (**134**) (Figure 6.2).<sup>2</sup> These compounds are structurally related to tetrapetalone A and only differ in oxidation of the ethyl group (**132**), oxidation of the tetramic acid moiety (**133**), or oxidation at both the ethyl group and the tetramic acid (**134**). The structures of **132** – **134** were assigned through various NMR studies and through analogy to **130**.

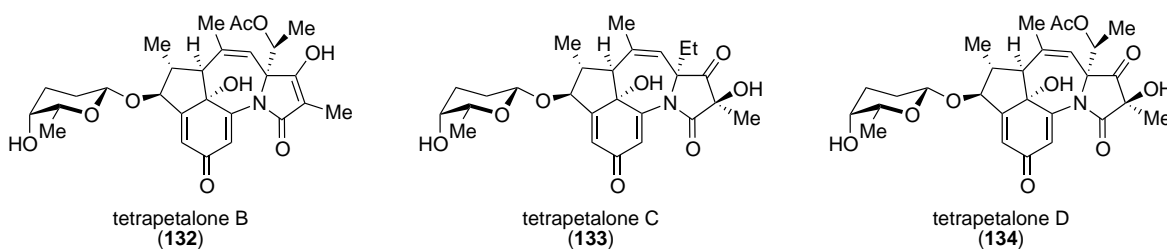


**Figure 6.2.** Tetrapetalones B (**132**), C (**133**), and D (**134**).

In 2008, Hirota and coworkers identified ansaetherone (**135**) from the same *Streptomyces* strain as the tetrapetalones while screening with a radical scavenging assay (Figure 6.3).<sup>3</sup> Ansaetherone was isolated as a colorless amorphous powder and found to have a molecular formula of  $C_{26}H_{33}NO_7$ . The structure was elucidated utilizing  $^1H$ ,  $^{13}C$ , DEPT,  $^1H$ - $^1H$  COSY, HMQC, and HMBC NMR experiments. The relative stereochemistry of **135** was assigned through NOE correlations and the absolute stereochemistry through analogy to the tetrapetalones, however the stereochemistry at C(2) and C(17) could not be assigned. Given the structural similarities, Hirota and coworkers proposed ansaetherone to be a biosynthetic precursor to the tetrapetalones.

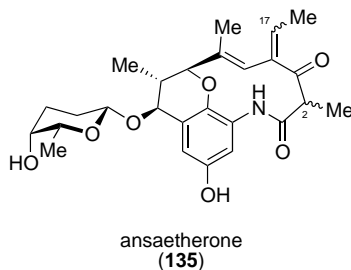
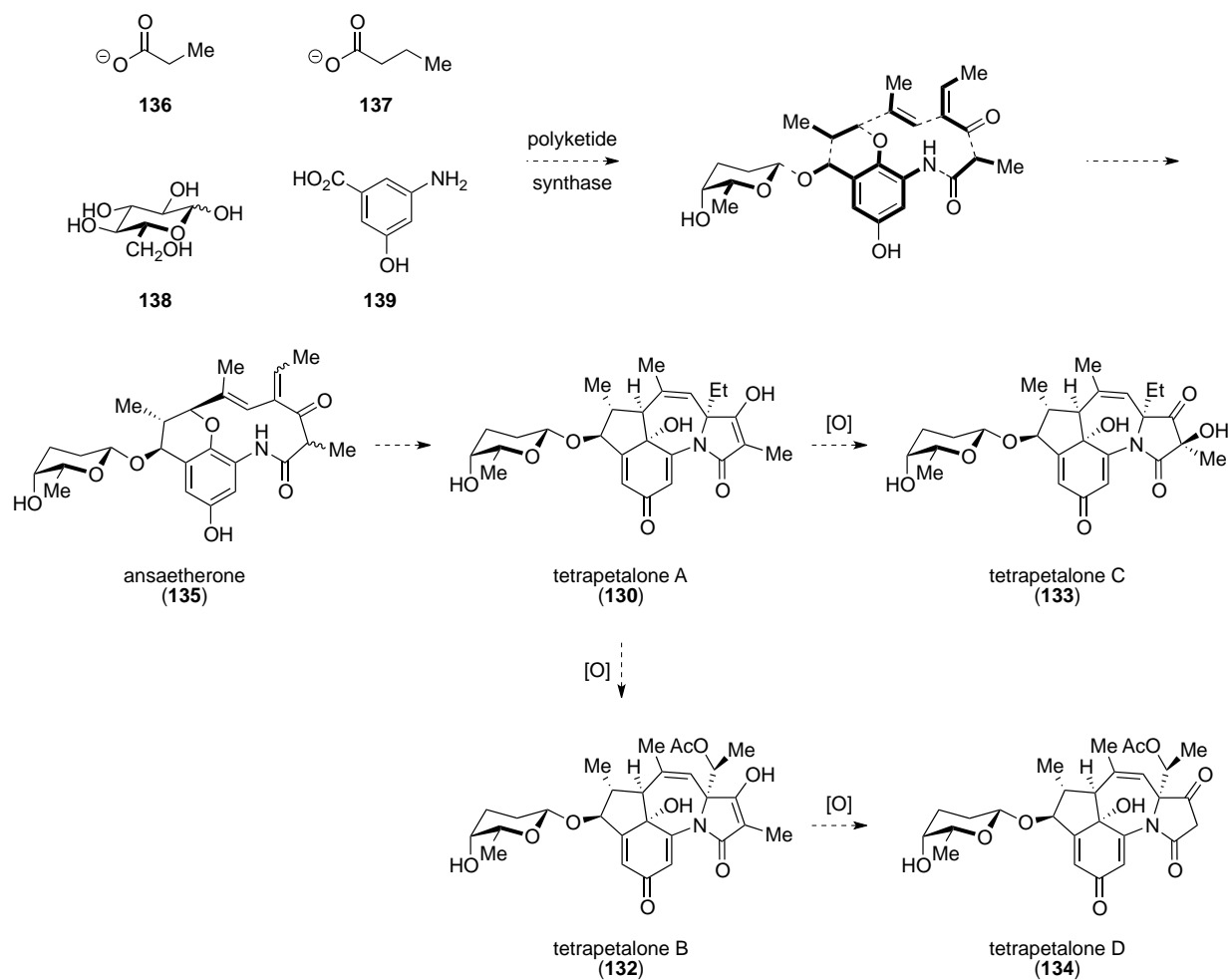


**Figure 6.3.** Structure of ansaetherone (**135**).

## 6.2 Biosynthesis

As noted above the Hirota group proposed that ansaetherone was a biosynthetic precursor to the tetrapetalones.<sup>3</sup> However, as they had isolated both the tetrapetalones and ansaetherone from the same *Streptomyces* strain, they were interested in further exploring the biosynthetic origins of these compounds. Through feeding studies of isotopically labeled precursors it was determined that the tetrapetalone core was derived from three molecules of propionate (**136**), one butyrate (**137**), one glucose (**138**), and one 3-amino-5-hydroxybenzoic acid (AHBA, **139**).<sup>4</sup> Thus, it was proposed that tetrapetalone A was biosynthesized by a polyketide synthase using **139** as a starter unit, and proceeding with ansaetherone as an intermediate. Oxidations to tetrapetalone A would lead to tetrapetalones B, C, and D (Scheme 6.2).



**Scheme 6.2.** Proposed biosynthetic pathway of the tetrapetalones.

## Chapter Seven

### Previous Synthetic Efforts

Although there have been no completed syntheses of any members of the tetrapetalones, there has been significant interest in the family. There are published reports in the literature from the Porco,<sup>5</sup> Sarpong,<sup>6</sup> and Hong<sup>7</sup> groups that outline progress towards the total synthesis of tetrapetalone A (**130**). There is also a single report from Yang *et al.* that outlines the syntheses of (+)-Q-1047H-A-A (**140**) and (+)-Q-1047H-R-A (**141**) (Figure 7.1),<sup>8</sup> which they propose could possibly be converted to tetrapetalone A. However, given the limited similarity to **130**, including the presence of a methyl group at C(4) instead of an ethyl and no clear way to form the C(4)–N or C(7)–C(15) bonds, further discussion of this report is omitted. If you search tetrapetalone in SciFinder you can find abstracts of posters presented at ACS meetings from the Frontier, Pettus, and Kobayashi groups. However, as these posters cannot be accessed their work will not be discussed here.

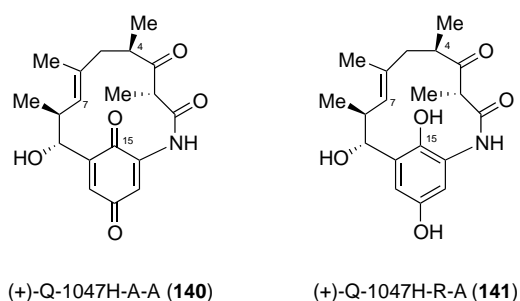
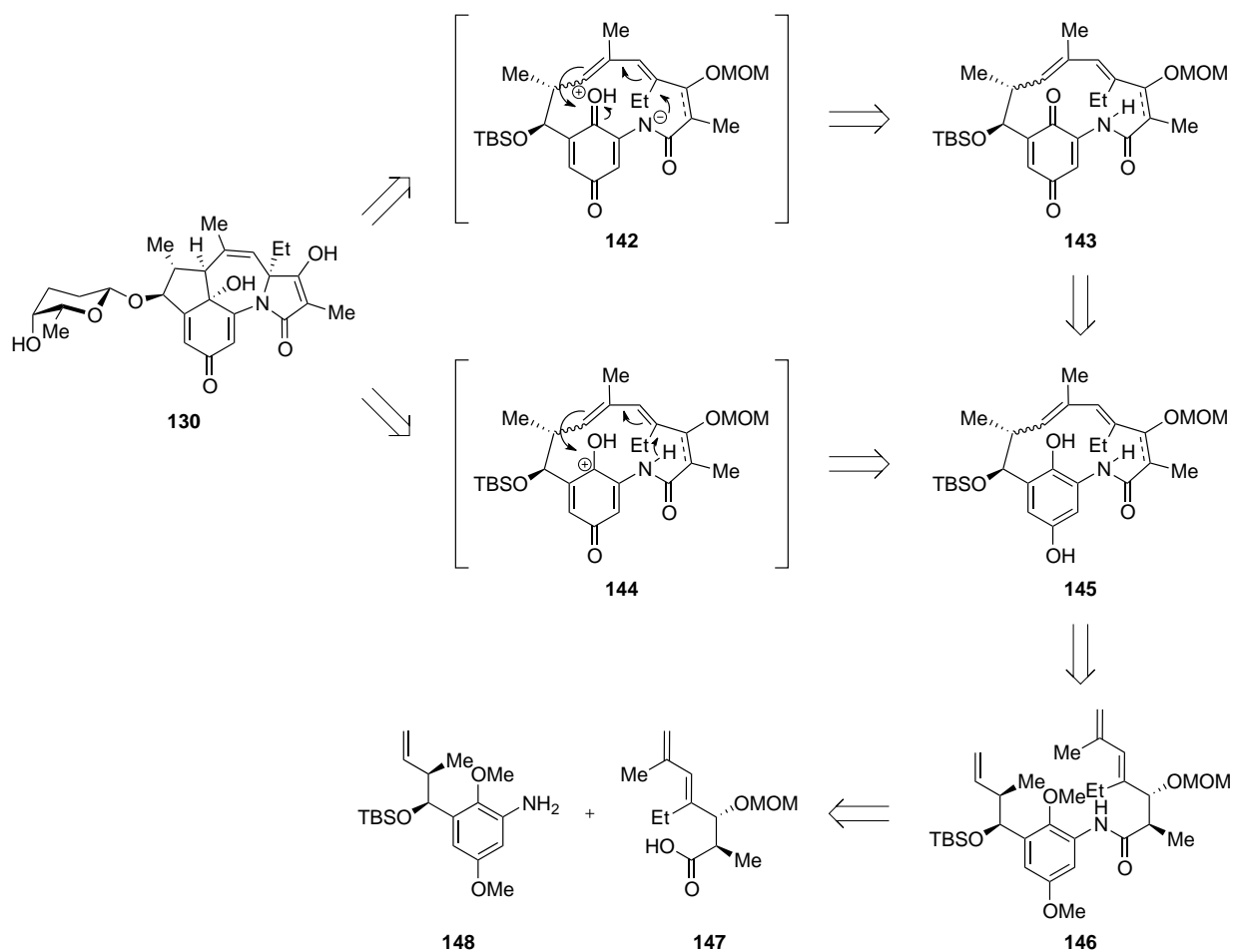


**Figure 7.1.** (+)-Q-1047H-A-A (**140**) and (+)-Q-1047H-R-A (**141**).

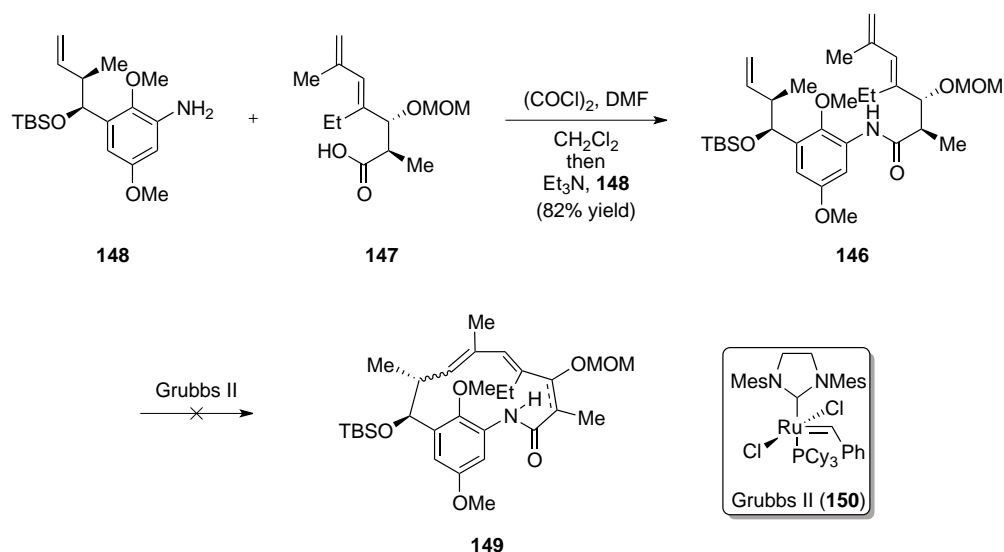
## 7.1 Porco's Efforts Towards Tetrapetalone A

Porco and coworkers envisioned constructing tetrapetalone A (**130**) through a late stage transannular [4+3] cyclization process (Scheme 7.1).<sup>5a</sup> They believed this could proceed via one of two pathways. Utilizing quinone **143** under UV irradiation would form intermediate **142** through an excited-state intramolecular proton transfer, which could undergo a formal [4+3] process. Conversely, hydroquinone **145** could be oxidized to oxonium **144** and undergo a formal [4+3] cycloaddition. Hydroquinone **145** would be formed from triene **146** by a ring-closing metathesis, and **146** would arise from an amidation of amide **148** with acid **147**.



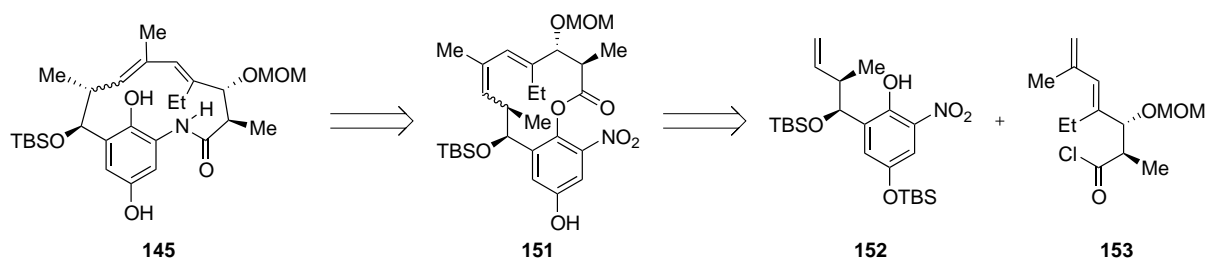
**Scheme 7.1.** Porco's retrosynthetic analysis of tetrapetalone A (**130**).

To explore this [4+3] cyclization process, Porco and coworkers set out to form protected hydroquinone **146** (Scheme 7.2). To accomplish this aniline **148**, available in three steps from known materials, was added to the *in situ* generated acid chloride of carboxylic acid **147**, which was available in three steps from known materials. Unfortunately, subjecting triene **146** under ring-closing metathesis conditions lead to no desired product. The authors believe that the catalyst was able to react with the monosubstituted olefin, but not the 1,1-disubstituted olefin. Furthermore, due to the *meta* relationship of the two pieces and the presence of the *ortho*-substituted methoxy group, it was speculated that considerable conformational strain prohibited proper overlap of the two double bond containing side chains.



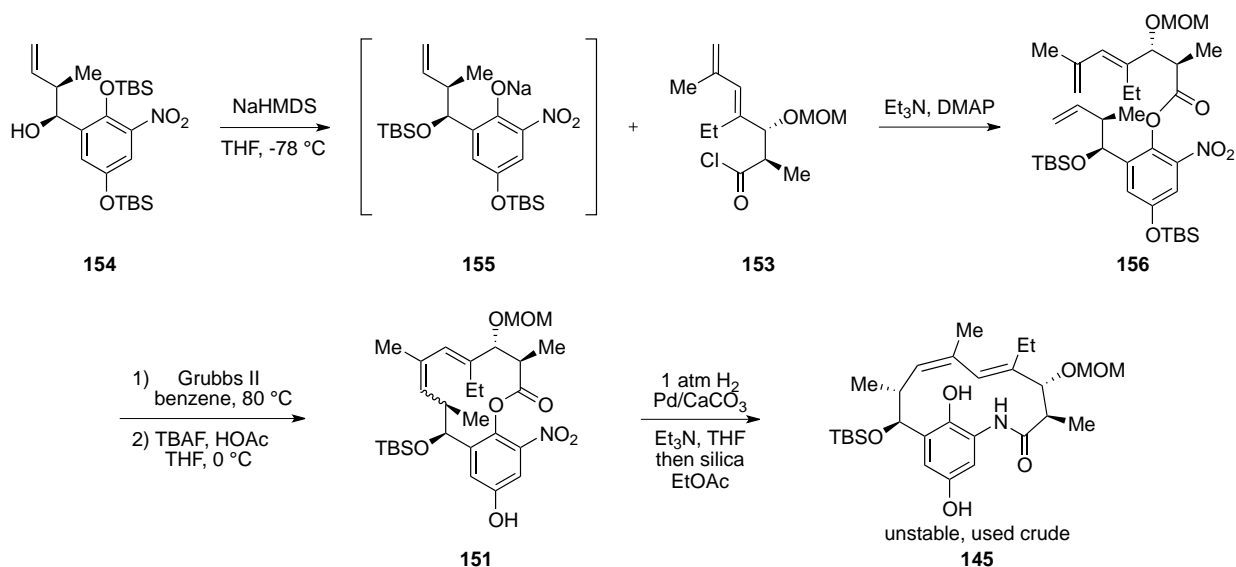
**Scheme 7.2.** Porco's attempted ring-closing metathesis of triene **146**.

Having failed at ring-closing metathesis, the Porco group next explored a pathway where hydroquinone **145** would derive from nitrobenzene **151** via reduction and acyl migration. This macrocycle would be formed from O-acylation followed by ring-closing metathesis, and would ultimately derive from nitrobenzene **152** and acid chloride **153** (Scheme 7.3).



**Scheme 7.3.** Porco's revised retrosynthetic analysis of intermediate **145**.

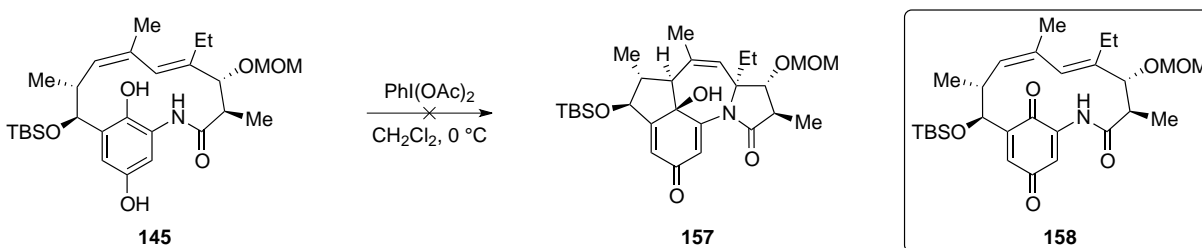
In the event, benzylic alcohol **154**, available in three steps from known materials, underwent a silyl migration to form intermediate alkoxide **155**, which could be reacted with acid chloride **153** to give ester **156**. Ring-closing metathesis followed by deprotection gave macrocycle **151**, which could be converted to the desired hydroquinone (**145**) following reduction of the nitro group and exposure to silica gel. Hydroquinone **145** was unstable and was therefore used directly in the next step.



**Scheme 7.4.** Porco's synthesis of hydroquinone **145**.

With access to hydroquinone **145**, the Porco group next explored their key transannular [4+3] cyclization. Upon exposure to iodobenzene diacetate the Porco group, although initially

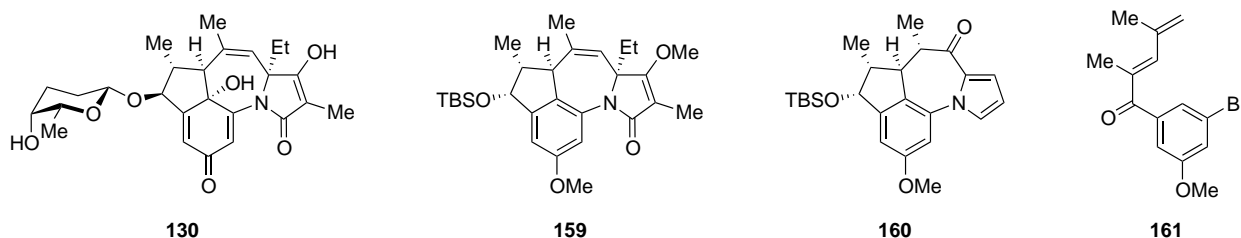
reporting tetracycle **157** was formed, did not obtain any of the desired product, instead isolating quinone **158** as the only product. This error was disclosed in a revision to the original manuscript (Scheme 7.5).<sup>5b</sup>



**Scheme 7.5.** Porco's attempted synthesis of tetracycle **157**.

## 7.2 Sarpong's Efforts Towards Tetrapetalone A

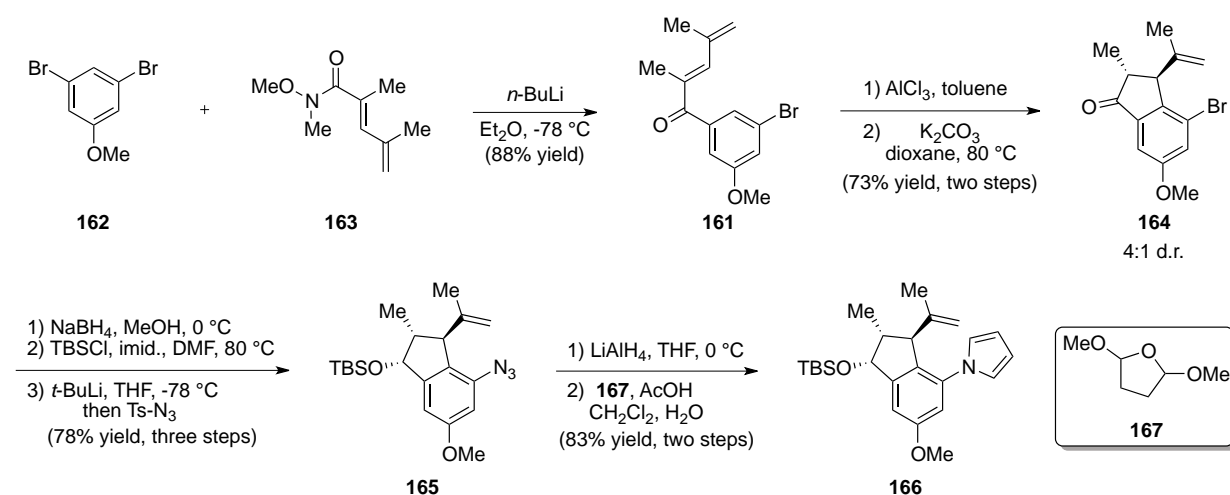
Sarpong and coworkers believed tetrapetalone A (**130**) could arise from late stage phenolic oxidation and glycosylation of tetracycle **159**.<sup>6b</sup> The tetramic acid moiety would be assembled from a corresponding pyrrole while the olefin in the seven membered ring would derive from the ketone in **160**. Pyrrole **160** would ultimately arrive from aryl bromide **161** in a number of steps including a key Nazarov cyclization.



**Scheme 7.6.** Sarpong's retrosynthetic analysis of tetrapetalone A (**130**).

Beginning with dibromide **162**, Sarpong and coworkers formed aryl ketone **161** after lithium–halogen exchange and addition of Weinreb amide **163**. The key Nazarov cyclization

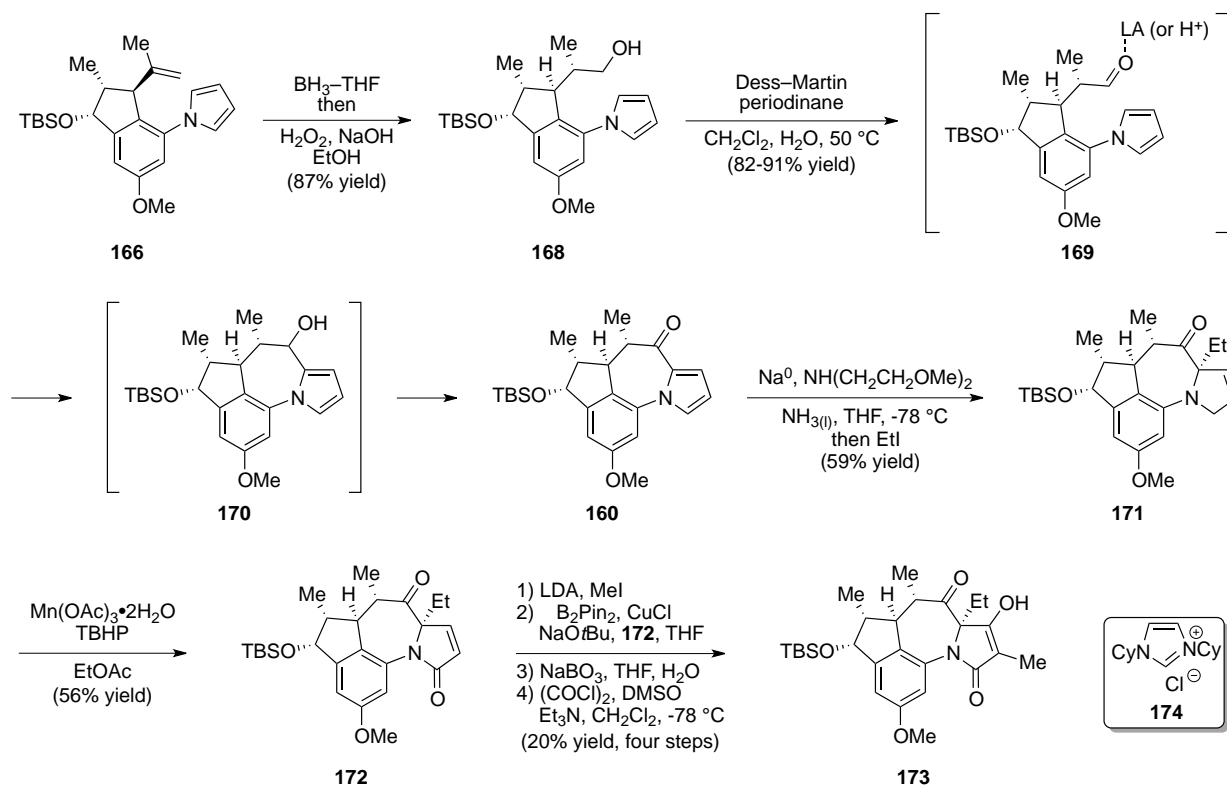
proceeded in the presence of  $\text{AlCl}_3$ , however gave a 9:1 mixture of the undesired *cis*-diastereomer of the product. Exposure of the undesired isomer to potassium carbonate in warm dioxane induced epimerization and furnished the desired *trans*-diastereomer **164** in a 4:1 diastereomeric ratio. Reduction and protection of the ketone followed by conversion of the aryl bromide to an aryl azide provided intermediate **165**. This could be converted to the desired aryl pyrrole **166** through reduction of the azide and condensation of the resultant aniline with 2,5-dimethoxytetrahydrofuran (**167**) (Scheme 7.7).



**Scheme 7.7.** Sarpong's synthesis of intermediate **166**.

The seven-membered ring of tetrapetalone A (**130**) was formed in an interesting two step protocol that began with a hydroboration–oxidation sequence applied to aryl pyrrole **166** to provide primary alcohol **168** and concluded with an oxidation that employed the Dess–Martin periodinane. The seven-membered ketone **160** was formed presumably after initial oxidation produced aldehyde **169**, which in turn underwent a Friedel–Crafts type reaction, possibly with the aid of an iodine Lewis Acid or hydronium ion, to give secondary alcohol **170**. This alcohol could then be oxidized a second time to generate the observed product. Reduction of the derived pyrrole and installation of the requisite ethyl group to furnish **171** was accomplished via exposure of **160** to dissolving metal conditions followed by ethyl iodide. Oxidation of **171** with

Mn(OAc)<sub>3</sub>•2H<sub>2</sub>O produced lactam **172**, which could be converted to the desired tetramic acid (**173**) in a four step sequence (Scheme 7.8). Tetracycline **173** is the most elaborated compound reported by Sarpong and coworkers. Major challenges left in their synthesis include conversion of the ketone in the seven-membered ring to an olefin, removal of the TBS group from the benzylic alcohol followed by inversion of that alcohol stereocenter, introduction of the sugar moiety, and phenolic oxidation.

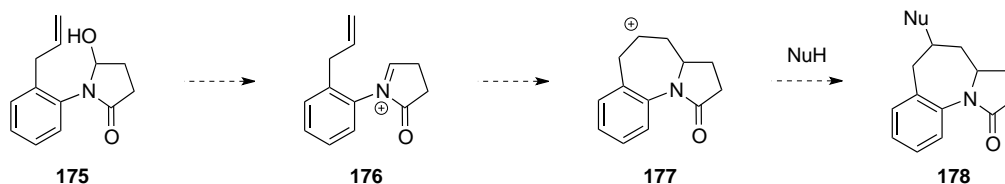


**Scheme 7.8.** Sarpong's synthesis of tetracycline **173**.

### 7.3 Hong's Synthetic Studies Towards the Core of Tetraketone A

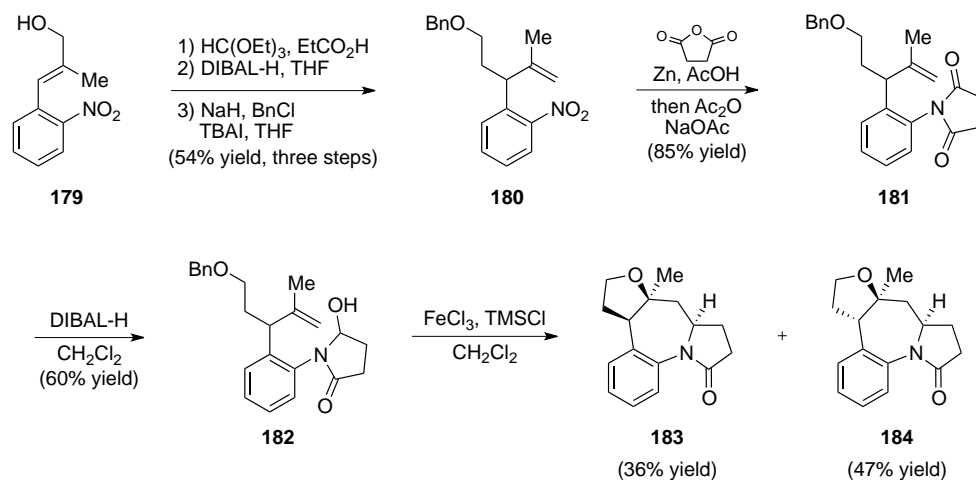
In 2009, Hong and coworkers published a report detailing synthetic studies on the tetraketones.<sup>7</sup> In their paper they detail a synthetic strategy for the core of tetraketone A

(130). Their strategy includes a key Speckamp cyclization, which involves formation of an *N*-acyl iminium ion (176) that can be trapped with the pendant olefin forming a secondary carbocation (177) that can be quenched with a nucleophile to form the six–seven–five system as seen in 178 (Scheme 7.9).



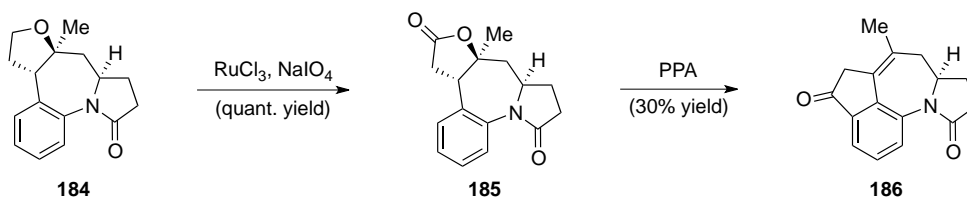
**Scheme 7.9.** Hong's proposed synthesis of the six–seven–five skeleton of tetrapetalone A.

Their synthesis began with allylic alcohol **179**. Johnson–Claisen rearrangement followed by reduction of the resultant ester to the primary alcohol and protection as the benzyl ether gave **180**. Reduction and condensation with succinic anhydride gave imide **181**, which could be monoreduced to give hydroxylactam **182**. Upon exposure to iron trichloride, hydroxylactam **182** underwent the key Speckamp cyclization giving a mixture of diastereomeric tetracycles **183** and **184** (Scheme 7.10).



**Scheme 7.10.** Hong's synthesis of tetracycles **183** and **184**.

The major diastereomer from the Speckamp cyclization (**184**) was oxidized to give lactone **185**. Exposure to polyphosphoric acid led to a Friedel–Crafts/ dehydration sequence that furnished tetracycle **186**. Although tetracycle **186** contains the carboskeleton required for tetrapetalone A, it lacks most of the functionality of the natural product. Although there are several interesting steps in the Hong synthesis, considerable effort remains for conversion of their most advanced intermediate to **130**.



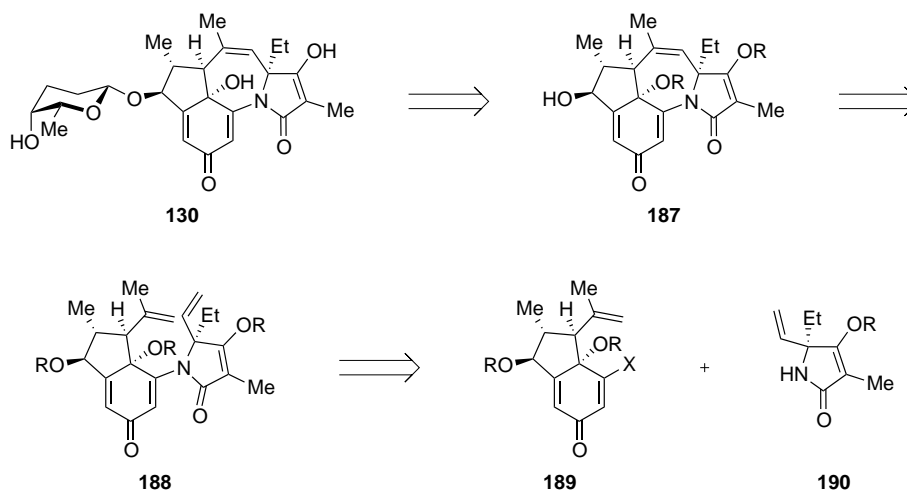
**Scheme 7.11.** Hong's synthesis of the barebone skeleton of tetrapetalone A.

## Chapter Eight

### Previous Approaches in the Wood Group

Prior to my taking over the tetrapetalone project a previous student, Dr. Jennifer Howell, had explored several strategies for incorporating various requisite functional groups. As my work was inspired by Dr. Howell's effort, it will be summarized here.<sup>9</sup>

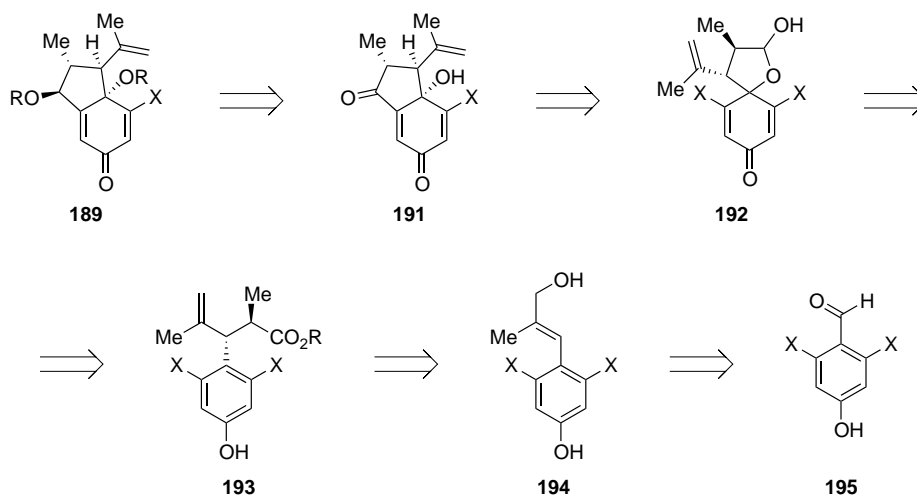
The first synthetic route studied in our group is outlined in Scheme 8.1. In that scenario tetrapetalone A (**130**) was envisioned as arising from late stage glycosylation and deprotection of tetracycle **187**. A key disconnect in this route was a ring-closing metathesis to form the seven membered ring employing diene **188** as a substrate. The two required olefin components would be installed via a Buchwald–Hartwig coupling of vinyl halide **189** and amide **190**.



**Scheme 8.1.** Initial retrosynthetic analysis of tetrapetalone A (**130**).

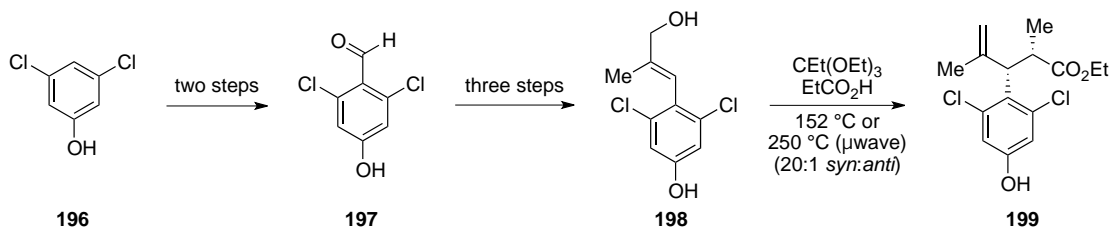
In order to explore the desired Buchwald-Hartwig coupling, initial efforts focused on the synthesis of vinyl halide **189**. To access this intermediate it was envisioned that ketone **191** would be reduced and protected. Ketone **191** would arise from an intramolecular Stetter reaction of lactol **192**, which itself would result from reduction and phenolic oxidation of ester

**193.** Ester **193** was seen as arising via a Claisen rearrangement applied to allylic alcohol **194**, the product of a Wittig olefination of benzaldehyde **195** (Scheme 8.2).



**Scheme 8.2.** Retrosynthetic analysis of vinyl halide **189**.

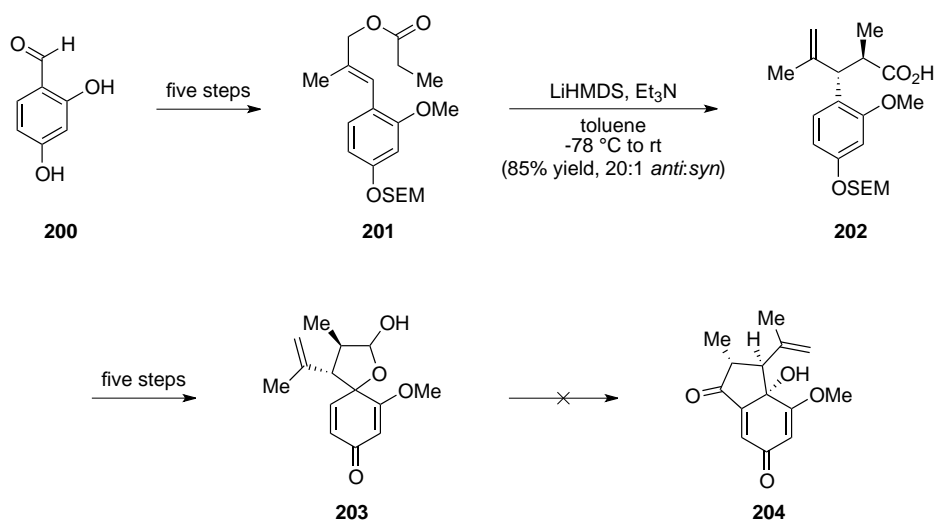
In accord with our retrosynthetic plan the synthesis began with a known two step sequence to form aldehyde **197** from phenol **196**.<sup>10</sup> Aldehyde **197** was then transformed in three steps to allylic alcohol **198**. Although subjecting **198** to a Johnson–Claisen rearrangement provided a rearranged product, it preferentially gave the undesired *syn*–diastereomer **199** in a 20:1 ratio over the desired *anti*–diastereomer (Scheme 8.3)



**Scheme 8.3.** Synthesis of undesired *syn* diastereomer **199**.

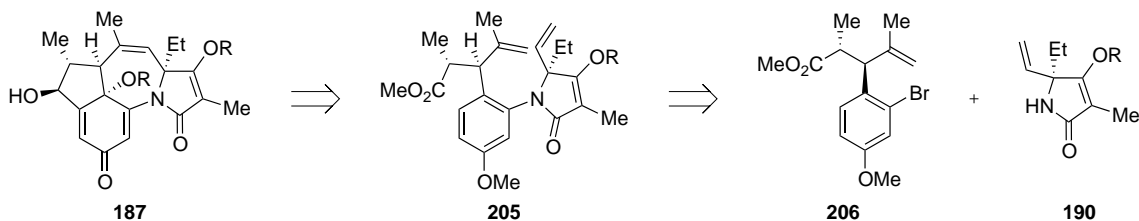
After extensive research, it was found that allylic ester **201** could be formed in five steps from benzaldehyde **200** and subjected to a lithium enolate variant of the Claisen rearrangement

that furnishes the desired *anti*-product **202**.<sup>11</sup> The latter was readily transformed into phenolic oxidation product **203** in five steps, however, efforts to employ **203** as a substrate in a Stetter reaction failed, presumably due to the sensitivity of this transformation to subtle changes in sterics (Scheme 8.4)



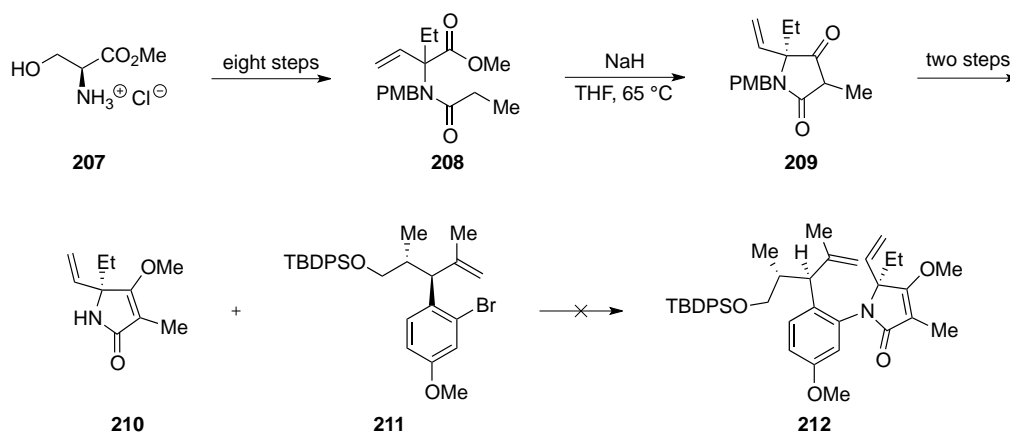
**Scheme 8.4.** Unsuccessful attempts of the Stetter reaction to form **204**.

Due to the difficulties encountered with the Stetter reaction, a new strategy was devised. Ultimately tetracyclic intermediate **187** would be formed from aryl bromide **206** and tetramic acid **190**. The key difference in this route is the aryl–amidation and the Stetter reaction would be performed in reverse order, and therefore the Buchwald–Hartwig coupling would occur between **206** and **190** (Scheme 8.5).



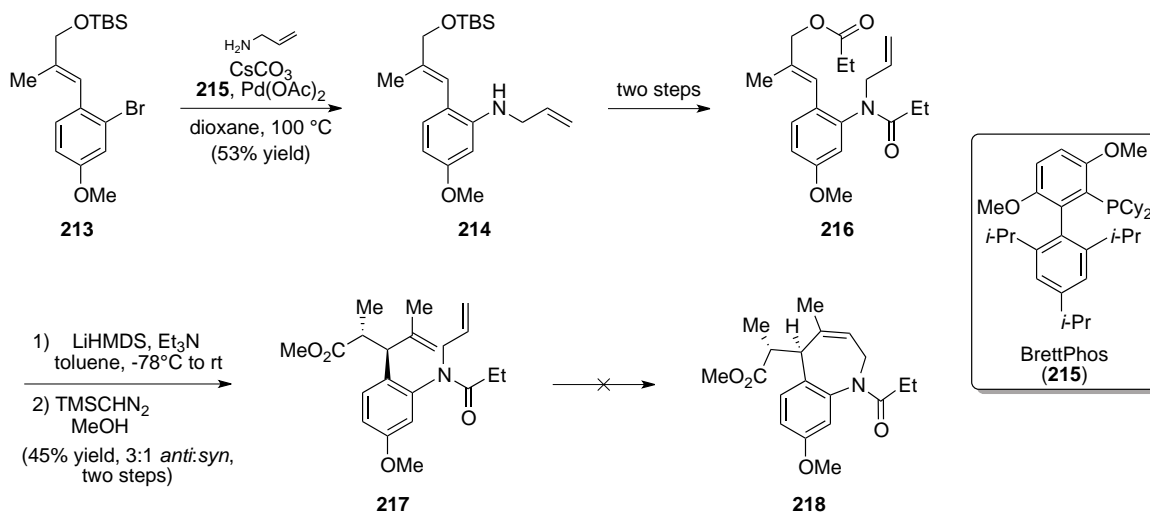
**Scheme 8.5.** Revised strategy for Buchwald–Hartwig coupling.

In accordance with this strategy, the requisite tetramic acid **210** was prepared from the corresponding amino acid derivative **208**, which was in turn available in eight steps from serine methyl ester hydrochloride (**207**). In the key step for the formation of tetramic acid **210**, a Dieckmann cyclization of **208** provided protected tetramic acid **209**, which could be converted to the desired tetramic acid **210** in two steps. However, all attempts to couple **210** with aryl bromide **211** or derivatives of **211** were unproductive (Scheme 8.6).



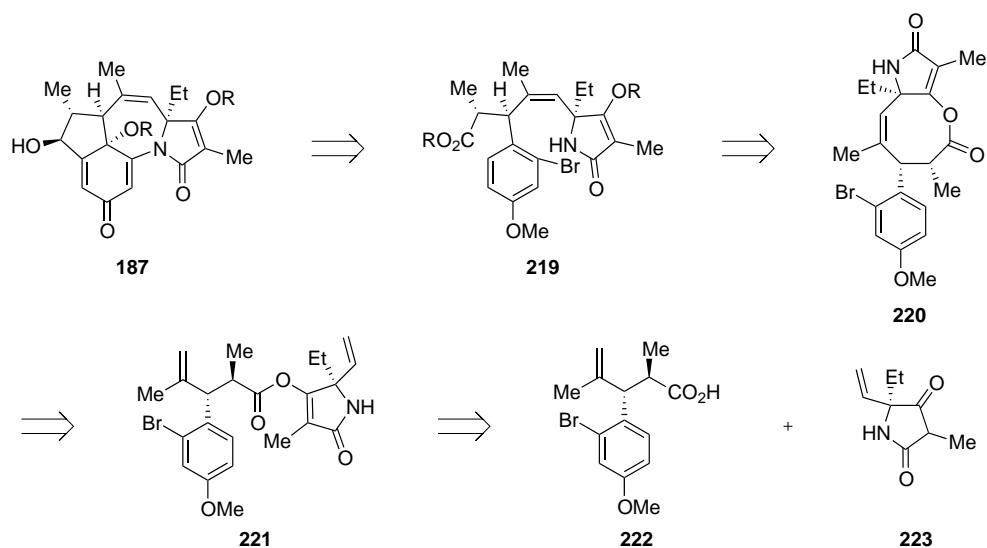
**Scheme 8.6.** Attempted Buchwald–Hartwig coupling to form **212**.

In order to circumvent this unsuccessful Buchwald–Hartwig coupling, the coupling partners were simplified (Scheme 8.7). In that regard, aryl bromide **213** and allyl amine were found to successfully form aryl amine **214** under palladium–catalyzed conditions. Conversion of **214** to allylic ester **216** via a two step sequence set the stage for a lithium enolate Claisen rearrangement analogous to that employed previously. Methylation of the derived product produced the RCM substrate **217**. Unfortunately, exhaustive efforts to implement the ring–closure failed to produce any of the desired product.



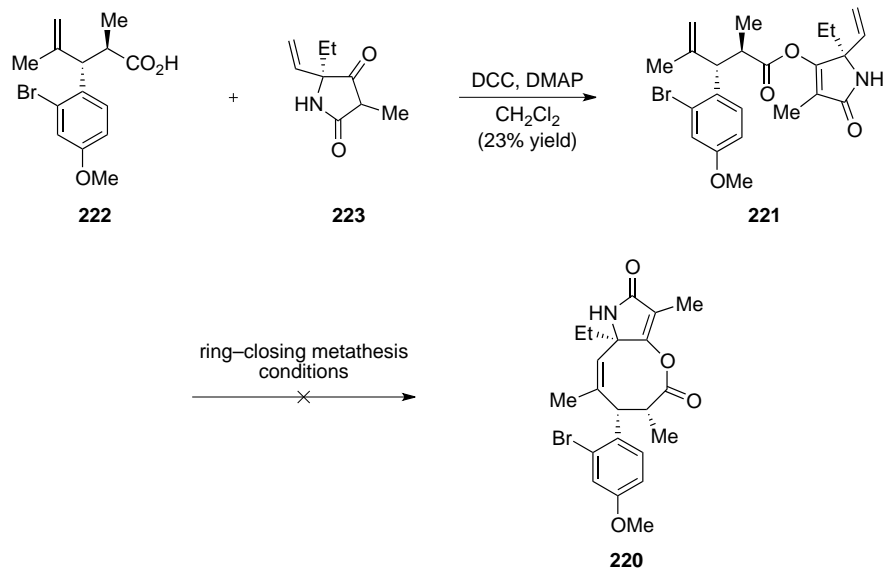
**Scheme 8.7.** Unsuccessful attempts at ring-closing metathesis.

After the unsuccessful attempts to perform a Buchwald–Hartwig coupling and subsequent ring-closing metathesis, Dr. Howell attempted to simply reverse the order of these steps (Scheme 8.8). Specifically, tetracyclic intermediate **187** was now seen as arising from an intramolecular Buchwald–Hartwig coupling of **219**, which itself would be the product of saponification of eight-membered lactone **220**. Lactone **220** would come from a ring-closing metathesis of ester **221**, which is the product of linking aryl bromide **222** with tetramic acid **223**.



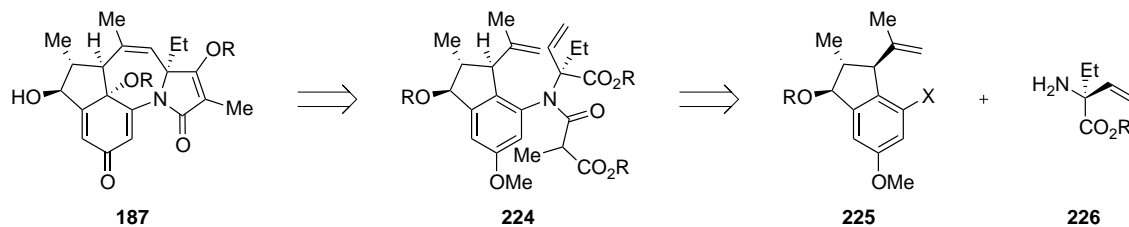
**Scheme 8.8.** Revised retrosynthetic analysis.

To explore the viability of this route for delivering tetrapetalone A (**130**), carboxylic acid **222** and tetramic acid **223** were coupled together to form lactone **221**. Unfortunately, the ring closing metathesis of **221** was unsuccessful and did not lead to any of the desired eight-membered lactone **220** (Scheme 8.9). Many variants of **221** were explored, including compounds bearing other tethers and compounds set up for relay ring-closing metathesis; however none of these variations lead to desired product. Thus a new route was established.



**Scheme 8.9.** Attempted ring-closing metathesis to form lactone **220**.

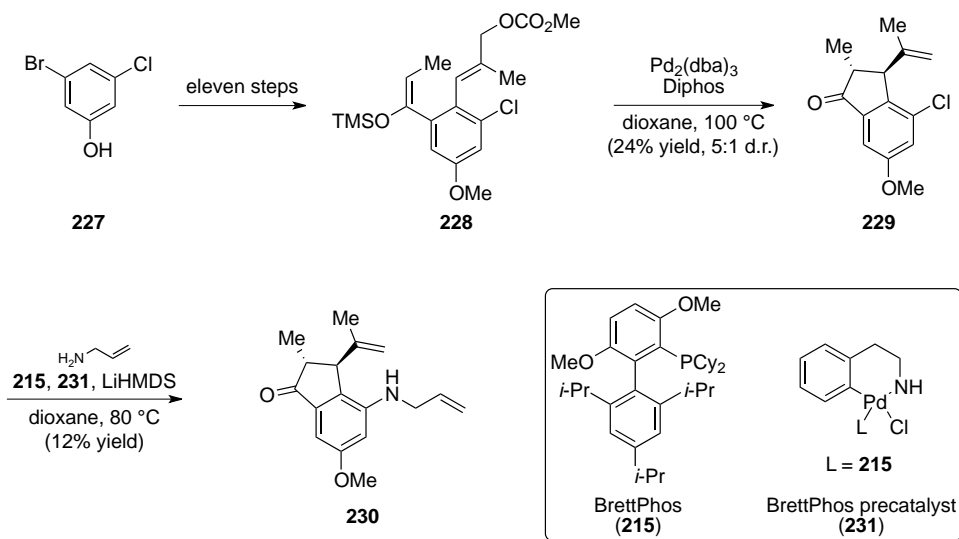
As outline in Scheme 8.10, a new route for the synthesis of tetrapetalone A (**130**) was designed wherein intermediate **187** was seen as arising from diene **224** via a sequence that would involve an RCM reaction to construct the seven-membered ring and a Dieckmann condensation to complete the tetramic acid. It was postulated that performing the ring-closing metathesis prior to Dieckmann condensation would be beneficial due to increased conformational flexibility in the substrate. Key intermediate **224** would be formed from a Buchwald-Hartwig coupling of aryl halide **225** and amino acid derivative **226**.



**Scheme 8.10.** Revised retrosynthetic analysis of intermediate **187**.

Efforts to implement this latest strategy began with the preparation of aryl chloride **229**. To this end, dihalophenol **227** was converted to silyl enol ether **228** over eleven steps.

Subjecting silyl enol ether **228** to an intramolecular Tsuji–Trost allylation furnished **229** in moderate yield. To test the viability of the required aryl–amidation reaction, aryl chloride **229** was reacted with allyl amine to give aniline **230**. Although the yield is low, it shows that this route may be viable in a synthesis of tetrapetalone A (**130**). This however, is where Dr. Jennifer Howell’s work towards **130** ended.



**Scheme 8.11.** Synthesis of aryl amine **230**.

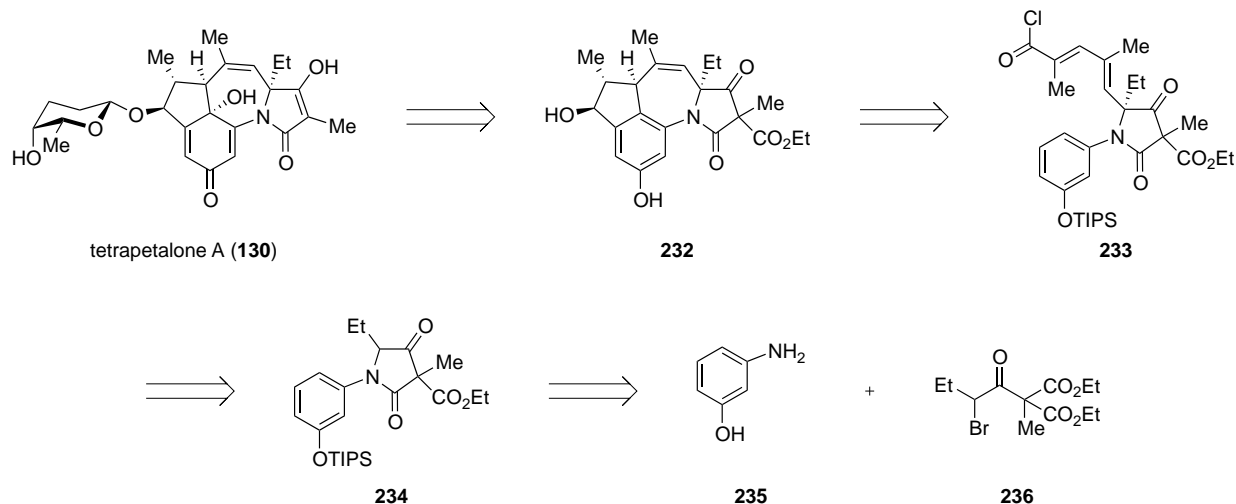
## Chapter Nine

### Formation of the Seven-Membered Ring Utilizing the Aromatic Ring as a Nucleophile

Although Dr. Jennifer Howell left a route in place towards tetrapetalone A (**130**) that was beginning to show some promise, concern over the limitation in scope of the requisite arylamidation reaction and numerous low yielding steps led us to consider a different approach.

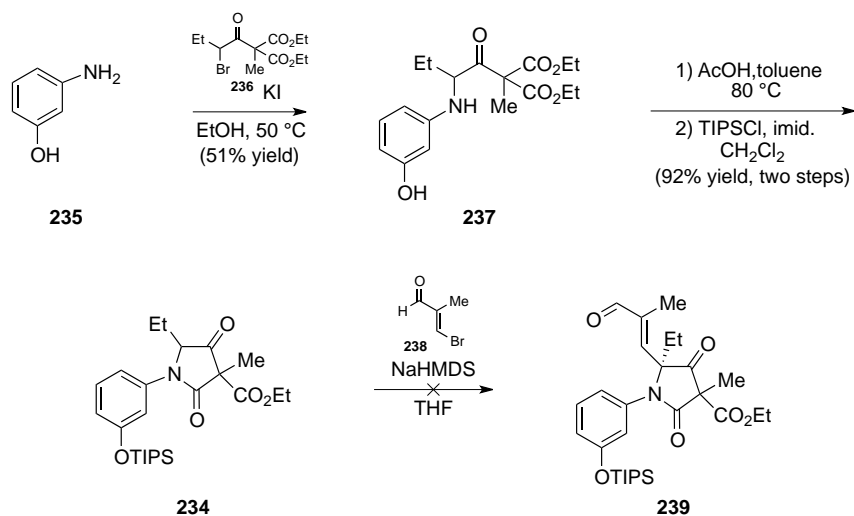
#### 9.1 Cascade Friedel-Crafts Approach

As illustrated in retrosynthetic fashion, our initial efforts to redesign the synthesis focused on a plan wherein a key cascade Friedel-Crafts reaction would furnish the tetracyclic core of **130**. Specifically, **130** was seen as arising from tetracycle **232** via a sequence involving phenolic oxidation, glycosylation, and decarboxylation (Scheme 9.1). Tetracycle **232** would, in turn, arise from the key cascade Friedel-Crafts sequence in which both the five- and seven-membered rings would be formed. To access **233**, tetramic acid **234** would be employed in a 1,4-addition followed by a Horner-Wadsworth-Emmons olefination. Tetramic acid **234** would be formed rapidly from simple precursors **235** and **236**.



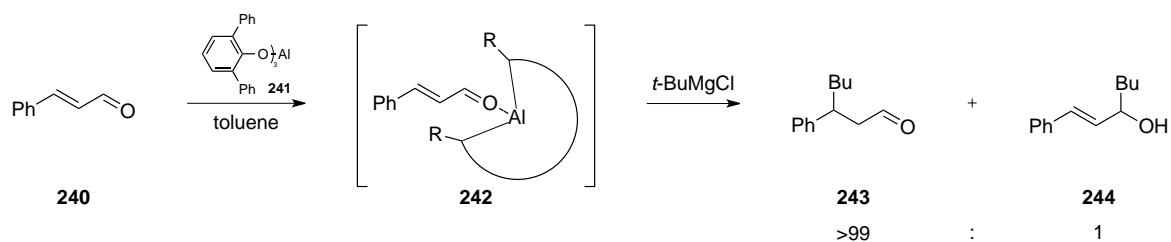
**Scheme 9.1.** Retrosynthetic analysis of tetrapetalone A (**130**).

In putting our plan into practice, commercially available 3-aminophenol (**233**) was alkylated with  $\alpha$ -bromo ketone **236** to give aniline **237**. Exposure to acetic acid in toluene provided the corresponding lactam, which was subsequently protected to give **234**. Ketone **234** could be successfully deprotonated; however, subjecting the derived enolate to aldehyde **238** gave a complex mixture of products including the presence of a 1,2-addition product and the desired 1,4-addition product in small amounts (Scheme 9.2).

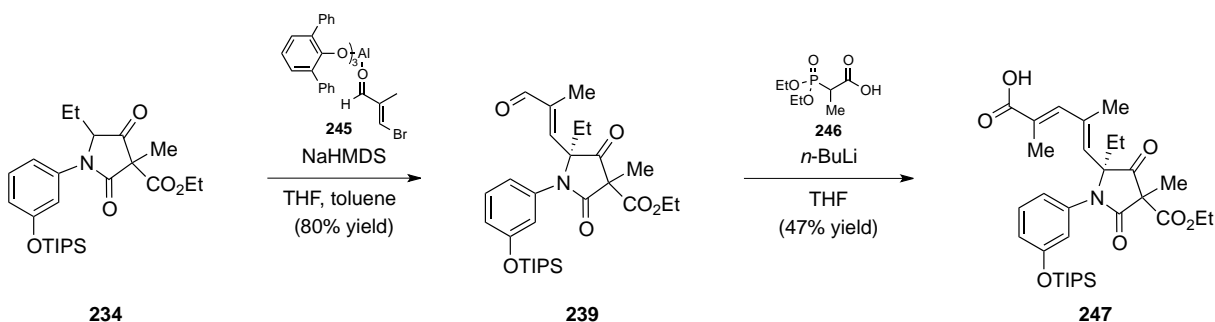


**Scheme 9.2.** Attempted synthesis of 1,4–adduct **239**.

Given the presence of a 1,2–addition product in our previous attempt, we sought a method to eliminate this possibility and favor the desired 1,4–adduct **239**. Upon searching the literature we became inspired by a report from Yamamoto and coworkers that detailed the use of a bulky Lewis acid (**241**) to help favor 1,4– and 1,6–addition to aldehydes such as **240** over the corresponding 1,2–addition product (Scheme 9.3).<sup>12</sup> They found that by initially forming the bulky Lewis acid–aldehyde complex **242**, then adding a nucleophile such as *t*–butyl magnesium chloride, they could obtain a >99:1 ratio of the desired 1,4–product **243** over 1,2–product **244**. Delightfully, applying this bulky Lewis acid led, presumably, to the preformed aldehyde complex (**245**) which, upon addition of the enolate derived from ketone **234** furnished exclusively the 1,4–addition product **239** in good yield. This could be further elaborated to acid **247** through a Horner–Wadsworth–Emmons reaction with phosphonate **246** (Scheme 9.4).



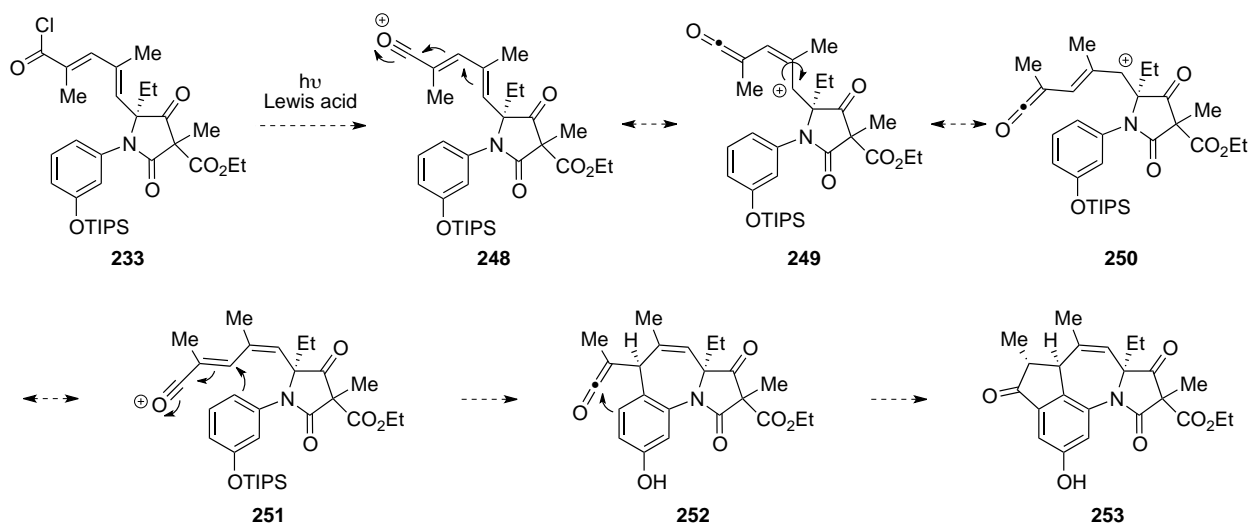
**Scheme 9.3.** Yamamoto's bulky Lewis acid.



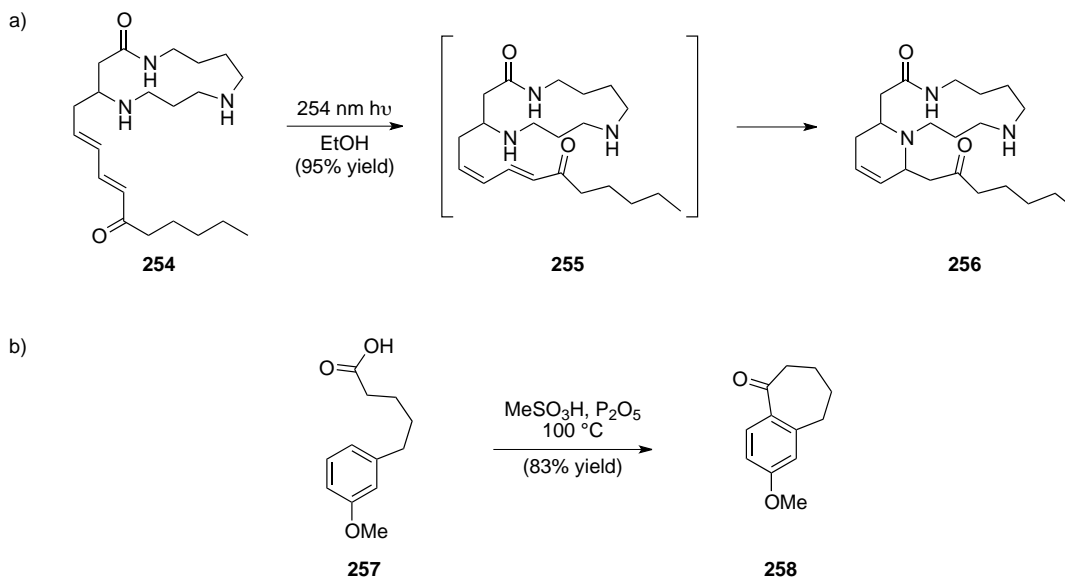
**Scheme 9.4.** Synthesis of acid **247**.

With acid **247** in hand we were next ready to investigate the key cascade Friedel–Crafts reaction. This reaction is imagined to proceed via the pathway outlined in Scheme 9.5. Exposing acid chloride **233** to a Lewis acid would activate the leaving group, forming acylium ion **248**. Exposure to light would promote a sequence wherein the undesired *E*-olefin could isomerize to the requisite *Z*-olefin (i.e. **248** to **251**). Oxonium **251** could be quenched via a Friedel–Crafts 1,4-addition from the electron rich aromatic ring forming ketene **252** and the seven-membered ring of tetrapetalone A. Nucleophilic attack from the aromatic ring towards the electrophilic ketene would eventually lead to tetracycle **253**. Although we recognized this was an ambitious sequence to propose, we were inspired by work from Wasserman and coworkers that showed in enone **254** they could effect an olefin isomerization in the presence of light before effecting a conjugate addition to form β-amino ketone **256** (Scheme 9.6.a).<sup>13</sup> Furthermore we had confidence in forming the seven-membered ring through a Friedel–Crafts type reaction based

on a number of reports including the formation of ketone **258** from carboxylic acid **257** (Scheme 9.6.b).<sup>14</sup>

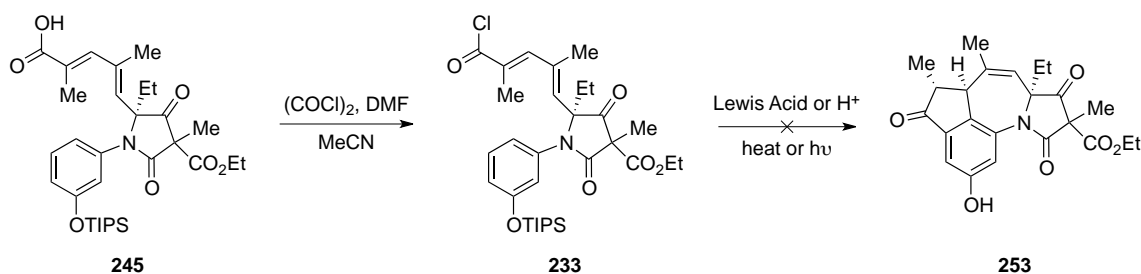


**Scheme 9.5.** Proposed cascade Friedel–Crafts to form tetracycle **253** from acid chloride **233**.

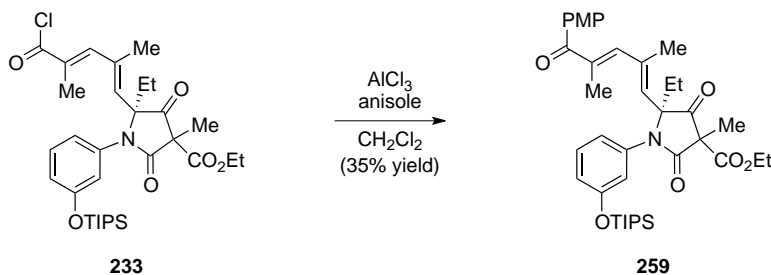


**Scheme 9.6.** Literature precedent showing a) an olefin isomerization before conjugate addition and b) a Friedel–Crafts type acylation forming a seven–membered ring.

In accordance with the above strategy carboxylic acid **245** was converted to acid chloride **233** and subjected to various conditions to perform the desired cascade Friedel–Crafts reaction (Scheme 9.7). Unfortunately, under none of the screened conditions was the desired product **253** obtained. To test the reactivity of acid chloride **233** in a Friedel–Crafts reaction, it was reacted with anisole and ketone **259** was obtained (Scheme 9.8). Thus it appeared the isomerization of the double bond was not occurring and a new strategy was devised.



**Scheme 9.7.** Attempts at cascade Friedel–Crafts pathway.

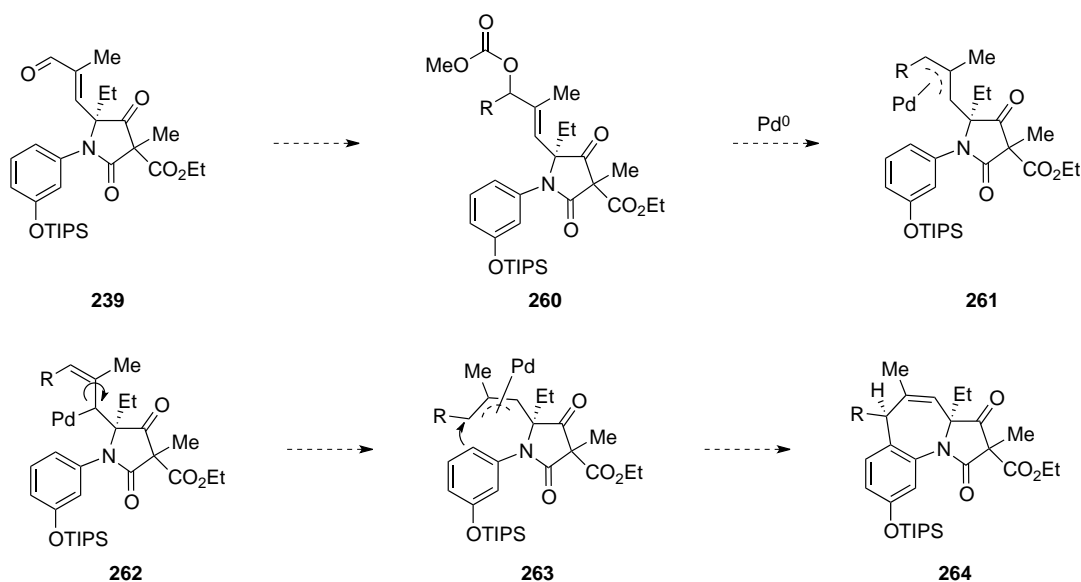


**Scheme 9.8.** Successful Friedel–Crafts with anisole.

## 9.2 Intramolecular $\pi$ -Allyl Approach

Given the difficulties that occurred in the isomerization event in the cascade Friedel–Crafts strategy, we became interested in other bond forming strategies that could both facilitate the double bond isomerization, and provide a sufficient electrophile to interact with the aromatic

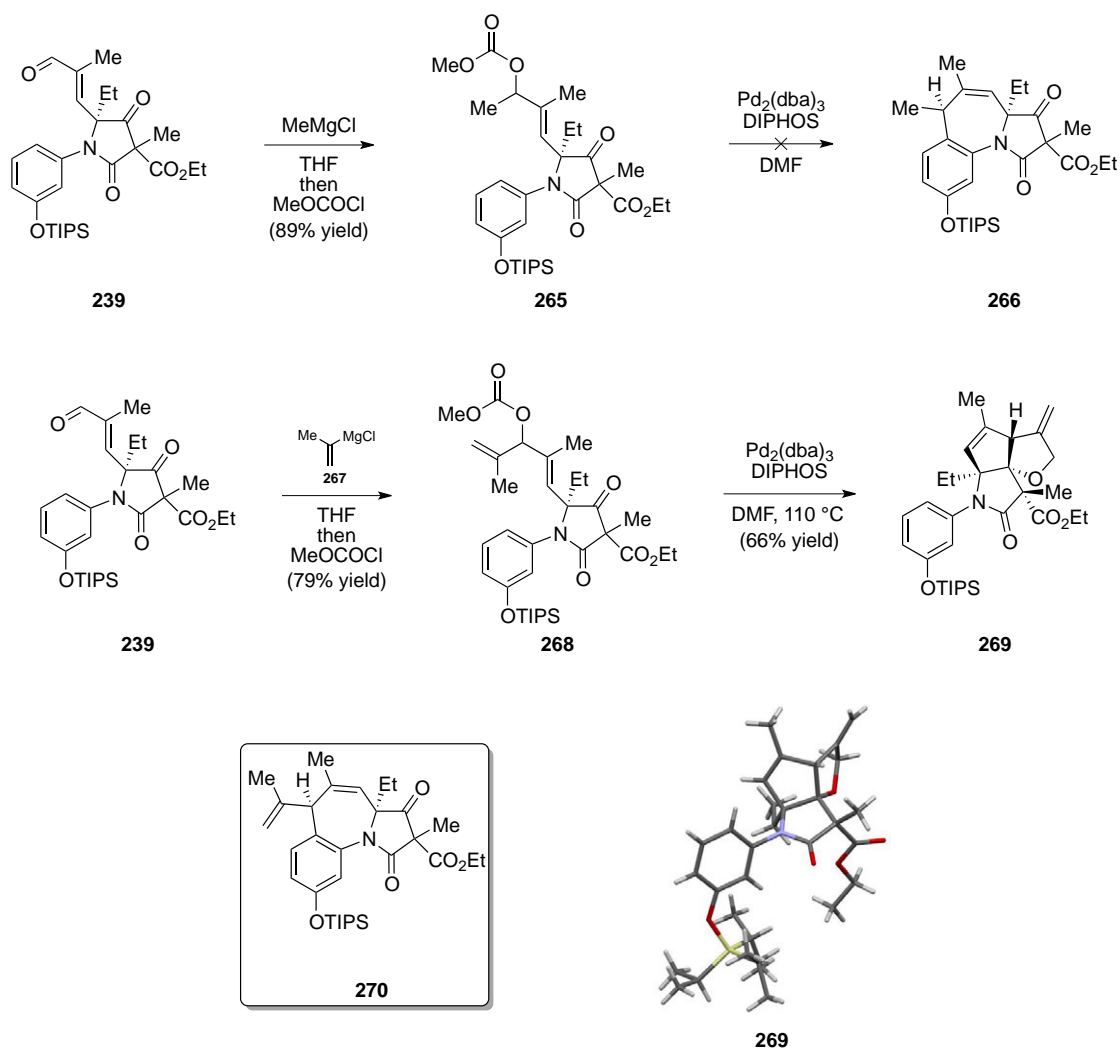
ring. We believed that a palladium  $\pi$ -allyl species offered a nice solution due to the fact that palladium  $\pi$ -allyls can exist in both  $\eta^1$  and  $\eta^3$  binding modes, and the presence of an  $\eta^1$ - $\pi$ -allyl would allow for bond rotation and olefin isomerization (Scheme 9.9). In that regard previously synthesized aldehyde **239** would be converted to allylic carbonate **260** by Grignard addition and trapping the resultant alkoxide with methyl chloroformate. Exposing allylic carbonate **260** to palladium(0) would form palladium  $\pi$ -allyl **261**, which could undergo an olefin isomerization event through an  $\eta^1$ - $\pi$ -allyl intermediate **262** to form  $\pi$ -allyl **263**. Attack from the aromatic ring would construct the requisite seven-membered ring giving intermediate **264**.



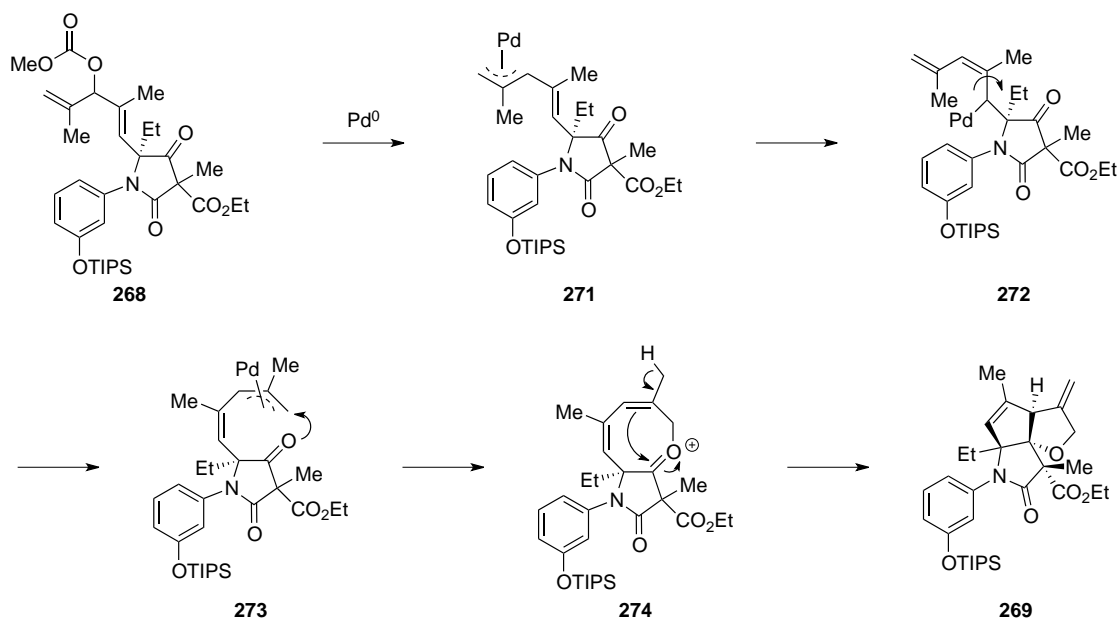
**Scheme 9.9.** Proposed  $\pi$ -allyl pathway to form the seven-membered ring (**264**).

To test the viability of the palladium  $\pi$ -allyl reaction, aldehyde **239** was reacted with methyl Grignard followed by methyl chloroformate to give allylic carbonate **265**. Subjecting **265** to palladium(0) resulted only in starting material and none of desired product **266**. In order to help promote this reaction, specifically to help with the oxidative addition, bisallyl carbonate **268** was synthesized in a similar fashion to **265**. Subjecting **268** to palladium(0) at 110 °C resulted in none of the desired product **270**, instead giving fused tricycle **269** (Scheme 9.10). A crystal

structure of **269** was obtained to verify its structure. A potential mechanism for the formation of this interesting compound is depicted in Scheme 9.11. Initial oxidative addition of allylic carbonate **268** forms  $\eta^3$ - $\pi$ -allyl **271**. Migration to  $\eta^1$ - $\pi$ -allyl **272** allows for bond rotation and subsequent formation of  $\eta^3$ - $\pi$ -allyl **273**. It is important to note that the olefin isomerization observed in this product is precisely what we desired in our planned reaction, and  $\eta^3$ - $\pi$ -allyl **273** is the intermediate we hoped to access. However at this point the reaction deviates from our plan. Instead of the aromatic ring acting as a nucleophile, we are observing nucleophilic attack from the ketone towards the  $\pi$ -allyl forming oxocarbenium **274**. A transannular Prins-type reaction then leads to observed fused tricycle **269**, the product of a formal [3+2] cycloaddition.

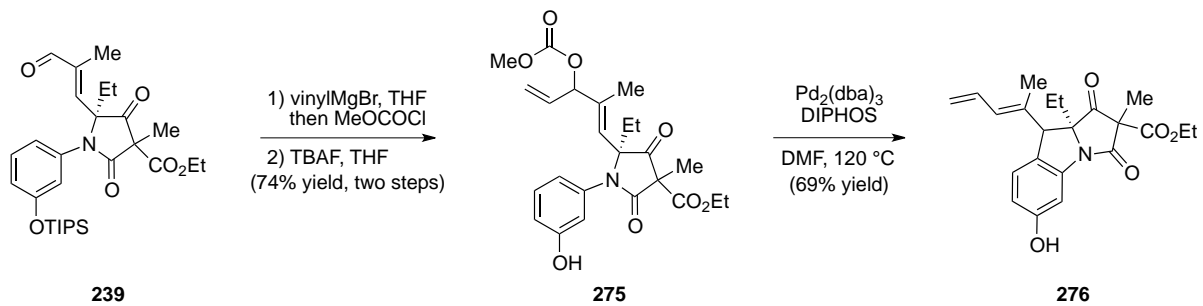


**Scheme 9.10.** Attempted palladium  $\pi$ -allyl reactions.



**Scheme 9.11.** Proposed mechanism for the formation of fused tricycle **269**.

In considering the mechanism leading to the production of **269** we became curious as to what effect removing the terminal methyl group would have on the course of the reaction. Elimination of a proton from this methyl group furnishes the exomethylene and was seen as potentially facilitating the observed Prins-type reaction. We hypothesized that removal of this methyl group entirely could potentially eliminate this undesired pathway thereby leading to reformation of palladium  $\pi$ -allyl species **273** and potentially the desired product. Gratifyingly, by utilizing the compound lacking the methyl group (**275**) none of this undesired formal [3+2] product was obtained. It also however, did not give the desired seven-membered product, instead giving undesired five-membered product **276** (Scheme 9.12). Although this mode of cyclization was a concern, we were uncertain to what extent ring strain and sterics would govern the 5- vs. 7-membered ring formation. Clearly this experiment establishes the regiochemical preference; however, more importantly it demonstrated that a  $\pi$ -allyl species could be formed and trapped with the aromatic nucleophile in our system. Thus we sought a way to bias the system into selectively forming the desired seven-membered ring.



**Scheme 9.12.** Synthesis of tricycle **276**.

## Chapter Ten

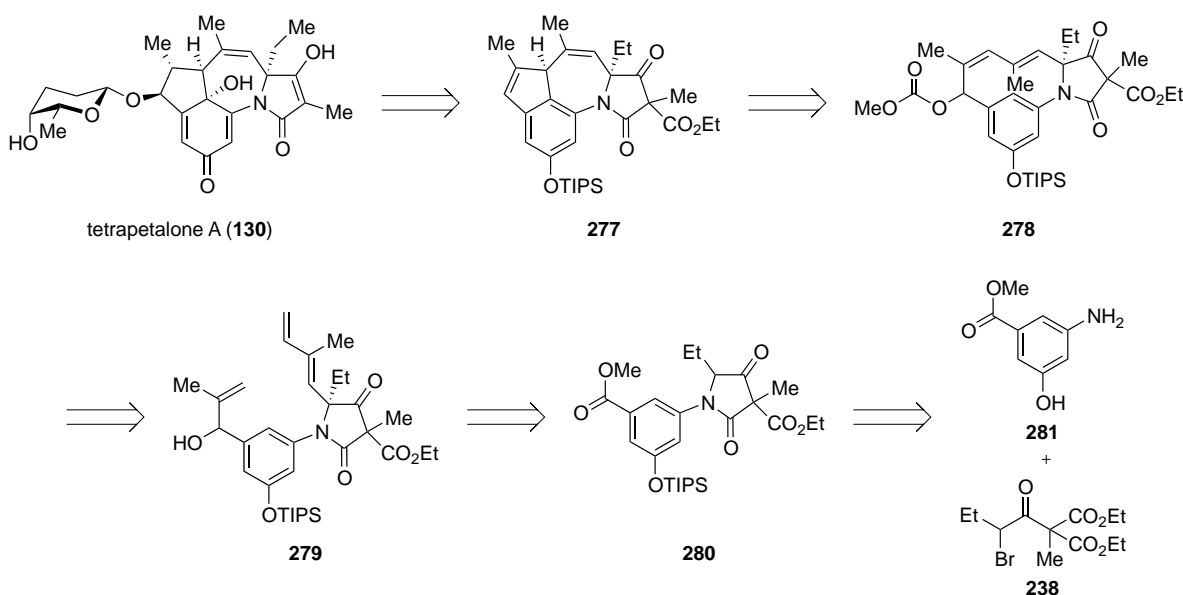
### A Transannular $\pi$ -Allyl Approach

Although in the previous approach we were unable to form our desired product, we established that a palladium  $\pi$ -allyl species could be formed and would undergo *E*-to-*Z* isomerization to furnish a  $\pi$ -allyl intermediate capable of undergoing nucleophilic attack by the pendant aromatic ring. Encouraged by these results we initiated an effort to adjust the regiochemical outcome so as to favor the formation of the desired seven-membered ring.

#### 10.1 A Transannular $\pi$ -Allyl Approach

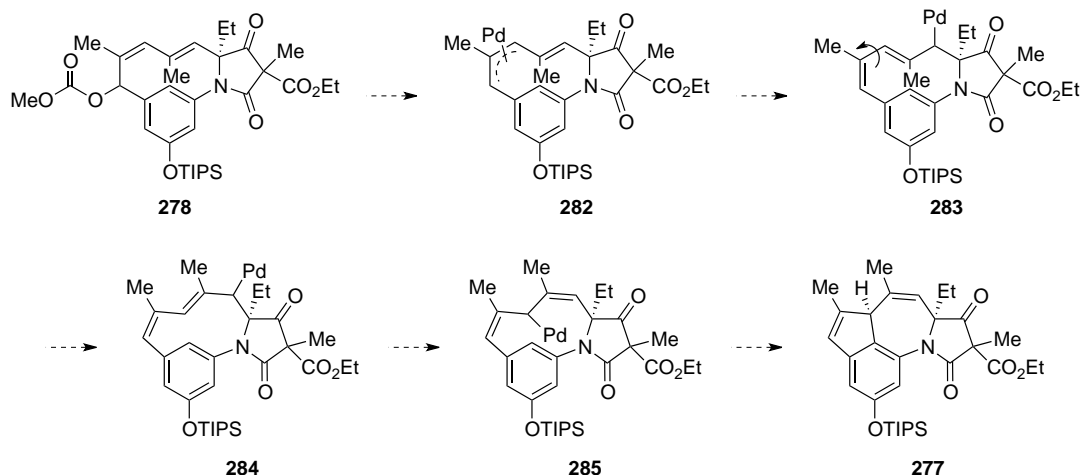
In order to control the regiochemistry, we envisioned starting with a ten-membered ring and forming the desired 5,7-ring system through a transannular attack from the aromatic ring onto a palladium  $\pi$ -allyl species. In accordance with this strategy tetrapetalone A (**130**) would ultimately arise from hydroboration, glycosylation, phenolic oxidation, and decarboxylation of **277**. Tetracycle **277** would be the product of the key transannular palladium  $\pi$ -allyl reaction, which would utilize allylic carbonate **278** as a starting point. It is important to note that while in this route we are choosing to start with the allylic carbonate shown, this reaction could be initiated from a regioisomeric allylic carbonate, and thus gives us flexibility in our synthetic approach. Nevertheless, allylic carbonate **278** would arise from triene **279** through a ring-closing metathesis. Although previous routes toward **130** employing a ring-closing metathesis have failed, we believed this particular substrate had advantages relative to the other approaches. The monosubstituted olefin is more remote to the fully substituted carbon rather than being neopentyl as in other approaches in our group (cf. Chapter 8). In comparison to Porco's failed ring-closing metathesis, wherein the substrate contained a *meta*-substituted

aromatic ring, there is only a proton in the *ortho* position compared to the bulkier methoxy group in their case (cf. **146** to **149**, Scheme 7.2). Triene **279** would come from ketone **280** after a 1,4-addition/ elimination followed by Wittig sequence and a Grignard addition into the methyl ester, and ketone **280** would be formed from aniline **281** and alkyl bromide **238** (Scheme 10.1).



**Scheme 10.1.** Retrosynthetic analysis of **130** utilizing a transannular  $\pi$ -allyl reaction.

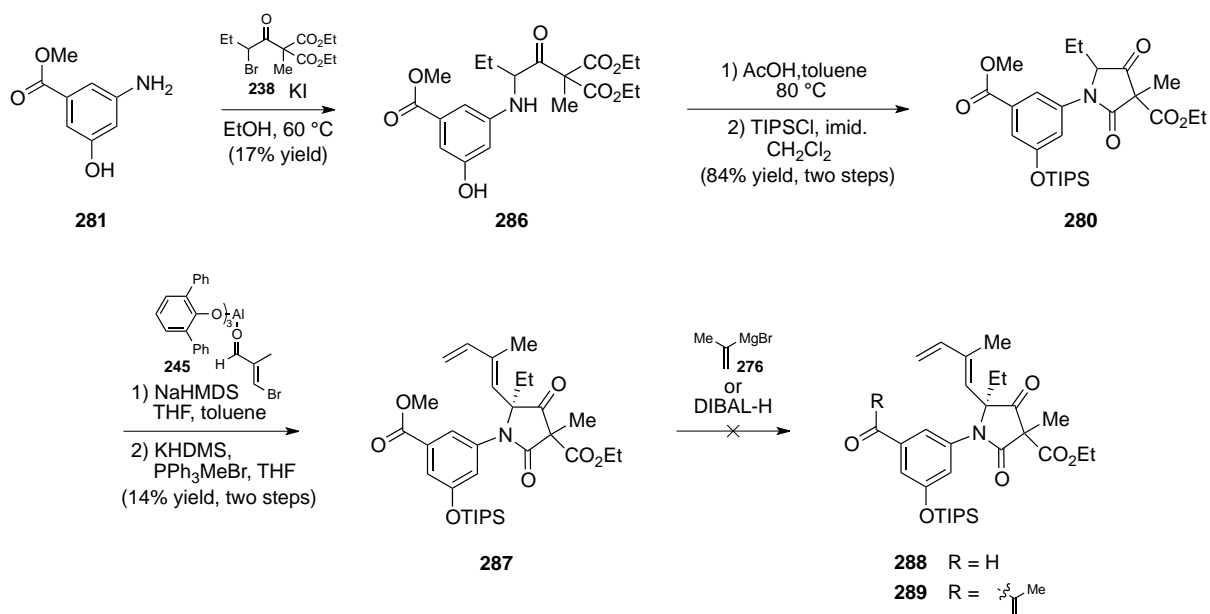
A more detailed mechanistic pathway for the proposed transannular palladium  $\pi$ -allyl reaction is outlined in Scheme 10.2. As illustrated, it was envisioned that initial oxidative addition to allylic carbonate **278** would provide  $\eta^3$ - $\pi$ -allyl **282**. By inspecting molecular models, it does not appear this palladium  $\pi$ -allyl species is accessible by the aromatic ring with the neighboring olefin in the *E* orientation. However, migration to  $\eta^1$ - $\pi$ -allyl **283** would allow for bond rotation and migration to give  $\eta^1$ - $\pi$ -allyl **285**, which now contains the requisite *Z*-double bond and appears to be conformationally accessible to undergo nucleophilic attack from the aromatic ring to lead to tetracycle **277**.



**Scheme 10.2.** Proposed transannular palladium  $\pi$ -allyl reaction.

To explore the plan outlined above, we initially set out to prepare triene **279**. Ester **281**<sup>15</sup> was chosen as a departure point due to the fact it was a known compound and we believed the presence of the methyl ester would be a good precursor to the allylic alcohol we eventually wanted to synthesize (i.e **279**, Scheme 10.1). With that in mind, ester **281** was alkylated with alkyl bromide **238** under the same conditions as used previously (see: **236** to **237** Scheme 9.2). Unfortunately, the presence of the electron withdrawing ester lessened the reactivity of the aniline and **286** was only formed in 17% yield. Efforts to increase this yield by changing the iodide source, adding base, or adding silver did not lead to improvement, only to similar yields in the best case or more decomposition in the worst. Although the yield was low we decided to move forward and explore the subsequent chemistry. Aniline **286** could be converted cleanly to tetramic acid **280** after ring-closure and TIPS protection. The requisite diene was installed with the 1,4-addition/ elimination sequence utilizing the bulky Lewis acid developed by Yamamoto and coworkers, and the resultant aldehyde olefinated under Wittig conditions. At this point the ester needed to be converted to the allylic carbonate, however this ester once again proved problematic, proving unreactive to either Grignard addition or reduction and in the best case

only giving trace product (Scheme 10.3). Given the deleterious influences of the methyl ester, we began to consider alternative routes wherein the ester has been removed.

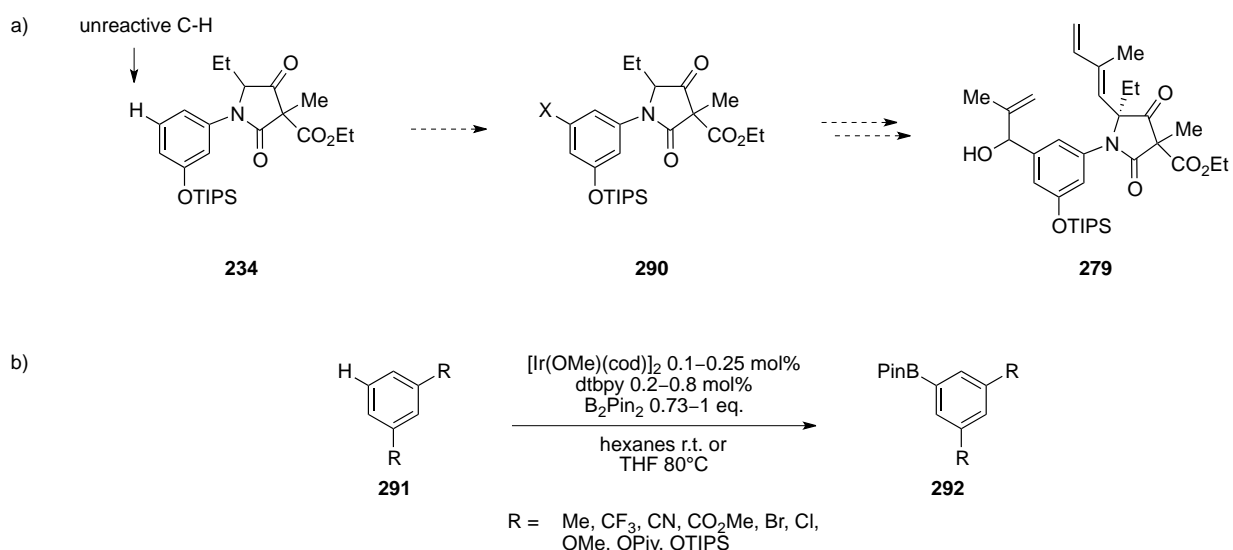


**Scheme 10.3.** Synthesis of unreactive ester **287**.

## 10.2 Implementation of Hartwig's Borylation Conditions

Given the difficulties with the ester we decided to return to the original method of building the tetramic acid by employing 3-aminophenol (**235**) as the aromatic precursor (cf. **235** to **234**, Scheme 9.2). Although removing the ester is advantageous for the production of **234**, it creates a new problem in that we have an unreactive C–H bond in **234** where we eventually need an allylic alcohol (Scheme 10.4.a). Therefore we sought a method to selectively functionalize this position to form an intermediate (**290**), which contains functionality that could eventually be transformed into allylic alcohol **279**. Due to the presence of the electron donating methoxy group, we believed classical electrophilic aromatic substitution would not be compatible with the substitution pattern we required. Instead we became inspired by the work of Hartwig and

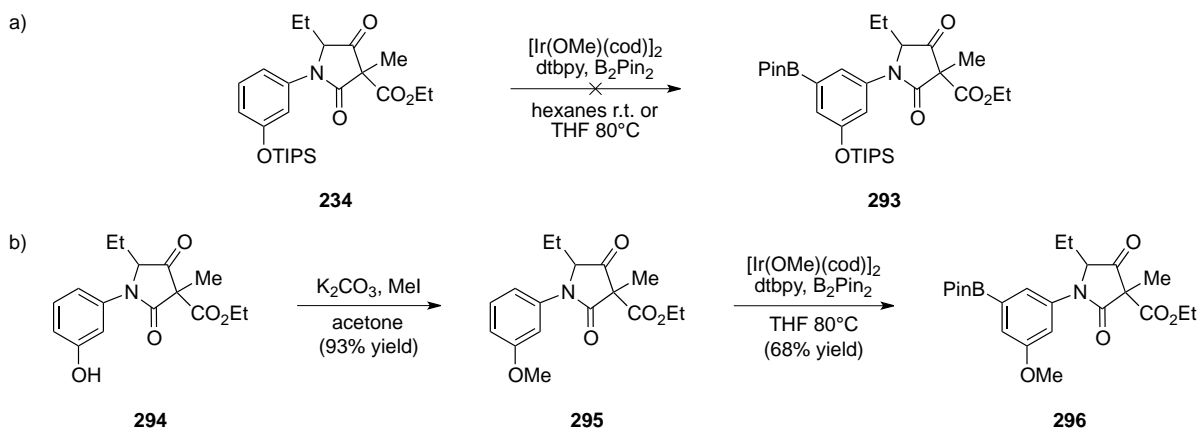
coworkers, who described that by employing a catalyst system based on  $[\text{Ir}(\text{OMe})(\text{cod})]_2$  and dtbpy as a ligand in the presence of  $\text{B}_2\text{Pin}_2$ , they could functionalize aromatic C–H bonds and obtain aryl boronic esters such as **292** as products (Scheme 10.4.b).<sup>16</sup> Furthermore they found that when the starting arene contained two substituents in a 1,3-orientation (i.e. **291**) they could exclusively obtain the 1,3,5-substituted product **292**. They propose that steric effects predominate in determining the observed regioselectivity in this reaction, and in fact they could utilize compounds bearing both electron donating and withdrawing groups successfully.



**Scheme 10.4.** Hartwig's iridium-catalyzed borylation.

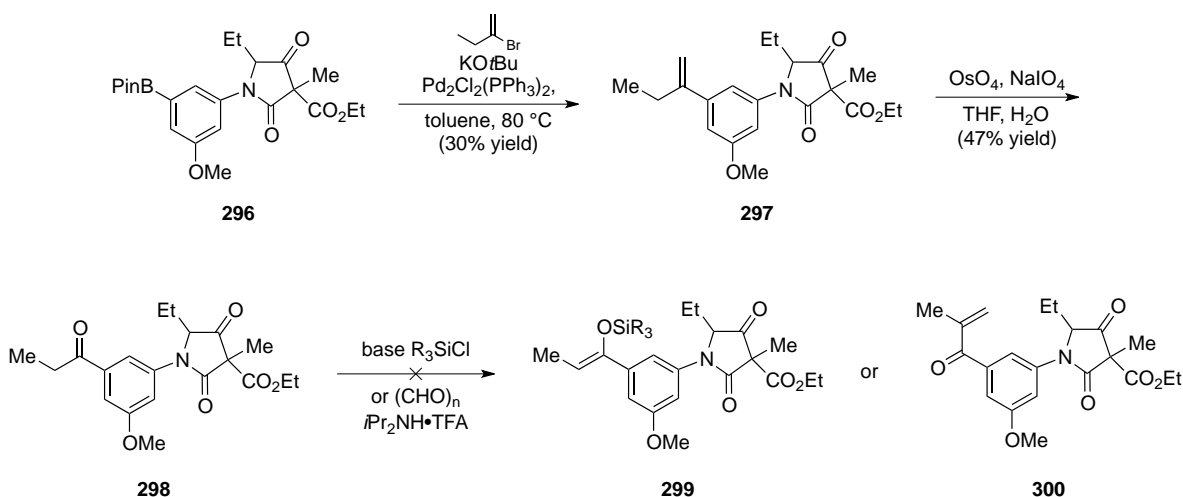
Excited by the possibilities this transformation could provide, TIPS-protected phenol **234** was subjected to the standard borylation conditions developed by Hartwig and coworkers. Unfortunately only starting material was obtained (Scheme 10.5.a). Although the Hartwig group was successful using one bulky group such as –OTIPS, they did not report any substrates possessing two bulky groups such as the –OTIPS and tetramic acid moieties in our substrate (**234**). In an effort to minimize the steric demand in our substrate, we opted to switch our TIPS protecting group to the sterically less demanding methyl, and therefore **295** was prepared in one

step from phenol **294**. Gratifyingly, subjecting methyl-protected phenol **295** to the borylation conditions delivered aryl boronic ester **296** in good yield (Scheme 10.5.b).



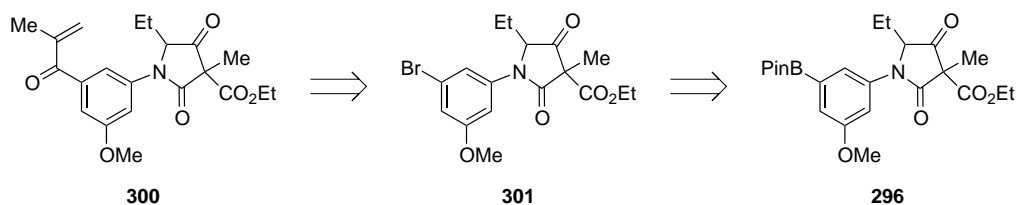
**Scheme 10.5.** a) Unsuccessful borylation of **234** and b) successful borylation of **295**.

With aryl boronic ester **296** in hand, we next explored methods to further elaborate this compound (Scheme 10.6). Our initial thoughts were to utilize boronic ester **296** directly in a Suzuki coupling. In accordance with this, aryl boronic ester **296** was coupled with 2-butenyl bromide to give styrene **297**. Exposure to a one-pot dihydroxylation/ oxidative cleavage furnished aryl ketone **298**. We hoped that we could selectively functionalize the kinetically more accessible aryl ketone by converting it to silyl enol ether **299** or enone **300**. However, this was met with no success.



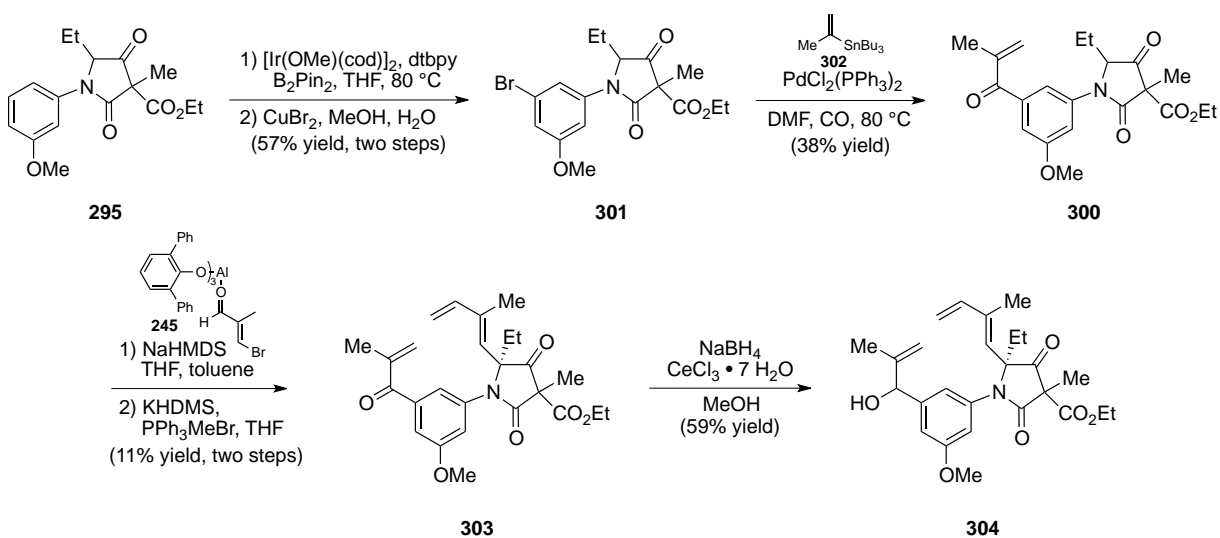
**Scheme 10.6.** Synthesis of bisketone **298**.

While we were exploring the reactivity of aryl ketone **298**, we also were investigating other routes to enone **300**. Given the two-step procedure we were utilizing for the production of **298** plus at least one more step for the installation of the exomethylene, we believed a more direct route could be realized. Specifically we imagined enone **300** could be formed directly from aryl bromide **301** through a carbonylative Stille reaction (Scheme 10.7).<sup>17</sup> Although we would have to access aryl bromide **301** from aryl boronic ester **296**, Hartwig and coworkers have shown that their iridium-catalyzed borylation products can be converted to aryl bromides by simply removing the solvent from the first step and, in the same pot, exposing the mixture to copper (II) bromide.<sup>18</sup>



**Scheme 10.7.** Revised retrosynthetic analysis of enone **300**.

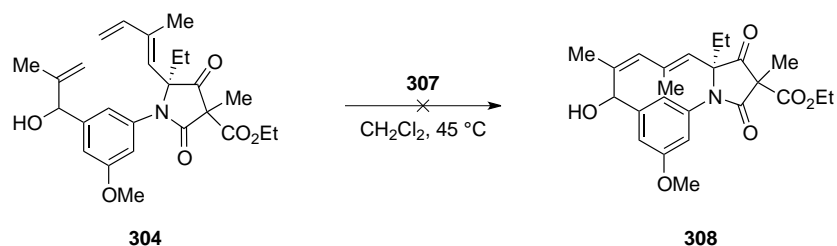
Thus protected phenol **295** could be subjected to the previously employed borylation conditions, and after simple removal of solvent, could be subjected to copper (II) bromide to form aryl bromide **301** in good yield and only one purification step. Aryl bromide **301** proved to be a valuable synthetic intermediate, as it was a competent cross-coupling partner. In the presence of vinyl stannane **302** and carbon monoxide carbonylative Stille product **300** was produced from **301** albeit in low and variable yields. Nevertheless, ketone **300** could participate in the 1,4-addition/ elimination followed by Wittig sequence to furnish triene **303**. Reduction of the enone under Luche conditions provided allylic alcohol **304**. With this synthetic route we were able to access two possible ring-closing metathesis precursors, **303** and **304**.



**Scheme 10.8.** Successful synthesis of ring-closing metathesis precursors **303** and **304**.

With trienes **303** and **304** in hand, we next explored the ring-closing metathesis.<sup>19</sup> We recognized this was going to be a difficult ring-closing metathesis from the outset. We are attempting to form a ten-membered ring, and while medium sized rings such as this are both enthalpically and entropically unfavored, others have had success forming these ring systems via ring-closing metathesis.<sup>20</sup> Although ten-membered rings have been formed via ring-closing metathesis, as far as we can tell there are no examples where a *meta*-substituted aromatic ring

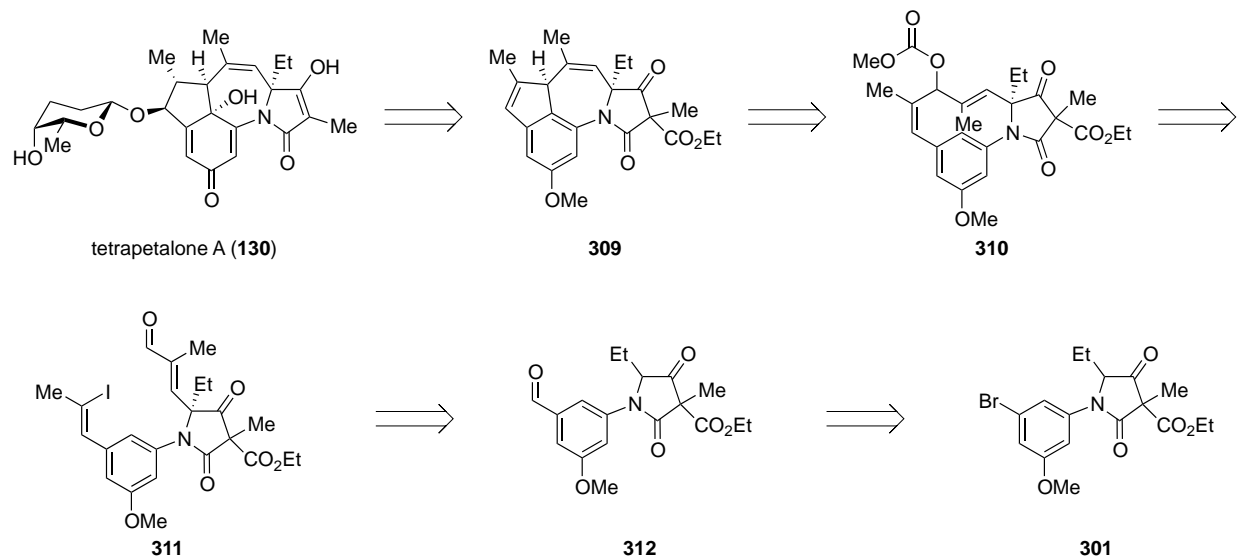




**Scheme 10.10.** Attempted ring-closing metathesis of allylic alcohol **304**.

### 10.3 A Nozaki–Hiyama–Kishi Approach to the Desired Ten–Membered Ring

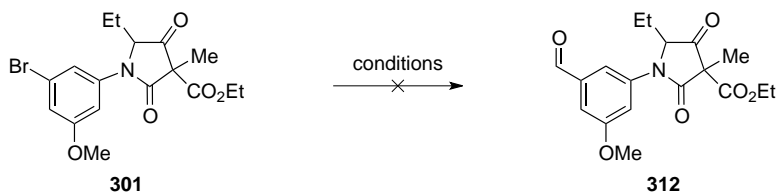
After unsuccessfully attempting to form the desired ten-membered ring needed for the transannular palladium  $\pi$ -allyl reaction through a ring-closing metathesis strategy, we opted to explore other routes. Specifically we believed that tetrapetalone A (**130**) could still arise from tetracycle **309**, which would be the product of the same type of transannular palladium  $\pi$ -allyl reaction as outlined in Scheme 10.2. The precursor in this instance, **310**, would be regioisomeric to the allylic carbonate previously targeted (cf. **278** Scheme 10.2). By transposing the allylic carbonate, **310** could be generated from a Nozaki–Hiyama–Kishi (NHK) reaction of vinyl iodide **311**, which would be the product of a modified Wittig–olefination and the 1,4–addition/ elimination sequence applied to aldehyde **312**. Aldehyde **312** would arise from formylation of bromide **301**.<sup>25</sup>



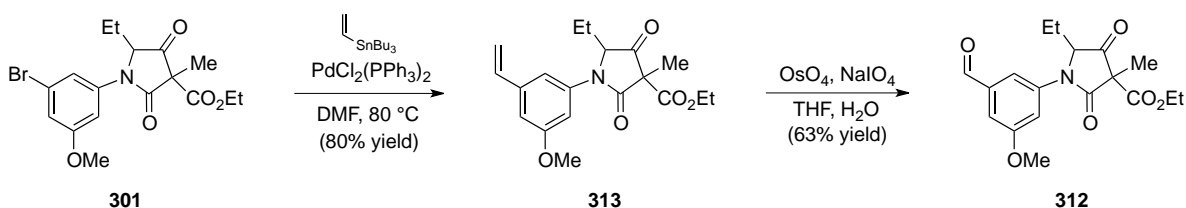
**Scheme 10.11.** Revised retrosynthetic analysis of tetrapetalone A (**130**).

To access benzaldehyde **312**, direct formylation of aryl bromide **301** was explored (Table 10.1). Subjecting **301** to palladium-catalyzed formylation conditions in the presence of carbon monoxide and a reductant unfortunately gave no product (entries 1 – 3). Lithium-halogen exchange followed by quenching with DMF only led to decomposition (entry 4). Although the direct formylation warrants further exploration, concurrent to these investigations the two-step procedure described in Scheme 10.12 was successfully implemented. In that sequence aryl bromide **301** was first converted to styrene **313** through a Stille coupling and benzaldehyde **312** was formed after a one-pot dihydroxylation/oxidative cleavage. Although a direct formylation would be a more efficient route, this two step process provided enough material to explore further reactions.

**Table 10.1.** Attempted formylations of aryl bromide **301**.

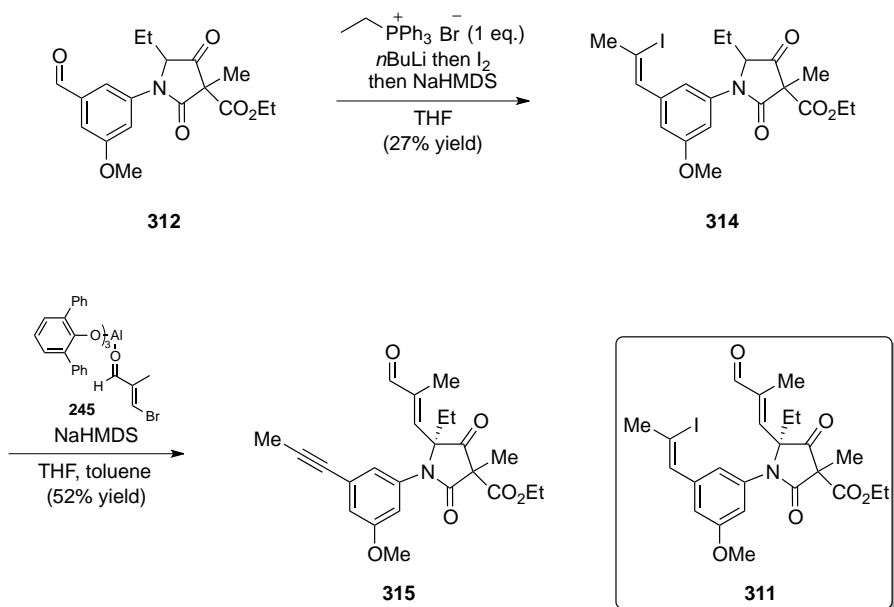


entry	conditions
1	$\text{PdCl}_2(\text{PPh}_3)_2$ , $\text{Na}_2\text{CO}_3$ , $\text{Et}_3\text{SiH}$ , DMF, CO, 90 °C
2	$\text{PdCl}_2(\text{PPh}_3)_2$ , $\text{NaCO}_2\text{H}$ , DMF, CO, 80 °C
3	$\text{PdCl}_2(\text{PPh}_3)_2$ , $\text{Bu}_3\text{SnH}$ , DMF, CO, 80 °C
4	$n\text{BuLi}$ , THF - 78 °C then DMF



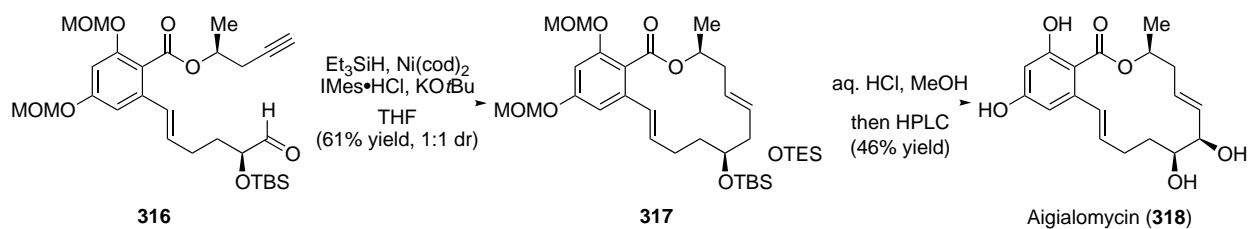
**Scheme 10.12.** Synthesis of aldehyde **312**.

With benzaldehyde **312** in hand we looked to elaborate this compound to the desired NHK precursor **311**. Thus **312** was subjected to modified Wittig conditions to install the desired vinyl iodide giving **314**, albeit in low yield.<sup>26</sup> While attempting to install the  $\alpha,\beta$ -unsaturated aldehyde applying our standard 1,4-addition/ elimination sequence, we observed none of the desired product **311**. We instead isolated a product (**315**) where the desired  $\alpha,\beta$ -unsaturated aldehyde was incorporated, however, the vinyl iodide also eliminated to form an alkyne. Unfortunately we were unable to attempt the Nozaki-Hiyama-Kishi reaction due to inability to form the proper precursor.



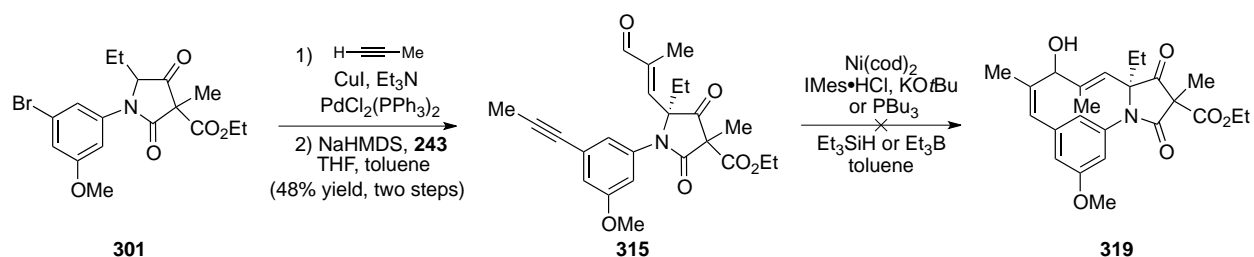
**Scheme 10.13.** Attempted synthesis of NHK precursor **311**.

Although we were unable to try the NHK reaction, we were intrigued by this alkyne byproduct. Specifically we became interested in utilizing this intermediate in a nickel-catalyzed reductive alkyne-aldehyde coupling.<sup>27</sup> We were intrigued by this reaction due to its use both to form medium to large ring systems, and in complex natural products synthesis. Montgomery and coworkers utilized this reaction in the late stages of their aigialoymycin (**318**) synthesis, forming protected allylic alcohol **317** from ynal **316** (Scheme 10.14).<sup>28</sup>



**Scheme 10.14.** Montgomery's synthesis of Aigialoymycin utilizing a reductive alkyne-aldehyde coupling.

Before we explored this chemistry we sought a more direct route to ynal **315**. To accomplish this, aryl bromide **301** was subjected to a Sonogashira coupling to install the alkyne and the  $\alpha,\beta$ -unsaturated aldehyde was installed in the usual fashion to give **315**. Unfortunately, subjecting this ynal to standard nickel catalyzed conditions provided none of the desired product, only giving recovered starting material (Scheme 10.15). This result is most likely due to the aldehyde and the alkyne not being able to adopt a conformation wherein the two reactive species are in close enough proximity to react.



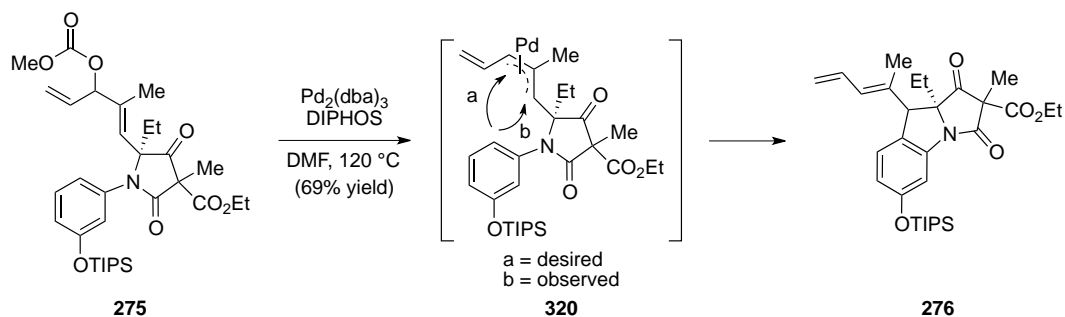
**Scheme 10.15.** Attempted nickel-catalyzed alkyne-aldehyde coupling.

At this point we had attempted multiple routes towards a transannular palladium  $\pi$ -allyl precursor and although we believed this is still an interesting and potentially useful synthetic transformation, we decided to explore other synthetic strategies towards tetrapetalone A due to the difficulties in accessing the desired *meta*-substituted ten-membered ring.

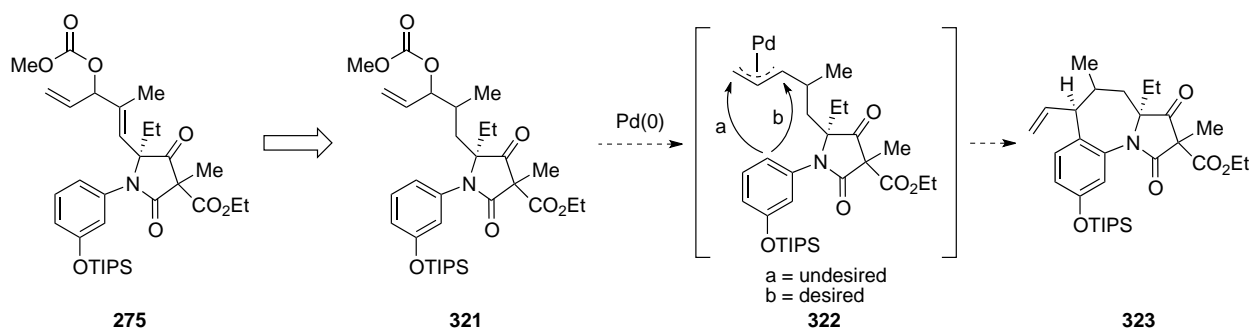
## Chapter Eleven

### Revisiting the Previous $\pi$ -Allyl Strategy

After unsuccessfully attempting a transannular palladium  $\pi$ -allyl approach to form the tetracyclic core of tetrapetalone A (**130**), we decided to take a step back and devise a new strategy. While we were still interested in forming the seven-membered ring of **130** through attack of the aromatic ring onto a palladium  $\pi$ -allyl species, we needed a way to bias the attack towards formation of the seven-membered ring. Recall that when allylic carbonate **275** was utilized in this reaction, none of the desired product was obtained, instead producing the undesired five-membered ring **276** (Scheme 11.1). This was due to initial formation of palladium  $\pi$ -allyl **320**, which we had hoped to access due to the need to isomerize that double bond. In intermediate **320**, there are two possible ways the aromatic ring could attack the palladium  $\pi$ -allyl species, either by forming the desired seven-membered ring (path a) or the undesired five-membered ring (path b). If we were to remove the double bond  $\alpha$  to the tetramic acid moiety, we now only have access to palladium  $\pi$ -allyl **322**, which cannot access a five-membered product, instead the attack can only occur to form an undesired nine-membered ring (path a) or the desired seven-membered ring (path b), which we believed would be more favorable (Scheme 11.2).



**Scheme 11.1.** Our previous  $\pi$ -allyl attempt that led to five-membered product **276**.

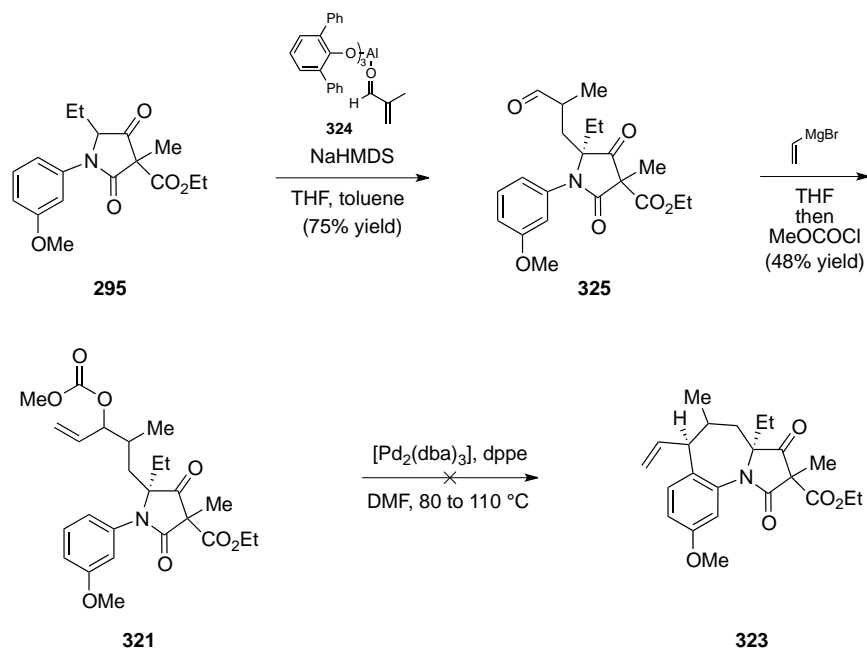


**Scheme 11.2.** Revised palladium  $\pi$ -allyl strategy.

### 11.1 Testing a New Palladium $\pi$ -Allyl Approach

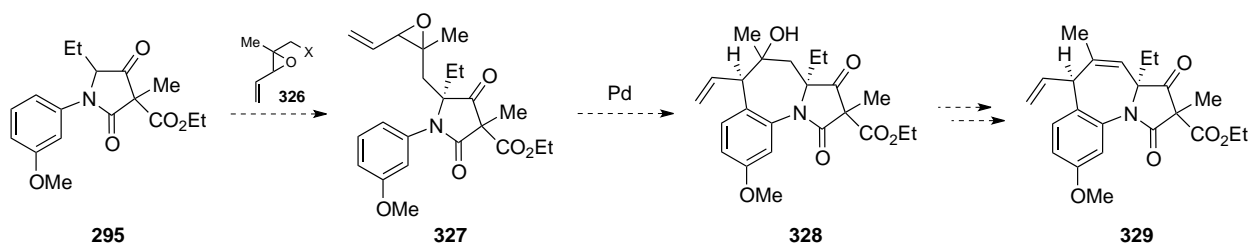
To test this new strategy, allylic carbonate **321** was synthesized in two steps. First ketone **295** was subjected to 1,4-addition conditions utilizing pre-coordinated methacrolein as the electrophile to furnish saturated aldehyde **325**. Then **325** was exposed to vinyl magnesium bromide followed by methyl chloroformate to provide allylic carbonate **321**. When heated to  $80\text{ }^\circ\text{C}$  in the presence of palladium(0) **321** only delivered recovered starting material. Raising the temperature did not help, and only led to decomposition of the starting material (Scheme 11.3). The unreactivity of **321** could be due to the removal of the double bond  $\alpha$  to the tetramic acid,

given that in our previous system (cf. **275** to **276**) a doubly allylic carbonate was required for the oxidative addition to proceed.



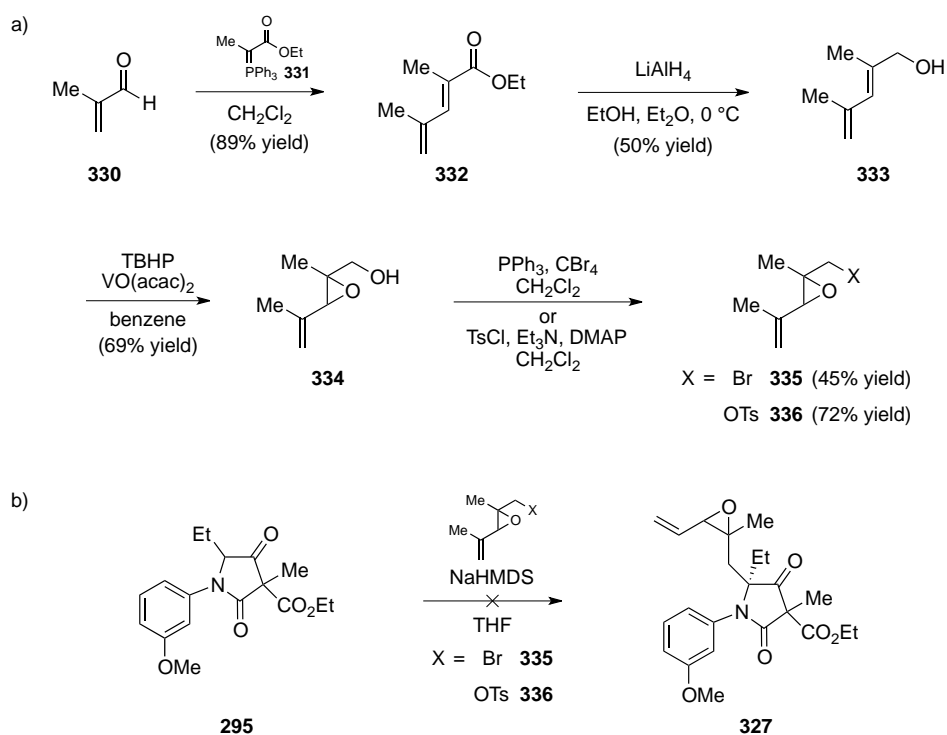
**Scheme 11.3.** Attempted palladium  $\pi$ -allyl reaction on substrate lacking double bond.

Concurrent to our investigations of allylic carbonate **321**, we also were interested in an allylic epoxide as the precursor for the palladium  $\pi$ -allyl reaction (Scheme 11.4). This was appealing due to the fact that the product (**328**) would contain an alcohol that could later be eliminated to form the double bond present in the natural product (i.e. **329**).



**Scheme 11.4.** Allylic epoxide palladium  $\pi$ -allyl approach.

To access the required epoxide **327**, acrolein was reacted with known ylide **331**<sup>29</sup> to form ester **332**, which was then reduced to give allylic alcohol **333**. The allylic double bond was selectively epoxidized in the presence of a vanadium catalyst to furnish **334**.<sup>30</sup> Alcohol **334** was then converted to bromide **335** and tosylate **336** under standard conditions (Scheme 11.5.a). We looked to incorporate this epoxide-containing piece into our system, however subjecting the enolate derived from ketone **295** with either **335** or **336** lead only to decomposition (Scheme 11.5.b).

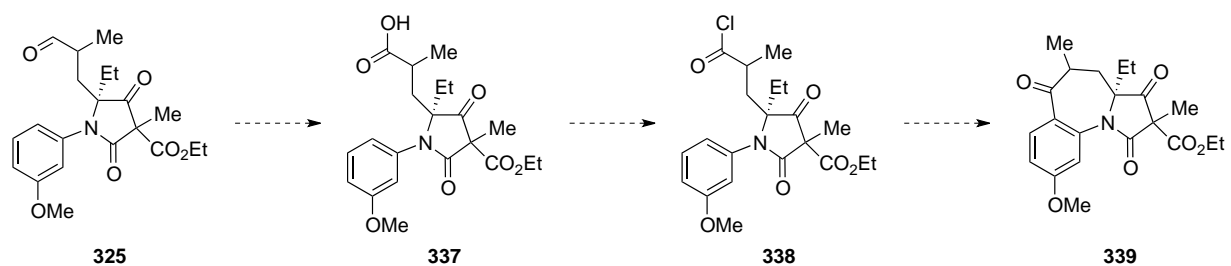


**Scheme 11.5.** a) Synthesis of epoxide **335** and **336** and b) attempts to form allylic epoxide **327**.

## 11.2 Revisiting the Friedel–Crafts Approach

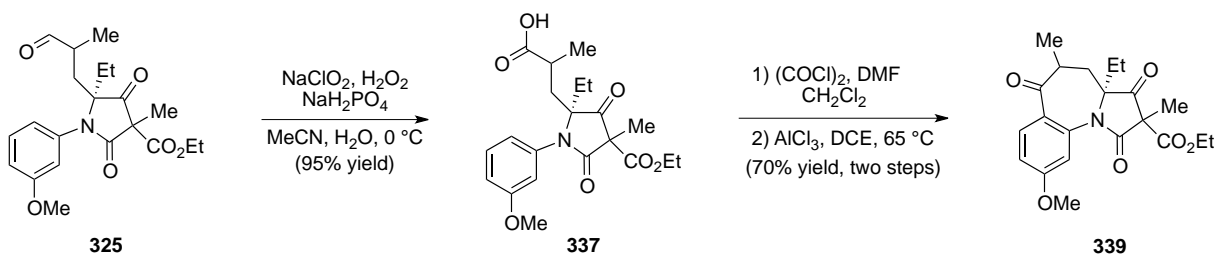
While we were encountering difficulties in the palladium  $\pi$ -allyl approach, we began to think about other methods to form the desired seven-membered ring. Given that we already

had aldehyde **325** in hand, we envisioned that ketone **339** could be accessed in quick fashion through a Friedel–Crafts acylation of acid chloride **338** (Scheme 11.6).<sup>14</sup> Since **338** lacked the olefin  $\alpha$  to the tetramic acid moiety, we believed this substrate was better suited for a Friedel–Crafts reaction compared to our previous approach (cf. Section 9.1).



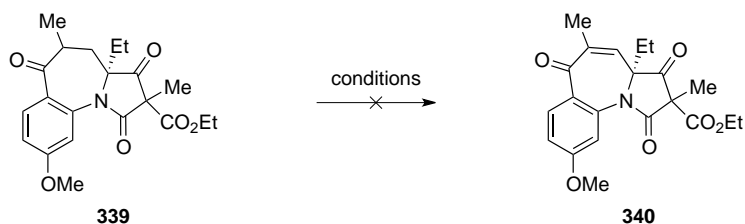
**Scheme 11.6.** Proposed Friedel–Crafts pathway to ketone **339**.

Carboxylic acid **337** was thus formed through a Pinnick oxidation of aldehyde **325**. We were delighted to find that by first converting **337** to the acid chloride and subjecting the crude material to aluminum trichloride in dichloroethane at 65 °C the desired seven–membered ketone (**339**) was obtained in good yield (Scheme 11.7). As we ultimately wanted a double bond in the seven–membered ring, we next explored oxidizing ketone **339** (Table 11.1). Although various conditions were attempted to form enone **340**, none of the desired product was obtained, instead returning recovered starting material in most cases.



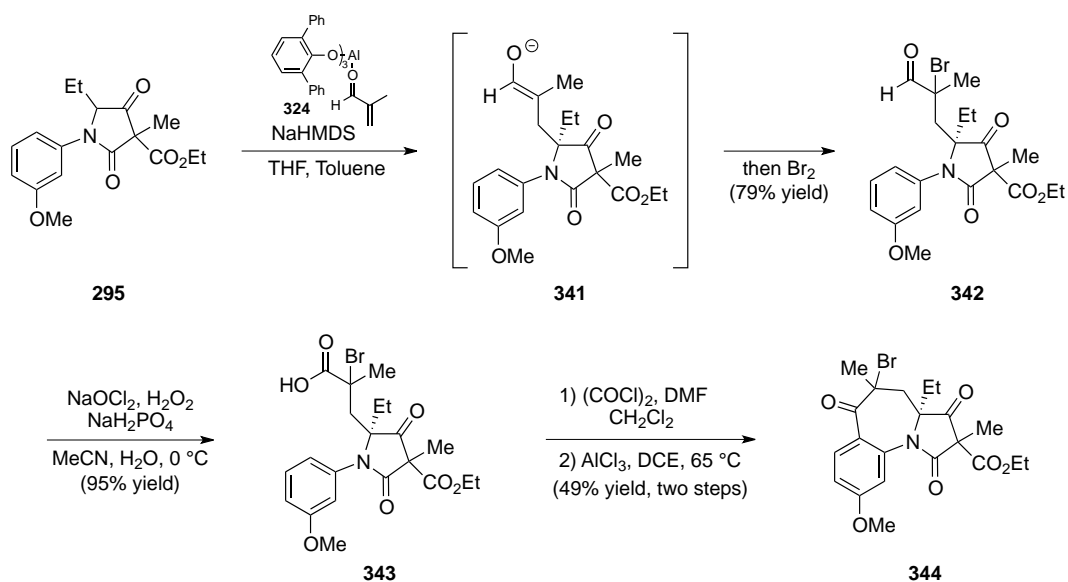
**Scheme 11.7.** Synthesis of ketone **339** via Friedel–Crafts reaction.

**Table 11.1.** Attempted oxidation of ketone **339** to enone **340**.



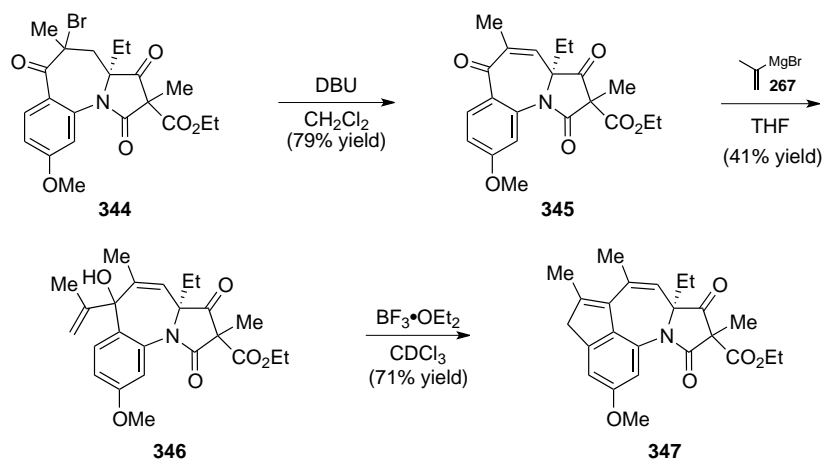
entry	conditions
1	IBX, DMSO, 60 °C
2	Br <sub>2</sub> , CCl <sub>4</sub> then DBU
3	NBS, CCl <sub>4</sub> then DBU
4	NaHMDS, PhSeBr then <i>m</i> CPBA
5	LDA, TMSCl then NBS then DBU

To circumvent the difficulties encountered in the oxidation to enone **340**, we looked to install a synthetic handle that could be eliminated after the Friedel–Crafts reaction. This was realized by subjecting ketone **295** to the same 1,4–addition conditions as before employing methacrolein pre-coordinated to the bulky Lewis acid developed by Yamamoto and coworkers followed by quenching the intermediate enolate (**341**) with bromine, to furnish  $\alpha$ –bromo aldehyde **342**. Gratifyingly **342** could undergo oxidation to carboxylic acid **343** followed by conversion to the acid chloride and Friedel–Crafts acylation to provide seven–membered ketone **344** (Scheme 11.8).



**Scheme 11.8.** Formation of  $\alpha$ -bromo ketone **344**.

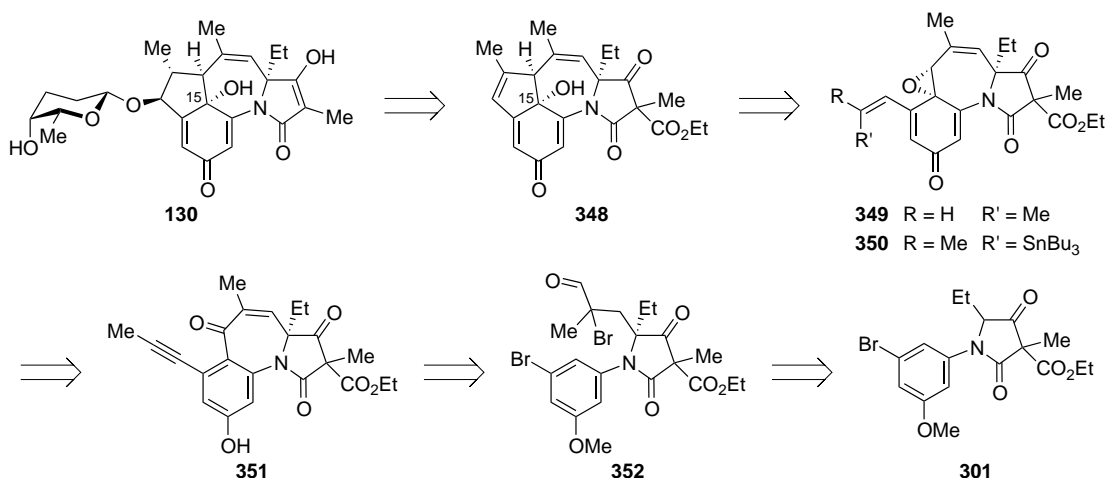
With  $\alpha$ -bromo ketone **344** in hand, we next looked to eliminate the bromide to form enone **345**, which was realized upon addition of DBU. To test the reactivity of enone **345**, isopropenyl magnesium bromide (**267**) was added and allylic alcohol **346** was formed. Furthermore, exposure of **346** to  $\text{BF}_3 \cdot \text{OEt}_2$  allowed access to tetracycle **347**, a compound that contains all the carbons present in the tetrapetalone A core. Although we were excited to access **347**, this compound would require significant functional group manipulations to access the natural product and thus we sought an alternate strategy to form this five-membered ring, one that would be better suited for the completion of the natural product.



**Scheme 11.9.** Elimination of  $\alpha$ -bromo ketone **344** to form enone **345** and elaboration to tetracycle **347**.

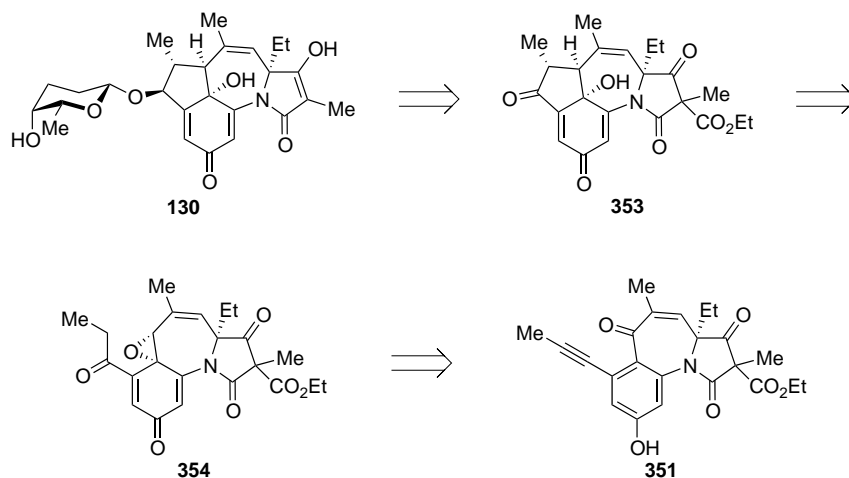
### 11.3 A New Strategy Towards Tetrapetalone A Utilizing the Friedel–Crafts Acylation

At this point we had developed an effective method to form the desired seven-membered ring, however the product we had obtained thus far (i.e. **345**) lacked the functionality necessary to access the natural product. We believed that by targeting tetracycle **348** as a late stage intermediate, we would be in good position to finish the natural product (Scheme 11.10). In the final steps of this scenario, tetracycle **348** would be subjected to a hydroboration/oxidation sequence followed by decarboxylation to furnish the natural product (**130**). Tetracycle **348** would in turn be derived from styrene **349** or vinyl stannane **350** through a palladium catalyzed opening of the allylic epoxide, which would both form the five-membered ring and deliver the C(15)–O bond present in the natural product. Both **349** and **350** could be produced from alkyne **351**, which would be derived from aldehyde **352** through Friedel–Crafts acylation and Sonogashira coupling.



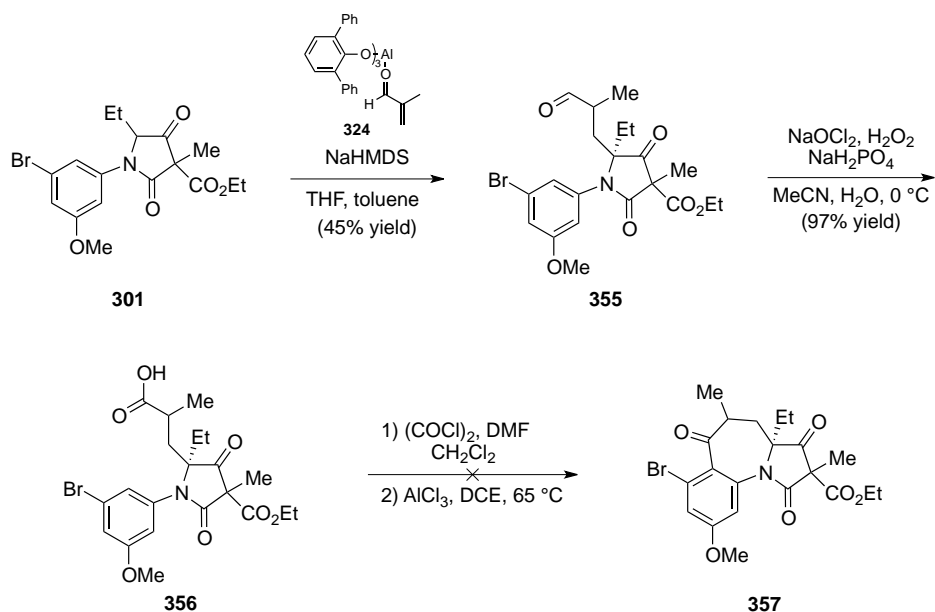
**Scheme 11.10.** Revised retrosynthetic analysis of tetrapetalone A (**130**).

An alternate strategy to tetrapetalone A (**130**) is outlined in Scheme 11.11 and differs from the approach in Scheme 11.10 in that the tetracyclic core of tetrapetalone (i.e. **353**) would be formed from intramolecular nucleophilic attack of ketone **354** onto the pendant epoxide with the aid of a Lewis acid or palladium. Ketone **354** would be derived by hydrolysis of alkyne **351**, which would prove to be a valuable departure point to explore the different strategies outlined in both Scheme 11.10 and Scheme 11.11.



**Scheme 11.11.** Alternate retrosynthetic analysis of tetrapetalone A (**130**).

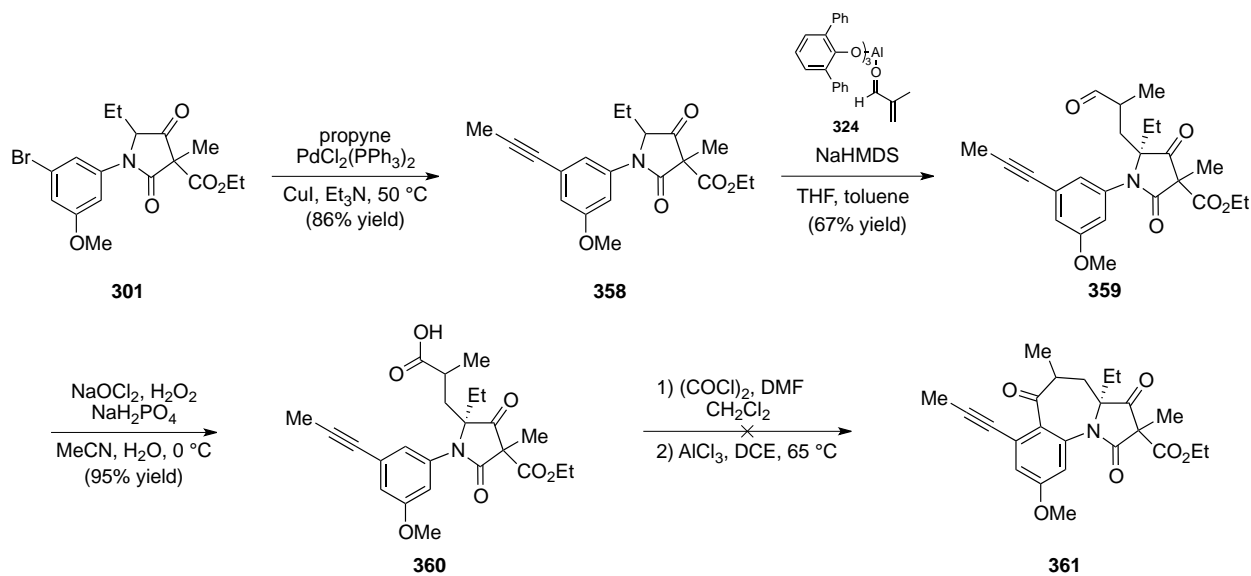
With a synthetic plan in place, we first looked to target alkyne **351**. As we had bromide **301** in hand from a previous route (cf. Scheme 10.8), we choose to first explore the Friedel–Crafts reaction on the compound with the bromide in place. To simplify the Friedel–Crafts reaction in our initial explorations, we choose to leave out the bromine quench and instead target aldehyde **355**, which was formed by subjecting aryl bromide **301** to the 1,4–addition sequence. Oxidation of **355** under Pinnick conditions provided carboxylic acid **356**. Unfortunately Friedel–Crafts acylation on the acid chloride derived from **356** only resulted in recovered acid chloride. Thus the Friedel–Crafts acylation was not compatible with the aryl bromide already in place (Scheme 11.12).



**Scheme 11.12.** Attempted Friedel–Crafts acylation of aryl bromide **356**.

To further investigate the Friedel–Crafts reaction with additional functionality, we choose to install the alkyne first. Coupling aryl bromide **301** with propyne proceeded uneventfully to provide aryl alkyne **358**, which could react with precoordinated methacrolein (**324**) to furnish aldehyde **359**. Oxidation under Pinnick conditions delivered acid **360**, which after being

converted to the acid chloride, was subjected to aluminum trichloride. Unfortunately this also led to no desired product, in this case only giving decomposition (Scheme 11.13).



**Scheme 11.13.** Attempted Friedel–Crafts acylation of aryl alkyne **360**.

#### 11.4 Installation of the Alkyne After the Friedel–Crafts Reaction

It seemed that the presence of an additional substituent on the aromatic ring completely shut down the Friedel–Crafts reaction. Therefore we decided that instead of starting with a substituent in place, we would look to install the desired functionality after the seven-membered ring had been formed (Scheme 11.14.a). However, in that case we would need to find a way to selectively functionalize the C–H bond *ortho* to the ketone. Around the time we were thinking about this transformation a paper by Dong and coworkers was published in the literature which outlined the use of ketones as directing groups in the C–H oxidation to form phenols (Scheme 11.14.b).<sup>31</sup>



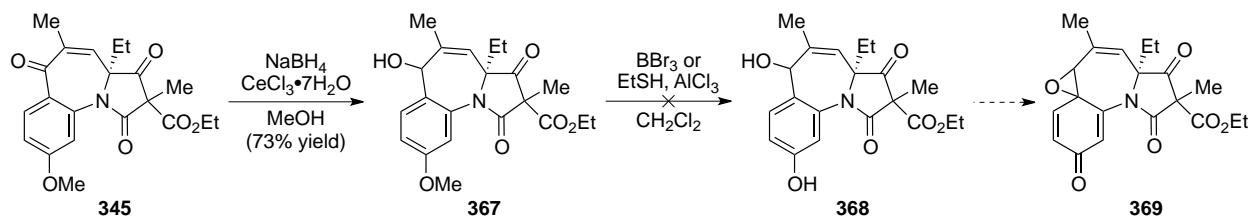
## Chapter Twelve

### Exploring the Phenolic Oxidation

While we were exploring ways to install the desired alkyne to form intermediate **351**, we also were investigating the phenolic oxidation to form the desired allylic epoxide.

#### 12.1 Deprotection Problems

In order to test the viability of the phenolic oxidation to form an allylic alcohol, the sequence starting with ketone **345** was initially explored (Scheme 12.1). To access phenolic oxidation precursor **368**, ketone **345** was reduced under Luche conditions to give allylic alcohol **367**. Interestingly it appeared that the ketone was being selectively reduced, which we hypothesized was based on the shape of the molecule, however at this point we were unsure which diastereomer was being favored. Nevertheless, **367** was subjected to conditions to remove the methyl protecting group; however this reaction was met with no success.

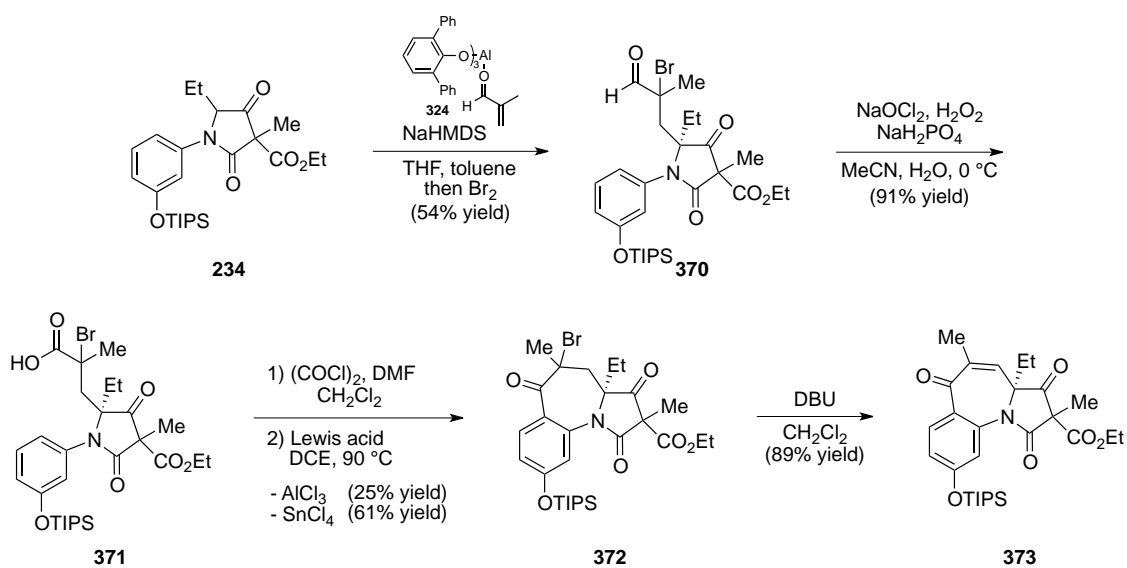


**Scheme 12.1.** Attempted removal of methyl protecting group.

Due to the difficulties encountered in methyl removal, we felt the best course of action was to explore other protecting groups. Recall we were initially utilizing a TIPS protecting group on the phenol and the only reason we had switched to the  $-\text{OMe}$  ether was to facilitate the iridium catalyzed borylation (cf. **294** to **295**, Scheme 10.5). Since our current route no longer

featured that transformation, we believed returning to the TIPS group would be worthwhile. Additionally, as we had previously utilized this protecting group, we were confident it would be compatible with our current chemistry, including the 1,4-addition, and be readily removed. The biggest question mark we had with the TIPS group was how it would fare in the Friedel–Crafts reaction.

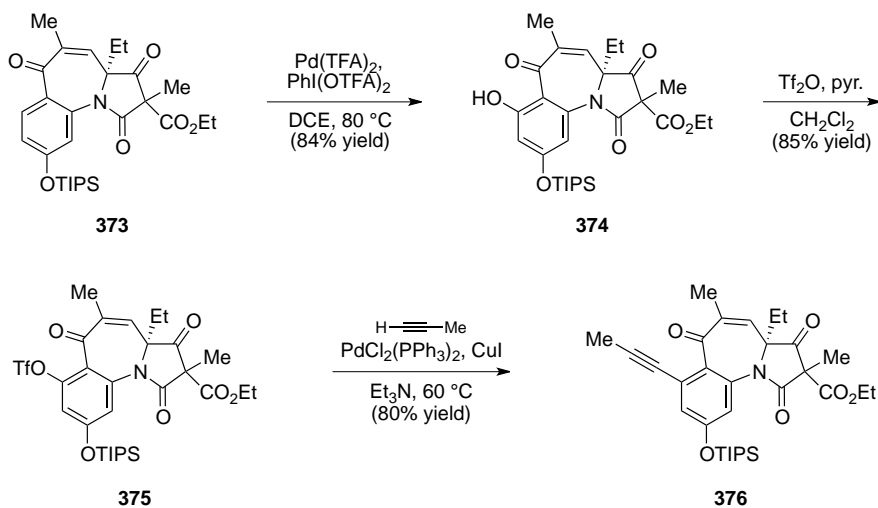
In that regard, previously accessed ketone **234** was converted to  $\alpha$ -bromo aldehyde **370** under the now standard conditions. Pinnick oxidation and conversion to the acid chloride proceeded smoothly, however exposure to the previously employed Friedel–Crafts conditions only provided **372** in a 25% yield, with a significant amount of TIPS removal observed. After a screen of Lewis acids it was found that tin tetrachloride was competent at promoting this reaction and a 61% yield of  $\alpha$ -bromo ketone **372** was obtained. Elimination of the bromide reliably produced enone **373** (Scheme 12.2).



**Scheme 12.2.** Synthesis of TIPS protected ketone **373**.

Although attempts to functionalize alkyne **376** will be discussed in later sections, we wanted to show that the chemistry to install this functionality was compatible in the –OTIPS

series. Therefore, ketone **373** was selectively oxidized to provide phenol **374**, which was converted to triflate **375**. Coupling with propyne under Sonogashira conditions delivered alkyne **376** in good yield (Scheme 12.3).

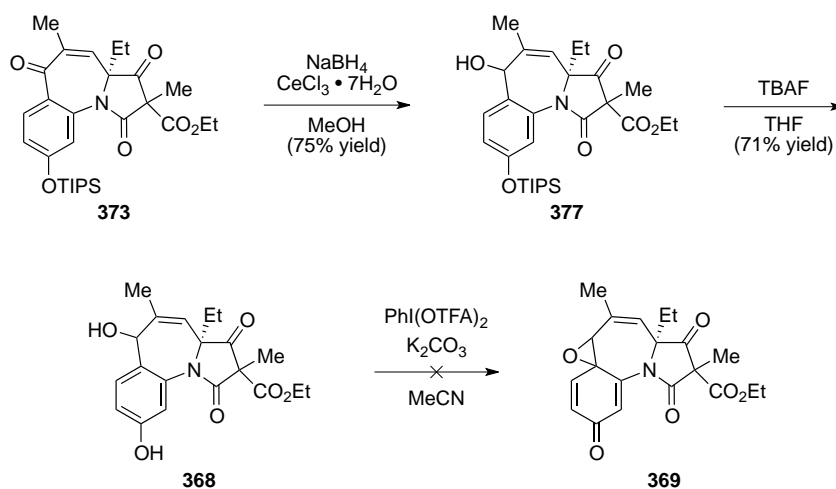


**Scheme 12.3.** Synthesis of TIPS protected alkyne **376**.

## 12.2 Phenolic Oxidation Attempts

With enone **373** in hand, we once again set out to explore the phenolic oxidation pathway to form allylic epoxide **369**. To that end, **373** was reduced under Luche conditions, which delivered allylic alcohol **377**. Gratifyingly, the TIPS protecting group could be removed upon exposure to TBAF. With a successful synthesis of phenolic oxidation precursor **368**, we looked to explore this transformation. Subjecting **368** to hypervalent iodine led to a complex mixture of products, with none of the desired product obtained (Scheme 12.4).<sup>32</sup> During the time we were exploring this reaction, in an effort to assign the stereochemical outcome of the Luche reduction, we were able to obtain a crystal structure of methyl protected allylic alcohol **367** (Figure 12.1). It is important to note that the crystal structure shown is the enantiomer of the

product shown; however this compound is racemic so the only important stereochemical information that can be obtained from this crystal structure is in the relative sense. Nevertheless, by inspecting the crystal structure, the relative stereochemistry of the newly formed allylic alcohol was found to be in the desired *syn* orientation to the ethyl group of the tetrasubstituted carbon. However, the allylic alcohol also appeared to be completely in the plane of the aromatic ring. This observation suggested to us that the phenolic oxidation that we were currently exploring was likely unable to proceed due to an inability to have significant overlap with the generated carbocation.



**Scheme 12.4.** Attempted phenolic oxidation to form epoxide **369**.

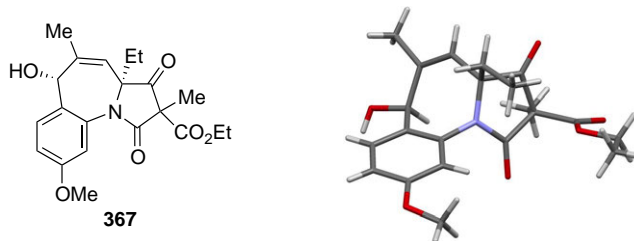
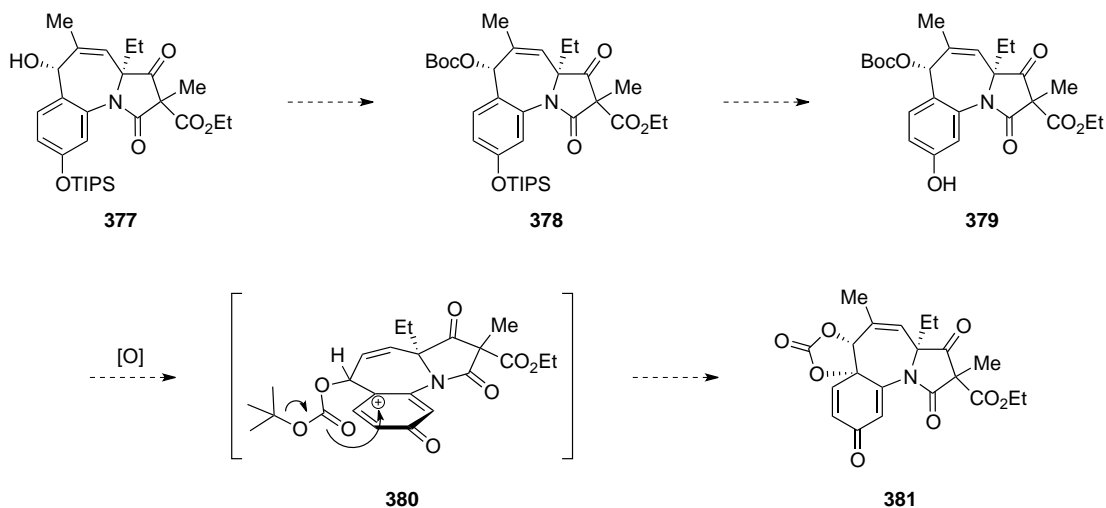
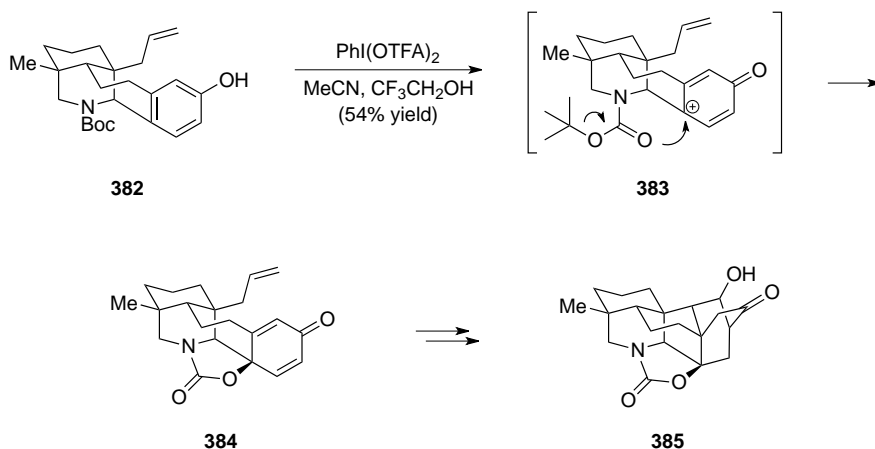


**Figure 12.1.** Crystal structure of allylic alcohol **367**.

Although spiroepoxide **369** appeared to be inaccessible, we were not deterred. To circumvent this conformational incompatibility, we opted to target cyclic carbonate **381** as a palladium  $\pi$ -allyl precursor instead. We believed that by exposing Boc-protected alcohol **379** to phenolic oxidation conditions we would access carbocation **380**. The Boc group should have sufficient flexibility that it can access a conformation (i.e. **380**), where the carbonyl can interact with the carbocation to form cyclic carbonate **381** (Scheme 12.5). Although to the best of our knowledge that are no reports of forming cyclic carbonates through this pathway, we were inspired by a recent report by Sarpong and coworkers outlining the synthesis of cyclic carbamate **384**, which they formed from phenol **382** through a similar intermediate (**383**) to the one we are proposing. They utilized intermediate **384** in their synthesis of the core structure (**385**) of the hetidine natural products.<sup>33</sup> Although we recognized that carbamates are better nucleophiles than carbonates, we believed this difference was minor and that our proposed transformation was feasible.

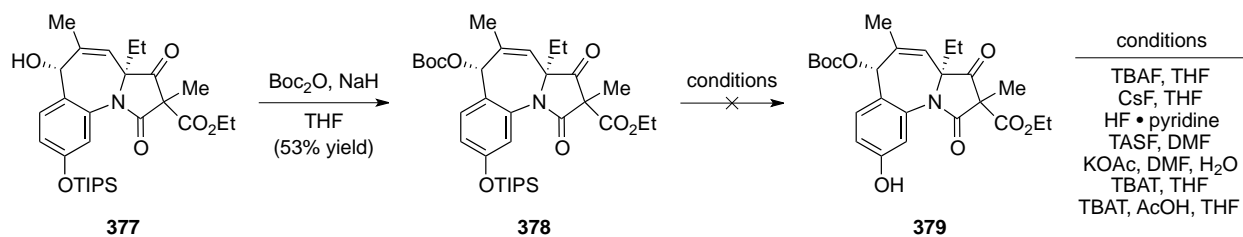


**Scheme 12.5.** Proposed synthesis of cyclic carbonate **381**.



**Scheme 12.6.** Sarpong's synthesis of **384**.

In accordance with this strategy, allylic alcohol **377** was protected with  $\text{Boc}_2\text{O}$  to give allylic carbonate **378**. With the requisite carbonate formed, we next explored methods to remove the TIPS group. Unfortunately, thus far we have been unable to remove the TIPS protecting group under a variety of fluoride-mediated conditions (Scheme 12.7). We are hesitant to expose **378** to strongly acidic conditions due to the presence of the acid sensitive carbonate. Although we have been unable to access phenol **379** thus far, we are still in the process of exploring methods to access this enticing intermediate.



**Scheme 12.7.** Attempted synthesis of phenol **379**.

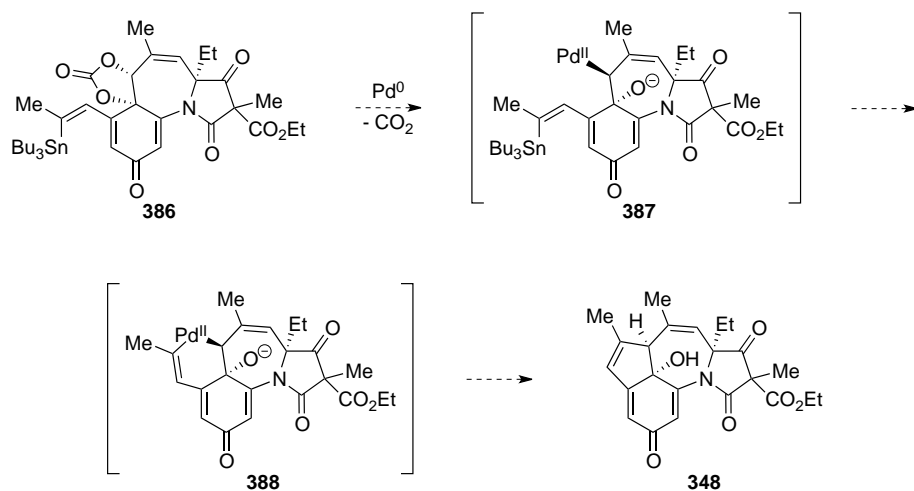
## Chapter Thirteen

### Elaboration of the Alkyne

To ultimately gain access to tetrapetalone A (**130**), we sought a method to form the final five-membered ring. We hoped to form this ring by elaborating alkyne **351** into a suitable nucleophile (cf. Schemes 11.10 and 11.11). We believed that vinyl stannanes, olefins, ketones, and silyl enol ethers would all be viable nucleophiles in this approach. Thus syntheses of these compounds were explored.

#### 13.1 Attempts to Form a Vinyl Stannane

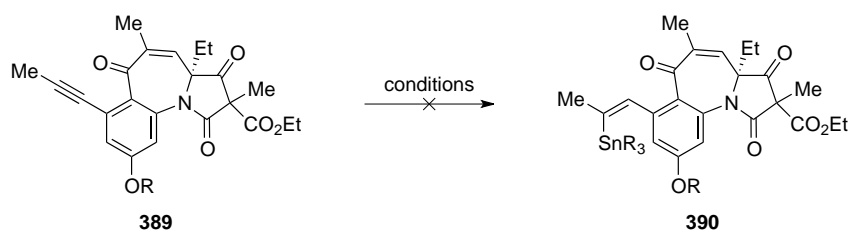
We first targeted a vinyl stannane, as vinyl stannanes have been reported in the literature to react intramolecularly with palladium  $\pi$ -allyl species.<sup>34</sup> Therefore our planned reaction pathway is outlined in Scheme 13.1. Oxidative addition into allylic carbonate **386** would, after loss of CO<sub>2</sub>, form palladium  $\pi$ -allyl **387**, which is represented as the  $\eta^1$ - $\pi$ -allyl. Transmetalation from the vinyl stannane would form palladium intermediate **388**, which could undergo reductive elimination to form tetracycle **348**.



**Scheme 13.1.** Proposed synthesis of tetracycle **348** from vinyl stannane **386**.

We hoped to install the requisite vinyl stannane by hydrostannylation of alkyne **389**. Because we hoped to access the *anti*-hydrostannylated product **390**, we were attracted to radical conditions to perform this transformation.<sup>35</sup> Initial experiments on alkyne **389** included the use of a trialkyl tin hydride and a radical initiator; however, none of the desired product was obtained (Table 13.1). We are currently in the process of screening other tin hydride species and radical initiators.

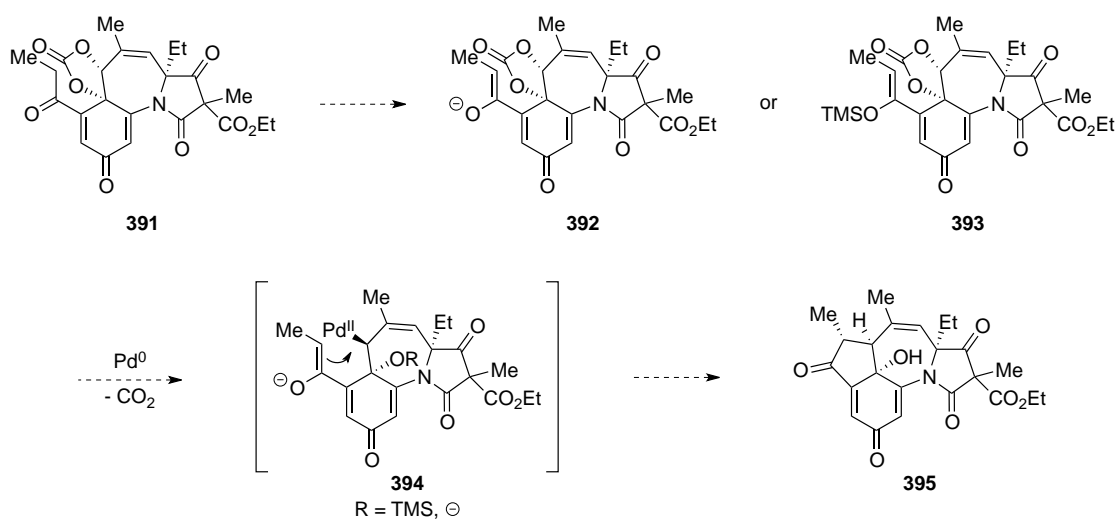
**Table 13.1.** Attempts to form vinyl stannane **390**.



entry	R	conditions
1	Me	<i>n</i> -Bu <sub>3</sub> SnH, B(OH) <sub>3</sub> toluene, 75 °C
2	TIPS	<i>n</i> -Bu <sub>3</sub> SnH, Et <sub>3</sub> B toluene, 75 °C
3	TIPS	Ph <sub>3</sub> SnH, Et <sub>3</sub> B toluene, 75 °C

## 13.2 Attempts to Form an Aryl Ketone

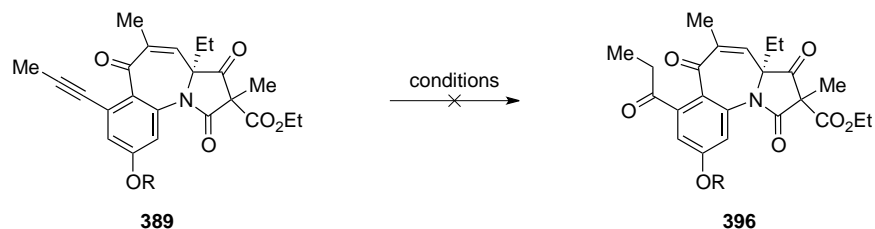
The most studied of the three nucleophiles that we want to approach is aryl ketone **391**, which would be formed from hydrolysis of the triple bond. The ketone could be utilized in our desired reaction as a nucleophile by transforming it to either enolate **392** upon reaction with a strong base such as LDA or silyl enol ether **393**. In either case a palladium  $\pi$ -allyl species (**394**) could be formed after oxidative addition into the allylic carbonate. Attack from the enolate onto the palladium  $\pi$ -allyl would then form tetracycle **395** (Scheme 13.2).



**Scheme 13.2.** Proposed synthesis of tetracycle **395** from ketone **391**.

The attempts to form ketone **391** are outlined in Table 13.2. In our screening we initially attempted hydroboration/ oxidation (entry 1) and acid hydrolysis (entry 2). After those failed we moved to metal mediated hydrolysis including: palladium (entry 3), silver (entry 4), and gold (entries 5, 6, and 7).<sup>36</sup> Unfortunately in all these attempts none of the desired product **396** was obtained, instead recovered starting material was obtained in most cases.

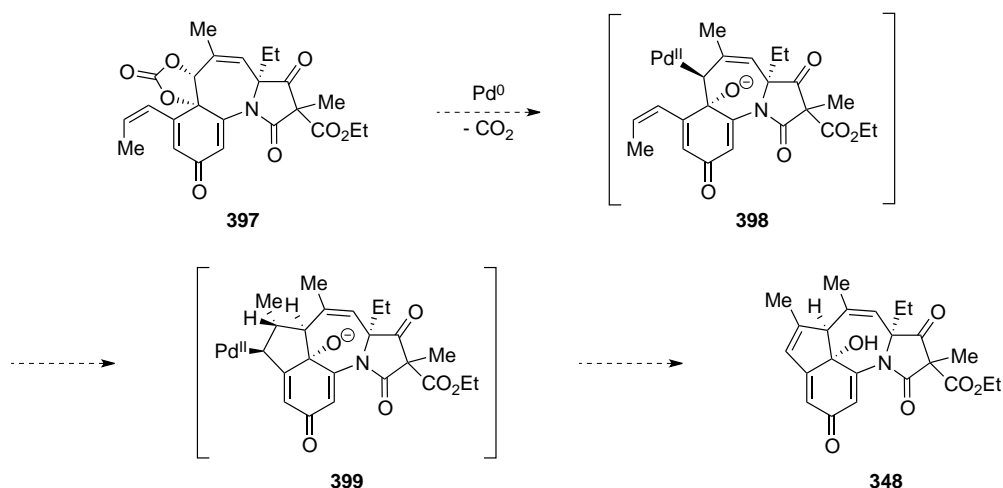
**Table 13.2.** Attempts to form ketone **396**.



entry	R	conditions
1	Me	BH <sub>3</sub> •SMe <sub>2</sub> , I <sub>2</sub> , CH <sub>2</sub> Cl <sub>2</sub> then NaOH, H <sub>2</sub> O <sub>2</sub> , MeOH
2	Me	<i>p</i> TsOH, EtOH, 60 °C
3	Me	Pd(PhCN) <sub>2</sub> Cl <sub>2</sub> MeCN, H <sub>2</sub> O, 60 °C
4	TIPS	AgOTf, toluene
5	TIPS	[Au(IPr)] <sub>2</sub> (OH)BF <sub>4</sub> , NaHCO <sub>3</sub> CH <sub>2</sub> Cl <sub>2</sub> , MeCN
6	TIPS	AuCl(PPh <sub>3</sub> ), AgSbF <sub>6</sub> , NaHCO <sub>3</sub> CH <sub>2</sub> Cl <sub>2</sub> , MeOH
7	TIPS	AuCl(PPh <sub>3</sub> ), Cu(OTf) <sub>2</sub> MeOH, H <sub>2</sub> O

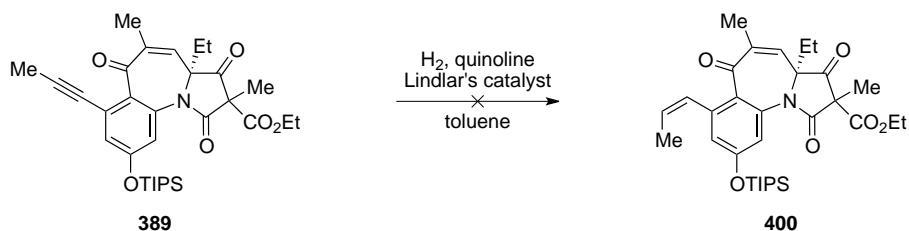
### 13.3 Attempts to Reduce the Alkyne to an Olefin

The last nucleophile we are interested in approaching is an olefin, which would be able to participate in a tandem palladium  $\pi$ -allyl/ Heck reaction. The reaction would be initiated by initial oxidative addition into allylic carbonate **397** to form palladium  $\pi$ -allyl **398**. Migratory insertion into the nearby double bond would provide **399**, which could undergo  $\beta$ -hydride elimination to give tetracycle **348**. One important consideration is in the  $\beta$ -hydride elimination the palladium and hydride must be *syn* to each other, therefore to undergo this desired reaction we must start with the *cis*-olefin shown (Scheme 13.3). While subsequent complexation and migratory insertion of olefins (i.e. Heck chemistry) has not been demonstrated for  $\pi$ -allyls, they have been shown to undergo complexation and migratory insertion of CO.<sup>37</sup>



**Scheme 13.3.** Proposed synthesis of tetracycle **348** from styrene **397**.

This transformation is in the most preliminary stages, as only one condition has been attempted. In the presence of hydrogen and Lindlar's catalyst, only starting material was obtained (Scheme 13.4). We are currently investigating this route further.

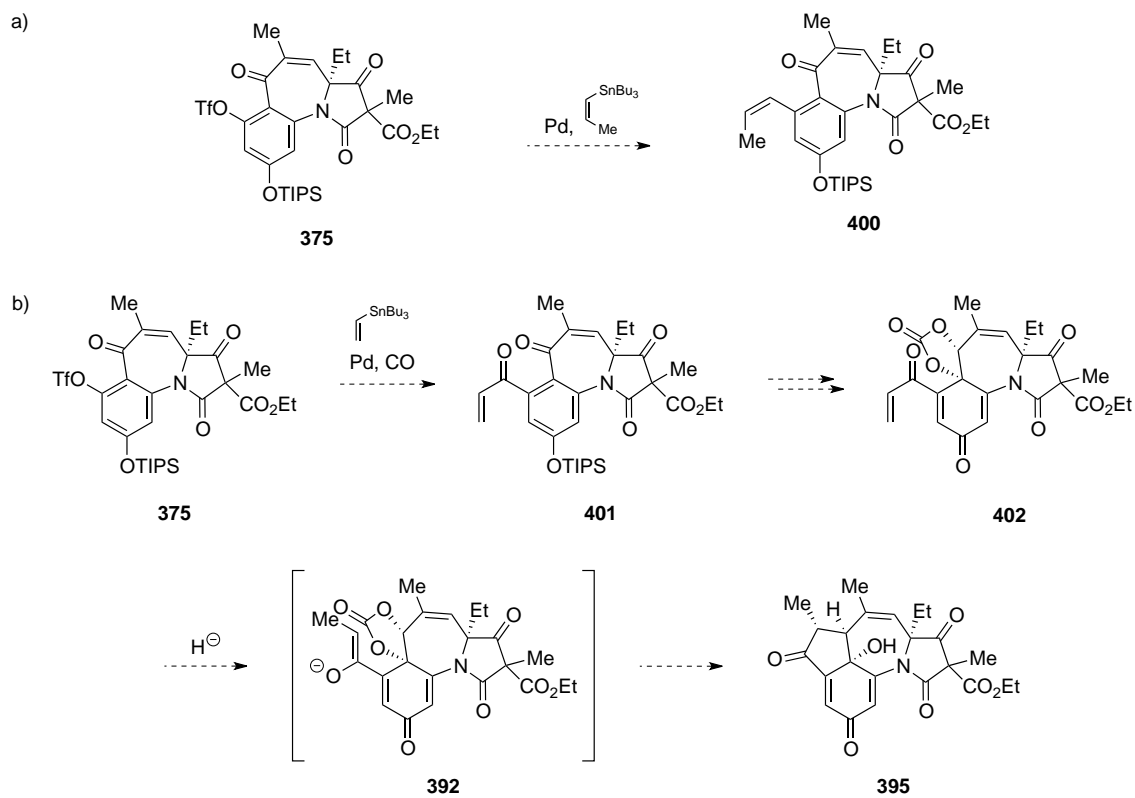


**Scheme 13.4.** Attempted reduction of alkyne **389**.

## 13.4 Conclusion and Future Work

At this point we have access to an alkyne that we are hopeful can be transformed into an appropriate nucleophile to react with a palladium  $\pi$ -allyl species that will be derived from an allylic carbonate. We have outlined three strategies in this chapter to functionalize the alkyne, all of which are in the very early stages of exploration. In addition to the approaches discussed

thus far, we have devised two routes starting from aryl triflate **375**. Direct Stille coupling of **375** with a vinyl stannane would deliver styrene **400**, the same product we are targeting through reduction of the alkyne (13.5.a). If instead the Stille reaction is performed in the presence of carbon monoxide, enone **401** could be accessed. After elaboration to cyclic carbonate **402**, conjugate reduction would provide enolate **392**, which could interact with the allylic carbonate either directly or with the aid of palladium or a Lewis acid (Scheme 13.5.b).

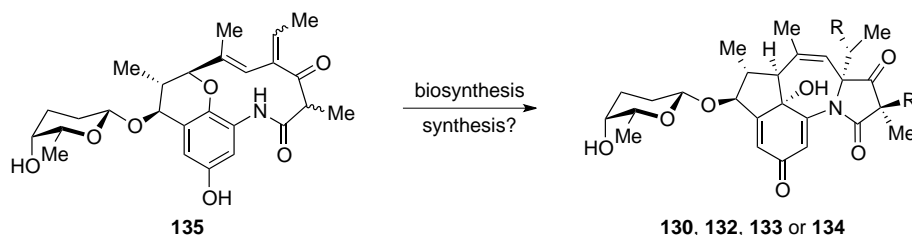


**Scheme 13.5.** Proposed reaction to form a) styrene **400** through a Stille coupling and b) tetracycle **395** through a carbonylative Stille coupling followed by conjugate reduction.

## Chapter Fourteen

### Ansaetherone

Concurrent to our studies toward the tetrapetalones, we also became interested in ansaetherone (**135**). This interest stemmed from the proposed biosynthetic pathway of the tetrapetalones, which included ansaetherone as an intermediate (cf. Scheme 6.2).<sup>3</sup> Thus if we could gain access to **135**, it may be possible to convert it to one of the tetrapetalones in a biomimetic fashion (Scheme 14.1).

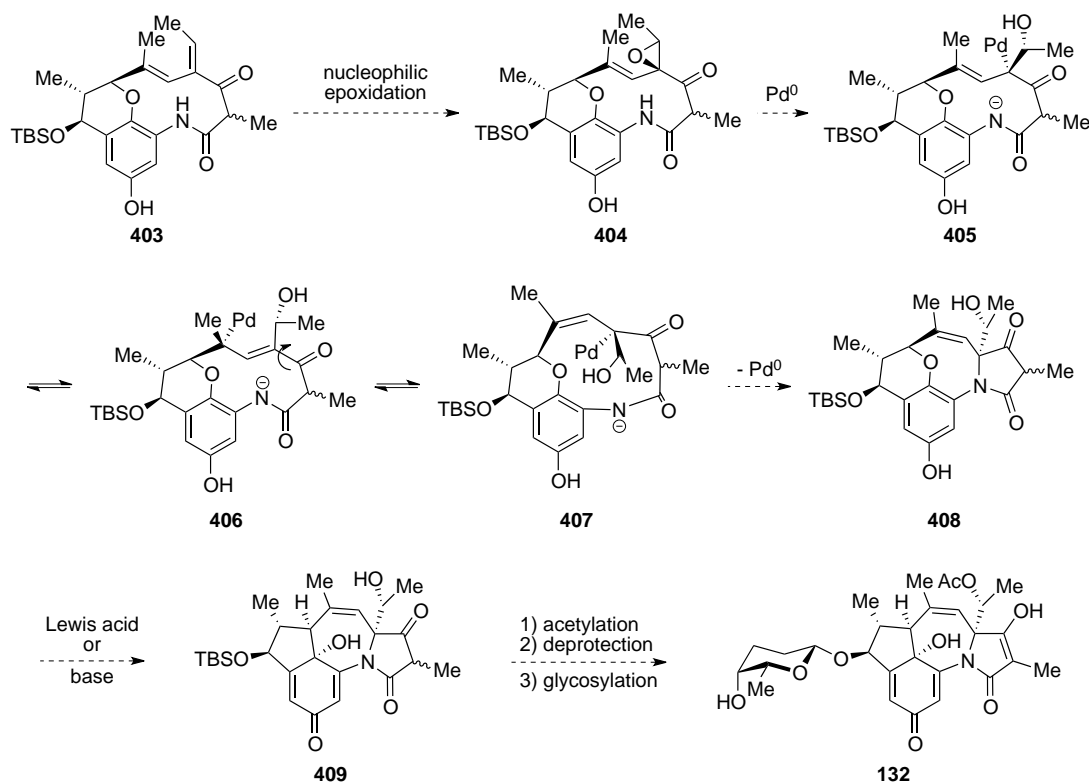


**Scheme 14.1.** Relationship between ansaetherone (**135**) and the tetrapetalones.

#### 14.1 Proposed Conversion of Ansaetherone to the Tetrapetalones

The main challenges associated with the conversion of ansaetherone (**135**) to the tetrapetalones are the contraction of the six to a five-membered ring and formation of the seven-five ring system, which can only take place after *trans/cis*-isomerization of the olefin in the eleven-membered ring. To address the olefin isomerization and formation of the five-membered tetramic acid moiety we envisioned utilizing allylic epoxide **404** as a substrate in a palladium-mediated transannular allylic amidation (Scheme 14.2). In the event ansaetherone derivative **403** would be selectively epoxidized under nucleophilic conditions to give allylic epoxide **404**. Exposure of **404** to palladium(0) would form intermediate  $\pi$ -allyl species **405**,

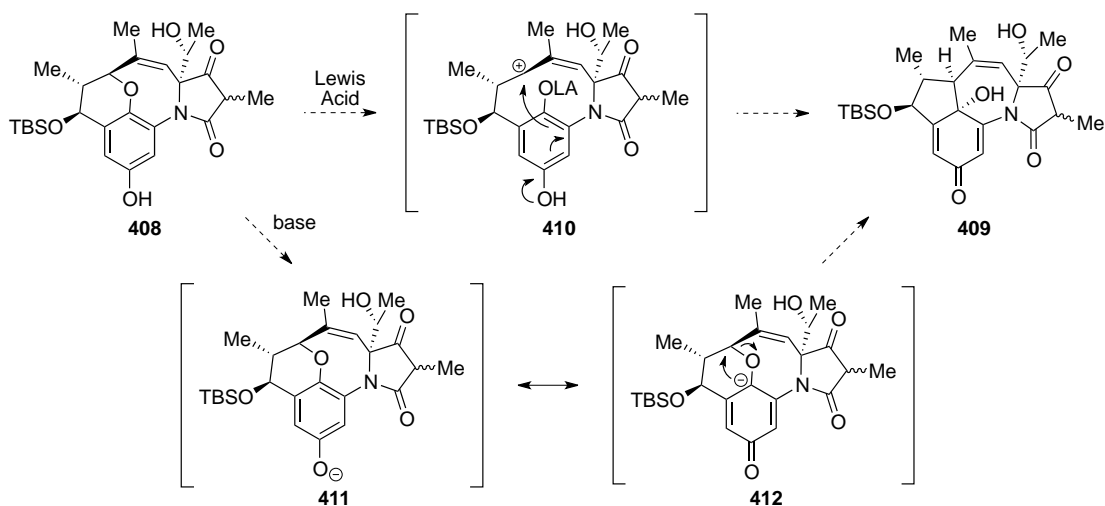
which upon migration to the corresponding  $\eta^1$ - $\pi$ -allyl (**406**) can undergo olefin isomerization and eventually deliver  $\eta^1$ - $\pi$ -allyl **407**. Ring closure by intramolecular attack of the amide nitrogen would furnish **408**. Inspection of molecular models indicates that cyclization prior to olefin isomerization is unlikely and the formation of **408** would be preferred. Having installed the tetramic acid moiety and set the olefin geometry only ring contraction followed by acetylation, deprotection, and glycosylation remains to form tetrapetalone B (**132**).



**Scheme 14.2.** Proposed conversion of ansaetherone (**135**) to tetrapetalone B (**132**).

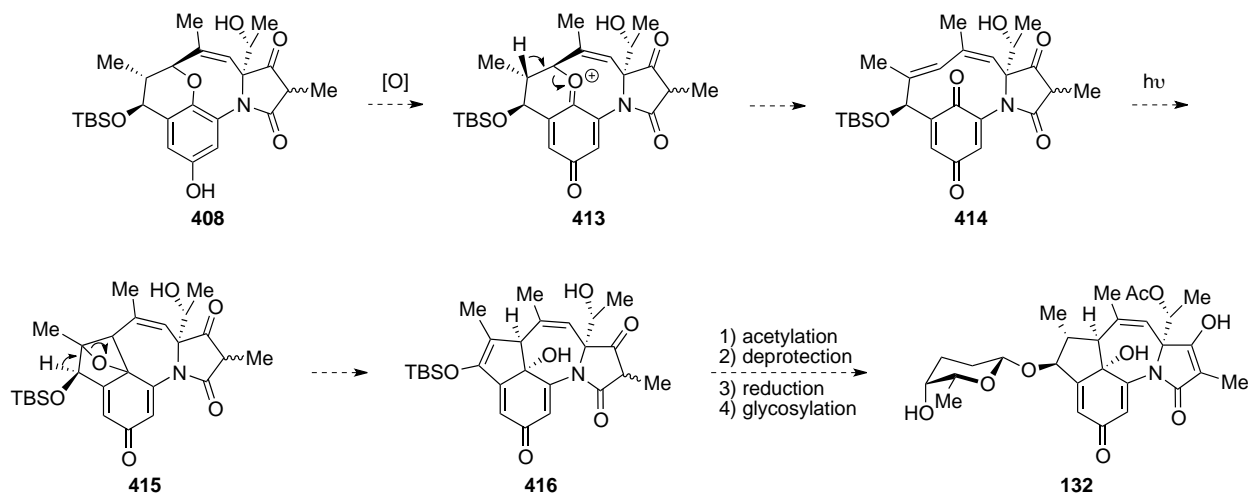
As depicted in Scheme 14.2 we envision the ring contraction to form the tetracyclic core of the tetrapetalones could proceed under Lewis acidic or basic conditions. A more detailed schematic showing how these processes are envisioned is outlined in Scheme 14.3. Exposure of dihydropyran **408** to Lewis acid would promote the formation of allylic cation **410**, which could be captured by the electron rich aromatic ring to provide tetracycle **409**. Alternatively, exposure

of the phenol **408** to basic conditions would result in phenoxide **411**, which could undergo a stereoselective 1,2-Wittig rearrangement of resonance structure **412** to deliver tetracycle **409**.

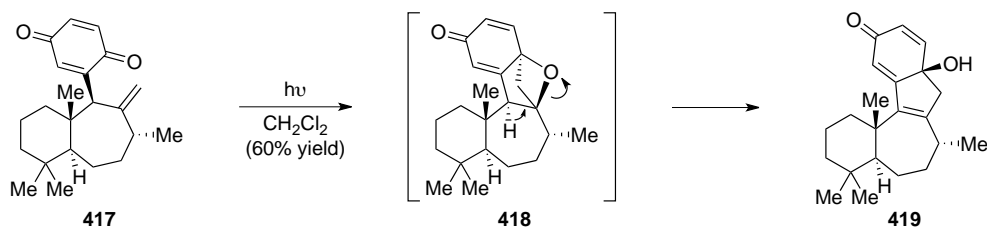


**Scheme 14.3.** Proposed synthesis of tetracycle **409** through a Lewis acidic or basic pathway.

An alternate pathway to convert phenol **408** to tetrapetalone B (**132**) is depicted in Scheme 14.4. Phenolic oxidation would initially form oxocarbenium **413**, which could eliminate to form *para*-quinone **414**. Exposure of **414** to UV light would promote a Paternó-Büchi reaction to give an intermediate oxetane (**415**) that upon ring opening and loss of a proton would furnish tetracycle **416**. Tetrapetalone B would then be completed by acetylation, deprotection, reduction, and glycosylation. This approach was inspired by George and coworkers' synthesis of tetracycle **419** through a Paternó-Büchi/ elimination route from *para*-quinone **417** (Scheme 14.5).<sup>38</sup>



**Scheme 14.4.** Proposed alternate synthesis of tetrapetalone B from phenol **408**.

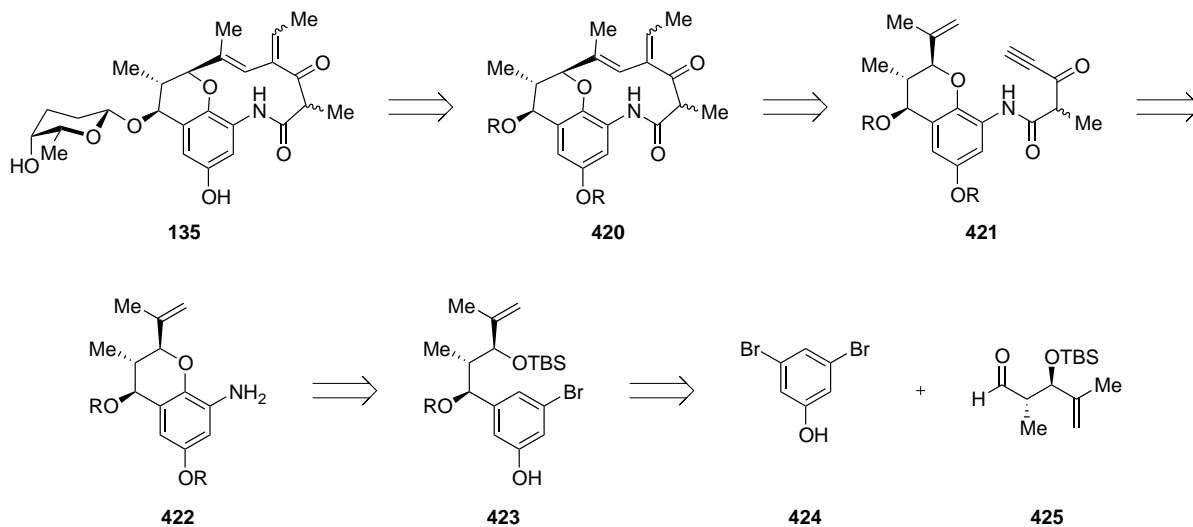


**Scheme 14.5.** George's Paternó-Büchi/ elimination route to tetracycle **419**.

## 14.2 A Phenolic Oxidation Pathway to Ansaetherone

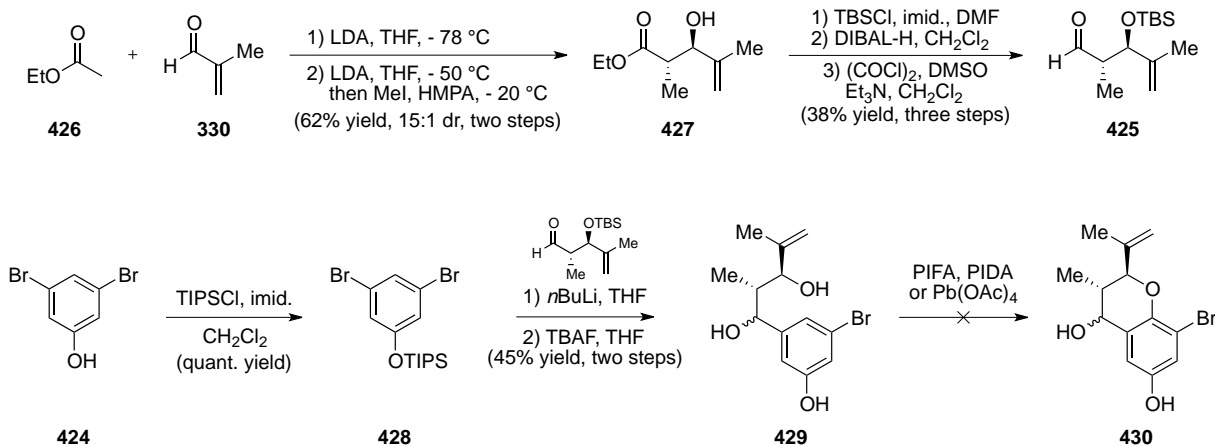
With a plan to convert ansaetherone (**135**) to tetrapetalone B (**132**) in place, we sought a method to access **135**. In that regard we envisioned **135** would ultimately arise from deprotection and glycosylation of diene **420**, the product of a tandem enyne/ cross metathesis starting from enyne **421**. Given that the olefin geometry of the exocyclic double bond is unknown in the natural product, late stage formation of this double bond will potentially lend access to both *E* and *Z* isomers and thus help lead to structural elucidation. Nevertheless, enyne **421** would be formed from an amidation of aniline **422**, which itself would be derived from

phenol **423** after a phenolic oxidation to form the dihydropyran and installation of the aniline nitrogen from the aryl bromide. Phenol **423** would ultimately arrive from dibromophenol **424** and aldehyde **425** (Scheme 14.6).



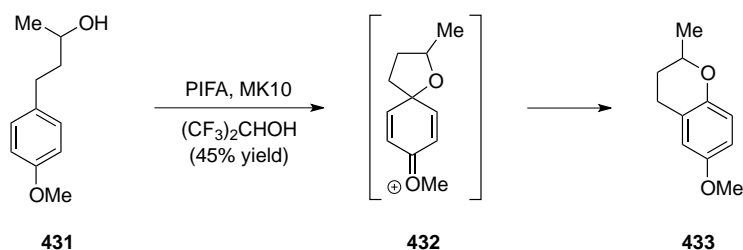
**Scheme 14.6.** Retrosynthetic analysis of ansaetherone (**135**).

The synthesis began with a known two-step sequence to access  $\beta$ -hydroxy ester **427** from ethyl acetate (**426**) and methacrolein (**330**).<sup>39</sup> Silyl protection followed by a two-step reduction/oxidation sequence furnished aldehyde **425**. Protected dibromophenol **428** was formed via TIPS protection of phenol **424** and then underwent mono lithium-halogen exchange and reaction with aldehyde **425**.<sup>6b</sup> Removal of both silyl protecting groups provided phenolic oxidation precursor **429**. Unfortunately, exposure of **429** to phenolic oxidation conditions led mostly to decomposition of the starting material.

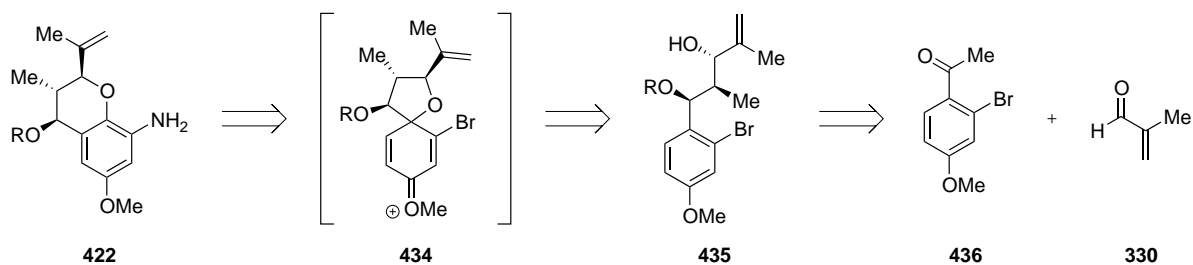


**Scheme 14.7.** Attempted phenolic oxidation of **429**.

Although difficulties were met with the phenolic oxidation of **429**, we still believed the dihydropyran moiety could be formed through a phenolic oxidation. Inspired by the work of Kita and coworkers, who showed that **433** could be formed by exposure of alcohol **431** to bisacetoxyiodo benzene and MK10, presumably through the intermediacy of **432** (Scheme 14.8),<sup>40</sup> the synthetic strategy outlined in Scheme 14.9 was devised. Specifically, intermediate **422** would now be formed from an alkyl migration/ elimination sequence from spirotetrahydrofuran **434**, which itself would be formed *in situ* from a phenolic oxidation and intramolecular trapping of alcohol **435**. Alcohol **435** would ultimately derive from known ketone **436** and methacrolein (**330**).

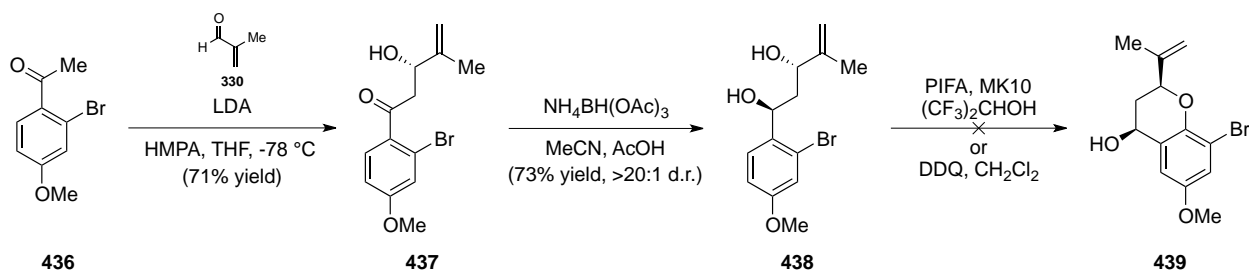


**Scheme 14.8.** Kita's synthesis of dihydropyran **433**.



**Scheme 14.9.** Revised retrosynthetic analysis of dihydropyran **422**.

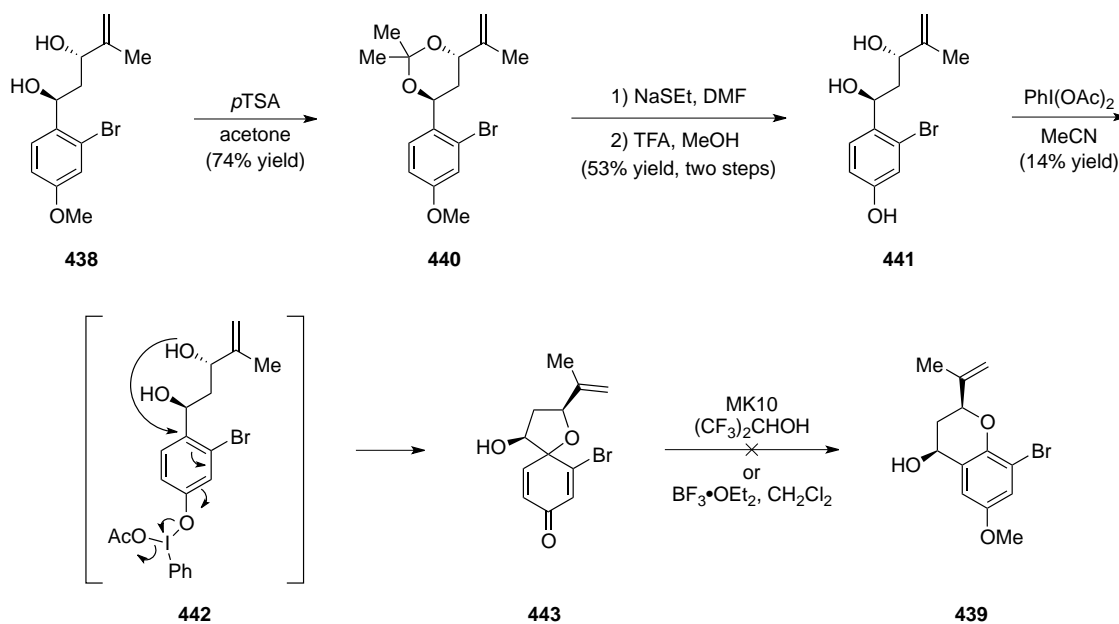
In the event known acetophenone **436** underwent an aldol reaction with methacrolein (**330**) to provide  $\beta$ -hydroxy ketone **437**. Although ketone **437** is lacking the required  $\alpha$ -methyl group, we decided to explore the subsequent chemistry on the desmethyl compound. With that in mind, **437** was reduced to selectively give *anti*-diol **438** as essentially one diastereomer. Protected phenol **438** was then explored in the phenolic oxidation step. However none of the desired product was obtained utilizing the conditions developed by Kita and coworkers or with DDQ (Scheme 14.10).



**Scheme 14.10.** Attempted synthesis of dihydropyran **439**.

We had utilized protected phenol **438** in this step because Kita and coworkers had used methyl protected phenols in their paper. However given our unsuccessful result we opted to look at the reaction with free phenol **441**, which would proceed via an alternate mechanistic pathway (i.e. intermediate **442**). To access free phenol **441**, diol **438** was converted to acetal **440**. Exposure to sodium ethane thiolate removed the methyl protecting group and TFA removed the

acetal to give phenolic oxidation precursor **441**. Gratifyingly, exposing **441** to iodobenzene diacetate provided spirotetrahydrofuran **443** albeit in low yields. Excited by this phenolic oxidation product we next explored the alkyl shift to form tetrahydropyran **439**. Subjecting **439** to the conditions developed by Kita and coworkers (i.e. MK10) resulted in no desired product formation, as did adding  $\text{BF}_3 \cdot \text{OEt}_2$ . Given the low yields of **443** and the inability to move it forward, we opted to explore other strategies toward ansaetherone (**135**).

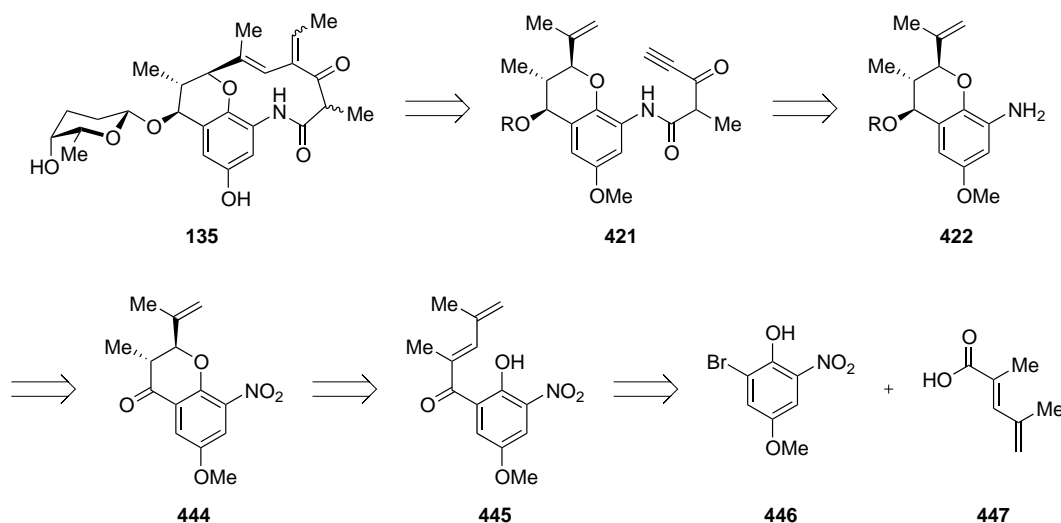


**Scheme 14.11.** Attempted synthesis of dihydropyran **439**.

### 14.3 Turning to a Fries Rearrangement

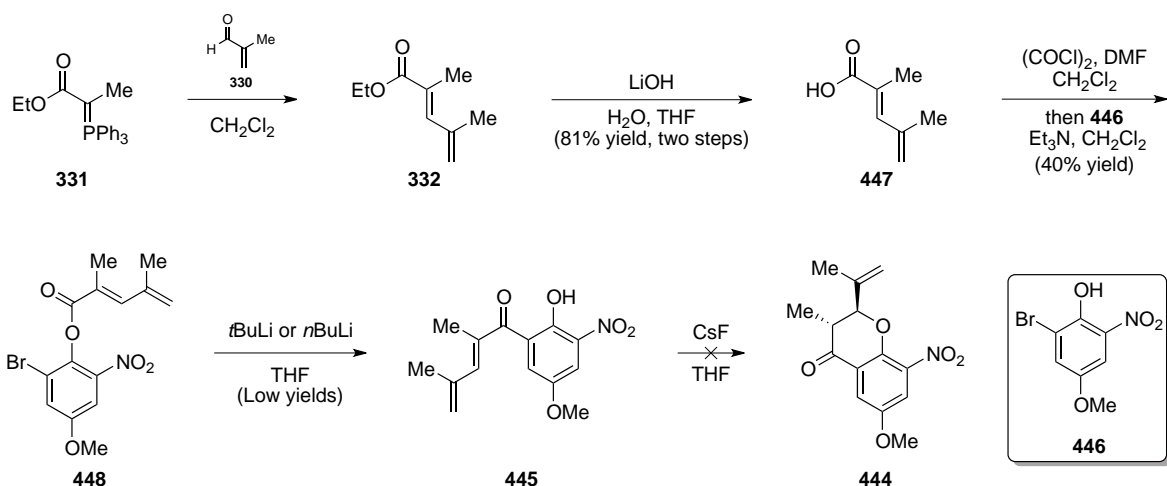
Given the difficulties encountered in trying to form the aromatic C–O bond, we decided to alter our approach and begin with that bond already in place. Therefore ansaetherone (**135**) would still arise from enyne **421**, which would be derived from aniline **422** as described in Scheme 14.6. However aniline **422** would come from reduction of nitrophenol **444**, the product of an intramolecular oxy–Michael addition of phenol **445**.<sup>41</sup> The key reaction in the formation of

phenol **445** would be an anionic Fries rearrangement of the ester derived from acylation of phenol **446** with acid **447** (Scheme 14.12).<sup>42</sup>



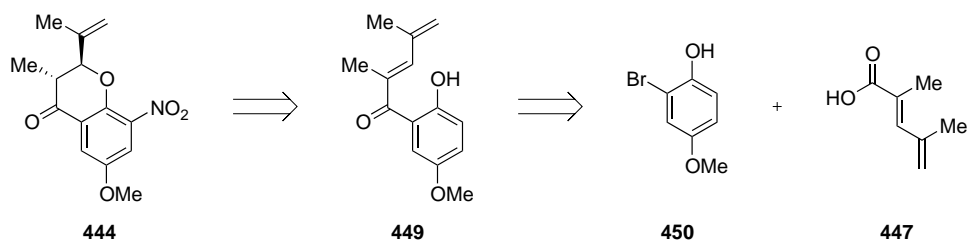
**Scheme 14.12.** Revised retrosynthetic analysis of ansaetherone (**135**).

To investigate the proposed anionic Fries rearrangement, known ylide **331** was reacted with methacrolein (**330**) and the resultant ester (**332**) was saponified to give acid **447**. Conversion to the acid chloride and addition of commercially available phenol **446** provided access to aryl ester **448** in moderate yield. Subjecting aryl bromide **448** to *n*-BuLi or *t*-BuLi provided the desired anionic Fries rearrangement product in very low yields. Furthermore the intramolecular oxy–Michael addition of phenol **445** did not provide any of the desired product **444** on the small scale.



**Scheme 14.13.** Attempted synthesis of oxy-Michael product **444**.

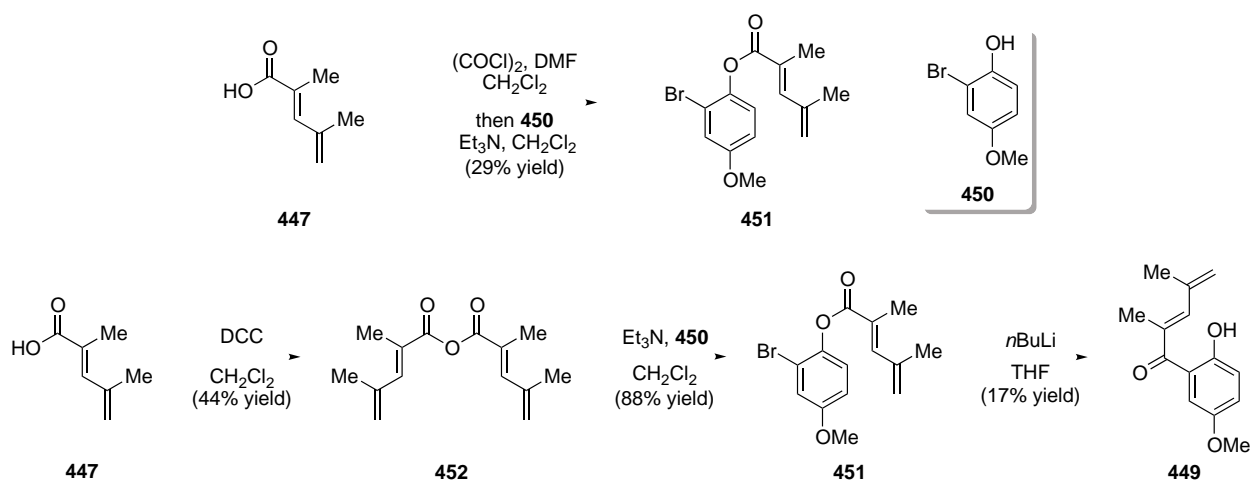
Although we were able to obtain small amounts of anionic Fries product **444**, it was clear this was not a viable route. We hypothesized that removal of the electron withdrawing nitro group may be beneficial for both the Fries rearrangement and the oxy-Michael addition. Thus we believed nitrobenzene **444** would be the product of the oxy-Michael addition followed by a nitration starting with phenol **449**, which would be derived from phenol **450** and acid **447** through an acylation/ anionic Fries rearrangement sequence (Scheme 14.14).



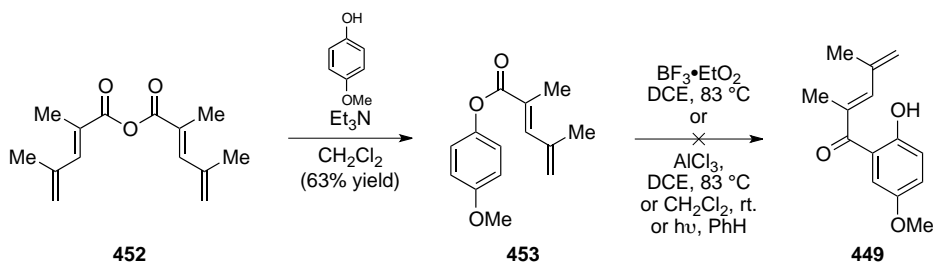
**Scheme 14.14.** Revised retrosynthetic analysis of nitrobenzene **444**.

Converting carboxylic acid **447** to the acid chloride then adding phenol **450** provided aryl ester **451** although in low yield once again. To help improve this acylation event, carboxylic acid **447** was converted to anhydride **452**, which proved to be a more effective acylating agent, giving **451** in good yield. Furthermore, aryl bromide **451** effectively underwent the desired

anionic Fries rearrangement to give aryl ketone **449** albeit still in low yield (Scheme 14.15). Employing other lithium or magnesium bases did not improve this reaction. Attempts to improve this rearrangement by utilizing Lewis acid-catalyzed Fries or photo Fries conditions were futile, leading either to recovered starting material or deacylated product (Scheme 14.16).



**Scheme 14.15.** Synthesis of aryl ketone **449**.

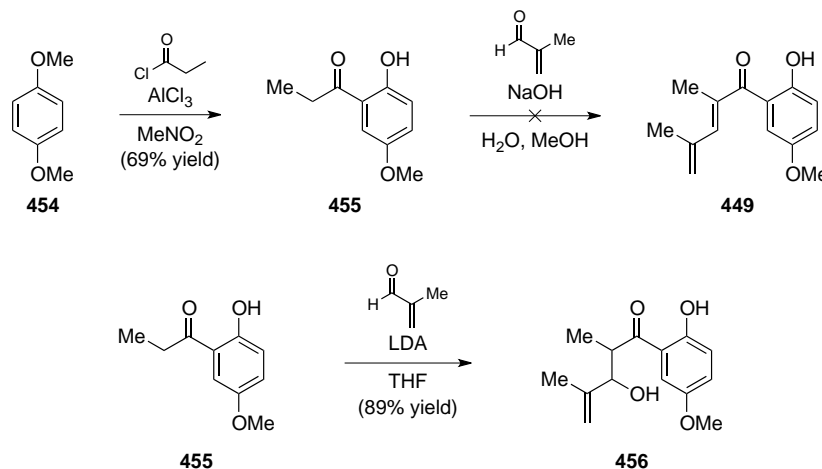


**Scheme 14.16.** Attempts at Fries or photo Fries rearrangements.

#### 14.4 Forming an Oxy-Michael Precursor Through an Aldol Reaction

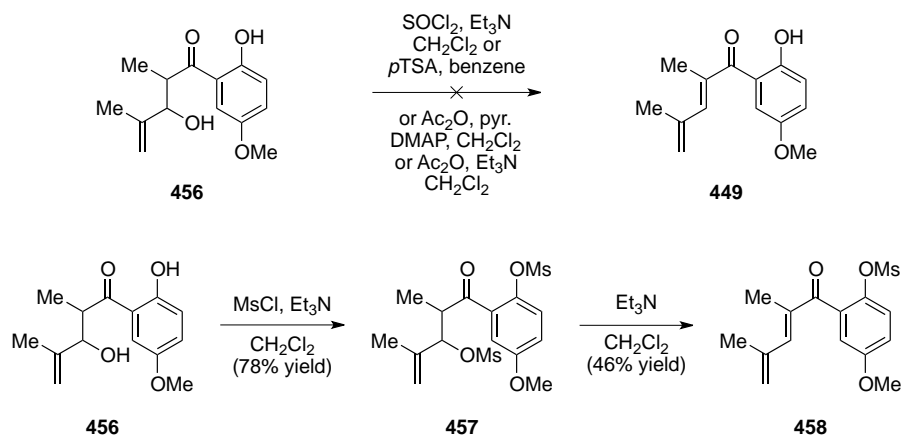
Although we were able to obtain aryl ketone **449** through an anionic Fries rearrangement, due to our inability to optimize this transformation we opted to explore other

ways to obtain this required compound. In that regard dimethoxyphenol (**454**) was transformed to ketophenol **455** under known conditions.<sup>43</sup> Subjecting **455** to aldol condensation conditions to give enone **449** directly only resulted only in recovered starting material, most likely due to a retro-aldol reaction occurring more readily than the desired dehydration. However, aldol adduct **456** could be obtained by switching to irreversible conditions utilizing LDA (Scheme 14.17).

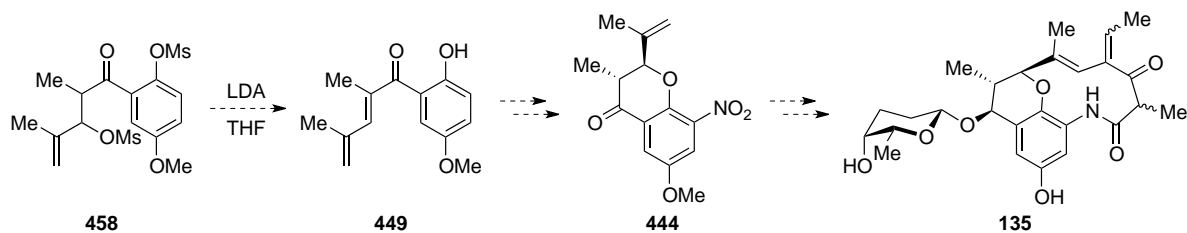


**Scheme 14.17.** Aldol Attempts to form aryl ketone **449**.

With  $\beta$ -hydroxy ketone **456** in hand we next looked to eliminate to form enone **449**. Direct elimination under a variety of conditions gave no desired product, instead in most cases giving retro-Aldol product. However **456** could be converted to bismesylate **457** and eliminated to give enone **458** (Scheme 14.18). Although the yield on this reaction is low, there has been no attempt to optimize this reaction as of yet. We believe the most direct pathway would involve subjecting **458** to two equivalents of LDA, which would both promote the elimination and removal of the phenolic mesylate in the same step.<sup>44</sup> With phenol **449** in hand we will be able to investigate the remaining steps of the synthesis towards ansaetherone (**135**) and eventually the tetrapetalones (Scheme 14.19).



**Scheme 14.18.** Synthesis of enone **458**.



**Scheme 14.19.** Proposed future work to obtain nitrobenzene **444**.

## References for Part Two

1. (a) Komoda, T.; Sugiyama, Y.; Abe, N.; Imachi, M.; Hirota, H.; Hirota, A. *Tetrahedron Lett.* **2003**, *44*, 1659-1661; (b) Komoda, T.; Sugiyama, Y.; Abe, N.; Imachi, M.; Hirota, H.; Koshino, H.; Hirota, A. *Tetrahedron Lett.* **2003**, *44*, 7417-7419; (c) Komoda, T.; Yoshida, K.; Abe, N.; Sugiyama, Y.; Imachi, M.; Hirota, H.; Koshino, H.; Hirota, A. *Biosci., Biotechnol., Biochem.* **2004**, *68*, 104-111.
2. Komoda, T.; Kishi, M.; Abe, N.; Sugiyama, Y.; Hirota, A. *Biosci., Biotechnol., Biochem.* **2004**, *68*, 903-908.
3. Komoda, T.; Akasaka, K.; Hirota, A. *Biosci., Biotechnol., Biochem.* **2008**, *72*, 2392-2397.
4. Komoda, T.; Sugiyama, Y.; Hirota, A. *Org. Biomol. Chem.* **2007**, *5*, 1615-1620.
5. (a) Wang, X.; Porco, J. A. *Angew. Chem. Int. Ed.* **2005**, *44*, 3067-3071; (b) Wang, X.; Porco, J. A. *Angew. Chem. Int. Ed.* **2006**, *45*, 6607-6607.
6. (a) Marcus, A. P.; Lee, A. S.; Davis, R. L.; Tantillo, D. J.; Sarpong, R. *Angew. Chem. Int. Ed.* **2008**, *47*, 6379-6383; (b) Marcus, A. P.; Sarpong, R. *Org. Lett.* **2010**, *12*, 4560-4563.
7. Li, C.; Li, X.; Hong, R. *Org. Lett.* **2009**, *11*, 4036-4039.
8. Yang, S.; Xi, Y.; Zhu, R.; Wang, L.; Chen, J.; Yang, Z. *Org. Lett.* **2013**, *15*, 812-815.
9. Howell, J. M. Synthetic Strategies Toward the Total Synthesis of Tetrapetalone A. Ph. D. Thesis, Colorado State University, Fort Collins, CO, 2012.
10. von Hirschheydt, T.; Voss, E. *Synthesis* **2004**, *2004*, 2062-2065.
11. Godenschwager, P. F.; Collum, D. B. *J. Am. Chem. Soc.* **2008**, *130*, 8726-8732.
12. Maruoka, K.; Imoto, H.; Saito, S.; Yamamoto, H. *J. Am. Chem. Soc.* **1994**, *116*, 4131-4132.
13. Wasserman, H. H.; Pearce, B. C. *Tetrahedron* **1988**, *44*, 3365-3372.

14. Negoro, N.; Sasaki, S.; Mikami, S.; Ito, M.; Suzuki, M.; Tsujihata, Y.; Ito, R.; Harada, A.; Takeuchi, K.; Suzuki, N.; Miyazaki, J.; Santou, T.; Odani, T.; Kanzaki, N.; Funami, M.; Tanaka, T.; Kogame, A.; Matsunaga, S.; Yasuma, T.; Momose, Y. *ACS Med. Chem. Lett.* **2010**, *1*, 290-294.
15. von Delius, M.; Geertsema, E. M.; Leigh, D. A. *Nat. Chem.* **2010**, *2*, 96-101.
16. Ishiyama, T.; Takagi, J.; Hartwig, J. F.; Miyaura, N. *Angew. Chem. Int. Ed.* **2002**, *41*, 3056-3058.
17. (a) Crisp, G. T.; Scott, W. J.; Stille, J. K. *J. Am. Chem. Soc.* **1984**, *106*, 7500-7506; (b) Stille, J. K. *Angew. Chem. Int. Ed.* **1986**, *25*, 508-524.
18. Murphy, J. M.; Liao, X.; Hartwig, J. F. *J. Am. Chem. Soc.* **2007**, *129*, 15434-15435.
19. (a) Fürstner, A. *Top. Catal.* **1997**, *4*, 285-299; (b) Fürstner, A. *Chem. Rev.* **1999**, *99*, 991-1046.
20. (a) Maier, M. E. *Angew. Chem. Int. Ed.* **2000**, *39*, 2073-2077; (b) Takao, K.-i., Tadano, K.-i. *Heterocycles* **2010**, *81*, 1603- 1629.
21. (a) Lemarchand, A.; Bach, T. *Tetrahedron* **2004**, *60*, 9659-9673; (b) Querolle, O.; Dubois, J.; Thoret, S.; Roussi, F.; Guëritte, F. o.; Guënard, D. *J. Med. Chem.* **2004**, *47*, 5937-5944; (c) Lemarchand, A.; Bach, T. *Synthesis* **2005**, *2005*, 1977-1990.
22. Majumdar, K. C.; Chattopadhyay, B.; Ansary, I. *Can. J. Chem.* **2009**, *87*, 472-477.
23. Chatterjee, A. K.; Choi, T.-L.; Sanders, D. P.; Grubbs, R. H. *J. Am. Chem. Soc.* **2003**, *125*, 11360-11370.
24. Stewart, I. C.; Ung, T.; Pletnev, A. A.; Berlin, J. M.; Grubbs, R. H.; Schrodi, Y. *Org. Lett.* **2007**, *9*, 1589-1592.
25. (a) Schoenberg, A.; Heck, R. F. *J. Am. Chem. Soc.* **1974**, *96*, 7761-7764; (b) Baillargeon, V. P.; Stille, J. K. *J. Am. Chem. Soc.* **1986**, *108*, 452-461.
26. Corminboeuf, O.; Overman, L. E.; Pennington, L. D. *J. Org. Chem.* **2009**, *74*, 5458-5470.

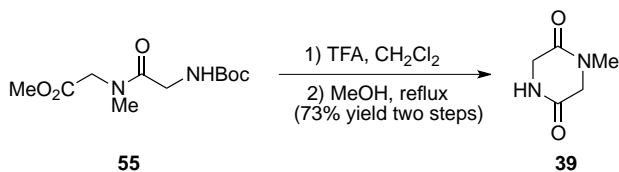
27. Montgomery, J. *Angew. Chem. Int. Ed.* **2004**, *43*, 3890-3908.
28. Chrovian, C. C.; Knapp-Reed, B.; Montgomery, J. *Org. Lett.* **2008**, *10*, 811-814.
29. Denmark, S. E.; Kobayashi, T.; Regens, C. S. *Tetrahedron* **2010**, *66*, 4745-4759.
30. Rodríguez-Berrios, R. I. R.; Torres, G.; Prieto, J. A. *Tetrahedron* **2011**, *67*, 830-836.
31. Mo, F.; Trzepakowski, L. J.; Dong, G. *Angew. Chem. Int. Ed.* **2012**, *51*, 13075-13079.
32. (a) Adler, E.; Holmberg, K.; Ryrfors, L.-O. *Acta Chem. Scand. Ser. B* **1974**, *28*, 883-887; (b) Ohkata, K.; Tamura, Y.; Shetuni, B. B.; Takagi, R.; Miyanaga, W.; Kojima, S.; Paquette, L. A. *J. Am. Chem. Soc.* **2004**, *126*, 16783-16792.
33. Hamlin, A. M.; de Jesus Cortez, F.; Lapointe, D.; Sarpong, R. *Angew. Chem. Int. Ed.* **2013**, *52*, 4854-4857.
34. (a) Keinan, E.; Peretz, M. *J. Org. Chem.* **1983**, *48*, 5302-5309; (b) Goliaszewski, A.; Schwartz, J. *Organometallics* **1985**, *4*, 417-419; (c) Trost, B. M.; Walchli, R. *J. Am. Chem. Soc.* **1987**, *109*, 3487-3488; (d) Del Valle, L.; Stille, J. K.; Hegedus, L. S. *J. Org. Chem.* **1990**, *55*, 3019-3023; (e) Farina, V.; Krishnan, B. *J. Am. Chem. Soc.* **1991**, *113*, 9585-9595; (f) Albéniz, A. C.; Espinet, P.; Martín-Ruiz, B. *Chem. Eur. J.* **2001**, *7*, 2481-2489; (g) White, J. D.; Carter, R. G.; Sundermann, K. F.; Wartmann, M. *J. Am. Chem. Soc.* **2001**, *123*, 5407-5413.
35. (a) Nozaki, K.; Oshima, K.; Uchimoto, K. *J. Am. Chem. Soc.* **1987**, *109*, 2547-2549; (b) Nozaki, K.; Oshima, K.; Utimoto, K. *Tetrahedron* **1989**, *45*, 923-933; (c) Doderio, V. n. I.; Koll, L. C.; Mandolesi, S. D.; Podestá, J. C. *J. Organomet. Chem.* **2002**, *650*, 173-180; (d) Chae, J.; Konno, T.; Kanda, M.; Ishihara, T.; Yamanaka, H. *J. Fluorine Chem.* **2003**, *120*, 185-193.
36. Gómez-Suárez, A. n.; Oonishi, Y.; Meiries, S.; Nolan, S. P. *Organometallics* **2013**, *32*, 1106-1111.
37. (a) Braunstein, P.; Zhang, J.; Welter, R. *Dalton Trans.* **2003**, 507-509; (b) Zhang, J.; Braunstein, P.; Welter, R. *Inorg. Chem.* **2004**, *43*, 4172-4177.
38. Pepper, H. P.; Kuan, K. K. W.; George, J. H. *Org. Lett.* **2012**, *14*, 1524-1527.
39. Fráter, G.; Müller, U.; Günther, W. *Tetrahedron* **1984**, *40*, 1269-1277.

40. Hata, K.; Hamamoto, H.; Shiozaki, Y.; Cämmerer, S. B.; Kita, Y. *Tetrahedron* **2007**, *63*, 4052-4060.
41. Ishikawa, T.; Oku, Y.; Kotake, K.-I. *Tetrahedron* **1997**, *53*, 14915-14928.
42. (a) Miller, J. A. *J. Org. Chem.* **1987**, *52*, 322-323; (b) Horne, S.; Rodrigo, R. *J. Org. Chem.* **1990**, *55*, 4520-4522; (c) Hardcastle, I. R.; Quayle, P. *Tetrahedron Lett.* **1994**, *35*, 1749-1750.
43. Zhang, Y.; Lee, Y. S.; Rothman, R. B.; Dersch, C. M.; Deschamps, J. R.; Jacobson, A. E.; Rice, K. C. *J. Med. Chem.* **2009**, *52*, 7570-7579.
44. Ritter, T.; Stanek, K.; Larrosa, I.; Carreira, E. M. *Org. Lett.* **2004**, *6*, 1513-1514.

## **Appendix One**

### Experimental

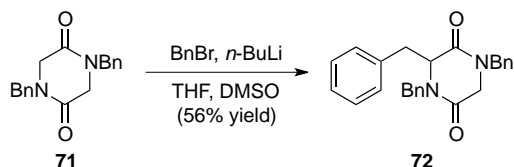
## Preparation of DKP 39



To a solution of dipeptide **55**<sup>1</sup> (1.287 g, 4.9 mmol) in CH<sub>2</sub>Cl<sub>2</sub> (49 mL) at 0 °C was added TFA (2.29 mL, 29.7 mmol). The solution was allowed to warm to room temperature and stirred overnight. The solvent was removed *in vacuo* and the crude material was used directly in the next reaction.

The crude TFA salt was dissolved in MeOH and refluxed. After two days the solvent was removed *in vacuo* and the crude material was purified by flash chromatography (5:1 CH<sub>2</sub>Cl<sub>2</sub>:MeOH) to yield DKP **39** as a white solid (0.461 g, 73% yield). Spectral data for DKP **39** was consistent with that published in the literature.<sup>1-2</sup>

## Preparation of DKP 72

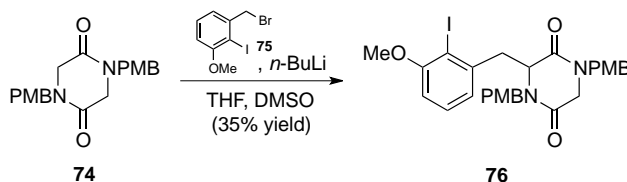


*n*-BuLi (1.93 M, 0.192 mL, 0.37 mmol) was added to a solution of THF (7 mL) and DMSO (3 mL) at 0 °C. The reaction was allowed to stir for 20 min at 0 °C then 10 min at room temperature then cooled back to 0 °C at which point known DKP **71**<sup>3</sup> (0.100 g, 0.34 mmol) in DMSO (3 mL) was added. The reaction was allowed to stir for 15 min at 0 °C then 15 min at room temperature. The reaction was cooled back to 0 °C and benzyl bromide (0.044 mL, 0.37 mmol) was added. After 1 h the reaction was warmed back to room temperature and water (20 mL) was added and extracted with EtOAc (3 × 20 mL). The combined organics were washed with water (2 × 20 mL) and brine (20 mL), dried over Na<sub>2</sub>SO<sub>4</sub>, filtered and concentrated *in*

*vacuo*. The crude material was purified by flash chromatography (6:1 CH<sub>2</sub>Cl<sub>2</sub>:Et<sub>2</sub>O) to yield DKP **72** (0.074 g, 56% yield).

<sup>1</sup>H-NMR (400 MHz; CDCl<sub>3</sub>): δ 7.36-7.25 (m, 8H), 7.19-7.13 (m, 3H), 7.06 (t, *J* = 7.6 Hz, 2H), 6.96 (d, *J* = 7.4 Hz, 2H), 5.44 (d, *J* = 14.8 Hz, 1H), 4.42 (d, *J* = 14.3 Hz, 1H), 4.28 (d, *J* = 14.3 Hz, 1H), 4.21 (t, *J* = 4.0 Hz, 1H), 3.92 (d, *J* = 14.8 Hz, 1H), 3.36 (d, *J* = 17.2 Hz, 1H), 3.22-3.10 (m, 2H), 2.33 (d, *J* = 17.1 Hz, 1H); <sup>13</sup>C-NMR (101 MHz, CDCl<sub>3</sub>): δ 165.80, 164.62, 135.33, 134.64, 134.39, 129.86, 128.99, 128.96, 128.72, 128.58, 128.43, 128.16, 128.07, 127.60, 59.98, 49.57, 48.49, 46.79, 36.74; FTIR (thin film): 3047, 3028, 2935, 1654, 1494, 1469, 1455, 1432, 1422, 1332, 1321, 1242, 1228, 1181, 1171, 1080, 1030, 1002 cm<sup>-1</sup>; HRMS (ESI-APCI) *m/z* calc'd for C<sub>25</sub>H<sub>24</sub>N<sub>2</sub>O<sub>2</sub> (M+H)<sup>+</sup>: 385.1916, found: 385.1916.

### Preparation of DKP **76**

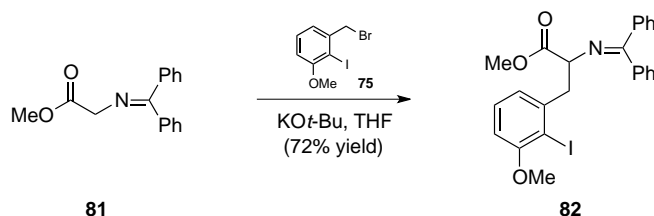


*n*-BuLi (1.93 M, 1.7 mL, 0.88 mmol) was added to a solution of DMSO (15 mL) and THF (35 mL) at 0 °C. After 35 min known DKP **74**<sup>3</sup> (0.550 g, 1.55 mmol) in DMSO (15 mL) was added. After 25 min benzyl bromide **75**<sup>4</sup> (0.558 g, 1.7 mmol) was added and allowed to stir for 2 h at which point the solution was allowed to warm to room temperature and water (30 mL) was added and extracted with EtOAc (3 × 30 mL). The combined organics were washed with water (2 × 30 mL) and brine (40 mL), dried over Na<sub>2</sub>SO<sub>4</sub>, filtered and concentrated *in vacuo*. The crude material was purified by flash chromatography (4:1 CH<sub>2</sub>Cl<sub>2</sub>:Et<sub>2</sub>O) to give DKP **76** (0.322 g, 35% yield).

<sup>1</sup>H-NMR (300 MHz; CDCl<sub>3</sub>): δ 7.16-7.04 (m, 5H), 6.88-6.81 (m, 4H), 6.76-6.70 (m, 2H), 5.24 (d, *J* = 14.9 Hz, 1H), 4.50 (d, *J* = 14.3 Hz, 1H), 4.37 (d, *J* = 14.3 Hz, 1H), 4.26 (t, *J* = 6.2

Hz, 1H), 3.90-3.89 (s, 3H), 3.83-3.79 (m, 6H), 3.67 (d,  $J = 17.1$  Hz, 1H), 3.47-3.37 (m, 3H);  $^{13}\text{C}$ -NMR (75 MHz,  $\text{CDCl}_3$ ):  $\delta$  166.01, 164.81, 159.67, 159.57, 158.62, 140.85, 130.19, 129.89, 129.40, 127.85, 127.40, 123.53, 114.48, 109.89, 93.84, 59.90, 56.78, 55.52, 49.29, 47.93, 42.58; FTIR (thin film): 3251, 2899, 2837, 1650, 1586, 1567, 1513, 1466, 1434, 1422, 1356, 1269, 1247, 1174, 1096, 1039, 1010  $\text{cm}^{-1}$ ; HRMS (ESI-APCI)  $m/z$  calc'd for  $\text{C}_{28}\text{H}_{29}\text{IN}_2\text{O}_5$  ( $\text{M}+\text{H}$ ) $^+$ : 601.1199, found: 601.1195.

### Preparation of protected amino acid **82**

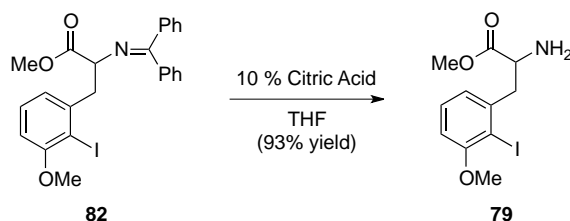


KOt-Bu (0.484 g, 4.3 mmol) was suspended in THF (18 mL) and cooled to  $-78$  °C. Known imine **81**<sup>5</sup> (0.916 g, 3.6 mmol) in THF (18 mL) was added via cannula to the suspension and allowed to stir for 30 min at which point known benzyl bromide **75**<sup>4</sup> (1.3 g, 3.97 mmol) in THF (18 mL) via cannula. After 5 h the reaction was warmed to room temperature and water (40 mL) was added and the THF was removed *in vacuo*. The aqueous solution was extracted with  $\text{CH}_2\text{Cl}_2$  (3  $\times$  20 mL) and the combined organics were washed with brine (40 mL), dried with  $\text{Na}_2\text{SO}_4$ , filtered and concentrated *in vacuo*. The crude material was purified by flash chromatography (5%  $\text{Et}_2\text{O}$ /benzene) to provide **82** as a white solid (1.299 g, 72% yield).

$^1\text{H}$ -NMR (400 MHz;  $\text{CDCl}_3$ ):  $\delta$  7.57-7.55 (m, 2H), 7.34-7.19 (m, 6H), 7.09 (t,  $J = 7.8$  Hz, 1H), 6.79 (dd,  $J = 7.6, 1.2$  Hz, 1H), 6.62-6.60 (m, 1H), 6.51-6.50 (m, 2H), 4.54 (dd,  $J = 10.0, 3.8$  Hz, 1H), 3.83 (s, 3H), 3.73 (s, 3H), 3.51 (dd,  $J = 13.3, 3.8$  Hz, 1H), 3.32 (dd,  $J = 13.3, 10.0$  Hz, 1H);  $^{13}\text{C}$ -NMR (101 MHz,  $\text{CDCl}_3$ ):  $\delta$  172.26, 171.44, 158.27, 142.26, 139.52, 136.06, 130.45, 129.05, 128.64, 128.33, 128.17, 127.84, 124.89, 109.09, 94.08, 64.53, 56.75, 52.49, 44.39; FTIR (thin film): : 3056, 2950, 2837, 1736, 1658, 1621, 1566, 1464, 1446, 1435, 1316, 1262,

1206, 1172, 1073, 1027, 1013  $\text{cm}^{-1}$ ; HRMS (ESI-APCI)  $m/z$  calc'd for  $\text{C}_{24}\text{H}_{22}\text{INO}_3$  ( $\text{M}+\text{H}$ ) $^+$ : 500.0723, found: 500.0719.

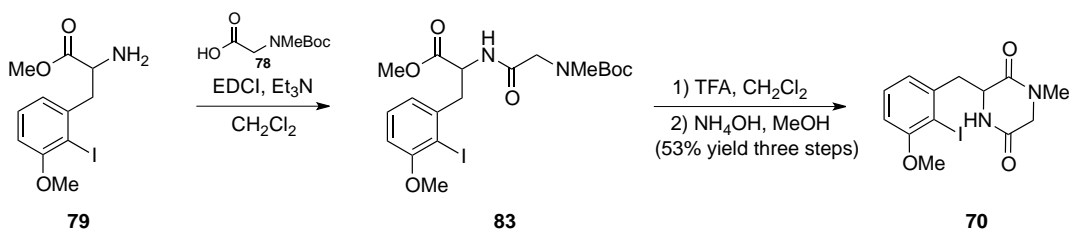
### Preparation of amino ester **79**



To a solution of imine **82** (4.82 g, 9.65 mmol) in THF (97 mL) was added a 10% solution of citric acid in water (32 mL) and allowed to stir for 16 h then the reaction was diluted with  $\text{Et}_2\text{O}$  (40 mL) and extracted with 1 N HCl (2  $\times$  30 mL). The acidic solution was washed with  $\text{Et}_2\text{O}$  (2  $\times$  30 mL) and basified with solid  $\text{K}_2\text{CO}_3$ . The basic aqueous solution was extracted with EtOAc (3  $\times$  30 mL), washed with brine (50 mL), dried with  $\text{MgSO}_4$ , filtered and concentrated *in vacuo* to yield crude **79** (3.0 g, 93% yield), which was used in the next step as is.

$^1\text{H-NMR}$  (300 MHz;  $\text{CDCl}_3$ ):  $\delta$  7.27-7.21 (m, 1H), 6.85 (dd,  $J = 7.5, 1.2$  Hz, 1H), 6.71 (dd,  $J = 8.2, 1.3$  Hz, 1H), 3.89 (s, 3H), 3.72 (s, 3H), 3.33 (dd,  $J = 13.5, 5.5$  Hz, 1H), 2.98 (dd,  $J = 13.5, 8.9$  Hz, 1H);  $^{13}\text{C-NMR}$  (75 MHz,  $\text{CDCl}_3$ ):  $\delta$  175.51, 158.55, 142.50, 129.15, 123.47, 109.47, 93.53, 56.76, 54.75, 52.29, 51.41, 46.38.

### Preparation of DKP **70**



To a solution of amine **79** (3.00 g, 8.95 mmol), Boc-sarcosine (**78**) (2.03 g, 10.7 mmol), and EDCI (1.72 g, 8.95 mmol) in  $\text{CH}_2\text{Cl}_2$  (18 mL) was added  $\text{Et}_3\text{N}$  (1.25 mL, 8.95 mmol) and the

reaction was allowed to stir for 20 h after which the reaction was diluted with CH<sub>2</sub>Cl<sub>2</sub> (20 mL) and washed with 10% HCl in water (20 mL) then sat. aq. NaHCO<sub>3</sub> (2 × 20 mL). The combined aqueous washes were extracted with CH<sub>2</sub>Cl<sub>2</sub> (2 × 20 mL) and the organics were combined and washed with brine (50 mL), dried over Na<sub>2</sub>SO<sub>4</sub>, filtered and concentrated *in vacuo*. The crude material was purified by flash chromatography (15:1 CH<sub>2</sub>Cl<sub>2</sub>:MeOH) to give dipeptide **83**.

<sup>1</sup>H-NMR (300 MHz; CDCl<sub>3</sub>): δ 7.22 (t, *J* = 7.9 Hz, 1H), 6.80 (dd, *J* = 7.6, 1.0 Hz, 1H), 6.69 (dd, *J* = 8.2, 1.0 Hz, 1H), 4.94-4.86 (m, 1H), 3.89-3.84 (s, 3H), 3.84-3.75 (m, 1H), 3.75-3.72 (s, 3H), 3.40 (dd, *J* = 14.0, 5.8 Hz, 1H), 3.25-3.18 (m, 1H), 2.83 (d, *J* = 5.1 Hz, 3H), 1.44-1.38 (s, 9H); <sup>13</sup>C-NMR (75 MHz, CDCl<sub>3</sub>): δ 171.91, 169.33, 158.52, 141.32, 129.35, 122.82, 109.66, 56.73, 52.75, 52.62, 51.39, 42.94, 35.81, 28.50.

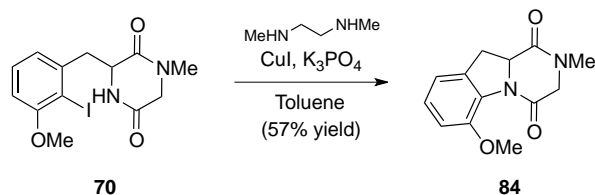
Dipeptide **83** was dissolved in CH<sub>2</sub>Cl<sub>2</sub> (90 mL) and TFA (4.1 mL, 53.7 mmol) was added. The reaction stirred overnight and the solvent was removed *in vacuo*. The crude material was purified by flash chromatography (12:1 CH<sub>2</sub>Cl<sub>2</sub>:MeOH). After column there was still a mixture of starting material and product, which was free based by dissolving in CH<sub>2</sub>Cl<sub>2</sub> (20 mL) and Et<sub>3</sub>N (1.25 mL, 8.95 mmol) was added. After stirring for 20 min, water (20 mL) was added and the solution was extracted with CH<sub>2</sub>Cl<sub>2</sub> (2 × 20 mL) and the combined organics were washed with brine (30 mL), dried over Na<sub>2</sub>SO<sub>4</sub>, filtered and concentrated *in vacuo*. The material was then used in the next step as is.

The deprotected dipeptide (2.11 g, 5.2 mmol) was dissolved in MeOH (54 mL) and NH<sub>4</sub>OH (28% in water, 5.36 mL) was added. After 1 h the solvent was removed *in vacuo*. The crude material was purified by flash chromatography (12:1 CH<sub>2</sub>Cl<sub>2</sub>:MeOH) to provide DKP **70** (1.761 g, 53% yield, three steps).

<sup>1</sup>H-NMR (300 MHz; CDCl<sub>3</sub>): δ 7.67-7.64 (m, 1H), 7.23-7.18 (m, 1H), 6.84-6.82 (m, 1H), 6.72-6.67 (m, 1H), 4.97-4.89 (m, 1H), 3.86 (s, 3H), 3.72-3.69 (s, 3H), 3.45-3.38 (m, 1H), 3.27-3.19 (m, 1H), 3.19-3.12 (m, 2H), 2.33-2.29 (s, 3H); <sup>13</sup>C-NMR (75 MHz, CDCl<sub>3</sub>): δ 172.26, 171.72, 158.49, 141.61, 129.25, 122.81, 109.60, 109.47, 93.87, 56.74, 54.60, 52.65, 52.26,

42.92, 36.87; FTIR (thin film): 3246, 2930, 1659, 1640, 1584, 1566, 1463, 1426, 1321, 1262, 1200, 1184, 1100, 1064, 1025, 1013  $\text{cm}^{-1}$ ; HRMS (ESI-APCI)  $m/z$  calc'd for  $\text{C}_{13}\text{H}_{15}\text{IN}_2\text{O}_3$  ( $\text{M}+\text{H}$ )<sup>+</sup>: 375.0206, found: 375.0199.

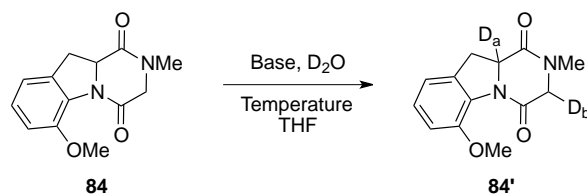
### Preparation of DKP **84**



To aryl iodide **70** (1.542 g, 4.1 mmol), CuI (0.078 g, 0.41 mmol), and K<sub>3</sub>PO<sub>4</sub> (1.741 g, 8.2 mmol) were added toluene (41 mL) then DMEDA (87.2  $\mu\text{L}$ , 0.82 mmol). The reaction was heated to 110  $^{\circ}\text{C}$  for 12 h then filtered and the solvent removed *in vacuo*. The crude material was filtered through a plug of silica gel (15:1  $\text{CH}_2\text{Cl}_2$ :MeOH) to yield DKP **84** (0.574 g, 57% yield).

<sup>1</sup>H-NMR (300 MHz;  $\text{CDCl}_3$ ):  $\delta$  7.16 (t,  $J = 7.9$  Hz, 1H), 6.91-6.88 (m, 2H), 4.80 (d,  $J = 0.6$  Hz, 1H), 4.47-4.41 (m, 1H), 3.93-3.88 (m, 4H), 3.34 (d,  $J = 9.8$  Hz, 2H), 3.06 (s, 3H); <sup>13</sup>C-NMR (75 MHz,  $\text{CDCl}_3$ ):  $\delta$  165.79, 159.61, 150.43, 134.08, 129.94, 127.94, 117.29, 112.78, 62.76, 56.68, 54.12, 35.50, 33.83; FTIR (thin film): 2937, 2838, 1653, 1606, 1486, 1464, 1461, 1418, 1406, 1343, 1292, 1271, 1213, 1145, 1122, 1065  $\text{cm}^{-1}$ ; HRMS (ESI-APCI)  $m/z$  calc'd for  $\text{C}_{13}\text{H}_{14}\text{N}_2\text{O}_3$  ( $\text{M}+\text{H}$ )<sup>+</sup>: 247.1083, found: 247.1074.

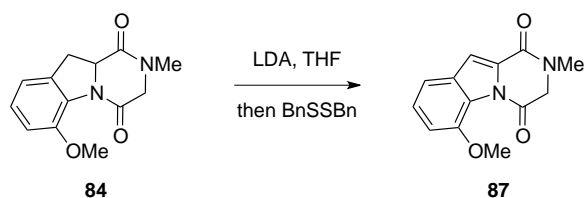
## Deuterium incorporation studies of DKP **84**



Entry	Base	Temperature (°C)	Incorporation (%)	
			D <sub>a</sub>	D <sub>b</sub>
1	LHMDS	-10	Decomp.	
2	LDA	-78	0	~100
3	LDA	0	~50	~100
4	NaH	0	~50	~100

DKP **84** (0.010 g, 0.040 mmol) was dissolved in THF (1 mL) and added to the appropriate base (2.1 equiv.) in THF (1 mL) at the given temperature. The reaction stirred for 30 min and was brought to 0 °C and D<sub>2</sub>O (1 mL) was added and stirred for 10 min. The solution was diluted with more D<sub>2</sub>O (5 mL) and extracted with EtOAc (3 × 5 mL). The combined organics were dried over MgSO<sub>4</sub>, filtered and concentrated *in vacuo*. The % deuterium incorporation was then found by integration of the relevant peaks in the crude NMR.

## Preparation of indole **87**

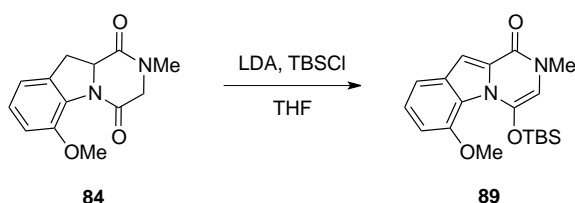


Indole **87** was obtained as a side product in various attempts outlined in Table 3.5. An example is given here. DKP (0.030 g, 0.12 mmol) in THF (4 mL) was added to a freshly prepared solution of LDA (prepared by adding *n*-BuLi (2.13 M, 0.169 mL, 0.36 mmol) to diisopropylamine (0.056 mL, 0.40 mmol) in THF (1.2 mL) at -78 °C and allowing it to stir for 30 min) at -78 °C. After 1 h BnSSBn (0.098 g, 0.040 mmol) was added and stirred for 1 h 45 min after which the reaction was warmed to 0 °C and stirred for 15 min. The reaction was quenched

with sat. aq.  $\text{NH}_4\text{Cl}$  (5 mL) and extracted with EtOAc (3  $\times$  5 mL). The combined organics were washed with brine (10 mL), dried over  $\text{MgSO}_4$ , filtered and concentrated *in vacuo*. The crude material was purified by flash chromatography (100% EtOAc) to provide DKP **87**.

$^1\text{H-NMR}$  (300 MHz;  $\text{CDCl}_3$ ):  $\delta$  7.47 (s, 1H), 7.38-7.28 (m, 2H), 7.05-7.02 (m, 1H), 4.43 (s, 2H), 4.02 (s, 3H), 3.17 (s, 3H).

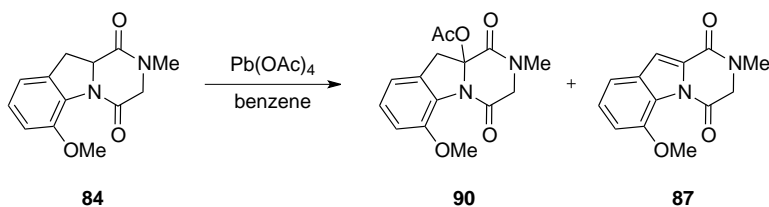
### Preparation of indole **89**



To a solution of DKP **84** (0.030 g, 0.122 mmol) in THF (1.2 mL) at 0 °C was added LDA (0.71 M, 0.38 mL, 0.268 mmol). After 1 h TBSCl (0.046 g, 0.305 mmol) in THF (1.2 mL) was added and the solution was allowed to warm to room temperature. After 3 h the reaction was quenched with sat. aq.  $\text{NH}_4\text{Cl}$  (5 mL) and extracted with EtOAc (3  $\times$  5 mL). The combined organics were washed with brine (10 mL), dried over  $\text{MgSO}_4$ , filtered and concentrated *in vacuo*. The crude material was purified by column chromatography (100% EtOAc) to provide indole **89** (0.009 g, 20% yield).

$^1\text{H-NMR}$  (400 MHz;  $\text{CDCl}_3$ ):  $\delta$  7.39 (s, 1H), 7.32 (d,  $J$  = 8.0 Hz, 1H), 7.17 (t,  $J$  = 7.9 Hz, 1H), 6.75 (d,  $J$  = 7.8 Hz, 1H), 5.67 (s, 1H), 3.85 (s, 3H), 3.36 (s, 3H), 0.86-0.82 (m, 9H), 0.10 (s, 6H).

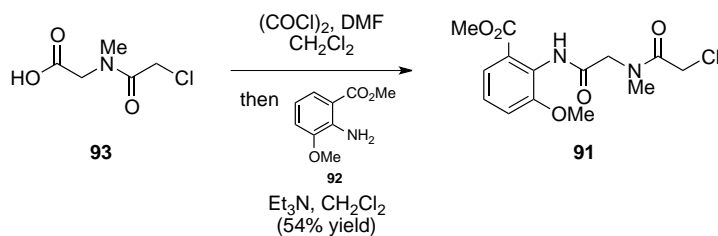
## Preparation of DKP **90** and indole **87**



To a solution of DKP **84** (0.015 g, 0.061 mmol) in benzene (1 mL) was added  $\text{Pb}(\text{OAc})_4$  (0.054 g, 0.122 mmol). After 7.5 h the reaction was filtered through celite and the solvent was removed *in vacuo*. The crude material was purified by flash chromatography (100% EtOAc) to provide DKP **90** and indole **87**.

$^1\text{H-NMR}$  (300 MHz;  $\text{CDCl}_3$ ):  $\delta$  7.22 (t,  $J = 7.9$  Hz, 1H), 6.94 (d,  $J = 7.8$  Hz, 2H), 4.70 (d,  $J = 15.4$  Hz, 1H), 3.90-3.85 (m, 4H), 3.45 (s, 2H), 3.03-3.02 (s, 3H), 2.00-1.99 (s, 3H).

## Preparation of amide **91**

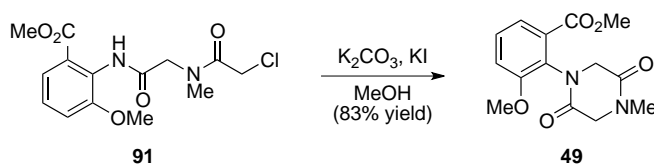


To a heterogeneous mixture of Acid **93** (11.0 g, 66.2 mmol) and  $\text{CH}_2\text{Cl}_2$  (276 mL) at 0 °C was added oxalyl chloride (6.47 mL, 71.8 mmol) followed by dimethylformamide (0.21 mL, 2.76 mmol). After 15 min the solution was allowed to warm to room temperature. After stirring for an additional 2.5 h the reaction was cooled back down to 0 °C and Aniline **92** (10.0 g, 55.2 mmol),  $\text{Et}_3\text{N}$  (17.7 mL, 127 mmol) and  $\text{CH}_2\text{Cl}_2$  (276 mL) were added slowly via an addition funnel. The solution was then allowed to warm to room temperature and stirred for 12 h. To the mixture was added 10% HCl (300 mL) and brine (100 mL) and the layers were separated. The aqueous layer was then extracted with  $\text{CH}_2\text{Cl}_2$  (100 mL) and EtOAc (2 × 100 mL) and the organic layers were combined and dried over sodium sulfate. After filtration the solvent was removed *in vacuo*

and the resulting oil was purified by flash chromatography (9:1→4:1 DCM:Et<sub>2</sub>O) to give **91** (9.8 g, 54% yield) as a yellow oil which slowly solidified.

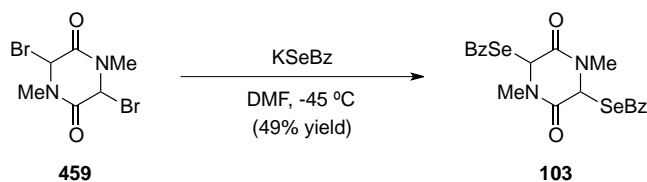
<sup>1</sup>H-NMR (300 MHz, Toluene – d<sub>8</sub>, 105 °C) δ 8.14 (br s, 1H), 7.36 (d, J = 8.0 Hz, 1H), 6.86 (t, J = 8.0 Hz, 1H), 6.65 (d, J = 8.2 Hz, 1H), 3.86 (s, 2H), 3.76 (s, 2H), 3.60 (s, 3H), 3.44 (s, 3H), 2.77 (s, 3H); <sup>13</sup>C-NMR (75 MHz, Toluene – d<sub>8</sub>, 105 °C) δ 166.9, 166.1, 154.0, 127.3, 127.1, 125.6, 122.3, 115.5, 56.0, 53.1, 51.5, 41.0, 35.8; FTIR (thin film) 3288, 3005, 2950, 2840, 1723, 1700, 1660, 1609, 1586, 1521, 1470, 1434, 1405, 1285, 1062, 751; HRMS (ESI–APCI) *m/z* calc'd for C<sub>14</sub>H<sub>17</sub>ClN<sub>2</sub>O<sub>5</sub> (M+H)<sup>+</sup>: 329.0899, found: 329.0898; m.p. 97 – 100 °C.

### Preparation of DKP **49**



A solution of Amide **91** (9.80 g, 29.8 mmol), potassium carbonate (4.94 g, 35.8 mmol), potassium iodide (1.24 g, 7.45 mmol) and MeOH (298 mL) was heated to 65 °C. After 1 h the reaction was allowed to cool to room temperature and the reaction mixture was filtered and the solvent removed *in vacuo*. The crude material was purified by flash chromatography (15:1 DCM:MeOH) to give **3** (7.2 g, 83% yield). Spectral data for DKP **49** was consistent with that published in the literature.<sup>6</sup>

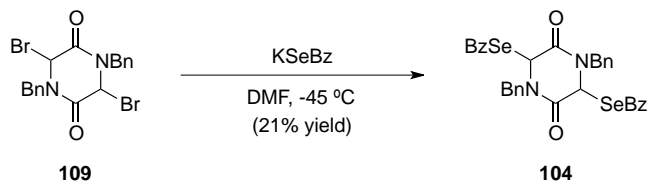
### Preparation of bisselenobenzoate **103**



Known dibromide **459**<sup>3</sup> (0.030 g, 0.1 mmol) was dissolved in DMF (1 mL) and cooled to –45 °C. KSeBz<sup>7</sup> (0.2 g, 0.045 mmol) was added and the solution was stirred for 4.5 h. The reaction was allowed to warm to room temperature and water (5 mL) was added. The solution was extracted with EtOAc (3 × 5 mL) and the combined organics were washed with water (2 × 10 mL) and brine (10 mL), dried over Na<sub>2</sub>SO<sub>4</sub>, filtered and concentrated *in vacuo*. The crude material was purified by flash chromatography (15%→30% EtOAc/hexanes) to yield bisselenobenzoate **103** (0.025 g, 49% yield).

<sup>1</sup>H-NMR (300 MHz; CDCl<sub>3</sub>): δ 7.99-7.90 (m, 4H), 7.72-7.63 (m, 2H), 7.58-7.48 (m, 4H), 6.06 (s, 2H), 3.10-2.96 (s, 6H); <sup>13</sup>C-NMR (101 MHz, CDCl<sub>3</sub>): δ 191.03, 165.21, 137.12, 134.78, 129.14, 127.94, 78.81, 60.87, 32.25; FTIR (thin film): 3061, 2927, 2854, 1729, 1677, 1447, 1396, 1291, 1242, 1200, 1171, 1062, 1037, 1023 cm<sup>-1</sup>; HRMS (ESI-APCI) *m/z* calc'd for C<sub>20</sub>H<sub>18</sub>N<sub>2</sub>O<sub>4</sub>Se<sub>2</sub> (M+H)<sup>+</sup>: 510.9675, found: 510.9666.

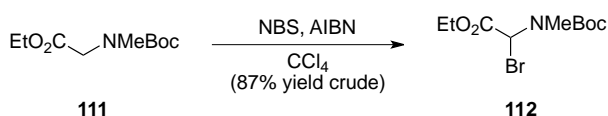
### Preparation of bisselenobenzoate **104**



The same procedure for the preparation of bisselenobenzoate **103** was followed. DKP **109** (0.384 g, 0.85 mmol) and KSeBz (0.386 g, 1.7 mmol) in DMF (8.5 mL) were used to produce bisselenobenzoate **104** (0.118 g, 21% yield).

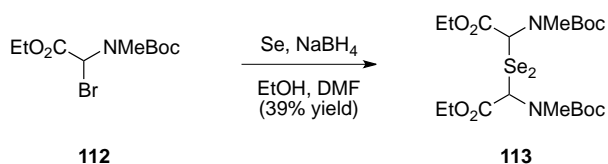
$^1\text{H-NMR}$  (400 MHz;  $\text{CDCl}_3$ ):  $\delta$  7.92-7.90 (m, 4H), 7.68-7.64 (m, 2H), 7.53-7.49 (m, 4H), 7.37-7.29 (m, 10H), 6.10 (s, 2H), 5.12 (d,  $J = 14.7$  Hz, 2H), 3.99 (d,  $J = 14.7$  Hz, 2H);  $^{13}\text{C-NMR}$  (101 MHz,  $\text{CDCl}_3$ ):  $\delta$  165.26, 135.05, 134.71, 129.10, 128.80, 128.71, 128.18, 127.99, 58.62, 47.99; FTIR (thin film): 3063, 3032, 2945, 1730, 1705, 1595, 1581, 1447, 1426, 1256, 1202, 1174, 1065  $\text{cm}^{-1}$ ; HRMS (ESI-APCI)  $m/z$  calc'd for  $\text{C}_{32}\text{H}_{26}\text{N}_2\text{O}_4\text{Se}_2$  ( $\text{M}+\text{H}$ ) $^+$ : 663.0301, found: 663.0299.

### Preparation of bromide **112**



Amino acid **111**<sup>8</sup> (0.600 g, 2.8 mmol), NBS (0.548 g, 3.1 mmol), AIBN (5 mg, 0.028 mmol) and  $\text{CCl}_4$  (28 mL) were added together and heated to 80 °C for 3 h at which point the reaction was cooled to room temperature, filtered and the solvent was removed *in vacuo* to give bromide **112** (0.723 g, 87% yield), which was used without further purification in the next step.

### Preparation of diselenide **113**

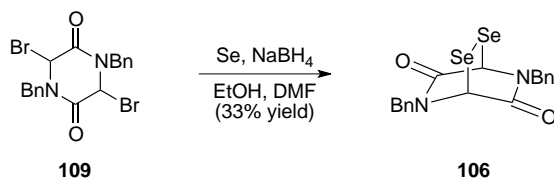


Absolute ethanol (0.12 mL, 2 mmol) was added drop wise to a flask containing selenium powder (0.027 g, 0.034 mmol) and  $\text{NaBH}_4$  (0.026 g, 0.675 mmol). The solution turned reddish brown then grey and hydrogen gas evolved. After 10 min DMF (0.7 mL) was added and the solution turned dark brown. The dark brown color slowly dissipated until it was light brown in color. After stirring for 1 h, 95% ethanol (0.080 mL) then selenium powder (0.027 g, 0.338) was added and the solution turned dark brown. After 20 min bromide **112** (0.2 g, 0.675 mmol) in

DMF (0.3 mL) was added. After 30 min the solution was heated to 70 °C and kept there for 35 min at which point the reaction was cooled to room temperature and water (10 mL) was added. The mixture was extracted with EtOAc (3 × 10 mL) and the combined organics were washed with brine (20 mL), dried over Na<sub>2</sub>SO<sub>4</sub>, filtered and concentrated *in vacuo*. The crude material was purified by flash chromatography (10% EtOAc/hexanes) to give diselenide **113** (0.078 g, 39% yield).

HRMS (ESI–APCI) *m/z* calc'd for (M+Na)<sup>+</sup>: 615.0700, found: 615.0711.

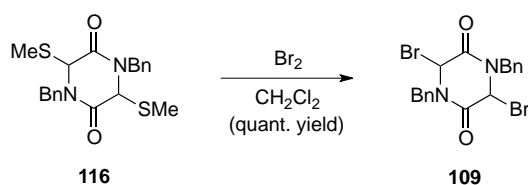
### Preparation of diselenide **106**



Absolute ethanol (0.12 mL, 2 mmol) was added drop wise to a flask containing selenium powder (0.026 g, 0.33 mmol) and NaBH<sub>4</sub> (0.025 g, 0.66 mmol). The solution turned reddish brown then white and hydrogen gas evolved. After 10 min DMF (0.66 mL) was added and the solution turned dark brown. The dark brown color slowly dissipated until the solution was colorless. After stirring for 1 h, 95% ethanol (0.077 mL) then selenium powder (0.026 g, 0.33 mmol) was added and the solution turned dark brown. After stirring for 45 min the flask was put in a MeCN/dry ice bath and dibromide **109** (0.3 g, 0.66 mmol) in DMF (2 mL) was added. The solution stirred for 1.5 h then water (10 mL) was added and extracted with EtOAc (3 × 10 mL). The combined organics were washed with water (2 × 20 mL) and brine (20 mL), dried over Na<sub>2</sub>SO<sub>4</sub>, filtered and concentrated *in vacuo* to give a reddish brown solid. The solid was purified by flash chromatography (5:45:50 Et<sub>2</sub>O:hexanes:CH<sub>2</sub>Cl<sub>2</sub>) to yield diselenide **106** as an orange solid (0.049 g, 33% yield).

$^1\text{H-NMR}$  (400 MHz,  $\text{CDCl}_3$ )  $\delta$  7.24–7.38 (m, 10H), 5.42 (s, 2H), 4.93 (d,  $J = 14.9$  Hz, 2H), 4.41 (d,  $J = 14.9$  Hz, 2H);  $^{13}\text{C-NMR}$  (100 MHz,  $\text{CDCl}_3$ )  $\delta$  189.5, 164.4, 134.0, 129.2, 128.6, 58.3, 47.6;  $^{77}\text{Se-NMR}$  (76 MHz,  $\text{CDCl}_3$ )  $\delta$  561.9; FTIR (thin film) 3065, 2975, 1671, 1444, 1418  $\text{cm}^{-1}$ ; Anal. calcd for  $\text{C}_{18}\text{H}_{16}\text{N}_2\text{O}_2\text{Se}_2$ : C, 48.02; H 3.58; N, 6.22; found C, 48.22; H, 3.65; N, 6.27; m.p. 164  $^\circ\text{C}$  (decomp.).

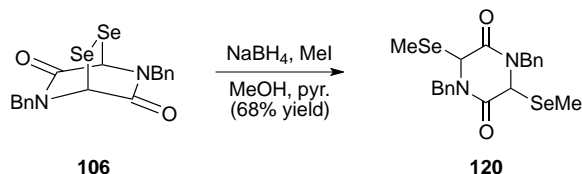
### Preparation of dibromide **109**



To a solution of bis(2-methylselenoethyl) ether **116** (0.281 g, 0.73 mmol) in  $\text{CH}_2\text{Cl}_2$  (7.3 mL) was added  $\text{Br}_2$  (0.082 mL, 1.6 mmol). After 20 min the solution was concentrated *in vacuo* to give the crude dibromide **109** (0.33 g, quant. yield) and due to instability was used crude in the next reaction.

$^1\text{H-NMR}$  (400 MHz,  $\text{CDCl}_3$ )  $\delta$  7.39–7.28 (m, 10H), 5.94 (s, 2H), 5.31 (d,  $J = 14.6$  Hz, 2H), 4.05 (d,  $J = 14.6$  Hz, 2H);  $^{13}\text{C-NMR}$  (100 MHz,  $\text{CDCl}_3$ )  $\delta$  161.5, 132.8, 129.3, 129.1, 129.0, 57.6, 48.3.

### Preparation of biselenoether **120**

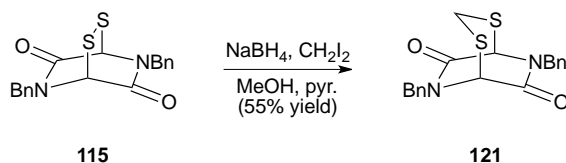


To a solution of diselenide **106** (0.128 g, 0.28 mmol) in MeOH (1.6 mL) was added pyridine (0.9 mL), MeI (0.6 mL) then  $\text{NaBH}_4$  (0.022 g, 0.57 mmol). After 1 h HCl (5 mL, 2 N in  $\text{H}_2\text{O}$ ) was added and extracted with EtOAc (3  $\times$  5 mL). The combined organics were washed

with brine (10 mL), dried over Na<sub>2</sub>SO<sub>4</sub>, filtered and concentrated *in vacuo* to give the crude bis-selenomethyl ether. The crude solid was purified by flash chromatography (15% EtOAc/hexanes) to give **120** as a white solid (0.091 g, 68% yield).

<sup>1</sup>H-NMR (400 MHz, CDCl<sub>3</sub>) δ 7.19–7.30 (m, 10H), 5.25 (d, *J* = 14.7 Hz, 2H), 4.68 (s, 2H), 4.01 (d, *J* = 14.7); <sup>13</sup>C-NMR (100 MHz, CDCl<sub>3</sub>) δ 165.1, 134.7, 129.0, 128.6, 128.3, 54.3, 47.4, 8.0; <sup>77</sup>Se-NMR (76 MHz, CDCl<sub>3</sub>) δ 250.8; FTIR (thin film) 3063, 3029, 2926, 1672, 1446, 1426 cm<sup>-1</sup>; Anal. calcd for C<sub>20</sub>H<sub>22</sub>N<sub>2</sub>O<sub>2</sub>Se<sub>2</sub>: C, 50.01; H, 4.62; N, 5.83; found C, 50.34; H, 4.75; N, 5.75; m.p. 105–108 °C.

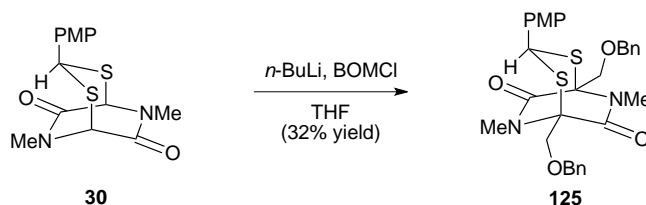
### Preparation of dithioacetal **121**



To a solution of disulfide **115** (0.1 g, 0.28 mmol) in MeOH (1.5 mL) was added pyridine (1 mL), CH<sub>2</sub>I<sub>2</sub> (0.6 mL) then NaBH<sub>4</sub> (0.021 g, 0.56 mmol). After 10 min another portion of CH<sub>2</sub>I<sub>2</sub> (0.6 mL) was added. After stirring for 2 h, HCl (10 mL, 2 N in H<sub>2</sub>O) was added and extracted with EtOAc (3 × 10 mL). The combined organics were washed with brine (15 mL), dried over Na<sub>2</sub>SO<sub>4</sub>, filtered and concentrated *in vacuo*. The crude material was purified by flash chromatography (10%→30% EtOAc/hexanes) to give diketopiperazine **121** as a white solid (0.057 g, 55% yield).

<sup>1</sup>H-NMR (400 MHz, CDCl<sub>3</sub>) δ 7.24–7.35 (m, 10H), 5.14 (d, *J* = 14.8, 2H), 4.85 (s, 2H), 4.16 (d, *J* = 14.8, 2H), 3.86 (s, 2H); <sup>13</sup>C-NMR (100 MHz, CDCl<sub>3</sub>) δ 189.5, 164.6, 134.1, 129.1, 128.5, 60.3, 47.9, 29.3; FTIR (thin film) 3064, 3031, 2966, 1676, 1447, 1423 cm<sup>-1</sup>; HRMS (ESI–APCI) *m/z* calc'd for C<sub>19</sub>H<sub>18</sub>N<sub>2</sub>O<sub>2</sub>S<sub>2</sub> (M+H)<sup>+</sup> 371.4964, found 371.0887; m.p. 189–192 °C.

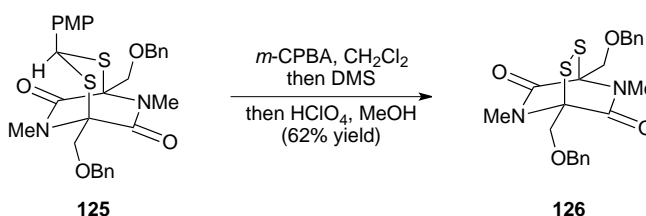
## Preparation of dithioacetal **125**



A solution of known dithioacetal **30**<sup>6a</sup> (1.7 g, 5.24 mmol) and BOMCl (7.3 mL, 52.4 mmol) in THF (210 mL) was cooled to  $-78^\circ\text{C}$ .  $n\text{-BuLi}$  (2.6 M, 4.64 mL, 12.05 mmol) was added over 1 h 15 min. After 40 min the reaction was allowed to warm to room temperature and stirred for 5 h. The reaction was quenched with sat. aq.  $\text{NH}_4\text{Cl}$  (150 mL) and extracted with EtOAc ( $3 \times 100$  mL). The combined organics were washed with brine (200 mL), dried over  $\text{MgSO}_4$ , filtered and concentrated *in vacuo*. The crude material was purified by flash chromatography (15%→30% EtOAc/hexanes then 1%  $\text{Et}_2\text{O}/\text{CH}_2\text{Cl}_2$ ) to give dithioacetal **125** (0.961 g, 32% yield).

$^1\text{H-NMR}$  (300 MHz;  $\text{CDCl}_3$ ):  $\delta$  7.38-7.24 (m, 12H), 6.83-6.80 (m, 2H), 4.94 (s, 1H), 4.76-4.66 (m, 2H), 4.55 (dd,  $J = 12.3$  Hz, 2H), 4.44 (d,  $J = 10.6$  Hz, 1H), 4.25 (d,  $J = 10.5$  Hz, 1H), 3.81-3.75 (m, 5H), 3.25-3.23 (s, 3H), 3.16 (s, 3H).

## Preparation of disulfide **126**

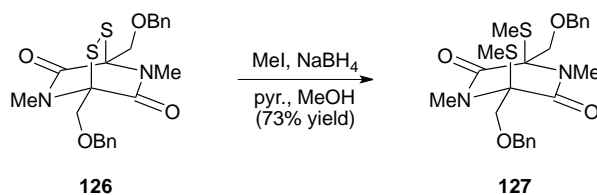


Dithioacetal **125** (0.300 g, 0.53 mmol) was dissolved in  $\text{CH}_2\text{Cl}_2$  (117 mL) and  $m\text{CPBA}$  (0.143 g, 0.83 mmol) was added. After stirring for 8 min DMS (0.050 mL, 0.64 mmol) and then 2 min later a 5:1 mixture of  $\text{MeOH}:\text{HClO}_4$  (1.06 mL) was added. After stirring for 19 h sat. aq.  $\text{NaHCO}_3$  (5 mL) was added and extracted with EtOAc ( $3 \times 5$  mL). The combined organics were washed with brine (10 mL), dried over  $\text{MgSO}_4$ , filtered and concentrated *in vacuo*. The crude

material was purified by flash chromatography (10%→20% EtOAc/hexanes) to give pure disulfide **126** (0.145 g, 62% yield).

$^1\text{H-NMR}$  (300 MHz;  $\text{CDCl}_3$ ):  $\delta$  7.39-7.29 (m, 10H), 4.77-4.67 (m, 4H), 4.29-4.21 (m, 4H), 3.16-3.14 (m, 6H).

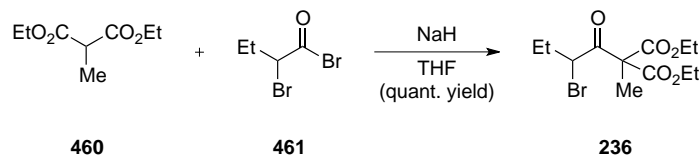
### Preparation of bisthiomethyl ether **127**



Disulfide **126** (0.270 g, 0.61 mmol) was dissolved in MeOH (3.4 mL), pyridine (2 mL), and MeI (1.4 mL) and cooled to 0 °C. Solid  $\text{NaBH}_4$  (0.046 g, 1.2 mmol) was added and after 15 min the reaction was allowed to warm to room temperature. After 3 h 15 min 1 N HCl (5 mL) was added and the mixture was extracted with EtOAc (3 × 5 mL). The combined organics were washed with brine (10 mL), dried over  $\text{MgSO}_4$ , filtered and concentrated *in vacuo*. The crude material was purified by flash chromatography (30% EtOAc/hexanes) to give bithiomethyl ether **127** (0.211 g, 73% yield).

$^1\text{H-NMR}$  (400 MHz;  $\text{CDCl}_3$ ):  $\delta$  7.34-7.19 (m, 10H), 4.45 (d,  $J = 12.2$  Hz, 2H), 4.31 (d,  $J = 12.2$  Hz, 2H), 4.17 (d,  $J = 10.1$  Hz, 2H), 3.71 (d,  $J = 10.1$  Hz, 2H), 3.08 (s, 6H), 2.19 (s, 6H);  $^{13}\text{C-NMR}$  (101 MHz,  $\text{CDCl}_3$ ):  $\delta$  165.00, 137.56, 128.31, 127.59, 126.92, 73.18, 70.90, 65.11, 65.08, 29.66, 13.52; FTIR (thin film): 3467, 3062, 3029, 2923, 2866, 1496, 1453, 1425, 1381, 1244, 1205, 1101, 1026  $\text{cm}^{-1}$ ; HRMS (ESI-APCI)  $m/z$  calc'd for  $\text{C}_{24}\text{H}_{30}\text{N}_2\text{NaO}_4\text{S}_2$  ( $\text{M}+\text{Na}$ ) $^+$ : 497.1545, found: 497.1541.

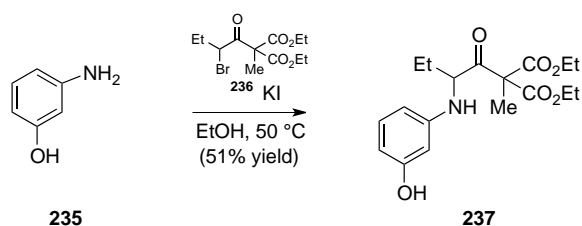
## Preparation of bromoketone **236**



NaH (60% in mineral oil, 7.0 g, 0.29 mol) was suspended in THF (265 mL) and cooled to 0 °C. Malonate **460** (27.1 mL, 0.159 mol) was added portionwise over 50 min while H<sub>2</sub> evolved. The reaction was warmed to room temperature, stirred at that temperature for 30 min, then was cooled back to 0 °C. Acid bromide **461** (21.1 mL, 0.175 mol) was added and the reaction was allowed to warm to room temperature. The solution became cloudy as NaBr crashed out and after stirring for 17 h was filtered through celite three times then silica gel once to provide bromoketone **236** as a yellow oil (51.9 g, quant. yield).

<sup>1</sup>H-NMR (400 MHz; CDCl<sub>3</sub>): δ 4.68 (dd, *J* = 9.0, 4.9 Hz, 1H), 4.27-4.17 (m, 4H), 2.05-1.99 (m, 2H), 1.67 (s, 3H), 1.26 (dt, *J* = 15.3, 7.1 Hz, 6H), 1.04 (t, *J* = 7.3 Hz, 3H); <sup>13</sup>C-NMR (101 MHz, CDCl<sub>3</sub>): δ 195.86, 168.47, 167.59, 66.32, 62.73, 62.33, 51.17, 26.96, 18.03, 13.83, 13.78, 11.81; FTIR (thin film): 2981, 2940, 2908, 2879, 1719, 1449, 1380, 1256, 1110, 1014 cm<sup>-1</sup>; HRMS (ESI-APCI) *m/z* calc'd for C<sub>12</sub>H<sub>19</sub>BrO<sub>5</sub> (M+H)<sup>+</sup>: 323.0494, found: 323.0493.

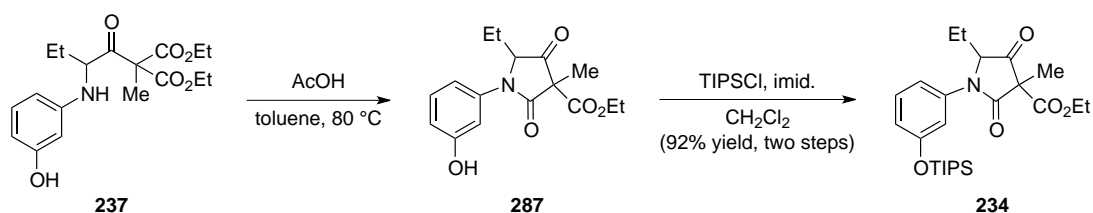
## Preparation of aniline **237**



A solution of 3-aminophenol (**235**) (2.18 g, 20.0 mmol), alkyl bromide **236** (3.23 g, 10 mmol), and KI (0.166 g, 1.0 mmol) was heated to 50 °C for 48 h. All volatiles were removed *in vacuo* and the crude mixture was purified via flash chromatography (30% EtOAc/hexanes) to yield aniline **237** (1.79 g, 51% yield) as a reddish brown oil.

$^1\text{H-NMR}$  (500 MHz;  $\text{CDCl}_3$ ):  $\delta$  6.99 (t,  $J = 8.0$  Hz, 1H), 6.21 (dd,  $J = 7.9, 1.7$  Hz, 1H), 6.17 (dd,  $J = 8.1, 1.6$  Hz, 1H), 6.09 (t,  $J = 2.1$  Hz, 1H), 5.29 (s, 1H), 4.40-4.34 (m, 2H), 4.22-4.14 (m, 2H), 3.94-3.89 (m, 2H), 1.96 (ddd,  $J = 14.1, 7.3, 4.6$  Hz, 1H), 1.72 (dt,  $J = 14.7, 6.3$  Hz, 1H), 1.65 (d,  $J = 22.3$  Hz, 3H), 1.26 (q,  $J = 6.8$  Hz, 3H), 1.14 (t,  $J = 7.1$  Hz, 3H), 0.92 (t,  $J = 7.4$  Hz, 3H);  $^{13}\text{C-NMR}$  (126 MHz,  $\text{CDCl}_3$ ):  $\delta$  203.88, 168.78, 168.67, 156.78, 147.79, 130.15, 106.16, 105.44, 100.30, 64.94, 62.41, 62.27, 61.15, 24.84, 19.25, 13.86, 13.73, 9.77; FTIR (thin film): 3396, 2980, 2940, 2908, 2878, 1717, 1600, 1517, 1498, 1451, 1378, 1264, 1161, 1114, 1017  $\text{cm}^{-1}$ ; HRMS (ESI-APCI)  $m/z$  calc'd for  $\text{C}_{18}\text{H}_{26}\text{NO}_6$  ( $\text{M}+\text{H}$ ) $^+$ : 352.1755, found: 352.1764.

### Preparation of ketone **239**



A solution of aniline **237** (1.79 g, 5.08 mmol) and acetic acid (5.0 mL) in toluene (50 mL) was heated to 80 °C overnight. All volatiles were removed *in vacuo* and the crude mixture was purified via flash chromatography (30% EtOAc/hexanes) to yield phenol **287** (1.44 g, 93% yield) as a separable mixture of diastereomers.

Higher  $R_f$  diastereomer:  $^1\text{H-NMR}$  (500 MHz;  $\text{CDCl}_3$ ):  $\delta$  7.26-7.23 (m, 1H), 7.03 (t,  $J = 2.1$  Hz, 1H), 6.83 (dd,  $J = 7.9, 1.2$  Hz, 1H), 6.75 (s, 1H), 6.75-6.71 (m, 1H), 4.77 (dd,  $J = 5.6, 2.9$  Hz, 1H), 4.23-4.18 (m, 2H), 1.97 (ddt,  $J = 14.8, 7.4, 3.7$  Hz, 1H), 1.81-1.75 (m, 1H), 1.63 (s, 3H), 1.29-1.23 (m, 3H), 0.75 (t,  $J = 7.4$  Hz, 2H);  $^{13}\text{C-NMR}$  (126 MHz,  $\text{CDCl}_3$ ):  $\delta$  204.90, 169.73, 165.11, 157.10, 136.22, 130.15, 115.31, 114.87, 112.39, 68.24, 62.96, 59.76, 21.28, 14.96, 13.90, 7.99; FTIR (thin film): 3331, 2972, 2939, 2881, 1778, 1747, 1683, 1608, 1596, 1492, 1460, 1407, 1298, 1222, 1159, 1126, 1108, 1048, 1009; HRMS (ESI-APCI)  $m/z$  calc'd for  $\text{C}_{16}\text{H}_{20}\text{NO}_5$  ( $\text{M}+\text{H}$ ) $^+$ : 306.1336, found: 306.1340.

Lower R<sub>f</sub> diastereomer: <sup>1</sup>H-NMR (500 MHz; CDCl<sub>3</sub>): δ 7.28-7.25 (m, 1H), 7.11 (t, *J* = 2.2 Hz, 1H), 6.82 (dt, *J* = 8.0, 0.9 Hz, 1H), 6.74 (ddd, *J* = 8.2, 2.4, 0.8 Hz, 1H), 6.35 (s, 1H), 4.52 (dd, *J* = 7.2, 3.7 Hz, 1H), 4.27-4.19 (m, 2H), 1.98 (ddd, *J* = 14.5, 7.5, 3.7 Hz, 1H), 1.87 (dt, *J* = 14.5, 7.3 Hz, 1H), 1.63 (s, 3H), 1.27-1.24 (m, 3H), 0.89 (t, *J* = 7.5 Hz, 3H); <sup>13</sup>C-NMR (126 MHz, CDCl<sub>3</sub>): δ 204.61, 169.54, 165.35, 156.88, 136.28, 130.13, 114.97, 114.51, 112.16, 67.54, 62.79, 59.66, 22.50, 17.19, 13.87, 8.67; FTIR (thin film): 3320, 2980, 2940, 2882, 1776, 1745, 1682, 1596, 1492, 1460, 1407, 1297, 1215, 1158, 1106, 1046, 1011.

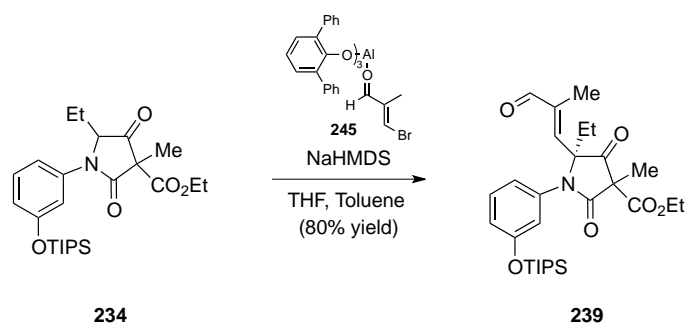
To a solution of phenol **287** (0.811 g, 2.66 mmol) in CH<sub>2</sub>Cl<sub>2</sub> (27 mL) was added imidazole (0.271 g, 3.98 mmol) and TIPSCl (0.739 mL, 3.45 mmol). The reaction mixture was stirred overnight at room temperature then quenched with water (30 mL). The phases were separated and the aqueous layer was extracted with CH<sub>2</sub>Cl<sub>2</sub> (2 x 20 mL). The combined organics were dried over MgSO<sub>4</sub>, filtered and concentrated *in vacuo*. The crude material was purified via flash chromatography (10% EtOAc/hexanes) to yield ketone **234** (1.21 g, 99% yield) as a separable mixture of diastereomers as an off-white waxy solid.

Higher R<sub>f</sub> diastereomer: <sup>1</sup>H-NMR (500 MHz; CDCl<sub>3</sub>): δ 7.27 (t, *J* = 8.0 Hz, 1H), 6.99 (t, *J* = 2.4 Hz, 2H), 6.82 (d, *J* = 8.1 Hz, 1H), 4.76 (dd, *J* = 5.2, 2.6 Hz, 1H), 4.19 (q, *J* = 7.1 Hz, 2H), 1.97 (s, 1H), 1.78 (d, *J* = 6.8 Hz, 1H), 1.58 (d, *J* = 12.8 Hz, 3H), 1.26 (m, 6H), 1.10 (s, 18H), 0.74 (t, *J* = 7.3 Hz, 3H); <sup>13</sup>C-NMR (126 MHz, CDCl<sub>3</sub>): δ 205.41, 168.61, 165.17, 156.74, 136.74, 129.81, 118.44, 116.63, 116.12, 67.78, 62.72, 59.58, 21.22, 17.86, 14.87, 13.86, 12.63, 7.89; FTIR (thin film): 2966, 2945, 2893, 2869, 1780, 1749, 1709, 1598, 1490, 1463, 1449, 1388, 1297, 1221, 1183, 1158, 1126, 1107, 1073, 1048, 1005; HRMS (ESI-APCI) *m/z* calc'd for C<sub>25</sub>H<sub>40</sub>NO<sub>5</sub>Si (M+H)<sup>+</sup>: 462.2670, found: 462.2676.

Lower R<sub>f</sub> diastereomer: <sup>1</sup>H-NMR (500 MHz; CDCl<sub>3</sub>): δ 7.28-7.25 (m, 1H), 7.01 (t, *J* = 2.1 Hz, 1H), 6.98 (d, *J* = 8.0 Hz, 1H), 6.81-6.80 (m, 1H), 4.49 (dd, *J* = 7.2, 3.6 Hz, 1H), 4.25 (dd, *J* = 7.1, 3.5 Hz, 2H), 1.87 (d, *J* = 7.3 Hz, 1H), 1.60 (s, 3H), 1.26 (dt, *J* = 14.3, 5.4 Hz, 6H), 1.11 (d, *J* = 7.3 Hz, 18H), 0.88 (t, *J* = 7.5 Hz, 3H); <sup>13</sup>C-NMR (126 MHz, CDCl<sub>3</sub>): δ 205.14, 168.67, 165.52,

156.70, 136.55, 129.79, 118.33, 116.27, 116.03, 67.24, 62.58, 22.46, 17.86, 17.17, 13.86, 12.61, 8.64; FTIR (thin film): 2945, 2894, 2869, 1775, 1732, 1702, 1599, 1496, 1447, 1395, 1306, 1255, 1232, 1160, 1127, 1107, 1052, 1005.

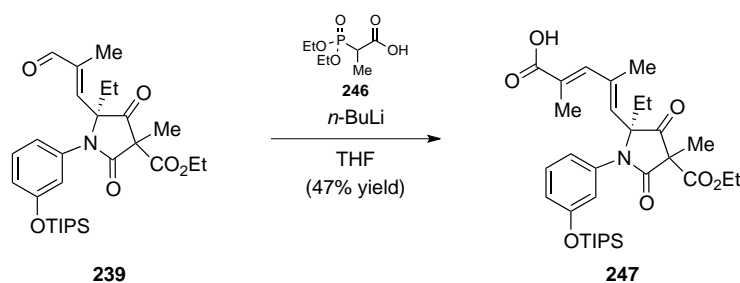
### Preparation of enal **239**



To a  $-78\text{ }^{\circ}\text{C}$  solution of ketone **234** (3.63 g 7.86 mmol) in THF (80 mL) was added NaHMDS (8.65 mL, 1.0 M in THF, 8.65 mmol) and the reaction mixture was allowed to warm slowly to  $-50\text{ }^{\circ}\text{C}$  then cooled to  $-78\text{ }^{\circ}\text{C}$ . Meanwhile, the vinyl bromide (1.76 g, 11.8 mmol) was added slowly to a solution of the bulky Lewis acid (generated from slow addition of  $\text{AlMe}_3$  (7.03 mL, 2.0 M in hexanes, 14.07 mmol) to a solution of 2,6-diphenylphenol (9.90 g, 40.2 mmol) in toluene (70 mL) at room temperature) at  $-78\text{ }^{\circ}\text{C}$  and maintained for 20 min. The solution containing aldehyde complex **245** was then transferred via cannula to the sodium enolate of ketone **234**. The reaction mixture was maintained at  $-78\text{ }^{\circ}\text{C}$  for 1 h then allowed to warm slowly to room temperature over 3 h. The reaction mixture was quenched with sat. aq. Rochelle's salt (100 mL), stirred vigorously overnight, and extracted with EtOAc (3 x 100 mL). The combined organics were dried over  $\text{MgSO}_4$ , filtered and concentrated *in vacuo*. The crude material was purified via flash chromatography (5%→10% EtOAc/hexanes) to yield enal **239** (3.33 g, 80% yield) as an inseparable mixture of diastereomers as a light brown oil. The major diastereomer is characterized.

$^1\text{H-NMR}$  (500 MHz;  $\text{CDCl}_3$ ):  $\delta$  9.40 (s, 1H), 7.25 (m, 1H), 6.97-6.95 (m, 1H), 6.92 (t,  $J = 2.2$  Hz, 1H), 6.84 (ddd,  $J = 8.2, 2.3, 0.7$  Hz, 1H), 6.47 (d,  $J = 1.4$  Hz, 1H), 4.28 (qd,  $J = 7.1, 3.0$  Hz, 2H), 2.42 (dd,  $J = 14.6, 7.3$  Hz, 1H), 2.18 (dd,  $J = 14.6, 7.4$  Hz, 1H), 1.89 (s, 3H), 1.62 (s, 3H), 1.29 (t,  $J = 7.2$  Hz, 3H), 1.25-1.18 (m, 3H), 1.10-1.04 (m, 18H), 0.83 (t,  $J = 7.4$  Hz, 3H);  $^{13}\text{C-NMR}$  (126 MHz,  $\text{CDCl}_3$ ):  $\delta$  203.07, 193.82, 169.39, 165.22, 156.64, 149.71, 142.03, 136.09, 129.88, 119.22, 117.50, 116.66, 62.89, 58.82, 27.78, 17.79, 13.87, 12.57, 10.30, 8.06; FTIR (thin film): 2946, 2868, 1777, 1751, 1710, 1598, 1491, 1463, 1378, 1354, 1284, 1225, 1124, 1004; HRMS (ESI-APCI)  $m/z$  calc'd for  $\text{C}_{29}\text{H}_{44}\text{NO}_6\text{Si}$  ( $\text{M}+\text{H}$ ) $^+$ : 530.2932, found: 530.2941.

### Preparation of carboxylic acid **247**

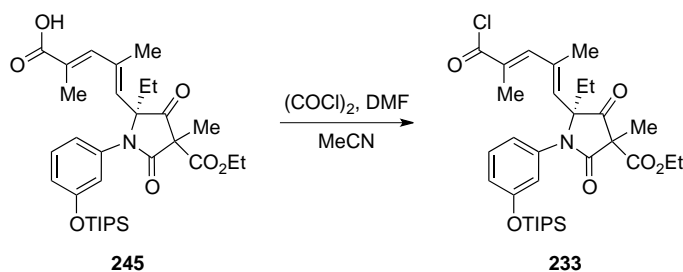


To a  $-78$  °C solution of phosphonate **246** (0.436 g 2.08 mmol) in THF (20 mL) was added  $n\text{-BuLi}$  (2.79 mL, 1.49 M, 4.15 mmol). After 40 min enal **239** (1.0 g, 1.89 mmol) in THF (5.0 mL) was added slowly. The reaction mixture was maintained at  $-78$  °C for 1 h then allowed to warm slowly to  $0$  °C and quenched with sat. aq.  $\text{NH}_4\text{Cl}$  (25 mL) and extracted with EtOAc (3 x 25 mL). The combined organics were dried over  $\text{MgSO}_4$ , filtered and concentrated *in vacuo*. The crude material was purified via flash chromatography (20%→30%→60% EtOAc/hexanes) to yield carboxylic acid **247** (0.515 g, 47% yield) as an inseparable mixture of diastereomers as a colorless oil and unreacted enal **239** (0.215 g, 22% yield). The major diastereomer of the product is characterized.

$^1\text{H-NMR}$  (500 MHz;  $\text{CDCl}_3$ ):  $\delta$  7.26-7.22 (m, 1H), 7.15 (s, 1H), 7.01 (dd,  $J = 8.1, 1.1$  Hz, 1H), 6.95 (t,  $J = 2.1$  Hz, 1H), 6.83 (dd,  $J = 8.2, 1.6$  Hz, 1H), 5.57 (s, 1H), 4.26 (q,  $J = 7.1$  Hz,

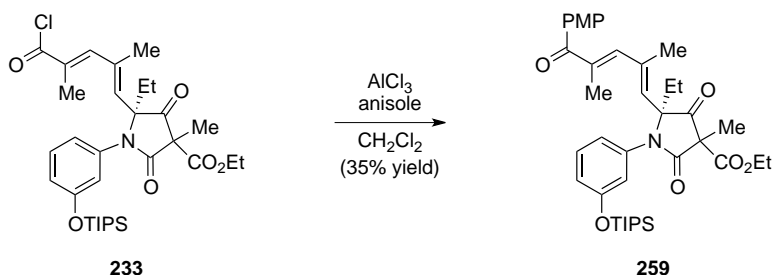
2H), 2.26 (dd,  $J = 14.5, 7.3$  Hz, 1H), 2.11 (dd,  $J = 14.5, 7.4$  Hz, 1H), 1.93 (s, 3H), 1.92 (s, 3H), 1.68 (s, 3H), 1.28 (t,  $J = 7.1$  Hz, 3H), 1.26-1.18 (m, 3H), 1.08 (dd,  $J = 7.4, 1.6$  Hz, 18H), 0.82 (q,  $J = 6.7$  Hz, 3H);  $^{13}\text{C-NMR}$  (126 MHz,  $\text{CDCl}_3$ ):  $\delta$  204.02, 169.59, 165.58, 156.51, 143.80, 138.05, 136.36, 132.22, 129.68, 119.11, 118.40, 117.38, 76.04, 62.76, 58.77, 50.69, 45.27, 28.84, 28.28, 17.78, 13.86, 12.60, 8.07; FTIR (thin film): 2946, 2869, 2653, 2529, 2253, 1775, 1748, 1714, 1635, 1598, 1489, 1463, 1379, 1285, 1122, 1004; HRMS (ESI-APCI)  $m/z$  calc'd for  $\text{C}_{32}\text{H}_{48}\text{NO}_7\text{Si}$  ( $\text{M}+\text{H}$ ) $^+$ : 586.3203, found: 586.3203.

### Preparation of acid chloride **233**



To a solution of carboxylic acid **245** (0.100 g, 0.171 mmol) in acetonitrile (5 mL) was added oxalyl chloride (0.017 mL, 0.205 mmol) and DMF (1 drop). The reaction was vented with a needle until effervescence ceased, then maintained under a positive pressure of  $\text{N}_2$  overnight. All volatiles were removed under full vacuum to yield acid chloride **233** (0.105 mg) as a crude oil, which was used without further purification.

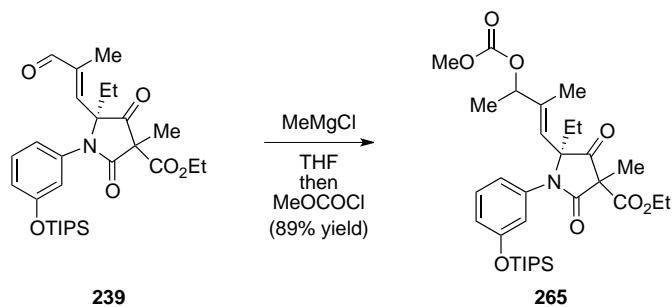
## Preparation of ketone **259**



To a 0 °C solution of acid chloride **233** (20.6 mg, 0.0341 mmol) in CH<sub>2</sub>Cl<sub>2</sub> (5.0 mL) was added AlCl<sub>3</sub> (0.009 g, 0.0683 mmol) and anisole (0.050 mL, 0.460 mmol). The reaction mixture was allowed to warm to room temperature and maintained overnight. After addition of sat. aq. Rochelle's salt (5 mL) the reaction was stirred vigorously for 2 h and the mixture was extracted with EtOAc (3 x 5 mL). The combined organics were dried over MgSO<sub>4</sub>, filtered and concentrated *in vacuo*. The crude material was purified by flash chromatography (20% EtOAc/hexanes) to yield ketone **259** (0.008 mg, 35% yield) as an inseparable mixture of diastereomers as a colorless oil. The major diastereomer of the product is characterized.

<sup>1</sup>H-NMR (500 MHz; CDCl<sub>3</sub>): δ 7.70 (d, *J* = 8.8 Hz, 2H), 7.23 (d, *J* = 8.1 Hz, 1H), 7.02-7.01 (m, 1H), 6.98 (d, *J* = 2.0 Hz, 1H), 6.93 (d, *J* = 8.8 Hz, 2H), 6.84-6.82 (m, 1H), 6.43 (s, 1H), 5.58 (s, 1H), 4.27 (q, *J* = 7.1 Hz, 2H), 3.88-3.86 (s, 3H), 2.27 (dd, *J* = 14.5, 7.3 Hz, 1H), 2.13 (dd, *J* = 14.5, 7.3 Hz, 1H), 2.04-2.02 (s, 3H), 1.90 (s, 3H), 1.69 (s, 3H), 1.29 (t, *J* = 7.1 Hz, 3H), 1.27-1.18 (m, 3H), 1.11-1.04 (m, 18H), 0.82 (q, *J* = 6.7 Hz, 3H); <sup>13</sup>C-NMR (126 MHz, CDCl<sub>3</sub>): δ 204.18, 197.78, 169.58, 165.63, 162.92, 156.49, 142.04, 138.08, 136.90, 136.48, 131.80, 131.10, 130.05, 129.63, 118.99, 118.22, 117.43, 113.55, 76.13, 62.75, 58.76, 55.44, 28.85, 18.07, 17.82, 14.88, 13.87, 12.58, 8.10; FTIR (thin film): 2943, 2868, 1774, 1748, 1708, 1647, 1599, 1509, 1490, 1461, 1376, 1354, 1283, 1254, 1173, 1149, 1111, 1005; HRMS (ESI-APCI) *m/z* calc'd for C<sub>39</sub>H<sub>54</sub>NO<sub>7</sub>Si (M+H)<sup>+</sup>: 676.3664, found: 676.3673.

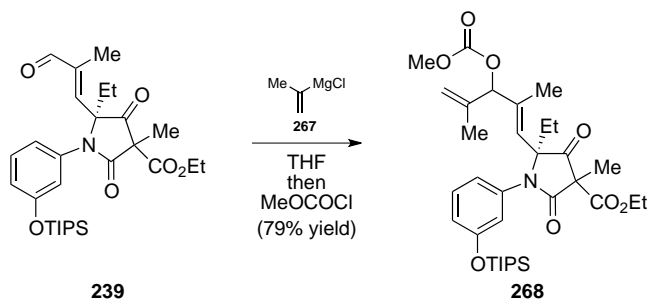
## Preparation of allylic carbonate **265**



To a solution of enal **239** (0.222 g, 0.419 mmol) in THF (5 mL) cooled to  $-78\text{ }^{\circ}\text{C}$  was added MeMgCl (0.210 mL, 3.0 M in THF, 0.630 mmol) and maintained for 1.5 h. Methyl chloroformate (0.097 mL, 1.26 mmol) was then added and the reaction mixture was allowed to warm slowly to room temperature then quenched with sat. aq.  $\text{NaHCO}_3$  (5 mL) and extracted with  $\text{Et}_2\text{O}$  (3 x 5 mL). The combined organics were dried over  $\text{MgSO}_4$ , filtered and concentrated *in vacuo*. The crude material was purified by flash chromatography (10%→30% EtOAc/hexanes) to yield allylic carbonate **265** (0.225 g, 89% yield) as an inseparable mixture of diastereomers as a colorless oil.

$^1\text{H-NMR}$  (500 MHz;  $\text{CDCl}_3$ ):  $\delta$  7.21 (q,  $J = 8.4$  Hz, 1H), 7.01 (dt,  $J = 15.8, 2.2$  Hz, 1H), 6.97-6.95 (m, 1H), 6.82-6.79 (m, 1H), 5.65 (d,  $J = 21.7$  Hz, 1H), 4.99 (dd,  $J = 6.5, 3.4$  Hz, 1H), 4.26-4.22 (m, 2H), 3.74 (d,  $J = 3.1$  Hz, 2H), 2.29-2.26 (m, 1H), 2.04 (td,  $J = 7.3, 3.4$  Hz, 1H), 1.76 (dd,  $J = 5.4, 1.1$  Hz, 3H), 1.63-1.60 (m, 3H), 1.35-1.31 (m, 3H), 1.29-1.20 (m, 6H), 1.09-1.04 (m, 18H), 0.74 (tt,  $J = 7.6, 3.9$  Hz, 3H);  $^{13}\text{C-NMR}$  (126 MHz,  $\text{CDCl}_3$ ):  $\delta$  204.22, 204.02, 169.63, 165.80, 165.78, 156.37, 154.78, 154.74, 140.99, 140.91, 136.49, 136.44, 129.51, 129.45, 126.59, 125.89, 118.73, 118.69, 117.80, 117.54, 117.47, 79.09, 78.89, 76.02, 75.95, 62.58, 62.56, 58.74, 58.67, 54.70, 27.80, 27.54, 19.15, 18.99, 17.83, 13.83, 13.63, 13.20, 12.57, 8.08, 8.06; FTIR (thin film): 2946, 2869, 1775, 1750, 1598, 1490, 1445, 1378, 1355, 1268, 1112, 1071; HRMS (ESI-APCI)  $m/z$  calc'd for  $\text{C}_{32}\text{H}_{50}\text{NO}_8\text{Si}$  ( $\text{M}+\text{H}$ ) $^+$ : 604.3300, found: 604.3310.

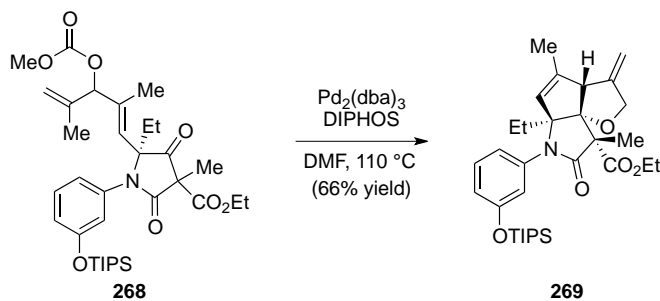
## Preparation of allylic carbonate **268**



To a solution of enal **239** (0.300 g, 0.566 mmol) in THF (6 mL) cooled to  $-78\text{ }^{\circ}\text{C}$  was added 2-propenylMgCl (1.70 mL, 0.5 M in THF, 0.849 mmol) and maintained for 1.5 h. Methyl chloroformate (0.131 mL, 1.70 mmol) was then added and the reaction mixture was allowed to warm slowly to room temperature and quenched with sat. aq.  $\text{NaHCO}_3$  and extracted with  $\text{Et}_2\text{O}$  (3 x 5 mL). The combined organics were dried over  $\text{MgSO}_4$ , filtered and concentrated *in vacuo*. The crude material was purified via flash chromatography (15%→20% EtOAc/hexanes) to yield allylic carbonate **268** (0.280 g, 79% yield) as an inseparable mixture of diastereomers as a colorless oil.

$^1\text{H-NMR}$  (500 MHz;  $\text{CDCl}_3$ ):  $\delta$  7.21 (q,  $J = 8.6$  Hz, 1H), 7.04 (d,  $J = 11.0$  Hz, 1H), 6.96 (t,  $J = 8.5$  Hz, 1H), 6.82-6.80 (m, 1H), 5.73 (d,  $J = 9.6$  Hz, 1H), 5.24 (s, 1H), 5.08 (s, 1H), 5.02 (s, 1H), 4.25 (td,  $J = 6.6, 5.1$  Hz, 2H), 3.80-3.77 (s, 3H), 2.32 (ddd,  $J = 14.5, 10.9, 7.3$  Hz, 1H), 2.05 (dd,  $J = 14.4, 7.1$  Hz, 1H), 1.71 (s, 3H), 1.62 (m, 6H), 1.25 (m, 6H), 1.13-1.05 (m, 18H), 0.76 (t,  $J = 7.1$  Hz, 3H);  $^{13}\text{C-NMR}$  (126 MHz,  $\text{CDCl}_3$ ):  $\delta$  204.21, 204.09, 169.60, 165.76, 165.74, 156.43, 156.42, 154.62, 154.57, 139.97, 139.91, 137.92, 137.85, 136.50, 136.45, 129.51, 129.42, 127.95, 127.39, 118.74, 118.66, 117.66, 117.62, 117.41, 114.96, 114.48, 84.84, 84.81, 76.20, 62.58, 58.68, 58.62, 54.85, 27.98, 27.72, 18.42, 18.09, 17.84, 14.05, 13.84, 13.49, 12.60, 8.13; FTIR (thin film): 2946, 2869, 1775, 1751, 1709, 1651, 1598, 1490, 1444, 1377, 1355, 1269, 1112; HRMS (ESI-APCI)  $m/z$  calc'd for  $\text{C}_{34}\text{H}_{52}\text{NO}_8\text{Si}$  ( $\text{M}+\text{H}$ ) $^+$ : 630.3480, found: 630.3480.

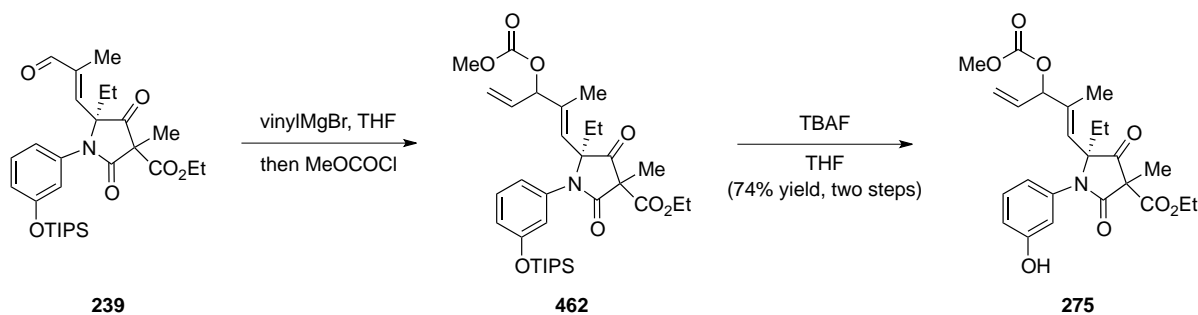
## Preparation of fused tricycle **269**



A flame dried vial was charged with methyl carbonate **268** (0.029 g, 0.0461 mmol), Pd<sub>2</sub>(dba)<sub>3</sub> (4.2 mg, 0.00461 mmol), and DIPHOS (3.7 mg, 0.00922 mmol) and vacuum purged under N<sub>2</sub>. DMF (3 mL) was then added and the reaction mixture heated to 110 °C overnight. Volatiles were removed *in vacuo* and the crude mixture was purified by flash chromatography (5% EtOAc/hexanes) to yield fused tricycle **269** (15 mg, 59% yield) as a colorless crystalline solid.

<sup>1</sup>H-NMR (500 MHz; CDCl<sub>3</sub>): δ 7.22 (t, *J* = 8.0 Hz, 1H), 6.85 (dd, *J* = 8.1, 1.1 Hz, 1H), 6.80 (d, *J* = 7.8 Hz, 1H), 6.74 (s, 1H), 5.40 (s, 1H), 5.13 (d, *J* = 0.7 Hz, 1H), 5.07 (d, *J* = 1.0 Hz, 1H), 4.47 (d, *J* = 12.7 Hz, 1H), 4.37-4.34 (m, 1H), 4.26 (q, *J* = 7.1 Hz, 2H), 3.83 (s, 1H), 2.17 (dd, *J* = 14.5, 7.4 Hz, 1H), 1.82 (s, 3H), 1.77 (dd, *J* = 14.5, 7.7 Hz, 1H), 1.49 (s, 2H), 1.34 (t, *J* = 7.1 Hz, 3H), 1.25 (dt, *J* = 15.0, 7.5 Hz, 3H), 1.10 (d, *J* = 7.4 Hz, 18H), 0.71 (t, *J* = 7.6 Hz, 3H); <sup>13</sup>C-NMR (126 MHz, CDCl<sub>3</sub>): δ 170.78, 170.31, 156.35, 146.44, 141.67, 138.07, 129.45, 129.40, 128.28, 128.23, 128.19, 121.45, 121.41, 121.38, 121.35, 120.52, 120.44, 119.55, 106.29, 106.25, 98.39, 79.18, 72.28, 61.34, 60.25, 57.30, 25.27, 17.86, 14.57, 13.96, 12.59, 9.53; FTIR (thin film): 2945, 2868, 1742, 1702, 1666, 1596, 1487, 1464, 1443, 1384, 1367, 1282, 1246, 1197, 1155, 1133, 1081, 1006; HRMS (ESI-APCI) *m/z* calc'd for C<sub>32</sub>H<sub>48</sub>NO<sub>5</sub>Si (M+H)<sup>+</sup>: 554.3296, found: 554.3287.

## Preparation of allylic carbonate 275



To a solution of enal **239** (0.112 g, 0.211 mmol) in THF (3 mL) cooled to  $-78\text{ }^{\circ}\text{C}$  was added vinylMgCl (0.317 mL, 1.0 M in THF, 0.317 mmol) and maintained for 1.5 h. Methyl chloroformate (0.049 mL, 0.634 mmol) was then added and the reaction mixture was allowed to warm slowly to room temperature and quenched with sat. aq.  $\text{NaHCO}_3$  and extracted with EtOAc (3 x 5 mL). The combined organics were dried over  $\text{MgSO}_4$ , filtered and concentrated *in vacuo*. The crude material was purified by flash chromatography (10% EtOAc/hexanes) to yield allylic carbonate **462** (0.096 g, 74% yield) as an inseparable mixture of diastereomers as a colorless oil.

$^1\text{H-NMR}$  (500 MHz;  $\text{CDCl}_3$ ):  $\delta$  7.21 (q,  $J = 7.6$  Hz, 1H), 7.00 (d,  $J = 14.1$  Hz, 1H), 6.96 (d,  $J = 8.1$  Hz, 1H), 6.81 (d,  $J = 8.2$  Hz, 1H), 5.73 (dd,  $J = 13.5, 8.0$  Hz, 2H), 5.35-5.27 (m, 3H), 4.26-4.22 (m, 2H), 3.77 (s, 3H), 2.28 (dd,  $J = 14.5, 7.3$  Hz, 1H), 2.04 (dd,  $J = 14.6, 7.4$  Hz, 1H), 1.75 (s, 3H), 1.61 (m, 3H), 1.27-1.20 (m, 6H), 1.07 (dd,  $J = 16.2, 7.3$  Hz, 18H), 0.77-0.72 (m, 3H);  $^{13}\text{C-NMR}$  (126 MHz,  $\text{CDCl}_3$ ):  $\delta$  204.14, 203.97, 169.61, 165.76, 156.39, 154.62, 154.57, 138.76, 136.47, 136.41, 133.46, 133.41, 129.52, 129.46, 127.81, 127.45, 118.77, 118.75, 118.68, 118.62, 117.77, 117.52, 117.50, 117.44, 82.86, 82.84, 76.12, 76.04, 62.57, 58.71, 58.66, 54.86, 27.78, 27.55, 13.99, 13.84, 13.72, 12.58, 8.08, 8.06; FTIR (thin film): 2946, 2869, 1776, 1752, 1709, 1598, 1490, 1444, 1377, 1355, 1262, 1113; HRMS (ESI-APCI)  $m/z$  calc'd for  $\text{C}_{33}\text{H}_{50}\text{NO}_8\text{Si}$  ( $\text{M}+\text{H}$ ) $^+$ : 616.3307, found: 616.3307.

To a solution of methyl carbonate **462** (130 mg, 0.211 mmol) in THF (4.5 mL) cooled to –15 °C was added TBAF (0.23 mL, 1.0 M in THF, 0.23 mmol). The reaction was monitored by TLC and after 5 min quenched with water (10 mL) and extracted with EtOAc (3 x 5 mL). The combined organics were dried over MgSO<sub>4</sub>, filtered and concentrated *in vacuo*. The crude material was purified via column chromatography (20% EtOAc/hexanes) to yield phenol **275** (0.097 mg, quant. yield) as an inseparable mixture of diastereomers as a colorless oil.

<sup>1</sup>H-NMR (500 MHz; CDCl<sub>3</sub>): δ 7.23 (tt, *J* = 7.3, 3.6 Hz, 1H), 6.99-6.95 (m, 2H), 6.76 (d, *J* = 7.6 Hz, 1H), 6.49 (d, *J* = 8.3 Hz, 1H), 5.81-5.74 (m, 1H), 5.64 (d, *J* = 4.0 Hz, 1H), 5.38-5.36 (m, 1H), 5.33 (m, 1H), 5.30 (m, 1H), 4.28-4.20 (m, 2H), 3.81-3.80 (s, 3H), 2.24-2.02 (m, 2H), 1.76-1.72 (m, 3H), 1.66-1.63 (m, 3H), 1.29-1.23 (m, 3H), 0.81-0.75 (m, 3H); <sup>13</sup>C-NMR (126 MHz, CDCl<sub>3</sub>): δ 203.97, 203.86, 169.85, 169.80, 165.57, 165.53, 156.75, 156.69, 156.66, 155.25, 155.21, 139.63, 139.42, 135.93, 135.90, 133.20, 133.04, 129.92, 129.88, 128.35, 127.24, 119.11, 118.45, 118.22, 118.01, 114.79, 114.75, 113.29, 113.24, 83.37, 83.18, 75.67, 75.24, 62.88, 62.83, 58.99, 58.87, 55.13, 29.15, 28.78, 17.75, 17.53, 14.59, 13.88, 13.33, 8.09, 7.96; FTIR (thin film): 3368, 2985, 2942, 1775, 1750, 1704, 1683, 1595, 1491, 1445, 1383, 1335, 1262, 1160, 1113; HRMS (ESI-APCI) *m/z* calc'd for C<sub>24</sub>H<sub>30</sub>NO<sub>8</sub> (M+H)<sup>+</sup>: 460.1971, found: 460.1977.

### Preparation of tricycle **276**

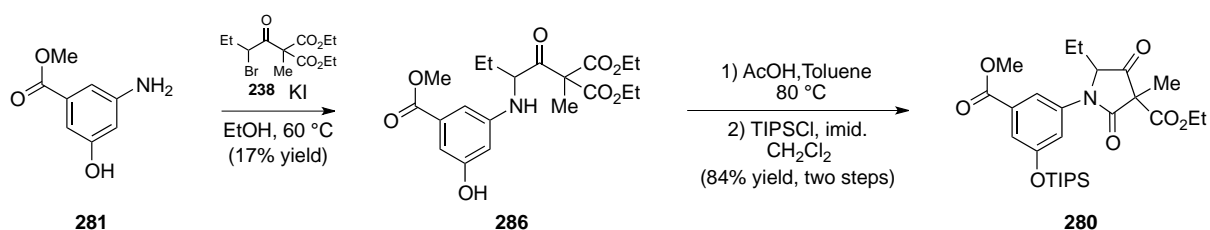


A flame dried vial was charged with methyl carbonate **275** (0.020 g, 0.0435 mmol), Pd<sub>2</sub>(dba)<sub>3</sub> (4.0 mg, 0.00435 mmol), and DIPHOS (3.5 mg, 0.00871 mmol) and vacuum purged

under N<sub>2</sub>. DMF (1 mL) and toluene (1 mL) was added and the reaction mixture heated to 120 °C overnight. The crude mixture was loaded directly on to silica gel and purified via flash chromatography (20% EtOAc/hexanes) to yield tricycle **276** (11.5 mg, 69% yield) as an inseparable mixture of diastereomers or olefin isomers as a colorless oil.

<sup>1</sup>H-NMR (500 MHz; CDCl<sub>3</sub>): δ 7.56 (s, 1H), 7.11-7.08 (m, 1H), 6.99-6.95 (m, 1H), 6.83-6.76 (m, 2H), 6.70 (dd, *J* = 8.3, 2.2 Hz, 1H), 5.95 (d, *J* = 10.9 Hz, 1H), 5.28 (d, *J* = 16.0 Hz, 1H), 5.21 (d, *J* = 10.2 Hz, 1H), 4.35 (s, 1H), 4.30-4.24 (m, 3H), 2.08-1.98 (m, 2H), 1.61-1.53 (m, 6H), 1.32-1.27 (m, 3H), 1.11-1.07 (m, 3H), 1.04-0.98 (m, 3H); <sup>13</sup>C-NMR (126 MHz, CDCl<sub>3</sub>): δ 200.57, 167.98, 165.69, 157.29, 139.43, 133.12, 131.40, 130.28, 126.29, 126.25, 124.96, 118.19, 118.14, 114.00, 113.77, 105.41, 105.35, 81.45, 63.16, 48.85, 32.05, 20.06, 17.04, 13.88, 7.80; FTIR (thin film): 3333, 2972, 2939, 1775, 1685, 1618, 1600, 1499, 1465, 1381, 1294, 1224, 1167, 1108, 1015; HRMS (ESI-APCI) *m/z* calc'd for C<sub>22</sub>H<sub>25</sub>NO<sub>5</sub> (M+H)<sup>+</sup>: 384.1811, found: 384.1815.

### Preparation of tetramic acid **280**



A solution of aniline **281**<sup>9</sup> (4.00 g, 23.9 mmol), bromide **238** (3.87 g, 12.0 mmol), and KI (0.199 g, 1.2 mmol) in EtOH (60 mL) was heated to 60 °C for 48 h. The solution was then cooled to room temperature and the volatiles were removed *in vacuo*. The crude material was purified by flash chromatography (10%→15%→20% EtOAc/hexanes) to give aniline **286** (1.703 g, 17% yield) as a mixture of diastereomers.

To aniline **286** (1.703 g, 4.16 mmol) was added toluene (42 mL) then AcOH (4.2 mL) and the reaction was heated to 80 °C for 16.5 h. The reaction was cooled to room temperature

and the volatiles were removed *in vacuo*. The crude mixture was purified by flash chromatography (20%→30% EtOAc/hexanes) to yield phenol **463** (1.324 g, 88% yield) as a mixture of diastereomers.

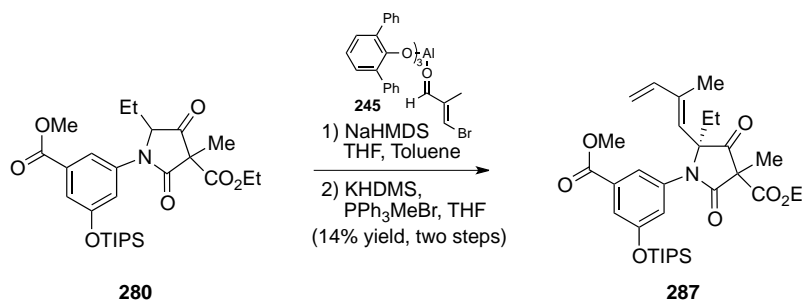
$^1\text{H-NMR}$  (400 MHz;  $\text{CDCl}_3$ ):  $\delta$  7.75 (s, 1H), 7.45 (t,  $J = 1.6$  Hz, 1H), 7.40-7.39 (m, 1H), 7.33 (t,  $J = 2.2$  Hz, 1H), 4.84 (dd,  $J = 5.6, 2.9$  Hz, 1H), 4.25-4.14 (m, 2H), 3.89-3.87 (s, 3H), 2.01-1.93 (m, 1H), 1.81-1.74 (m, 1H), 1.58 (s, 3H), 1.25-1.21 (m, 3H), 0.72 (t,  $J = 7.4$  Hz, 3H);  $^1\text{H-NMR}$  (400 MHz;  $\text{CDCl}_3$ ):  $\delta$  7.82 (s, 1H), 7.42 (t,  $J = 1.6$  Hz, 1H), 7.40-7.39 (m, 1H), 7.37 (t,  $J = 2.2$  Hz, 1H), 4.59 (dd,  $J = 7.1, 3.6$  Hz, 1H), 4.25-4.14 (m, 2H), 3.88 (s,  $J = 3.6, 1.6$  Hz, 1H), 2.01-1.93 (m, 1H), 1.87-1.79 (m, 1H), 1.62 (s, 3H), 1.23-1.19 (m, 3H), 0.85 (t,  $J = 7.5$  Hz, 3H);  $^{13}\text{C-NMR}$  (101 MHz,  $\text{CDCl}_3$ ):  $\delta$  204.22, 203.88, 194.67, 191.40, 170.13, 166.33, 165.13, 157.49, 157.47, 136.16, 132.06, 116.92, 116.82, 115.83, 115.81, 115.67, 115.47, 68.02, 67.56, 63.12, 62.95, 59.77, 59.72, 52.51, 22.38, 21.15, 17.16, 14.96, 13.88, 13.82, 8.56, 7.92; FTIR (thin film): 3339, 2979, 2941, 1777, 1746, 1704, 1681, 1598, 1455, 1437, 1330, 1295, 1209, 1107, 1006  $\text{cm}^{-1}$ ; HRMS (ESI-APCI)  $m/z$  calc'd for  $\text{C}_{18}\text{H}_{22}\text{NO}_7$  ( $\text{M}+\text{H}$ ) $^+$ : 364.1396, found: 364.1394.

To a solution of phenol **463** (1.324 g, 3.64 mmol) and imidazole (0.372 g, 5.46 mmol) in  $\text{CH}_2\text{Cl}_2$  (36 mL) was added TIPSCI (1.0 mL, 4.74 mmol). The reaction was stirred for 17.5 h then water (30 mL) was added and the mixture was extracted with  $\text{CH}_2\text{Cl}_2$  (3  $\times$  20 mL). The combined organics were washed with brine (50 mL), dried over  $\text{MgSO}_4$ , filtered and concentrated *in vacuo*. The crude material was purified by flash chromatography to yield tetramic acid **280** (1.818 g, 96% yield) as a mixture of diastereomers.

$^1\text{H-NMR}$  (400 MHz;  $\text{CDCl}_3$ ):  $\delta$  7.58 (t,  $J = 0.8$  Hz, 1H), 7.44-7.43 (m, 1H), 7.28 (t,  $J = 2.1$  Hz, 1H), 4.82 (dd,  $J = 5.5, 2.7$  Hz, 1H), 4.20-4.15 (m, 2H), 3.89 (s, 3H), 2.00-1.94 (m, 1H), 1.81-1.76 (m, 1H), 1.56 (s, 3H), 1.31-1.19 (m, 6H), 1.08 (s, 18H), 0.70 (t,  $J = 7.4$  Hz, 3H);  $^1\text{H-NMR}$  (400 MHz;  $\text{CDCl}_3$ ):  $\delta$  7.55 (t,  $J = 0.8$  Hz, 1H), 7.43 (t,  $J = 1.2$  Hz, 1H), 7.30 (t,  $J = 2.1$  Hz, 1H), 4.56 (dd,  $J = 7.0, 3.5$  Hz, 1H), 4.26-4.21 (m, 2H), 3.89 (s, 3H), 1.96 (m, 1H), 1.86 (m, 1H), 1.59 (s, 3H), 1.31-1.19 (m, 6H), 1.09 (d,  $J = 7.4$  Hz, 18H), 0.85 (t,  $J = 7.4$  Hz, 3H);  $^{13}\text{C-NMR}$  (101

MHz, CDCl<sub>3</sub>):  $\delta$  204.83, 204.59, 168.83, 166.11, 165.35, 164.95, 156.78, 156.74, 136.84, 136.66, 132.03, 132.01, 120.56, 119.14, 119.11, 116.90, 116.60, 67.50, 66.98, 62.84, 62.67, 59.55, 59.43, 52.40, 22.31, 21.09, 17.82, 17.19, 14.89, 13.86, 13.83, 12.56, 12.53, 8.50, 7.81; FTIR (thin film): 2945, 2893, 2868, 1777, 1707, 1593, 1453, 1386, 1372, 1331, 1243, 1212, 1104, 1013 cm<sup>-1</sup>; HRMS (ESI-APCI) *m/z* calc'd for C<sub>27</sub>H<sub>42</sub>NO<sub>7</sub>Si (M+H)<sup>+</sup>: 520.2731, found: 520.2723.

### Preparation of diene **287**

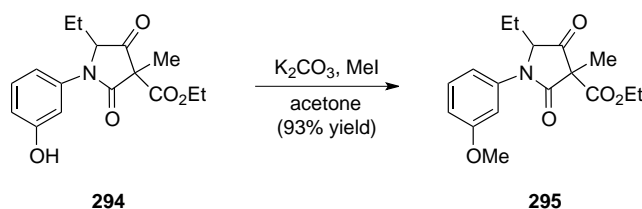


To a  $-78$  °C solution of ketone **280** (1.318 g 2.54 mmol) in THF (25 mL) was added NaHMDS (2.79 mL, 1.0 M in THF, 2.79 mmol) and the reaction mixture was allowed to warm slowly to  $-50$  °C then cooled to  $-78$  °C. Meanwhile, the vinyl bromide (0.568 g, 3.81 mmol) was added slowly to a solution of the Lewis acid (generated from slow addition of AlMe<sub>3</sub> (2.29 mL, 2.0 M in hexanes, 4.57 mmol) to a solution of 2,6-diphenylphenol (3.128 g, 12.7 mmol) in toluene (25 mL) at room temperature) at  $-78$  °C and maintained for 20 min. The solution containing aldehyde complex **245** was then transferred via cannula to the sodium enolate of ketone **280**. The reaction mixture was maintained at  $-78$  °C for 1 h then allowed to warm slowly to room temperature over 3 h. The reaction mixture was quenched with sat. aq. Rochelle's salt (50 mL), stirred vigorously overnight, and extracted with EtOAc (3 x 25 mL). The combined organics were dried over MgSO<sub>4</sub>, filtered and concentrated *in vacuo*. The crude material was purified via flash chromatography (5%→10%→20% EtOAc/hexanes) to yield an intermediate enal (0.812 g, 54% yield) as an inseparable mixture of diastereomers.

KHMDS (0.5 M in THF, 2.8 mL, 1.4 mmol) was added to PPh<sub>3</sub>MeBr (0.536g, 1.5 mmol). After 1 h the enal from the last step (0.287 g, 0.489 mmol) in THF (5 mL) was added. After 10 min sat. aq. NH<sub>4</sub>Cl (10 mL) was added. The mixture was extracted with EtOAc (3 × 5 mL) and the combined organics were washed with brine (10 mL), dried over MgSO<sub>4</sub>, filtered and concentrated *in vacuo*. The crude material was purified by flash chromatography (10% EtOAc/hexanes) to give triene **287** (0.071 g, 25% yield).

<sup>1</sup>H-NMR (400 MHz; CDCl<sub>3</sub>): δ 7.72 (t, *J* = 1.7 Hz, 1H), 7.46-7.44 (m, 1H), 7.12 (t, *J* = 2.2 Hz, 1H), 6.35-6.28 (dd, *J* = 17.3, 10.7 Hz, 1H), 5.52 (s, 1H), 5.29 (d, *J* = 17.3 Hz, 1H), 5.14 (d, *J* = 10.7 Hz, 1H), 4.28-4.22 (m, 2H), 3.89-3.87 (s, 3H), 2.24 (dt, *J* = 14.6, 7.3 Hz, 1H), 2.10-2.03 (m, 1H), 1.82 (s, 3H), 1.65-1.63 (s, 3H), 1.29-1.26 (m, 3H), 1.25-1.16 (m, 3H), 1.05 (d, *J* = 4.2 Hz, 18H), 0.75 (t, *J* = 7.4 Hz, 3H); <sup>13</sup>C-NMR (101 MHz, CDCl<sub>3</sub>): δ 222.27, 203.87, 194.65, 191.46, 169.72, 166.14, 165.59, 156.44, 140.74, 139.58, 136.63, 131.93, 130.28, 120.99, 119.76, 119.30, 119.27, 114.85, 76.08, 62.78, 58.76, 52.33, 28.66, 18.00, 17.85, 17.79, 17.67, 13.84, 12.95, 12.51, 8.07; FTIR (thin film): 2945, 2893, 2868, 1776, 1708, 1592, 1453, 1376, 1361, 1312, 1239, 1186, 1146, 1107, 1020 cm<sup>-1</sup>; HRMS (ESI-APCI) *m/z* calc'd for C<sub>32</sub>H<sub>48</sub>NO<sub>7</sub>Si (M+H)<sup>+</sup>: 586.3200, found: 586.3201.

### Preparation of tetramic acid **295**

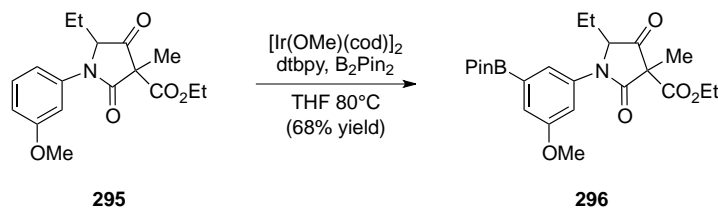


A solution of phenol **294** (10.9 g, 35.8 mmol), K<sub>2</sub>CO<sub>3</sub> (14.9 g, 107 mmol), and MeI (13.4 mL, 215 mmol) in acetone (358 mmol) was heated to 60 °C for 5.5 h. The reaction was cooled to room temperature and the solvent removed *in vacuo*. The crude material was run through a

plug of silica gel (100% EtOAc) to yield tetramic acid **295** (10.6 g, 93% yield) as a mixture of diastereomers.

$^1\text{H-NMR}$  (400 MHz;  $\text{CDCl}_3$ ):  $\delta$  7.31 (td,  $J = 8.1, 4.1$  Hz, 1H), 7.03 (s, 1H), 6.94 (d,  $J = 7.7$  Hz, 1H), 6.81 (ddd,  $J = 8.1, 5.3, 2.6$  Hz, 1H), 4.77 (dd,  $J = 5.5, 2.9$  Hz, 1H), 4.15 (dt,  $J = 13.6, 6.5$  Hz, 2H), 3.79 (s, 3H), 1.95 (dddt,  $J = 14.5, 10.8, 7.2, 3.5$  Hz, 1H), 1.83-1.71 (m, 1H), 1.55 (s, 3H), 1.22-1.18 (m, 3H), 0.72 (t,  $J = 7.4$  Hz, 3H);  $^1\text{H-NMR}$  (400 MHz;  $\text{CDCl}_3$ ):  $\delta$  7.31 (td,  $J = 8.1, 4.1$  Hz, 1H), 7.03 (s, 1H), 6.94 (d,  $J = 7.7$  Hz, 1H), 6.81 (ddd,  $J = 8.1, 5.3, 2.6$  Hz, 1H), 4.50 (dd,  $J = 7.1, 3.6$  Hz, 1H), 4.15 (dt,  $J = 13.6, 6.5$  Hz, 2H), 3.79 (s, 3H), 1.95 (dddt,  $J = 14.5, 10.8, 7.2, 3.5$  Hz, 1H), 1.88-1.80 (m, 1H), 1.57 (s, 3H), 1.24 (dd,  $J = 7.4, 6.9$  Hz, 3H), 0.88-0.81 (m, 3H);  $^{13}\text{C-NMR}$  (101 MHz,  $\text{CDCl}_3$ ):  $\delta$  205.24, 205.03, 194.66, 194.64, 191.46, 168.86, 168.83, 165.52, 165.13, 160.20, 160.17, 136.79, 136.65, 129.96, 129.92, 116.05, 115.97, 112.41, 112.28, 110.47, 110.39, 67.78, 67.26, 62.76, 62.64, 59.57, 59.47, 55.41, 22.45, 21.19, 17.18, 14.88, 13.88, 8.64, 7.94; FTIR (thin film): 2974, 2939, 2881, 1775, 1744, 1603, 1589, 1493, 1455, 1386, 1291, 1123, 1106, 1039, 1010  $\text{cm}^{-1}$ ; HRMS (ESI-APCI)  $m/z$  calc'd for  $\text{C}_{17}\text{H}_{22}\text{NO}_5$  (M+H) $^+$ : 320.1498, found: 320.1488.

### Preparation of aryl boronic ester **296**

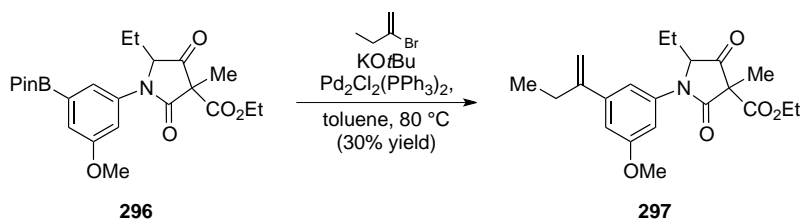


Tetramic acid **295** (2.33 g, 7.3 mmol),  $[\text{Ir}(\text{OMe})(\text{cod})]_2$  (0.048 g, 0.073 mmol), dtbpy (0.063 g, 0.23 mmol),  $\text{B}_2\text{Pin}_2$  (1.85 g, 7.3 mmol), and THF (15 mL) were added to a Schlenk flask and the solvent was degassed by the freeze/ pump/ thaw method (3x). The mixture was then heated to  $80^\circ\text{C}$  and maintained that that temperature for 18 h. The reaction was cooled to room temperature and the solvent was removed *in vacuo*. The crude material was purified by

flash chromatography (15%→30% EtOAc/hexanes) to yield aryl boronic ester **296** (2.194 g, 68% yield).

$^1\text{H-NMR}$  (400 MHz;  $\text{CDCl}_3$ ):  $\delta$  7.28 (d,  $J = 2.0$  Hz, 1H), 7.17 (t,  $J = 2.9$  Hz, 1H), 7.10 (dd,  $J = 5.0, 2.5$  Hz, 1H), 4.78 (dd,  $J = 5.5, 2.8$  Hz, 1H), 4.20-4.07 (m, 2H), 3.77-3.75 (m, 3H), 1.95-1.85 (m, 1H), 1.76-1.70 (m, 1H), 1.48 (d,  $J = 6.5$  Hz, 3H), 1.25 (d,  $J = 4.6$  Hz, 12H), 1.21-1.11 (m, 3H), 0.67-0.64 (m, 3H);  $^1\text{H-NMR}$  (400 MHz;  $\text{CDCl}_3$ ):  $\delta$  7.25 (t,  $J = 2.3$  Hz, 1H), 7.17 (t,  $J = 2.9$  Hz, 1H), 7.10 (dd,  $J = 5.0, 2.5$  Hz, 1H), 4.52 (t,  $J = 3.4$  Hz, 1H), 4.20-4.13 (m, 2H), 3.77-3.75 (m, 3H), 1.95-1.85 (m, 1H), 1.78 (t,  $J = 7.3$  Hz, 1H), 1.48 (d,  $J = 6.5$  Hz, 3H), 1.25 (d,  $J = 4.6$  Hz, 12H), 1.21-1.11 (m, 3H), 0.79 (t,  $J = 7.3$  Hz, 3H);  $^{13}\text{C-NMR}$  (101 MHz,  $\text{CDCl}_3$ ):  $\delta$  205.20, 205.07, 194.71, 168.76, 165.55, 165.11, 159.65, 159.61, 136.34, 136.22, 121.87, 121.72, 117.56, 117.50, 114.56, 114.51, 114.20, 84.05, 67.76, 67.22, 62.66, 62.65, 62.49, 59.42, 59.31, 55.44, 55.41, 24.76, 22.40, 21.18, 17.09, 14.89, 13.82, 8.52, 7.91; FTIR (thin film): 2978, 2938, 1777, 1745, 1702, 1588, 1450, 1430, 1372, 1359, 1294, 1252, 1166, 1143, 1105, 1048, 1010, 968, 954  $\text{cm}^{-1}$ ; HRMS (ESI-APCI)  $m/z$  calc'd for  $\text{C}_{17}\text{H}_{21}\text{NO}_5$  ( $\text{M}+\text{H}$ ) $^+$ : 446.2350, found: 446.2351.

### Preparation of styrene **297**

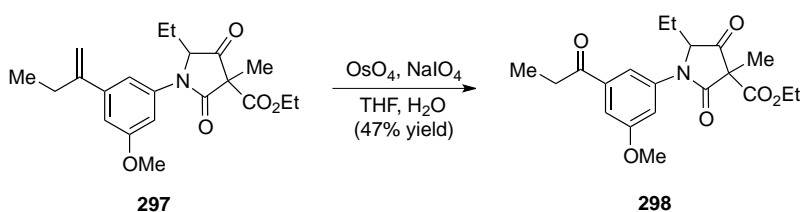


Aryl boronic ester **296** (0.460 g, 1.04 mmol),  $\text{PdCl}_2(\text{PPh}_3)_2$  (0.073 g, 0.104 mmol),  $\text{KO}^t\text{Bu}$  (0.350 g, 3.12 mmol), 2-bromobutene (0.13 mL, 1.25 mmol), and toluene (3.2 mL) were added together and heated to 80 °C. After 14 h the reaction was cooled to room temperature and water (10 mL) was added. The solution was extracted with EtOAc (3 × 5 mL) and the combined organics were washed with brine (15 mL), dried over  $\text{MgSO}_4$ , filtered and concentrated *in vacuo*.

The crude material was purified by flash chromatography (15%→20% EtOAc/hexanes) to yield styrene **297** (0.116 g, 30% yield) as a mixture of diastereomers.

$^1\text{H-NMR}$  (300 MHz;  $\text{CDCl}_3$ ):  $\delta$  7.00 (m, 1H), 6.96 (m, 1H), 6.89-6.85 (m, 1H), 5.30-5.26 (m, 1H), 5.10-5.08 (m, 1H), 4.82-4.52 (m, 1H), 4.28-4.16 (m, 2H), 3.84-3.78 (m, 3H), 2.52-2.43 (m, 2H), 2.06-1.72 (m, 2H), 1.60-1.55 (m, 3H), 1.33-1.04 (m, 6H), 0.95-0.71 (m, 3H).

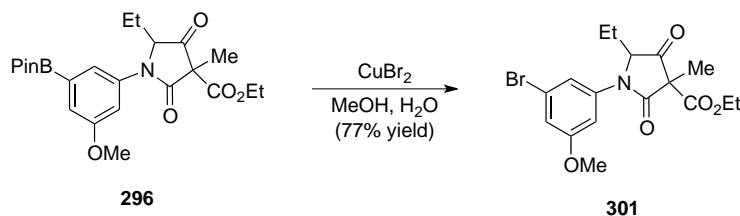
### Preparation of ketone **298**



Styrene **297** (0.155 g, 0.415 mmol) was dissolved in THF (3 mL) and water (1.5 mL) and  $\text{OsO}_4$  (0.08 M, 0.052 mL, 0.0415 mmol) and  $\text{NaIO}_4$  (0.462 g, 2.2 mmol) were added. The reaction was stirred for 3 h the water (5 mL) was added and the solution was extracted with EtOAc (3  $\times$  5 mL). The combined organics were washed with brine (10 mL), dried over  $\text{MgSO}_4$ , filtered and concentrated *in vacuo*. The crude material was purified by flash chromatography (25% EtOAc/hexanes) to yield ketone **298** (0.073 g, 47% yield) as a mixture of diastereomers.

$^1\text{H-NMR}$  (300 MHz;  $\text{CDCl}_3$ ):  $\delta$  7.59 (m, 1H), 7.40 (m, 1H), 7.29 (m, 1H), 4.88-4.58 (m, 1H), 4.29-4.16 (m, 2H), 3.90-3.84 (m, 3H), 3.04-2.96 (m, 2H), 2.05-1.76 (m, 2H), 1.61-1.52 (m, 3H), 1.30-1.17 (m, 6H), 0.93-0.69 (m, 3H).

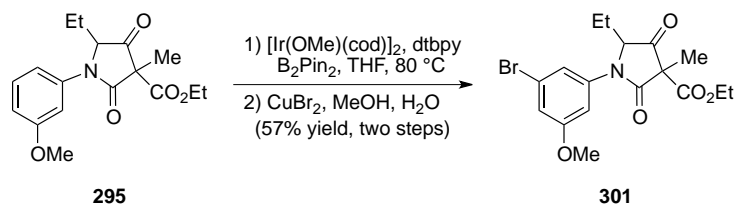
## Preparation of aryl bromide **301** from aryl boronic ester **296**



CuBr<sub>2</sub> (0.599 g, 2.68 mmol) was dissolved in water (11.2 mL). In a separate flask aryl boronic ester **296** (0.397 g, 0.89 mmol) was dissolved in MeOH (11.2 mL). The solution of **296** in MeOH was then poured into the aqueous solution and heated to 80 °C. The reaction was stirred for 4.5 h then cooled to room temperature and brine (20 mL) was added. The mixture was extracted with EtOAc (3 × 20 mL). The combined organics were washed with brine (50 mL), dried over MgSO<sub>4</sub>, filtered and concentrated *in vacuo*. The crude material was purified by flash chromatography (15% EtOAc/hexanes) to yield aryl bromide **301** (0.262 g, 77% yield) as a mixture of diastereomers.

<sup>1</sup>H-NMR (400 MHz; CDCl<sub>3</sub>): δ 7.12 (m, 1H), 6.95 (m, 1H), 6.95-6.90 (m, 1H), 4.72 (dd, *J* = 5.4, 2.7 Hz, 1H), 4.20-4.10 (m, 2H), 3.74 (s, 3H), 1.97-1.73 (m, 2H), 1.53-1.49 (m, 3H), 1.23-1.14 (m, 3H), 0.73-0.65 (m, 3H); <sup>1</sup>H-NMR (400 MHz; CDCl<sub>3</sub>): δ 7.12 (m, 1H), 6.95 (m, 1H), 6.95-6.90 (m, 1H), 4.47 (dd, *J* = 7.2, 3.6 Hz, 1H), 4.20-4.10 (m, 2H), 3.74 (s, 3H), 1.97-1.73 (m, 2H), 1.53-1.49 (m, 3H), 1.23-1.14 (m, 3H), 0.84-0.78 (m, 3H); <sup>13</sup>C-NMR (101 MHz, CDCl<sub>3</sub>): δ 204.54, 204.37, 194.65, 194.63, 194.62, 168.86, 168.80, 165.31, 164.86, 160.69, 160.64, 137.66, 137.58, 122.96, 122.90, 121.38, 118.89, 118.87, 118.75, 116.34, 116.28, 115.42, 115.25, 115.16, 112.00, 111.81, 109.50, 109.43, 67.50, 67.00, 62.85, 62.69, 59.51, 59.41, 55.69, 55.66, 55.62, 22.34, 21.11, 17.13, 14.88, 13.87, 8.56, 7.90; FTIR (thin film): 2975, 2939, 2880, 1777, 1744, 1702, 1598, 1571, 1449, 1381, 1287, 1251, 1179, 1106, 1042, 1010 cm<sup>-1</sup>; HRMS (ESI-APCI) *m/z* calc'd for C<sub>17</sub>H<sub>21</sub>BrNO<sub>5</sub> (M+H)<sup>+</sup>: 398.0603, found: 398.0580.

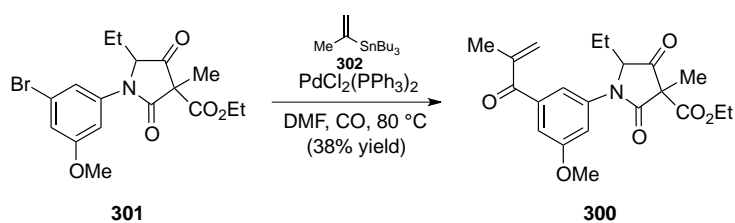
## Preparation of aryl bromide **301** from arene **295**



Alternative to the two-step procedure, aryl bromide **301** can be synthesized from arene **295** by subjecting the crude material of the borylation reaction directly into the bromination step. This was performed as followed:

Arene **295** (3.91 g, 12.6 mmol),  $[\text{Ir}(\text{OMe})(\text{cod})]_2$  (0.084 g, 0.126 mmol), dtbpy (0.108 g, 0.40 mmol),  $\text{B}_2\text{Pin}_2$  (3.20 g, 12.6 mmol), and THF (25 mL) were added to a Schlenk flask and the solvent was degassed by the freeze/ pump/ thaw method (3x). The mixture was then heated to 80 °C and maintained that that temperature for 13.5 h. The reaction was cooled to room temperature and the solvent was removed *in vacuo*. The crude material was dissolved in MeOH (158 mL) and added to a solution of  $\text{CuBr}_2$  (8.44 g, 37.8 mmol) in water (158 mL). The reaction was stirred for 5 h then cooled to room temperature and brine (150 mL) was added. The mixture was extracted with EtOAc (3 × 150 mL). The combined organics were washed with brine (300 mL), dried over  $\text{MgSO}_4$ , filtered and concentrated *in vacuo*. The crude material was purified by flash chromatography (15% EtOAc/hexanes) to yield aryl bromide **301** (2.745 g, 57% yield, two steps) as a mixture of diastereomers. All spectral data was identical to the material produced in the two step procedure.

## Preparation of enone **300**

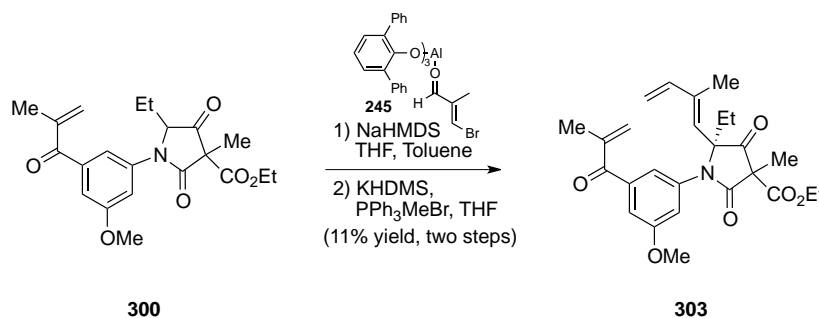


Aryl bromide **301** (0.439 g, 1.15 mmol), vinyl stannane **302** (1.52 g, 4.58 mmol), PdCl<sub>2</sub>(PPh<sub>3</sub>)<sub>2</sub> (0.081 g, 0.115 mmol), and DMF (11.5 mL) were added to a steel bomb. The bomb was flushed with CO by filling to 30 bar and venting three times. The bomb was then filled with CO to 30 bar and heated to 80 °C. The reaction was stirred for 19 h then cooled to room temperature. The bomb was vented and water (30 mL) was added. The mixture was extracted with EtOAc (3 × 20 mL) and the combined organics were washed with brine (30 mL), dried over MgSO<sub>4</sub>, filtered and concentrated *in vacuo*. The crude material was purified by flash chromatography (15% EtOAc/hexanes) to give enone **300** (0.164 g, 38% yield) as a mixture of diastereomers and starting material **301** (0.174 g, 40% recovery).

<sup>1</sup>H-NMR (400 MHz; CDCl<sub>3</sub>): δ 7.33-7.29 (m, 1H), 7.24-7.22 (m, 1H), 7.16-7.13 (m, 1H), 5.93 (s, 1H), 5.69 (d, *J* = 4.9 Hz, 1H), 4.81 (dd, *J* = 5.5, 2.7 Hz, 1H), 4.17 (td, *J* = 6.6, 3.0 Hz, 2H), 3.83 (s, 3H), 2.03 (s, 3H), 2.03-1.79 (m, 2H), 1.56 (m, 3H), 1.20 (t, *J* = 6.8 Hz, 3H), 0.70 (t, *J* = 7.2 Hz, 3H); <sup>1</sup>H-NMR (400 MHz; CDCl<sub>3</sub>): δ 7.33-7.29 (m, 1H), 7.24-7.22 (m, 1H), 7.16-7.13 (m, 1H), 5.93 (s, 1H), 5.69 (m, 1H), 4.55 (dd, *J* = 7.1, 3.5 Hz, 1H), 4.21 (dt, *J* = 12.2, 5.7 Hz, 2H), 3.83 (s, 3H), 2.03 (s, 3H), 2.03-1.79 (m, 2H), 1.57 (s, 3H), 1.24 (td, *J* = 7.1, 3.6 Hz, 3H), 0.85 (t, *J* = 7.4 Hz, 3H); <sup>13</sup>C-NMR (101 MHz, CDCl<sub>3</sub>): δ 204.65, 204.46, 203.26, 196.96, 196.94, 169.02, 168.97, 165.35, 164.92, 160.02, 159.98, 159.93, 143.34, 139.49, 136.59, 136.50, 127.95, 116.95, 116.76, 113.85, 113.82, 112.57, 112.42, 67.48, 66.98, 62.86, 62.72, 59.56, 59.46, 55.71, 55.67, 55.65, 22.37, 21.08, 18.52, 18.49, 18.08, 17.19, 14.91, 13.87, 8.58, 7.90; FTIR (thin film): 2977, 2939, 2844, 1777, 1745, 1704, 1656, 1626, 1592, 1453, 1435, 1338,

1214, 1182, 1108, 1061, 1034, 1011  $\text{cm}^{-1}$ ; HRMS (ESI-APCI)  $m/z$  calc'd for  $\text{C}_{21}\text{H}_{26}\text{NO}_6$  ( $\text{M}+\text{H}$ ) $^+$ : 388.1760, found: 388.1765.

### Preparation of triene 303



To a  $-78$  °C solution of ketone **300** (0.164 g 0.49 mmol) in THF (4.4 mL) was added NaHMDS (0.48 mL, 1.0 M in THF, 0.48 mmol) and the reaction mixture was allowed to warm slowly to  $-50$  °C then cooled to  $-78$  °C. Meanwhile, the vinyl bromide (0.098 g, 0.66 mmol) was added slowly to a solution of the Lewis acid (generated from slow addition of  $\text{AlMe}_3$  (0.40 mL, 2.0 M in hexanes, 0.79 mmol) to a solution of 2,6-diphenylphenol (0.542 g, 2.2 mmol) in toluene (4.4 mL) at room temperature) at  $-78$  °C and maintained for 20 min. The solution containing aldehyde complex **245** was then transferred via cannula to the sodium enolate of ketone **300**. The reaction mixture was maintained at  $-78$  °C for 1 h then allowed to warm slowly to room temperature over 3 h. The reaction mixture was quenched with sat. aq. Rochelle's salt (10 mL), stirred vigorously overnight, and extracted with EtOAc (3 x 10 mL). The combined organics were dried over  $\text{MgSO}_4$ , filtered and concentrated *in vacuo*. The crude material was purified via flash chromatography (15%→30% EtOAc/hexanes) to provide enal **464** (0.088 g, 44% yield) as an inseparable mixture of diastereomers.

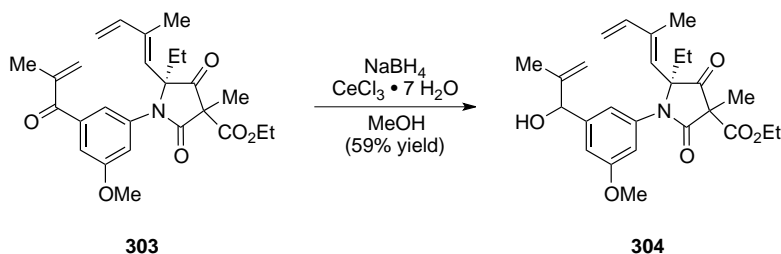
$^1\text{H-NMR}$  (400 MHz;  $\text{CDCl}_3$ ):  $\delta$  9.41 (s, 1H), 7.29 (s, 1H), 7.18 (s, 1H), 7.10 (s, 1H), 6.45 (s, 1H), 5.92 (t,  $J = 5.6$  Hz, 1H), 5.66 (s, 1H), 4.29-4.21 (m, 2H), 3.85-3.82 (s, 3H), 2.45-2.39 (m, 1H), 2.20-2.15 (m, 1H), 2.03-1.99 (s, 3H), 1.86-1.83 (s, 3H), 1.61-1.58 (s, 3H), 1.31-1.20 (m,

3H), 0.89-0.77 (m, 3H);  $^{13}\text{C}$ -NMR (101 MHz,  $\text{CDCl}_3$ ):  $\delta$  202.49, 196.65, 193.96, 193.70, 193.67, 169.68, 165.01, 160.11, 160.02, 149.47, 149.03, 148.87, 143.42, 142.11, 139.52, 135.93, 129.97, 127.81, 127.75, 118.92, 118.39, 117.28, 115.16, 112.55, 112.37, 111.86, 63.03, 58.80, 55.68, 27.88, 27.82, 18.51, 17.92, 16.09, 14.03, 13.90, 10.33, 8.62, 8.11; FTIR (thin film): 2981, 2940, 2842, 1777, 1747, 1659, 1628, 1595, 1493, 1455, 1376, 1358, 1284, 1221, 1162, 1125,  $1032\text{ cm}^{-1}$ ; HRMS (ESI-APCI)  $m/z$  calc'd for  $\text{C}_{25}\text{H}_{30}\text{NO}_7$  (M+H) $^+$ : 456.2022, found: 456.2021.

NaHMDS (1 M in THF, 0.22 mL, 0.22 mmol) was added to  $\text{PPh}_3\text{MeBr}$  (0.086 g, 0.24 mmol). After 1 h enal **464** (0.088 g, 0.20 mmol) in THF (2 mL) was added. After 10 min sat. aq.  $\text{NH}_4\text{Cl}$  (10 mL) was added. The mixture was extracted with EtOAc ( $3 \times 5$  mL) and the combined organics were washed with brine (10 mL), dried over  $\text{MgSO}_4$ , filtered and concentrated *in vacuo*. The crude material was purified by flash chromatography (10% EtOAc/hexanes) to give triene **303** (0.021 g, 24% yield) as a mixture of diastereomers.

$^1\text{H}$ -NMR (400 MHz;  $\text{CDCl}_3$ ):  $\delta$  7.35 (d,  $J = 1.2$  Hz, 1H), 7.20 (dd,  $J = 6.9, 1.6$  Hz, 1H), 7.13 (t,  $J = 2.1$  Hz, 1H), 6.96 (dd,  $J = 4.4, 2.1$  Hz, 1H), 6.31 (ddd,  $J = 17.3, 10.7, 2.8$  Hz, 1H), 5.90 (s, 1H), 5.66 (s, 1H), 5.52 (d,  $J = 6.5$  Hz, 1H), 5.29 (dd,  $J = 17.3, 3.0$  Hz, 1H), 5.12 (dt,  $J = 10.5, 5.2$  Hz, 1H), 4.25 (dt,  $J = 11.0, 5.3$  Hz, 2H), 3.85-3.78 (m, 3H), 2.24 (ddd,  $J = 14.4, 7.3, 5.5$  Hz, 1H), 2.08 (ddd,  $J = 14.6, 7.3, 3.8$  Hz, 1H), 2.03 (s, 3H), 1.82 (s, 3H), 1.65 (s, 3H), 1.27 (tdd,  $J = 7.7, 6.9, 6.0$  Hz, 3H), 0.78 (td,  $J = 7.4, 1.9$  Hz, 3H);  $^{13}\text{C}$ -NMR (101 MHz,  $\text{CDCl}_3$ ):  $\delta$  204.22, 203.70, 169.88, 169.71, 165.78, 165.56, 159.87, 143.35, 140.92, 140.69, 139.71, 139.42, 139.16, 136.56, 136.23, 130.59, 130.13, 129.63, 127.56, 119.55, 118.01, 115.77, 115.02, 114.74, 112.64, 112.35, 111.93, 76.67, 62.81, 62.69, 58.81, 58.78, 55.61, 55.30, 28.83, 28.71, 18.58, 17.91, 17.85, 13.89, 13.10, 13.06, 8.14.

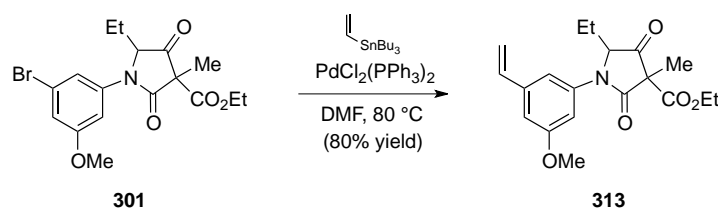
## Preparation of allylic alcohol **304**



Enone **303** (0.017 g, 0.037 mmol) was dissolved in MeOH (0.4 mL) and cooled to 0 °C. CeCl<sub>3</sub> · 7H<sub>2</sub>O (0.015 g, 0.041 mmol) was added and after 7 min NaBH<sub>4</sub> (0.002 g, 0.041 mmol) was added. After 1 h CeCl<sub>3</sub> · 7H<sub>2</sub>O (0.015 g, 0.041 mmol) then NaBH<sub>4</sub> (0.002 g, 0.041 mmol) was added again. After 10 min the reaction was allowed to warm to room temperature. After 2 h the reaction mixture was concentrated *in vacuo*. The crude material was purified by flash chromatography (15%→20%→30% EtOAc/hexanes) to give allylic alcohol **304** (0.010 g, 59% yield).

<sup>1</sup>H-NMR (400 MHz; CDCl<sub>3</sub>): δ 6.97 (d, *J* = 7.2 Hz, 1H), 6.89-6.87 (m, 2H), 6.33-6.26 (m, 1H), 5.49 (d, *J* = 2.4 Hz, 1H), 5.27 (d, *J* = 17.1 Hz, 1H), 5.14-5.07 (m, 3H), 4.92-4.91 (m, 1H), 4.25 (qd, *J* = 7.1, 0.9 Hz, 2H), 3.81-3.77 (m, 3H), 2.25-2.19 (m, 1H), 2.06 (ddd, *J* = 13.8, 6.6, 3.5 Hz, 1H), 1.80 (dd, *J* = 2.5, 1.1 Hz, 3H), 1.65-1.62 (m, 3H), 1.59-1.56 (m, 3H), 1.29-1.22 (m, 3H), 0.77 (tt, *J* = 7.4, 3.7 Hz, 3H); <sup>13</sup>C-NMR (101 MHz, CDCl<sub>3</sub>): δ 204.16, 204.15, 169.71, 165.74, 159.98, 159.94, 146.33, 146.28, 144.12, 141.37, 140.85, 139.48, 139.46, 136.41, 136.38, 130.41, 130.39, 130.03, 116.32, 116.27, 114.69, 111.99, 111.73, 111.07, 111.05, 110.70, 110.52, 62.73, 62.71, 58.83, 58.82, 55.43, 55.39, 29.67, 28.94, 28.87, 17.97, 17.86, 17.76, 13.88, 13.09, 13.07, 12.89, 8.13, 8.12; FTIR (thin film): 3456, 2979, 2940, 2849, 1774, 1745, 1599, 1461, 1378, 1288, 1226, 1152, 1126, 1052 cm<sup>-1</sup>; HRMS (ESI-APCI) *m/z* calc'd for C<sub>26</sub>H<sub>34</sub>NO<sub>6</sub> (M+H)<sup>+</sup>: 456.2386, found: 456.2386.

### Preparation of styrene **313**



Aryl bromide **301** (0.507 g, 1.32 mmol), PdCl<sub>2</sub>(PPh<sub>3</sub>)<sub>2</sub> (0.093 g, 0.132 mmol), vinyl stannane (0.77 mL, 2.64 mmol), and DMF (13.2 mL) were heated to 80 °C. After 16 h the reaction was cooled to room temperature and water (20 mL) was added. The mixture was extracted with EtOAc (3 × 15 mL) and the combined organics were washed with water (2 × 20 mL) then brine (30 mL), dried over MgSO<sub>4</sub>, filtered and concentrated *in vacuo*. The crude material was purified by flash chromatography (15%→20% EtOAc/hexanes) to give styrene **313** (0.367 g, 80% yield).

<sup>1</sup>H-NMR (300 MHz; CDCl<sub>3</sub>): δ 7.03 (q, *J* = 1.8 Hz, 1H), 6.93 (t, *J* = 2.1 Hz, 1H), 6.88 (t, *J* = 1.9 Hz, 1H), 6.68 (dd, *J* = 17.5, 10.9 Hz, 1H), 5.76 (d, *J* = 17.5 Hz, 1H), 5.32 (d, *J* = 10.9 Hz, 1H), 4.66 (m, *J* = 3.3 Hz, 1H), 4.28-4.17 (m, 2H), 3.84 (s, 3H), 1.92 (m, 2H), 1.59 (m, 3H), 1.31-1.22 (m, 3H), 0.94-0.73 (m, 3H).

### Preparation of benzaldehyde **312**

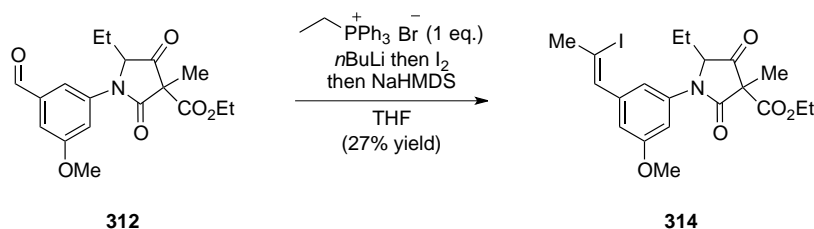


Styrene **313** (0.367 g, 1.06 mmol) was dissolved in THF (7 mL) and water (3.5 mL) and OsO<sub>4</sub> (0.08 M, 1.33 mL, 0.106 mmol) and NaIO<sub>4</sub> (1.18 g, 5.51 mmol) were added. The reaction was stirred for 3 h the water (10 mL) was added and the solution was extracted with EtOAc (3 × 10 mL). The combined organics were washed with brine (20 mL), dried over MgSO<sub>4</sub>, filtered

and concentrated *in vacuo*. The crude material was purified by flash chromatography (20% EtOAc/hexanes) to yield ketone **312** (0.231 g, 63% yield) as a mixture of diastereomers.

$^1\text{H-NMR}$  (400 MHz;  $\text{CDCl}_3$ ):  $\delta$  9.98-9.94 (m, 1H), 7.52 (dd,  $J = 1.9, 1.2$  Hz, 1H), 7.35 (dt,  $J = 5.7, 2.2$  Hz, 1H), 7.30 (ddd,  $J = 4.0, 2.5, 1.3$  Hz, 1H), 4.85 (dd,  $J = 5.6, 2.8$  Hz, 1H), 4.29-4.21 (m, 2H), 3.89-3.88 (m, 3H), 2.03-1.98 (m, 1H), 1.82-1.80 (m, 1H), 1.60-1.56 (m, 3H), 1.24-1.20 (m, 3H), 0.73 (q,  $J = 7.5$  Hz, 3H);  $^{13}\text{C-NMR}$  (101 MHz,  $\text{CDCl}_3$ ):  $\delta$  204.42, 204.20, 194.70, 191.14, 169.10, 165.28, 164.82, 160.80, 160.77, 138.18, 137.69, 137.58, 119.42, 119.23, 117.25, 117.10, 116.45, 116.43, 111.54, 111.23, 67.37, 66.89, 62.95, 62.81, 59.59, 59.49, 55.85, 22.33, 21.05, 17.28, 14.95, 13.91, 8.55, 7.89; FTIR (thin film): 2976, 2939, 2880, 2849, 1777, 1744, 1595, 1458, 1384, 1291, 1214, 1153, 1107, 1079, 1010  $\text{cm}^{-1}$ ; HRMS (ESI-APCI)  $m/z$  calc'd for  $\text{C}_{18}\text{H}_{22}\text{NO}_6$  ( $\text{M}+\text{H}$ ) $^+$ : 348.1447, found: 348.1440.

### Preparation of vinyl iodide **314**

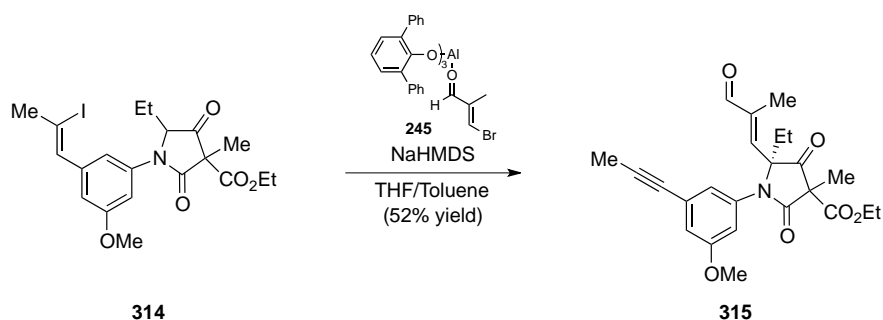


*n*-BuLi (1.6 M in hexanes, 0.14 mL, 0.216 mmol) was added to EtPPh<sub>3</sub>Br (0.080 g, 0.216 mmol) in THF (0.43 mL) at room temperature. After 30 min this solution was added via cannula to a mixture of I<sub>2</sub> (0.055 g, 0.216 mmol) in THF (1.3 mL) at  $-78$  °C. The reaction was slowly warmed to  $-10$  °C over 1 hr 15 min then cooled to  $-45$  °C at which point NaHMDS (1.0 M in THF, 0.216 mL, 0.216 mmol) was added. After stirring for 15 min benzaldehyde **312** (0.075 g,

0.216 mmol) in THF (3 mL) was added and the mixture was allowed to slowly warm to room temperature. After 1 hr 45 min MeOH (5 mL) was added and the volatiles were removed *in vacuo*. The crude material was purified by flash chromatography (20% EtOAc/hexanes) to provide vinyl iodide **314** (0.028 g, 27% yield).

$^1\text{H-NMR}$  (300 MHz;  $\text{CDCl}_3$ ):  $\delta$  7.04 (m, 2H), 6.90-6.88 (m, 1H), 6.63 (s, 1H), 4.67 (m,  $J = 3.3$  Hz, 1H), 4.29-4.07 (m, 2H), 3.84 (s, 3H), 2.71-2.68 (m, 3H), 2.06-1.82 (m, 2H), 1.63-1.55 (m, 3H), 1.31-1.19 (m, 3H), 0.93-0.73 (m, 3H).

### Preparation of alkyne **315**

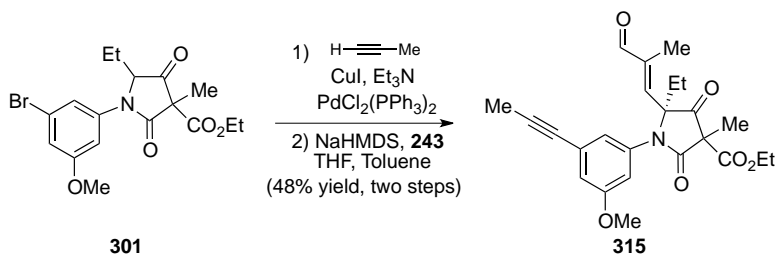


To a  $-78$  °C solution of ketone **314** (0.052 g 0.107 mmol) in THF (1.1 mL) was added NaHMDS (0.12 mL, 1.0 M in THF, 0.12 mmol) and the reaction mixture was allowed to warm slowly to  $-50$  °C then cooled to  $-78$  °C. Meanwhile, the vinyl bromide (0.024 g, 0.161 mmol) was added slowly to a solution of the Lewis acid (generated from slow addition of  $\text{AlMe}_3$  (0.096 mL, 2.0 M in hexanes, 0.193 mmol) to a solution of 2,6-diphenylphenol (0.132 g, 0.535 mmol) in toluene (1.1 mL) at room temperature) at  $-78$  °C and maintained for 20 min. The solution containing aldehyde complex **245** was then transferred via cannula to the sodium enolate of ketone **314**. The reaction mixture was maintained at  $-78$  °C for 1 h then allowed to warm slowly to room temperature over 3 h. The reaction mixture was quenched with sat. aq. Rochelle's salt (5 mL), stirred vigorously overnight, and extracted with EtOAc ( $3 \times 5$  mL). The combined organics were dried over  $\text{MgSO}_4$ , filtered and concentrated *in vacuo*. The crude material was

purified via flash chromatography (5%→10%→20% EtOAc/hexanes) to yield alkyne **315** (0.024 g, 52% yield).

$^1\text{H-NMR}$  (400 MHz;  $\text{CDCl}_3$ ):  $\delta$  9.41 (s, 1H), 6.90 (d,  $J = 1.3$  Hz, 1H), 6.87 (t,  $J = 2.2$  Hz, 1H), 6.84 (d,  $J = 2.2$  Hz, 1H), 6.44 (t,  $J = 1.3$  Hz, 1H), 4.25 (qd,  $J = 7.1, 1.2$  Hz, 2H), 3.77-3.75 (m, 3H), 2.39 (dd,  $J = 14.6, 7.3$  Hz, 1H), 2.17 (dd,  $J = 14.6, 7.4$  Hz, 1H), 2.01 (d,  $J = 2.4$  Hz, 3H), 1.88-1.85 (m, 3H), 1.63-1.57 (m, 3H), 1.28-1.24 (m, 3H), 0.87-0.80 (m, 3H);  $^{13}\text{C-NMR}$  (101 MHz,  $\text{CDCl}_3$ ):  $\delta$  202.82, 194.68, 194.00, 165.14, 159.78, 149.35, 142.07, 136.05, 125.90, 120.16, 115.09, 111.87, 87.25, 78.84, 62.95, 58.77, 55.44, 27.77, 17.95, 13.91, 10.31, 8.12, 4.32; FTIR (thin film): 2981, 2940, 2847, 1776, 1747, 1589, 1450, 1428, 1378, 1361, 1319, 1299, 1285, 1222, 1201, 1171, 1124, 1062, 1014  $\text{cm}^{-1}$ ; HRMS (ESI-APCI)  $m/z$  calc'd for  $\text{C}_{24}\text{H}_{28}\text{NO}_6$  ( $\text{M}+\text{H}$ ) $^+$ : 426.1917, found: 426.1901.

### Preparation of alkyne **315**

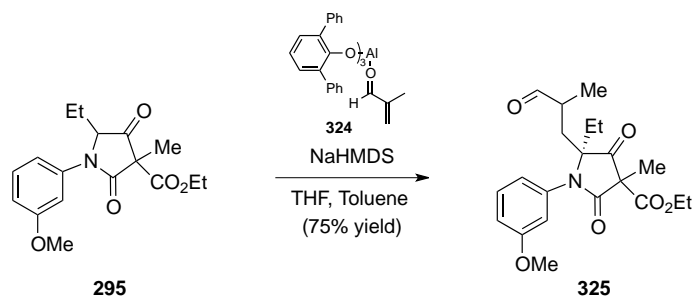


In a Schlenk flask was added  $\text{PdCl}_2(\text{PPh}_3)_2$  (0.043 g, 0.061 mmol) and  $\text{CuI}$  (0.006 g, 0.0304 mmol) then aryl bromide **301** (0.233 g, 0.608 mmol) in  $\text{Et}_3\text{N}$  (6.1 mL). Propyne gas was then bubble through the solution for 30 s and the Schlenk flask was closed under the propyne atmosphere. The reaction was heated at 50 °C for 19 h then was cooled to room temperature and sat. aq.  $\text{NH}_4\text{Cl}$  (15 mL) was added. The mixture was extracted with  $\text{EtOAc}$  ( $3 \times 10$  mL) and the combined organics were washed with brine (15 mL), dried over  $\text{MgSO}_4$ , filtered and concentrated *in vacuo*. The crude material was purified by flash chromatography (20%  $\text{EtOAc}$ /hexanes) to give alkyne **358** (0.160 g, 74% yield).

$^1\text{H-NMR}$  (400 MHz;  $\text{CDCl}_3$ ):  $\delta$  7.15 (t,  $J = 1.6$  Hz, 1H), 7.01-6.95 (m, 2H), 4.74 (dd,  $J = 5.5, 2.8$  Hz, 1H), 4.25-4.16 (m, 2H), 3.80 (s, 3H), 2.02 (s, 3H), 1.99-1.87 (m, 2H), 1.59-1.56 (s, 3H), 1.27-1.24 (m, 3H), 0.90-0.86 (m, 3H);  $^1\text{H-NMR}$  (400 MHz;  $\text{CDCl}_3$ ):  $\delta$  7.15 (t,  $J = 1.6$  Hz, 1H), 7.01-6.95 (m, 2H), 4.47 (dd,  $J = 7.2, 3.6$  Hz, 1H), 4.25-4.16 (m, 2H), 3.79 (s, 3H), 2.02 (s, 4H), 1.99-1.87 (m, 2H), 1.55 (s, 3H), 1.22 (td,  $J = 4.6, 2.5$  Hz, 3H), 0.72 (td,  $J = 7.4, 2.9$  Hz, 3H);  $^{13}\text{C-NMR}$  (101 MHz,  $\text{CDCl}_3$ ):  $\delta$  205.07, 204.38, 168.88, 168.86, 168.76, 165.31, 165.03, 160.69, 159.92, 159.90, 137.57, 136.67, 134.07, 128.40, 128.33, 125.77, 123.01, 118.99, 118.89, 115.50, 115.36, 114.93, 114.78, 110.61, 109.53, 109.45, 86.95, 78.92, 67.63, 67.04, 62.80, 62.76, 59.46, 55.73, 55.51, 22.41, 21.15, 17.24, 14.91, 13.91, 13.90, 8.60, 7.92, 4.28; FTIR (thin film): 2974, 2939, 1777, 1744, 1703, 1593, 1572, 1449, 1435, 1289, 1251, 1202, 1174, 1107  $\text{cm}^{-1}$ ; HRMS (ESI-APCI)  $m/z$  calc'd for  $\text{C}_{20}\text{H}_{24}\text{NO}_5$  (M+H) $^+$ : 358.1654, found: 358.1645.

To a  $-78$  °C solution of alkyne **358** (0.160 g 0.448 mmol) in THF (4.5 mL) was added NaHMDS (0.49 mL, 1.0 M in THF, 0.49 mmol) and the reaction mixture was allowed to warm slowly to  $-50$  °C then cooled to  $-78$  °C. Meanwhile, the vinyl bromide (0.100 g, 0.672 mmol) was added slowly to a solution of the Lewis acid (generated from slow addition of  $\text{AlMe}_3$  (0.40 mL, 2.0 M in hexanes, 0.806 mmol) to a solution of 2,6-diphenylphenol (0.552 g, 2.24 mmol) in toluene (4.5 mL) at room temperature) at  $-78$  °C and maintained for 20 min. The solution containing aldehyde complex **243** was then transferred via cannula to the sodium enolate of ketone **358**. The reaction mixture was maintained at  $-78$  °C for 1 h then allowed to warm slowly to room temperature over 3 h. The reaction mixture was quenched with sat. aq. Rochelle's salt (15 mL), stirred vigorously overnight, and extracted with EtOAc (3  $\times$  10 mL). The combined organics were dried over  $\text{MgSO}_4$ , filtered and concentrated *in vacuo*. The crude material was purified via flash chromatography (5% $\rightarrow$ 10% $\rightarrow$ 20% EtOAc/hexanes) to yield alkyne **315** (0.024 g, 65% yield). The spectral data was identical to that obtained when alkyne **315** was synthesized from vinyl iodide **314**.

## Preparation of synthesis of aldehyde **325**

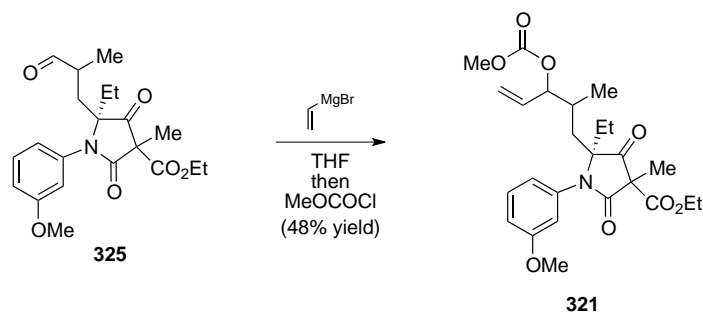


To a solution of **295** (0.500 g, 1.57 mmol) in THF (20 mL) was added NaHMDS (1 M in THF, 1.9 mL, 1.88 mmol) dropwise at  $-78\text{ }^{\circ}\text{C}$  and the mixture was allowed to stir for 20 min at this temperature. Meanwhile,  $\text{AlMe}_3$  (2 M in toluene, 1.4 mL, 2.82 mmol) was added to a solution of 2,6-diphenylphenol (1.97 g, 7.99 mmol) in toluene (20 mL). After 10 min stirring at room temperature the toluene solution was cooled to  $-78\text{ }^{\circ}\text{C}$  and methacrolein (0.20 mL, 2.35 mmol) was added, which resulted in the formation of a bright yellow solution. The THF solution of the sodium enolate of **295** was then transferred via cannula to the methacrolein–Lewis Acid complex at  $-78\text{ }^{\circ}\text{C}$ , the solution stirred for another 10 min at  $-78\text{ }^{\circ}\text{C}$  and then slowly warmed to room temperature. After stirring for 1 h at room temperature the reaction was quenched by addition of saturated aqueous Rochelle's salt (30 mL) and the mixture stirred vigorously for 30 min. Then diethyl ether (10 mL) was added and the phases separated. The aqueous phase was extracted with diethyl ether ( $2 \times 10\text{ mL}$ ) and the combined organic phase was washed with brine (30 mL), dried over  $\text{MgSO}_4$ , filtered and concentrated *in vacuo*. The crude material was purified by flash chromatography (5:1→2:1 hexanes:EtOAc) to yield aldehyde **325** (0.460 g, 75% yield) as a mixture of diastereomers.

$^1\text{H-NMR}$  (400 MHz;  $\text{CDCl}_3$ ):  $\delta$  9.47-9.36 (m, 1H), 7.35 (t,  $J = 8.0\text{ Hz}$ , 1H), 6.92 (dd,  $J = 8.0, 6.1\text{ Hz}$ , 1H), 6.80 (d,  $J = 7.9\text{ Hz}$ , 1H), 6.74 (s, 1H), 4.31-4.16 (m, 2H), 2.80-2.40 (m, 3H), 1.99 (m,  $J = 7.5\text{ Hz}$ , 1H), 1.89-1.77 (m, 1H), 1.60-1.50 (m, 3H), 1.33-1.20 (m, 3H), 1.07-1.00 (m, 3H), 0.96-0.88 (m, 3H);  $^{13}\text{C-NMR}$  (101 MHz,  $\text{CDCl}_3$ ):  $\delta$  208.08, 207.93, 207.79, 207.08, 202.61, 202.19, 202.04, 201.76, 170.31, 170.09, 170.03, 165.43, 165.35, 165.31, 165.10, 160.35,

160.33, 160.31, 149.57, 135.54, 135.48, 135.39, 130.26, 130.21, 130.14, 120.72, 120.65, 120.54, 115.87, 114.86, 114.84, 114.74, 114.68, 114.07, 114.02, 113.94, 113.29, 75.73, 75.55, 75.24, 74.81, 63.08, 62.90, 62.68, 62.58, 58.62, 58.58, 58.38, 55.39, 41.63, 41.11, 40.99, 40.88, 36.94, 36.91, 36.51, 36.32, 29.62, 29.00, 28.43, 28.22, 18.00, 17.34, 16.40, 16.17, 15.94, 15.77, 15.75, 14.02, 13.92, 13.86, 8.90, 8.81, 8.56, 8.54; FTIR (thin film): 2977, 2940, 2883, 2838, 1772, 1702, 1603, 1588, 1512, 1492, 1455, 1383, 1288, 1270, 1218, 1038  $\text{cm}^{-1}$ ; HRMS (ESI-APCI)  $m/z$  calc'd for  $\text{C}_{21}\text{H}_{28}\text{NO}_6$  ( $\text{M}+\text{H}$ ) $^+$ : 390.1917, found: 390.1907.

### Preparation of vinyl carbonate **321**

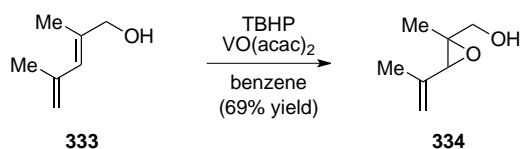


To a solution of aldehyde **325** (0.150 g, 0.385 mmol) in THF (5 mL) was added vinylmagnesium bromide (1.1 M in THF, 0.42 mL, 0.462 mmol) at  $-78$  °C and the mixture stirred for 1 h at this temperature. Methyl chloroformate (75 mL, 0.963 mmol) was added and the mixture was allowed to warm to room temperature. Aqueous saturated sodium bicarbonate (10 mL) and diethylether (10 mL) were added and the phases separated. The aqueous phase was extracted with diethyl ether ( $2 \times 5$  mL) and the combined organic phase was washed with brine (20 mL), dried over  $\text{MgSO}_4$ , filtered and concentrated *in vacuo*. The crude material was purified by flash chromatography (3:1 $\rightarrow$ 2:1 hexanes:EtOAc) to provide vinyl carbonate **321** (0.087 g, 48% yield) as a mixture of diastereomers.

$^1\text{H-NMR}$  (400 MHz;  $\text{CDCl}_3$ ):  $\delta$  7.34 (m, 1H), 6.94-6.90 (m, 1H), 6.86-6.82 (m, 1H), 6.79 (m, 1H), 5.69-5.60 (m, 1H), 5.29-5.23 (m, 1H), 4.85-4.77 (m, 1H), 4.26-4.16 (m, 2H), 3.82-3.69

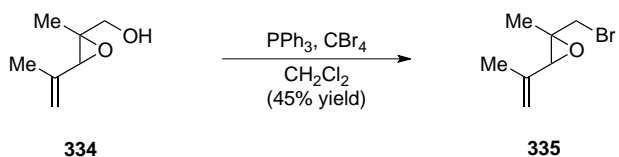
(m, 7H), 2.18-1.80 (m, 5H), 1.70-1.62 (m, 3H), 1.28-1.18 (m, 3H), 1.01-0.84 (m, 6H);  $^{13}\text{C}$ -NMR (101 MHz,  $\text{CDCl}_3$ ):  $\delta$  207.63, 207.31, 170.41, 170.19, 165.67, 165.58, 160.24, 160.20, 154.99, 135.61, 132.72, 132.69, 130.07, 129.99, 120.76, 120.66, 120.57, 120.51, 119.58, 118.90, 114.86, 114.81, 114.53, 113.85, 113.72, 96.97, 82.18, 75.81, 75.61, 62.64, 62.56, 62.52, 58.84, 58.63, 58.58, 55.44, 55.38, 55.33, 55.30, 54.99, 54.70, 40.27, 40.21, 34.52, 32.04, 31.33, 28.80, 28.76, 18.58, 18.52, 18.42, 17.94, 17.42, 17.27, 17.20, 13.87, 9.03, 8.69, 8.59; FTIR (thin film): 2979, 2941, 1770, 1745, 1701, 1602, 1587, 1492, 1442, 1381, 1134, 1036, 1018  $\text{cm}^{-1}$ ; HRMS (ESI-APCI)  $m/z$  calc'd for  $\text{C}_{25}\text{H}_{34}\text{NO}_8$  ( $\text{M}+\text{H}$ ) $^+$ : 476.2284, found: 476.2277.

### Preparation of epoxide **334**



To a suspension of known allylic alcohol **333**<sup>10</sup> (1.50 g, 13.37 mmol) and  $\text{VO}(\text{acac})_2$  (196 mg, 0.76 mmol) in benzene (50 mL) was added TBHP (7.3 M in  $\text{H}_2\text{O}$ , 2.3 mL, 16.79 mmol) at room temperature. The dark reddish-brown solution was stirred for 14 h at ambient temperature before  $\text{MgSO}_4$  was added. The mixture was stirred for 30 min, filtered and concentrated *in vacuo*. The crude material was purified by flash chromatography (5:1→4:1 hexanes:EtOAc) to provide allylic epoxide **334** (1.18 g, 69% yield). All spectral data matched that known in the literature for **334**.<sup>10</sup>

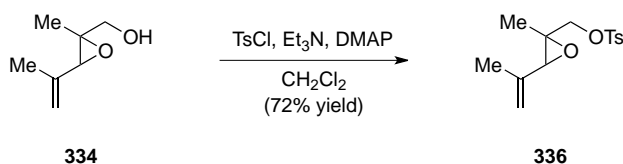
### Preparation of bromide **335**



Triphenylphosphine (675 mg, 2.575 mmol) was suspended in acetonitrile (5 mL) and cooled to 0 °C before bromine (130 mL, 2.575 mmol) was added dropwise. The tan suspension was stirred for 20 min at 0 °C then a solution of allylic epoxide **334** (300 mg, 2.341 mmol) and triethylamine (390 mL, 2.809 mmol) in acetonitrile (1 mL) was added. The mixture was allowed to warm to room temperature and stirred for 30 min before diethyl ether (10 mL) was added. The precipitate was filtered off, the filtrate concentrated *in vacuo* and the crude material was purified by flash chromatography (50:1→20:1 hexanes:EtOAc) to furnish allylic bromide **335** (202 mg, 45% yield).

$^1\text{H-NMR}$  (400 MHz;  $\text{CDCl}_3$ ):  $\delta$  4.97 (s, 1H), 4.88 (s, 1H), 3.42 (d,  $J = 10.2$  Hz, 1H), 3.29 (d,  $J = 10.3$  Hz, 1H), 3.26 (s, 1H), 1.74 (s, 3H), 1.28 (s, 3H);  $^{13}\text{C-NMR}$  (101 MHz,  $\text{CDCl}_3$ ):  $\delta$  138.26, 112.47, 66.03, 61.31, 38.99, 19.58, 13.71; FTIR (thin film): 3093, 2970, 2935, 2857, 1656, 1446, 1423, 1384, 1216, 1070, 1040, 1015  $\text{cm}^{-1}$ .

### Preparation of tosylate **336**

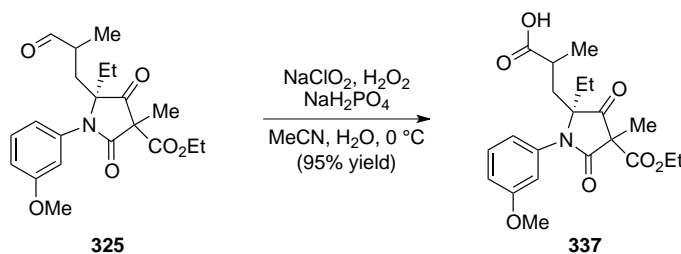


To an ice cold solution of epoxy alcohol **334** (300 mg, 2.341 mmol) in  $\text{CH}_2\text{Cl}_2$  (10 mL) was added  $\text{DMAP}$  (30 mg, 0.234 mmol), triethylamine (0.35 mL, 2.575 mmol) and *p*- $\text{TsCl}$  (470 mg, 2.458 mmol). The white suspension formed was stirred for 30 min at 0 °C and then warmed to room temperature where it was stirred for 1 h. The mixture was quenched by addition of saturated aqueous ammonium chloride (10 mL). The aqueous phase was extracted with  $\text{CH}_2\text{Cl}_2$

(3 × 5 mL) and the combined organic phases were washed with brine (20 mL), dried over MgSO<sub>4</sub>, filtered and concentrated *in vacuo*. The crude material was purified by flash chromatography (10:1 hexanes:EtOAc) to give allylic tosylate **336** (473 mg, 72% yield).

<sup>1</sup>H-NMR (400 MHz; CDCl<sub>3</sub>): δ 7.78-7.76 (d, *J* = 8.1 Hz, 2H), 7.33 (d, *J* = 8.1 Hz, 2H), 4.97 (s, 1H), 4.87 (s, 1H), 4.00 (d, *J* = 10.7 Hz, 1H), 3.99-3.95 (d, *J* = 10.7 Hz, 1H), 3.20 (s, 1H), 2.42 (s, 3H), 1.70 (s, 3H), 1.16 (s, 3H); <sup>13</sup>C-NMR (101 MHz, CDCl<sub>3</sub>): δ 145.04, 137.69, 132.62, 129.89, 127.91, 112.83, 73.72, 62.67, 59.55, 21.62, 19.60, 12.76; FTIR (thin film): 2975, 2939, 1656, 1598, 1495, 1448, 1359, 1175, 1096 cm<sup>-1</sup>; HRMS (ESI-APCI) *m/z* calc'd for C<sub>14</sub>H<sub>18</sub>NaO<sub>4</sub>S (M+Na)<sup>+</sup>: 305.0823, found: 305.0810.

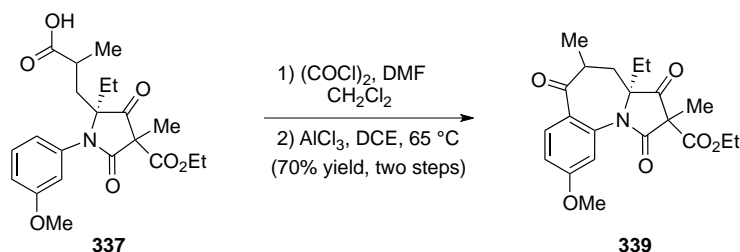
### Preparation of carboxylic acid **337**



To a solution of aldehyde **325** (570 mg, 1.46 mmol) in acetonitrile (3 mL) was added a solution of NaH<sub>2</sub>PO<sub>2</sub> (53 mg, 0.438 mmol) in water (1.5 mL) followed by H<sub>2</sub>O<sub>2</sub> (30% (w/w) in H<sub>2</sub>O, 0.15 mL, 1.42 mmol). The biphasic mixture was cooled to 0 °C and stirred vigorously, while a solution of NaClO<sub>2</sub> (80% (w/w), 232 mg, 2.05 mmol) in water (1.5 mL) was added over 45 min. After stirring for 1 h at 0 °C the reaction was quenched by addition of saturated aqueous sodium bisulfite solution (1 mL) and saturated aqueous ammonium chloride (5 mL). Then EtOAc (10 mL) was added and the phases separated. The aqueous phase was extracted with EtOAc (2 × 10 mL) and the combined organic phase was washed with brine (50 mL), dried over MgSO<sub>4</sub>, filtered and concentrated *in vacuo* to provide carboxylic acid **337** (460 mg, 91% yield) as a mixture of diastereomers in form of an off white foam.

$^1\text{H-NMR}$  (400 MHz;  $\text{CDCl}_3$ ):  $\delta$  7.34 (m, 1H), 6.92 (m, 1H), 6.85-6.78 (m, 1H), 6.75 (m, 1H), 4.25-4.16 (m, 2H), 3.79-3.77 (m, 3H), 2.59 (m, 1H), 2.35-2.31 (m, 1H), 1.97-1.67 (m, 3H), 1.65-1.52 (m, 3H), 1.33-1.21 (m, 3H), 1.17-1.10 (m, 3H), 0.91 (m, 3H);  $^{13}\text{C-NMR}$  (101 MHz,  $\text{CDCl}_3$ ):  $\delta$  207.70, 207.40, 207.13, 206.42, 181.57, 181.10, 180.91, 180.62, 170.60, 170.58, 170.34, 170.21, 165.49, 165.39, 165.33, 164.86, 160.34, 160.29, 136.50, 135.58, 135.55, 135.37, 135.32, 130.25, 130.18, 130.12, 120.80, 120.68, 120.58, 120.56, 114.86, 114.67, 114.60, 114.17, 114.14, 113.92, 75.83, 75.62, 75.57, 74.89, 65.79, 62.98, 62.88, 62.65, 62.57, 58.70, 58.67, 58.57, 58.50, 55.39, 55.35, 55.27, 40.63, 39.85, 39.76, 39.20, 34.77, 34.67, 34.44, 34.06, 29.63, 29.19, 28.42, 27.74, 27.18, 20.16, 20.01, 19.95, 19.89, 17.88, 17.78, 15.68, 15.63, 15.12, 14.01, 13.86, 13.78, 8.92, 8.74, 8.54, 8.52; FTIR (thin film): 3084, 2979, 2941, 2885, 1772, 2740, 1603, 1588, 1492, 1455, 1385, 1288, 1269, 1217, 1177, 1149  $\text{cm}^{-1}$ ; HRMS (ESI-APCI)  $m/z$  calc'd for  $\text{C}_{21}\text{H}_{28}\text{NO}_7$  ( $\text{M}+\text{H}$ ) $^+$ : 406.1866, found: 406.1845.

### Preparation of ketone **339**

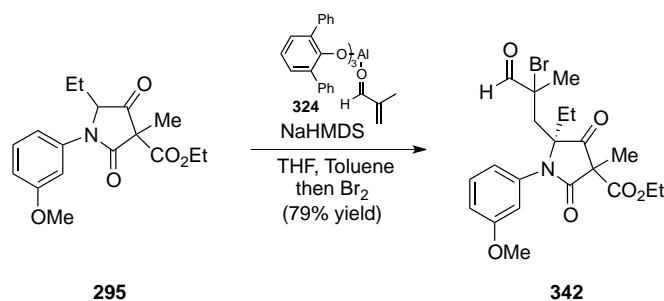


To a solution of carboxylic acid **337** (530 mg, 1.31 mmol) in  $\text{CH}_2\text{Cl}_2$  (5 mL) was added oxalyl chloride (0.22 mL, 2.61 mmol) followed by a drop of DMF. The solution was stirred for 30 min and then concentrated *in vacuo*. The residue was dissolved in 1,2-dichloroethane (20 mL) and  $\text{AlCl}_3$  (261 mg, 1.96 mmol) was added and the suspension heated at  $65\text{ }^\circ\text{C}$  for 4 h. The yellowish mixture was then cooled to room temperature and a saturated aqueous Rochelle's salt (20 mL) was added and the mixture stirred vigorously for 30 min. The mixture was then diluted with water (10 mL) and  $\text{CH}_2\text{Cl}_2$  (5 mL) and the phases separated. The aqueous phase was

extracted with CH<sub>2</sub>Cl<sub>2</sub> (2 × 5 mL) and the combined organic phase was washed with brine (15 mL), dried over MgSO<sub>4</sub>, filtered and concentrated *in vacuo*. The crude material was purified by flash chromatography (4:1→3:1 hexanes:EtOAc) to yield ketone **339** (356 mg, 70% yield) as a mixture of diastereomers.

<sup>1</sup>H-NMR (400 MHz; CDCl<sub>3</sub>): δ 8.11 (m, 1H), 7.01-6.94 (m, 2H), 4.29-4.18 (m, 2H), 3.86 (m, 3H), 2.47-2.38 (m, 2H), 1.84-1.70 (m, 3H), 1.67-1.59 (m, 3H), 1.31-1.17 (m, 6H), 0.79 (m, 3H); <sup>13</sup>C-NMR (101 MHz, CDCl<sub>3</sub>): δ 208.16, 206.63, 197.99, 197.57, 169.11, 165.32, 165.19, 163.71, 163.62, 136.72, 136.60, 132.52, 125.57, 114.48, 114.43, 114.37, 113.76, 75.56, 75.10, 62.99, 62.88, 58.42, 58.39, 55.81, 55.76, 42.39, 41.98, 41.45, 40.56, 31.10, 30.76, 17.03, 16.91, 15.80, 15.63, 13.90, 8.83, 7.99; FTIR (thin film): 2977, 2938, 2873, 1775, 1745, 1704, 1673, 1600, 1496, 1445, 1378, 1298, 1151, 1112, 1032 cm<sup>-1</sup>; HRMS (ESI-APCI) *m/z* calc'd for C<sub>21</sub>H<sub>26</sub>NO<sub>6</sub> (M+H)<sup>+</sup>: 388.1760, found: 388.1762.

### Preparation of aldehyde **342**

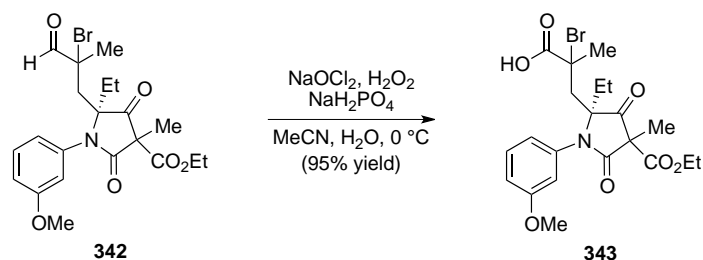


To a solution of ketone **295** (1.00 g, 3.13 mmol) in THF (30 mL) was added NaHMDS (1 M in THF, 3.7 mL, 3.76 mmol) dropwise at -78 °C and the mixture was allowed to stir for 20 min. Meanwhile, AlMe<sub>3</sub> (2 M in toluene, 2.8 mL, 2.82 mmol) was added to a solution of 2,6-diphenylphenol (3.94 g, 15.98 mmol) in toluene (30 mL). After 10 min stirring at room temperature the toluene solution was cooled to -78 °C and methacrolein (0.40 mL, 4.70 mmol) was added, which resulted in the formation of a bright yellow solution. The THF solution of the sodium enolate of **325** was then transferred via cannula to the methacrolein-Lewis Acid

complex at  $-78\text{ }^{\circ}\text{C}$ . The solution was stirred for another 10 min at  $-78\text{ }^{\circ}\text{C}$  and then was allowed to slowly warm to room temperature. After stirring for 1 h at room temperature the reaction was cooled to  $-78\text{ }^{\circ}\text{C}$  and bromine (0.24 mL, 4.70 mmol) was added dropwise. The reaction mixture was allowed to warm to room temperature and quenched by addition of saturated aqueous Rochelle's salt solution (50 mL), which was stirred vigorously for 30 min. The aqueous phase was extracted with diethyl ether ( $3 \times 20\text{ mL}$ ) and the combined organic phases were washed with brine (50 mL), dried over  $\text{MgSO}_4$ , filtered and concentrated *in vacuo*. The crude material was purified by flash chromatography (5:1 $\rightarrow$ 3:1 hexanes:EtOAc) to give aldehyde **342** (1.16 g, 79% yield) as a mixture of diastereomers in form of a brownish oil.

$^1\text{H-NMR}$  (400 MHz;  $\text{CDCl}_3$ ):  $\delta$  9.23-9.10 (m, 1H), 7.42-7.35 (m, 1H), 6.98-6.74 (m, 3H), 4.34-4.16 (m, 2H), 3.81-3.75 (m, 3H), 3.10 (m, 1H), 2.63-2.44 (m, 1H), 2.25-1.97 (m, 2H), 1.94-1.84 (m, 3H), 1.76-1.51 (m, 3H), 1.38-1.21 (m, 3H), 0.94-0.86 (m, 3H);  $^{13}\text{C-NMR}$  (101 MHz,  $\text{CDCl}_3$ ):  $\delta$  207.02, 206.75, 205.95, 205.54, 192.36, 190.64, 189.86, 189.64, 169.92, 169.78, 169.76, 165.33, 165.17, 164.85, 160.44, 160.33, 135.38, 135.37, 135.14, 134.85, 130.48, 130.45, 130.27, 130.26, 121.05, 120.70, 120.64, 120.62, 115.09, 115.03, 114.89, 114.75, 114.69, 114.27, 114.22, 114.18, 114.10, 75.95, 75.84, 74.83, 74.65, 66.64, 66.42, 65.64, 65.20, 63.29, 63.21, 62.94, 62.79, 59.10, 58.82, 58.79, 58.57, 55.42, 46.31, 45.08, 44.76, 42.25, 31.76, 31.54, 28.99, 28.37, 27.62, 25.18, 24.72, 24.53, 18.20, 17.31, 15.69, 15.33, 14.05, 13.96, 13.89, 8.95, 8.77, 8.66, 8.62; FTIR (thin film): 2980, 2941, 2838, 1773, 1602, 1587, 1492, 1451, 1380, 1312, 1269, 1235, 1209, 1158, 1138, 1038  $\text{cm}^{-1}$ ; HRMS (ESI-APCI) *m/z* calc'd for  $\text{C}_{21}\text{H}_{26}\text{BrNO}_6\text{Na}$  ( $\text{M}+\text{Na}$ ) $^+$ : 490.0841, found: 490.0834.

### Preparation of carboxylic acid **343**

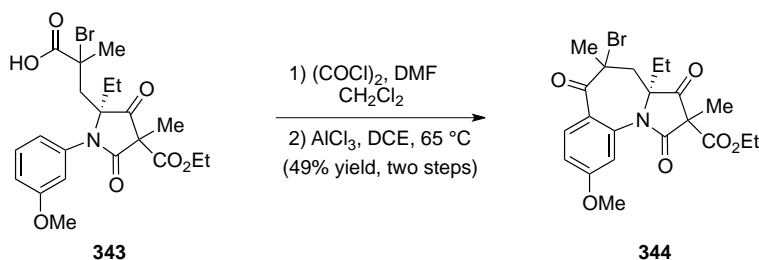


To a solution of aldehyde **342** (1.00 g, 2.135 mmol) in acetonitrile (5 mL) was added a solution of NaH<sub>2</sub>PO<sub>2</sub> (77 mg, 0.641 mmol) in water (3 mL) followed by H<sub>2</sub>O<sub>2</sub> (30% (w/w) in H<sub>2</sub>O, 0.22 mL, 2.24 mmol). The biphasic mixture was cooled to 0 °C and stirred vigorously while a solution of NaClO<sub>2</sub> (80% (w/w), 483 mg, 4.27 mmol) in water (2 mL) was added over 45 min. After stirring for 1 h at 0 °C the reaction was quenched by addition of saturated aqueous sodium bisulfite solution (2 mL) and saturated aqueous ammonium chloride (10 mL). The aqueous phase was extracted with EtOAc (3 × 20 mL) and the combined organic phase was washed with brine (50 mL), dried over MgSO<sub>4</sub>, filtered and concentrated *in vacuo* to yield carboxylic acid **343** (400 mg, 97% yield) as a mixture of diastereomers, which was used without further purification.

<sup>1</sup>H-NMR (400 MHz; CDCl<sub>3</sub>): δ 7.41-7.27 (m, 1H), 6.98-6.73 (m, 3H), 4.31-4.16 (m, 2H), 3.84-3.73 (m, 3H), 3.36-3.18 (m, 1H), 2.96 (m, 1H), 2.67-2.26 (m, 2H), 2.09-1.94 (m, 3H), 1.73-1.48 (m, 3H), 1.39-1.18 (m, 3H), 0.97-0.83 (m, 3H); <sup>13</sup>C-NMR (101 MHz, CDCl<sub>3</sub>): δ 206.31, 205.82, 205.64, 205.35, 204.81, 177.58, 177.44, 174.14, 173.85, 173.53, 173.10, 171.65, 171.54, 170.98, 170.68, 170.33, 170.27, 170.11, 165.44, 165.30, 164.90, 164.48, 160.40, 160.28, 160.25, 160.20, 137.13, 135.26, 135.24, 135.10, 134.77, 130.43, 130.33, 130.28, 130.24, 130.20, 130.06, 121.02, 120.97, 120.82, 120.48, 120.35, 115.01, 114.97, 114.79, 114.70, 114.51, 114.39, 114.33, 114.31, 114.28, 113.51, 109.98, 83.18, 77.93, 76.03, 75.53, 74.95, 71.75, 64.48, 63.35, 63.21, 62.81, 62.72, 62.70, 62.38, 60.53, 59.09, 58.95, 58.58, 58.01, 57.62, 56.58, 55.43, 55.39, 55.37, 49.09, 48.86, 47.69, 46.73, 46.15, 44.39, 30.86, 30.71, 30.55, 29.64, 29.34, 29.19, 28.94, 28.87, 28.72, 28.38, 27.50, 25.92, 25.33, 21.01, 20.97, 19.06, 18.45,

18.26, 17.37, 15.90, 15.67, 15.48, 14.13, 14.04, 14.00, 13.96, 13.87, 13.69, 13.66, 9.30, 8.95, 8.73, 8.68, 8.47, 8.10; HRMS (ESI-APCI)  $m/z$  calc'd for  $C_{21}H_{27}BrNO_7$  (M+H)<sup>+</sup>: 470.1001, found: 470.1004.

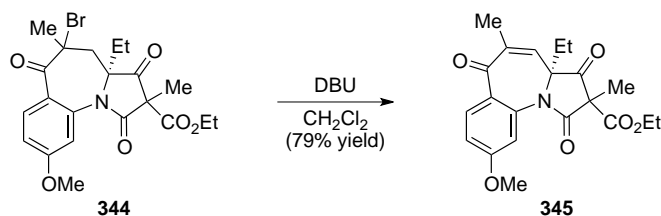
### Preparation of ketone **344**



To a solution of carboxylic acid **343** (1.27 g, 2.62 mmol) in  $CH_2Cl_2$  (10 mL) was added oxalyl chloride (0.44 mL, 5.24 mmol) followed by a drop of DMF. The solution was stirred for 30 min and then concentrated *in vacuo*. The residue was dissolved in 1,2-dichloroethane (20 mL) and  $AlCl_3$  (699 mg, 5.24 mmol) was added and the suspension was heated at  $65\text{ }^\circ\text{C}$  for 4 h. The yellowish mixture was cooled to room temperature and saturated aqueous Rochelle's salt (20 mL) was added and the mixture was stirred vigorously for 30 min. The aqueous phase was extracted with  $CH_2Cl_2$  ( $3 \times 5$  mL) and the combined organic phases were washed with brine (15 mL), dried over  $MgSO_4$ , filtered and concentrated *in vacuo*. The crude material was purified by flash chromatography (5:1→2:1 hexanes:EtOAc) to yield ketone **344** (0.254 g, 21% yield, higher  $R_f$  diastereomer contaminated with inseparable acid chloride intermediate; 0.345 g, 28% yield, lower  $R_f$  diastereomer, pure). Only the lower  $R_f$  diastereomer is characterized.

$^1H$ -NMR (300 MHz;  $CDCl_3$ ):  $\delta$  8.06 (d,  $J = 8.9$  Hz, 1H), 7.08 (d,  $J = 2.5$  Hz, 1H), 6.98 (dd,  $J = 8.9, 2.5$  Hz, 1H), 4.29 (q,  $J = 7.1$  Hz, 3H), 3.90 (s, 3H), 3.19-3.14 (m, 1H), 2.21-2.15 (m, 1H), 1.99 (s, 3H), 1.78 (s, 3H), 1.33 (t,  $J = 7.2$  Hz, 3H), 0.80 (t,  $J = 7.5$  Hz, 3H).

## Preparation of enone 345

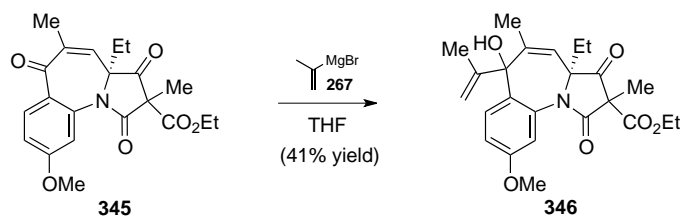


To a solution of  $\alpha$ -bromo ketone **344** (345 mg, 0.740 mmol) in  $\text{CH}_2\text{Cl}_2$  (5 mL) was added DBU (220 mL, 1.48 mmol) and the dark solution was stirred for 2 h at ambient temperature. The reaction mixture was diluted with saturated aqueous ammonium chloride (10 mL) and the aqueous phase was extracted with  $\text{CH}_2\text{Cl}_2$  (3  $\times$  5 mL). The combined organic phases were washed with brine (15 mL), dried over  $\text{MgSO}_4$ , filtered and concentrated *in vacuo*. The crude material was purified by flash chromatography (5:1 $\rightarrow$ 4:1 hexanes:EtOAc) to furnish **345** (226 mg, 79% yield) of a separable mixture of diastereomers.

Diastereomer A:  $^1\text{H-NMR}$  (400 MHz;  $\text{CDCl}_3$ ):  $\delta$  7.92 (d,  $J = 8.9$  Hz, 1H), 7.01 (d,  $J = 2.5$  Hz, 1H), 6.95 (dd,  $J = 8.9, 2.5$  Hz, 1H), 6.48 (s, 1H), 4.14-4.02 (m, 2H), 3.87 (s, 3H), 2.04-1.98 (m, 4H), 1.66-1.58 (m, 4H), 1.09 (t,  $J = 7.1$  Hz, 3H), 0.76 (t,  $J = 7.3$  Hz, 3H);  $^{13}\text{C-NMR}$  (101 MHz,  $\text{CDCl}_3$ ):  $\delta$  205.13, 194.71, 188.23, 168.32, 164.30, 163.11, 139.76, 136.92, 133.78, 133.41, 128.45, 114.47, 112.41, 62.90, 57.68, 55.81, 27.57, 20.91, 15.23, 13.69, 8.47.

Diastereomer B:  $^1\text{H-NMR}$  (400 MHz;  $\text{CDCl}_3$ ):  $\delta$  7.95 (d,  $J = 8.9$  Hz, 1H), 7.03 (d,  $J = 2.5$  Hz, 1H), 6.96 (dd,  $J = 8.9, 2.5$  Hz, 1H), 6.46 (s, 1H), 4.27 (q,  $J = 7.1$  Hz, 2H), 3.88 (s, 3H), 2.06-2.00 (m, 4H), 1.69 (dd,  $J = 14.7, 7.4$  Hz, 1H), 1.57 (s, 3H), 1.29 (t,  $J = 7.1$  Hz, 3H), 0.84 (t,  $J = 7.4$  Hz, 3H);  $^{13}\text{C-NMR}$  (101 MHz,  $\text{CDCl}_3$ ):  $\delta$  204.98, 194.96, 187.48, 168.60, 165.17, 163.28, 139.27, 138.48, 134.14, 133.51, 127.96, 114.36, 112.75, 62.82, 57.94, 55.73, 28.08, 21.03, 18.91, 13.93, 8.41. HRMS (ESI-APCI)  $m/z$  calc'd for  $\text{C}_{21}\text{H}_{24}\text{NO}_6$  ( $\text{M}+\text{H}$ ) $^+$ : 386.1604, found: 386.1590.

## Preparation of alcohol **346**



To a solution of enone **345** (94 mg, 0.244 mmol) in THF (4 mL) was added isopropenylmagnesium bromide (0.5 M in THF, 540 mL, 0.268 mmol) at  $-78$  °C. The dark green mixture was stirred for 15 min at  $-78$  °C and then warmed to 0 °C. After 1 h at 0 °C the reaction was quenched by addition of saturated aqueous ammonium chloride solution (10 mL) and the aqueous phase extracted with diethyl ether (3  $\times$  5 mL). The combined organic phases were washed with brine (15 mL), dried over  $\text{MgSO}_4$ , filtered and concentrated *in vacuo*. The crude material was purified by flash chromatography (4:1  $\rightarrow$  3:1 hexanes:EtOAc) to provide allylic alcohol **346** (43 mg, 41% yield) and starting material (**345**, 30 mg, 32% yield).

$^1\text{H-NMR}$  (400 MHz;  $\text{CDCl}_3$ ):  $\delta$  7.76 (d,  $J = 8.8$  Hz, 1H), 6.92 (dd,  $J = 8.9, 2.7$  Hz, 1H), 6.86 (d,  $J = 2.7$  Hz, 1H), 5.65 (s, 1H), 4.87 (s, 1H), 4.83 (s, 1H), 4.24 (q,  $J = 7.2$  Hz, 2H), 3.82-3.81 (m, 3H), 2.00-1.99 (m, 3H), 1.73 (m, 2H), 1.48-1.46 (m, 6H), 1.28 (m, 3H), 0.76 (t,  $J = 7.4$  Hz, 3H);  $^{13}\text{C-NMR}$  (101 MHz,  $\text{CDCl}_3$ ):  $\delta$  206.44, 205.33, 167.55, 167.24, 165.68, 165.39, 159.20, 159.09, 148.09, 147.24, 140.55, 138.95, 133.47, 132.62, 129.14, 127.73, 125.81, 123.30, 114.63, 113.89, 113.49, 113.42, 113.36, 112.90, 112.85, 111.58, 78.93, 73.47, 62.75, 62.66, 62.59, 62.43, 62.40, 57.75, 57.31, 55.51, 55.45, 31.21, 29.65, 23.67, 23.61, 22.77, 18.34, 18.10, 17.71, 16.31, 13.91, 8.71, 8.30; FTIR (thin film): 3475, 2979, 2940, 1776, 1745, 1701, 1609, 1502, 1448, 1380, 1276, 1261, 1233, 1110, 1036  $\text{cm}^{-1}$ ; HRMS (ESI-APCI)  $m/z$  calc'd for  $\text{C}_{24}\text{H}_{30}\text{NO}_6$  ( $\text{M}+\text{H}$ ) $^+$ : 428.2073, found: 428.2072.

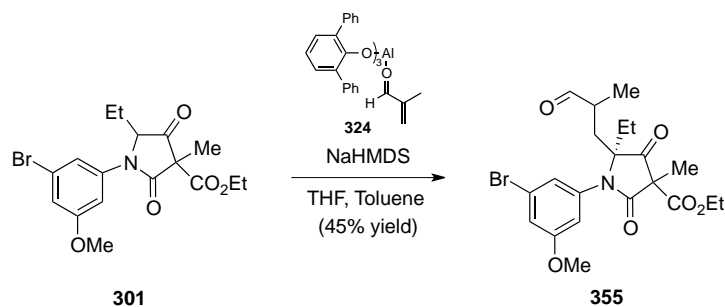
## Preparation of tetracycle **347**



To a solution of allylic alcohol **346** (83 mg, 0.194 mmol) in  $\text{CH}_2\text{Cl}_2$  (3 mL) was added  $\text{BF}_3 \cdot \text{OEt}_2$  (50 mL, 0.388 mmol) at  $-78^\circ\text{C}$ . The yellowish solution was stirred for 10 min at  $-78^\circ\text{C}$  and then warmed to  $0^\circ\text{C}$ . After 20 min at  $0^\circ\text{C}$ , the reaction was quenched by addition of saturated aqueous sodium bicarbonate solution (5 mL) and the aqueous phase was extracted with  $\text{CH}_2\text{Cl}_2$  ( $3 \times 5$  mL). The combined organic phases were washed with brine (15 mL), dried over  $\text{MgSO}_4$ , filtered and concentrated *in vacuo*. The crude material was purified by flash chromatography (5:1→4:1 hexanes:EtOAc) to provide tetracycle **347** (56 mg, 71% yield).

$^1\text{H-NMR}$  (400 MHz;  $\text{CDCl}_3$ ):  $\delta$  7.24 (s, 2H), 6.85 (s, 1H), 5.54 (s, 1H), 4.24 (q,  $J = 7.1$  Hz, 2H), 3.88-3.79 (s, 3H), 3.40 (s, 2H), 2.28 (s, 3H), 2.16 (s, 3H), 2.05-2.00 (m, 1H), 1.87-1.82 (m, 1H), 1.63-1.58 (m, 3H), 1.29-1.21 (m, 3H), 0.77-0.71 (m, 3H);  $^{13}\text{C-NMR}$  (101 MHz,  $\text{CDCl}_3$ ):  $\delta$  207.58, 167.93, 165.83, 157.35, 144.08, 142.71, 142.08, 135.95, 133.65, 130.10, 128.92, 128.50, 127.94, 108.93, 108.76, 108.19, 75.61, 62.47, 58.69, 55.75, 55.71, 45.65, 31.55, 28.35, 28.25, 25.38, 25.23, 18.66, 17.82, 17.78, 15.59, 14.10, 13.89, 13.81, 8.92, 8.63; FTIR (thin film): 2979, 2938, 1776, 1746, 1702, 1653, 1609, 1480, 1456, 1445, 1384, 1289, 1232, 1132, 1043  $\text{cm}^{-1}$ ; HRMS (ESI-APCI)  $m/z$  calc'd for  $\text{C}_{24}\text{H}_{28}\text{NO}_5$  ( $\text{M}+\text{H}$ ) $^+$ : 410.1967, found: 410.1963.

## Preparation of aldehyde **355**

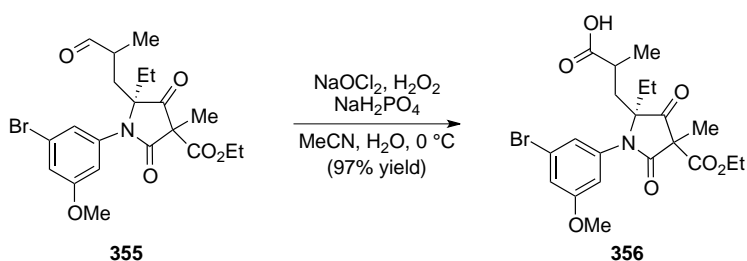


To a solution of aryl bromide **301** (300 mg, 0.753 mmol) in THF (10 mL) was added NaHMDS (1 M in THF, 0.83 mL, 0.829 mmol) dropwise at  $-78\text{ }^{\circ}\text{C}$  and the mixture allowed to stir for 20 min. Meanwhile,  $\text{AlMe}_3$  (2 M in toluene, 0.68 mL, 1.36 mmol) was added to a solution of 2,6-diphenylphenol (946 mg, 3.84 mmol) in toluene (10 mL). After 10 min stirring at room temperature the toluene solution was cooled to  $-78\text{ }^{\circ}\text{C}$  and methacrolein (95 mL, 1.13 mmol) was added, which resulted in the formation of a bright yellow solution. The THF solution of the sodium enolate of **301** was then transferred via cannula to the methacrolein–Lewis Acid complex at  $-78\text{ }^{\circ}\text{C}$ . The reaction was stirred for another 10 min at  $-78\text{ }^{\circ}\text{C}$  and then was allowed to slowly warm to room temperature. After stirring for 1 h at room temperature the reaction was quenched by addition of saturated aqueous Rochelle's salt solution (15 mL) and the mixture stirred vigorously for 30 min. The aqueous phase was extracted with diethyl ether ( $3 \times 10\text{ mL}$ ) and the combined organic phases were washed with brine (20 mL), dried over  $\text{MgSO}_4$ , filtered and concentrated *in vacuo*. The crude material was purified by flash chromatography (5:1→3:1 hexanes:EtOAc) to furnish aldehyde **355** (160 mg, 45% yield) as a mixture of diastereomers in form of a yellowish oil.

$^1\text{H-NMR}$  (400 MHz;  $\text{CDCl}_3$ ):  $\delta$  9.57-9.37 (m, 1H), 7.07 (m, 1H), 6.96-6.91 (m, 1H), 6.69 (s, 1H), 4.22-4.07 (m, 2H), 3.79-3.76 (m, 3H), 2.59-2.44 (m, 3H), 1.81 (m, 2H), 1.58-1.51 (m, 3H), 1.26-1.20 (m, 3H), 1.10-1.02 (m, 3H), 0.95-0.88 (m, 3H);  $^{13}\text{C-NMR}$  (101 MHz,  $\text{CDCl}_3$ ):  $\delta$  207.57, 207.36, 207.27, 206.53, 202.83, 202.46, 202.02, 201.84, 201.64, 171.09, 170.28, 170.24, 170.02, 169.95, 165.23, 165.17, 165.11, 164.88, 160.82, 160.80, 160.78, 160.57,

155.71, 143.27, 136.51, 136.43, 136.32, 123.79, 123.75, 123.68, 123.66, 123.24, 123.19, 123.12, 122.73, 122.61, 117.34, 117.28, 117.18, 115.81, 114.36, 114.27, 114.16, 114.12, 112.99, 75.83, 75.61, 75.34, 74.89, 64.30, 63.23, 63.03, 62.81, 62.71, 60.34, 58.71, 58.57, 58.54, 58.32, 55.76, 55.73, 55.72, 55.70, 55.64, 53.21, 51.03, 45.87, 41.62, 41.08, 40.95, 40.86, 36.85, 36.75, 36.29, 36.20, 30.58, 29.58, 29.00, 28.41, 28.16, 21.01, 20.97, 19.07, 17.96, 17.32, 16.38, 16.20, 16.16, 15.98, 15.74, 15.71, 14.16, 14.04, 13.92, 13.88, 13.67, 11.68, 8.89, 8.79, 8.57, 8.54; FTIR (thin film): 2976, 2940, 2877, 1772, 1702, 1596, 1571, 1448, 1426, 1306, 1276, 1233, 1213, 1078, 1054, 1037  $\text{cm}^{-1}$ ; HRMS (ESI-APCI)  $m/z$  calc'd for  $\text{C}_{21}\text{H}_{27}\text{BrNO}_6$  (M+H)<sup>+</sup>: 470.1001, found: 470.1004.

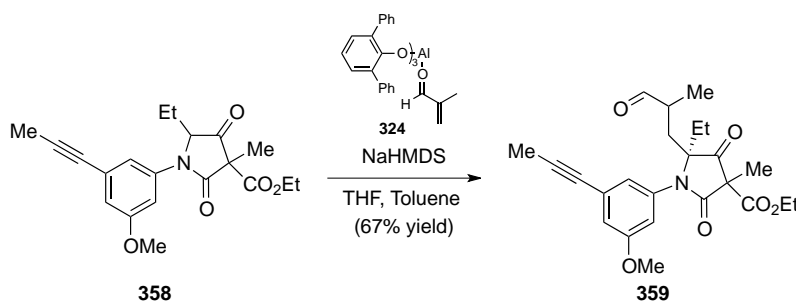
### Preparation of carboxylic acid **356**



To a solution of aldehyde **355** (255 mg, 0.544 mmol) in acetonitrile (1 mL) was added a solution of  $\text{NaH}_2\text{PO}_2$  (20 mg, 0.163 mmol) in water (0.5 mL) followed by  $\text{H}_2\text{O}_2$  (30% (w/w) in  $\text{H}_2\text{O}$ , 0.60 mL, 0.566 mmol). The biphasic mixture was cooled to  $0\text{ }^\circ\text{C}$  and stirred vigorously, while a solution of  $\text{NaClO}_2$  (80% (w/w), 86 mg, 1.09 mmol) in water (0.5 mL) was added over 45 min. After stirring for 1 h at  $0\text{ }^\circ\text{C}$  the reaction was quenched by addition of saturated aqueous sodium bisulfite solution (1 mL) and saturated aqueous ammonium chloride (5 mL). The aqueous phase was extracted with  $\text{EtOAc}$  ( $3 \times 5\text{ mL}$ ) and the combined organic phases were washed with brine (20 mL), dried over  $\text{MgSO}_4$ , filtered and concentrated *in vacuo* to provide carboxylic acid **356** (250 mg, 95% yield) as a mixture of diastereomers, which was used without further purification.

$^1\text{H-NMR}$  (400 MHz;  $\text{CDCl}_3$ ):  $\delta$  7.07 (m, 1H), 6.94 (m, 1H), 6.76-6.68 (m, 1H), 4.27-4.14 (m, 2H), 3.79-3.72 (m, 3H), 2.73-2.51 (m, 2H), 2.30 (m, 1H), 2.06-1.69 (m, 2H), 1.67-1.59 (m, 3H), 1.28-1.21 (m, 3H), 1.21-1.10 (m, 3H), 0.94-0.86 (m, 3H);  $^{13}\text{C-NMR}$  (101 MHz,  $\text{CDCl}_3$ ):  $\delta$  207.12, 206.83, 206.49, 205.85, 181.51, 180.95, 180.82, 180.56, 180.03, 170.81, 170.78, 170.48, 170.39, 165.30, 165.21, 165.17, 164.71, 160.82, 160.77, 160.49, 156.06, 143.21, 136.40, 136.17, 123.78, 123.74, 123.68, 123.62, 123.26, 123.19, 123.11, 122.81, 122.49, 117.49, 117.45, 117.28, 115.94, 114.35, 114.18, 114.07, 114.03, 112.84, 76.03, 75.79, 75.17, 63.27, 63.15, 62.91, 62.86, 58.74, 58.51, 55.78, 55.74, 55.70, 55.65, 53.31, 52.82, 40.46, 39.70, 39.61, 39.02, 38.36, 34.77, 34.70, 34.41, 34.03, 29.21, 28.58, 27.84, 27.18, 20.18, 20.03, 19.98, 19.85, 17.78, 17.76, 15.68, 15.64, 14.54, 14.03, 13.89, 13.80, 8.94, 8.73, 8.53; FTIR (thin film): 3086, 2978, 2940, 1773, 1704, 1596, 1571, 1449, 1426, 1383, 1276, 1210, 1176, 1038  $\text{cm}^{-1}$ ; HRMS (ESI-APCI)  $m/z$  calc'd for  $\text{C}_{21}\text{H}_{27}\text{BrNO}_7$  ( $\text{M}+\text{H}$ ) $^+$ : 484.0971, found: 484.0958.

### Preparation of aldehyde **359**

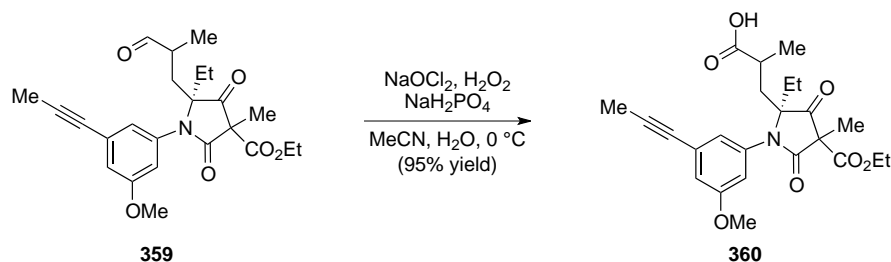


To a solution of alkyne **358** (810 mg, 2.27 mmol) in THF (25 mL) was added NaHMDS (1 M in THF, 2.70 mL, 2.72 mmol) dropwise at  $-78$  °C and the mixture was allowed to stir for 20 min. Meanwhile,  $\text{AlMe}_3$  (2 M in toluene, 2.00 mL, 4.08 mmol) was added to a solution of 2,6-diphenylphenol (2.85 g, 11.56 mmol) in toluene (25 mL). After 10 min stirring at room temperature the toluene solution was cooled to  $-78$  °C and methacrolein (290 mL, 3.40 mmol) was added, which resulted in the formation of a bright yellow solution. The THF solution of the sodium enolate of **358** was then transferred via cannula to the methacrolein-Lewis Acid

complex at  $-78\text{ }^{\circ}\text{C}$ . The solution was stirred for another 10 min at  $-78\text{ }^{\circ}\text{C}$  and then slowly warmed to room temperature. After stirring for 1 h the reaction was quenched by addition of saturated aqueous Rochelle's salt solution (50 mL) and the mixture stirred vigorously for 30 min. The aqueous phase was extracted with diethyl ether ( $3 \times 20\text{ mL}$ ) and the combined organic phases were washed with brine (50 mL), dried over  $\text{MgSO}_4$ , filtered and concentrated *in vacuo*. The crude material was purified by flash chromatography (5:1 $\rightarrow$ 2:1 hexanes:EtOAc) to give aldehyde **359** (652 mg, 67% yield) as a mixture of diastereomers.

$^1\text{H-NMR}$  (400 MHz;  $\text{CDCl}_3$ ):  $\delta$  9.46-9.36 (m, 1H), 6.93 (m, 1H), 6.81 (m, 1H), 6.66 (s, 1H), 4.31-4.18 (m, 2H), 3.77 (m, 3H), 2.69-2.42 (m, 3H), 2.04-2.00 (m, 3H), 1.88-1.75 (m, 2H), 1.68-1.51 (m, 3H), 1.37-1.20 (m, 3H), 1.07-1.01 (m, 3H), 0.96-0.87 (m, 3H);  $^{13}\text{C-NMR}$  (101 MHz,  $\text{CDCl}_3$ ):  $\delta$  207.94, 207.79, 207.66, 206.91, 202.57, 202.15, 201.95, 201.66, 170.17, 169.95, 169.88, 165.39, 165.29, 165.25, 165.03, 160.00, 135.47, 135.39, 135.28, 126.25, 126.22, 126.14, 123.93, 123.86, 123.70, 116.53, 116.44, 116.41, 115.03, 115.00, 114.95, 114.86, 87.40, 87.37, 87.34, 78.75, 78.73, 75.72, 75.50, 75.23, 74.74, 63.13, 62.94, 62.71, 62.60, 58.69, 58.58, 58.54, 58.33, 55.50, 55.48, 55.46, 55.44, 41.63, 41.09, 40.97, 40.88, 37.02, 36.83, 36.43, 36.24, 29.66, 28.89, 28.33, 28.23, 18.09, 17.35, 16.40, 16.17, 15.94, 15.77, 15.70, 14.15, 14.04, 13.93, 13.87, 8.93, 8.84, 8.61, 8.57, 4.29; FTIR (thin film): 2977, 2940, 2882, 2242, 1772, 1702, 1590, 1451, 1426, 1385, 1297, 1217, 1201, 1171, 1062  $\text{cm}^{-1}$ ; HRMS (ESI-APCI)  $m/z$  calc'd for  $\text{C}_{24}\text{H}_{30}\text{NO}_6$  ( $\text{M}+\text{H}$ ) $^+$ : 428.2073, found: 428.2076.

## Preparation of carboxylic acid **360**

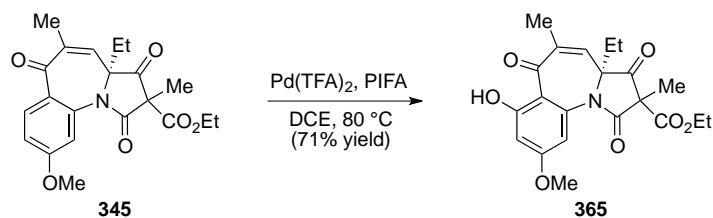


To a solution of aldehyde **359** (200 mg, 0.468 mmol) in acetonitrile (1 mL) was added a solution of NaH<sub>2</sub>PO<sub>2</sub> (17 mg, 0.140 mmol) in water (0.5 mL) followed by H<sub>2</sub>O<sub>2</sub> (30% (w/w) in H<sub>2</sub>O, 0.50 mL, 0.487 mmol). The biphasic mixture was cooled to 0 °C and stirred vigorously while a solution of NaClO<sub>2</sub> (80% (w/w), 106 mg, 0.936 mmol) in water (0.5 mL) was added over 45 min. After stirring for 1 h at 0 °C the reaction was quenched by addition of saturated aqueous sodium bisulfite solution (1 mL) and saturated aqueous ammonium chloride (5 mL). The aqueous phase was extracted with EtOAc (3 × 5 mL) and the combined organic phases were washed with brine (20 mL), dried over MgSO<sub>4</sub>, filtered and concentrated *in vacuo* to furnish carboxylic acid **360** (197 mg, 95% yield) as a mixture of diastereoisomers, which was used without further purification.

<sup>1</sup>H-NMR (400 MHz; CDCl<sub>3</sub>): δ 6.96-6.93 (m, 1H), 6.87-6.81 (m, 1H), 6.72-6.66 (m, 1H), 4.28-4.15 (m, 2H), 3.82-3.75 (m, 3H), 2.68-2.54 (m, 2H), 2.32 (ddd, *J* = 14.5, 8.0, 3.3 Hz, 1H), 2.06-2.00 (m, 3H), 2.00-1.70 (m, 2H), 1.64-1.50 (m, 3H), 1.35-1.21 (m, 3H), 1.20-1.12 (m, 3H), 0.95-0.88 (m, 3H); <sup>13</sup>C-NMR (101 MHz, CDCl<sub>3</sub>): δ 207.60, 207.32, 207.00, 206.29, 181.69, 181.13, 181.02, 180.75, 170.44, 170.17, 170.06, 165.45, 165.33, 165.30, 164.79, 160.02, 159.99, 135.53, 135.46, 135.27, 135.24, 126.24, 126.21, 126.19, 126.11, 124.03, 123.91, 123.80, 123.68, 116.65, 116.63, 116.45, 116.40, 115.11, 115.03, 114.90, 114.81, 87.35, 87.29, 78.77, 75.79, 75.54, 74.79, 63.04, 62.93, 62.68, 62.59, 58.65, 58.53, 58.45, 55.49, 55.44, 40.74, 39.80, 39.70, 39.12, 34.75, 34.62, 34.43, 34.04, 31.55, 29.23, 28.29, 27.70, 27.19, 25.23, 22.61, 20.17, 20.03, 19.96, 19.91, 18.00, 17.80, 15.68, 15.59, 14.08, 14.04, 13.87, 13.80, 8.97, 8.77,

8.57, 4.30; FTIR (thin film): 3058, 2978, 2940, 2242, 1773, 1740, 1590, 1452, 1426, 1386, 1325, 1265, 1200, 1171, 1148, 1126, 1061, 1017  $\text{cm}^{-1}$ ; HRMS (ESI-APCI)  $m/z$  calc'd for  $\text{C}_{24}\text{H}_{30}\text{NO}_7$  ( $\text{M}+\text{H}$ )<sup>+</sup>: 444.2022, found: 444.2025.

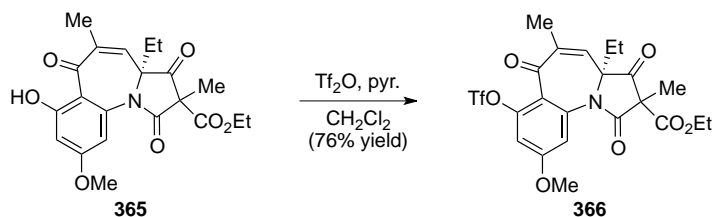
### Preparation of phenol **365**



To a solution of enone **345** (172 mg, 0.446 mmol), [bis(trifluoroacetoxy)iodo]benzene (384 mg, 893  $\mu\text{mol}$ ) and palladium(II) acetate (5 mg, 0.022 mmol) in 1,2-dichloroethane (4.5 mL) was added trifluoroacetic acid (0.5 mL) and the mixture was heated at 80  $^\circ\text{C}$  for 2.5 h. After cooling to room temperature, the mixture was diluted with saturated aqueous sodium bicarbonate solution (10 mL) and extracted with  $\text{CH}_2\text{Cl}_2$  (3  $\times$  5 mL). The combined organic phases were washed with brine (15 mL), dried over  $\text{MgSO}_4$ , filtered and concentrated *in vacuo*. The crude material was purified by flash chromatography (5:1  $\rightarrow$  4:1 hexanes:EtOAc) to give phenol **365** (127 mg, 71% yield).

$^1\text{H-NMR}$  (400 MHz;  $\text{CDCl}_3$ ):  $\delta$  13.47 (m, 1H), 6.59 (m, 1H), 6.50-6.45 (m, 2H), 4.29-4.06 (m, 2H), 3.85 (m, 3H), 2.08-1.99 (m, 4H), 1.71 (td,  $J = 16.2, 7.4$  Hz, 1H), 1.58 (m, 3H), 1.30-1.11 (m, 3H), 0.81 (m, 3H);  $^{13}\text{C-NMR}$  (101 MHz,  $\text{CDCl}_3$ ):  $\delta$  204.97, 204.77, 191.52, 191.13, 168.61, 168.29, 167.42, 167.20, 164.98, 164.83, 164.65, 164.36, 141.22, 140.48, 139.47, 137.80, 135.09, 134.80, 111.94, 111.78, 108.88, 108.68, 101.08, 101.03, 76.45, 75.67, 62.88, 57.80, 57.50, 55.79, 55.75, 27.37, 26.93, 21.16, 21.13, 18.72, 15.52, 13.94, 13.78, 8.07; FTIR (thin film): 2981, 2939, 1781, 1713, 1617, 1578, 1447, 1429, 1375, 1347, 1289, 1239, 1210, 1167, 1123, 1057  $\text{cm}^{-1}$ ; HRMS (ESI-APCI)  $m/z$  calc'd for  $\text{C}_{21}\text{H}_{24}\text{NO}_7$  ( $\text{M}+\text{H}$ )<sup>+</sup>: 402.1553, found: 402.1548.

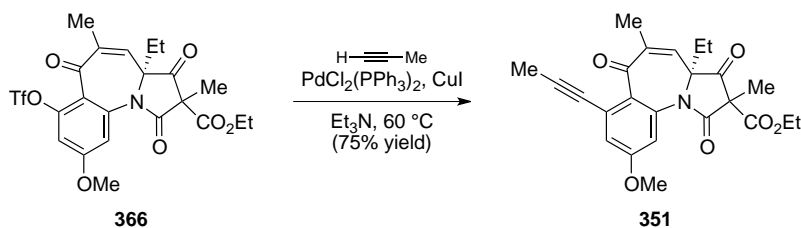
## Preparation of triflate **366**



To a solution of phenol **365** (112 mg, 0.279 mmol) in  $\text{CH}_2\text{Cl}_2$  (5 mL) was added pyridine (45 mL, 0.558 mmol) followed by triflic anhydride (0.71 mL, 0.419 mmol) at  $-78^\circ\text{C}$ . The mixture was warmed to  $0^\circ\text{C}$  and stirred for 2 h before it was quenched by addition of saturated aqueous ammonium chloride solution (2 mL). The aqueous phase was extracted with  $\text{CH}_2\text{Cl}_2$  ( $3 \times 5$  mL) and the combined organic phases were washed with brine (15 mL), dried over  $\text{MgSO}_4$ , filtered and concentrated *in vacuo*. The crude material was purified by flash chromatography (4:1 hexanes:EtOAc) to deliver aryl triflate **366** (112 mg, 76% yield).

$^1\text{H-NMR}$  (400 MHz;  $\text{CDCl}_3$ ):  $\delta$  7.02 (d,  $J = 2.4$  Hz, 1H), 6.86 (d,  $J = 2.4$  Hz, 1H), 6.36 (m, 1H), 4.29-4.05 (m, 2H), 3.89 (s, 3H), 2.04-2.00 (m, 4H), 1.71 (t,  $J = 7.4$  Hz, 1H), 1.60-1.55 (m, 3H), 1.29 (t,  $J = 7.1$  Hz, 2H), 0.87-0.77 (m, 3H);  $^{13}\text{C-NMR}$  (101 MHz,  $\text{CDCl}_3$ ):  $\delta$  203.70, 203.60, 188.23, 187.57, 168.76, 168.61, 164.92, 163.81, 162.05, 161.90, 148.15, 147.88, 138.36, 137.95, 137.73, 137.33, 134.56, 134.16, 124.90, 124.49, 120.08, 120.07, 116.88, 113.14, 112.93, 109.63, 77.81, 77.08, 63.18, 62.98, 57.81, 57.63, 56.33, 56.27, 28.39, 27.71, 20.53, 20.35, 18.96, 15.00, 13.93, 13.60, 8.40, 8.35;  $^{19}\text{F-NMR}$  (376 MHz,  $\text{CDCl}_3$ ):  $\delta$  -73.07; FTIR (thin film): 2983, 2941, 2851, 1782, 1750, 1716, 1660, 1614, 1426, 1381, 1358, 1290, 1211, 1171, 1140, 1114,  $1009\text{ cm}^{-1}$ ; HRMS (ESI-APCI)  $m/z$  calc'd for  $\text{C}_{22}\text{H}_{23}\text{F}_3\text{NO}_9\text{S}$  ( $\text{M}+\text{H}$ ) $^+$ : 534.1046, found: 534.1037.

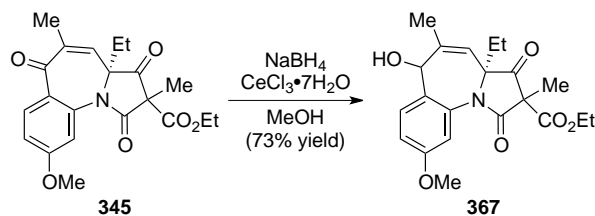
## Preparation of alkyne 351



Triflate **366** (40 mg, 0.075 mmol),  $\text{PdCl}_2(\text{PPh}_3)_2$  (5.3 mg, 7.5 mmol) and copper(I) iodide (0.7 mg, 3.7 mmol) were suspended in triethylamine (3 mL). Propyne gas was bubbled into the solution for 10 s and the mixture was heated to 60 °C. After 30 min at elevated temperature propyne was again bubbled in for 10 seconds and the mixture stirred at 60 °C for an additional 4 hours. The dark reaction mixture was cooled to room temperature, diluted with diethyl ether (10 mL) and saturated aqueous ammonium chloride solution (10 mL) was added. The aqueous phase was extracted with diethyl ether (3 × 5 mL) and the combined organic phases were washed with brine (20 mL), dried over  $\text{MgSO}_4$ , filtered and concentrated *in vacuo*. The crude material was purified by flash chromatography (4:1→3:1 hexanes:EtOAc) to furnish alkyne **351** (24 mg, 75% yield) as a brown crystalline solid.

$^1\text{H-NMR}$  (400 MHz;  $\text{CDCl}_3$ ):  $\delta$  7.02 (m, 1H), 6.85 (m, 1H), 6.23 (m, 1H), 4.26-4.03 (m, 2H), 3.83 (m, 3H), 2.02-2.01 (m, 6H), 1.95 (m, 1H), 1.66 (m, 1H), 1.56-1.52 (m, 3H), 1.28-1.06 (m, 3H), 0.82 (m, 3H);  $^{13}\text{C-NMR}$  (101 MHz,  $\text{CDCl}_3$ ):  $\delta$  204.38, 204.35, 191.35, 190.29, 168.71, 168.66, 165.17, 164.14, 160.94, 160.80, 138.32, 137.42, 136.63, 136.10, 133.23, 133.20, 132.80, 132.62, 126.30, 125.94, 119.28, 119.19, 113.46, 113.30, 90.76, 90.70, 63.00, 62.77, 57.89, 57.70, 55.76, 55.72, 28.05, 27.53, 20.76, 20.58, 19.02, 14.98, 13.90, 13.53, 8.30, 8.26, 4.64, 4.56; FTIR (thin film): 2980, 2939, 2237, 1778, 1747, 1710, 1659, 1594, 1567, 1431, 1385, 1357, 1317, 1292, 1241, 1147, 1126, 1103  $\text{cm}^{-1}$ ; HRMS (ESI-APCI)  $m/z$  calc'd for  $\text{C}_{24}\text{H}_{26}\text{NO}_6$  ( $\text{M}+\text{H}$ ) $^+$ : 424.1760, found: 424.1747.

## Preparation of allylic alcohol **367**



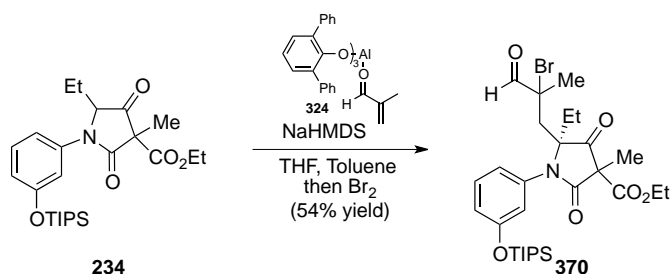
To a solution of enone **345** (37 mg, 0.096 mmol) and cerium(III) chloride heptahydrate (39 mg, 0.106 mmol) in MeOH (2.5 mL) and THF (0.5 mL) was added sodium borohydride (4.4 mg, 0.115 mmol) at 0 °C. After 40 minutes the reaction was quenched by addition of saturated aqueous ammonium chloride (5 mL). The aqueous phase was extracted with diethyl ether (3 × 5 mL) and the combined organic phases were washed with brine (15 mL), dried over MgSO<sub>4</sub>, filtered and concentrated *in vacuo*. The crude material was purified by flash chromatography (4:1→3:1 hexanes:EtOAc) to provide allylic alcohol **367** (27 mg, 73% yield) as a separable mixture of diastereomers. Single crystals suitable for X-ray analysis were obtained by slow diffusion of hexane into a concentrated solution of **367** in diethyl ether/CH<sub>2</sub>Cl<sub>2</sub>.

Diastereomer A: <sup>1</sup>H-NMR (400 MHz; CDCl<sub>3</sub>): δ 7.49 (d, *J* = 8.7 Hz, 1H), 6.94 (dd, *J* = 8.6, 2.5 Hz, 1H), 6.82 (d, *J* = 2.5 Hz, 1H), 5.82 (d, *J* = 0.3 Hz, 1H), 5.16 (s, 1H), 4.17-4.00 (m, 2H), 3.80 (s, 3H), 2.37 (d, *J* = 4.9 Hz, 1H), 1.88 (s, 3H), 1.80 (dd, *J* = 14.6, 7.4 Hz, 1H), 1.63-1.59 (m, 3H), 1.32 (dd, *J* = 14.6, 7.4 Hz, 1H), 1.17 (t, *J* = 7.2 Hz, 3H), 0.80 (t, *J* = 7.4 Hz, 3H); FTIR (thin film): 3455, 2976, 2940, 1774, 1743, 1691, 1661, 1612, 1585, 1500, 1447, 1383, 1290, 1218, 1169, 1111, 1044, 1031, 1010 cm<sup>-1</sup>; HRMS (ESI-APCI) *m/z* calc'd for C<sub>21</sub>H<sub>26</sub>NO<sub>6</sub> (M+H)<sup>+</sup>: 388.1760, found: 388.1755.

Diastereomer B: <sup>1</sup>H-NMR (400 MHz; CDCl<sub>3</sub>): δ 7.49-7.46 (m, 1H), 6.93 (dd, *J* = 8.6, 2.6 Hz, 1H), 6.88 (d, *J* = 2.6 Hz, 1H), 5.43 (s, 1H), 5.17 (s, 1H), 4.30-4.19 (m, 2H), 3.82 (s, 3H), 2.50 (d, *J* = 5.0 Hz, 1H), 1.89 (s, 3H), 1.88-1.81 (m, 1H), 1.60 (s, 3H), 1.46 (dd, *J* = 14.6, 7.4 Hz, 1H), 1.27 (t, *J* = 7.1 Hz, 3H), 0.85 (t, *J* = 7.4 Hz, 3H); <sup>13</sup>C-NMR (101 MHz, CDCl<sub>3</sub>): δ 205.20, 194.80, 169.63, 165.56, 159.13, 141.33, 134.59, 131.89, 124.76, 121.26, 114.46, 114.05, 74.47, 67.84,

62.65, 58.27, 55.57, 29.58, 20.89, 18.96, 13.89, 7.95; FTIR (thin film): 3444, 2981, 2935, 2852, 1774, 1740, 1613, 1586, 1503, 1448, 1391, 1292, 1238, 1228, 1139, 1109, 1072, 1032  $\text{cm}^{-1}$ ; HRMS (ESI-APCI)  $m/z$  calc'd for  $\text{C}_{21}\text{H}_{26}\text{NO}_6$  ( $\text{M}+\text{H}$ ) $^+$ : 388.1760, found: 388.1767.

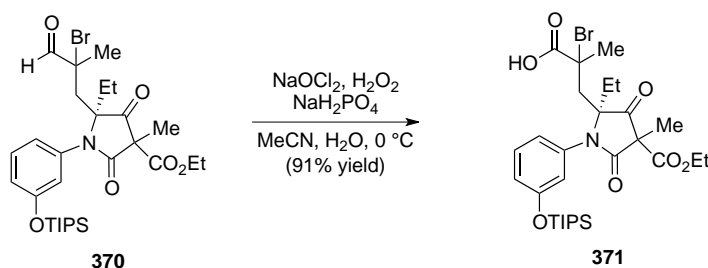
### Preparation of aldehyde **370**



To a solution of ketone **234** (11.02 g, 23.88 mmol) in THF (250 mL) was added NaHMDS (1 M in THF, 26.3 mL, 26.27 mmol) dropwise at  $-78$  °C and the mixture was stirred for 30. Meanwhile,  $\text{AlMe}_3$  (neat, 4.3 mL, 42.98 mmol) was added to a solution of 2,6-diphenylphenol (30.0 g, 121.8 mmol) in toluene (250 mL). After 10 min the toluene solution was cooled to  $-78$  °C and methacrolein (3.0 mL, 35.82 mmol) was added, which resulted in the formation of a bright yellow solution. The THF solution of the sodium enolate of **234** was then transferred via cannula to the methacrolein–Lewis Acid complex at  $-78$  °C. The solution was stirred for another 10 min at  $-78$  °C and then slowly warmed to room temperature. After stirring for 2 h at room temperature the reaction was cooled to  $-78$  °C and bromine (2.2 mL, 42.98 mmol) was added dropwise. The reaction mixture was allowed to warm to room temperature and quenched by addition of saturated aqueous Rochelle's salt (200 mL) and the mixture stirred vigorously for 30 min. The aqueous phase was extracted with diethyl ether ( $3 \times 50$  mL) and the combined organic phases were washed with brine (200 mL), dried over  $\text{MgSO}_4$ , filtered and concentrated *in vacuo*. The crude material was purified by flash chromatography (20:1→3:1 hexanes:EtOAc) to furnish aldehyde **370** (7.84 g, 54% yield) as a mixture of diastereoisomers in form of a brownish oil.

$^1\text{H-NMR}$  (400 MHz;  $\text{CDCl}_3$ ):  $\delta$  9.09 (m, 1H), 7.31 (m, 1H), 6.98-6.84 (m, 2H), 6.79-6.75 (m, 1H), 4.32-4.20 (m, 2H), 3.03 (d,  $J = 15.2$  Hz, 1H), 2.66-2.59 (m, 1H), 1.92-1.84 (m, 4H), 1.65-1.47 (m, 4H), 1.36 (t,  $J = 7.2$  Hz, 3H), 1.25 (m, 3H), 1.08 (m, 18H), 0.90 (m, 3H);  $^{13}\text{C-NMR}$  (101 MHz,  $\text{CDCl}_3$ ):  $\delta$  206.05, 205.70, 190.54, 189.53, 169.72, 169.63, 165.15, 164.83, 157.01, 156.91, 135.33, 134.67, 130.39, 130.17, 121.00, 120.89, 120.86, 120.67, 120.54, 120.36, 75.95, 74.81, 66.70, 65.41, 63.17, 62.91, 58.68, 58.49, 45.00, 42.77, 31.56, 28.25, 24.45, 24.40, 17.90, 17.28, 15.71, 14.01, 13.86, 12.58, 12.55, 8.74, 8.61; FTIR (thin film): 2945, 2892, 2868, 1777, 1746, 1706, 1596, 1486, 1464, 1446, 1381, 1282, 1205, 1060, 1015, 1005  $\text{cm}^{-1}$ ; HRMS (ESI-APCI)  $m/z$  calc'd for  $\text{C}_{29}\text{H}_{45}\text{BrNO}_6\text{Si}$  ( $\text{M}+\text{H}$ ) $^+$ : 610.2200, found: 610.2188.

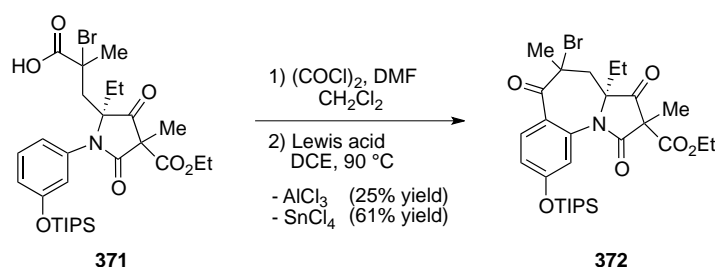
### Preparation of carboxylic acid **371**



To a solution of aldehyde **370** (7.80 g, 12.80 mmol) in acetonitrile (30 mL) was added a solution of  $\text{NaH}_2\text{PO}_2$  (768 mg, 6.40 mmol) in water (5 mL) followed by  $\text{H}_2\text{O}_2$  (30% (w/w) in  $\text{H}_2\text{O}$ , 1.3 mL, 13.44 mmol). The biphasic mixture was cooled to 0  $^\circ\text{C}$  and stirred vigorously, while a solution of  $\text{NaClO}_2$  (80% (w/w), 2.89 g, 25.61 mmol, 2.0 equiv) in water (20 mL) was added over 45 min. After stirring for 1 h at 0  $^\circ\text{C}$ , the reaction was quenched by addition of saturated aqueous ammonium chloride (50 mL). The aqueous phase was extracted with diethyl ether (3  $\times$  30 mL) and the combined organic phases were washed with brine (100 mL), dried over  $\text{MgSO}_4$ , filtered and concentrated *in vacuo* to provide carboxylic acid **371** (7.22 g, 91% yield) as a mixture of diastereomers, which was used without further purification.

$^1\text{H-NMR}$  (400 MHz;  $\text{CDCl}_3$ ):  $\delta$  7.31 (td,  $J = 8.0, 0.9$  Hz, 1H), 6.97-6.75 (m, 3H), 4.30-4.09 (m, 2H), 3.05-2.95 (m, 1H), 2.62 (m, 1H), 2.03-1.97 (m, 3H), 1.88 (td,  $J = 7.4, 4.2$  Hz, 1H), 1.73-1.52 (m, 3H), 1.39-1.19 (m, 6H), 1.08-1.05 (m, 18H), 0.91 (m,  $J = 6.1$  Hz, 3H);  $^{13}\text{C-NMR}$  (101 MHz,  $\text{CDCl}_3$ ):  $\delta$  206.04, 205.49, 174.96, 174.75, 169.95, 169.78, 169.77, 165.38, 164.90, 156.87, 135.01, 134.58, 130.27, 130.15, 121.14, 121.03, 121.01, 120.96, 120.75, 120.66, 75.39, 63.15, 62.79, 58.77, 58.47, 57.13, 56.14, 56.13, 46.60, 46.46, 29.12, 28.65, 28.45, 25.87, 18.30, 17.83, 15.72, 14.16, 14.02, 13.85, 12.56, 12.53, 8.68, 8.50; FTIR (thin film): 2945, 2892, 2868, 1777, 1743, 1706, 1671, 1596, 1488, 1462, 1384, 1284, 1265, 1215, 1157, 1136, 1015, 1005,  $996\text{ cm}^{-1}$ ; HRMS (ESI-APCI)  $m/z$  calc'd for  $\text{C}_{29}\text{H}_{45}\text{BrNO}_7\text{Si}$  ( $\text{M}+\text{H}$ ) $^+$ : 626.2149, found: 626.2153.

### Preparation of ketone **372**

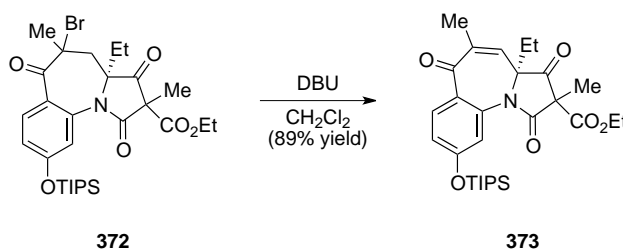


To a solution of carboxylic acid **371** (7.22 g, 11.52 mmol) in  $\text{CH}_2\text{Cl}_2$  (50 mL) was added oxalyl chloride (1.95 mL, 23.05 mmol) followed by three drops of DMF. The solution was stirred for 30 min and then concentrated *in vacuo*. The residue was then dissolved in 1,2-dichloroethane (80 mL) and  $\text{SnCl}_4$  (2.7 mL, 23.05 mmol) was added and the suspension was heated at  $90\text{ }^\circ\text{C}$  for 8 h.  $^1\text{H-NMR}$  analysis of the reaction mixture revealed the presence of starting material, therefore more  $\text{SnCl}_4$  (0.5 mL, 4.25 mmol) was added and the suspension heated at  $90\text{ }^\circ\text{C}$  for 11 h. The dark mixture was then cooled to room temperature and filtered over a short plug of celite, which was washed with  $\text{CH}_2\text{Cl}_2$  (50 mL) and the  $\text{CH}_2\text{Cl}_2$  was removed *in vacuo*. The crude material was purified by flash chromatography (15:1→5:1 hexanes:EtOAc)

to provide  $\alpha$ -bromo ketone **372** (4.25 g, 61% yield) as a mixture of diastereomers in form of a brownish oil.

$^1\text{H-NMR}$  (400 MHz;  $\text{CDCl}_3$ ):  $\delta$  7.96 (d,  $J = 8.8$  Hz, 1H), 7.07 (d,  $J = 2.4$  Hz, 1H), 6.92 (dd,  $J = 8.8, 2.4$  Hz, 1H), 4.28-4.23 (m, 2H), 3.12 (d,  $J = 16.1$  Hz, 1H), 2.18 (m, 1H), 1.96 (s, 3H), 1.85 (dd,  $J = 14.4, 7.0$  Hz, 1H), 1.76 (m, 3H), 1.70 (m, 1H), 1.31-1.22 (m, 6H), 1.08 (m,  $J = 13.6$  Hz, 18H), 0.76 (t,  $J = 7.5$  Hz, 3H);  $^1\text{H-NMR}$  (400 MHz;  $\text{CDCl}_3$ ):  $\delta$  7.91 (d,  $J = 8.8$  Hz, 1H), 7.29 (d,  $J = 2.3$  Hz, 1H), 6.84 (dd,  $J = 8.8, 2.3$  Hz, 1H), 4.28-4.23 (m, 2H), 3.32 (d,  $J = 16.2$  Hz, 1H), 2.22 (d,  $J = 16.2$  Hz, 1H), 1.96 (s, 3H), 1.85 (dd,  $J = 14.4, 7.0$  Hz, 1H), 1.76 (m, 3H), 1.70 (dd,  $J = 14.1, 7.2$  Hz, 1H), 1.31-1.22 (m, 6H), 1.08 (d,  $J = 13.6$  Hz, 18H), 0.51 (t,  $J = 7.2$  Hz, 3H);  $^{13}\text{C-NMR}$  (101 MHz,  $\text{CDCl}_3$ ):  $\delta$  206.19, 204.03, 193.32, 191.65, 168.80, 168.46, 165.64, 165.06, 161.45, 160.82, 136.88, 136.12, 133.99, 132.85, 123.95, 122.38, 121.02, 120.22, 119.86, 118.74, 117.02, 74.09, 73.02, 63.05, 62.97, 62.59, 60.02, 58.97, 57.76, 50.48, 46.06, 31.71, 31.56, 30.99, 28.92, 18.57, 17.87, 17.84, 17.79, 17.77, 17.67, 14.04, 13.86, 12.58, 12.56, 8.56, 7.73; FTIR (thin film): 2945, 2893, 2868, 1777, 1712, 1671, 1595, 1493, 1463, 1426, 1376, 1284, 1262, 1228, 1139, 1118, 1055, 983  $\text{cm}^{-1}$ ; HRMS (ESI-APCI)  $m/z$  calc'd for  $\text{C}_{29}\text{H}_{43}\text{BrNO}_6\text{Si}$  ( $\text{M}+\text{H}$ ) $^+$ : 610.2023, found: 610.2019.

### Preparation of enone **373**

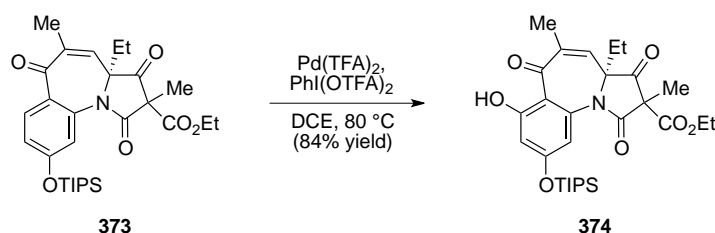


To a solution of  $\alpha$ -bromo ketone **372** (4.25 g, 7.00 mmol) in  $\text{CH}_2\text{Cl}_2$  (50 mL) was added DBU (2.1 mL, 14.01 mmol) and the dark solution stirred for 2 h at ambient temperature. The reaction mixture was diluted with saturated aqueous ammonium chloride (50 mL) and the

aqueous phase was extracted with CH<sub>2</sub>Cl<sub>2</sub> (3 × 20 mL). The combined organic phases were washed with brine (50 mL), dried over MgSO<sub>4</sub>, filtered and concentrated *in vacuo*. The crude material was purified by flash chromatography (5:1→4:1 hexanes:EtOAc) to give enone **373** (3.31 g, 89% yield) of a clear oil that solidified upon standing.

<sup>1</sup>H-NMR (400 MHz; CDCl<sub>3</sub>): δ 7.88 (m, 1H), 7.02 (m, 1H), 6.93 (m, 1H), 6.47 (m, 1H), 4.26 (dd, *J* = 14.7, 7.2 Hz, 2H), 2.03-2.00 (m, 4H), 1.61-1.57 (m, 4H), 1.27 (m, *J* = 3.7 Hz, 6H), 1.10-1.09 (m, 18H), 0.78 (t, *J* = 7.4 Hz, 3H); <sup>13</sup>C-NMR (101 MHz, CDCl<sub>3</sub>): δ 205.29, 205.06, 188.37, 187.42, 168.52, 168.13, 165.10, 164.33, 160.43, 160.22, 139.79, 139.19, 138.58, 136.92, 133.99, 133.64, 133.37, 133.20, 128.77, 128.04, 120.46, 120.16, 118.50, 118.44, 77.03, 76.22, 62.87, 62.72, 57.91, 57.66, 28.02, 27.54, 21.00, 20.87, 18.88, 17.88, 17.85, 17.76, 17.74, 17.65, 17.61, 15.22, 13.81, 13.67, 12.60, 12.57, 12.51, 12.25, 8.37; FTIR (thin film): 2944, 2892, 2867, 1781, 1751, 1714, 1633, 1497, 1492, 1430, 1378, 1359, 1291, 1258, 1235, 1149, 1103, 1015, 997, 985 cm<sup>-1</sup>; HRMS (ESI-APCI) *m/z* calc'd for C<sub>29</sub>H<sub>42</sub>NO<sub>6</sub>Si (M+H)<sup>+</sup>: 528.2781, found: 528.2779.

### Preparation of phenol **374**

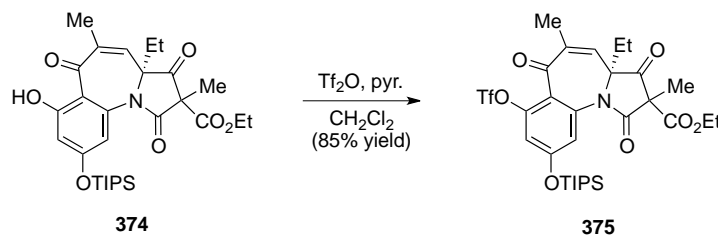


A solution of enone **373** (1.00 g, 1.895 mmol), [bis(trifluoroacetoxy)iodo] benzene (1.63 g, 3.79 mmol) and palladium(II) trifluoroacetate (31 mg, 0.095 mmol) in 1,2-dichloroethane (15 mL) was heated at 80 °C for 4 h. After cooling to room temperature the mixture was diluted with aqueous ammonium hydroxide (1M, 30 mL) and CH<sub>2</sub>Cl<sub>2</sub> (15 mL). The aqueous phase was extracted with CH<sub>2</sub>Cl<sub>2</sub> (3 × 10 mL) and the combined organic phases were washed with brine (50 mL), dried over MgSO<sub>4</sub>, filtered and concentrated *in vacuo*. The crude material was purified

by flash chromatography (15:1→10:1 hexanes:EtOAc) to furnish phenol **374** (870 mg, 84% yield).

$^1\text{H-NMR}$  (400 MHz;  $\text{CDCl}_3$ ):  $\delta$  13.23 (s, 1H), 6.60-6.45 (m, 3H), 4.28-4.05 (m, 2H), 2.05-1.99 (m, 4H), 1.68 (m, 1H), 1.61-1.54 (m, 3H), 1.32-1.23 (m, 6H), 1.15-1.09 (m, 18H), 0.79 (t,  $J$  = 7.3 Hz, 3H);  $^{13}\text{C-NMR}$  (101 MHz,  $\text{CDCl}_3$ ):  $\delta$  205.10, 191.60, 168.62, 168.22, 166.80, 166.55, 164.38, 162.21, 161.99, 141.22, 140.38, 139.60, 137.86, 135.15, 134.88, 112.88, 112.83, 112.56, 112.34, 108.41, 108.14, 76.41, 75.65, 62.89, 62.82, 57.80, 57.49, 29.66, 27.25, 26.85, 21.10, 18.74, 17.76, 17.74, 17.73, 17.70, 15.53, 13.82, 13.78, 12.60, 12.58, 8.05, 8.03; HRMS (ESI-APCI)  $m/z$  calc'd for  $\text{C}_{29}\text{H}_{42}\text{NO}_7\text{Si}$  ( $\text{M}+\text{H}$ ) $^+$ : 544.2731, found: 544.2726.

### Preparation of triflate **375**

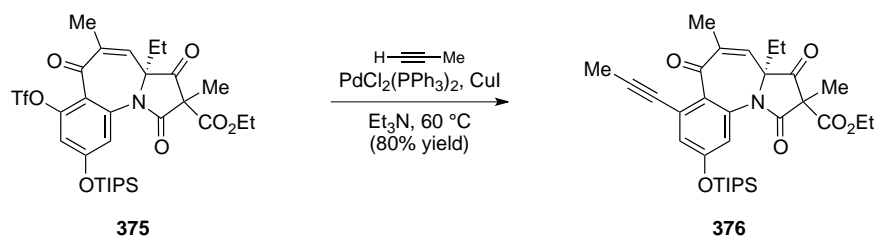


To a solution of phenol **374** (850 mg, 1.563 mmol) in  $\text{CH}_2\text{Cl}_2$  (10 mL) was added pyridine (0.50 mL, 6.253 mmol) followed by triflic anhydride (530  $\mu\text{L}$ , 3.127 mmol) at  $-78$  °C. The mixture was warmed to  $0$  °C and stirred for 2 h before it was quenched by addition of saturated aqueous ammonium chloride (10 mL). The aqueous phase extracted with  $\text{CH}_2\text{Cl}_2$  ( $3 \times 10$  mL) and the combined organic phases were washed with brine (30 mL), dried over  $\text{MgSO}_4$ , filtered and concentrated *in vacuo*. The crude material was purified by flash chromatography (4:1 hexanes:EtOAc) to provide aryl triflate **375** (896 mg, 85% yield).

$^1\text{H-NMR}$  (400 MHz;  $\text{CDCl}_3$ ):  $\delta$  7.01 (d,  $J$  = 2.3 Hz, 1H), 6.83 (t,  $J$  = 2.6 Hz, 1H), 6.36 (m, 1H), 4.26 (dd,  $J$  = 9.7, 7.2 Hz, 2H), 2.02 (m, 4H), 1.56 (s, 3H), 1.29-1.23 (m, 6H), 1.10-1.06 (m, 18H), 0.79 (t,  $J$  = 7.4 Hz, 3H);  $^{13}\text{C-NMR}$  (101 MHz,  $\text{CDCl}_3$ ):  $\delta$  203.82, 203.63, 188.29, 187.50, 168.67, 168.43, 164.82, 163.82, 159.22, 159.05, 148.06, 147.72, 138.36, 137.99, 137.83,

137.28, 134.35, 133.98, 125.21, 124.70, 120.08, 119.18, 119.02, 116.89, 115.05, 114.74, 77.69, 63.14, 62.86, 57.74, 57.62, 28.39, 27.69, 20.49, 20.30, 18.87, 17.63, 17.61, 14.97, 13.80, 13.58, 12.49, 12.46, 12.24, 8.31, 8.29;  $^{19}\text{F}$ -NMR (376 MHz,  $\text{CDCl}_3$ ):  $\delta$  -73.41, -73.50; FTIR (thin film): 2946, 2894, 2869, 1782, 1752, 1718, 1660, 1608, 1427, 1360, 1291, 1243, 1140, 1113, 1015  $\text{cm}^{-1}$ ; HRMS (ESI-APCI)  $m/z$  calc'd for  $\text{C}_{30}\text{H}_{41}\text{F}_3\text{NO}_9\text{SSi}$  ( $\text{M}+\text{H}$ ) $^+$ : 676.2223, found: 676.2220.

### Preparation of alkyne **376**

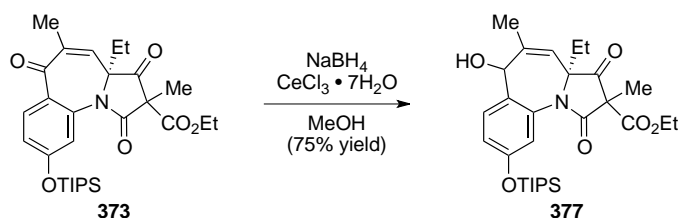


Triflate **375** (300 mg, 0.444 mmol),  $\text{PdCl}_2(\text{PPh}_3)_2$  (31 mg, 0.044 mmol) and  $\text{CuI}$  (4.2 mg, 0.022 mmol) were suspended in triethylamine (10 mL). Propyne gas was bubbled into the solution for 10 s and the mixture was heated to  $50\text{ }^\circ\text{C}$ . After 30 min at elevated temperature propyne was bubbled through the solution for 10 s and the mixture stirred at  $50\text{ }^\circ\text{C}$  for 4 hours. The dark reaction mixture was cooled to room temperature and diluted with diethyl ether (50 mL) and saturated aqueous ammonium chloride solution (50 mL). The aqueous phase was extracted with diethyl ether ( $3 \times 10\text{ mL}$ ) and the combined organic phases were washed with brine (50 mL), dried over  $\text{MgSO}_4$ , filtered and concentrated *in vacuo*. The crude material was purified by flash chromatography (20:1 $\rightarrow$ 10:1 hexanes:EtOAc) to give alkyne **376** (200 mg, 80% yield) as a brown crystalline solid.

$^1\text{H}$ -NMR (400 MHz;  $\text{CDCl}_3$ ):  $\delta$  6.99 (d,  $J = 2.3\text{ Hz}$ , 1H), 6.82 (d,  $J = 2.3\text{ Hz}$ , 1H), 6.22 (m, 1H), 5.25 (s, 1H), 4.24-4.01 (m, 2H), 2.00 (s, 3H), 1.97-1.94 (m, 1H), 1.67 (m, 1H), 1.55-1.51 (m, 3H), 1.27-1.18 (m, 6H), 1.04 (m, 18H), 0.79 (t,  $J = 7.4\text{ Hz}$ , 3H);  $^{13}\text{C}$ -NMR (101 MHz,  $\text{CDCl}_3$ ):  $\delta$  204.44, 204.31, 191.56, 190.24, 168.66, 168.52, 165.09, 164.13, 157.92, 157.74, 138.26, 137.34, 136.69, 136.15, 133.54, 133.10, 132.75, 132.69, 126.18, 125.86, 125.70, 125.39,

118.86, 118.64, 90.60, 90.56, 77.16, 76.55, 62.97, 62.68, 57.83, 57.69, 28.00, 27.46, 20.73, 20.53, 18.93, 17.76, 17.73, 17.62, 17.60, 14.92, 13.76, 13.51, 12.55, 12.51, 12.44, 12.23, 8.28, 8.24, 4.63, 4.55; FTIR (thin film): 3421, 2945, 2894, 2868, 2235, 2159, 1780, 1750, 1654, 1593, 1561, 1541, 1463, 1427, 1387, 1317, 1293, 1243, 1206, 1124, 1014  $\text{cm}^{-1}$ ; HRMS (ESI-APCI)  $m/z$  calc'd for  $\text{C}_{32}\text{H}_{44}\text{NO}_6\text{Si}$  ( $\text{M}+\text{H}$ ) $^+$ : 566.2938, found: 566.2933.

### Preparation of allylic alcohol **377**

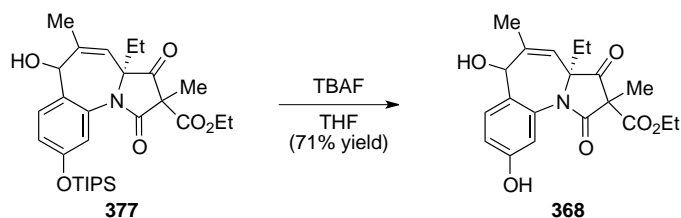


To a solution of enone **373** (528 mg, 1.00 mmol) and cerium(III) chloride heptahydrate (410 mg, 1.1 mmol) in  $\text{MeOH}$  (10 mL) and THF (5 mL) was added sodium borohydride (42 mg, 1.1 mmol) at 0 °C. After 1 h the reaction was quenched by addition of saturated aqueous ammonium chloride (5 mL). The aqueous phase was extracted with diethyl ether (3 × 5 mL) and the combined organic phases were washed with brine (15 mL), dried over  $\text{MgSO}_4$ , filtered and concentrated *in vacuo*. The crude material was purified by flash chromatography (10:1→5:1 hexanes:EtOAc) to give allylic alcohol **377** (398 mg, 75% yield).

$^1\text{H-NMR}$  (400 MHz;  $\text{CDCl}_3$ ):  $\delta$  7.40 (m, 1H), 6.88 (m, 1H), 6.80 (m, 1H), 5.21 (s, 1H), 5.11 (m, 1H), 4.21 (m, 2H), 3.25 (d,  $J = 5.0$  Hz, 1H), 1.85-1.82 (m, 3H), 1.82-1.76 (m, 1H), 1.54 (s, 3H), 1.39 (m, 1H), 1.28-1.17 (m, 6H), 1.12-1.01 (m, 18H), 0.82-0.73 (m, 3H);  $^{13}\text{C-NMR}$  (101 MHz,  $\text{CDCl}_3$ ):  $\delta$  205.55, 205.19, 169.63, 169.38, 165.52, 165.04, 155.37, 155.27, 141.78, 141.19, 136.02, 135.17, 131.50, 131.31, 125.03, 124.50, 120.97, 120.95, 120.29, 119.75, 119.69, 75.44, 74.50, 67.59, 67.58, 62.74, 62.58, 58.26, 58.09, 29.43, 29.29, 21.04, 20.62, 18.82, 17.80, 15.43, 13.77, 13.57, 12.57, 12.55, 8.01, 7.91; FTIR (thin film): 3492, 2944, 2893, 2867, 1776, 1748, 1691, 1608, 1579, 1497, 1462, 1448, 1431, 1383, 1290, 1109, 1013, 976  $\text{cm}^{-1}$

$^1$ : 2344, 2894, 2868, 1782, 1752, 1614, 1574, 1462, 1402, 1369, 1344, 1236, 1196, 1178, 1144, 1122, 1101, 1072, 1056, 1015, 997, 993  $\text{cm}^{-1}$ ; HRMS (ESI-APCI)  $m/z$  calc'd for  $\text{C}_{29}\text{H}_{44}\text{NO}_6\text{Si}$  ( $\text{M}+\text{H}$ ) $^+$ : 530.2938, found: 530.2941.

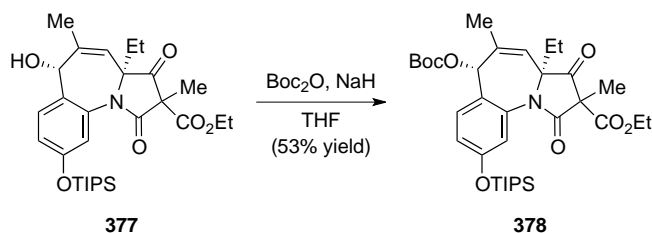
### Preparation of phenol **368**



To a solution of allylic alcohol **377** (40 mg, 0.076 mmol) in THF (1 mL) was added TBAF (1M in THF, 150 mL, 0.151 mmol) at room temperature. After stirring for 1 h at ambient temperature the reaction was quenched by addition of saturated aqueous ammonium chloride (1 mL). The aqueous phase was extracted with diethyl ether (3  $\times$  1 mL) and the combined organic phases were dried over  $\text{MgSO}_4$ , filtered and concentrated *in vacuo*. The crude material was purified by flash chromatography (1:1 hexanes:EtOAc) to supply diol **368** (20 mg, 71% yield).

$^1\text{H-NMR}$  (400 MHz; acetone- $d_6$ ):  $\delta$  7.49 (d,  $J = 8.5$  Hz, 1H), 6.91 (m, 1H), 6.84 (m, 1H), 5.51 (s, 1H), 5.20 (m, 1H), 4.78 (d,  $J = 5.7$  Hz, 1H), 4.24-4.10 (m, 2H), 1.91 (m, 3H), 1.84 (m, 2H), 1.49 (s, 3H), 1.27-1.17 (m, 3H), 0.85 (t,  $J = 7.4$  Hz, 3H);  $^{13}\text{C-NMR}$  (101 MHz, acetone- $d_6$ ):  $\delta$  168.77, 168.44, 165.75, 165.34, 156.60, 156.42, 143.11, 142.33, 135.19, 134.45, 132.47, 132.18, 125.04, 124.82, 120.80, 120.74, 115.50, 115.38, 115.35, 115.24, 74.97, 74.11, 67.11, 66.98, 62.28, 62.11, 57.93, 57.65, 29.58, 29.49, 20.40, 20.24, 18.08, 15.01, 13.30, 13.17, 7.55, 7.49; HRMS (ESI-APCI)  $m/z$  calc'd for  $\text{C}_{20}\text{H}_{24}\text{NO}_6$  ( $\text{M}+\text{H}$ ) $^+$ : 374.1604, found: 374.1598

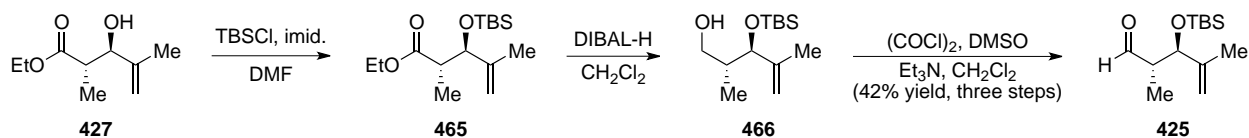
## Preparation of carbonate **378**



To a solution of allylic alcohol **377** (340 mg, 0.642 mmol) in THF (7 mL) was added  $\text{Boc}_2\text{O}$  (420 mg, 1.925 mmol) and sodium hydride (60% in mineral oil, 77 mg, 1.925 mmol). The suspension was stirred for 20 h at ambient temperature and then quenched by addition of saturated aqueous ammonium chloride (10 mL). The aqueous phase was extracted with diethyl ether ( $3 \times 5$  mL) and the combined organic phases were washed with brine (20 mL), dried over  $\text{MgSO}_4$ , filtered and concentrated *in vacuo*. The crude material was purified by flash chromatography (10:1→5:1 hexanes:EtOAc) to provide allylic carbonate **378** (215 mg, 53% yield) starting material (**377**, 99 mg, 29% yield).

$^1\text{H-NMR}$  (400 MHz;  $\text{CDCl}_3$ ):  $\delta$  7.36 (m, 1H), 6.90 (m, 2H), 6.37 (s, 1H), 5.24 (m, 1H), 4.25 (m, 2H), 1.79 (m, 2H), 1.70 (s, 3H), 1.49-1.47 (m, 6H), 1.29-1.20 (m, 6H), 1.09 (m, 18H), 0.86 (t,  $J = 7.4$  Hz, 3H);  $^{13}\text{C-NMR}$  (101 MHz,  $\text{CDCl}_3$ ):  $\delta$  205.20, 169.29, 165.61, 155.84, 152.66, 138.43, 131.88, 130.99, 124.63, 122.50, 120.35, 120.30, 82.89, 74.14, 72.26, 62.54, 58.37, 29.83, 27.67, 27.63, 20.34, 19.10, 17.82, 17.76, 17.74, 13.81, 12.56, 7.92; HRMS (ESI-APCI)  $m/z$  calc'd for  $\text{C}_{34}\text{H}_{52}\text{NO}_8\text{Si}$  ( $\text{M}+\text{H}$ ) $^+$ : 630.3462, found: 630.3451.

## Preparation of aldehyde **425**



Known  $\beta$ -hydroxy ester **427**<sup>11</sup> (5.0 g, 29 mmol) and imidazole (4.34 g, 63.8 mmol) were dissolved in DMF (36 mL) and TBSCl (5.25 g, 34.8 mmol) and allowed to stir overnight. Water

(50 mL) was added and the mixture was extracted with EtOAc (3 × 40 mL) and the combined organics were washed with brine (75 mL), dried over MgSO<sub>4</sub>, filtered and concentrated *in vacuo*. The crude material was purified by flash chromatography (5% EtOAc/hexanes) to give silyl ether **465** (7.875 g, 95% yield). This compound was contaminated with a small amount of a compound lacking the α-methyl group due to incomplete conversion in the previous step. This compound could however be removed after the next step.

<sup>1</sup>H-NMR (400 MHz; CDCl<sub>3</sub>): δ 4.87-4.85 (m, 2H), 4.16 (d, *J* = 9.7 Hz, 1H), 4.09 (qd, *J* = 7.2, 0.8 Hz, 2H), 2.56-2.52 (m, 1H), 1.62 (s, 3H), 1.26-1.22 (m, 3H), 0.91 (d, *J* = 7.1 Hz, 3H), 0.83-0.81 (m, 9H), -0.01 (s, 3H), -0.04 (s, 3H); <sup>13</sup>C-NMR (101 MHz, CDCl<sub>3</sub>): δ 175.63, 144.62, 114.31, 79.74, 60.22, 44.72, 17.95, 15.81, 14.11, 13.99, -4.85, -5.59; FTIR (thin film): 2955, 2930, 2887, 2857, 1736, 1473, 1463, 1389, 1376, 1362, 1251, 1175, 1071 cm<sup>-1</sup>; HRMS (ESI-APCI) *m/z* calc'd for C<sub>15</sub>H<sub>31</sub>O<sub>3</sub>Si (M+H)<sup>+</sup>: 287.2042, found: 287.2034.

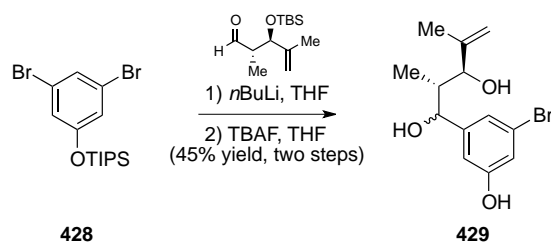
Ester **465** (1.5 g, 5.24 mmol) was dissolved in CH<sub>2</sub>Cl<sub>2</sub> (52 mL) and cooled to -78 °C. DIBAL-H (1 M in hexanes, 15.7 mL, 15.7 mmol) was added and the reaction was allowed to warm to room temperature. After 1 h 45 min sat. aq. Rochelles salt (50 mL) was added. The mixture was extracted with CH<sub>2</sub>Cl<sub>2</sub> (3 × 30 mL) and the combined organics were washed with brine (75 mL), dried over MgSO<sub>4</sub>, filtered and concentrated *in vacuo*. The crude material was purified by flash chromatography (10% EtOAc/hexanes) to give alcohol **466** (0.679 g, 53% yield).

<sup>1</sup>H-NMR (400 MHz; CDCl<sub>3</sub>): δ 4.86 (t, *J* = 0.9 Hz, 1H), 4.83 (t, *J* = 1.5 Hz, 1H), 3.87 (d, *J* = 7.4 Hz, 1H), 3.57 (d, *J* = 5.6 Hz, 2H), 2.85 (s, 1H), 1.78-1.75 (m, 1H), 1.64 (s, 3H), 0.84 (d, *J* = 7.7 Hz, 9H), 0.81 (d, *J* = 8.4 Hz, 3H), 0.04 (s, 3H), -0.03 (s, 3H); <sup>13</sup>C-NMR (101 MHz, CDCl<sub>3</sub>): δ 145.78, 112.80, 82.44, 66.24, 37.98, 25.76, 18.02, 17.17, 14.26, -4.61, -5.33; FTIR (thin film): 3388, 2957, 2930, 2886, 2858, 1472, 1463, 1388, 1373, 1256, 1065, 1040 cm<sup>-1</sup>; HRMS (ESI-APCI) *m/z* calc'd for C<sub>13</sub>H<sub>29</sub>O<sub>2</sub>Si (M+H)<sup>+</sup>: 245.1937, found: 245.1925.

Oxalyl chloride (0.57 mL, 6.53 mmol) was added to a solution of DMSO (0.78 mL, 11.04 mmol) in CH<sub>2</sub>Cl<sub>2</sub> (26 mL) at -78 °C. After 10 min alcohol **466** (1.228 g, 5.02 mmol) in CH<sub>2</sub>Cl<sub>2</sub> (26 mL) was added. The reaction was stirred for 45 min then Et<sub>3</sub>N (3.5 mL, 25.1 mmol) was added. After 45 min the reaction was warmed to room temperature and the reaction was quenched with sat. aq. NH<sub>4</sub>Cl (50 mL). The mixture was extracted with CH<sub>2</sub>Cl<sub>2</sub> (3 × 40 mL) and the combined organics were washed with brine (100 mL), dried over MgSO<sub>4</sub>, filtered and concentrated *in vacuo*. The crude material was purified by flash chromatography (10% EtOAc/hexanes) to give aldehyde **425** (1.028 g, 84% yield).

<sup>1</sup>H-NMR (400 MHz; CDCl<sub>3</sub>): δ 9.73 (s, 1H), 4.92-4.90 (m, 2H), 4.14 (d, *J* = 8.1 Hz, 1H), 2.52 (ddd, *J* = 7.9, 7.1, 2.8 Hz, 1H), 0.90 (d, *J* = 7.0 Hz, 3H), 0.85 (s, 9H), 0.03 (s, 3H), -0.01 (s, 3H); <sup>13</sup>C-NMR (101 MHz, CDCl<sub>3</sub>): δ 204.94, 144.52, 113.78, 78.64, 49.82, 25.64, 18.05, 16.63, 11.01, -4.64, -5.37; FTIR (thin film): 2956, 2930, 2886, 2857, 1727, 1472, 1462, 1389, 1373, 1362, 1251, 1117, 1065 cm<sup>-1</sup>; HRMS (ESI-APCI) *m/z* calc'd for C<sub>13</sub>H<sub>27</sub>O<sub>3</sub>Si (hydrate of the aldehyde) (M-H)<sup>-</sup>: 259.1729, found: 259.1725.

### Preparation of phenol **429**



*n*-BuLi (1.6 M in hexanes, 3.18 mL, 5.09 mmol) was added to aryl bromide **428**<sup>12</sup> (2.077 g, 5.09 mmol) in THF (11.3 mL) at -78 °C. After 10 min aldehyde **425** (1.028 g, 4.24 mmol) in THF (2.1 mL) was added. The reaction was stirred for 20 min then warmed to room temperature. After 20 min the reaction was quenched with sat. aq. NH<sub>4</sub>Cl (10 mL) and extracted with EtOAc (3 × 10 mL). The combined organics were washed with brine (20 mL), dried over

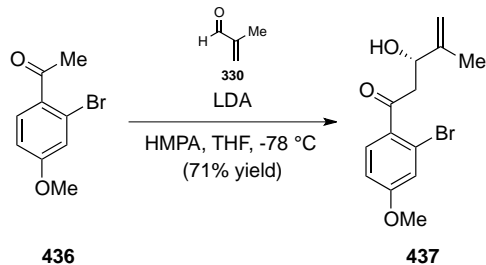
MgSO<sub>4</sub>, filtered and concentrated *in vacuo*. The crude material was purified by flash chromatography (10% EtOAc/hex) to give alcohol **467** (2.4 g, quant. yield).

<sup>1</sup>H-NMR (400 MHz; CDCl<sub>3</sub>): δ 6.98 (s, 1H), 6.87 (t, *J* = 2.0 Hz, 1H), 6.74 (d, *J* = 1.1 Hz, 1H), 5.11 (s, 1H), 5.04 (s, 1H), 5.01 (s, 1H), 4.12 (s, 1H), 3.41 (s, 1H), 1.78 (m, 1H), 1.74 (s, 3H), 1.27-1.19 (m, 3H), 1.11-1.03 (m, 18H), 0.94-0.91 (s, 9H), 0.77 (d, *J* = 7.1 Hz, 3H), 0.10-0.08 (s, 3H), 0.04 (s, 3H); <sup>13</sup>C-NMR (101 MHz, CDCl<sub>3</sub>): δ 156.56, 147.27, 146.17, 145.41, 144.81, 122.90, 122.22, 122.02, 121.35, 121.10, 117.91, 116.06, 114.62, 112.66, 84.84, 80.51, 78.80, 71.21, 42.80, 41.92, 25.96, 25.87, 25.82, 25.78, 18.98, 18.09, 17.90, 17.85, 17.76, 16.38, 14.29, 12.63, 12.57, 10.16, -4.23, -4.67, -5.27, -5.30; FTIR (thin film): 3487, 2946, 2930, 2893, 2867, 1596, 1567, 1471, 1463, 1442, 1278, 1257, 1151, 1106, 1090, 1061, 1013, 1001 cm<sup>-1</sup>; HRMS (ESI-APCI) *m/z* calc'd for C<sub>28</sub>H<sub>51</sub>BrNaO<sub>3</sub>Si<sub>2</sub> (M+Na)<sup>+</sup>: 595.2437, found: 595.2434.

TBAF (1 M in THF, 4.12 mL, 4.12 mmol) was added to alcohol **467** (1.07 g, 1.87 mmol) in THF (18.7 mL). After 1 h the solvent was removed *in vacuo* and the crude material was purified by flash chromatography (30%→50% EtOAc/hexanes) to give phenol **429** (0.254 g, 45% yield).

<sup>1</sup>H-NMR (400 MHz; CDCl<sub>3</sub>): δ 6.89 (s, 1H), 6.86 (s, 1H), 6.78 (s, 1H), 5.01 (s, 1H), 4.96 (m, 2H), 4.06 (d, *J* = 6.9 Hz, 1H), 3.81-3.76 (m, 1H), 3.00-2.95 (m, 1H), 2.00-1.96 (m, 1H), 1.74 (s, 3H), 0.77-0.76 (m, 3H); <sup>13</sup>C-NMR (101 MHz, CDCl<sub>3</sub>): δ 156.61, 146.01, 145.24, 122.46, 121.19, 117.52, 113.01, 112.04, 79.32, 73.55, 40.70, 17.96, 10.93; FTIR (thin film): 3310, 2972, 2921, 1597, 1576, 1377, 1266, 1149, 1090 cm<sup>-1</sup>; HRMS (ESI-APCI) *m/z* calc'd for C<sub>13</sub>H<sub>17</sub>BrClO<sub>3</sub> (M+Cl): 337.0029, found: 337.0032.

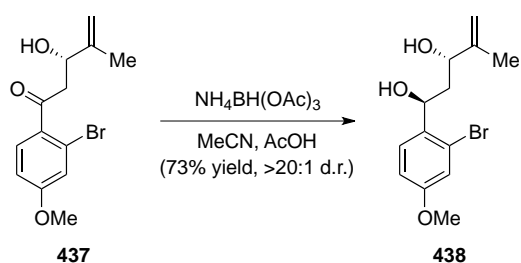
## Preparation of $\beta$ -hydroxy ketone **437**



LDA was prepared by addition of *n*-BuLi (1.6 M in hexanes, 3.0 mg, 4.802 mmol) to a solution of diisopropylamine (730 mL, 5.239 mmol) in THF (10 mL). After stirring for 30 min at  $-78\text{ }^\circ\text{C}$ , acetophenone **436** (1.00 g, 4.356 mmol) in THF (2 mL) was added and the orange solution was stirred for 45 min at  $-78\text{ }^\circ\text{C}$ . Methacrolein (80%, 450 mL, 4.365 mmol) was added and the greenish solution formed was stirred for another 45 min at  $-78\text{ }^\circ\text{C}$  before it was quenched by addition of acetic acid (0.5 mL) in THF (1 mL). The mixture was then warmed to room temperature and the white suspension was diluted with water (30 mL). The aqueous phase was extracted with diethyl ether ( $3 \times 10\text{ mL}$ ) and the combined organic phases were washed with brine (40 mL), dried over  $\text{MgSO}_4$ , filtered and concentrated *in vacuo*. The crude material was purified by flash chromatography (3:1 hexanes:EtOAc) to furnish allylic alcohol **437** (921 mg, 71% yield) along with a minor amount of inseparable debrominated product.

$^1\text{H-NMR}$  (400 MHz;  $\text{CDCl}_3$ ):  $\delta$  7.53 (d,  $J = 8.7\text{ Hz}$ , 1H), 7.12 (d,  $J = 2.5\text{ Hz}$ , 1H), 6.85 (dd,  $J = 8.7, 2.5\text{ Hz}$ , 1H), 5.03 (s, 1H), 4.85 (s, 1H), 4.60 (m, 1H), 3.80 (s, 3H), 3.21-3.07 (m, 3H), 1.75 (s, 3H);  $^{13}\text{C-NMR}$  (101 MHz,  $\text{CDCl}_3$ ):  $\delta$  201.65, 162.01, 145.73, 132.22, 131.46, 130.43, 119.62, 113.79, 113.12, 111.32, 71.62, 55.71, 47.19, 43.18, 18.50, 18.41; FTIR (thin film): 3445, 2970, 2941, 2915, 2840, 1676, 1593, 1488, 1457, 1439, 1261, 1229, 1170, 1027  $\text{cm}^{-1}$ ; HRMS (ESI-APCI)  $m/z$  calc'd for  $\text{C}_{13}\text{H}_{16}\text{BrO}_3$  ( $\text{M}+\text{H}$ ) $^+$ : 299.0283, found: 299.0268.

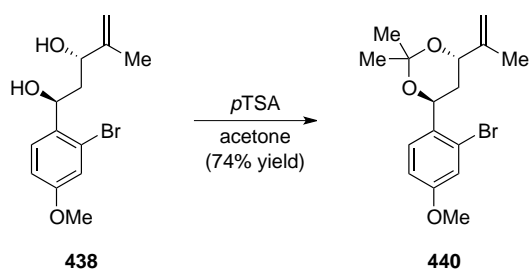
## Preparation of diol **438**



Tetramethylammonium triacetoxyborohydride (2.11 g, 8.02 mmol) was dissolved in a mixture of acetonitrile (3 mL) and acetic acid (3 mL) and the mixture was stirred for 30 min. Then a solution of allylic alcohol **437** (300 mg, 1.00 mmol) in acetonitrile (1 mL) was added and the mixture was stirred for 2 h at ambient temperature. The mixture was then diluted with saturated aqueous Rochelle's salt solution (10 mL) and diethyl ether (10 mL) followed by slow addition of saturated aqueous sodium bicarbonate solution (10 mL). The aqueous phase was extracted with diethyl ether (3 × 10 mL) and the combined organic phases were washed with saturated aqueous sodium bicarbonate (30 mL) and brine (30 mL), dried over  $\text{MgSO}_4$ , filtered and concentrated *in vacuo*. The crude material was purified by flash chromatography (9:1→3:1 hexanes:EtOAc) to provide diol **438** (221 mg, 73% yield).

$^1\text{H-NMR}$  (400 MHz;  $\text{CDCl}_3$ ):  $\delta$  7.50 (d,  $J = 8.7$  Hz, 1H), 7.02 (d,  $J = 2.6$  Hz, 1H), 6.87 (dd,  $J = 8.7, 2.6$  Hz, 1H), 5.23 (dt,  $J = 7.7, 3.7$  Hz, 1H), 5.06 (s, 1H), 4.91 (s, 1H), 4.27-4.26 (m, 1H), 3.77 (s, 3H), 3.38 (d,  $J = 3.6$  Hz, 1H), 2.79 (d,  $J = 4.4$  Hz, 1H), 1.96-1.92 (m, 2H), 1.74 (s, 3H);  $^{13}\text{C-NMR}$  (101 MHz,  $\text{CDCl}_3$ ):  $\delta$  159.10, 146.83, 135.06, 128.10, 121.39, 117.67, 113.70, 110.39, 73.28, 70.36, 55.50, 40.19, 18.99; FTIR (thin film): 3340, 2942, 2917, 2836, 1604, 1589, 1490, 1455, 1439, 1285, 1234, 1070, 1027  $\text{cm}^{-1}$ ; HRMS (ESI-APCI)  $m/z$  calc'd for  $\text{C}_{13}\text{H}_{21}\text{BrNO}_3$  ( $\text{M}+\text{NH}_4$ ) $^+$ : 318.0705, found: 318.069.

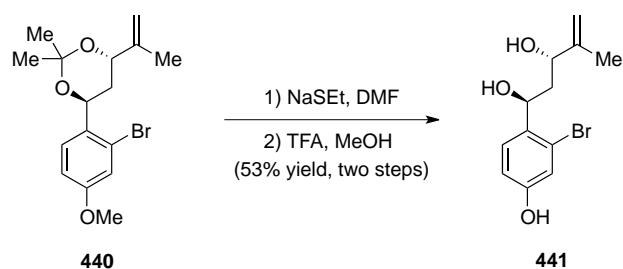
## Preparation of acetal 440



Diol **438** (450 mg, 1.49 mmol) and *p*-TsOH (28 mg, 0.15 mmol) were dissolved in 2,2-dimethoxypropane (2 mL) and heated to 56 °C for 3 h. The mixture was cooled to room temperature and diluted with diethyl ether (10 mL) and saturated aqueous sodium bicarbonate solution (10 mL). The aqueous phase was extracted with diethyl ether (3 × 5 mL) and the combined organic phases were washed with brine (20 mL), dried over MgSO<sub>4</sub>, filtered and concentrated *in vacuo*. The crude material was purified by flash chromatography (20:1 hexanes:EtOAc) to provide acetal **440** (379 mg, 74% yield).

<sup>1</sup>H-NMR (400 MHz; CDCl<sub>3</sub>): δ 7.49 (d, *J* = 8.7 Hz, 1H), 7.05 (t, *J* = 2.5 Hz, 1H), 6.89 (dd, *J* = 8.7, 2.6 Hz, 1H), 5.17 (dd, *J* = 9.7, 5.8 Hz, 1H), 5.04 (s, 1H), 4.86 (s, 1H), 4.37 (t, *J* = 7.5 Hz, 1H), 3.77 (s, 3H), 2.24 (ddd, *J* = 13.2, 8.6, 5.8 Hz, 1H), 1.85-1.77 (m, 4H), 1.49 (s, 3H), 1.48 (s, 3H); <sup>13</sup>C-NMR (101 MHz, CDCl<sub>3</sub>): δ 159.14, 145.09, 134.03, 128.28, 121.91, 117.50, 114.02, 110.71, 100.91, 69.93, 67.62, 55.52, 37.13, 25.44, 25.06, 18.62; FTIR (thin film): 2987, 2940, 2836, 1604, 1567, 1494, 1457, 1439, 1377, 1167, 1130, 1096, 1029 cm<sup>-1</sup>.

## Preparation of phenol **441**



To a suspension of sodium hydride (60% in mineral oil, 101 mg, 2.514 mmol) in DMF (3 mL) was added ethanethiol (181 mL, 2.514 mmol) and the foaming mixture was stirred for 15 min until a clear solution was obtained. A solution of acetal **440** (286 mg, 0.838 mmol) in DMF (1 mL) was then added and the mixture was heated to 90 °C for 20 h. The reaction mixture was then cooled to room temperature and diluted with diethyl ether (10 mL) and saturated aqueous ammonium chloride solution (10 mL). The aqueous phase was extracted with diethyl ether (3 × 5 mL) and the combined organic phases were washed with brine (2 × 20 mL), dried over MgSO<sub>4</sub>, filtered and concentrated *in vacuo*. The crude material was purified by flash chromatography (20:1→10:1 hexanes:EtOAc) to provide phenol **468** (220 mg, 80% yield).

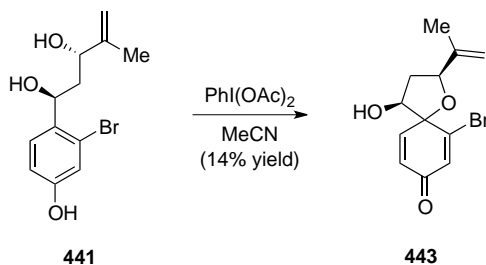
<sup>1</sup>H-NMR (400 MHz; CDCl<sub>3</sub>): δ 7.40 (dd, *J* = 8.6, 4.1 Hz, 1H), 6.96 (dd, *J* = 4.8, 2.6 Hz, 1H), 6.76-6.73 (m, 1H), 5.99-5.92 (m, 1H), 5.20 (dd, *J* = 9.8, 5.7 Hz, 1H), 5.05 (s, 1H), 4.88 (s, 1H), 4.39 (t, *J* = 7.4 Hz, 1H), 2.22 (ddd, *J* = 13.5, 8.2, 5.5 Hz, 1H), 1.92-1.83 (m, 1H), 1.79 (s, 2H), 1.51 (s, 3H), 1.48 (s, 3H); <sup>13</sup>C-NMR (101 MHz, CDCl<sub>3</sub>): δ 155.54, 155.52, 144.86, 133.32, 128.63, 128.59, 122.16, 119.42, 119.40, 115.24, 111.08, 101.21, 72.56, 70.20, 67.79, 36.77, 25.50, 25.08, 18.65; FTIR (thin film): 3347, 2989, 2936, 2159, 2030, 1976, 1608, 1583, 1495, 1434, 1319, 1220, 1161, 1132, 1089, 1031, 1008 cm<sup>-1</sup>; HRMS (ESI-APCI) *m/z* calc'd for C<sub>15</sub>H<sub>18</sub>BrO<sub>3</sub> (M-H)<sup>-</sup>: 325.0439, found: 325.0442.

Acetal **468** (200 mg, 0.611 mmol) was dissolved in methanol (2 mL), cooled to 0 °C and TFA (14 mL, 0.183 mmol) was added. The solution was stirred 3 h at 0 °C and for an additional 3 h at room temperature before it was diluted with diethyl ether (10 mL) and saturated aqueous

sodium bicarbonate (10 mL). The aqueous phase was extracted with diethyl ether (3 × 5 mL) and the combined organic phases were washed with brine (20 mL), dried over MgSO<sub>4</sub>, filtered and concentrated *in vacuo*. The crude material was purified by flash chromatography (4:1→2:1 hexanes:EtOAc) to furnish phenol **441** (117 mg, 66% yield).

<sup>1</sup>H-NMR (400 MHz; acetone-d<sub>6</sub>): δ 8.65 (s, 1H), 7.47 (d, *J* = 8.5 Hz, 1H), 7.00 (m, 1H), 6.85 (d, *J* = 8.5 Hz, 1H), 5.21 (dt, *J* = 9.3, 3.4 Hz, 1H), 5.00 (s, 1H), 4.79-4.77 (m, 1H), 4.60 (d, *J* = 4.1 Hz, 1H), 4.32 (m, 1H), 4.24 (d, *J* = 4.7 Hz, 1H), 1.85 (m, *J* = 2.8 Hz, 1H), 1.77-1.70 (m, 4H); <sup>13</sup>C-NMR (101 MHz, acetone-d<sub>6</sub>): δ 205.52, 156.91, 148.24, 135.46, 128.47, 118.68, 114.92, 109.04, 71.94, 69.10, 42.55, 17.98; HRMS (ESI-APCI) *m/z* calc'd for C<sub>12</sub>H<sub>14</sub>BrO<sub>3</sub> (M-H)<sup>-</sup>: 285.0126, found: 285.0123.

#### Preparation of spirotetrahydrofuran **443**

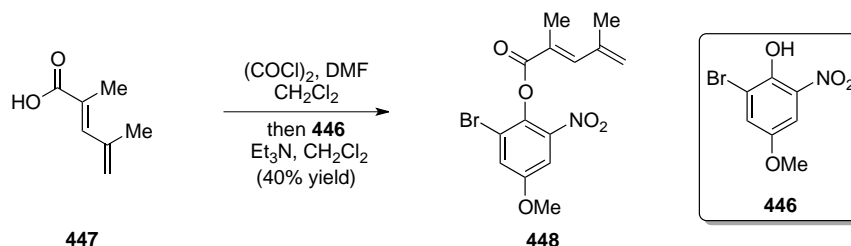


To a solution of triol **441** (50 mg, 0.174 mmol) in acetonitrile (3 mL) was added PhI(OAc)<sub>2</sub> (112 mg, 0.348 mmol) and the solution was stirred for 6 h. The orange solution was then diluted with diethyl ether (10 mL) and saturated aqueous sodium bicarbonate (10 mL). The aqueous phase was extracted with diethyl ether (3 × 5 mL) and the combined organic phases were washed with brine (20 mL), dried over MgSO<sub>4</sub>, filtered and concentrated *in vacuo*. The crude material was purified by flash chromatography (3:1→2:1 hexanes:EtOAc) to give spirotetrahydrofuran **443** (7 mg, 14% yield).

<sup>1</sup>H-NMR (400 MHz; CDCl<sub>3</sub>): δ 6.93 (s, 1H), 6.74 (m, 1H), 6.55-6.51 (m, 1H), 5.03 (s, 1H), 4.91 (s, 1H), 4.36-4.32 (m, 1H), 3.97 (t, *J* = 5.9 Hz, 1H), 2.07-1.99 (m, 2H), 1.78-1.73 (m, 3H);

$^{13}\text{C}$ -NMR (101 MHz,  $\text{CDCl}_3$ ):  $\delta$  183.10, 146.45, 145.82, 143.77, 136.45, 136.40, 133.26, 111.86, 72.90, 64.57, 58.06, 34.10, 17.77.

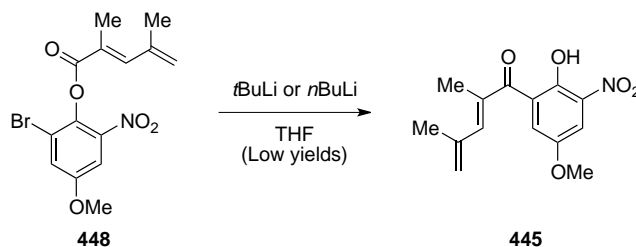
### Preparation of ester **448**



DMF (0.006 mL, 0.08 mmol) was added to a solution of acid **447**<sup>13</sup> (0.244 g, 1.94 mmol) and oxalyl chloride (0.29 mL, 3.22 mmol) in  $\text{CH}_2\text{Cl}_2$  (8 mL) at 0 °C. After 30 min the reaction was warmed to room temperature and after 30 min a solution of phenol **446** (0.400 g, 1.61 mmol) and  $\text{Et}_3\text{N}$  (0.45 mL, 3.22 mmol) in  $\text{CH}_2\text{Cl}_2$  (8 mL) was added. After stirring for 2 h sat. aq.  $\text{NH}_4\text{Cl}$  (20 mL) was added and the mixture was extracted with  $\text{CH}_2\text{Cl}_2$  (3  $\times$  15 mL). The combined organics were washed with sat. aq.  $\text{NaHCO}_3$  (40 mL), dried over  $\text{MgSO}_4$ , filtered and concentrated *in vacuo*. The crude mixture was purified by flash chromatography (5% EtOAc/hexanes) to give ester **448** (0.229 g, 40% yield).

$^1\text{H}$ -NMR (400 MHz;  $\text{CDCl}_3$ ):  $\delta$  7.53-7.50 (m, 1H), 7.42 (dt,  $J = 7.3, 3.6$  Hz, 1H), 7.39 (d,  $J = 9.2$  Hz, 1H), 7.00 (t,  $J = 0.5$  Hz, 1H), 5.32 (s, 1H), 5.21 (s, 1H), 3.87-3.81 (m, 3H), 2.18-2.13 (m, 3H), 2.00-1.98 (m, 3H);  $^{13}\text{C}$ -NMR (101 MHz,  $\text{CDCl}_3$ ):  $\delta$  165.68, 156.98, 144.11, 142.91, 140.49, 125.48, 124.10, 124.05, 121.84, 120.02, 109.83, 56.33, 22.64, 13.98; FTIR (thin film): 3092, 2929, 2850, 1741, 1614, 1537, 1476, 1436, 1347, 1302, 1197, 1072, 1041  $\text{cm}^{-1}$ ; HRMS (ESI-APCI)  $m/z$  calc'd for  $\text{C}_{14}\text{H}_{15}\text{BrNO}_5$  ( $\text{M}+\text{H}$ )<sup>+</sup>: 356.0134, found: 356.0132.

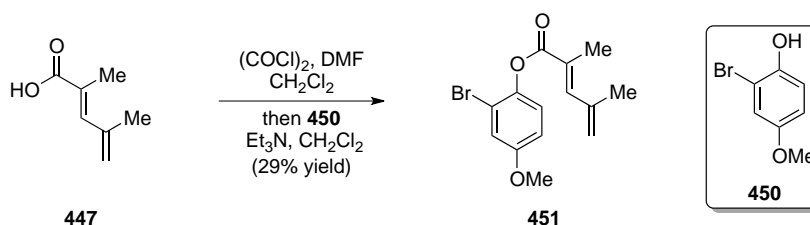
## Preparation of enone 445



$n\text{-BuLi}$  (1.67 M in hexanes, 0.16 mL, 0.26 mmol) was added to aryl bromide **448** (0.085 g, 0.24 mmol) in THF (2.4 mL) at  $-78\text{ }^\circ\text{C}$ . After 2.5 h the reaction was warmed to room temperature and sat. aq.  $\text{NH}_4\text{Cl}$  (5 mL) was added. The mixture was extracted with EtOAc (3  $\times$  5 mL) and the combined organics washed with brine (15 mL), dried over  $\text{MgSO}_4$ , filtered and concentrated *in vacuo*. The crude material was purified by flash chromatography (5% $\rightarrow$ 10% EtOAc/hexanes) to give enone **445** (0.006 g, 9% yield).

$^1\text{H-NMR}$  (300 MHz;  $\text{CDCl}_3$ ):  $\delta$  10.59 (s, 1H), 7.61 (d,  $J = 3.0$  Hz, 1H), 7.17 (d,  $J = 3.2$  Hz, 1H), 6.59 (d,  $J = 0.6$  Hz, 1H), 5.29 (d,  $J = 0.6$  Hz, 1H), 5.11 (s, 1H), 3.82 (s, 3H), 2.12 (s, 3H), 1.94 (s, 3H).

## Preparation of ester 451

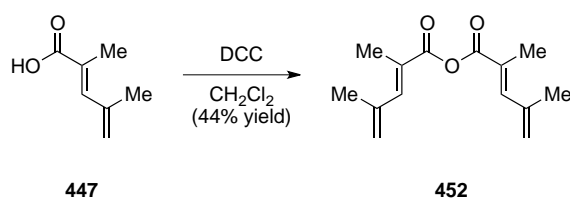


DMF (3 drops) was added to a solution of acid **447** (1.24 g, 9.85 mmol) and oxalyl chloride (1.11 mL, 12.33 mmol) in  $\text{CH}_2\text{Cl}_2$  (25 mL) at  $0\text{ }^\circ\text{C}$ . After 30 min the reaction was warmed to room temperature and after 30 min a solution of phenol **450** (1.00 g, 4.93 mmol) and  $\text{Et}_3\text{N}$  (1.72 mL, 12.33 mmol) in  $\text{CH}_2\text{Cl}_2$  (25 mL) was added. After stirring for 2 h sat. aq.  $\text{NH}_4\text{Cl}$  (50 mL) was added and the mixture was extracted with  $\text{CH}_2\text{Cl}_2$  (3  $\times$  30 mL). The combined

organics were washed with sat. aq.  $\text{NaHCO}_3$  (75 mL), dried over  $\text{MgSO}_4$ , filtered and concentrated *in vacuo*. The crude mixture was purified by flash chromatography (2%→3%→5% EtOAc/hexanes) to give ester **451** (0.444 g, 29% yield).

$^1\text{H-NMR}$  (400 MHz;  $\text{CDCl}_3$ ):  $\delta$  7.38 (s, 1H), 7.12 (d,  $J = 2.8$  Hz, 1H), 7.06 (d,  $J = 8.9$  Hz, 1H), 6.85 (dd,  $J = 8.9, 2.9$  Hz, 1H), 5.30 (s, 1H), 5.18 (s, 1H), 3.77 (s, 3H), 2.15 (s, 3H), 1.99 (s, 3H);  $^{13}\text{C-NMR}$  (101 MHz,  $\text{CDCl}_3$ ):  $\delta$  166.80, 157.61, 142.83, 142.15, 140.64, 126.35, 123.93, 121.03, 118.06, 116.31, 114.10, 55.78, 22.73, 14.03; FTIR (thin film): 2962, 2940, 2837, 1771, 1727, 1600, 1580, 1488, 1439, 1263, 1229, 1181, 1082, 1030  $\text{cm}^{-1}$ ; HRMS (ESI-APCI)  $m/z$  calc'd for  $\text{C}_{14}\text{H}_{16}\text{BrO}_3$  ( $\text{M}+\text{H}$ ) $^+$ : 311.0283, found: 311.2080.

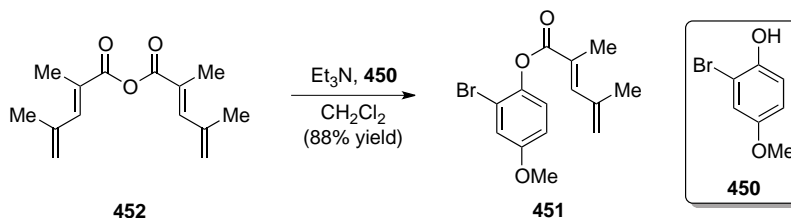
### Preparation of anhydride **452**



DCC (0.577 g, 2.79 mmol) was added to acid **447** (0.863 g, 5.6 mmol) in  $\text{CH}_2\text{Cl}_2$  (28 mL) at 0 °C. After 35 min the solution was warmed to room temperature. After 1 h 20 min the reaction was placed in the freezer overnight. The solution was then filtered through a pad of silica while still cold. The solvent was removed *in vacuo* to provide anhydride **452** (0.574 g, 44% yield), which was used in the next step as is.

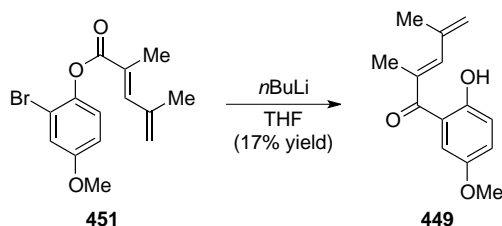
$^1\text{H-NMR}$  (300 MHz;  $\text{CDCl}_3$ ):  $\delta$  7.20 (s, 2H), 5.33 (s, 2H), 5.17 (s, 2H), 2.08 (s, 6H), 1.99 (s, 6H);  $^{13}\text{C-NMR}$  (75 MHz,  $\text{CDCl}_3$ ):  $\delta$  165.27, 144.51, 140.65, 127.12, 122.08, 22.79, 14.00; FTIR (thin film): 2970, 2929, 1769, 1710, 1633, 1623, 1446, 1388, 1265, 1187, 1003  $\text{cm}^{-1}$ ; HRMS (ESI-APCI)  $m/z$  calc'd for  $\text{C}_{14}\text{H}_{18}\text{NaO}_3$  ( $\text{M}+\text{Na}$ ) $^+$ : 257.1154, found: 257.1157.

### Preparation of ester **451**



Anhydride **452** (0.574 g, 2.45 mmol), phenol **450** (0.452 g, 2.23 mmol), Et<sub>3</sub>N (0.34 mL, 2.45 mmol), and CH<sub>2</sub>Cl<sub>2</sub> (22 mL) were combined and heated to 45 °C. After 15 h the reaction was cooled to room temperature and sat. aq. NH<sub>4</sub>Cl (25 mL) was added and extracted with CH<sub>2</sub>Cl<sub>2</sub> (3 × 15 mL). The combined organics were washed with 1 N NaOH (50 mL) and brine (50 mL), dried over MgSO<sub>4</sub>, filtered and concentrated *in vacuo*. The crude material was purified by flash chromatography (2.5%→5% EtOAc/hexanes) to give ester **451** (0.612 g, 88% yield). All spectral data matched that from the acid chloride procedure.

### Preparation of enone **449**

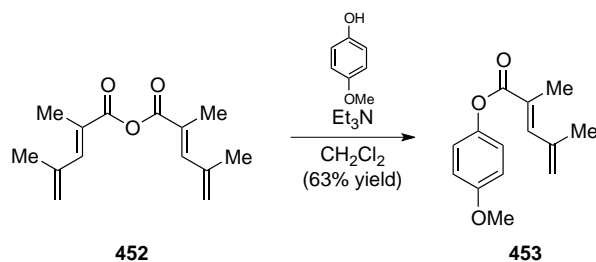


*n*-BuLi (1.67 M in hexanes, 1.28 mL, 2.14 mmol) was added to aryl bromide **451** (0.444 g, 1.43 mmol) in THF (14.3 mL) at -78 °C. The reaction was allowed to warm to room temperature and stir of 17 h. MeOH (10 mL) was added and the volatiles were removed *in vacuo*. The crude material was purified by flash chromatography (5% EtOAc/hexanes) to give enone **449** (0.056 g, 17% yield).

<sup>1</sup>H-NMR (400 MHz; CDCl<sub>3</sub>): δ 11.33 (s, 1H), 7.12 (d, *J* = 3.0 Hz, 1H), 7.08 (t, *J* = 6.0 Hz, 1H), 6.94 (m, 1H), 6.40 (s, 1H), 5.24 (s, 1H), 5.10 (s, 1H), 3.74 (s, 3H), 2.14 (s, 3H), 1.97 (s, 3H); <sup>13</sup>C-NMR (101 MHz, CDCl<sub>3</sub>): δ 203.82, 157.11, 151.24, 140.30, 139.99, 134.51, 123.42,

119.91, 119.12, 115.66, 113.79, 55.87, 15.10, 14.07; FTIR (thin film): 2955, 2933, 2871, 2860, 2836, 1726, 1630, 1599, 1483, 1323, 1281, 1254, 1218, 1138, 1039  $\text{cm}^{-1}$ ; HRMS (ESI-APCI)  $m/z$  calc'd for  $\text{C}_{14}\text{H}_{15}\text{O}_3$  (M-H) $^-$ : 231.1021, found: 231.1023.

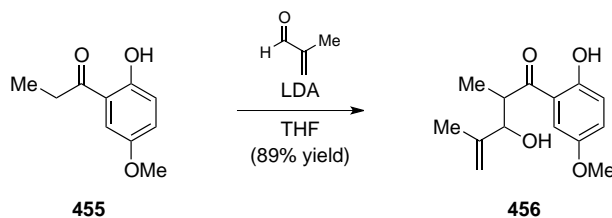
### Preparation of ester **453**



Anhydride **452** (0.519 g, 2.22 mmol), *p*-methoxyphenol (0.25 g, 2.01 mmol),  $\text{Et}_3\text{N}$  (0.31 mL, 2.22 mmol), and  $\text{CH}_2\text{Cl}_2$  (20 mL) were combined and heated to 45 °C. After stirring for 15 h the reaction was cooled to room temperature and sat. aq.  $\text{NH}_4\text{Cl}$  (20 mL) was added and extracted with  $\text{CH}_2\text{Cl}_2$  (3  $\times$  15 mL). The combined organics were washed with 1 N NaOH (30 mL) and brine (30 mL), dried over  $\text{MgSO}_4$ , filtered and concentrated *in vacuo*. The crude material was purified by flash chromatography (2% $\rightarrow$ 10% EtOAc/hexanes) to give ester **453** (0.292 g, 63% yield).

$^1\text{H-NMR}$  (400 MHz;  $\text{CDCl}_3$ ):  $\delta$  7.31 (s, 1H), 7.02 (dd,  $J = 9.7, 3.0$  Hz, 2H), 6.91-6.87 (m, 2H), 5.28 (s, 1H), 5.15 (s, 1H), 3.78 (s, 3H), 2.12 (d,  $J = 1.2$  Hz, 3H), 1.98 (s, 3H);  $^{13}\text{C-NMR}$  (101 MHz,  $\text{CDCl}_3$ ):  $\delta$  167.67, 157.08, 144.59, 142.12, 140.68, 126.92, 122.37, 120.56, 114.39, 114.37, 55.54, 22.76, 14.01; FTIR (thin film): 2958, 2934, 2836, 1721, 1633, 1610, 1596, 1504, 1455, 1442, 1229, 1090, 1031  $\text{cm}^{-1}$ ; HRMS (ESI-APCI)  $m/z$  calc'd for  $\text{C}_{14}\text{H}_{17}\text{O}_3$  (M+H) $^+$ : 233.1178, found: 233.1176.

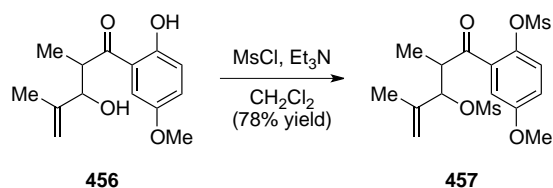
## Preparation of Aldol product 456



LDA was prepared by adding *n*-BuLi (1.67 M in hexanes, 2.19 mL, 3.65 mmol) to *i*-Pr<sub>2</sub>NH (0.58 mL, 4.2 mmol) in THF (16 mL) at  $-78$  °C. After stirring for 30 min ketone **455**<sup>14</sup> (0.300 g, 1.66 mmol) in THF (5 mL) was added. After 25 min methacrolein (80%, 0.21 mL, 2.49 mmol) was added. After 40 min the reaction was quenched with AcOH (2 mL) and allowed to warm to room temperature. Sat. aq. NaHCO<sub>3</sub> (40 mL) was added and the solution was extracted with EtOAc (3 × 20 mL). The combined organics were washed with brine (50 mL), dried over MgSO<sub>4</sub>, filtered and concentrated *in vacuo*. The crude material was purified by flash chromatography (10%→30% EtOAc/hexanes) to give aldol product **456** (0.371 g, 89% yield).

<sup>1</sup>H-NMR (400 MHz; CDCl<sub>3</sub>):  $\delta$  11.82 (s, 1H), 7.14 (d, *J* = 2.9 Hz, 1H), 7.08-7.05 (m, 1H), 6.87 (d, *J* = 9.0 Hz, 1H), 5.04 (s, 1H), 4.89 (s, 1H), 4.42 (s, 1H), 3.74 (s, 3H), 3.62-3.57 (m, 1H), 1.71 (s, 3H), 1.21 (d, *J* = 7.1 Hz, 3H); <sup>13</sup>C-NMR (101 MHz, CDCl<sub>3</sub>):  $\delta$  209.78, 157.49, 157.19, 151.71, 144.51, 143.81, 124.35, 124.02, 119.66, 119.29, 119.02, 117.71, 114.37, 113.46, 112.69, 112.59, 78.25, 74.72, 55.87, 42.96, 42.76, 19.26, 16.87, 15.49, 11.71; FTIR (thin film): 3495, 2975, 2939, 2836, 1639, 1611, 1590, 1484, 1373, 1269, 1245, 1173, 1038 cm<sup>-1</sup>; HRMS (ESI-APCI) *m/z* calc'd for C<sub>14</sub>H<sub>17</sub>O<sub>4</sub> (M-H)<sup>-</sup>: 249.1127, found: 249.1129.

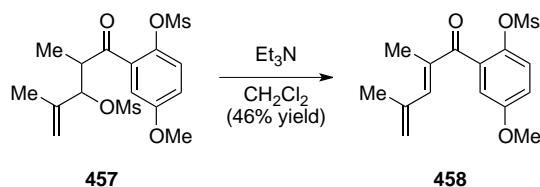
### Preparation of bismesylate **457**



MsCl (0.14 mL, 1.83 mmol) was added to alcohol **456** (0.207 g, 0.83 mmol) and Et<sub>3</sub>N (0.46 mL, 3.32 mmol) in CH<sub>2</sub>Cl<sub>2</sub> (8.3 mL). The reaction was stirred for 16 h then sat. aq. NH<sub>4</sub>Cl (10 mL) was added and extracted with CH<sub>2</sub>Cl<sub>2</sub> (3 × 10 mL). The combined organics were washed with brine (20 mL), dried over MgSO<sub>4</sub>, filtered and concentrate *in vacuo*. The crude material was purified by flash chromatography (40% EtOAc/hexanes) to give bismesylate **457** (0.262 g, 78% yield) as a mixture of diastereomers.

<sup>1</sup>H-NMR (400 MHz; CDCl<sub>3</sub>): δ 7.32-7.30 (m, 1H), 7.02 (d, *J* = 1.9 Hz, 1H), 7.01 (d, *J* = 2.5 Hz, 1H), 5.27 (t, *J* = 5.1 Hz, 1H), 5.16-5.15 (m, 1H), 5.04 (t, *J* = 1.3 Hz, 1H), 3.79 (t, *J* = 4.1 Hz, 3H), 3.66 (t, *J* = 6.8 Hz, 1H), 3.11 (s, 3H), 2.97 (s, 3H), 1.70 (s, 3H), 1.27 (d, *J* = 7.0 Hz, 3H); <sup>13</sup>C-NMR (101 MHz, CDCl<sub>3</sub>): δ 200.71, 158.18, 140.18, 139.43, 133.23, 124.43, 118.19, 116.93, 114.91, 85.12, 55.87, 47.11, 38.98, 37.63, 18.11, 12.60; FTIR (thin film): 3389, 3022, 2979, 2941, 1697, 1582, 1486, 1459, 1415, 1351, 1331, 1274, 1197, 1032 cm<sup>-1</sup>; HRMS (ESI-APCI) *m/z* calc'd for (M+H)<sup>+</sup>: 429.0654, found: 429.0653.

### Preparation of enone **458**



To a solution of bismesylate **457** (0.984 g, 2.42 mmol) in CH<sub>2</sub>Cl<sub>2</sub> (24 mL) was added Et<sub>3</sub>N (1.35 mL, 9.68 mmol). The reaction was allowed to stir at room temperature for 3 d the saturated aqueous ammonium chloride (30 mL) was added. The aqueous layer was extracted

with CH<sub>2</sub>Cl<sub>2</sub> (3 × 25 mL) and the combined organics were washed with brine (50 mL), dried over MgSO<sub>4</sub>, filtered and concentrated *in vacuo*. The crude material was purified by column chromatography (30% EtOAc/hexanes) to provide enone **458** (0.349 g, 46% yield).

<sup>1</sup>H-NMR (400 MHz; CDCl<sub>3</sub>): δ 7.32-7.29 (m, 1H), 6.93 (dt, *J* = 9.0, 2.8 Hz, 1H), 6.80 (dd, *J* = 3.0, 1.6 Hz, 1H), 6.57 (d, *J* = 1.0 Hz, 1H), 5.23 (d, *J* = 1.5 Hz, 1H), 5.06 (s, 1H), 3.76-3.75 (m, 3H), 3.01-3.01 (m, 3H), 2.05 (s, 3H), 1.89 (s, 3H); <sup>13</sup>C-NMR (101 MHz, CDCl<sub>3</sub>): δ 196.55, 157.67, 147.26, 147.21, 140.69, 139.31, 136.17, 134.22, 124.08, 121.90, 116.31, 114.38, 55.74, 37.56, 22.56, 12.78; FTIR (thin film): 3058, 2966, 2940, 2840, 1652, 1611, 1583, 1485, 1464, 1445, 1414, 1367, 1331, 1266, 1198, 1161, 1031 cm<sup>-1</sup>; HRMS (ESI-APCI) *m/z* calc'd for (M+H)<sup>+</sup>: 311.0953, found: 311.0947.

## References for Appendix One

1. López-Cobeñas, A.; Cledera, P.; Sánchez, J. D.; López-Alvarado, P.; Ramos, M. T.; Avendaño, C.; Menéndez, J. C. *Synthesis* **2005**, *2005*, 3412-3422.
2. Levene, P. A.; Bass, L. W.; Steiger, R. E. *J. Biol. Chem.* **1929**, *81*, 697-702.
3. Williams, R. M.; Armstrong, R. W.; Maruyama, L. K.; Dung, J. S.; Anderson, O. P. *J. Am. Chem. Soc.* **1985**, *107*, 3246-3253.
4. Piers, E.; Harrison, C. L.; Zetina-Rocha, C. *Org. Lett.* **2001**, *3*, 3245-3247.
5. (a) Danner, P.; Bauer, M.; Phukan, P.; Maier, Martin E. *Eur. J. Org. Chem.* **2005**, *2005*, 317-325; (b) O'Donnell, M. J.; Boniece, J. M.; Earp, S. E. *Tetrahedron Lett.* **1978**, *19*, 2641-2644.
6. (a) Fukuyama, T.; Nakatsuka, S.-I.; Kishi, Y. *Tetrahedron* **1981**, *37*, 2045-2078; (b) Kishi, Y.; Fukuyama, T.; Nakatsuka, S. *J. Am. Chem. Soc.* **1973**, *95*, 6492-6493.
7. Ishihara, H.; Hirabayashi, Y. *Chem. Lett.* **1976**, *5*, 203-204.
8. Bélanger, G.; April, M.; Dauphin, É.; Roy, S. *J. Org. Chem.* **2007**, *72*, 1104-1111.
9. von Delius, M.; Geertsema, E. M.; Leigh, D. A. *Nat. Chem.* **2010**, *2*, 96-101.
10. Narjes, F.; Schaumann, E. *Liebigs Ann. Chem.* **1993**, *1993*, 841-846.
11. Fráter, G.; Müller, U.; Günther, W. *Tetrahedron* **1984**, *40*, 1269-1277.
12. Shetty, R. S.; Lee, Y.; Liu, B.; Husain, A.; Joseph, R. W.; Lu, Y.; Nelson, D.; Mihelcic, J.; Chao, W.; Moffett, K. K.; Schumacher, A.; Flubacher, D.; Stojanovic, A.; Bukhtiyarova, M.; Williams, K.; Lee, K.-J.; Ochman, A. R.; Saporito, M. S.; Moore, W. R.; Flynn, G. A.; Dorsey, B. D.; Springman, E. B.; Fujimoto, T.; Kelly, M. J. *J. Med. Chem.* **2010**, *54*, 179-200.
13. Marcus, A. P.; Lee, A. S.; Davis, R. L.; Tantillo, D. J.; Sarpong, R. *Angew. Chem. Int. Ed.* **2008**, *47*, 6379-6383.

14. Zhang, Y.; Lee, Y. S.; Rothman, R. B.; Dersch, C. M.; Deschamps, J. R.; Jacobson, A. E.; Rice, K. C. *J. Med. Chem.* **2009**, *52*, 7570-7579.

## **Appendix Two**

### Spectra

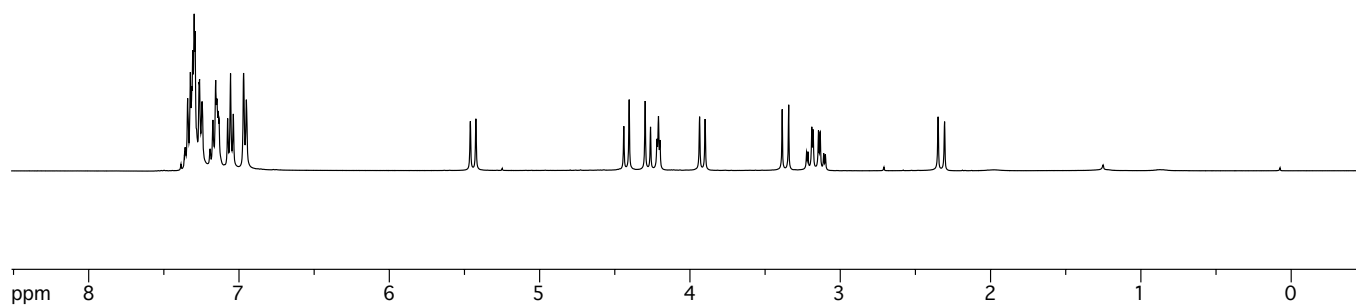
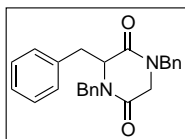


**Figure A2.1.** <sup>1</sup>H-NMR of DKP 72.

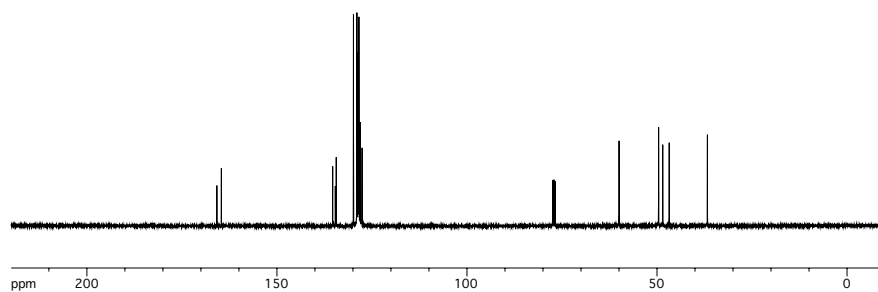


Figure A2.2.  $^{13}\text{C-NMR}$  of DKP 72.

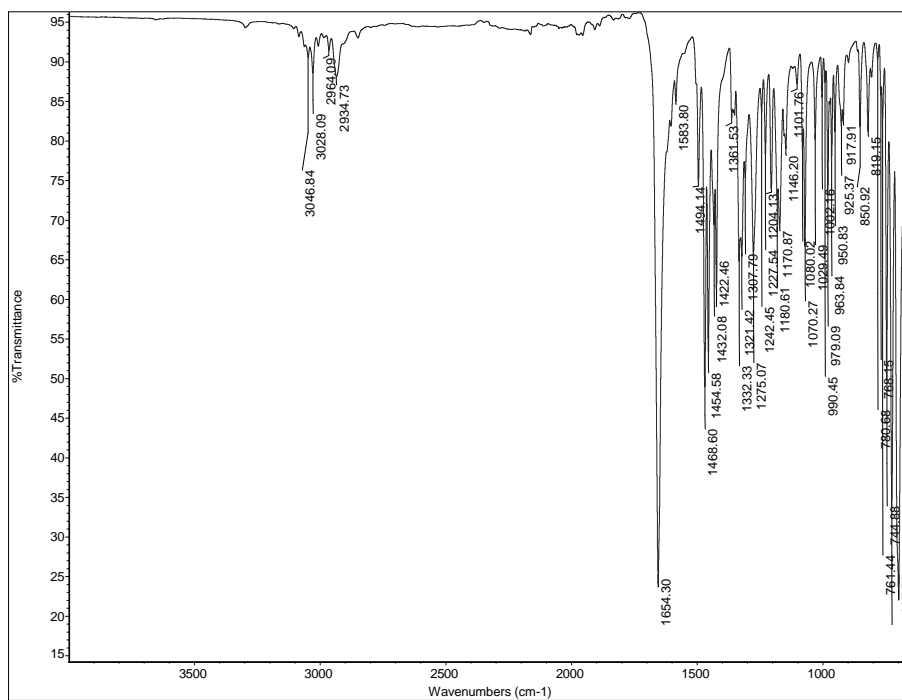
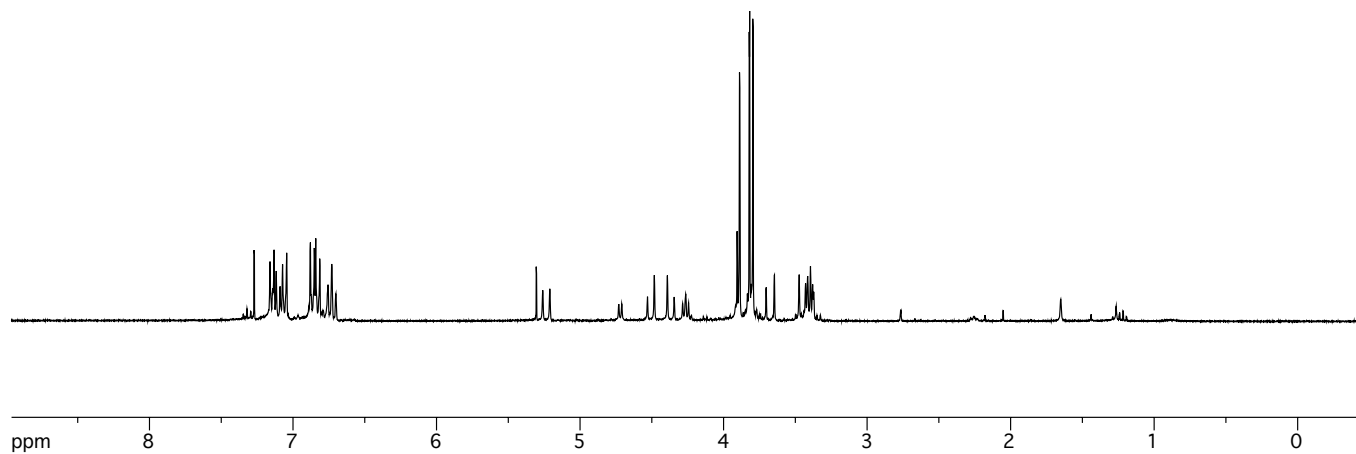
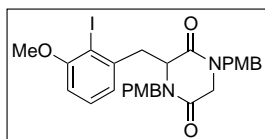


Figure A2.3. FTIR of DKP 72.



**Figure A2.4.** <sup>1</sup>H-NMR of DKP 76.

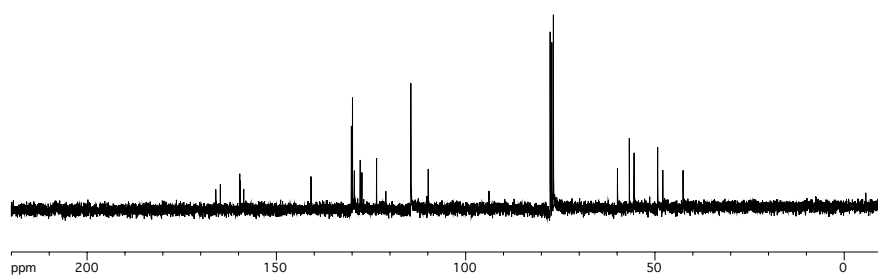


Figure A2.5. <sup>13</sup>C-NMR of DKP 76.

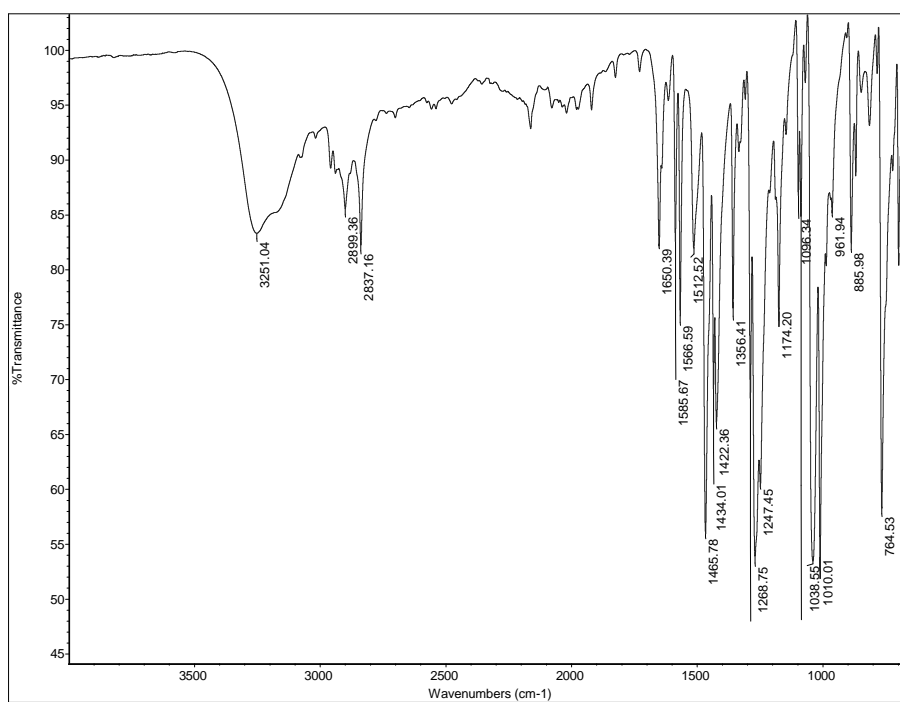
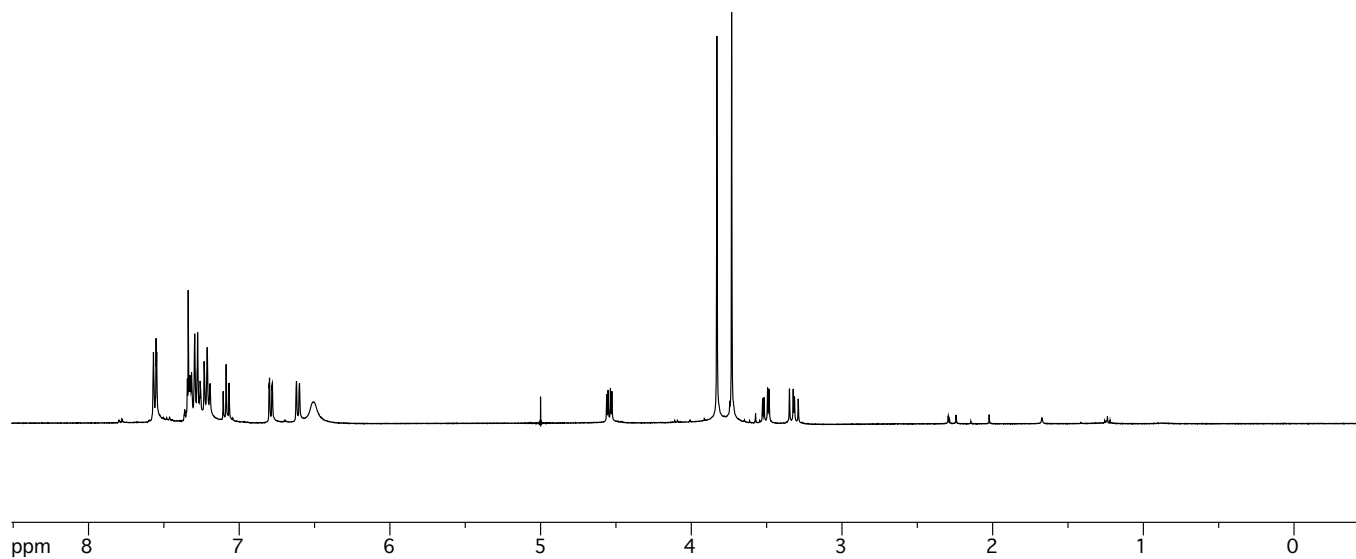
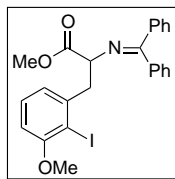
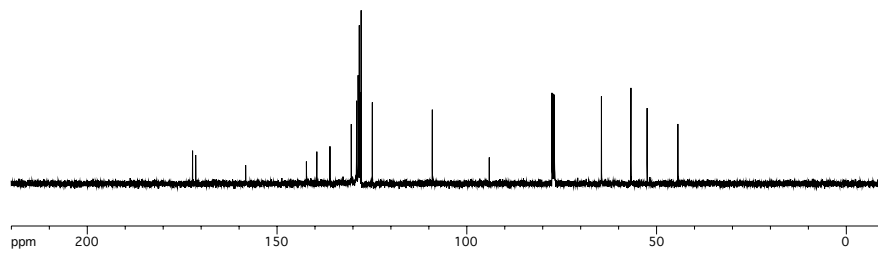


Figure A2.6. FTIR of DKP 76.



**Figure A2.7.** <sup>1</sup>H-NMR of protected amino acid **82**.



**Figure A2.8.**  $^{13}\text{C}$ -NMR of protected amino acid **82**.

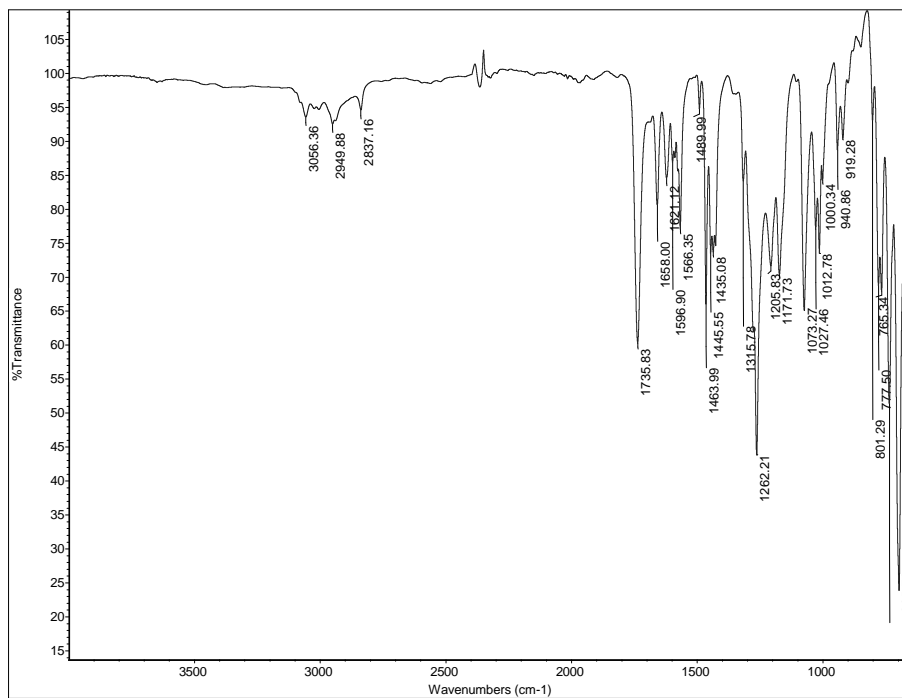


**Figure A2.9.** FTIR of protected amino acid **82**.

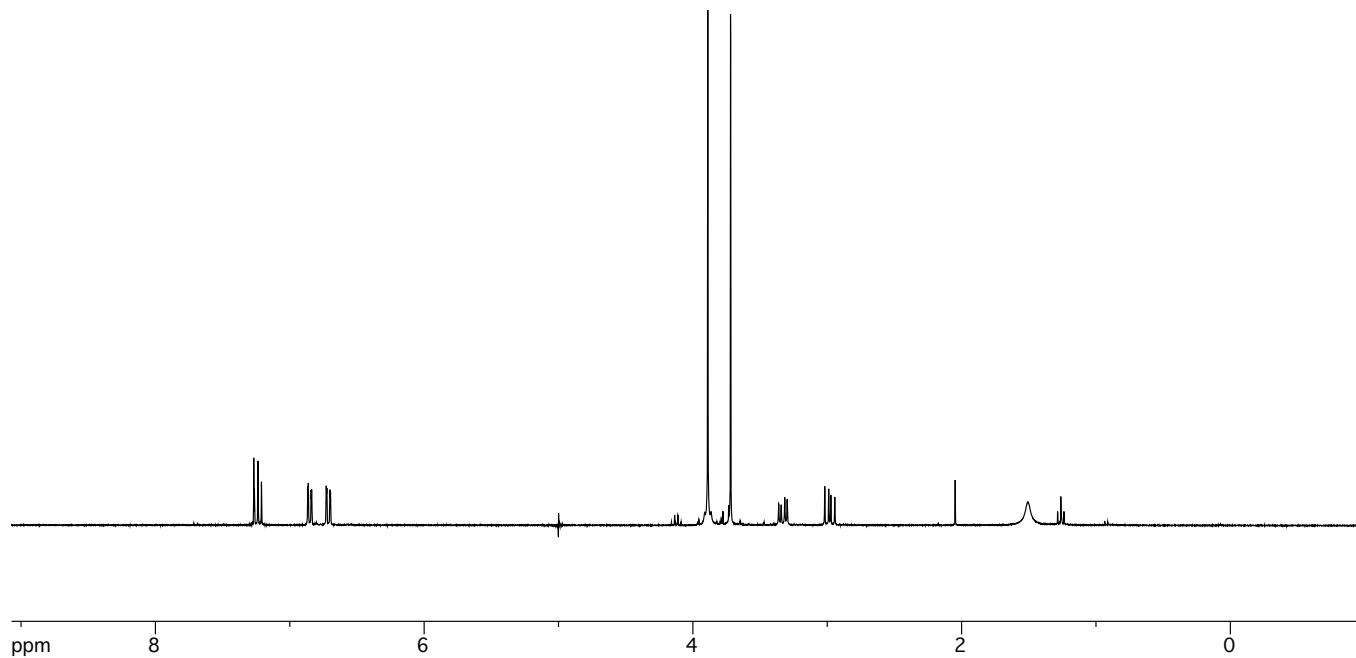
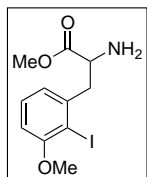


**Figure A2.10.** <sup>1</sup>H-NMR of amino ester **79**.

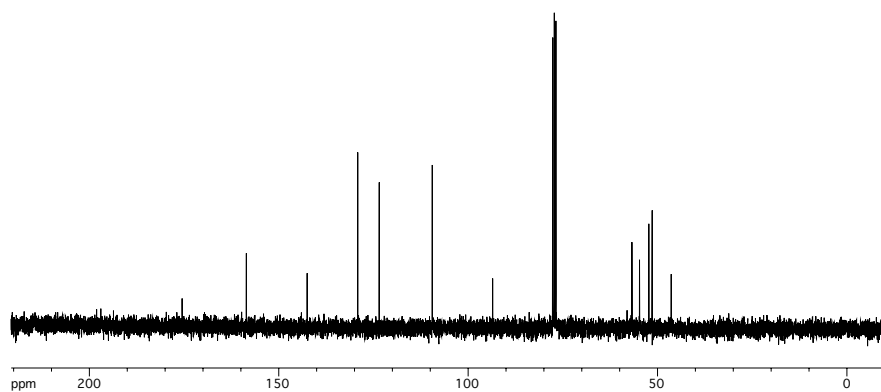


**Figure A2.11.**  $^{13}\text{C}$ -NMR of amino ester **79**.

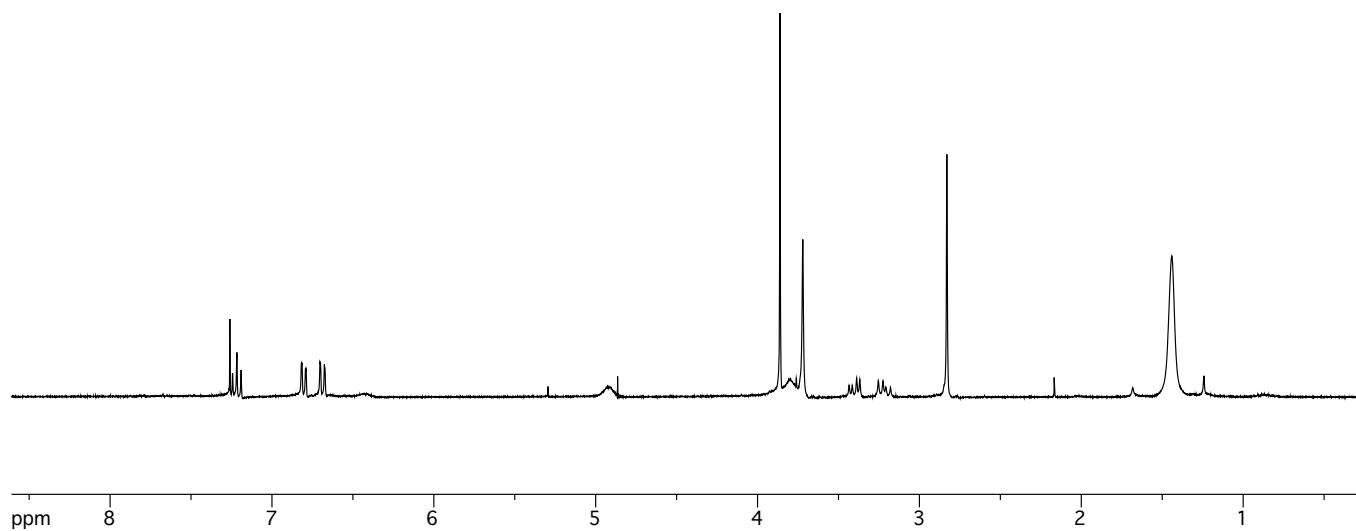
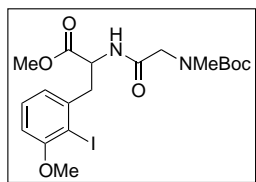


**Figure A2.12.** <sup>1</sup>H-NMR of dipeptide **83**.

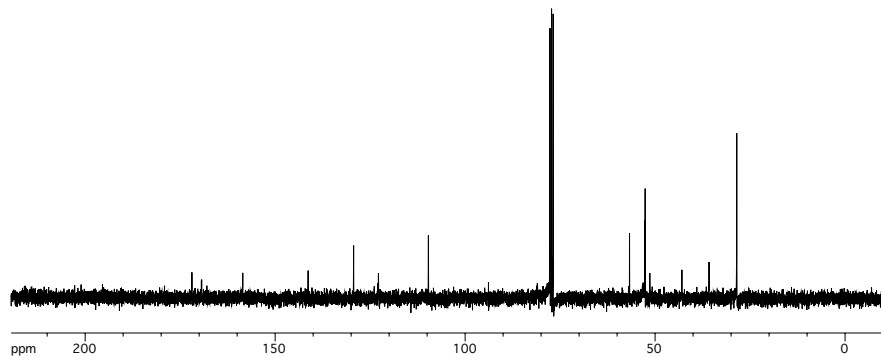


**Figure A2.13.**  $^{13}\text{C}$ -NMR of dipeptide **83**.

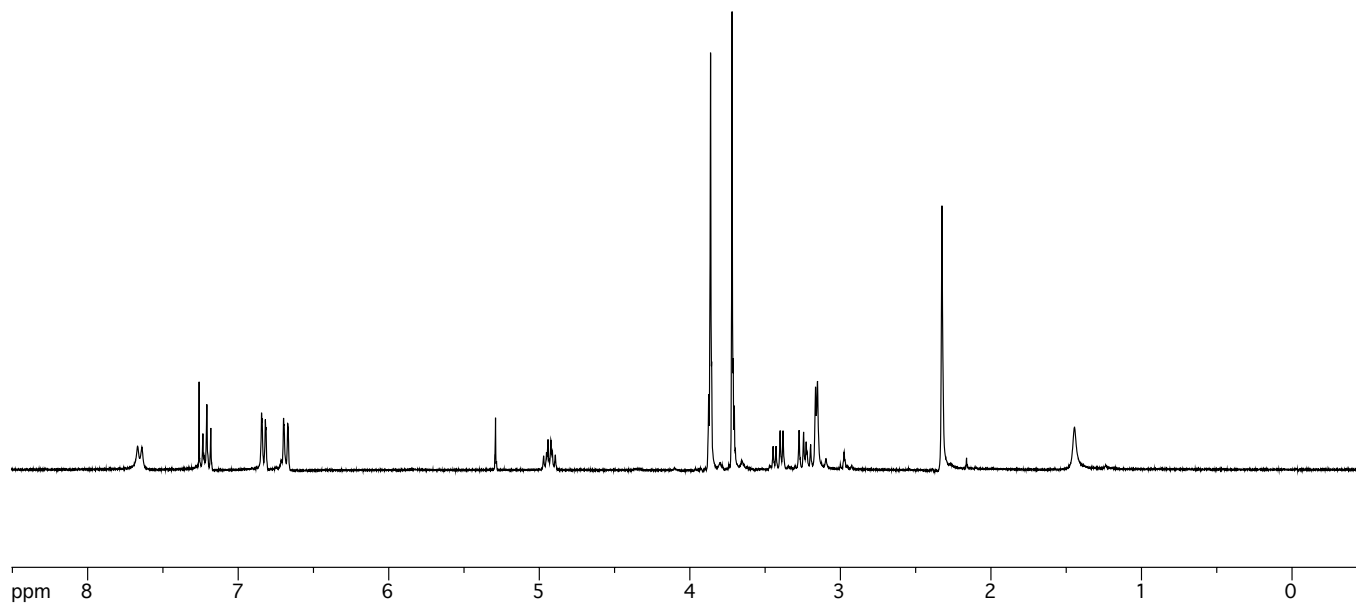
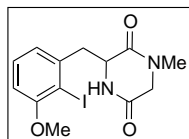
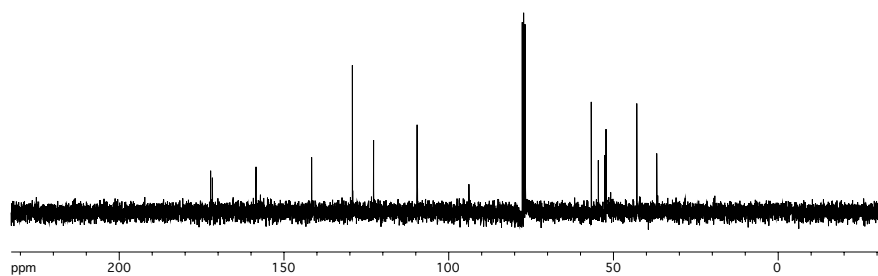
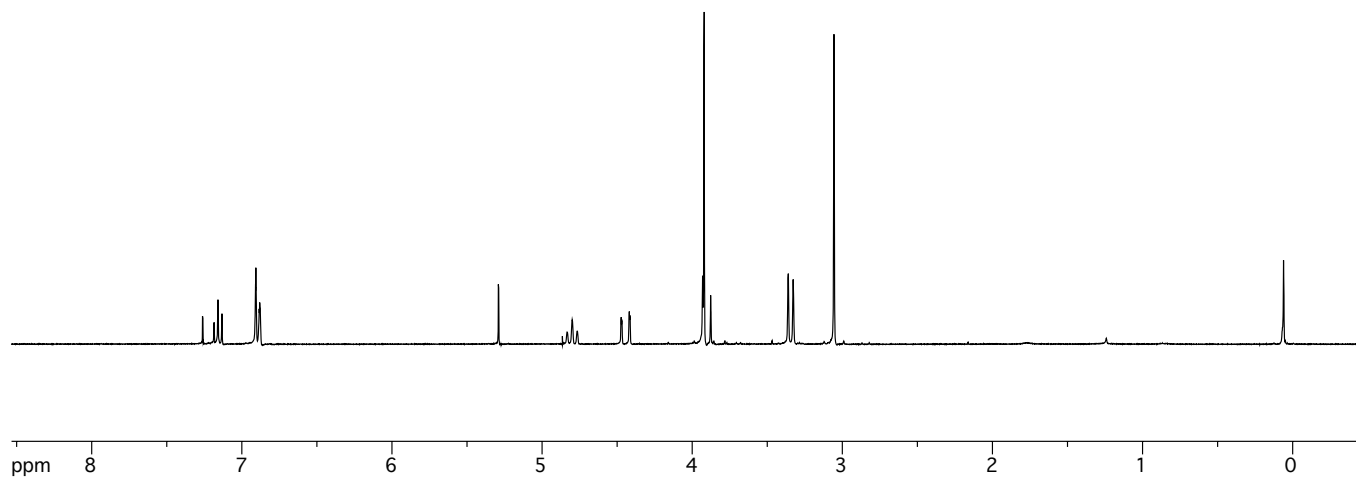
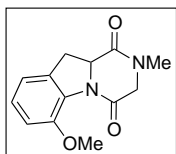


Figure A2.14. <sup>1</sup>H-NMR of DKP 70.



**Figure A2.15.**  $^{13}\text{C}$ -NMR of DKP 70.



**Figure A2.16.** <sup>1</sup>H-NMR of DKP 84.

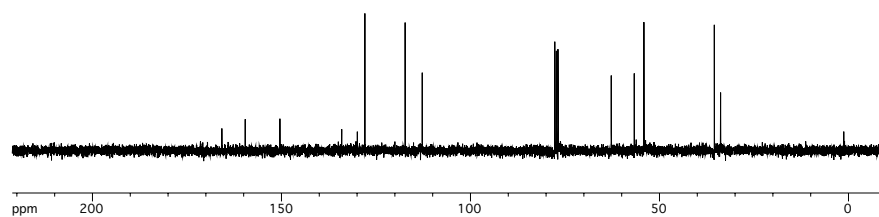


Figure A2.17. <sup>13</sup>C-NMR of DKP 84.

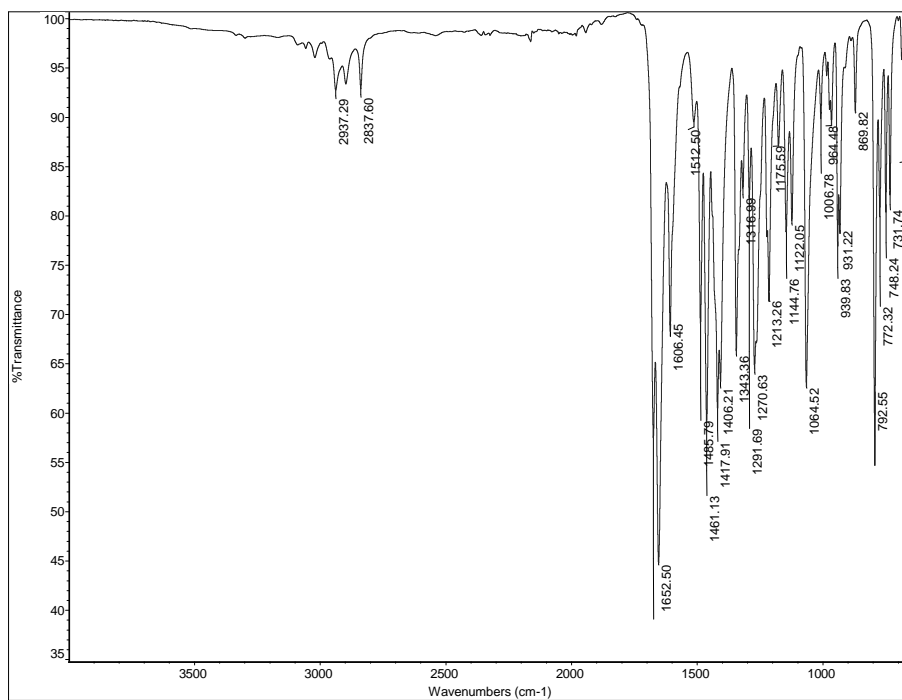


Figure A2.18. FTIR of DKP 84.

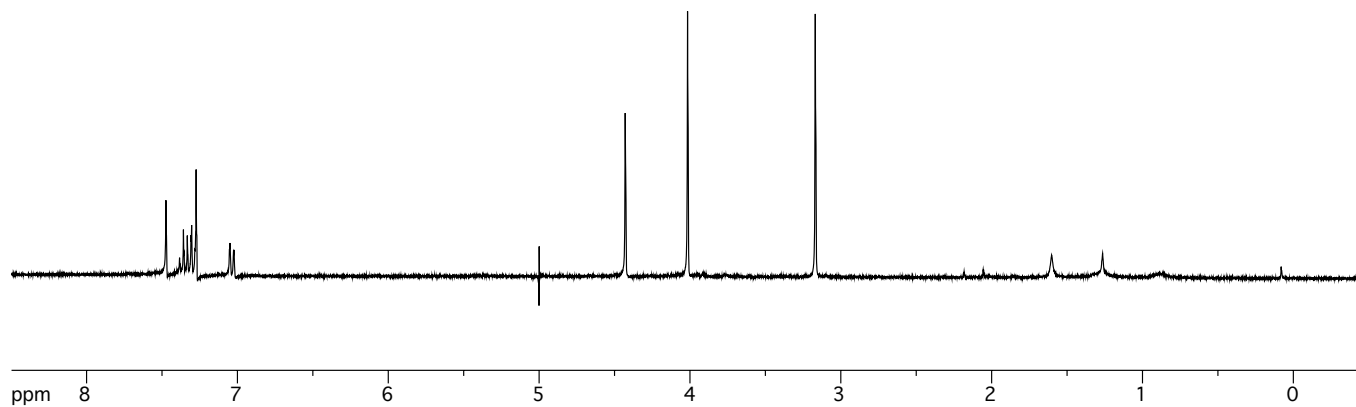
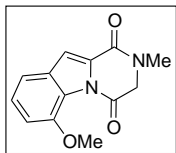


Figure A2.19. <sup>1</sup>H-NMR of indole 87.

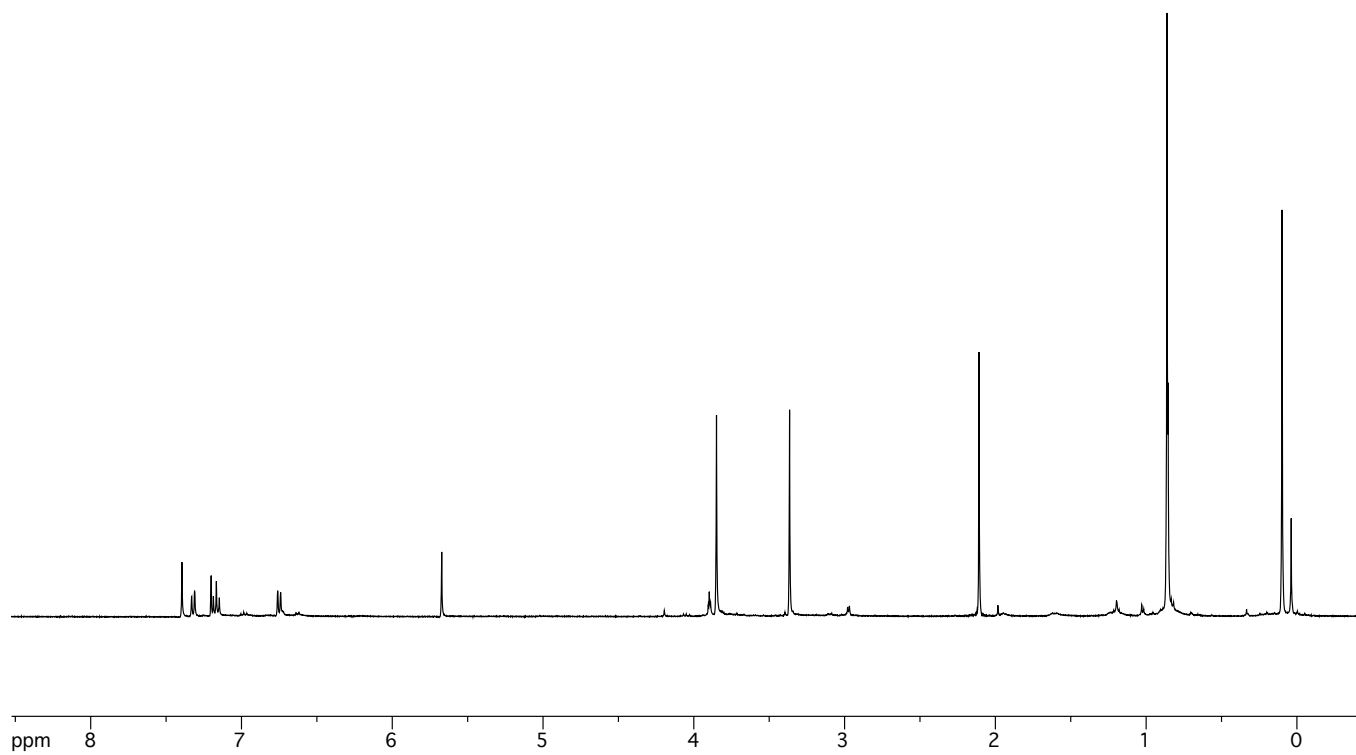
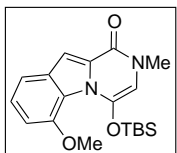


Figure A2.20. <sup>1</sup>H-NMR of indole **89**.

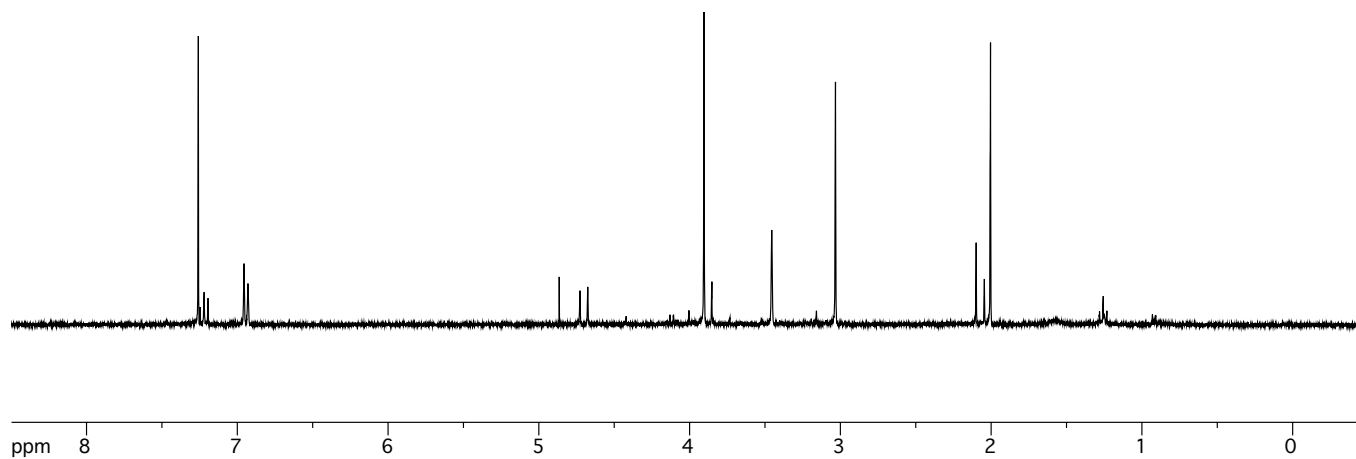
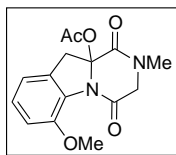
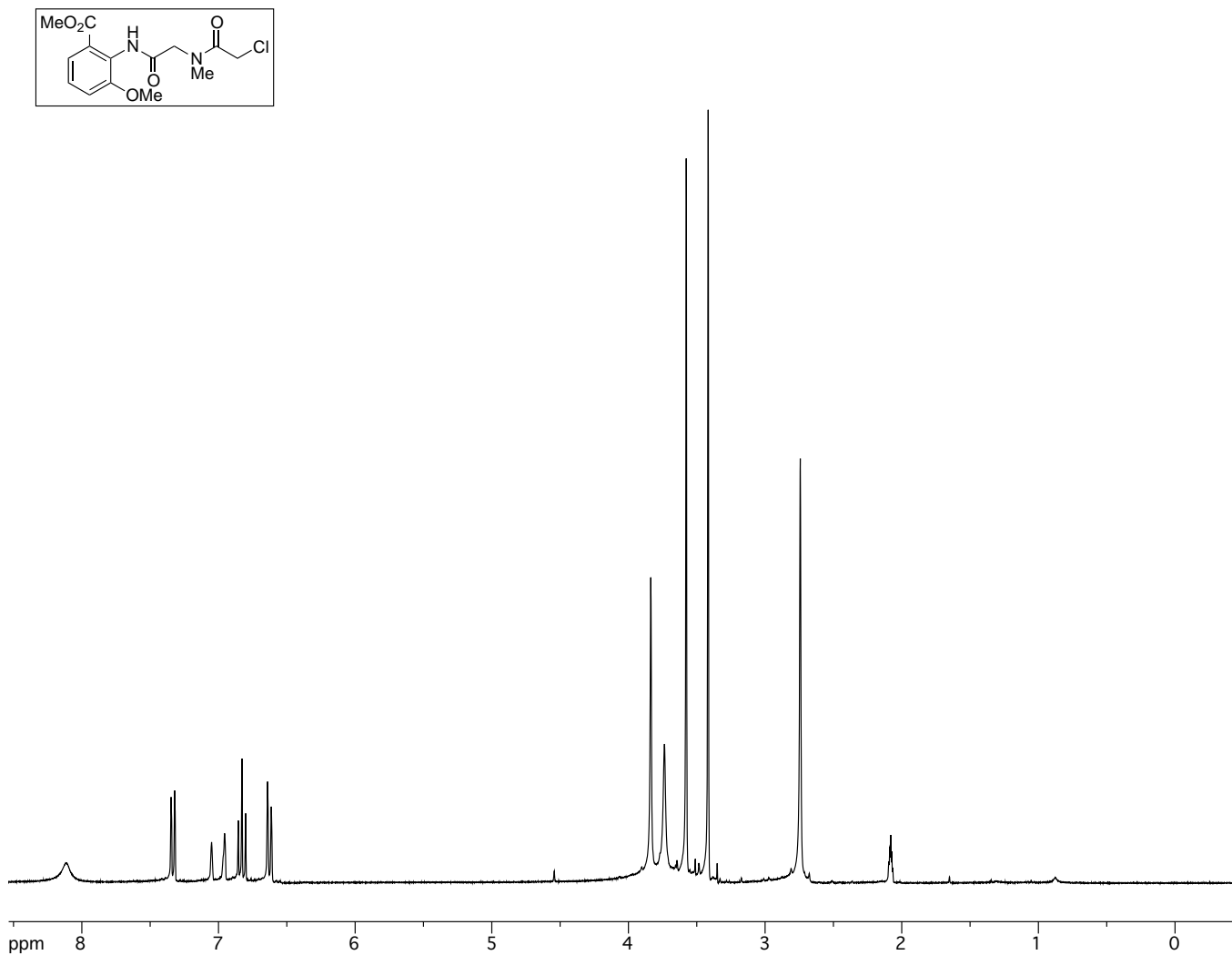


Figure A2.21. <sup>1</sup>H-NMR of DKP 90.



**Figure A2.22.** <sup>1</sup>H-NMR of amide **91**.

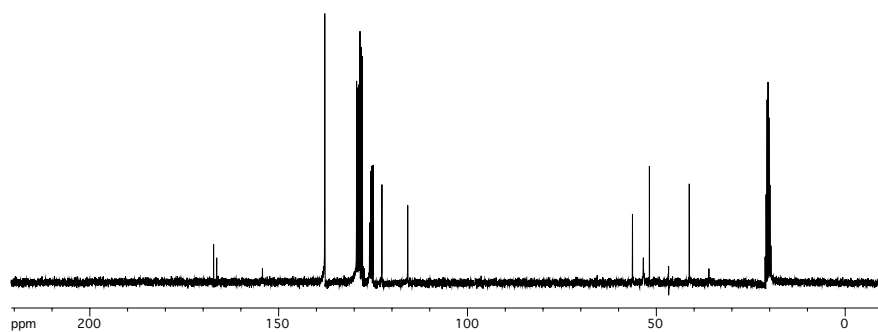


Figure A2.23.  $^{13}\text{C-NMR}$  of amide 91.

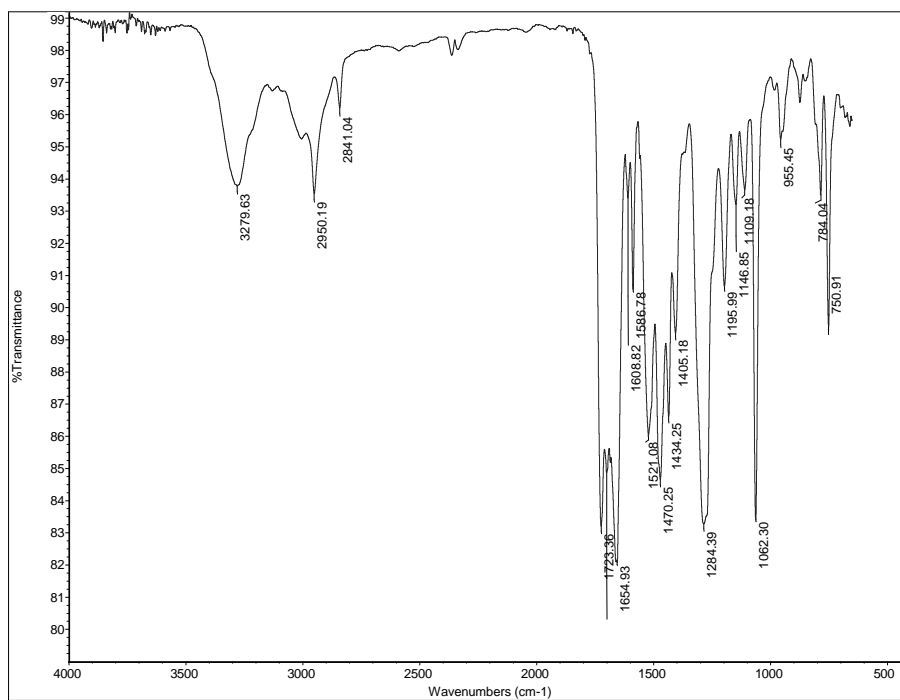
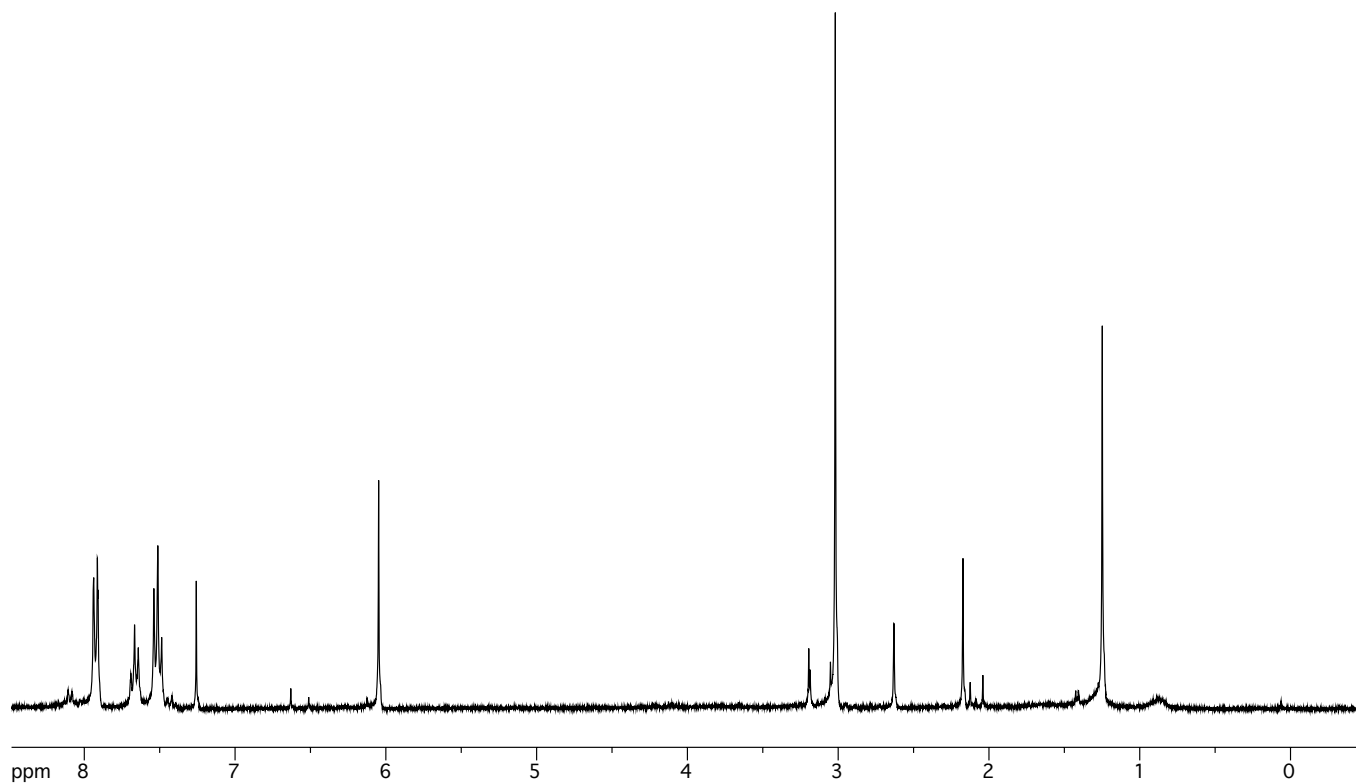
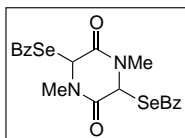
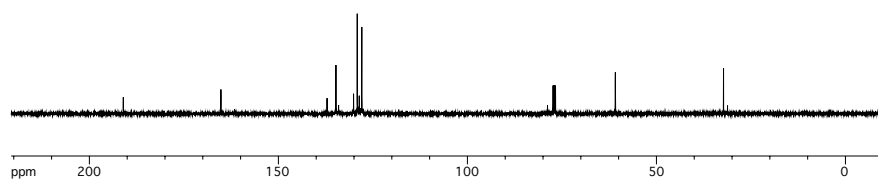


Figure A2.24. FTIR of amide 91.



**Figure A2.25.** <sup>1</sup>H-NMR of biselenobenzoate **103**.



**Figure A2.26.**  $^{13}\text{C-NMR}$  of bisselenbenzoate **103**.

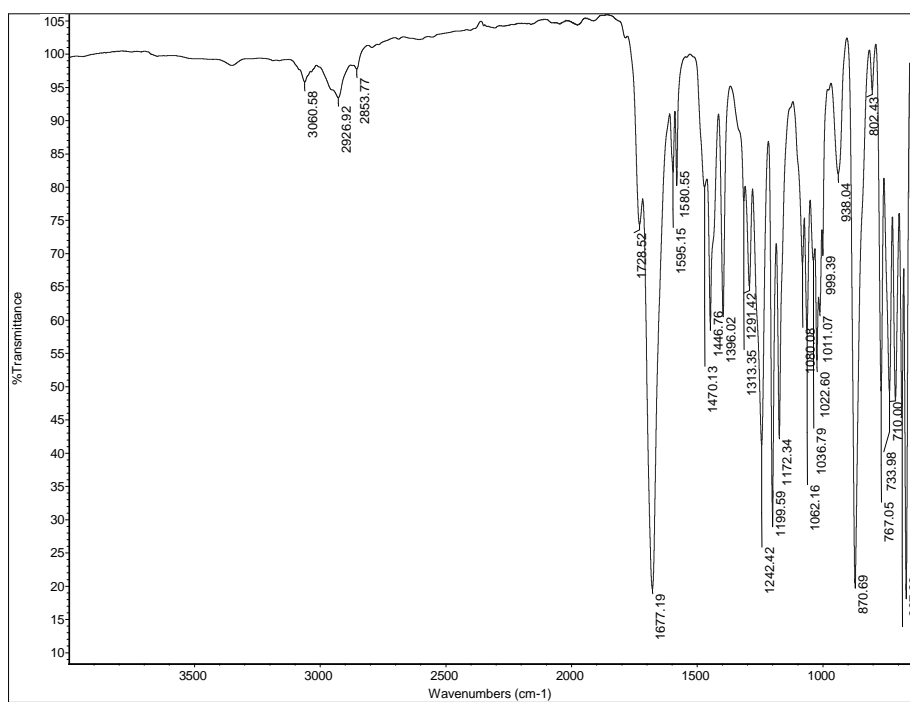


**Figure A2.27.** FTIR of bisselenbenzoate **103**.

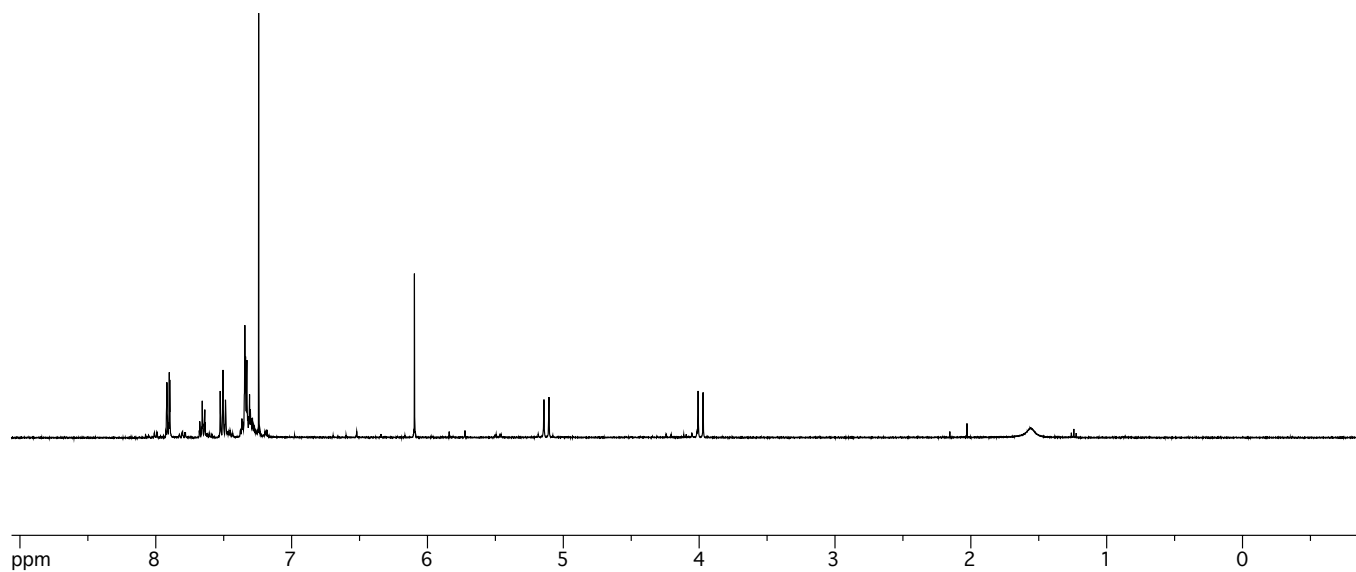
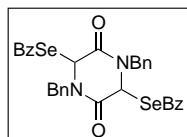


**Figure A2.28.** <sup>1</sup>H-NMR of biselenobenzoate **104**.

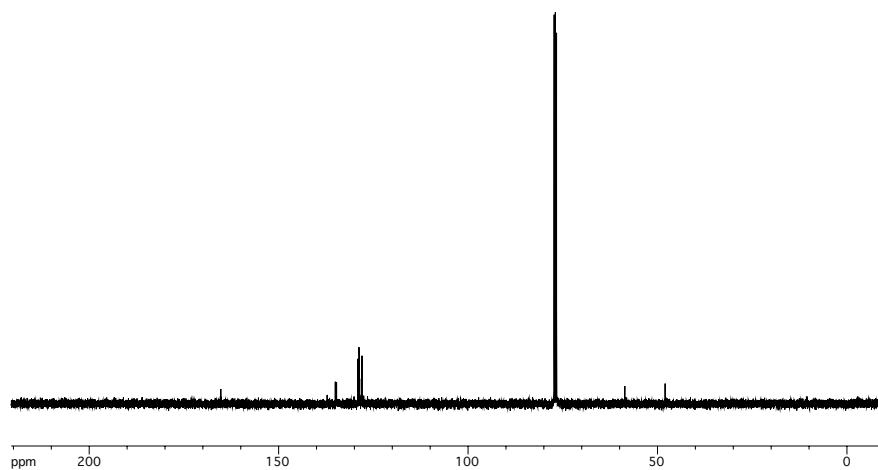


Figure A2.29.  $^{13}\text{C}$ -NMR of bisselenobenzoate **104**.

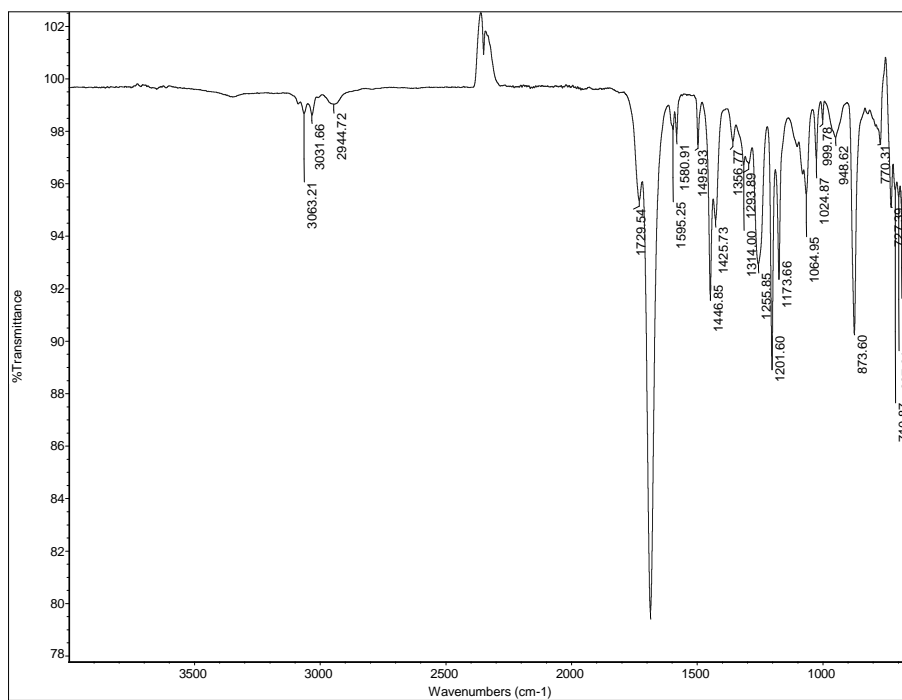
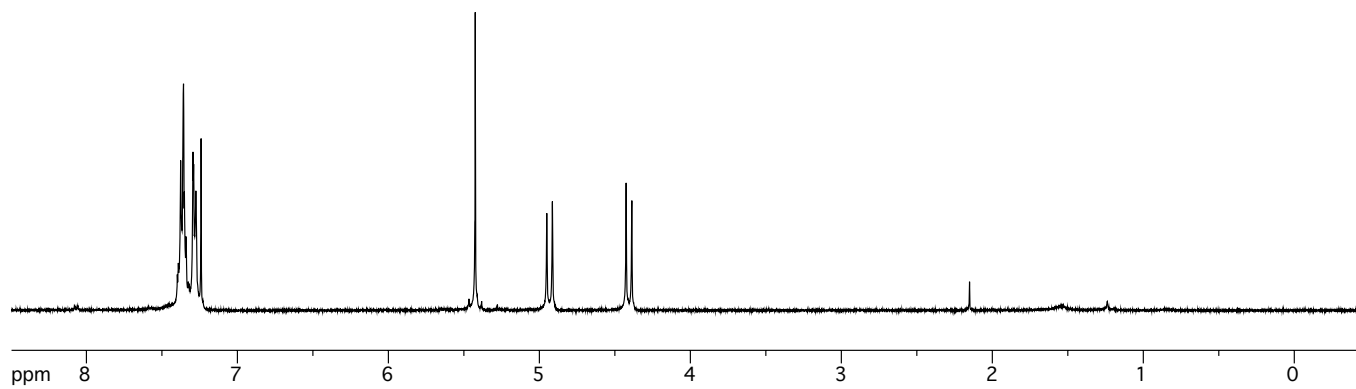
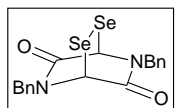
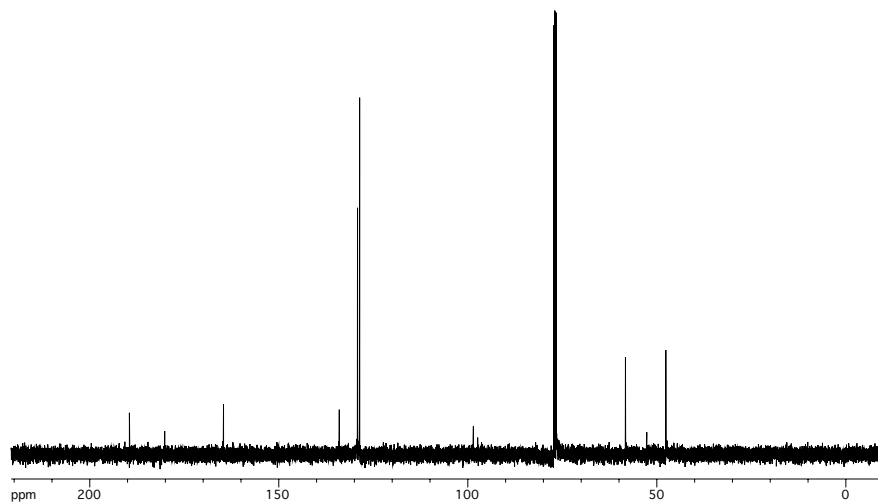


Figure A2.30. FTIR of bisselenobenzoate **104**.



**Figure A2.31.** <sup>1</sup>H-NMR of diselenide **106**.



**Figure A2.32.**  $^{13}\text{C}$ -NMR of diselenide **106**.

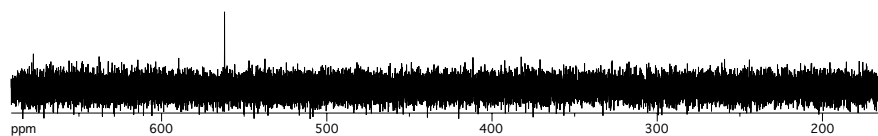
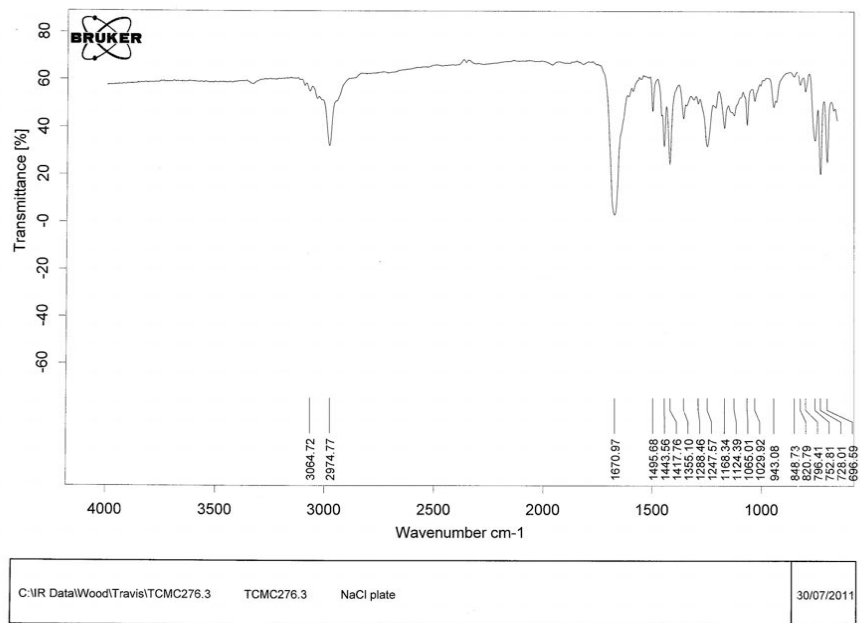


**Figure A2.33.**  $^{77}\text{Se}$ -NMR of diselenide **106**.



Page 1/1

Figure A2.34. FTIR of diselenide 106.

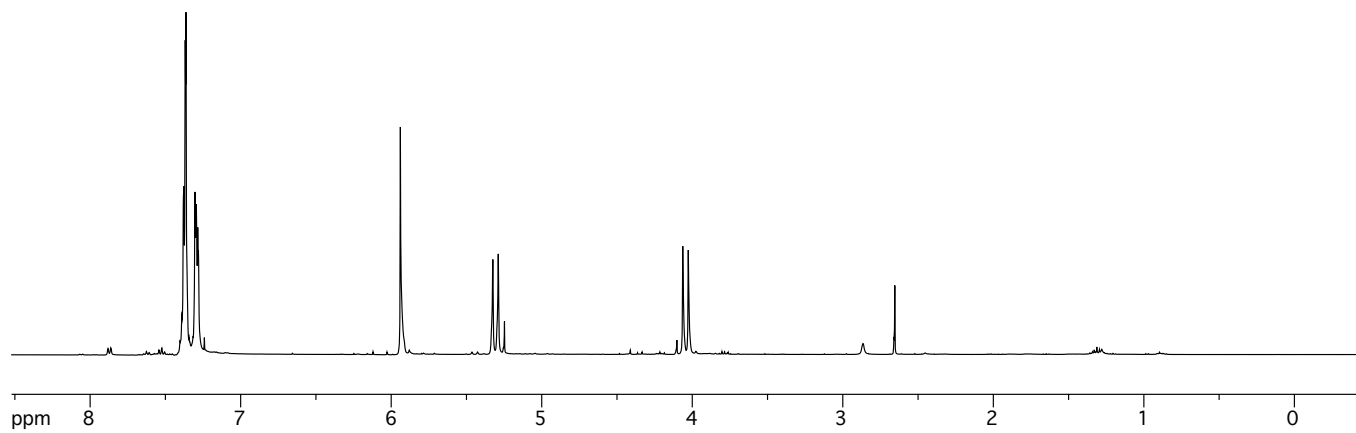
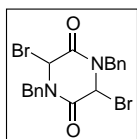


**Figure A2.35.** <sup>1</sup>H-NMR of dibromide **109**.

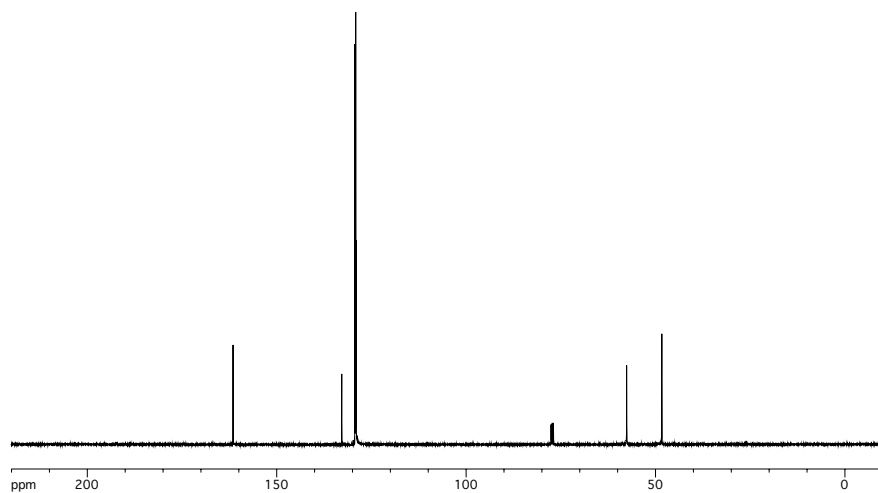


**Figure A2.36.**  $^{13}\text{C}$ -NMR of dibromide **109**.

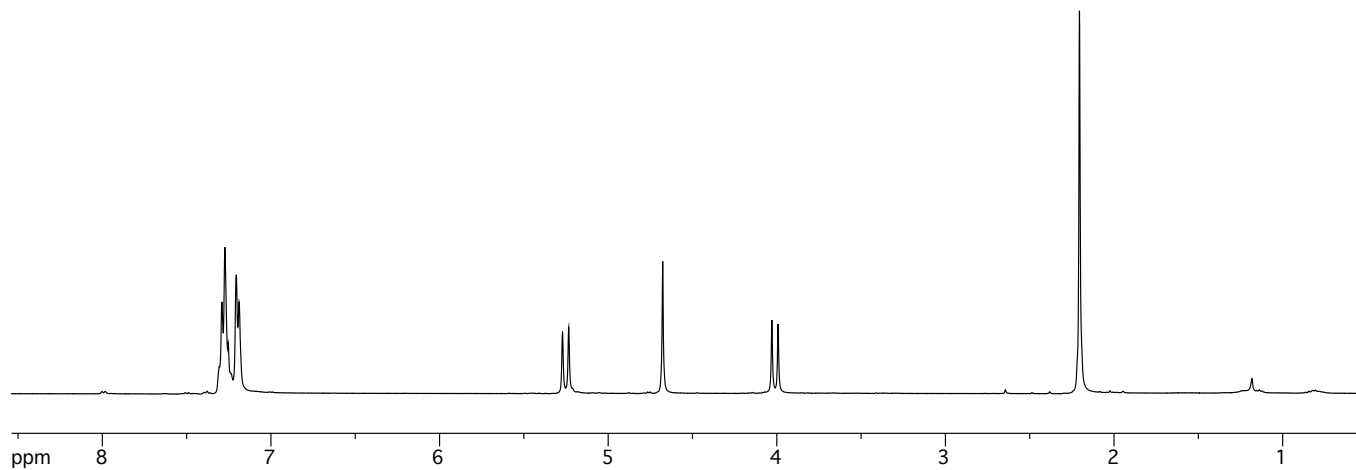
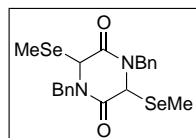


**Figure A2.37.** <sup>1</sup>H-NMR of bis-selenoether **120**.

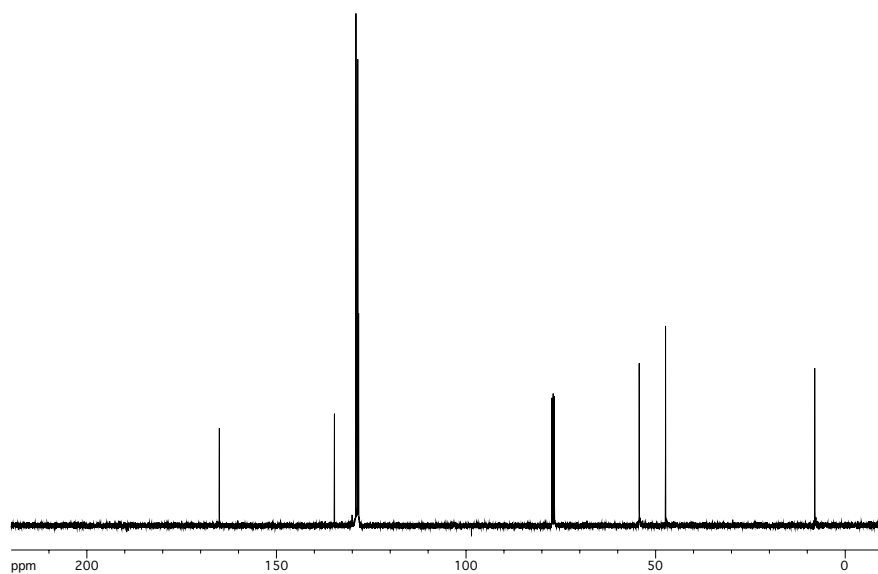


**Figure A2.38.**  $^{13}\text{C}$ -NMR of bisselenoether **120**.

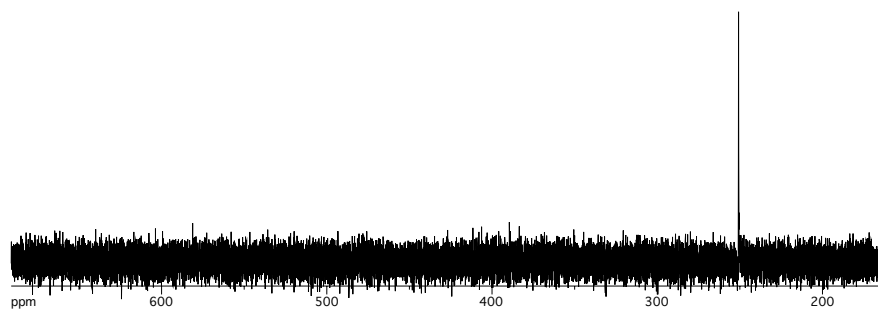


**Figure A2.39.**  $^{77}\text{Se}$ -NMR of bisselenoether **120**.

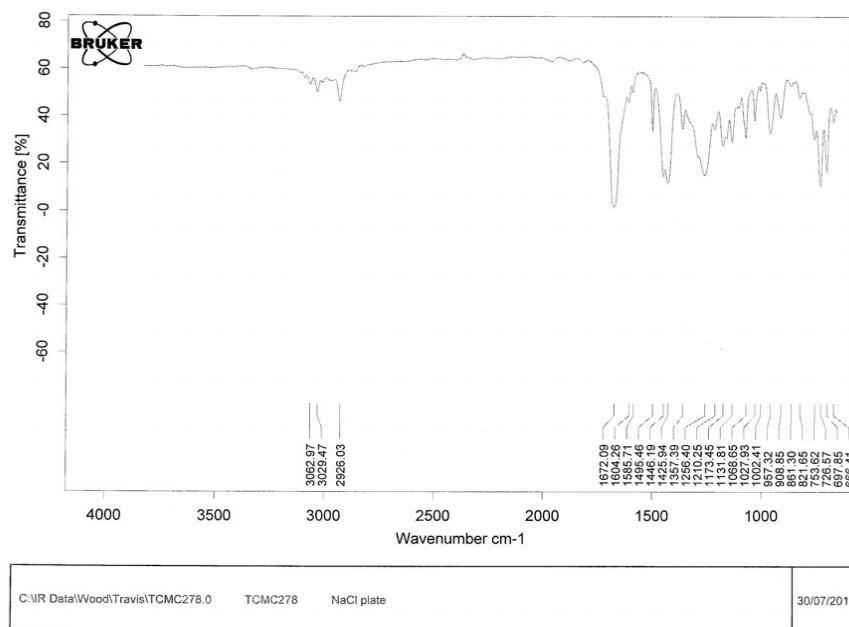
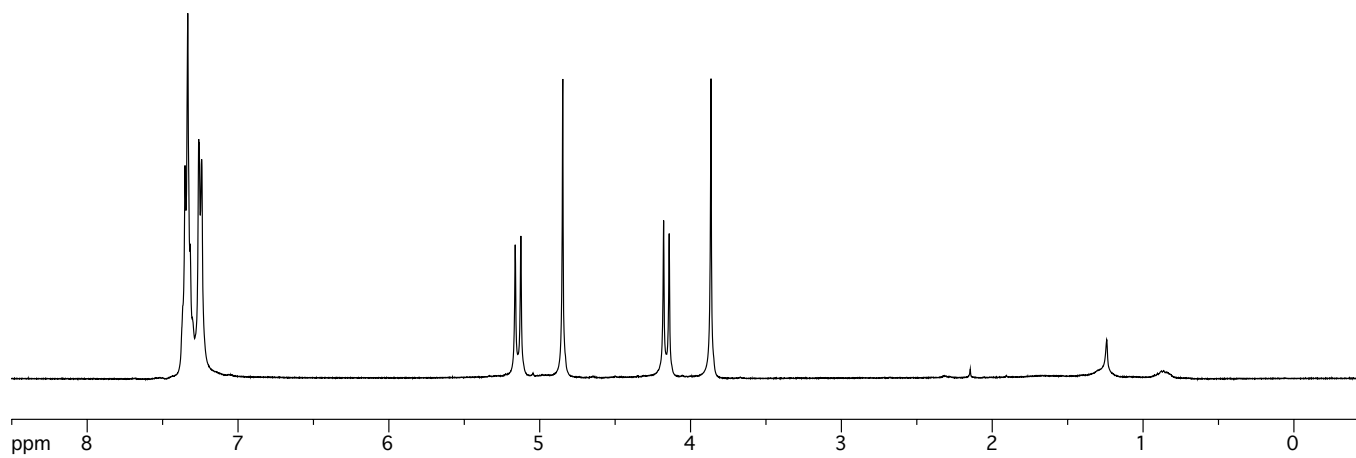
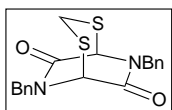


Figure A2.40. FTIR of biselenoether 120.



**Figure A2.41.** <sup>1</sup>H-NMR of dithioacetal **121**.

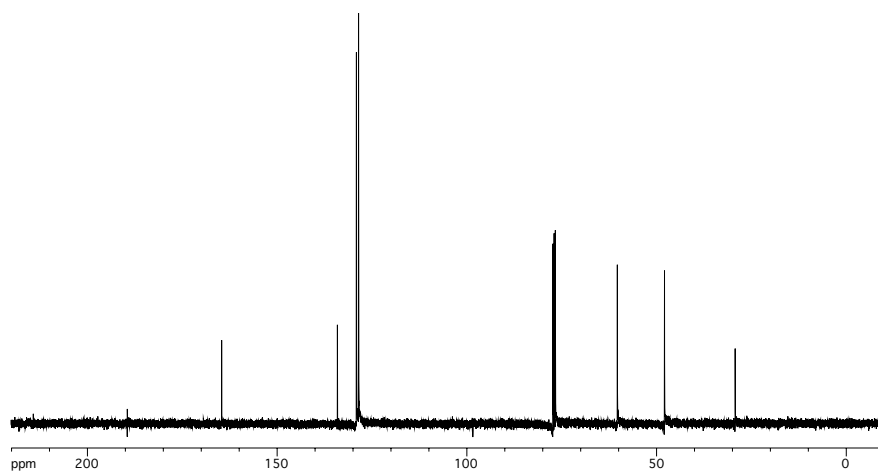
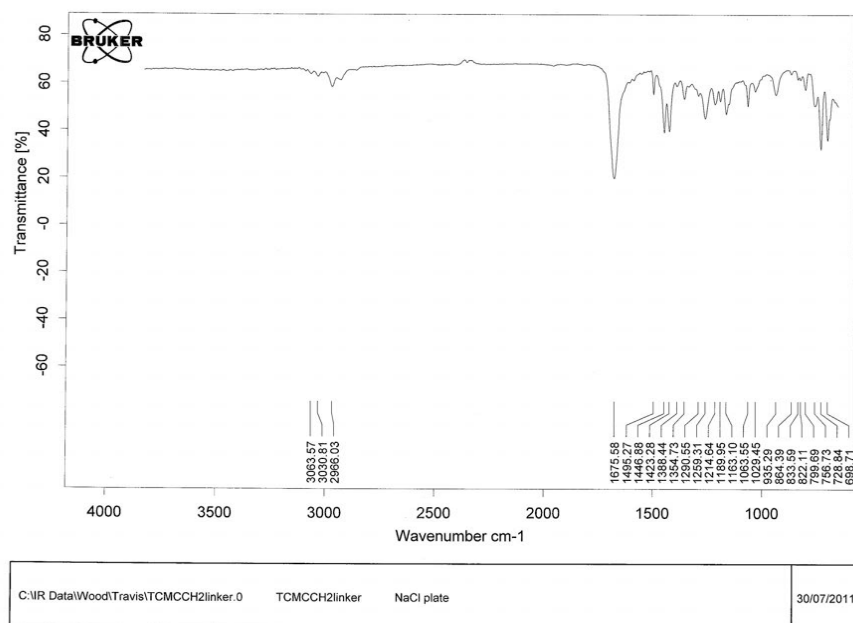
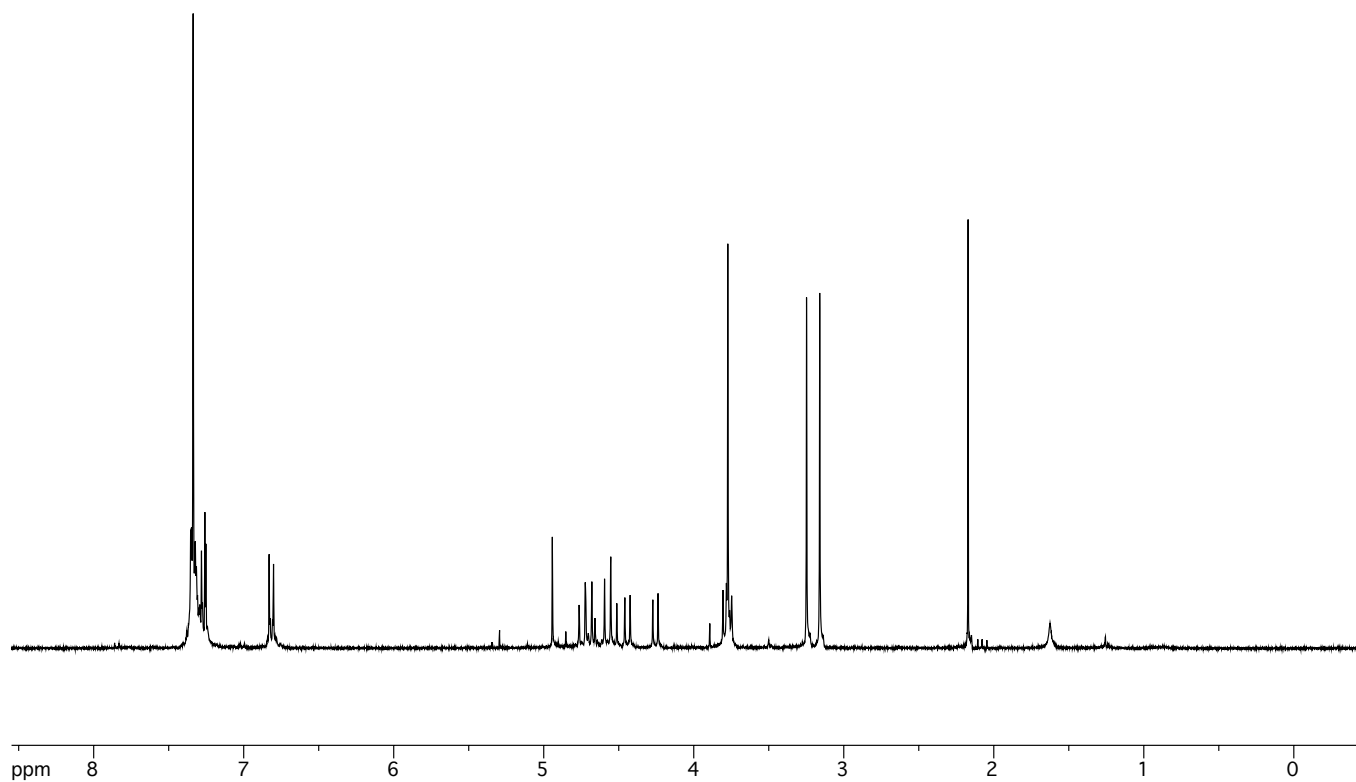
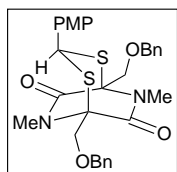


Figure A2.42.  $^{13}\text{C}$ -NMR of dithioacetal 121.



Page 1/1

Figure A2.43. FTIR of dithioacetal 121.



**Figure A2.44.**  $^1\text{H-NMR}$  of dithioacetal **125**.

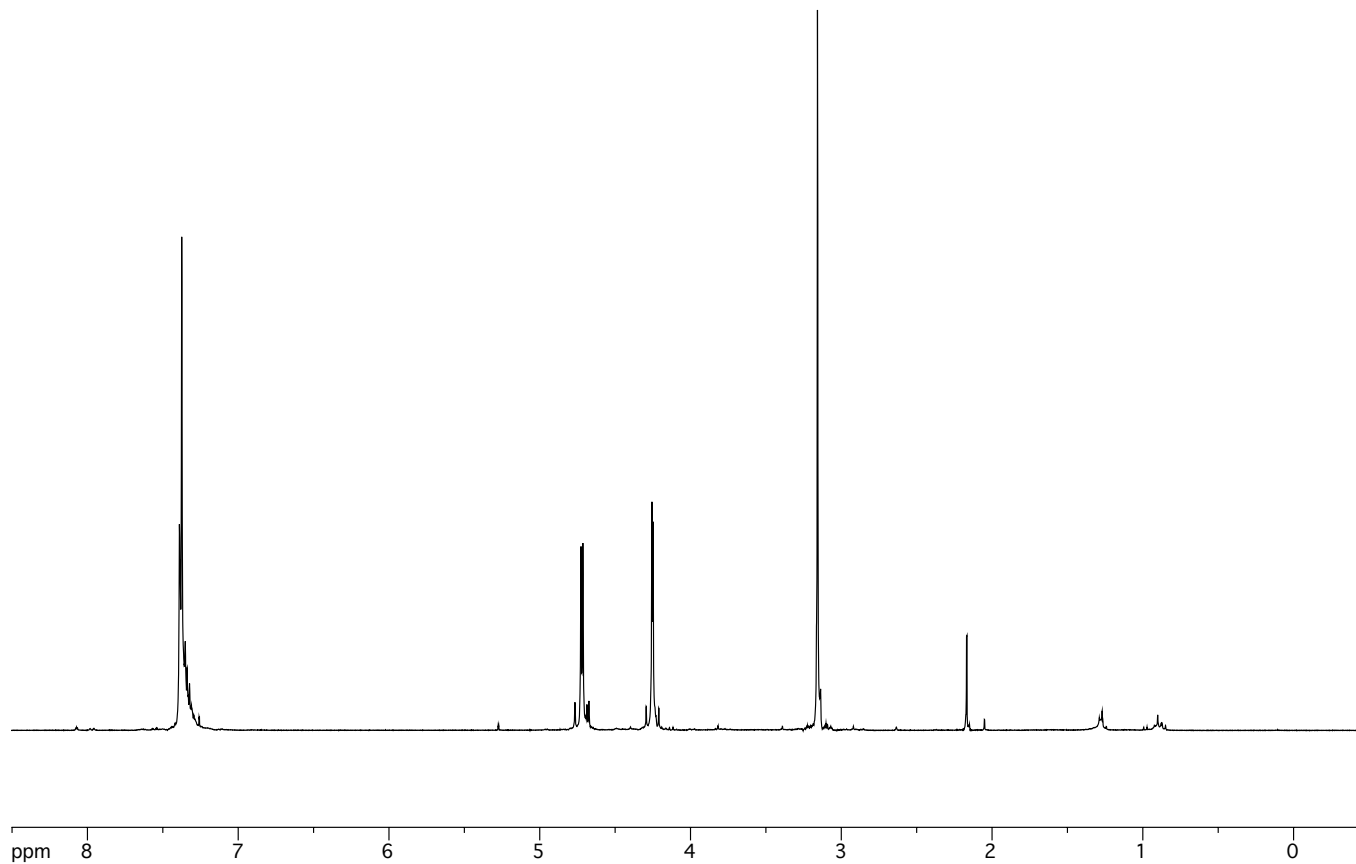
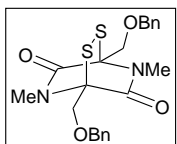
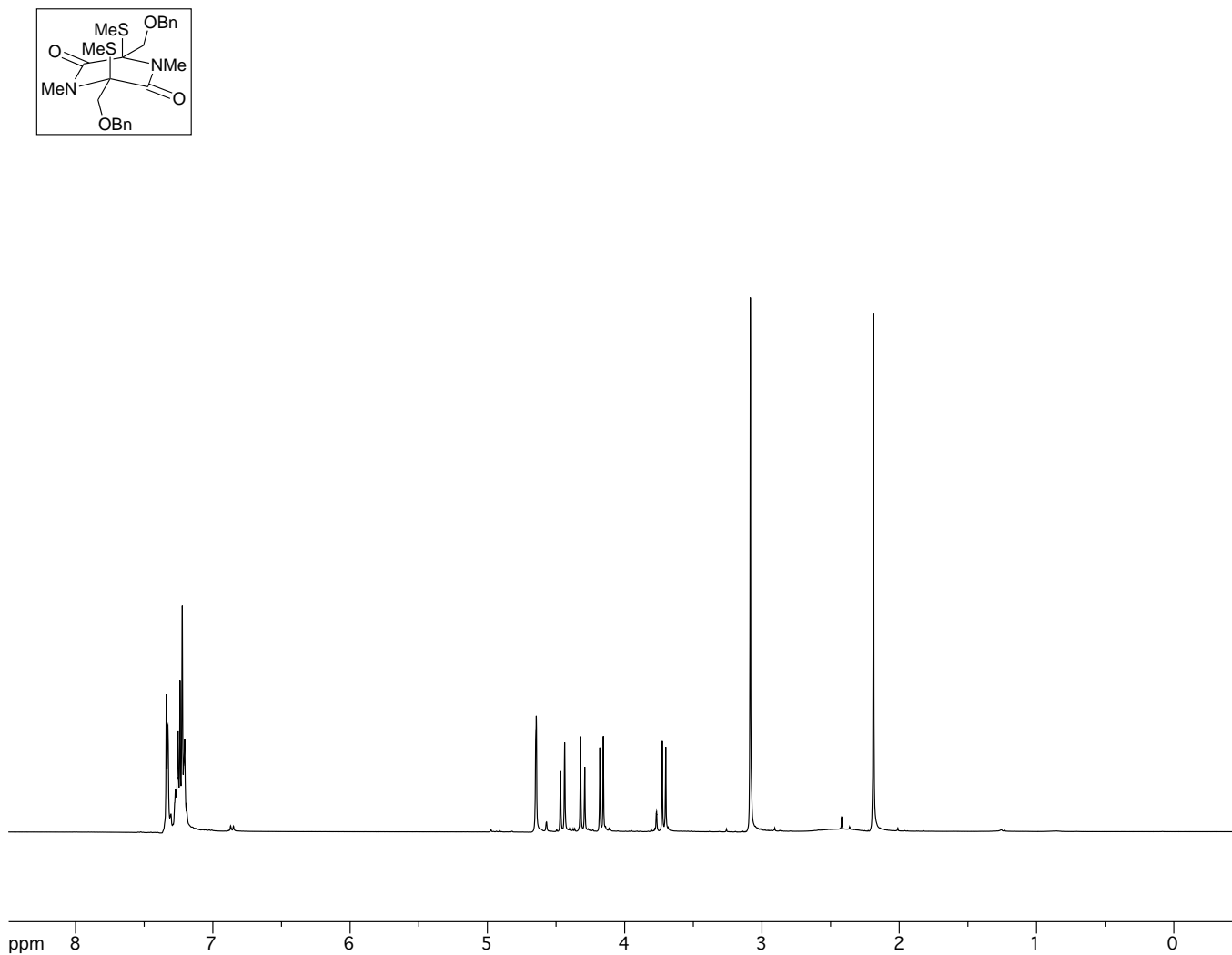


Figure A2.45. <sup>1</sup>H-NMR of disulfide 126.



**Figure A2.46.** <sup>1</sup>H-NMR of bithiomethyl ether **127**.

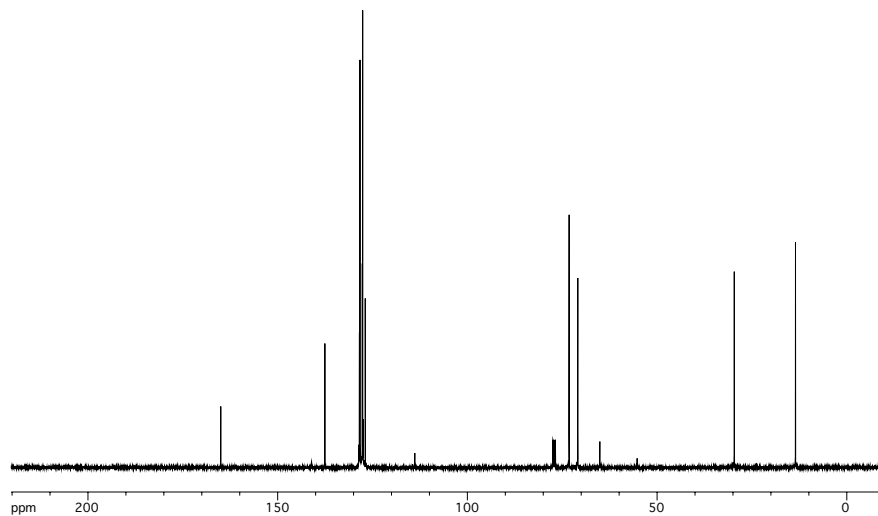


Figure A2.47.  $^{13}\text{C}$ -NMR of bithiomethyl ether **127**.

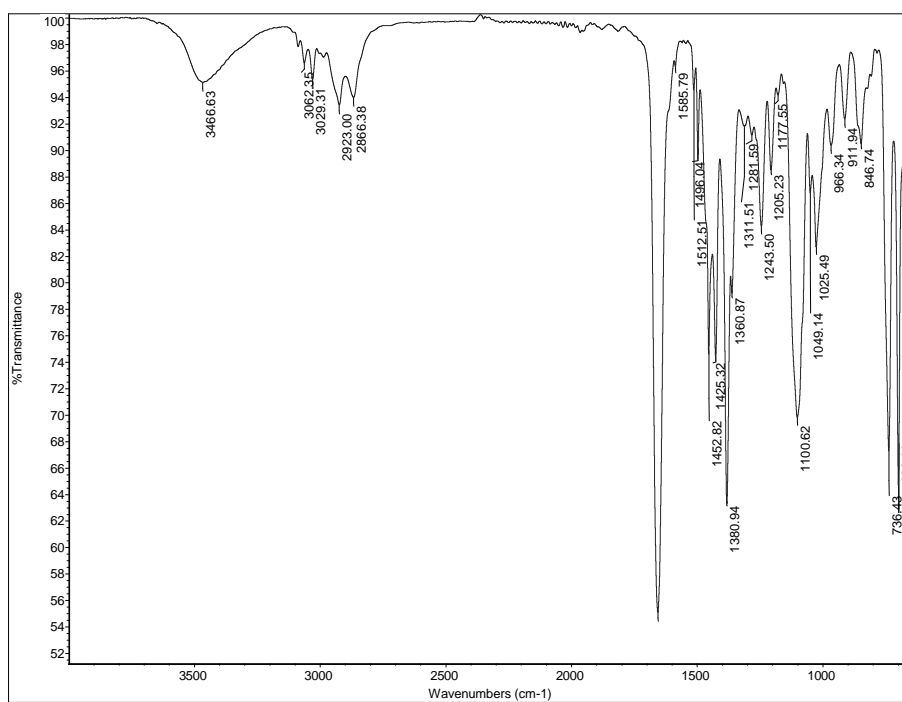


Figure A2.48. FTIR of bithiomethyl ether **127**.

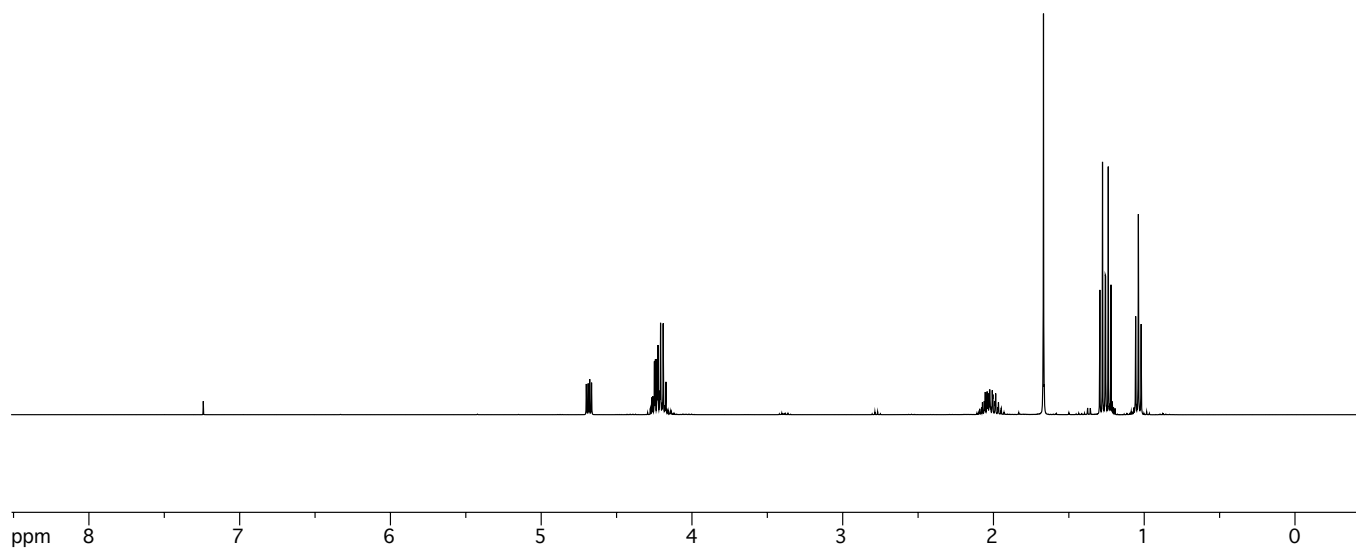
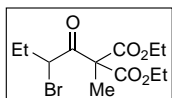
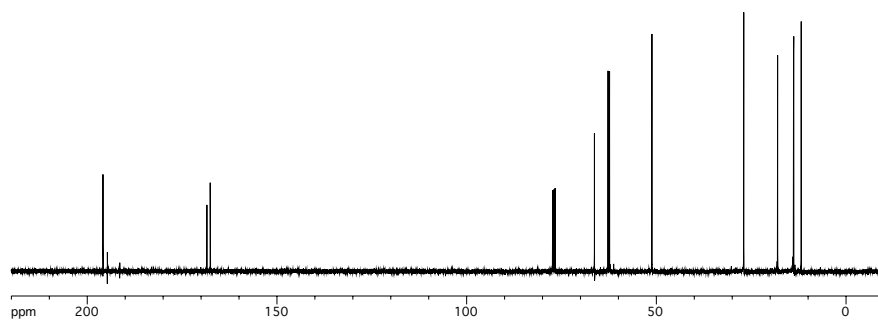
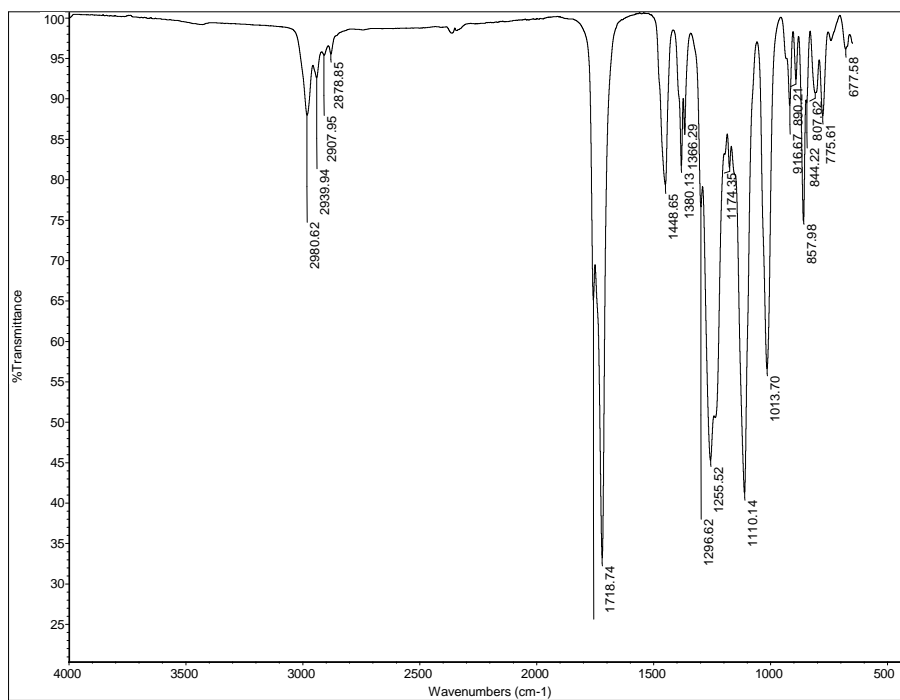


Figure A2.49.  $^1\text{H-NMR}$  of bromoketone **236**.



**Figure A2.50.**  $^{13}\text{C}$ -NMR of bromoketone **236**.



**Figure A2.51.** FTIR of bromoketone **236**.

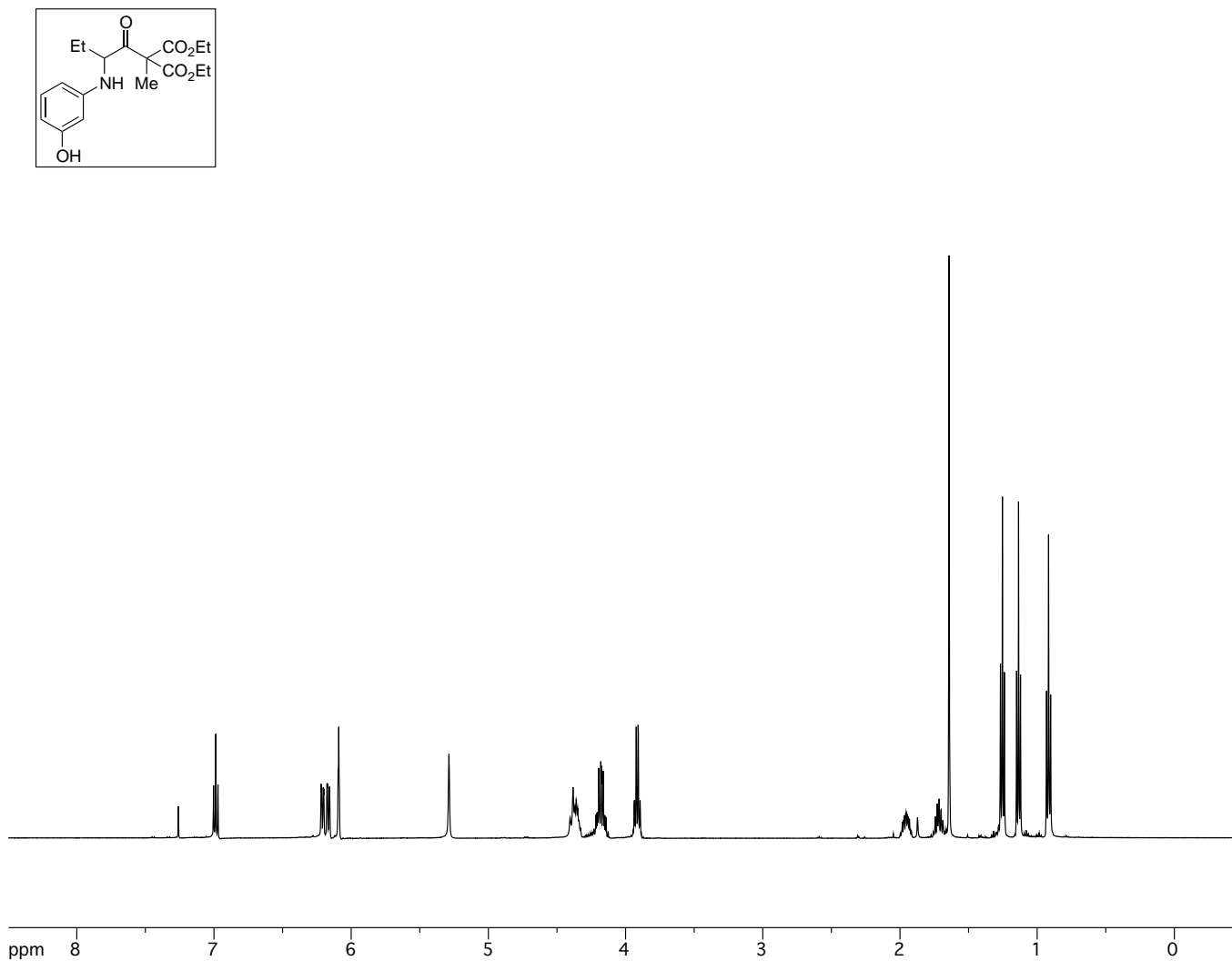


**Figure A2.52.** <sup>1</sup>H-NMR of aniline 237.

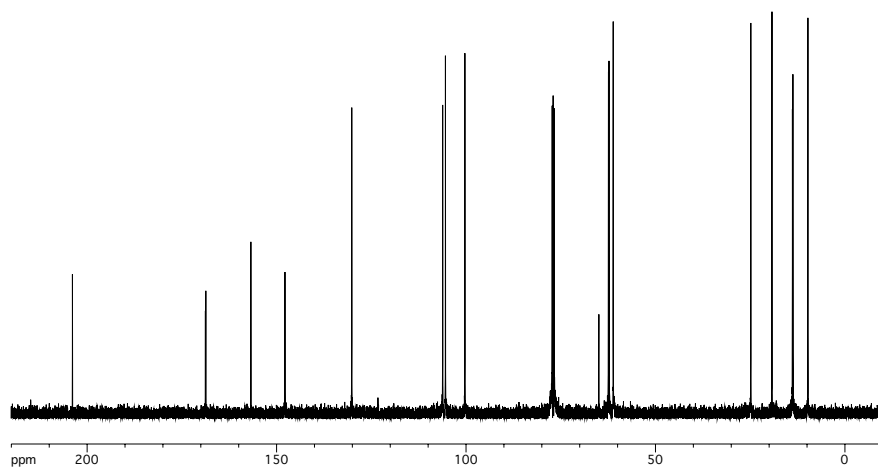


Figure A2.53. <sup>13</sup>C-NMR of aniline 237.

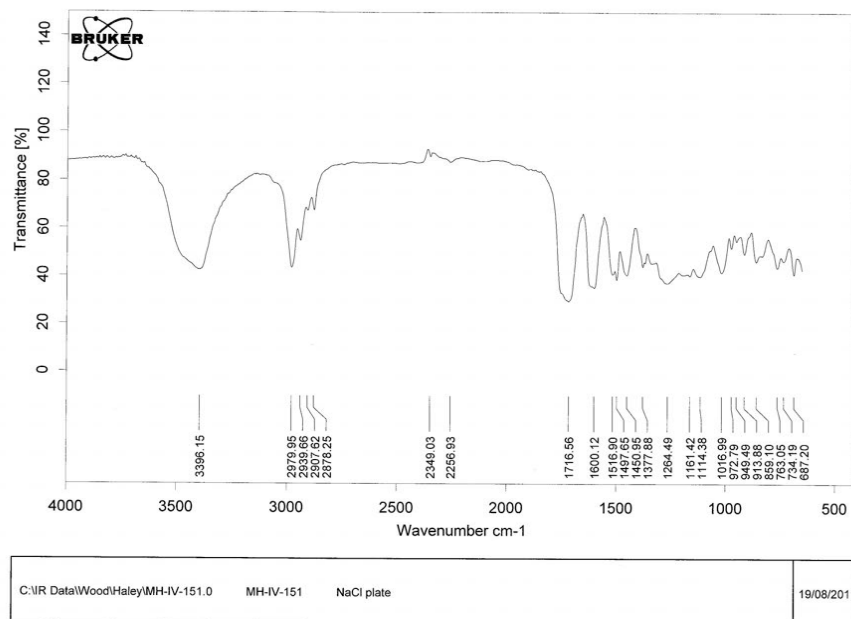
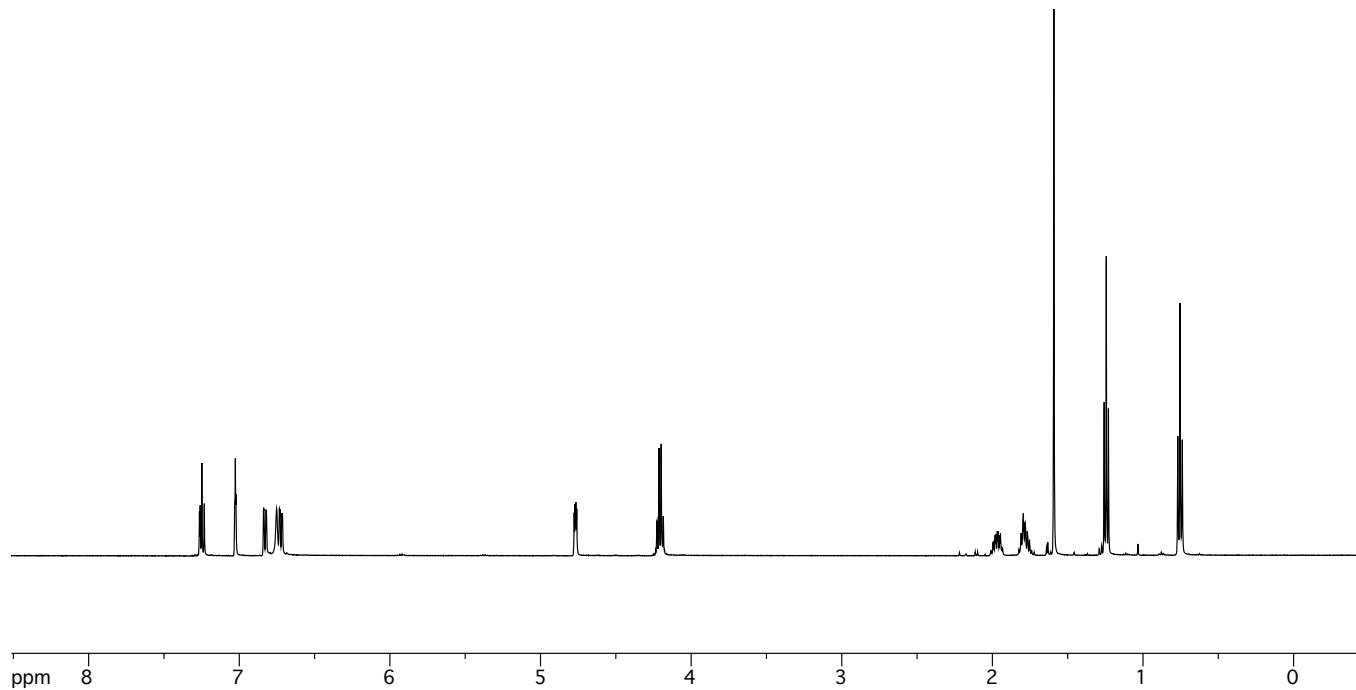
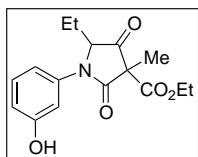


Figure A2.54. FTIR of aniline 237.



**Figure A2.55.** <sup>1</sup>H-NMR of phenol **287** (higher R<sub>f</sub> diastereomer).

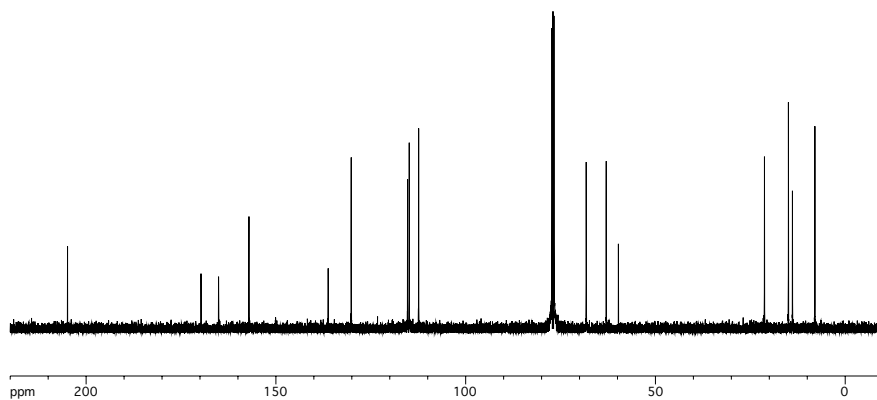
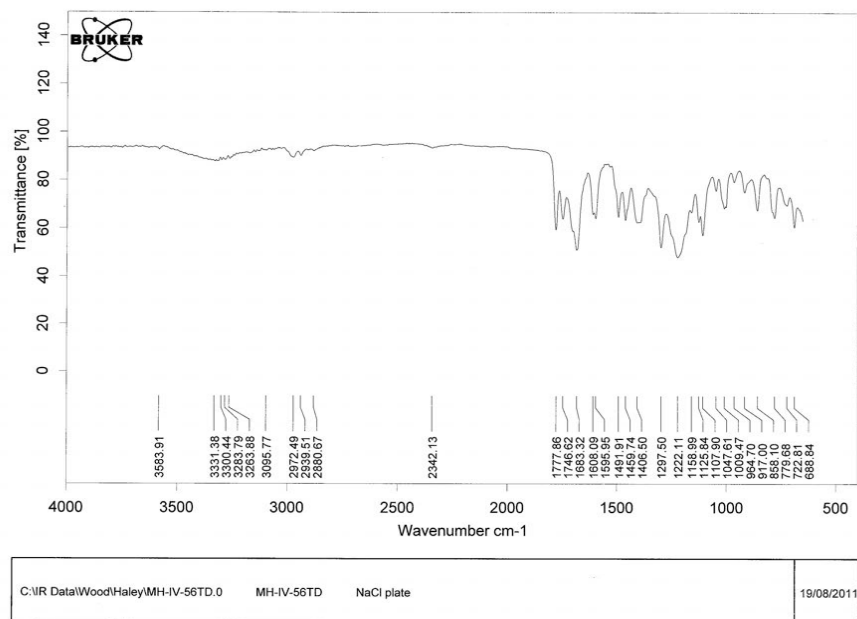
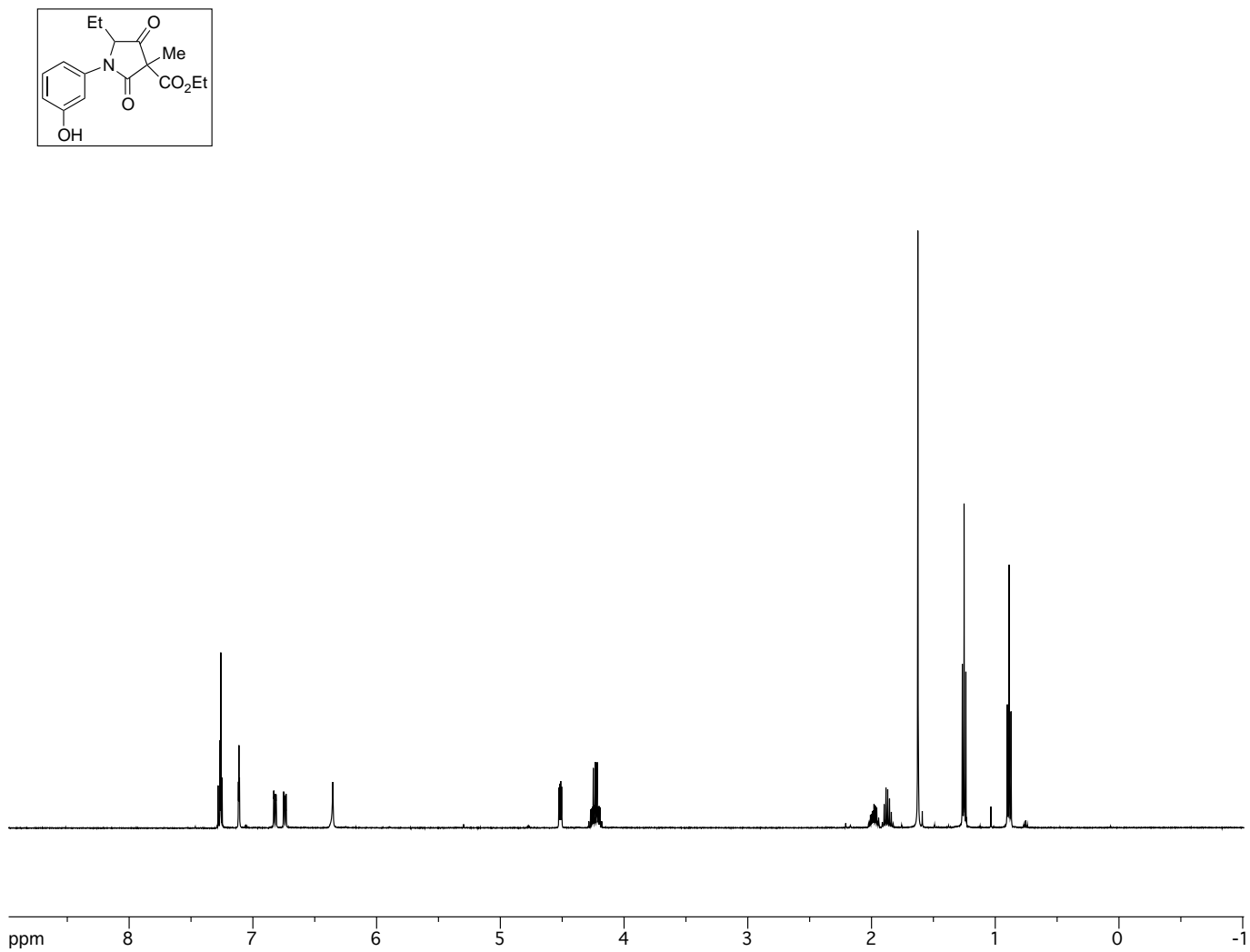


Figure A2.56.  $^{13}\text{C}$ -NMR of phenol **287** (higher  $R_f$  diastereomer).



Page 1/1

Figure A2.57. FTIR of phenol **287** (higher  $R_f$  diastereomer).



**Figure A2.58.** <sup>1</sup>H-NMR of phenol **287** (lower R<sub>f</sub> diastereomer).

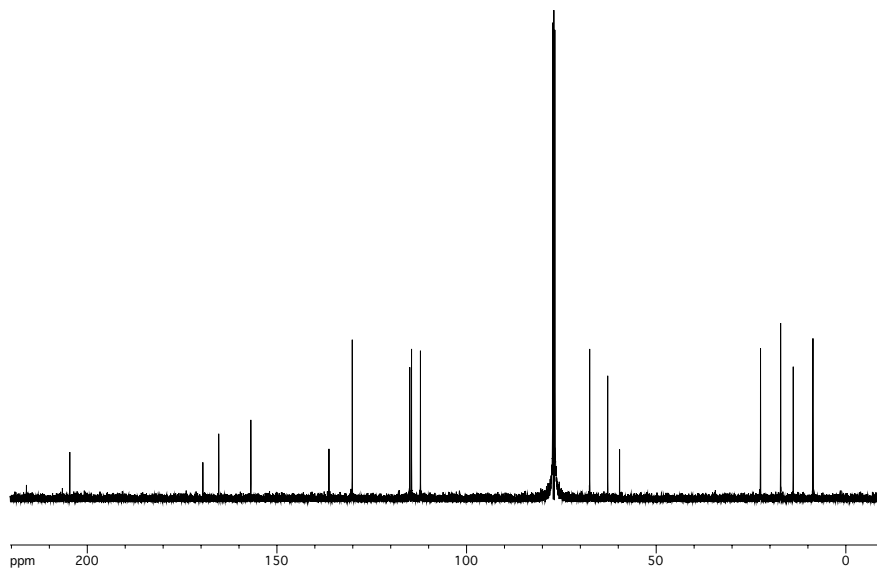


Figure A2.59.  $^{13}\text{C}$ -NMR of phenol **287** (lower  $R_f$  diastereomer).

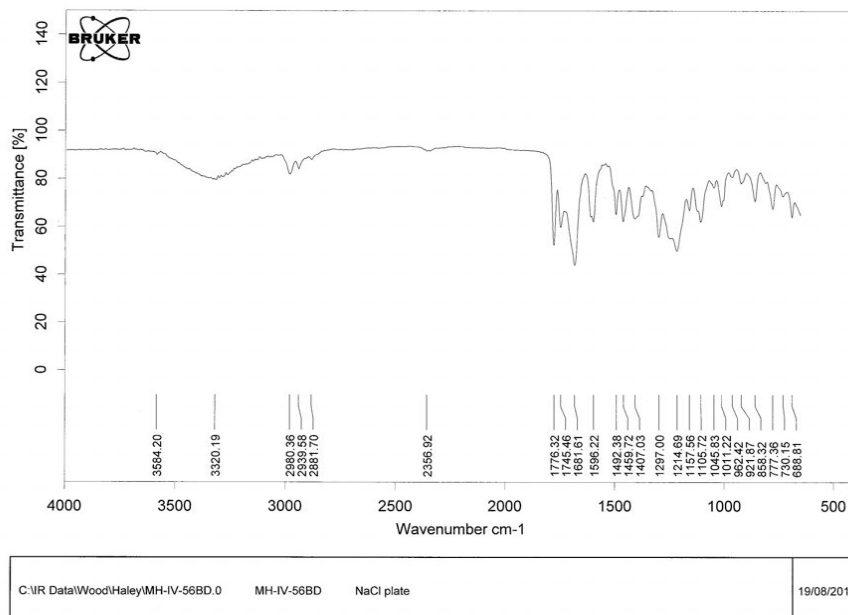
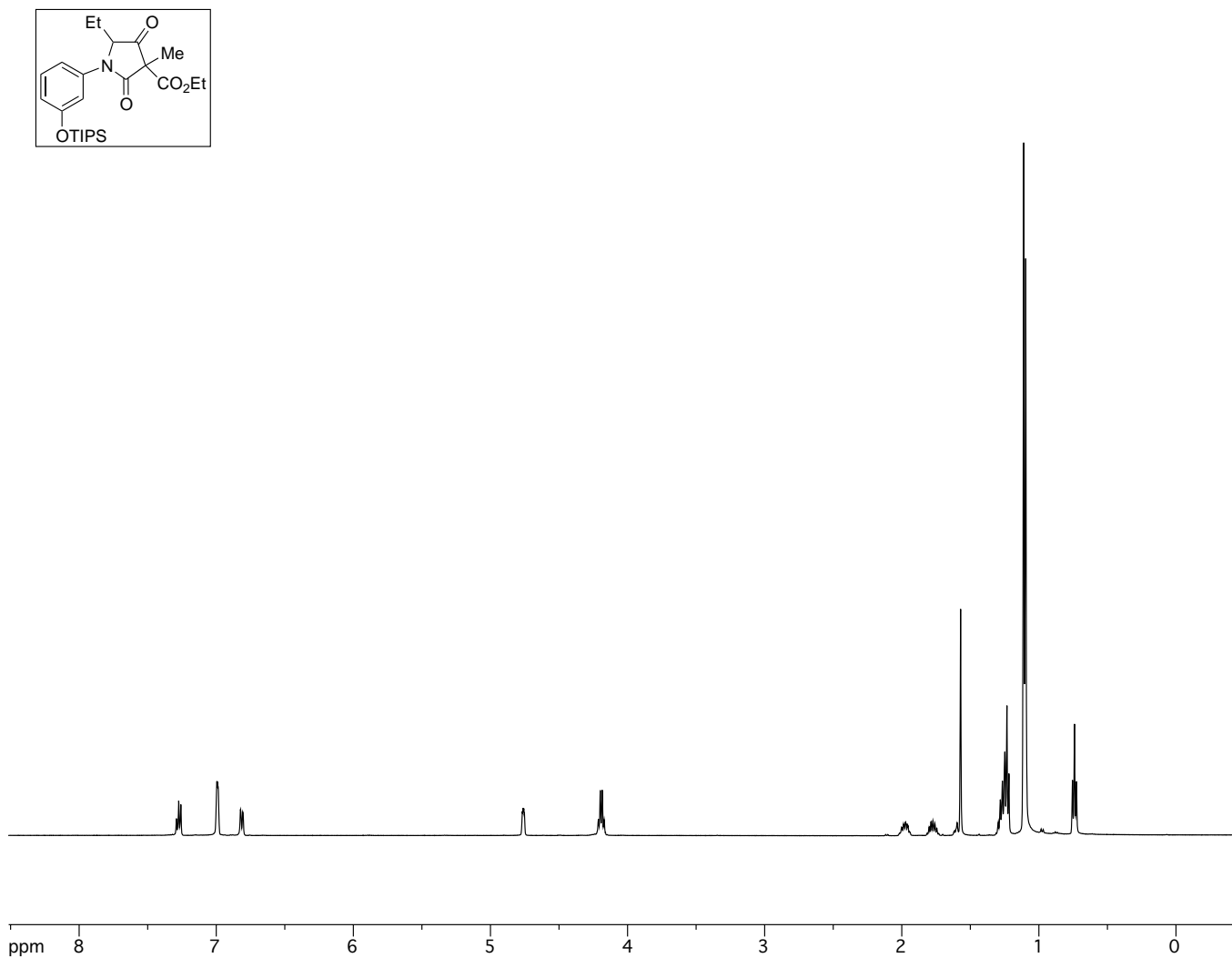


Figure A2.60. FTIR of phenol **287** (lower  $R_f$  diastereomer).



**Figure A2.61.** <sup>1</sup>H-NMR of ketone **234** (higher R<sub>f</sub> diastereomer).

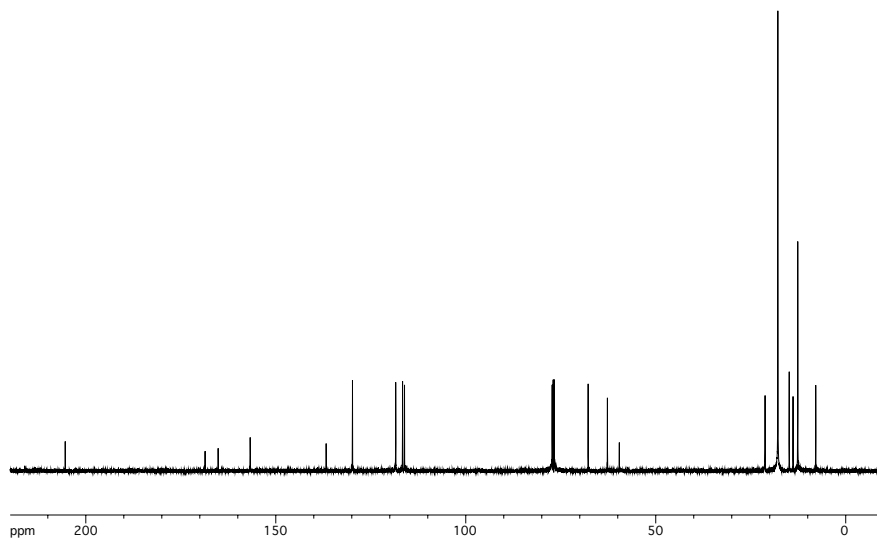
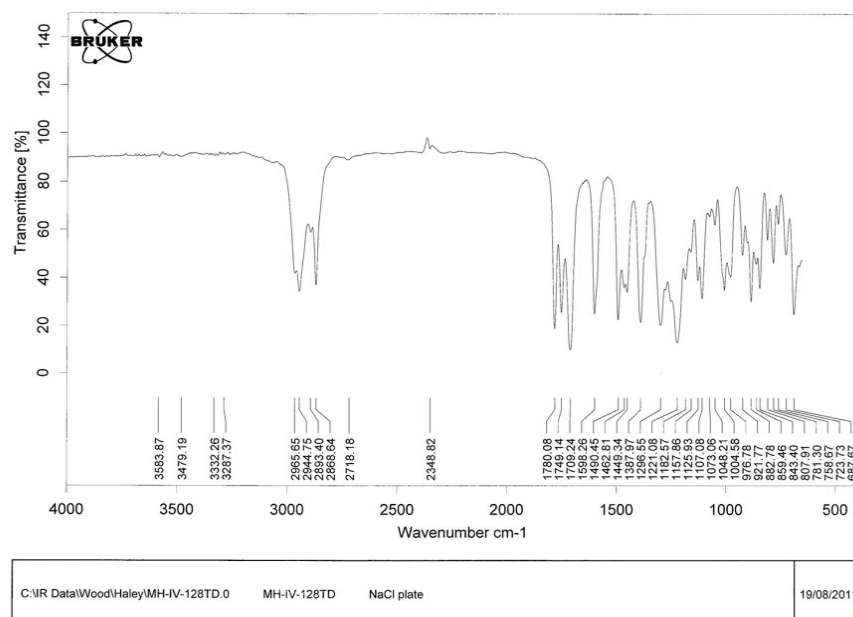
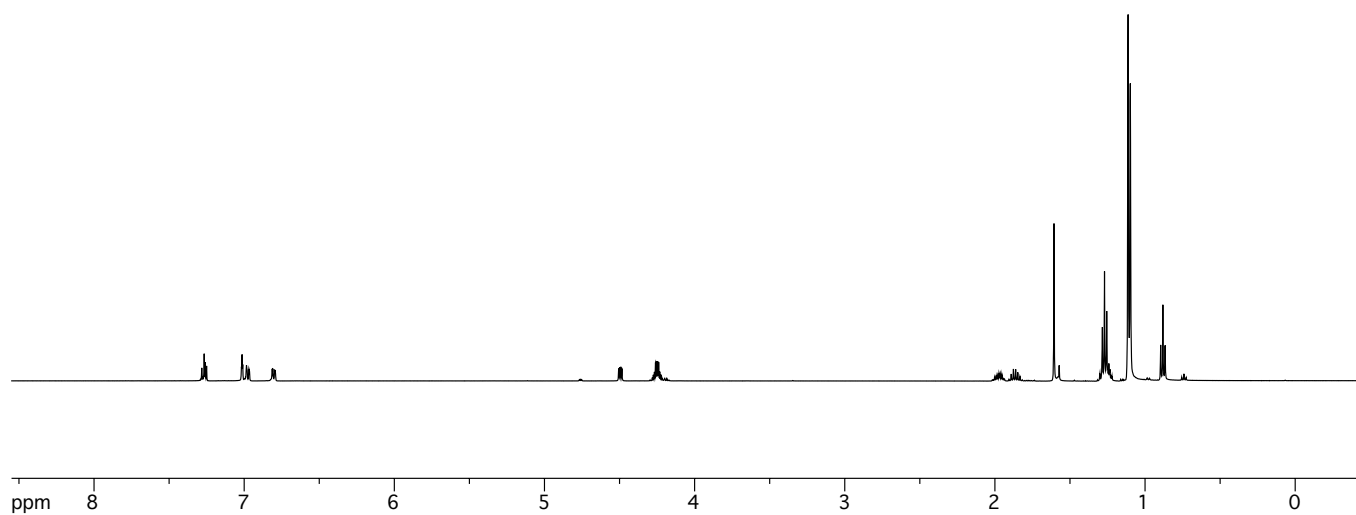
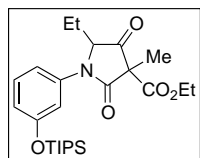


Figure A2.62.  $^{13}\text{C}$ -NMR of ketone **234** (higher  $R_f$  diastereomer).



Page 1/1

Figure A2.63. FTIR of ketone **234** (higher  $R_f$  diastereomer).



**Figure A2.64.** <sup>1</sup>H-NMR of ketone **234** (lower R<sub>f</sub> diastereomer).

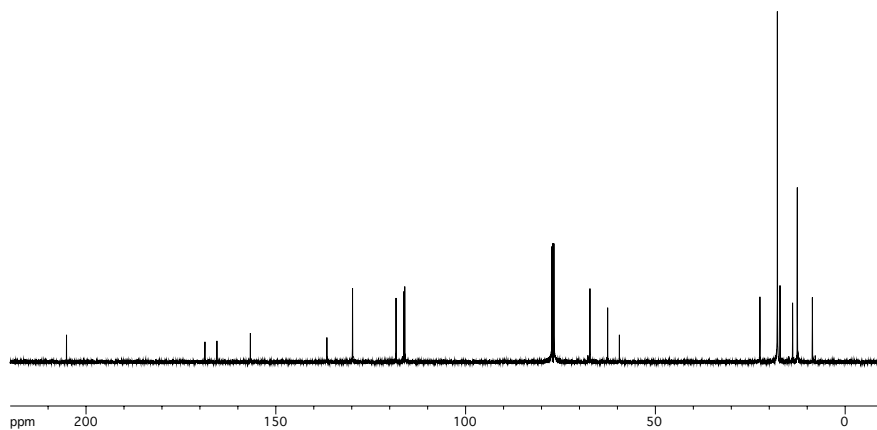
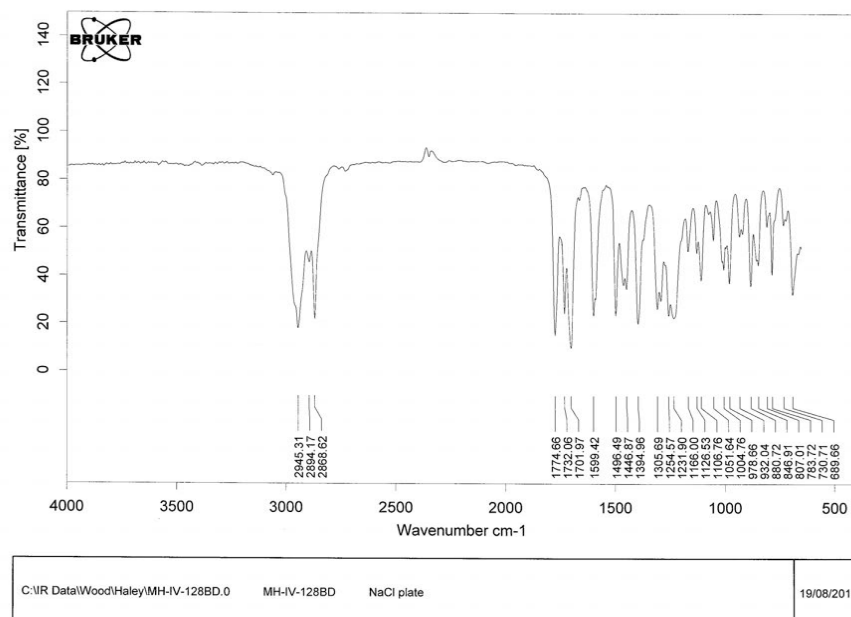
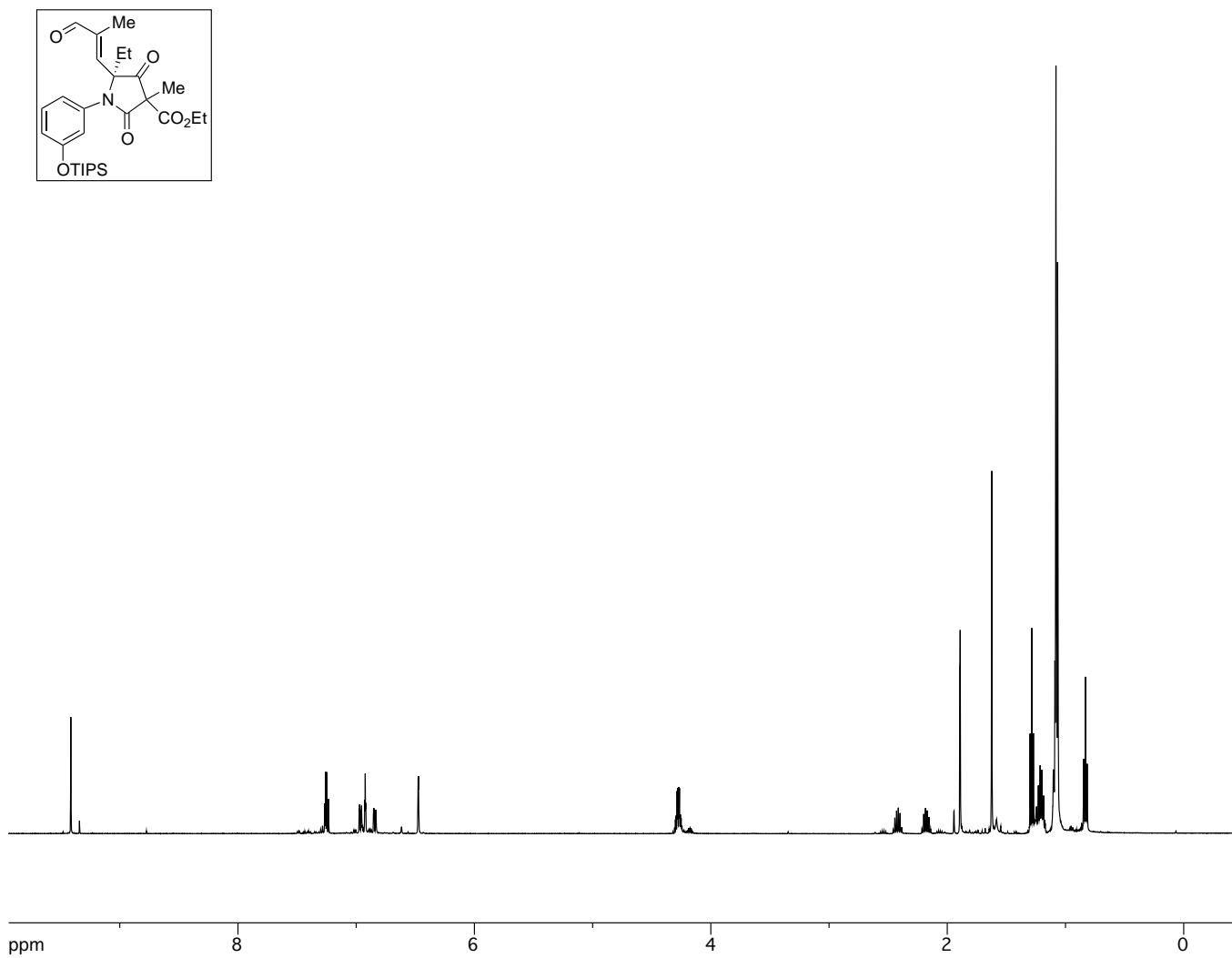


Figure A2.65.  $^{13}\text{C}$ -NMR of ketone **234** (lower  $R_f$  diastereomer).



Page 1/1

Figure A2.66. FTIR of ketone **234** (lower  $R_f$  diastereomer).



**Figure A2.67.** <sup>1</sup>H-NMR of enal 239.

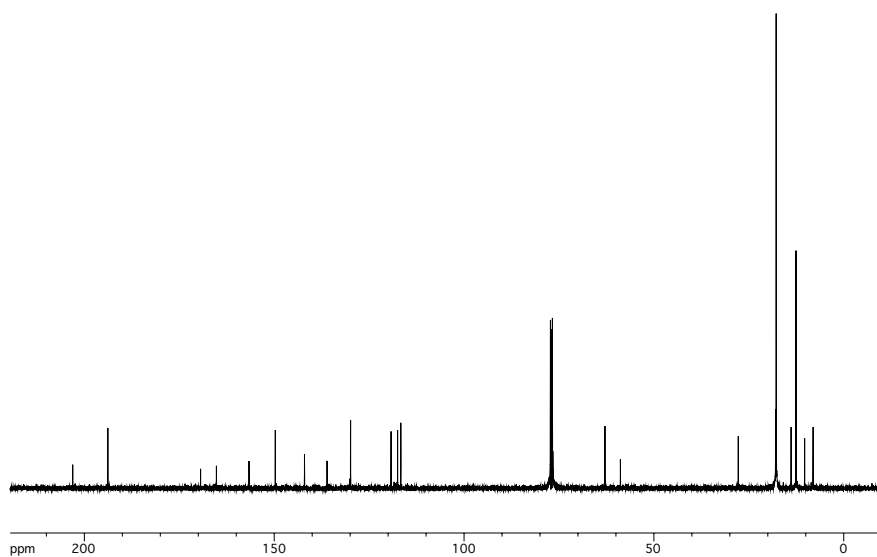


Figure A2.68.  $^{13}\text{C-NMR}$  of enal **239**.

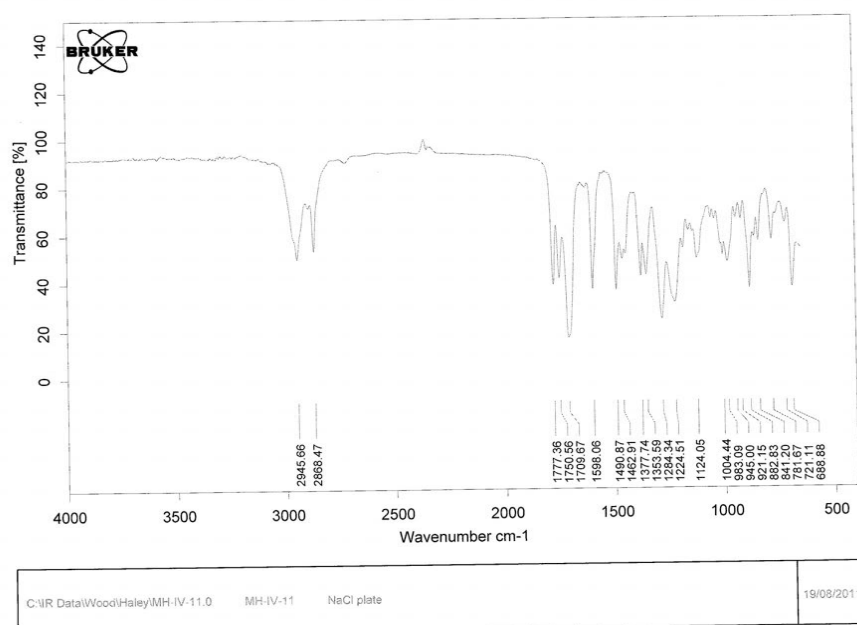
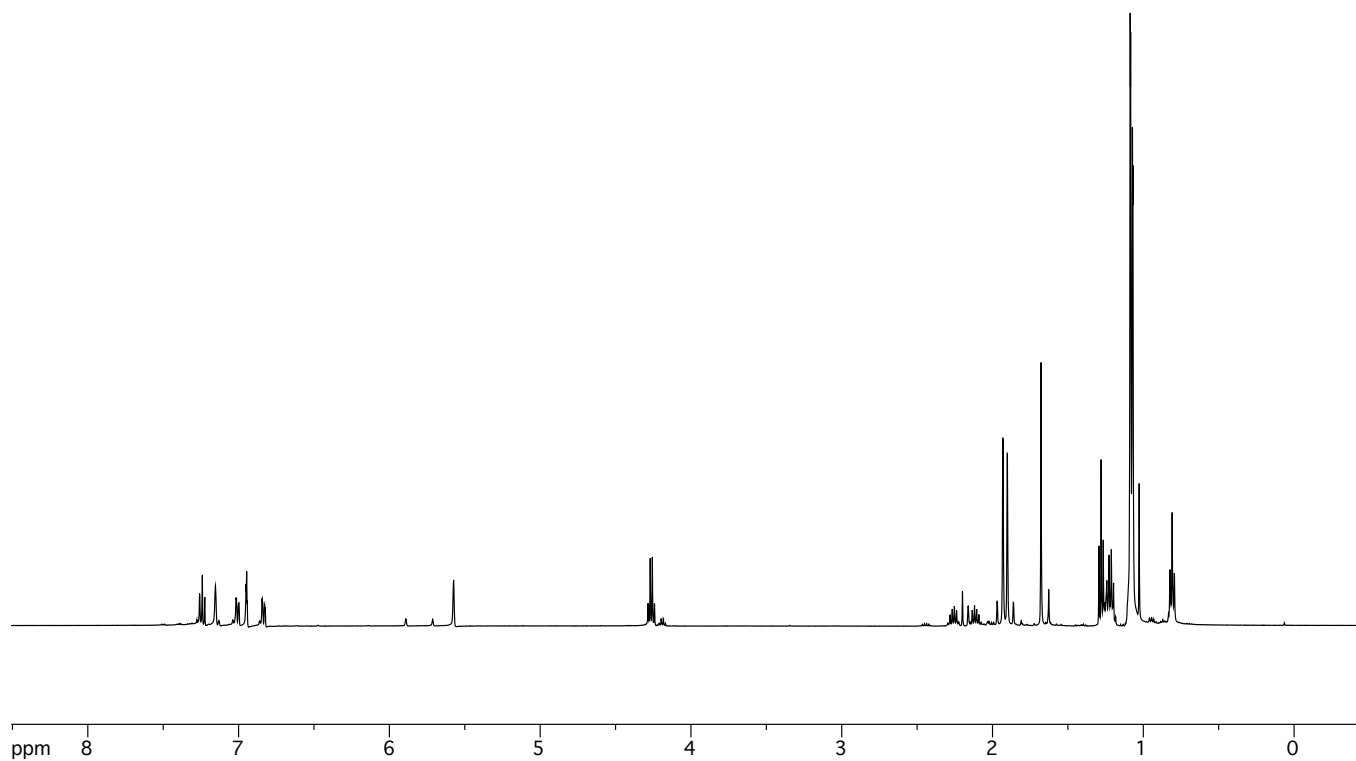
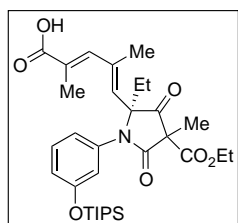


Figure A2.69. FTIR of enal **239**.



**Figure A2.70.**  $^1\text{H-NMR}$  of carboxylic acid **247**.

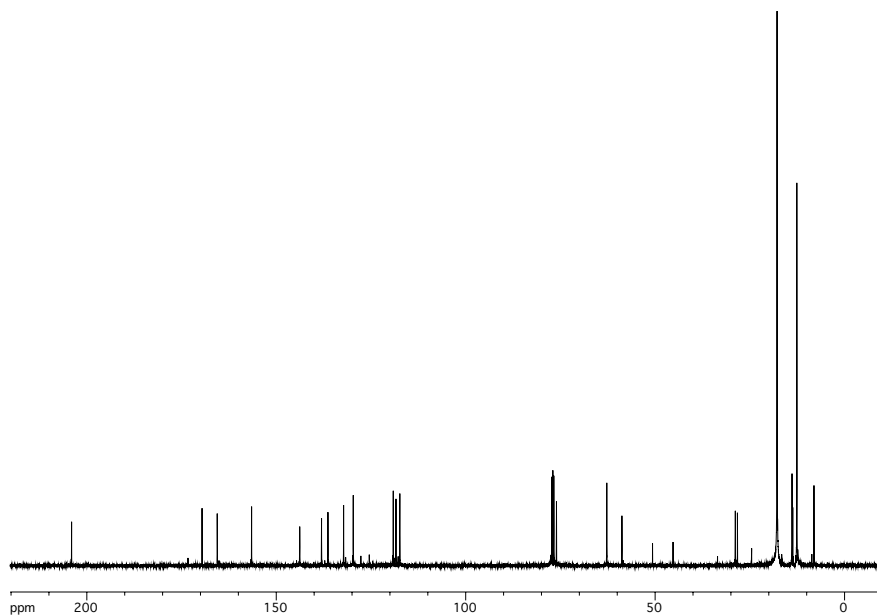
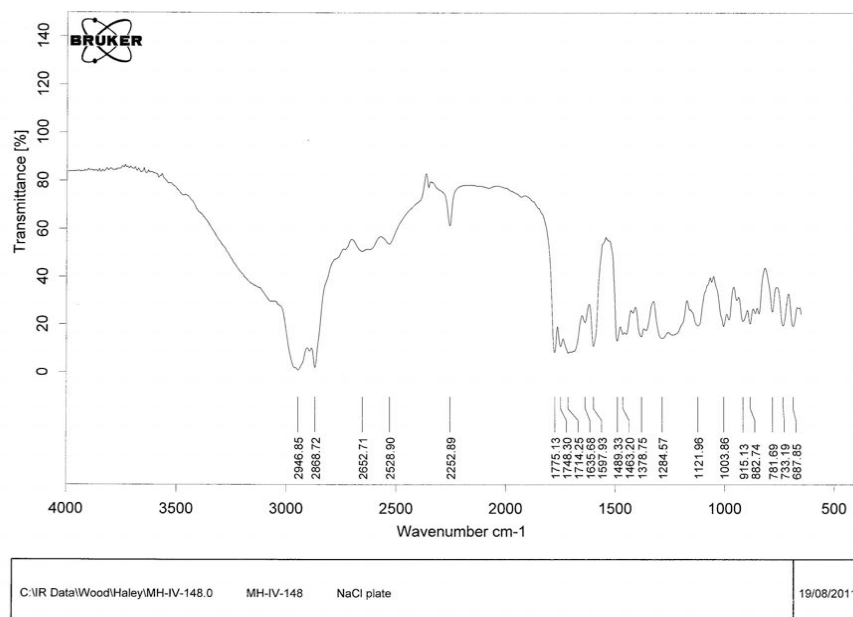
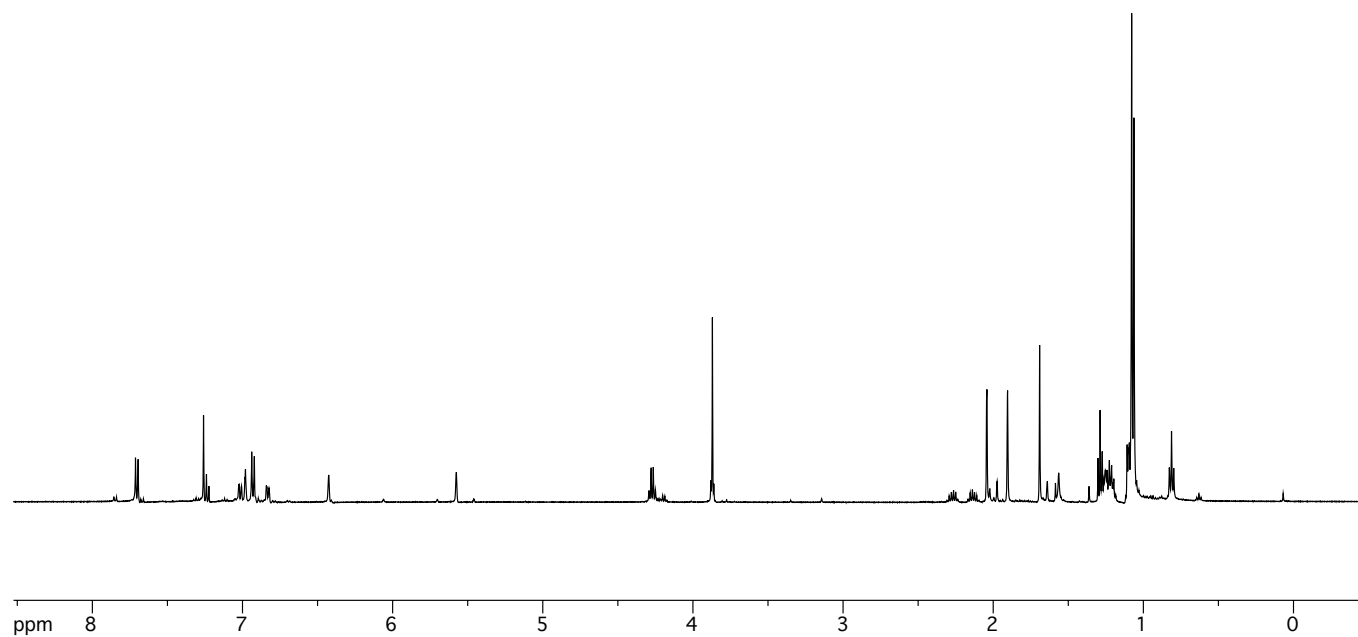
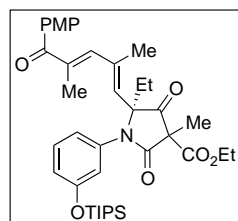


Figure A2.71. <sup>13</sup>C-NMR of carboxylic acid **247**.



Page 1/1

Figure A2.72. FTIR of carboxylic acid **247**.



**Figure A2.73.** <sup>1</sup>H-NMR of ketone **259**.

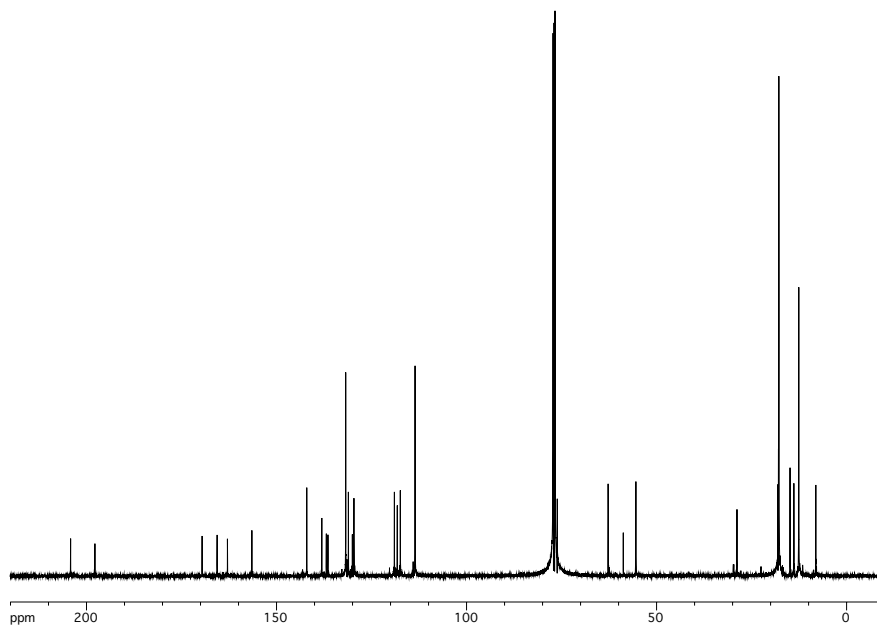
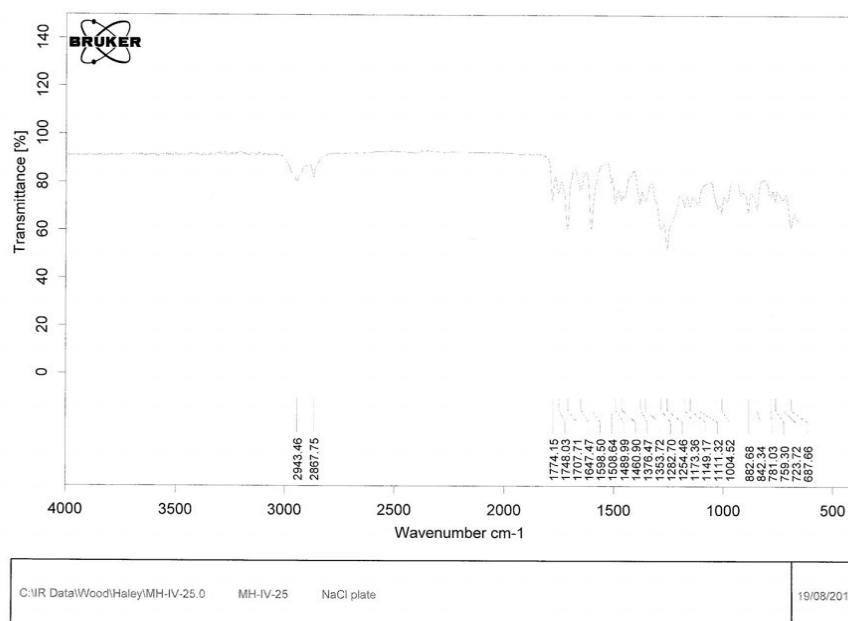
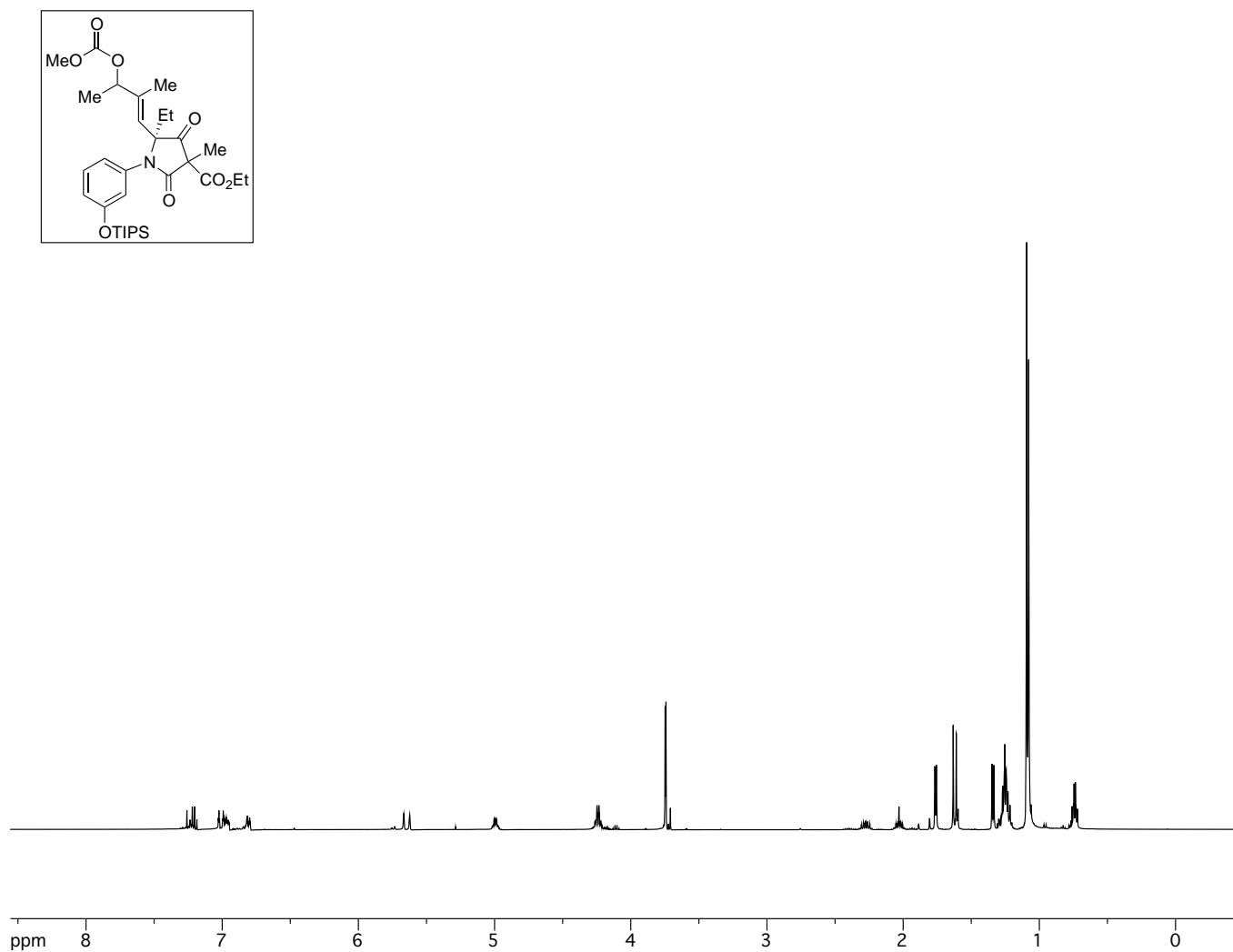


Figure A2.74.  $^{13}\text{C}$ -NMR of ketone 259.



Page 1/1

Figure A2.75. FTIR of ketone 259.



**Figure A2.76.** <sup>1</sup>H-NMR of allylic carbonate **265**.

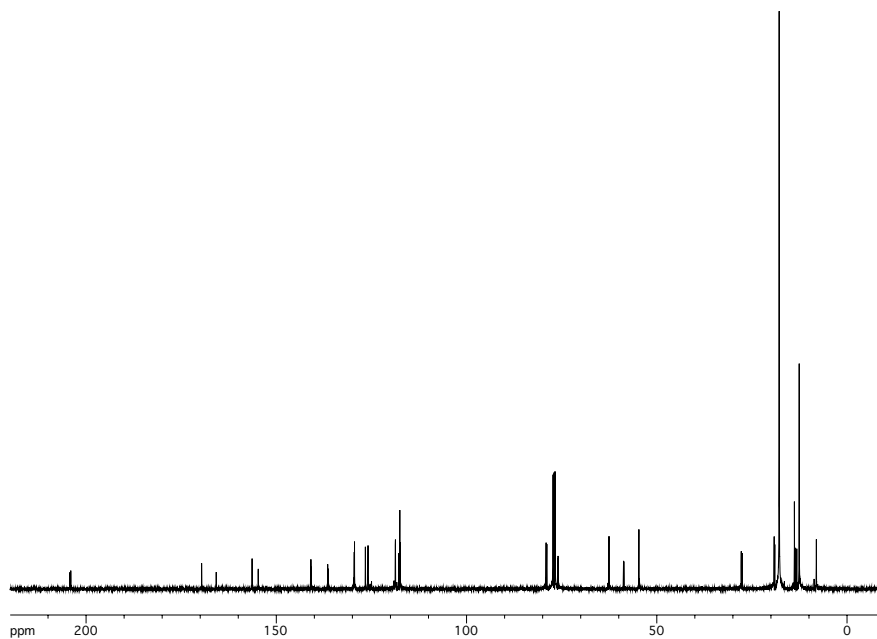
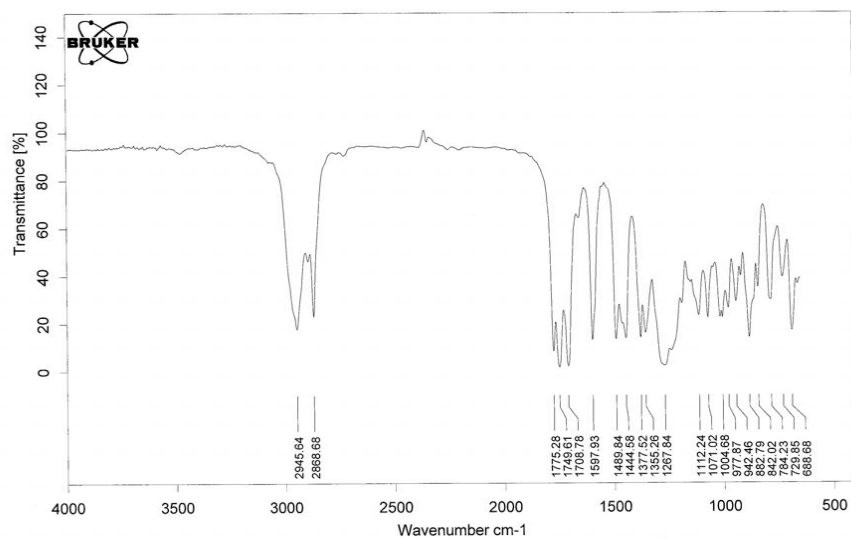
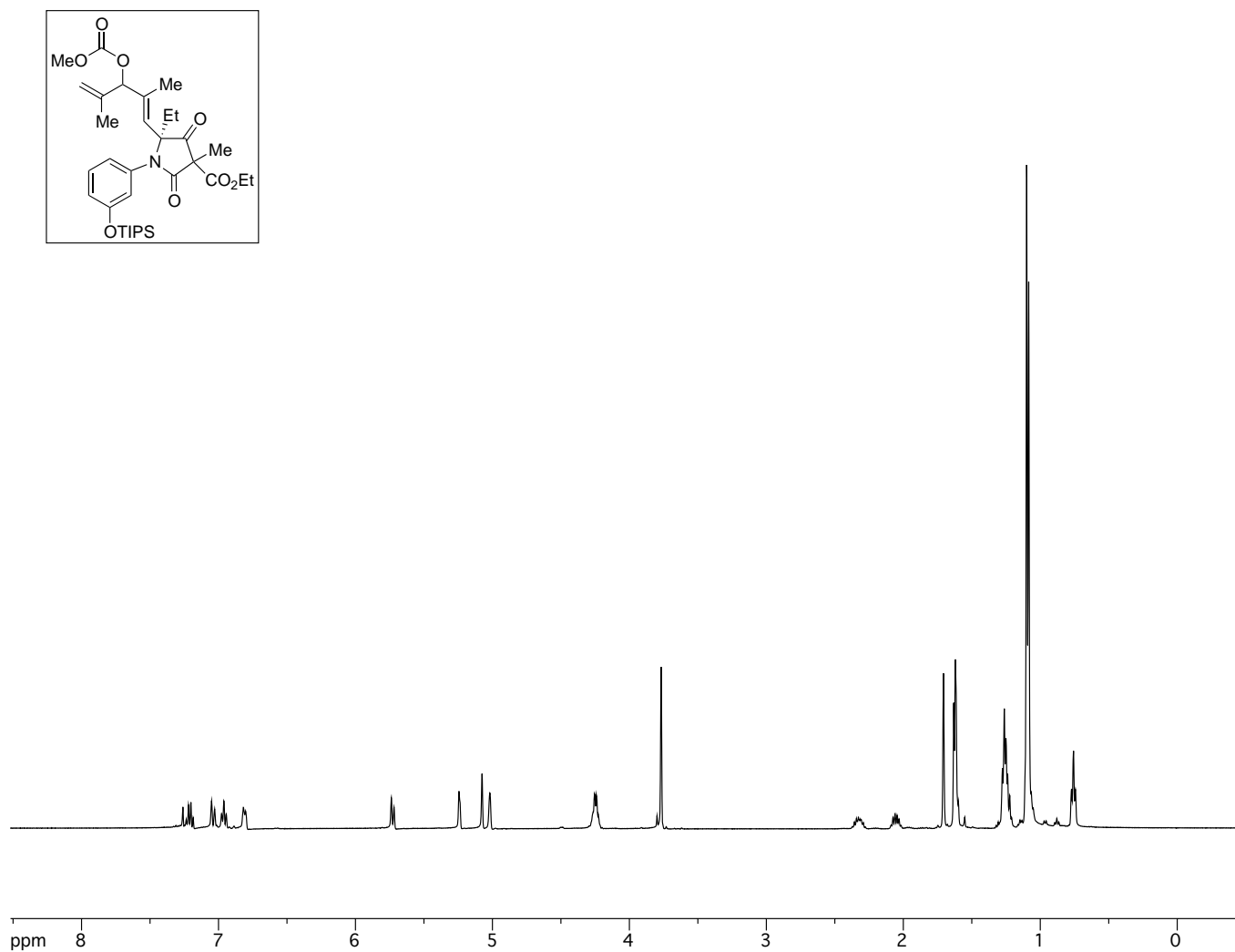


Figure A2.77.  $^{13}\text{C}$ -NMR of allylic carbonate **265**.



C:\IR Data\Wood\Haley\MH-IV-66.0	MH-IV-66	NaCl plate	19/08/2011
----------------------------------	----------	------------	------------

Figure A2.78. FTIR of allylic carbonate **265**.



**Figure A2.79.** <sup>1</sup>H-NMR of allylic carbonate **268**.

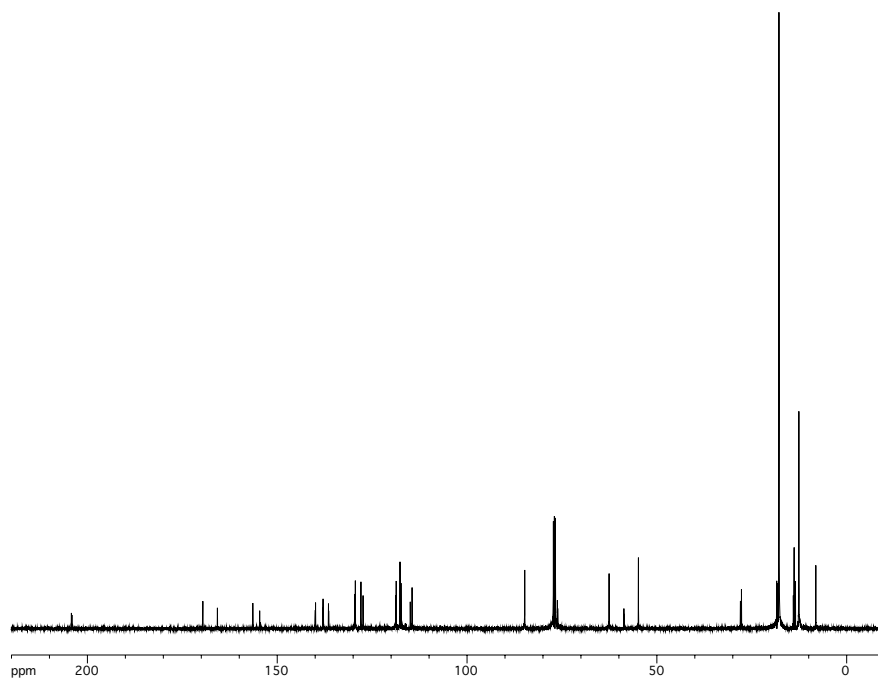


Figure A2.80.  $^{13}\text{C}$ -NMR of allylic carbonate **268**.

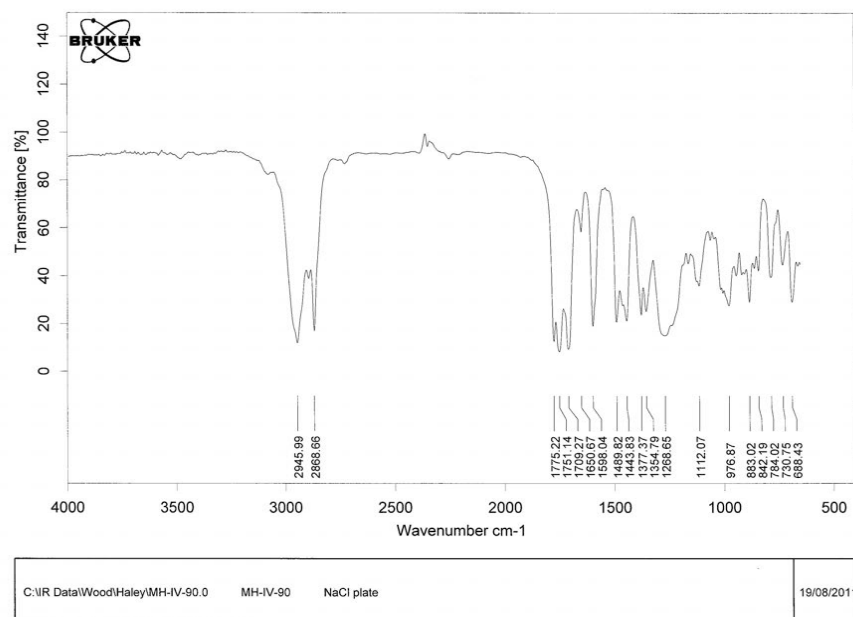
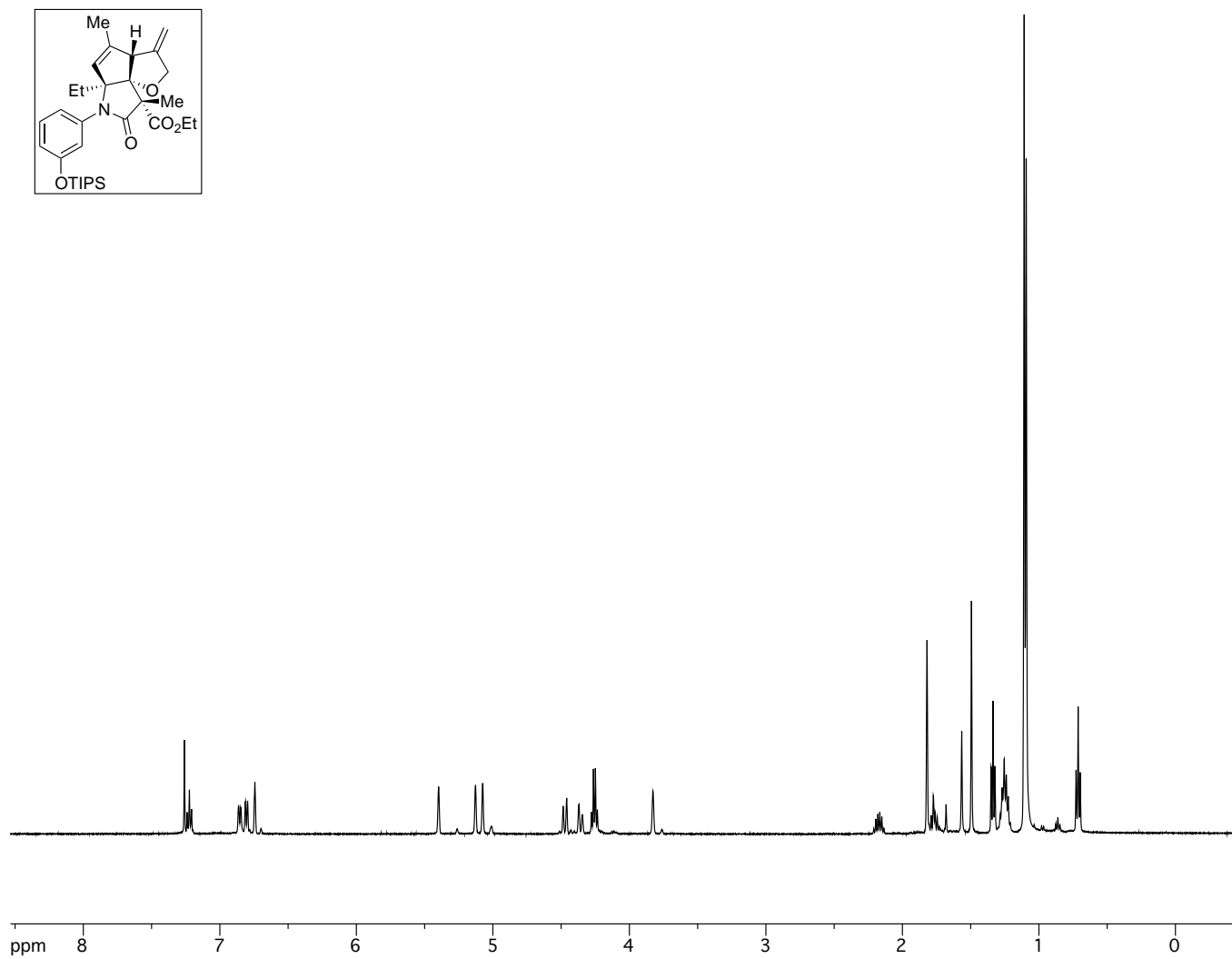


Figure A2.81. FTIR of allylic carbonate **268**.



**Figure A2.82.** <sup>1</sup>H-NMR of fused tricycle **269**.

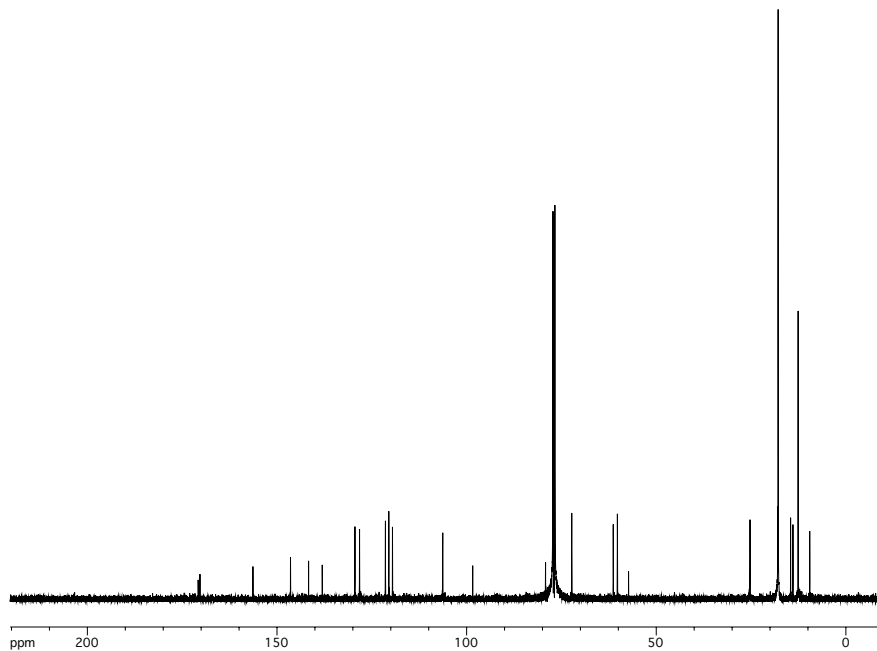
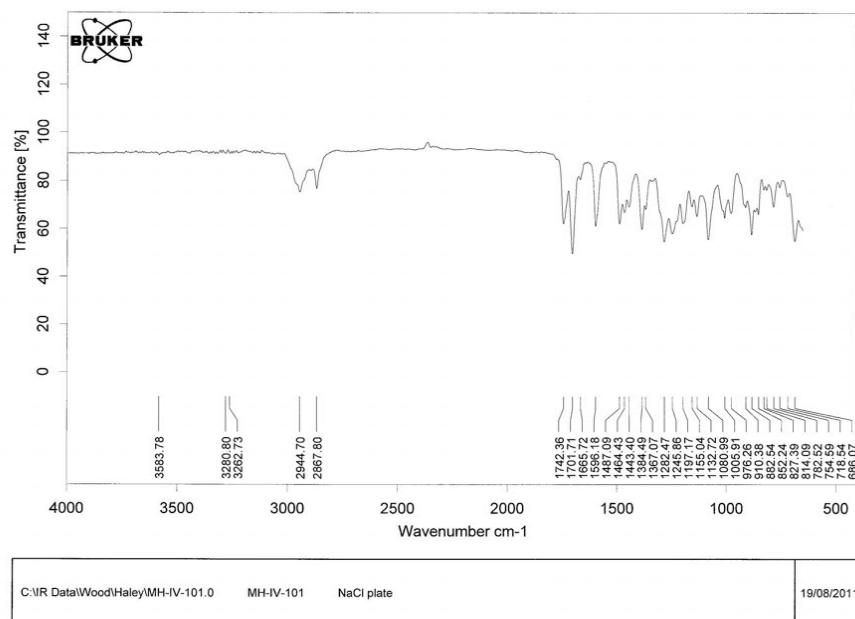
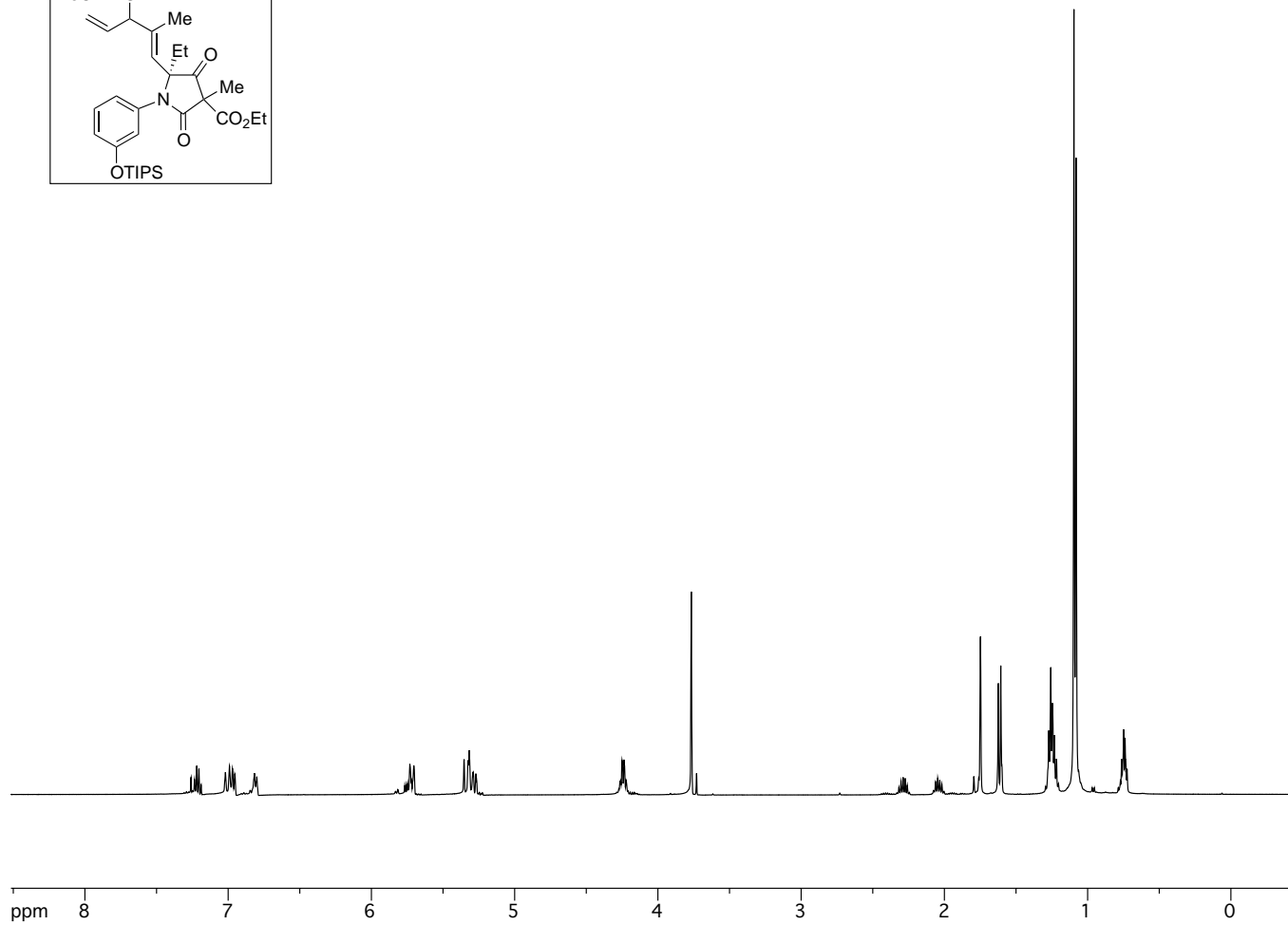
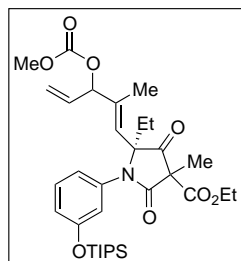


Figure A2.83.  $^{13}\text{C}$ -NMR of fused tricycle **269**.



Page 1/1

Figure A2.84. FTIR of fused tricycle **269**.



**Figure A2.85.** <sup>1</sup>H-NMR of allylic carbonate **462**.

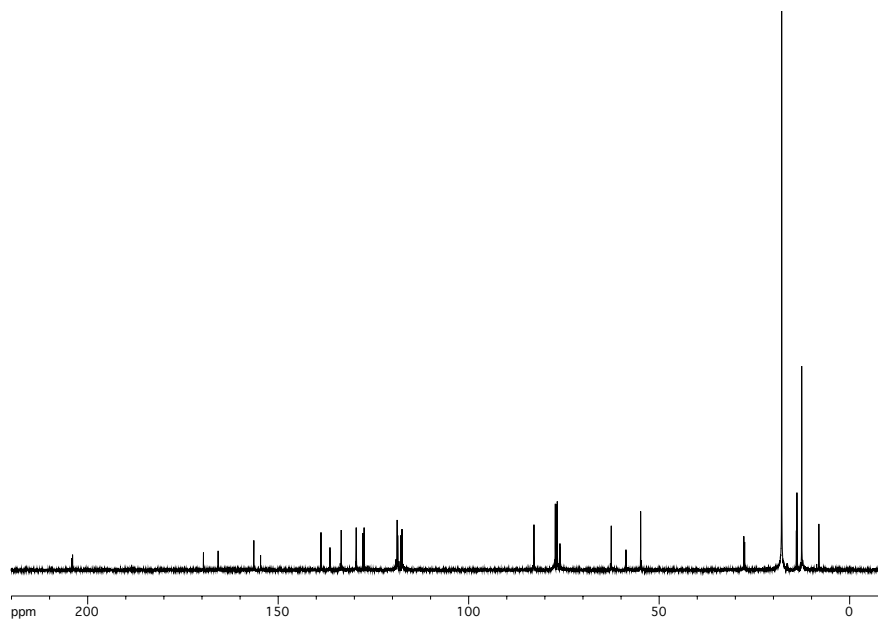


Figure A2.86.  $^{13}\text{C}$ -NMR of allylic carbonate **462**.

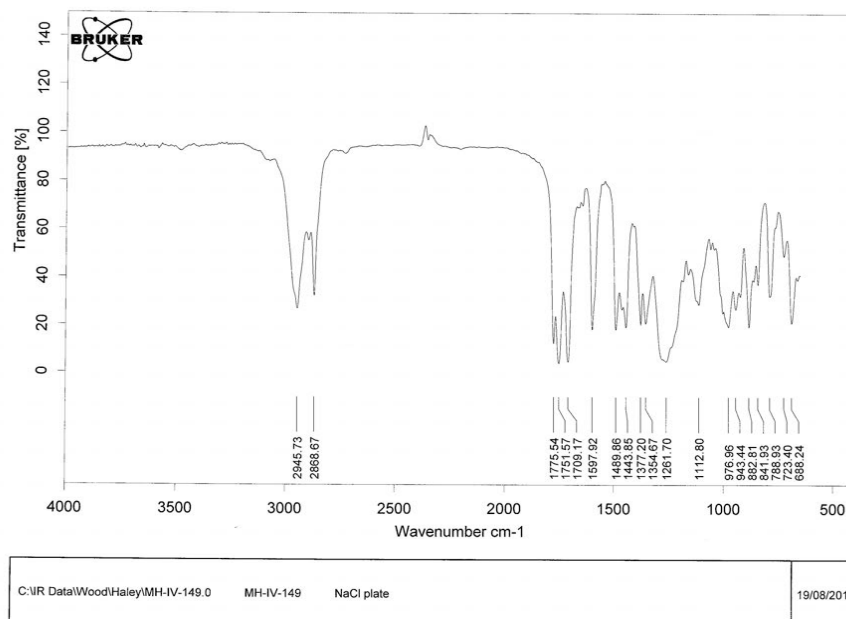
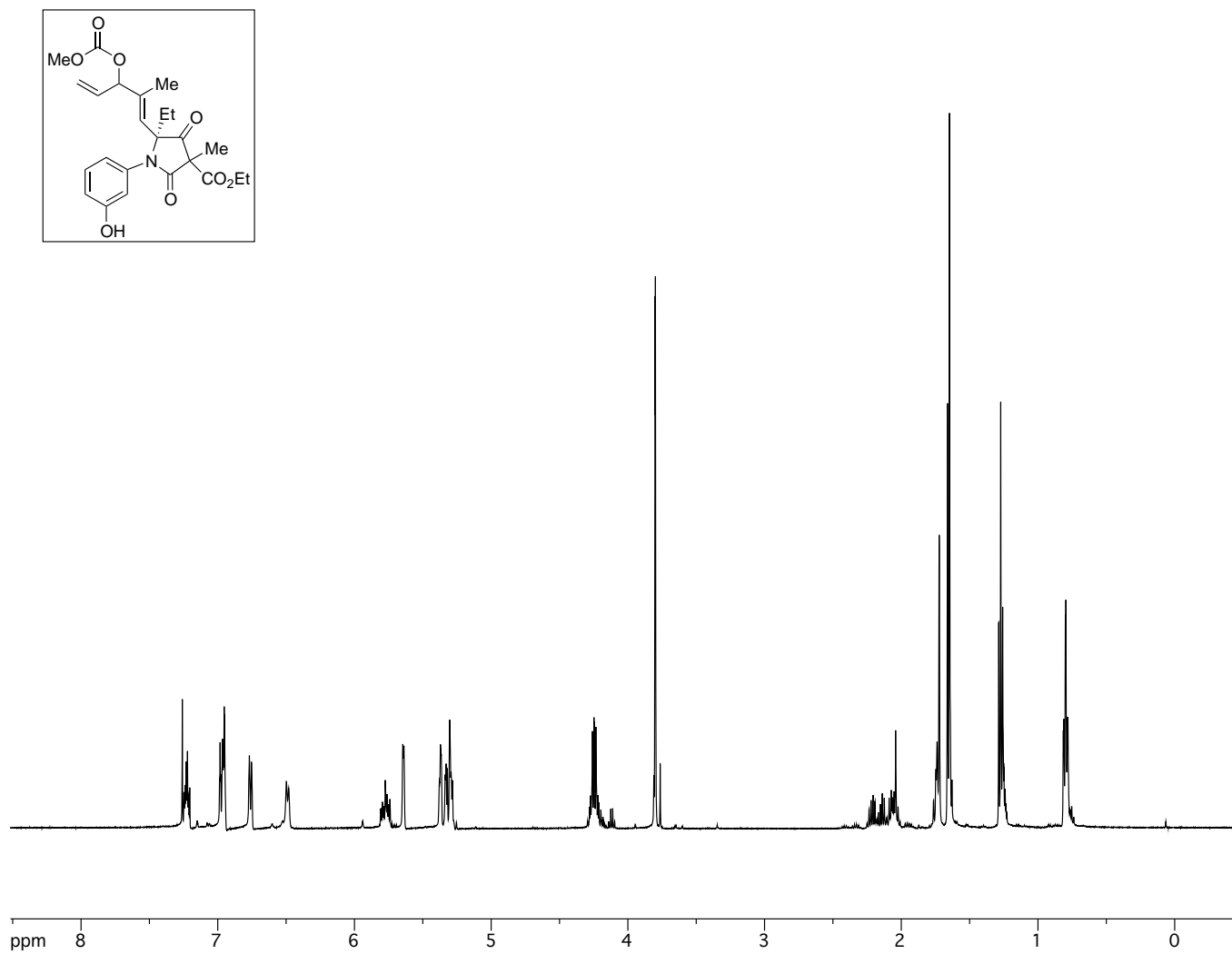


Figure A2.87. FTIR of allylic carbonate **462**.



**Figure A2.88.** <sup>1</sup>H-NMR of allylic carbonate **275**.

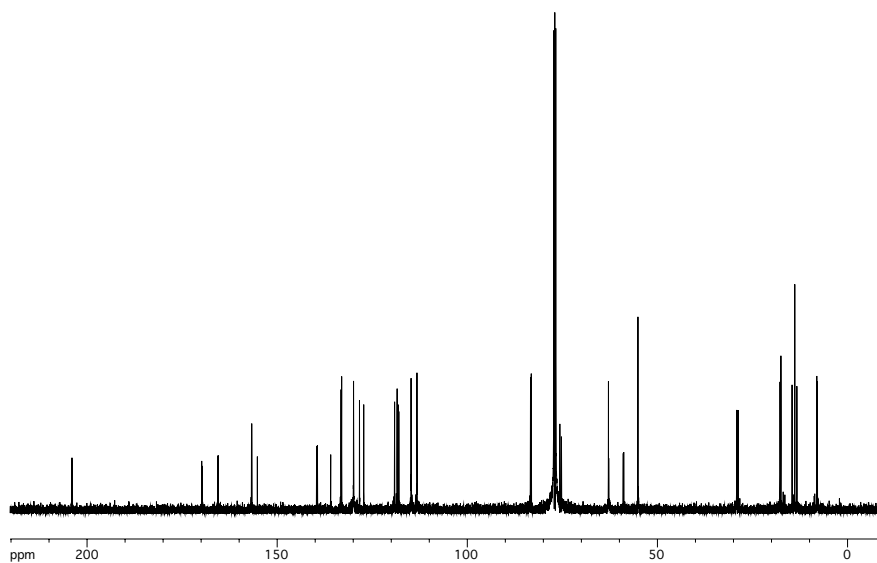
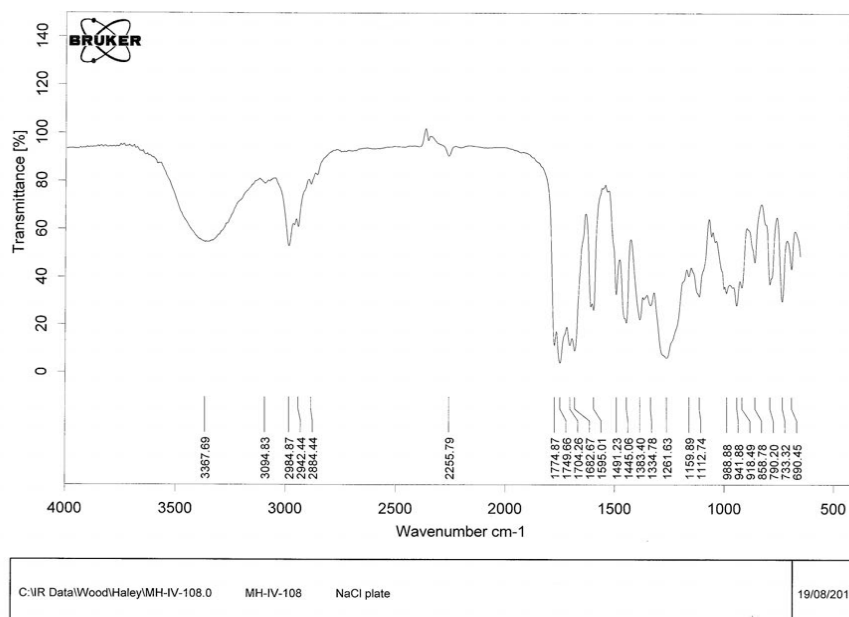
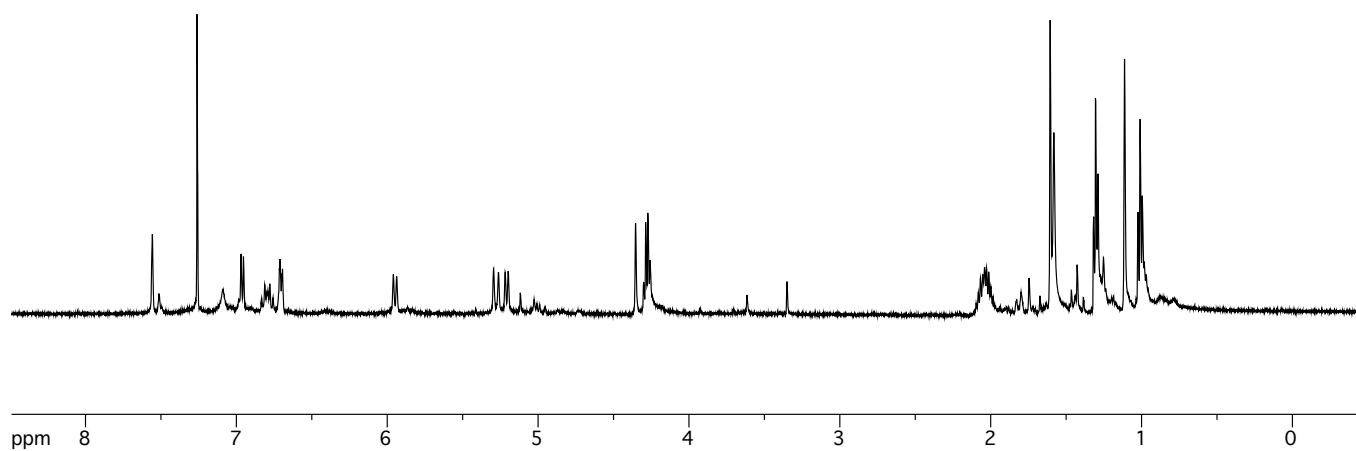
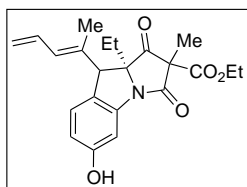


Figure A2.89.  $^{13}\text{C}$ -NMR of allylic carbonate **275**.



Page 1/1

Figure A2.90. FTIR of allylic carbonate **275**.



**Figure A2.91.** <sup>1</sup>H-NMR of tricycle **276**.

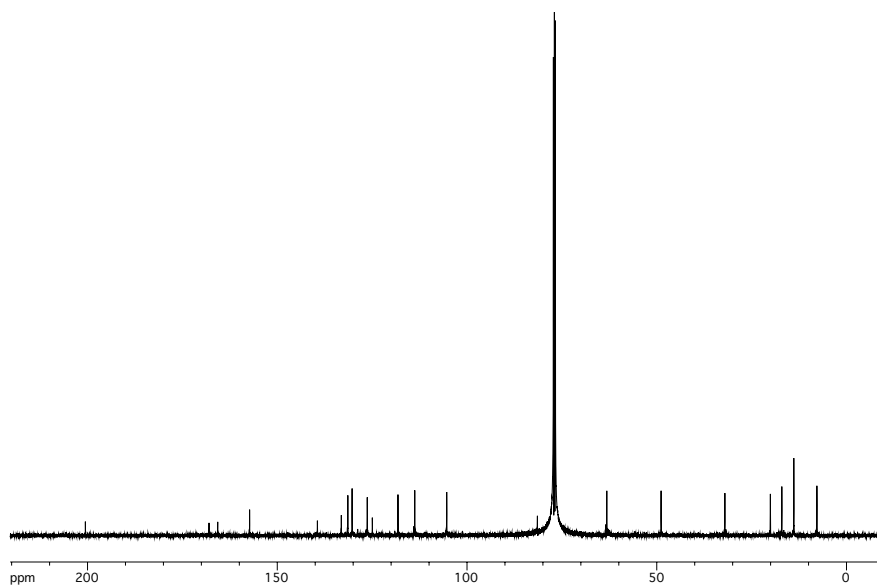
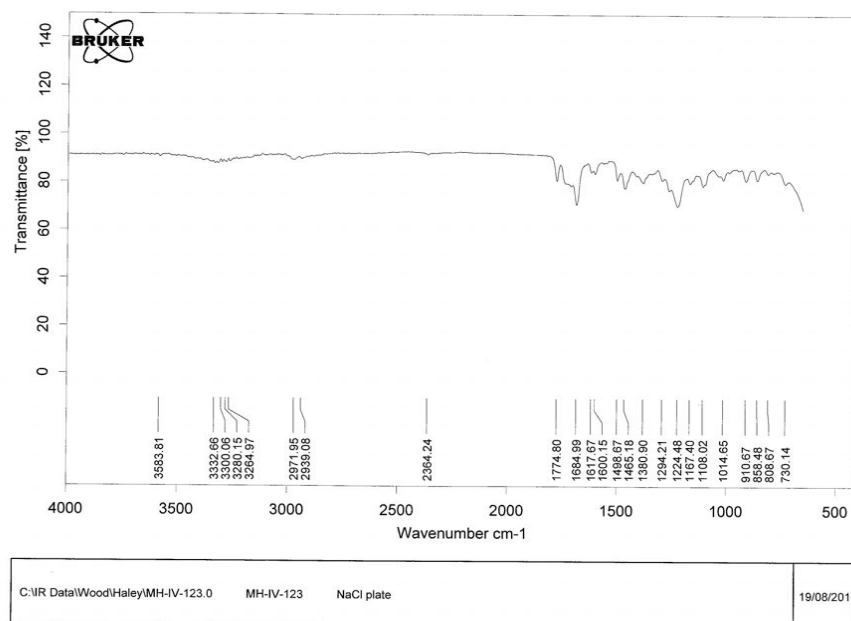
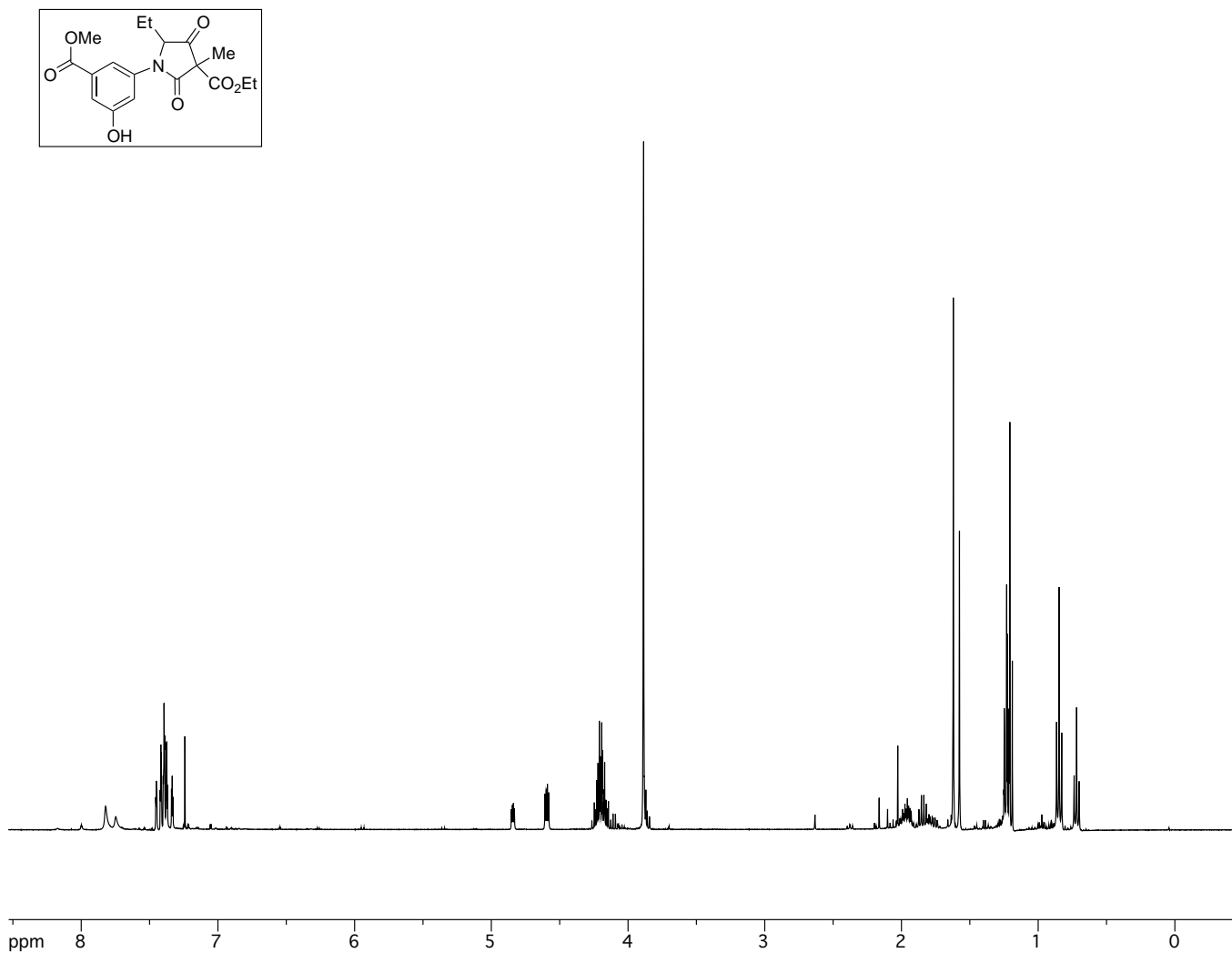


Figure A2.92.  $^{13}\text{C}$ -NMR of tricycle 276.



Page 1/1

Figure A2.93. FTIR of tricycle 276.



**Figure A2.94.** <sup>1</sup>H-NMR of phenol 463.

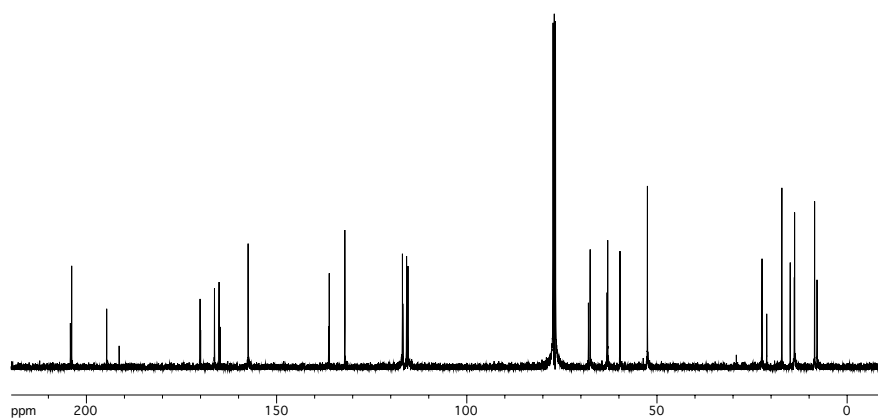


Figure A2.95.  $^{13}\text{C-NMR}$  of phenol 463.

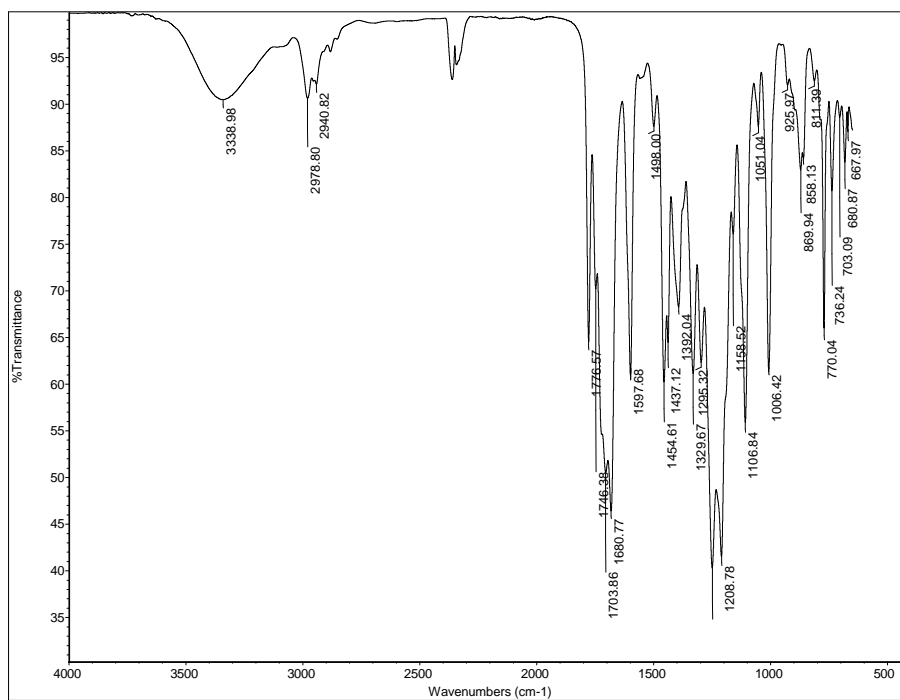
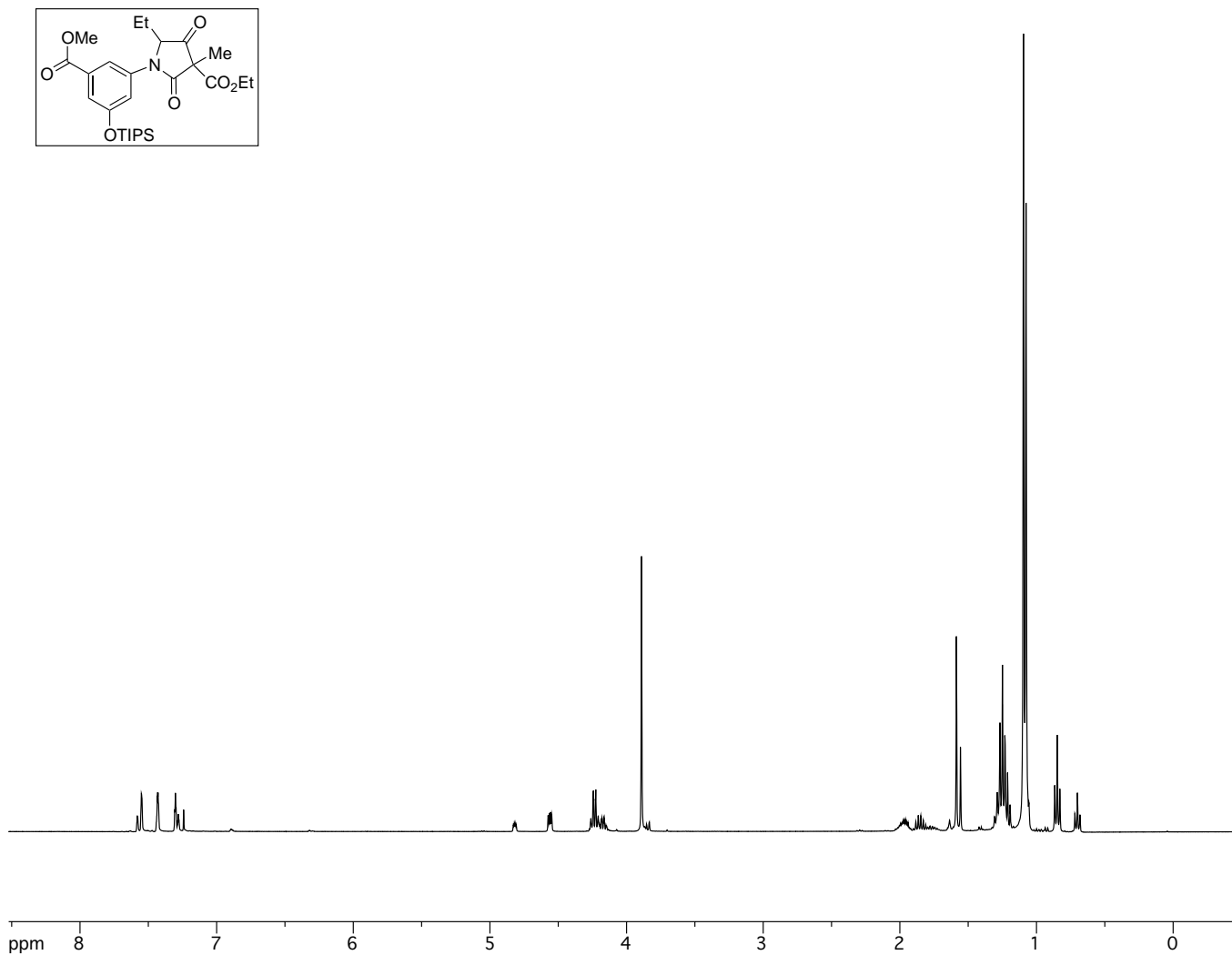
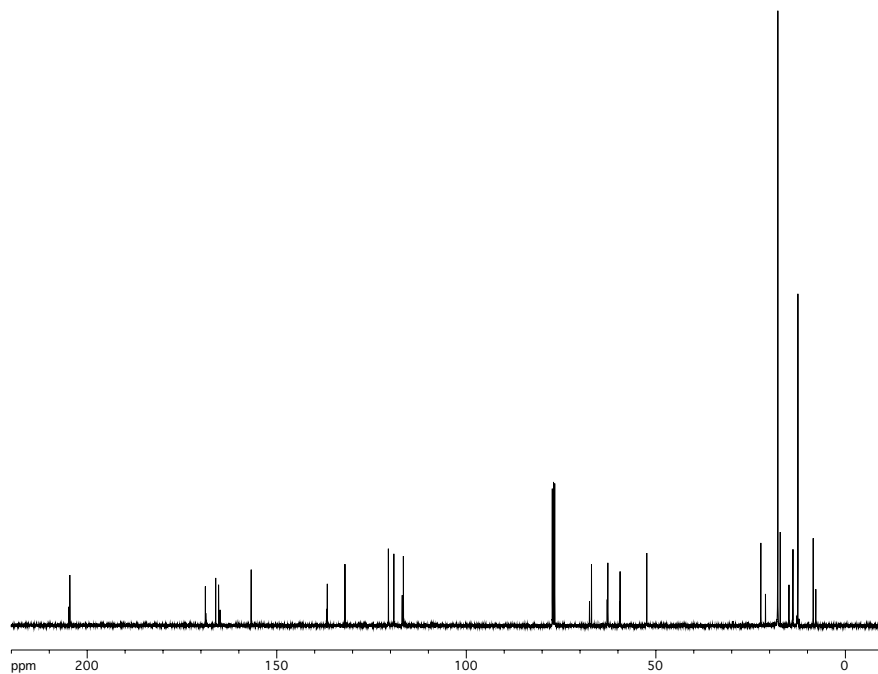


Figure A2.96. FTIR of phenol 463.



**Figure A2.97.** <sup>1</sup>H-NMR of tetramic acid **280**.



**Figure A2.98.**  $^{13}\text{C-NMR}$  of tetramic acid **280**.

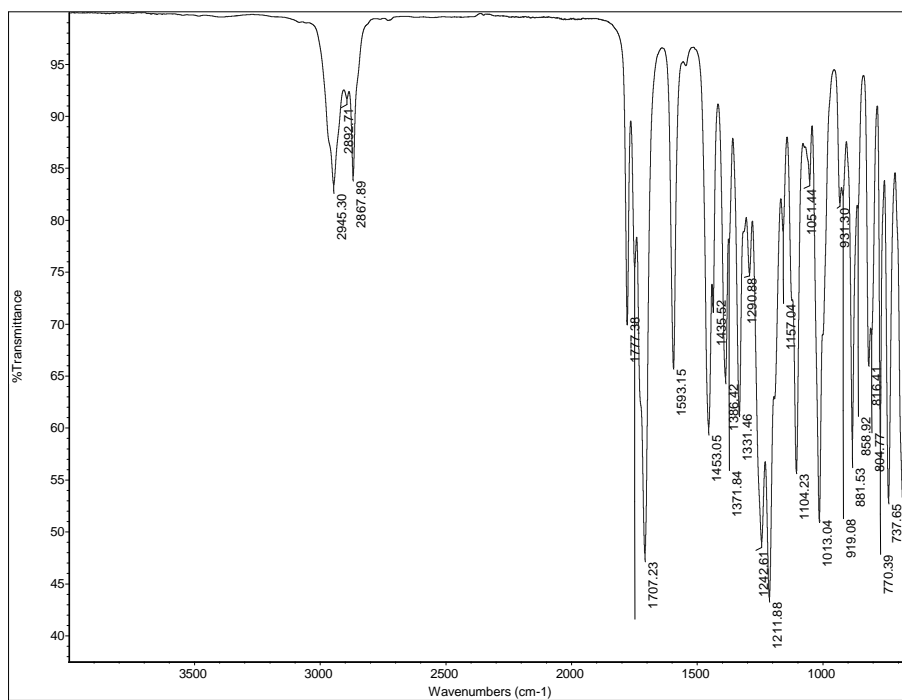


**Figure A2.99.** FTIR of tetramic acid **280**.

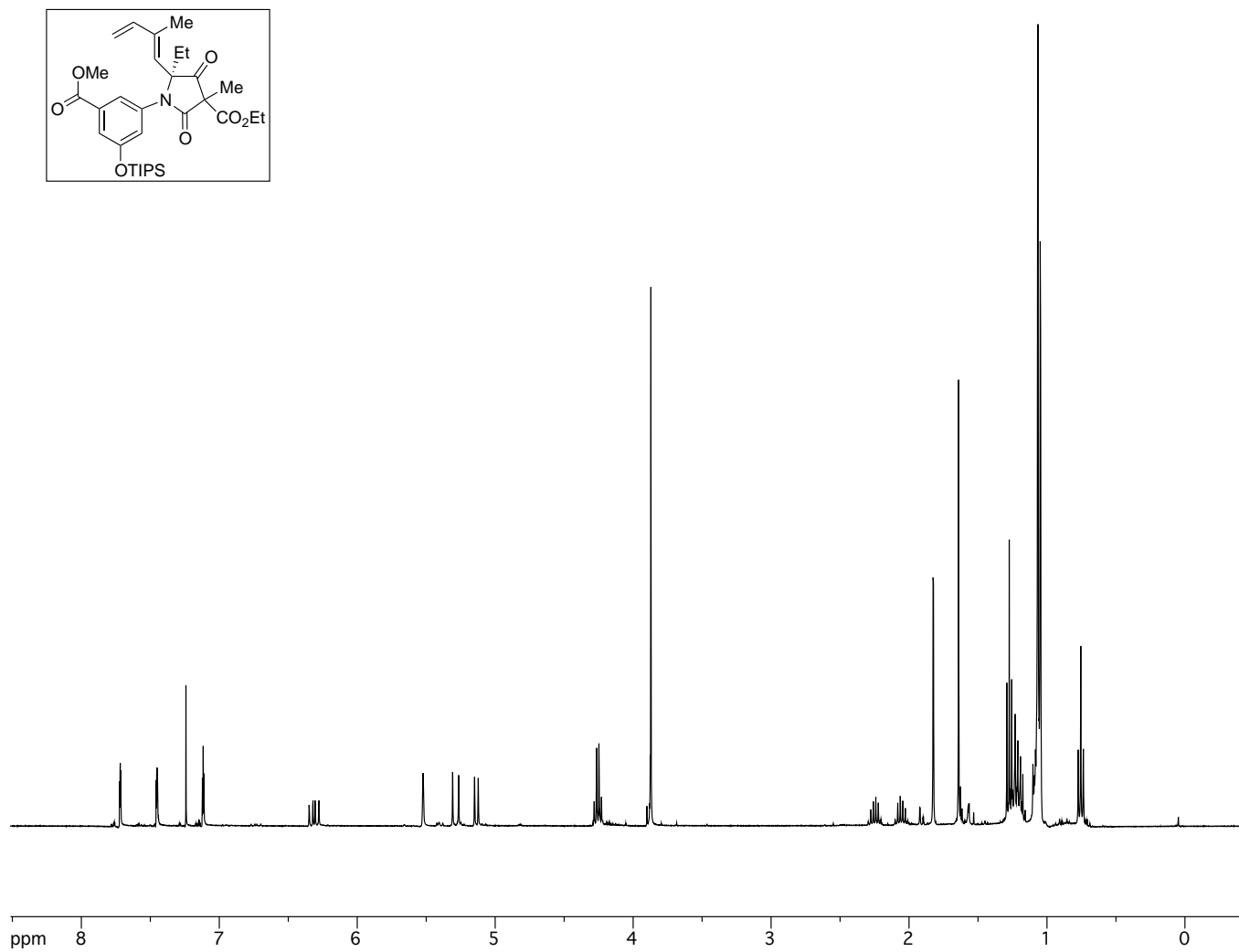


**Figure A2.100.** <sup>1</sup>H-NMR of diene 287.

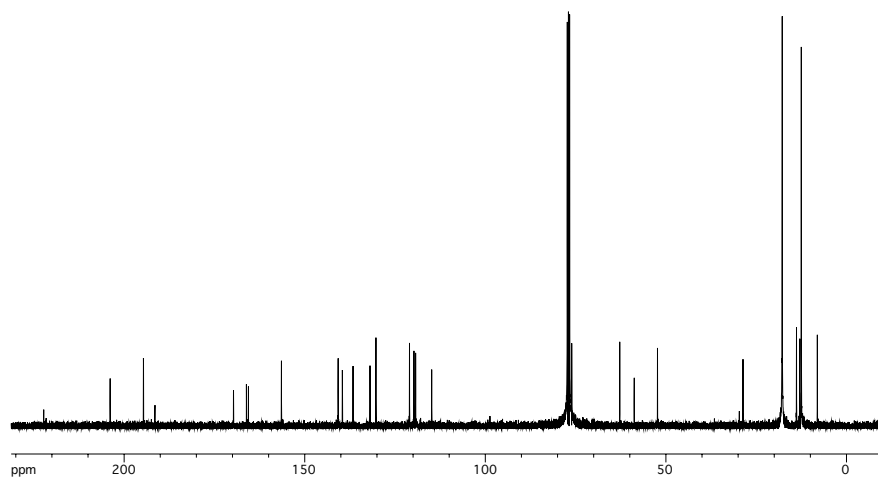


Figure A2.101.  $^{13}\text{C-NMR}$  of diene 287.

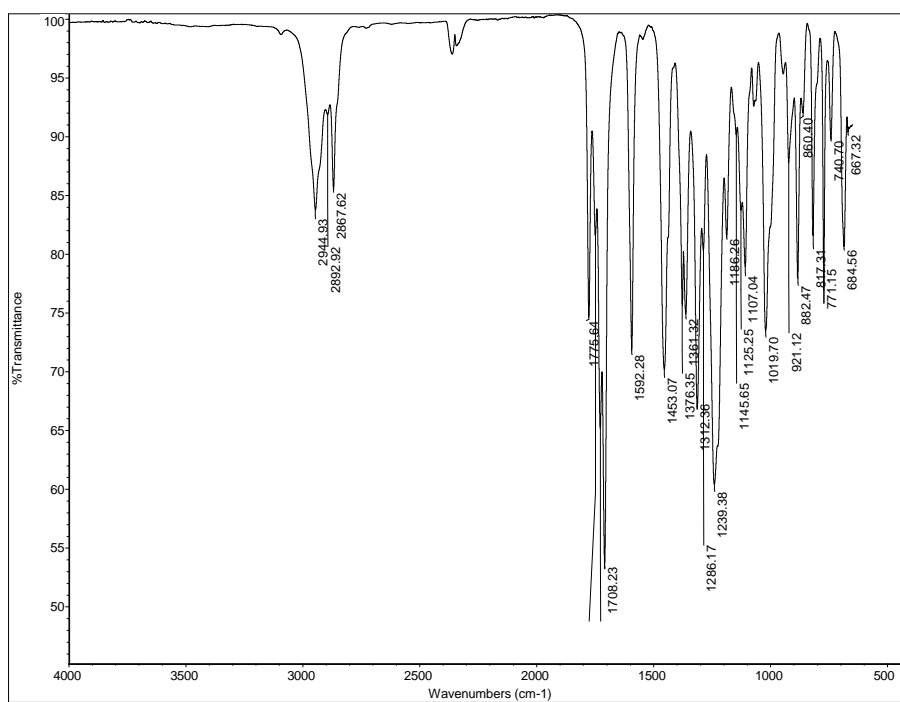
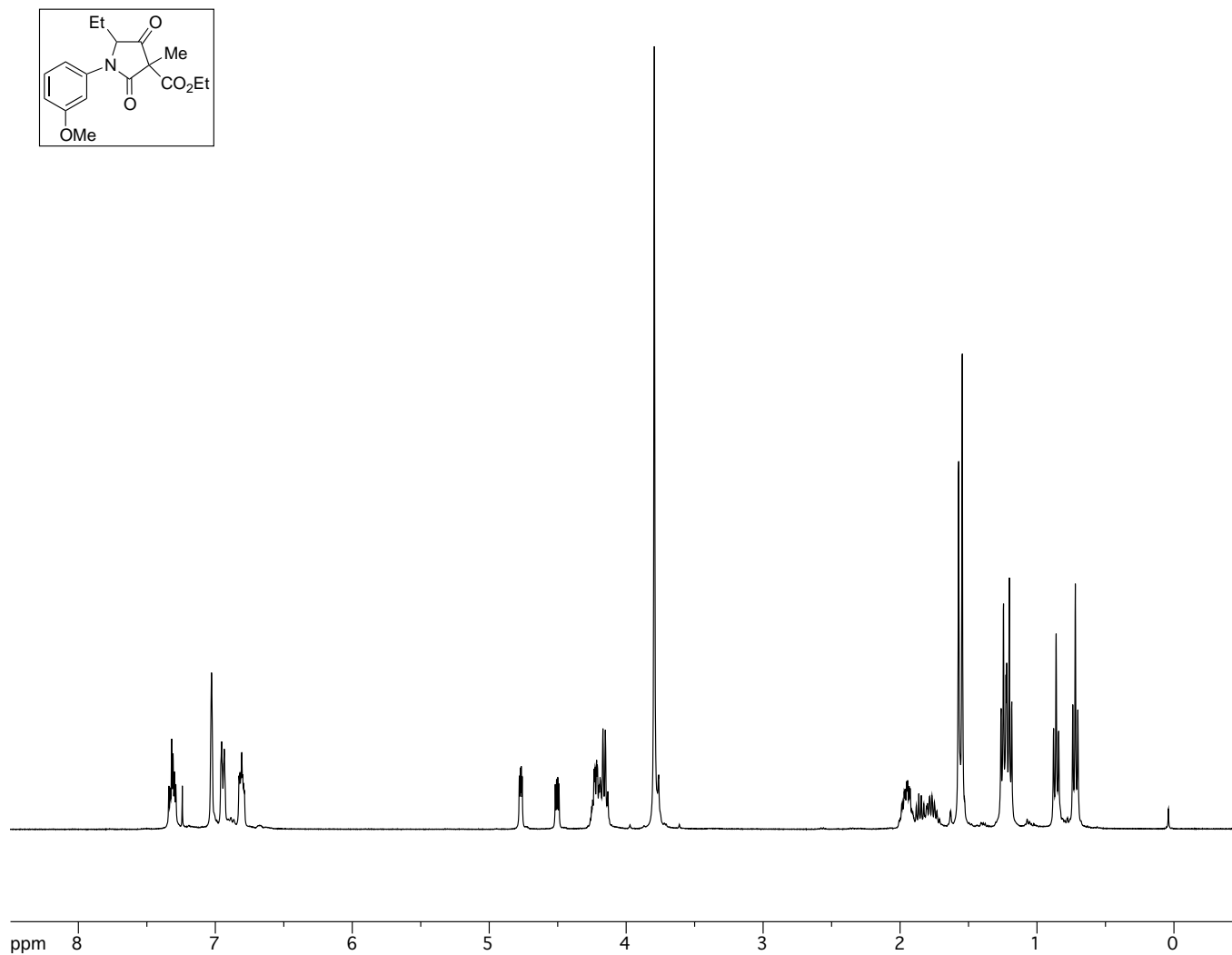


Figure A2.102. FTIR of diene 287.



**Figure A2.103.** <sup>1</sup>H-NMR of tetramic acid **295**.

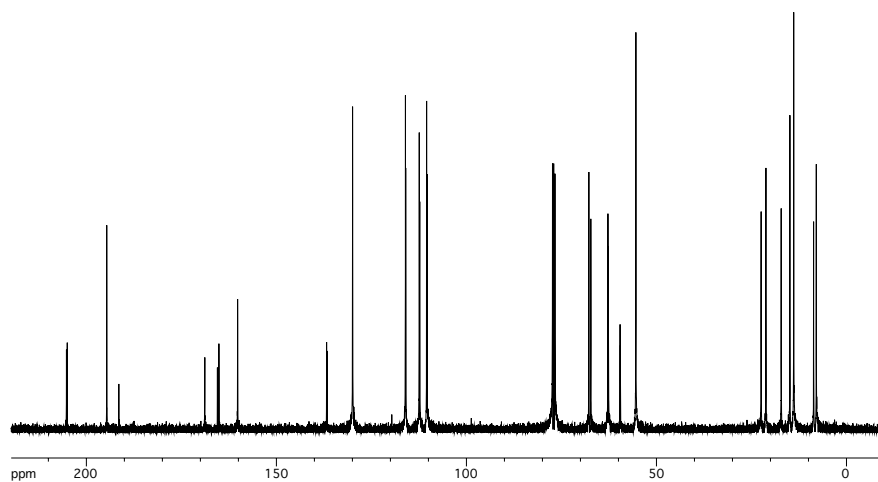


Figure A2.104.  $^{13}\text{C-NMR}$  of tetramic acid 295.

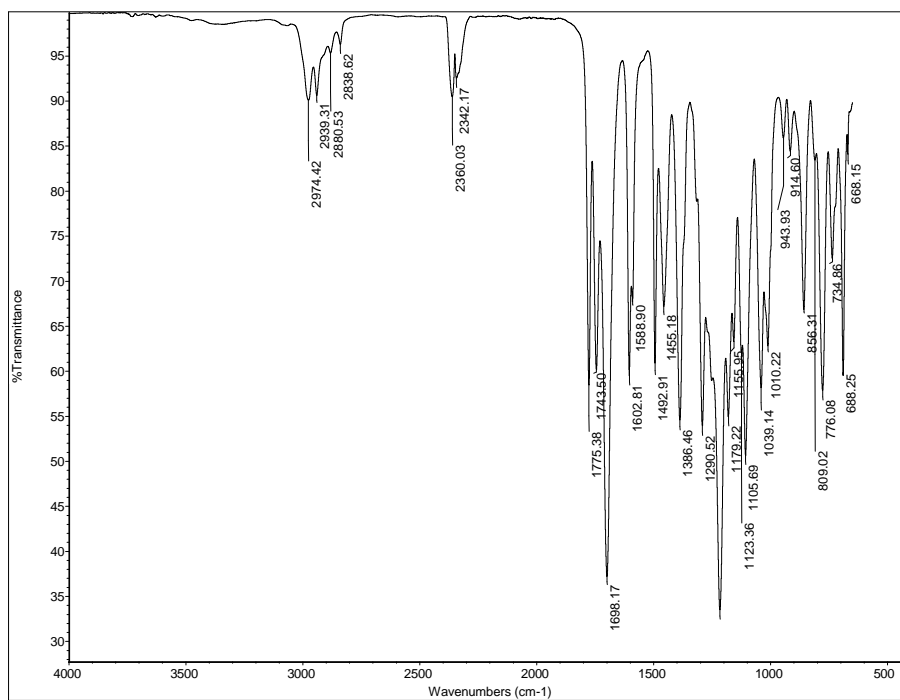
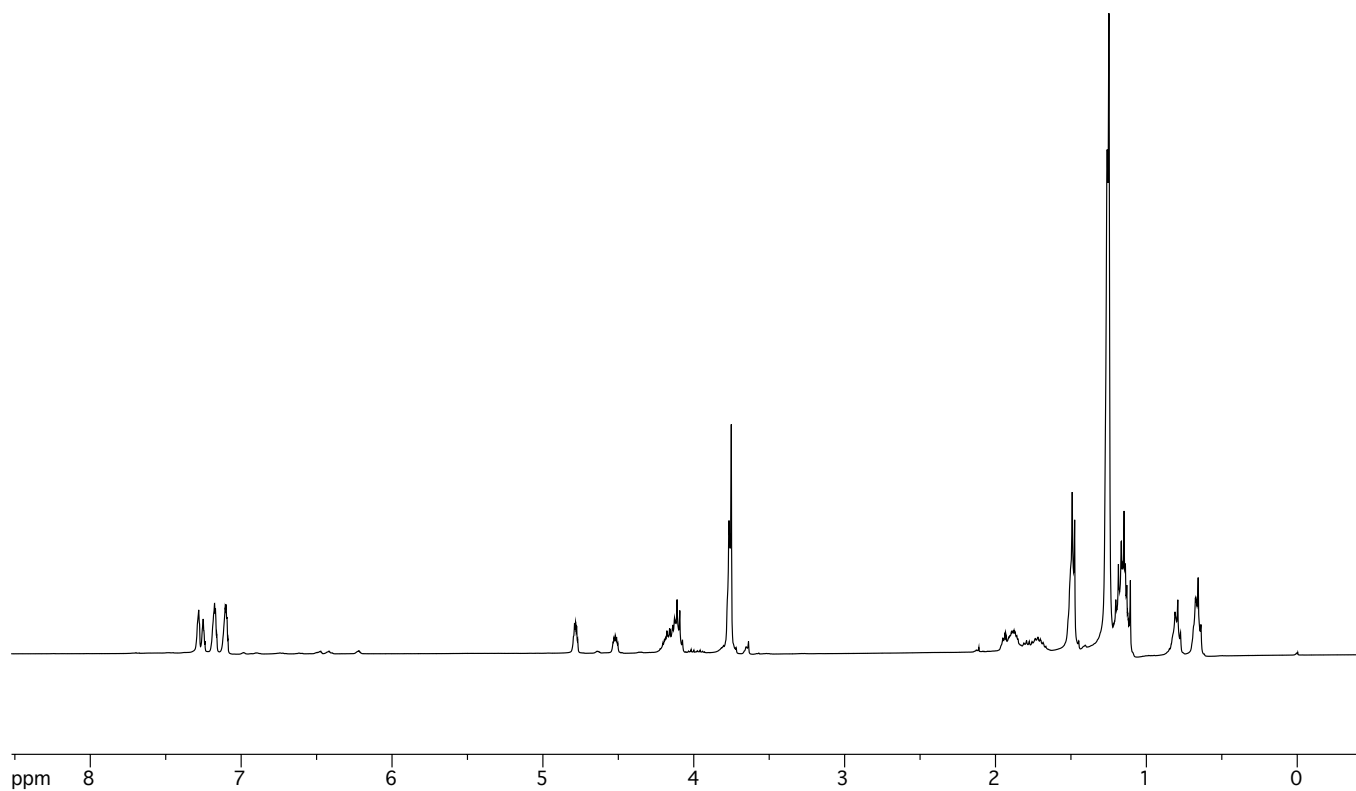
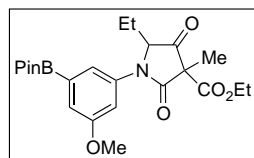


Figure A2.105. FTIR of tetramic acid 295.



**Figure A2.106.**  $^1\text{H-NMR}$  of aryl boronic ester **296**.

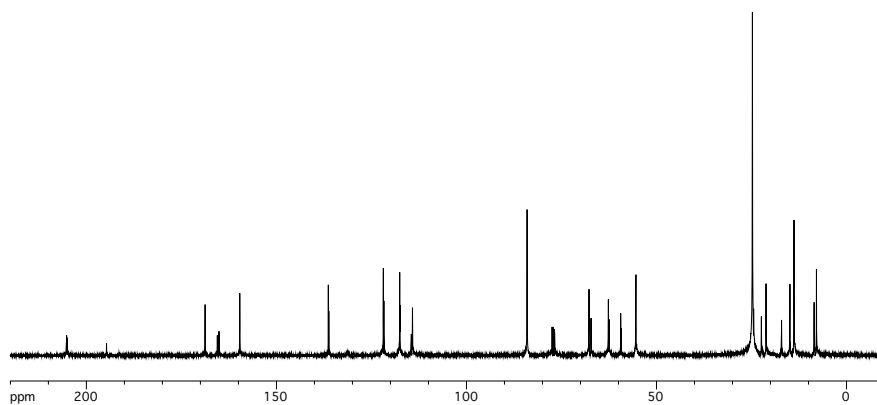


Figure A2.107.  $^{13}\text{C-NMR}$  of aryl boronic ester **296**.

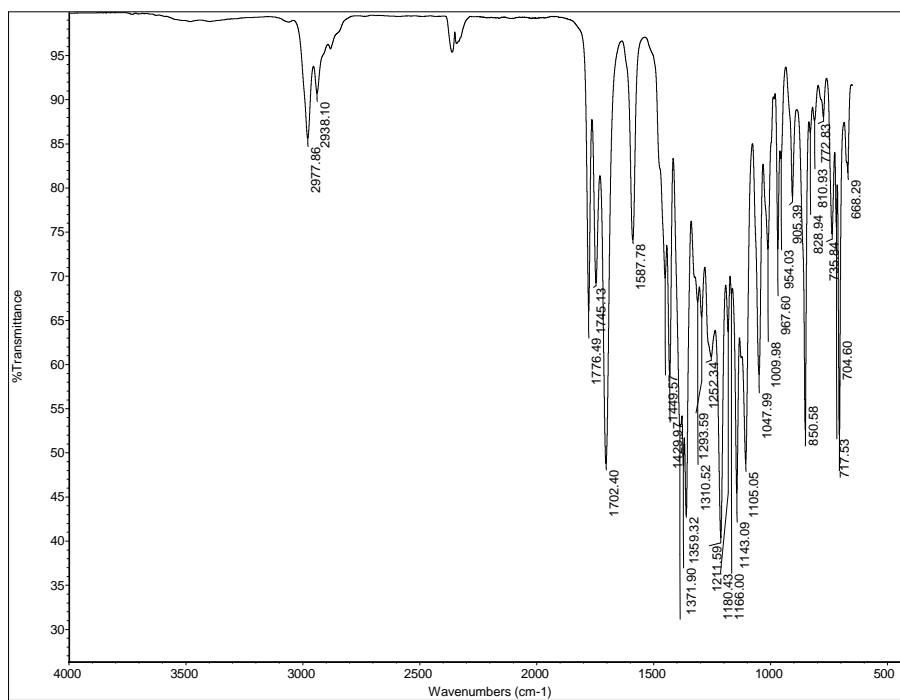


Figure A2.108. FTIR of aryl boronic ester **296**.

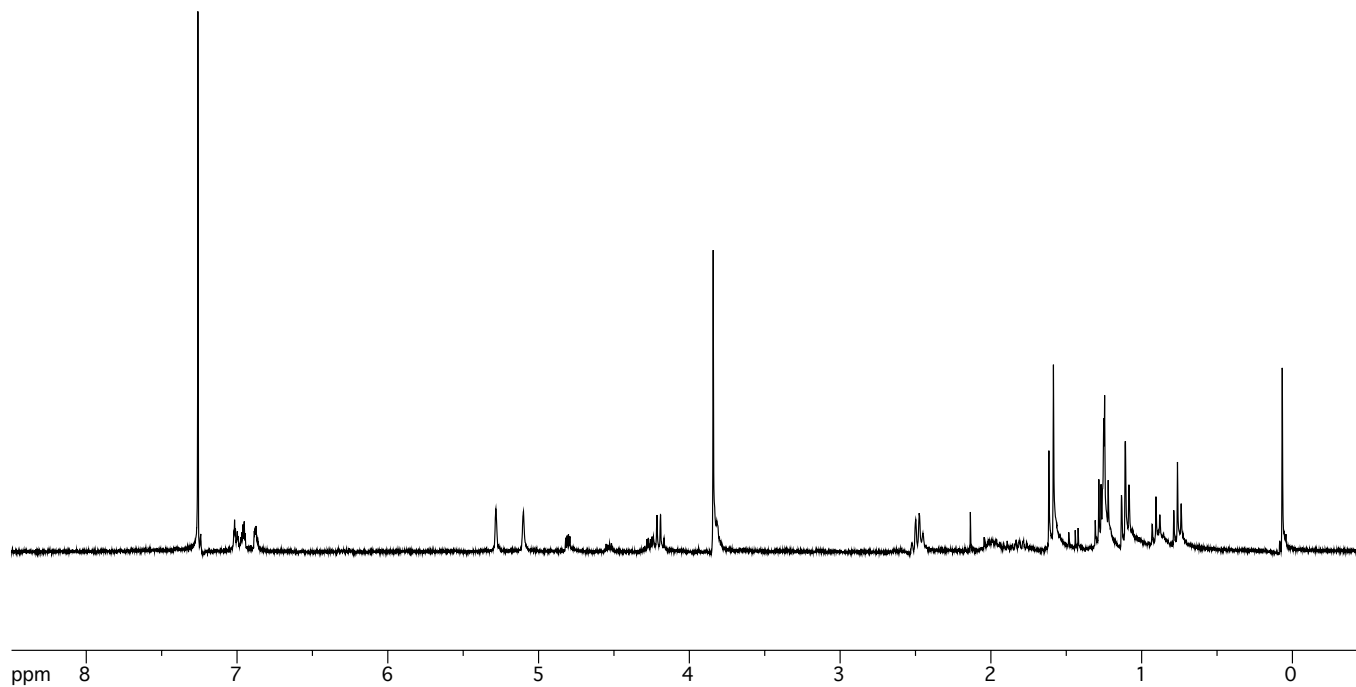
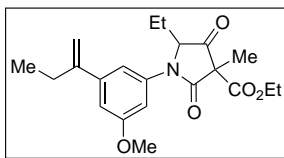
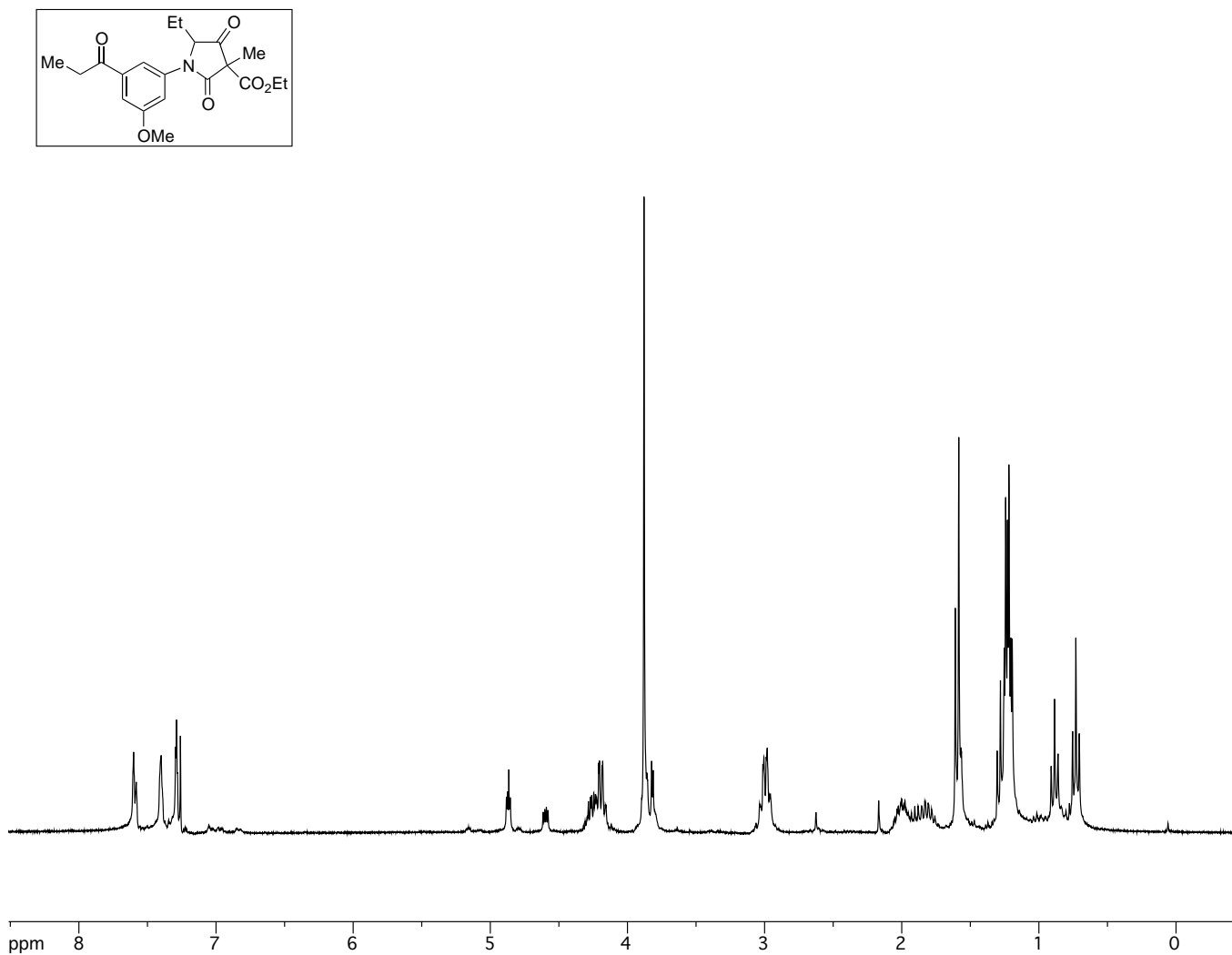
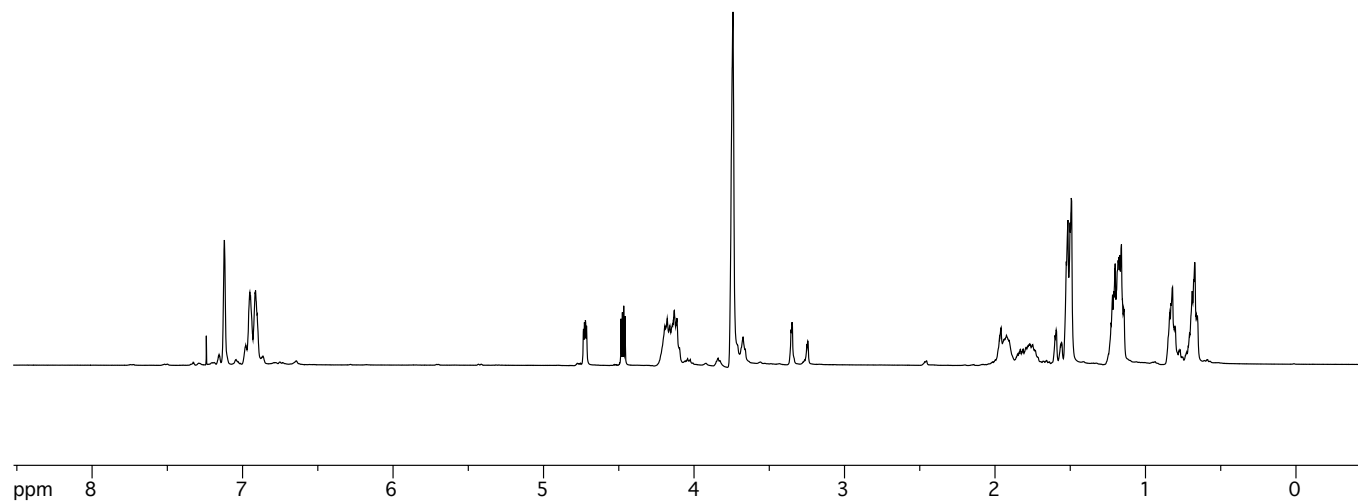
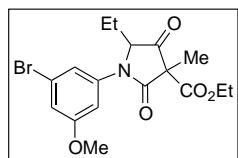


Figure A2.109. <sup>1</sup>H-NMR of styrene 297.



**Figure A2.110.** <sup>1</sup>H-NMR of ketone **298**.



**Figure A2.111.** <sup>1</sup>H-NMR of aryl bromide **301**.

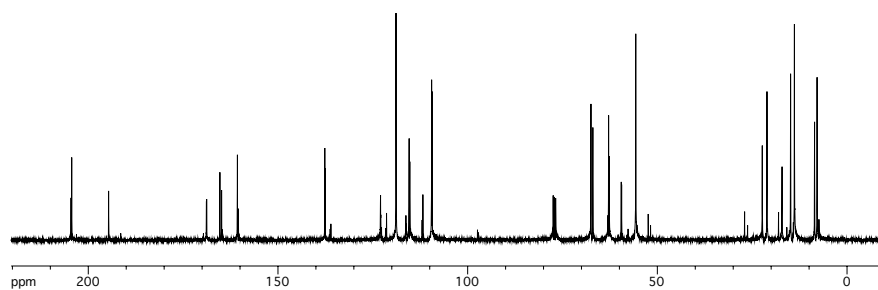


Figure A2.112.  $^{13}\text{C-NMR}$  of aryl bromide **301**.

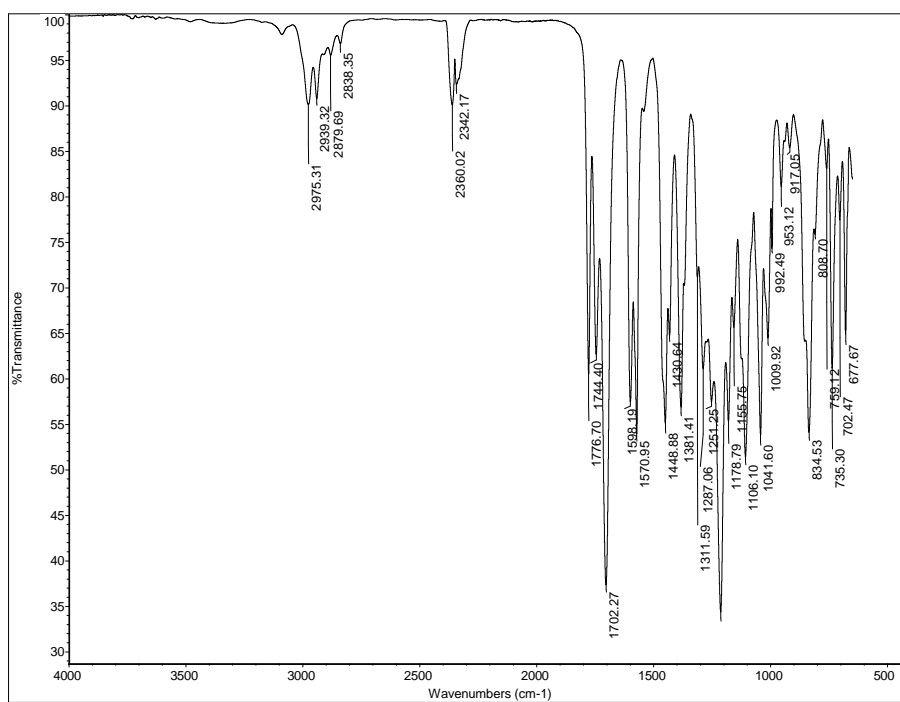
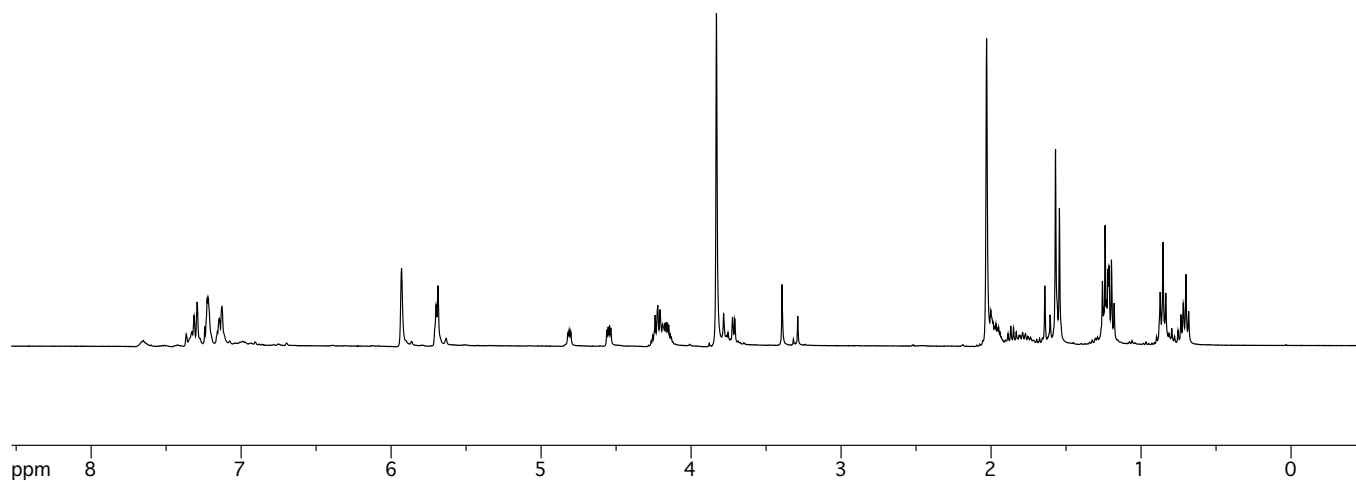
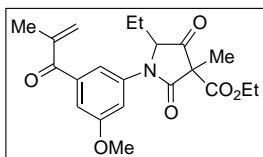


Figure A2.113. FTIR of aryl bromide **301**.



**Figure A2.114.** <sup>1</sup>H-NMR of enone **300**.

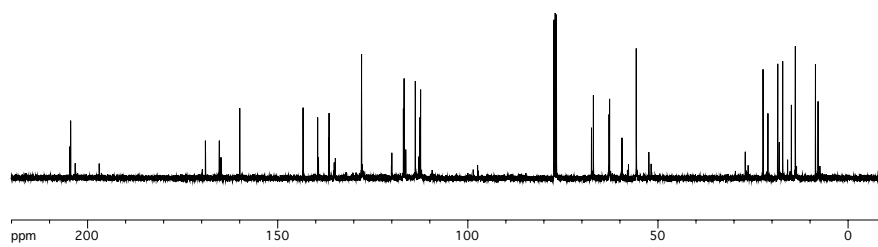


Figure A2.115.  $^{13}\text{C-NMR}$  of enone 300.

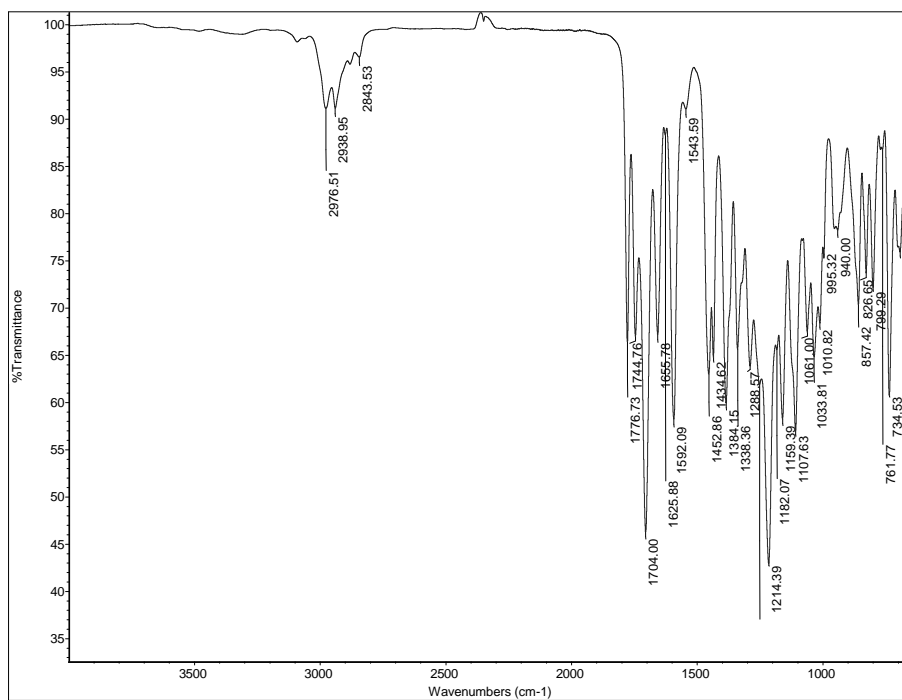
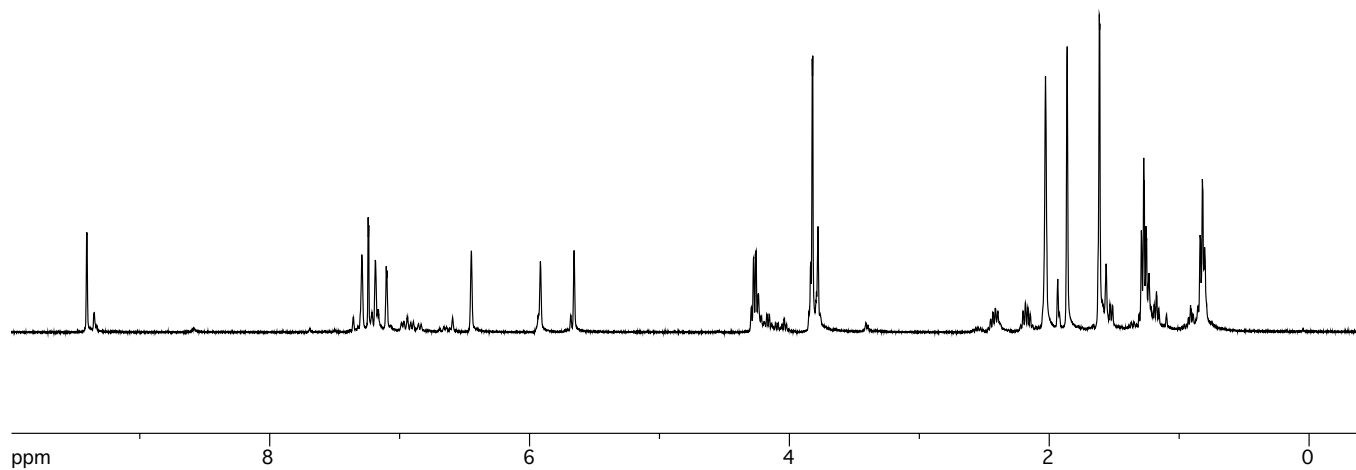
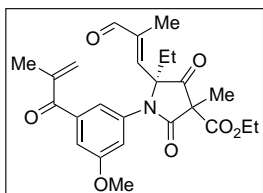


Figure A2.116. FTIR of enone 300.



**Figure A2.117.** <sup>1</sup>H-NMR of enal **464**.

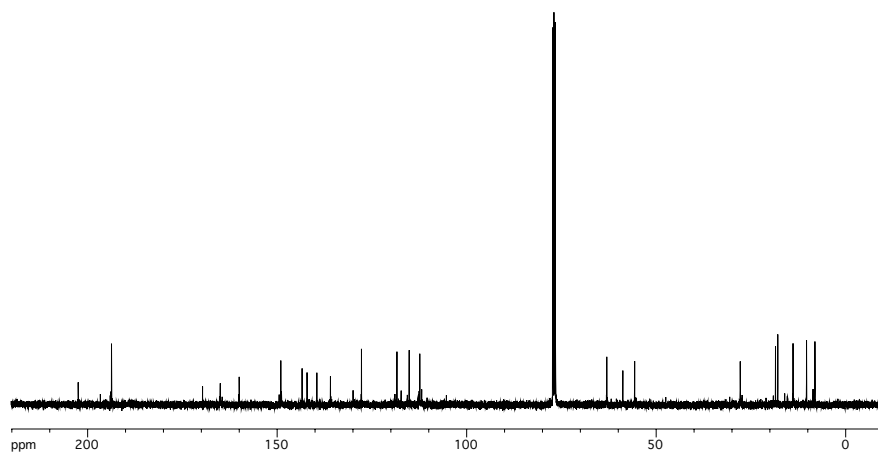


Figure A2.118. <sup>13</sup>C-NMR of enal 464.

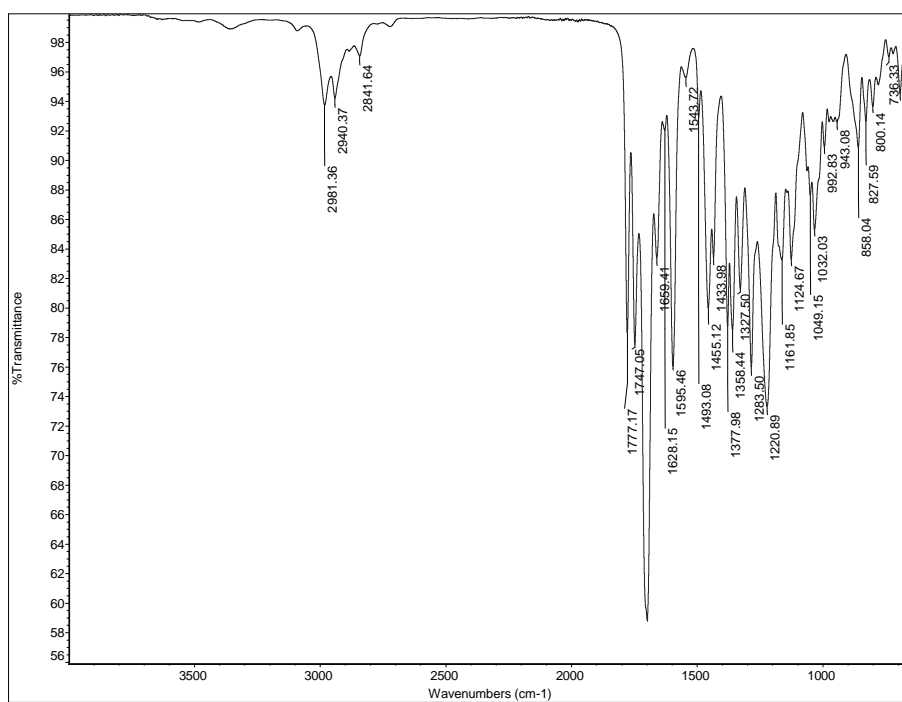
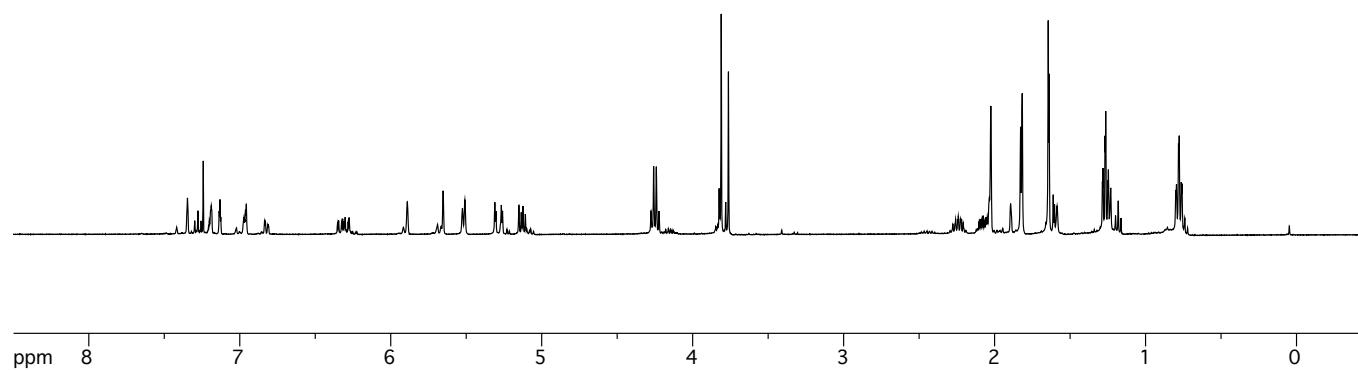
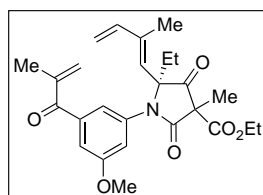
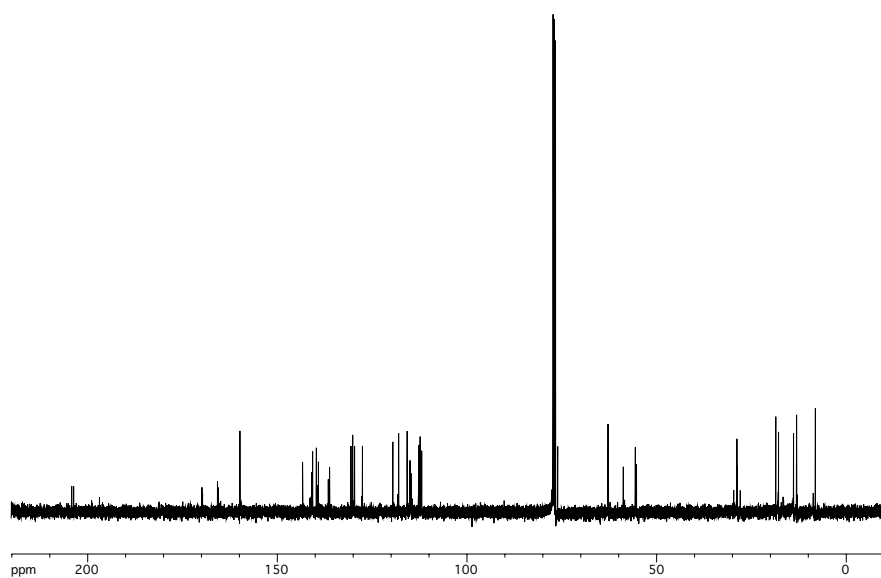


Figure A2.119. FTIR of enal 464.



**Figure A2.120.** <sup>1</sup>H-NMR of triene **303**.



**Figure A2.121.**  $^{13}\text{C}$ -NMR of triene **303**.

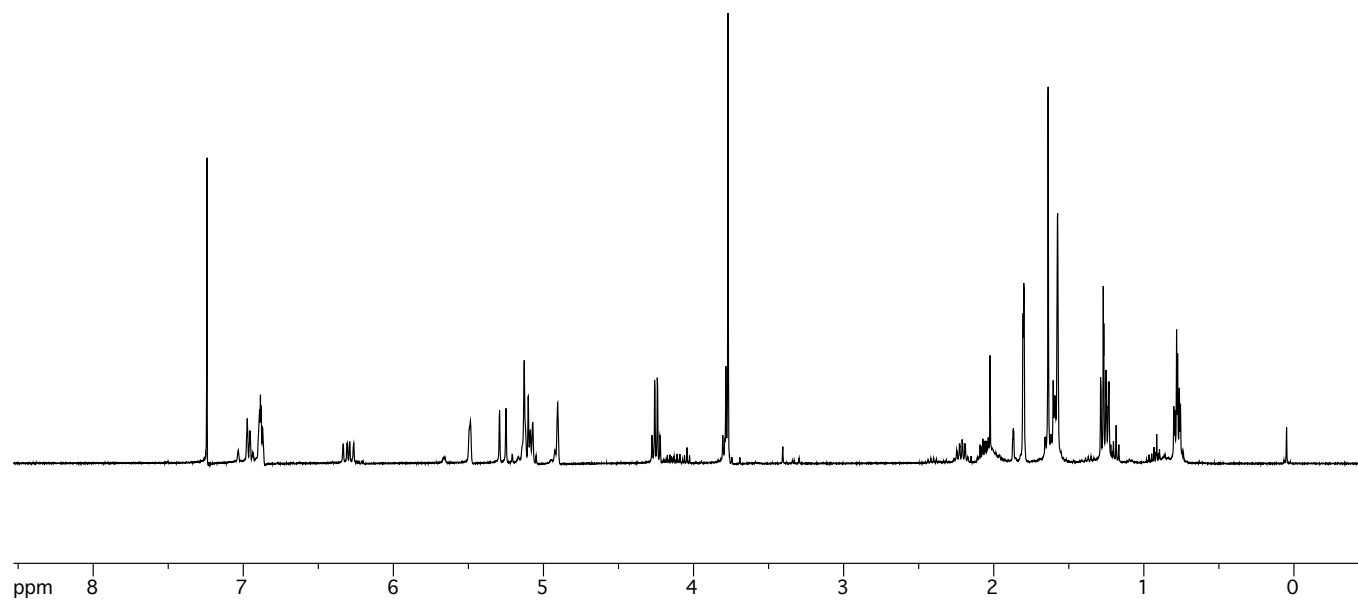
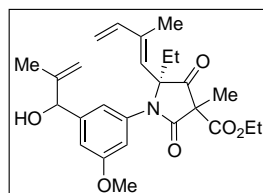


**Figure A2.122.** <sup>1</sup>H-NMR of allylic alcohol **304**.

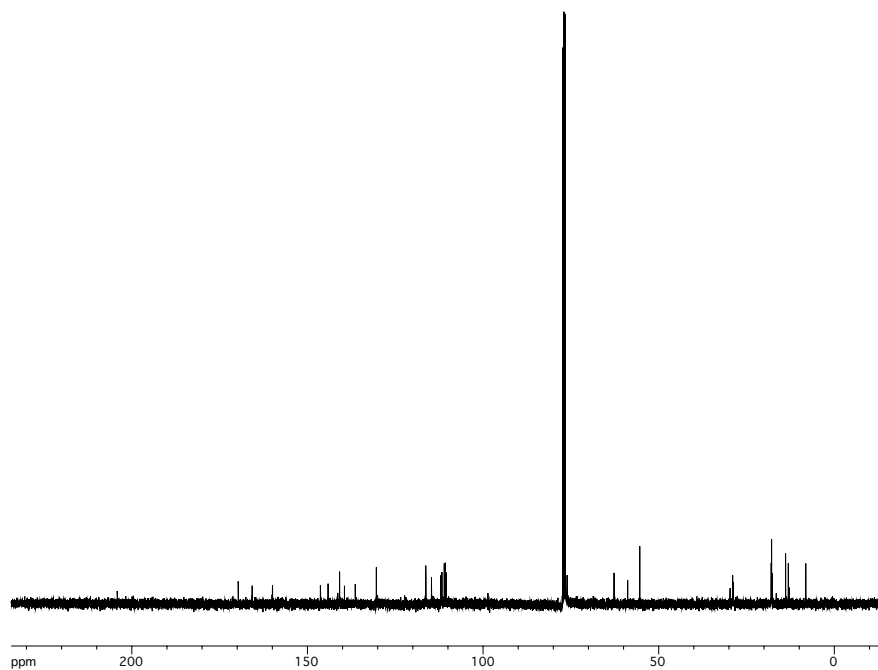


Figure A2.123.  $^{13}\text{C}$ -NMR of allylic alcohol **304**.

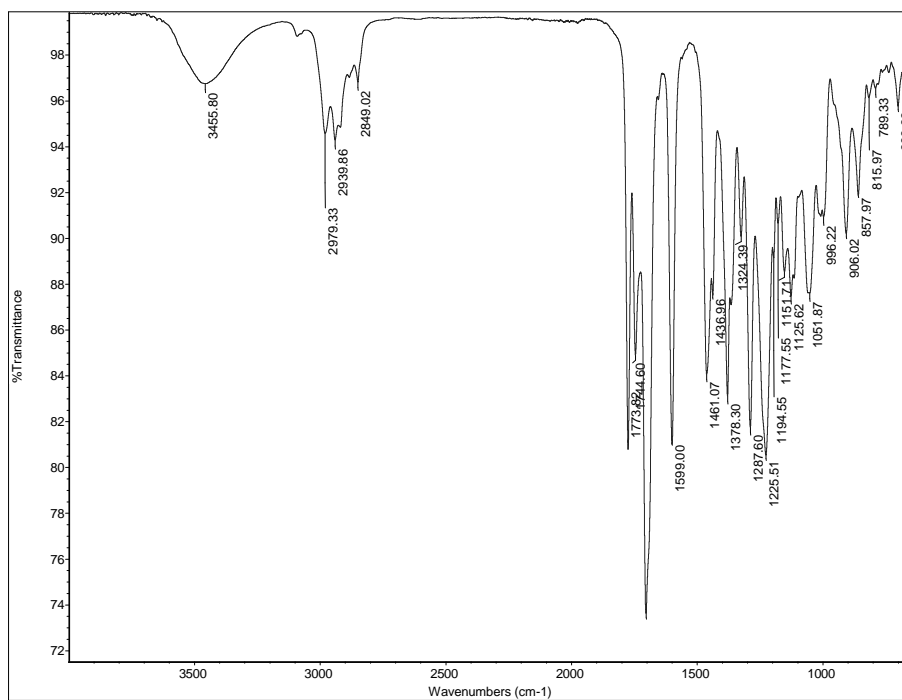


Figure A2.124. FTIR of allylic alcohol **304**.

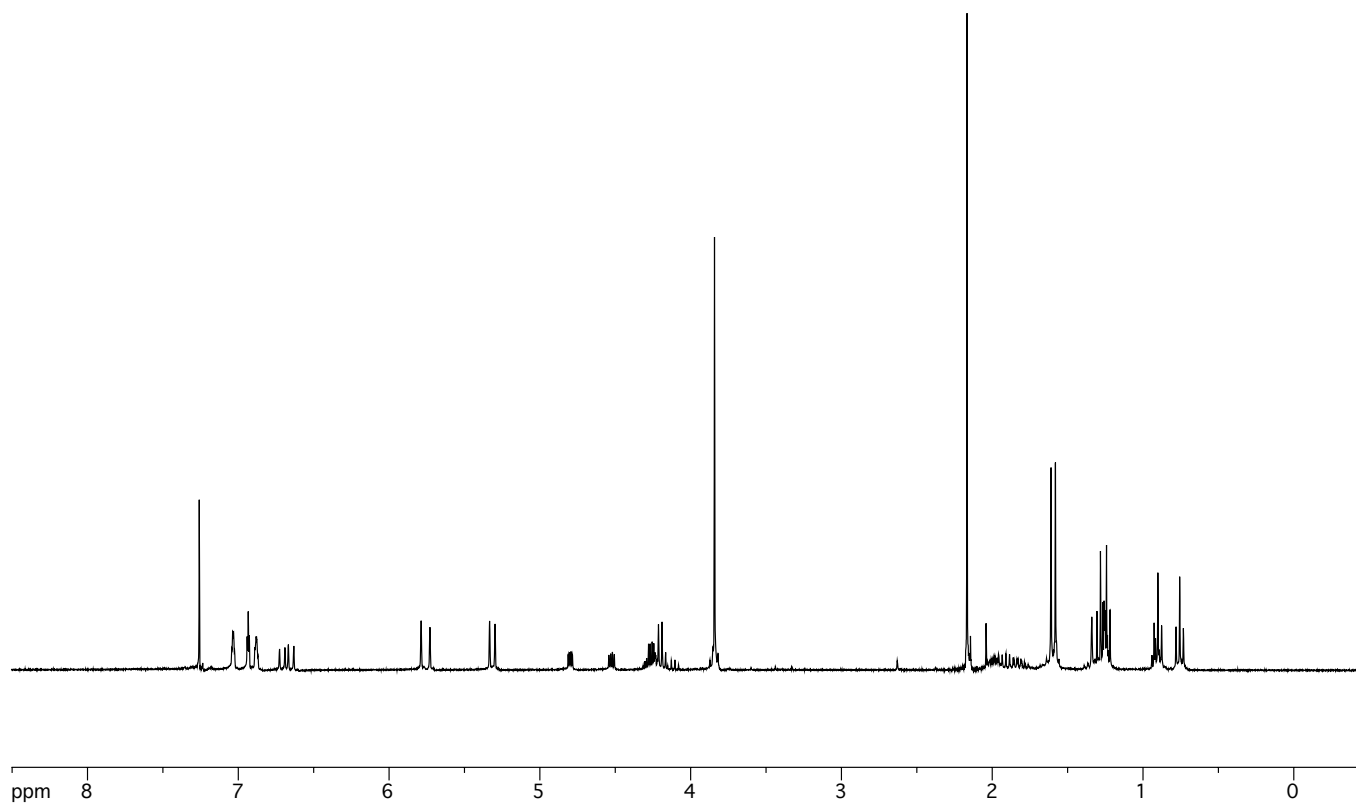
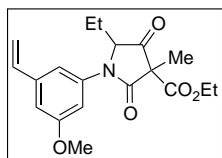
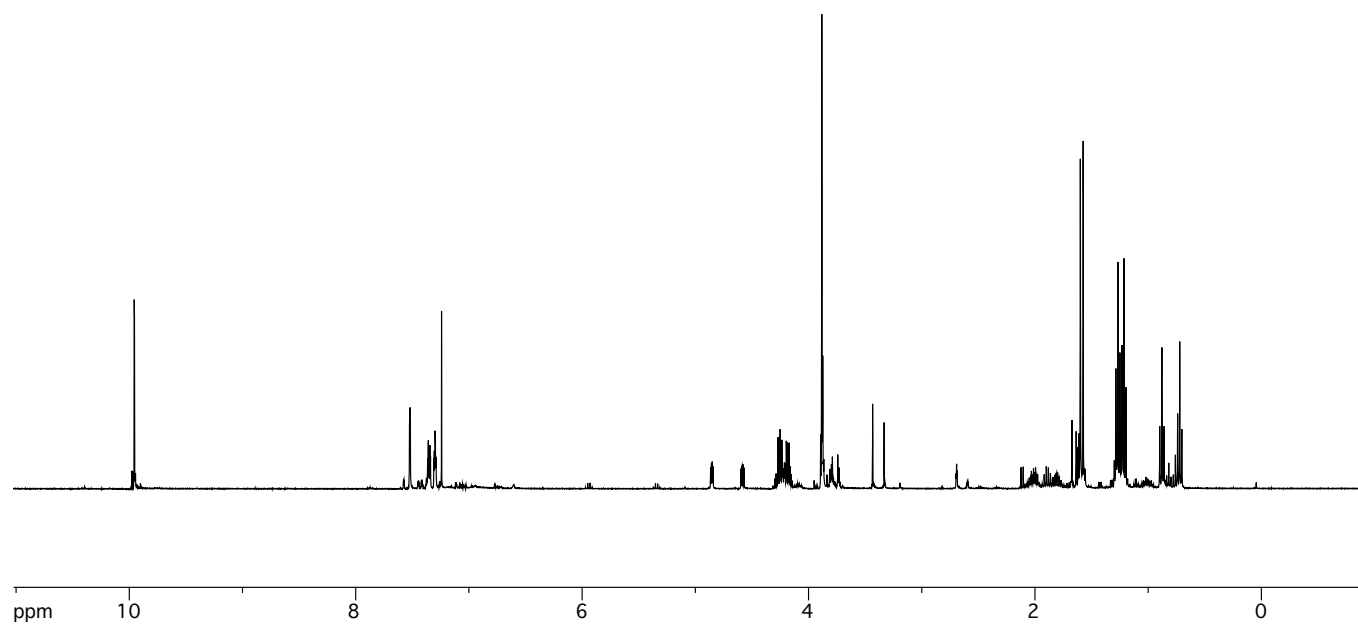
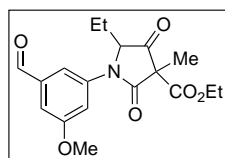


Figure A2.125. <sup>1</sup>H-NMR of styrene 313.



**Figure A2.126.** <sup>1</sup>H-NMR of benzaldehyde **312**.

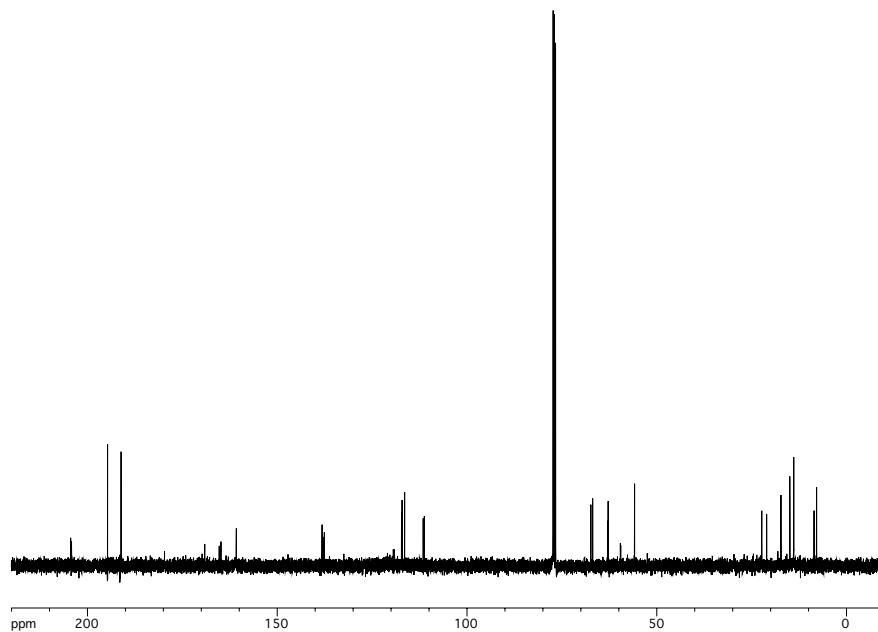


Figure A2.127. <sup>13</sup>C-NMR of benzaldehyde **312**.

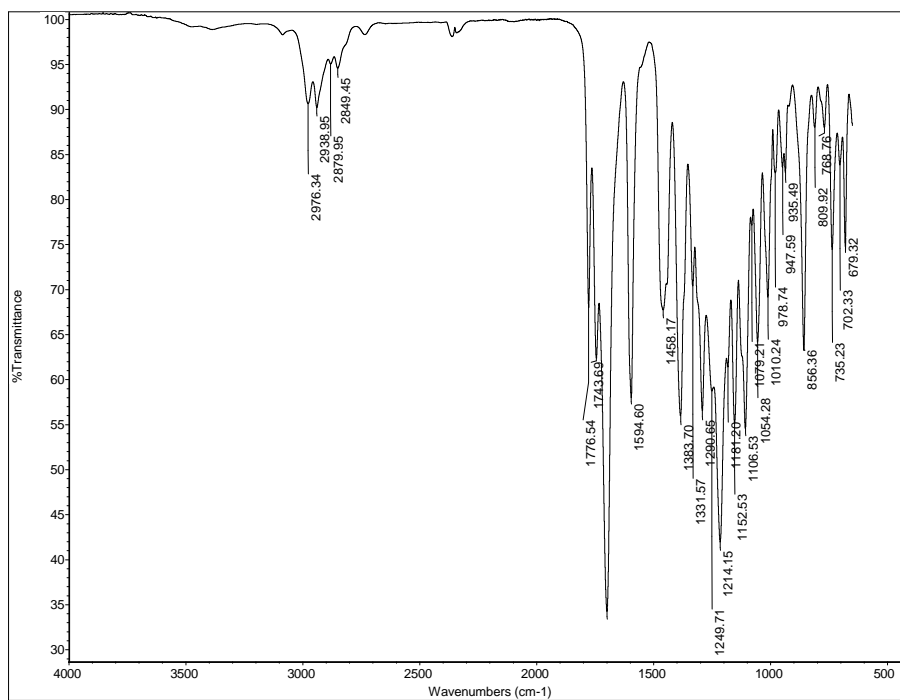


Figure A2.128. FTIR of benzaldehyde **312**.

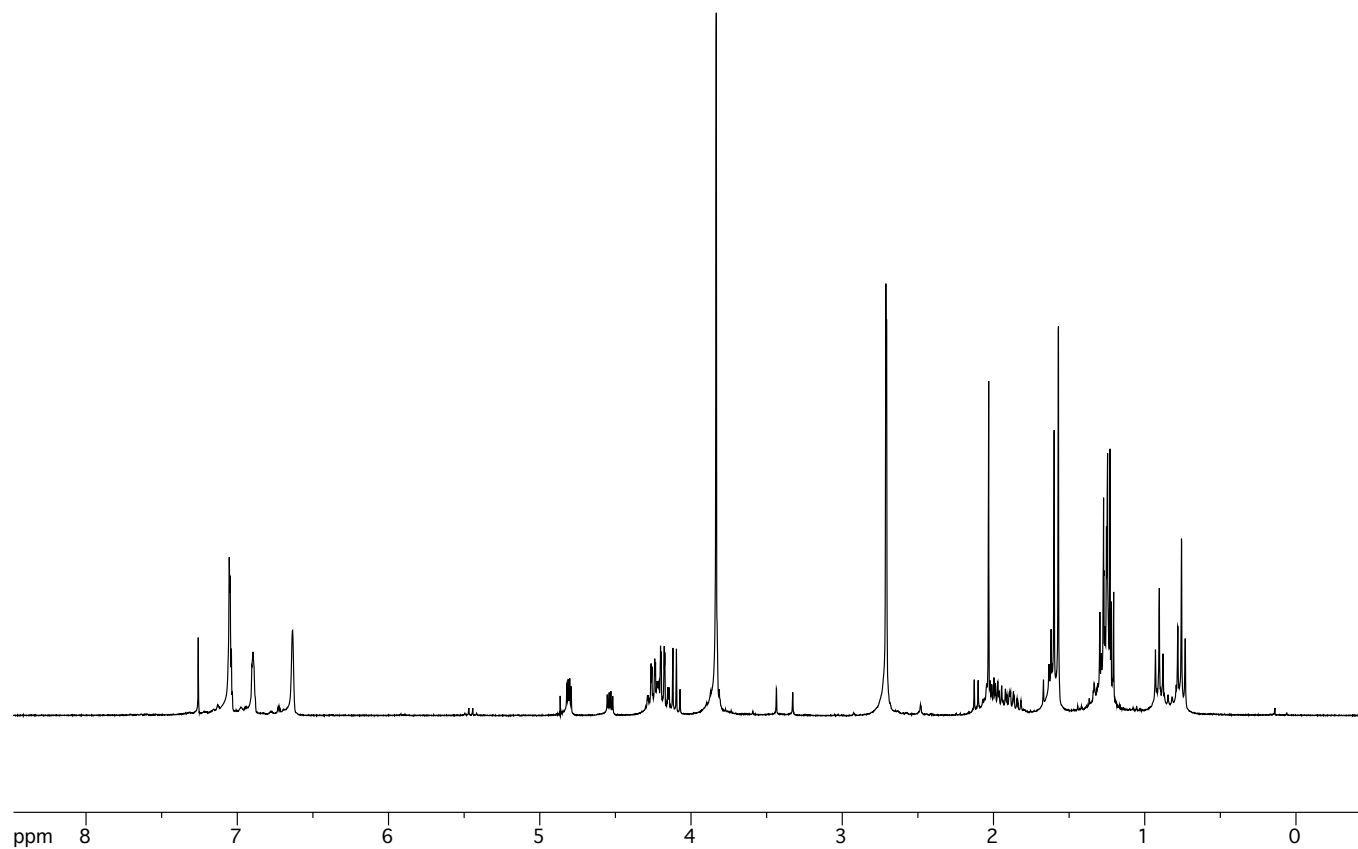
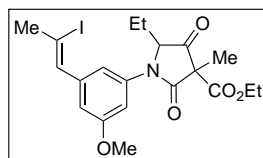


Figure A2.129. <sup>1</sup>H-NMR of vinyl iodide 314.

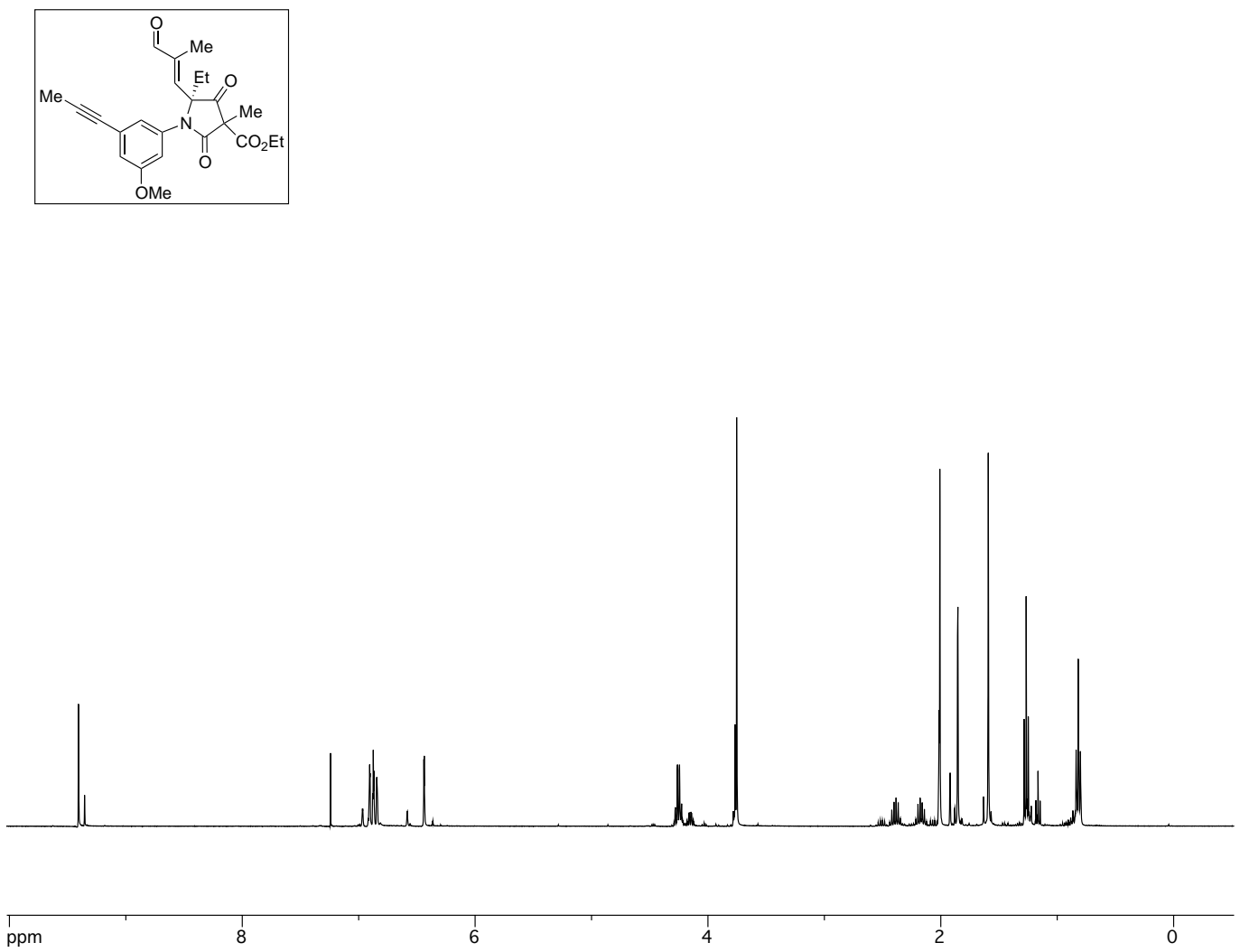


Figure A2.130. <sup>1</sup>H-NMR of alkyne 315.

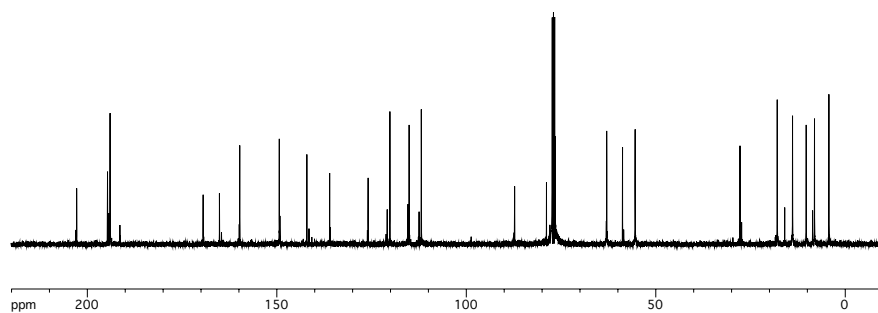


Figure A2.131.  $^{13}\text{C}$ -NMR of alkyne **315**.

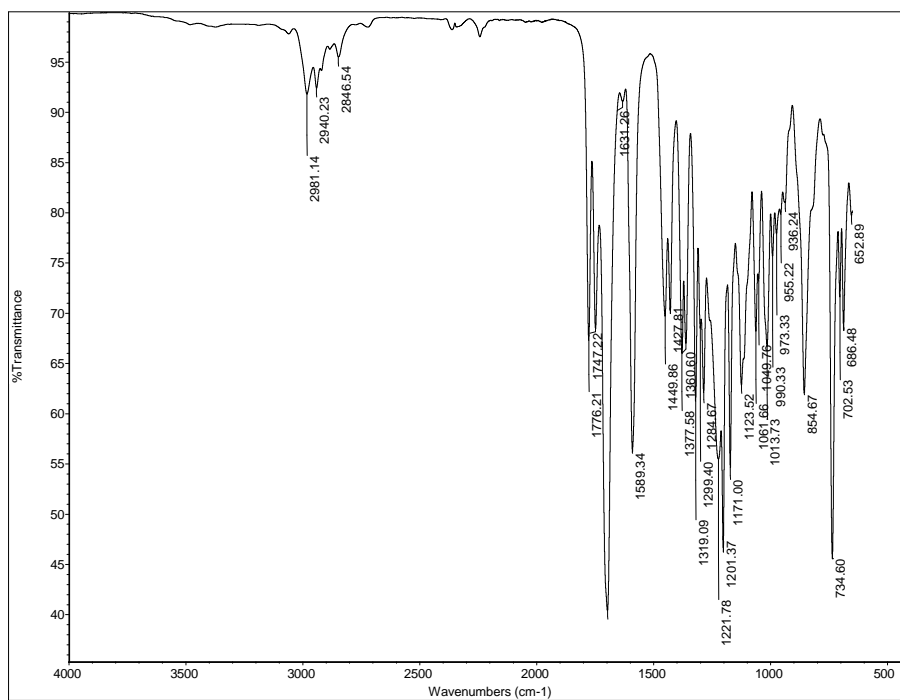
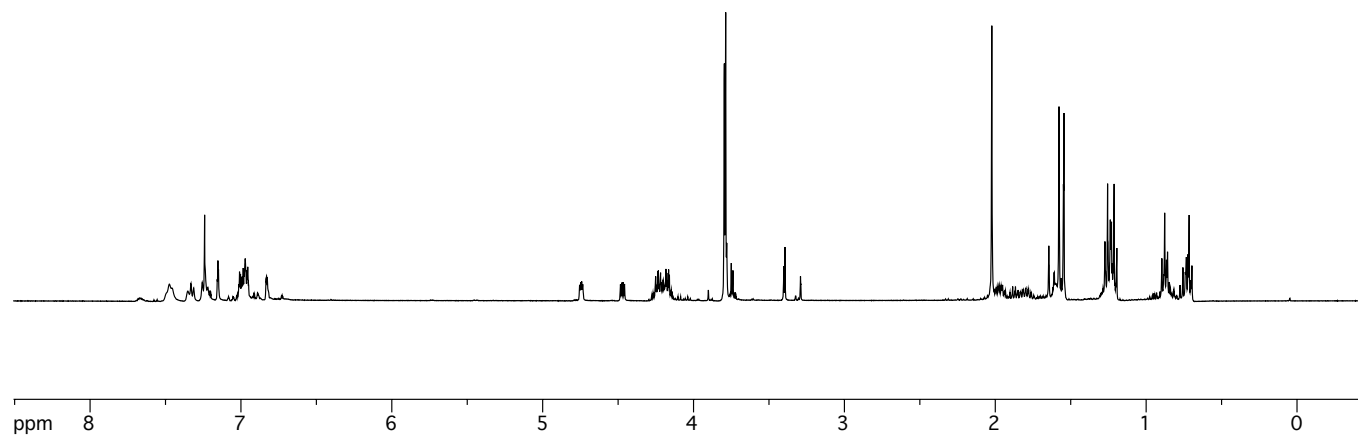
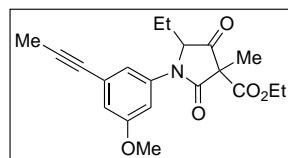


Figure A2.132. FTIR of alkyne **315**.



**Figure A2.133.** <sup>1</sup>H-NMR of alkyne **358**.

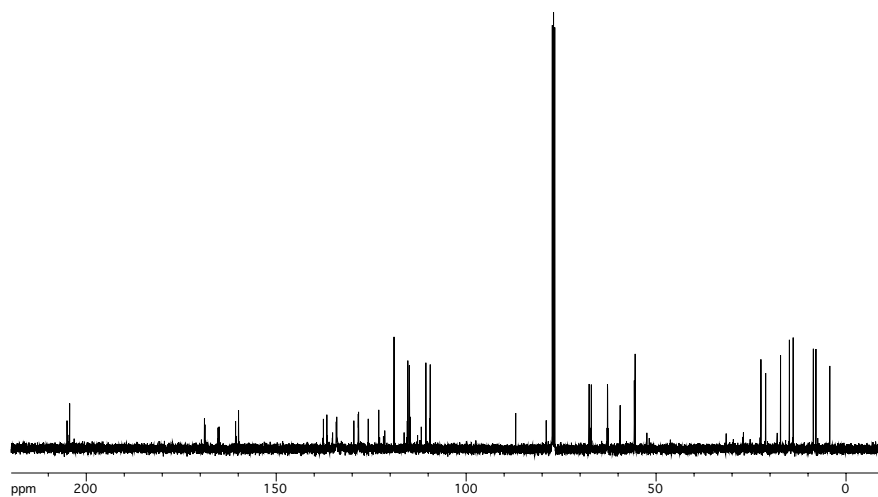


Figure A2.134.  $^{13}\text{C}$ -NMR of alkyne 358.

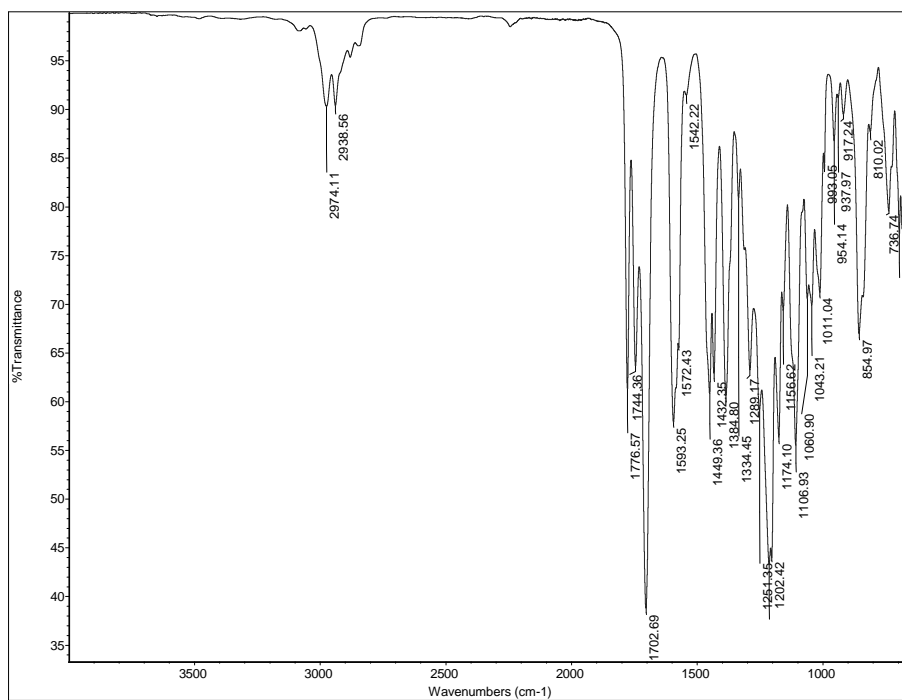
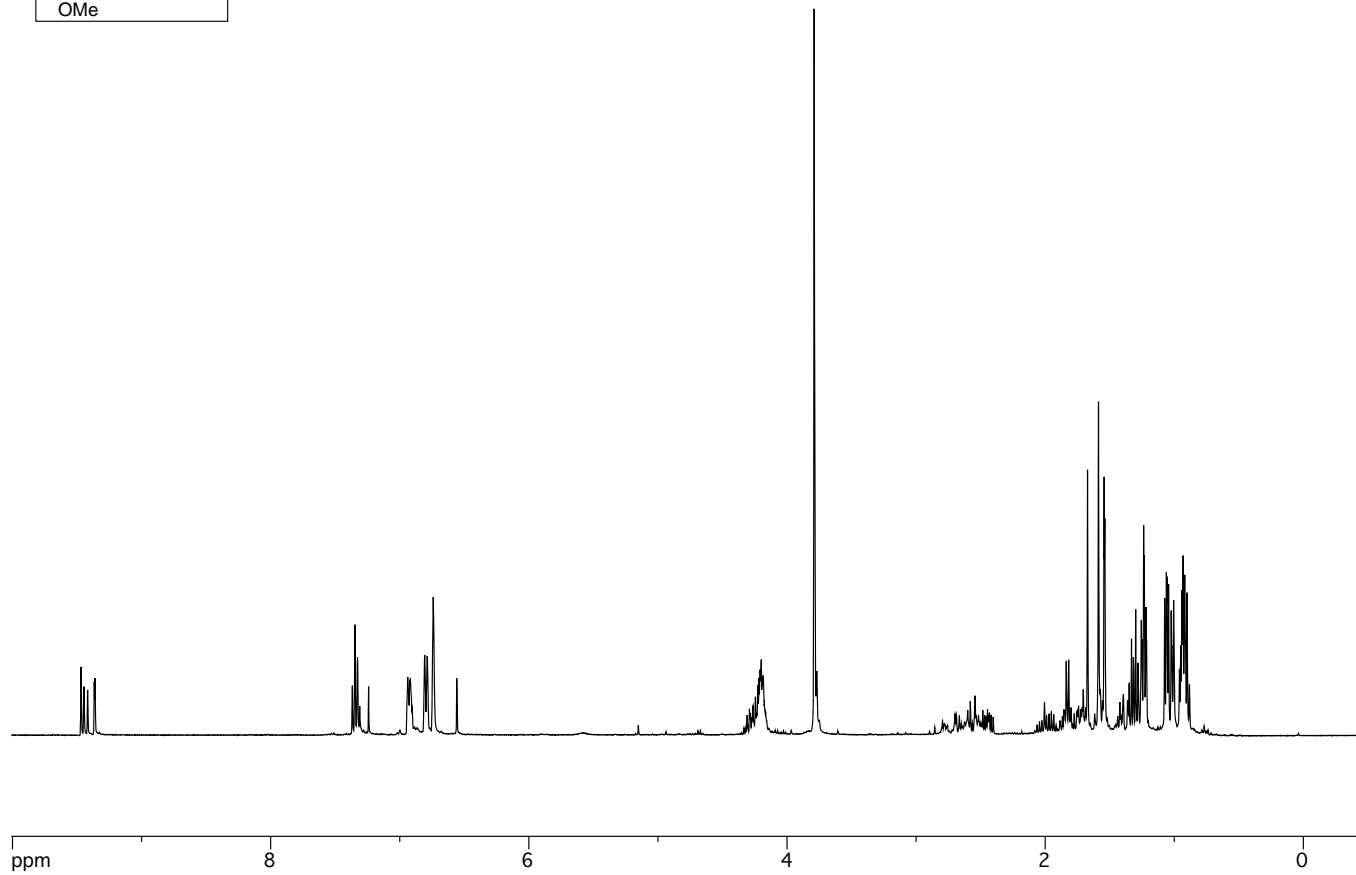
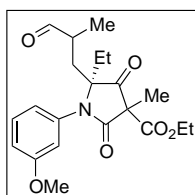


Figure A2.135. FTIR of alkyne 358.



**Figure A2.136.** <sup>1</sup>H-NMR of aldehyde **325**.

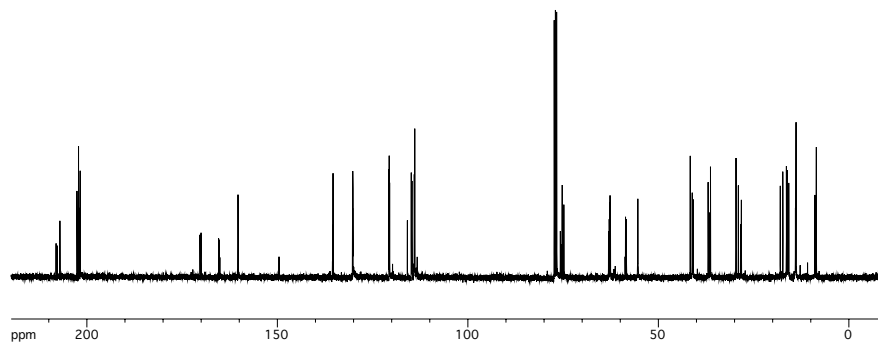


Figure A2.137.  $^{13}\text{C}$ -NMR of aldehyde **325**.

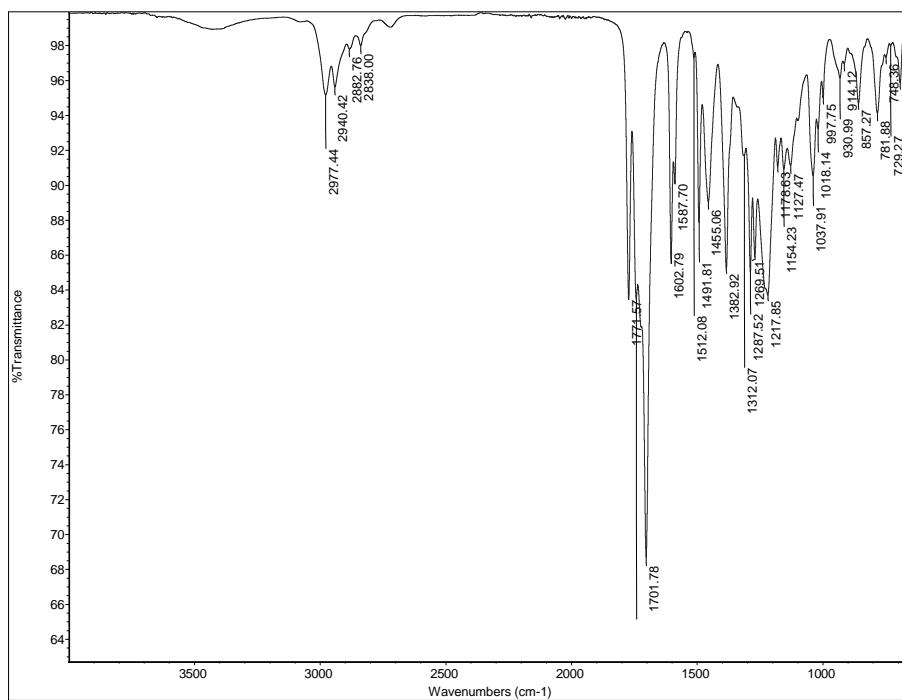
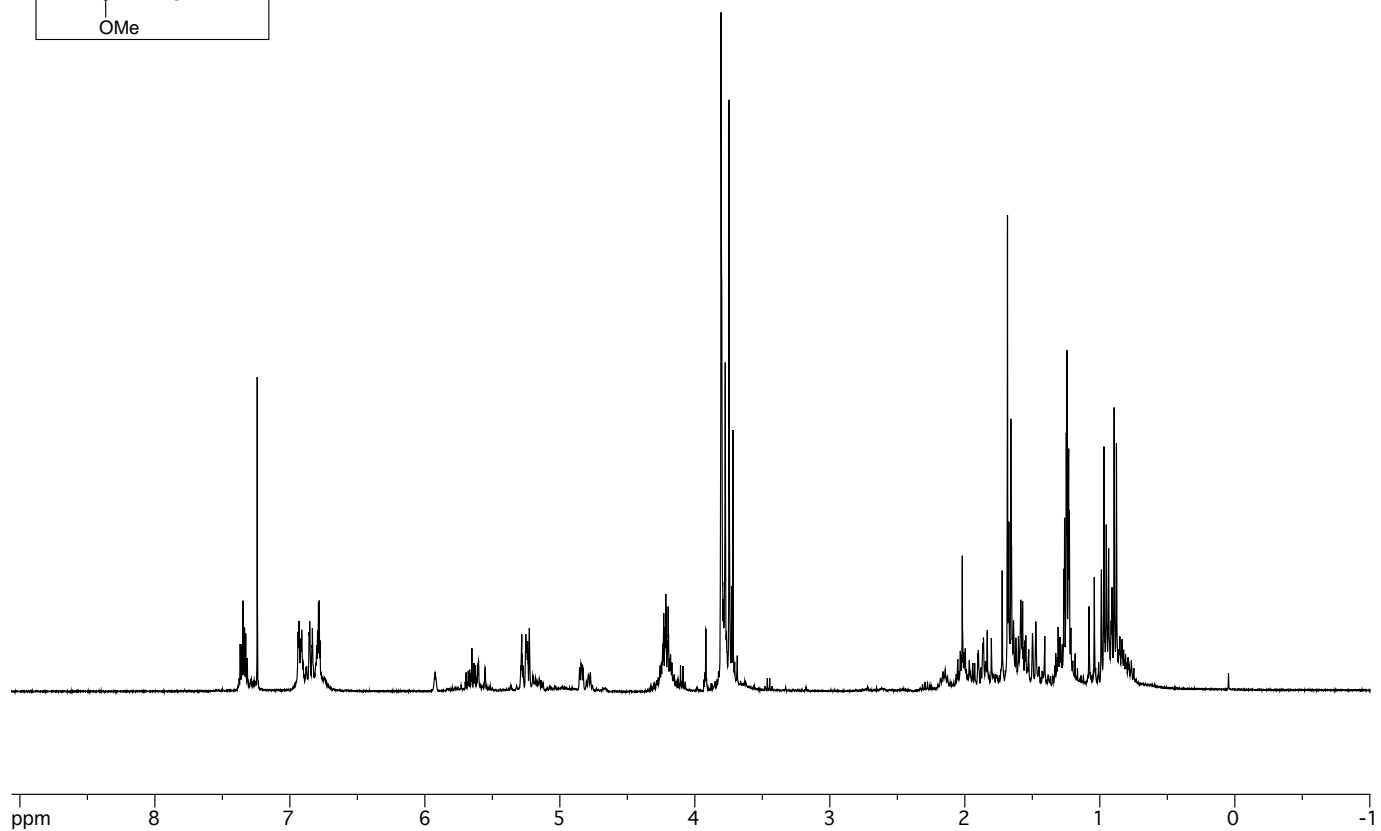
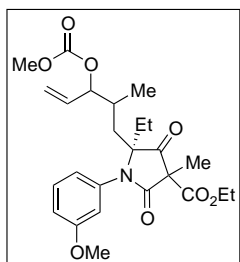


Figure A2.138. FTIR of aldehyde **325**.



**Figure A2.139.** <sup>1</sup>H-NMR of vinyl carbonate **321**.

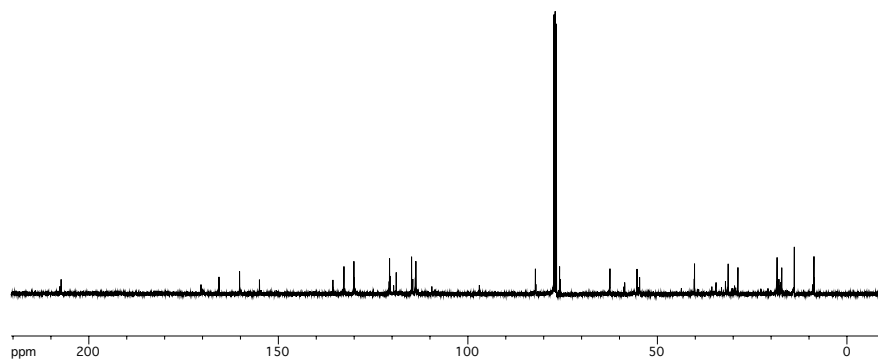


Figure A2.140. <sup>13</sup>C-NMR of vinyl carbonate 321.

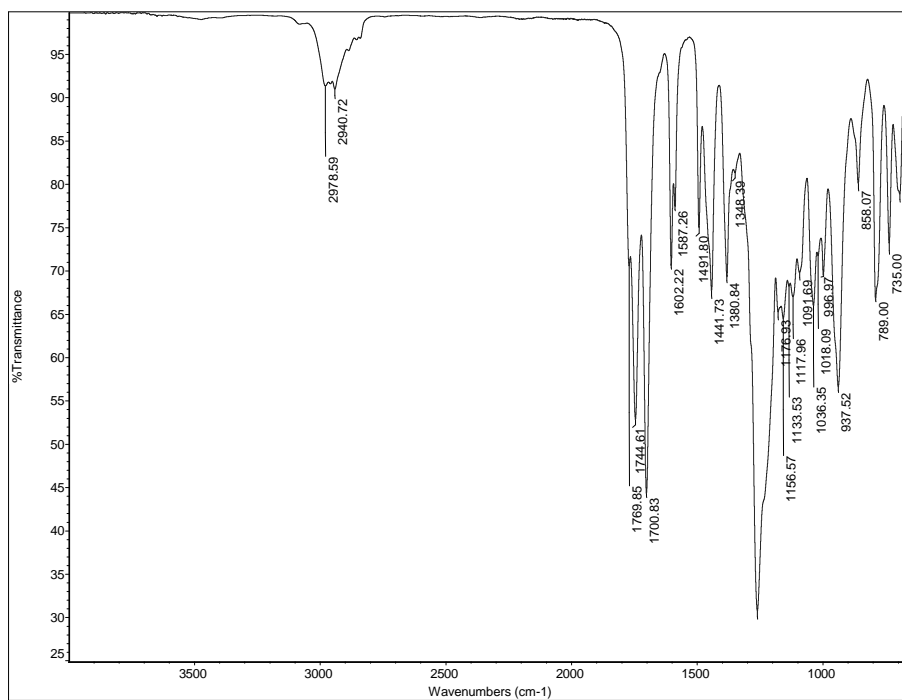
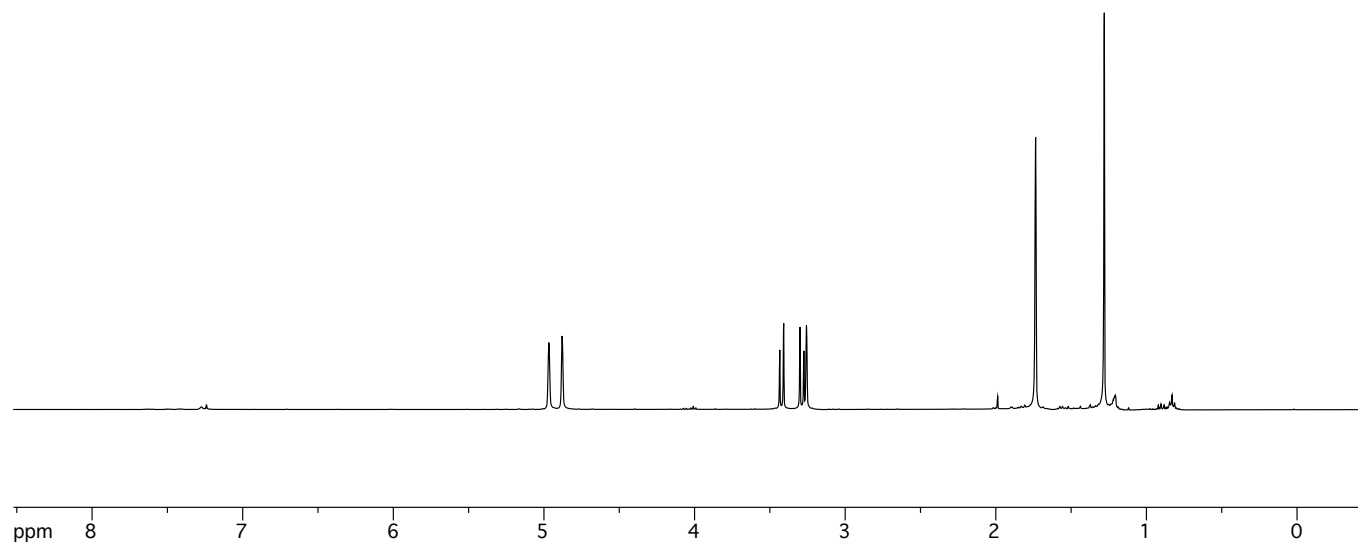
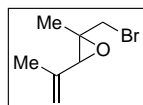


Figure A2.141. FTIR of vinyl carbonate 321.



**Figure A2.142.**  $^1\text{H-NMR}$  of bromide **335**.

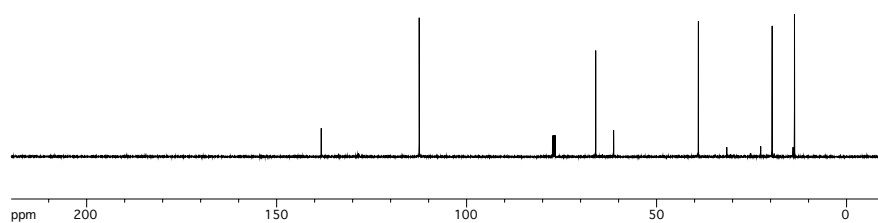


Figure A2.143. <sup>13</sup>C-NMR of bromide 335.

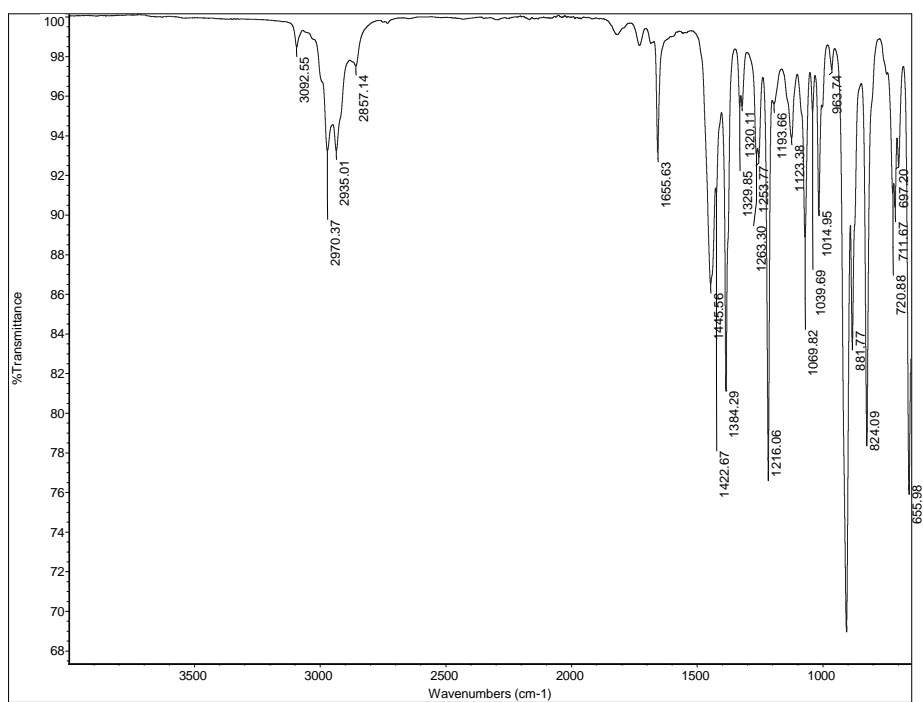
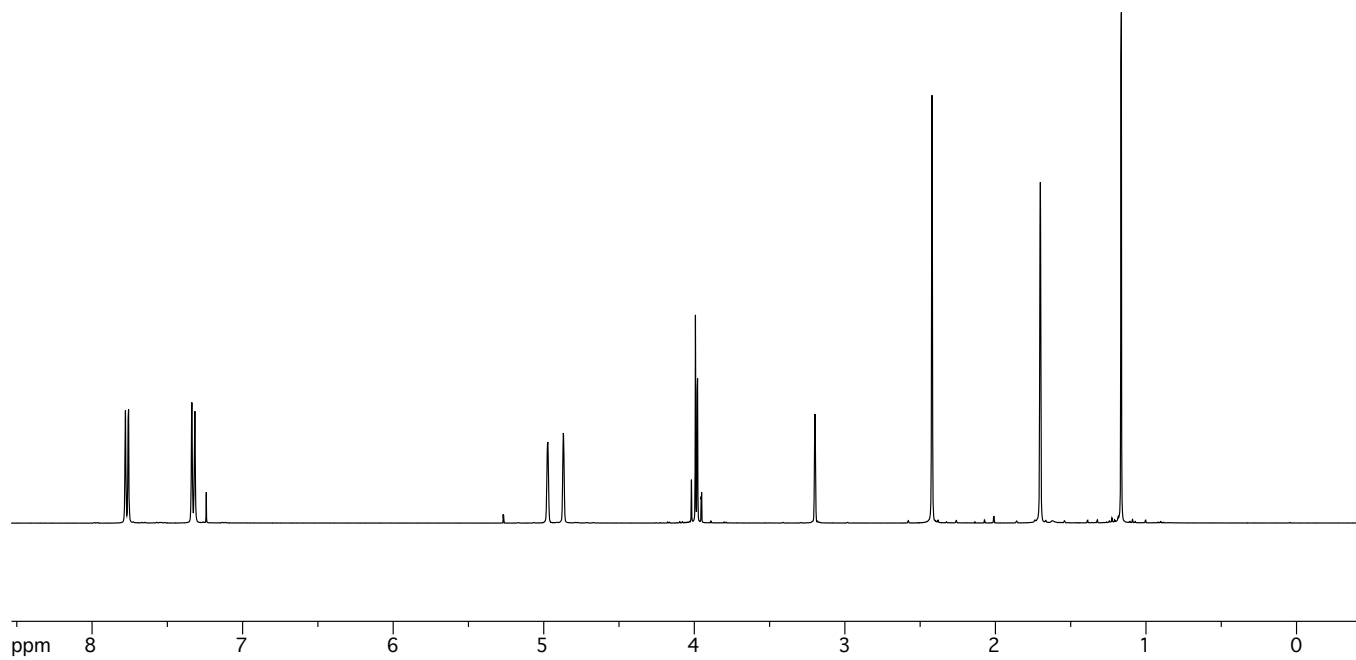
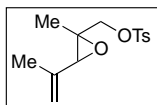


Figure A2.144. FTIR of bromide 335.



**Figure A2.145.** <sup>1</sup>H-NMR of tosylate 336.

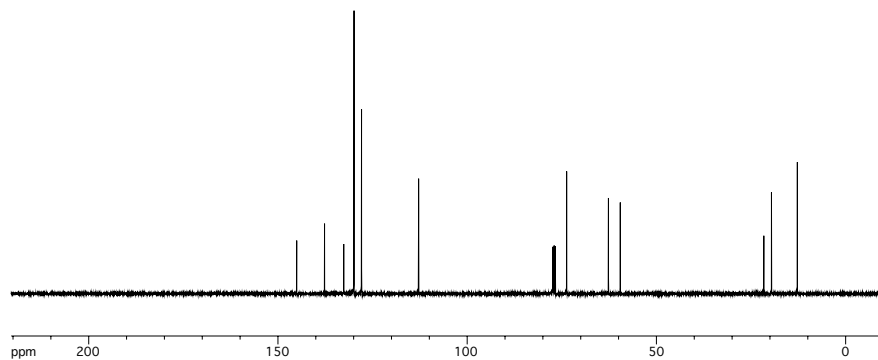


Figure A2.146.  $^{13}\text{C}$ -NMR of tosylate 336.

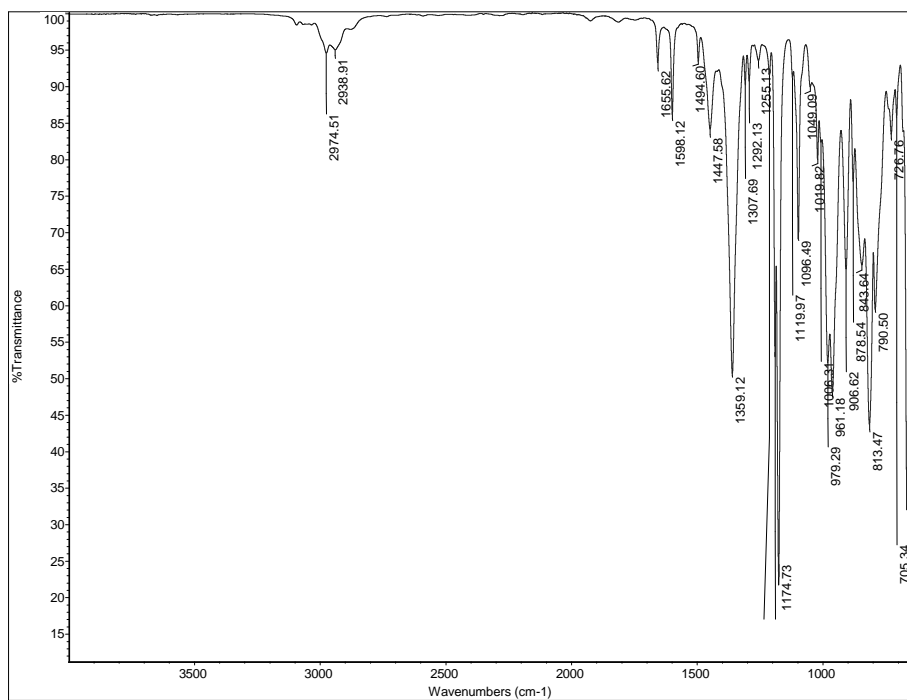
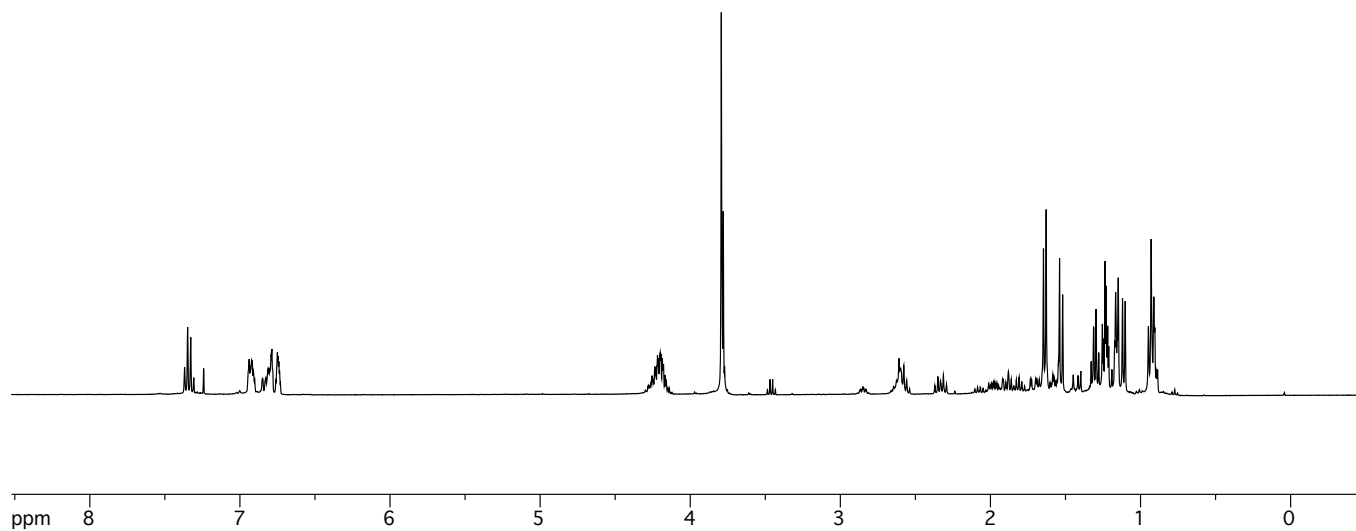
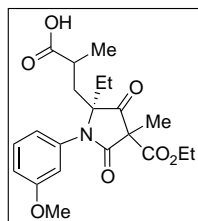


Figure A2.147. FTIR of tosylate 336.



**Figure A2.148.** <sup>1</sup>H-NMR of carboxylic acid 337.

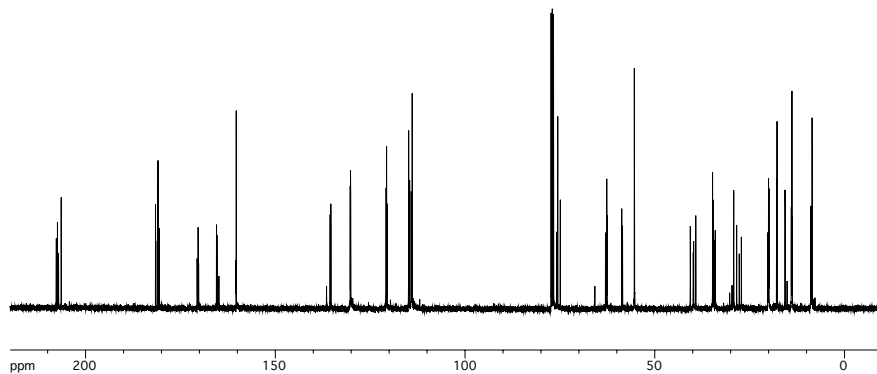


Figure A2.149.  $^{13}\text{C}$ -NMR of carboxylic acid **337**.

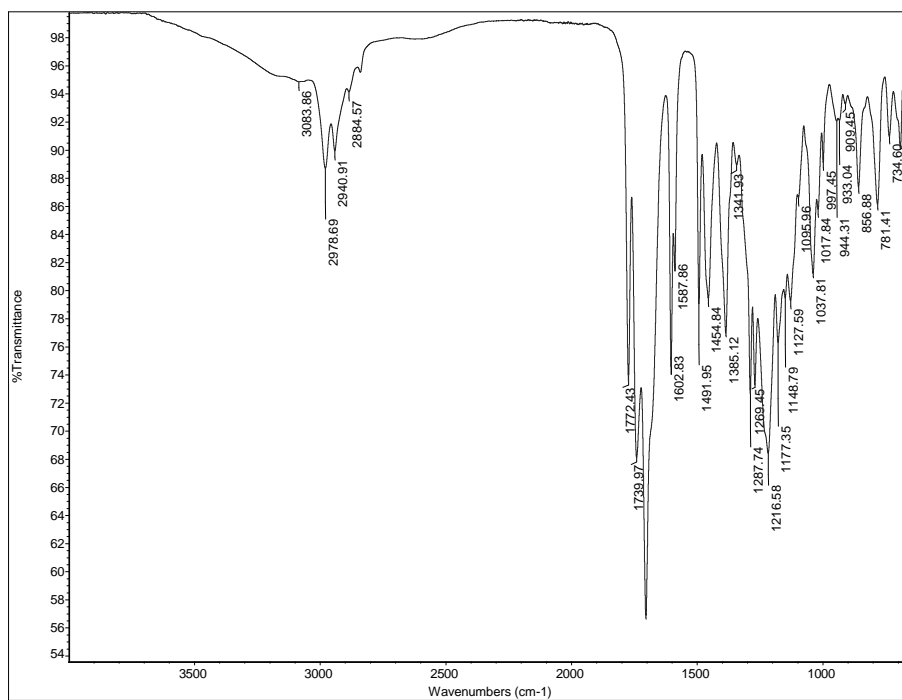
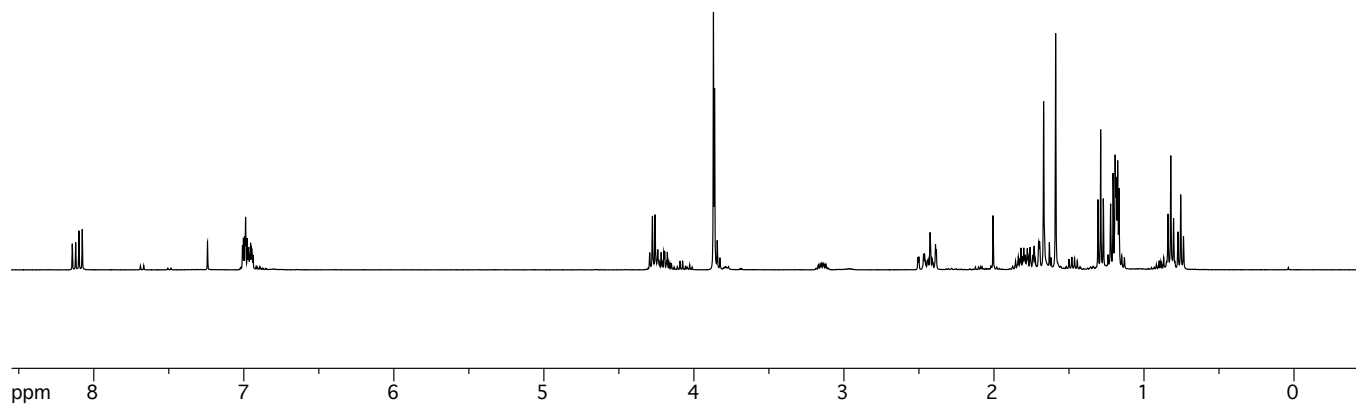
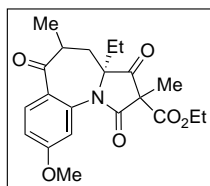


Figure A2.150. FTIR of carboxylic acid **337**.



**Figure A2.151.** <sup>1</sup>H-NMR of ketone **339**.

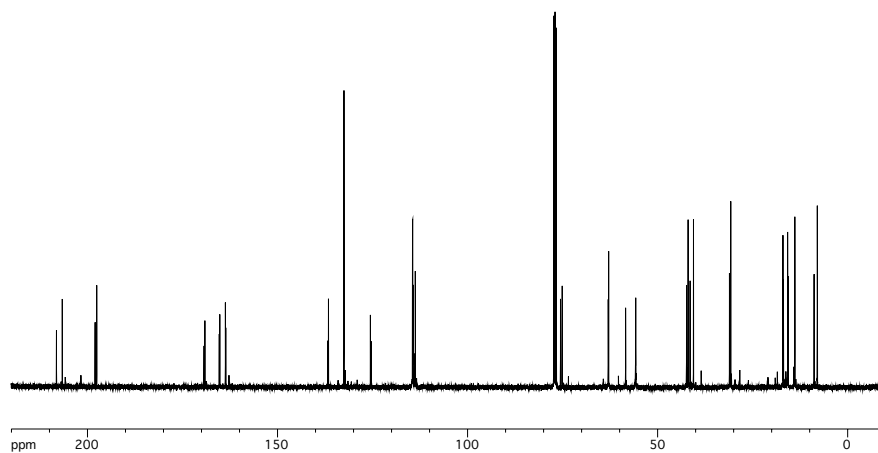


Figure A2.152.  $^{13}\text{C}$ -NMR of ketone 339.

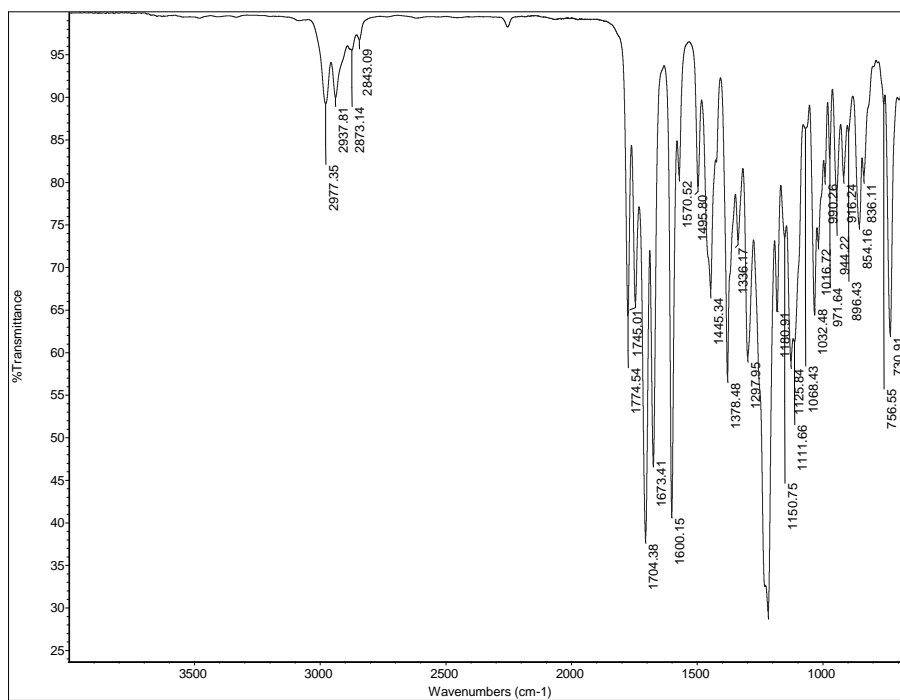


Figure A2.153. FTIR of ketone 339.

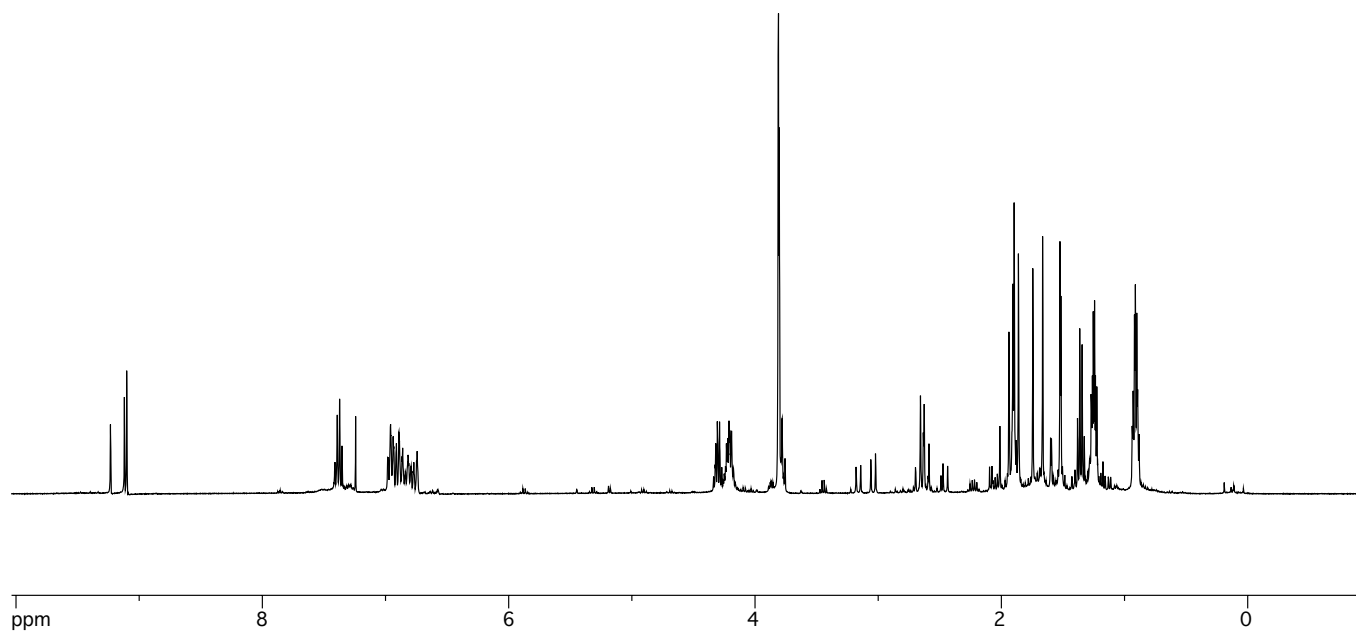
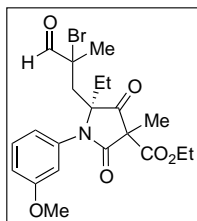


Figure A2.154. <sup>1</sup>H-NMR of aldehyde 342.

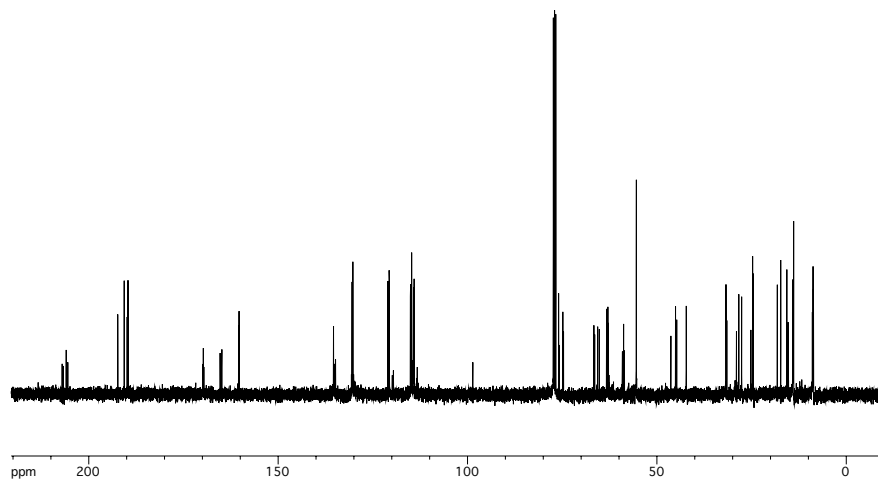


Figure A2.155.  $^{13}\text{C-NMR}$  of aldehyde 342.

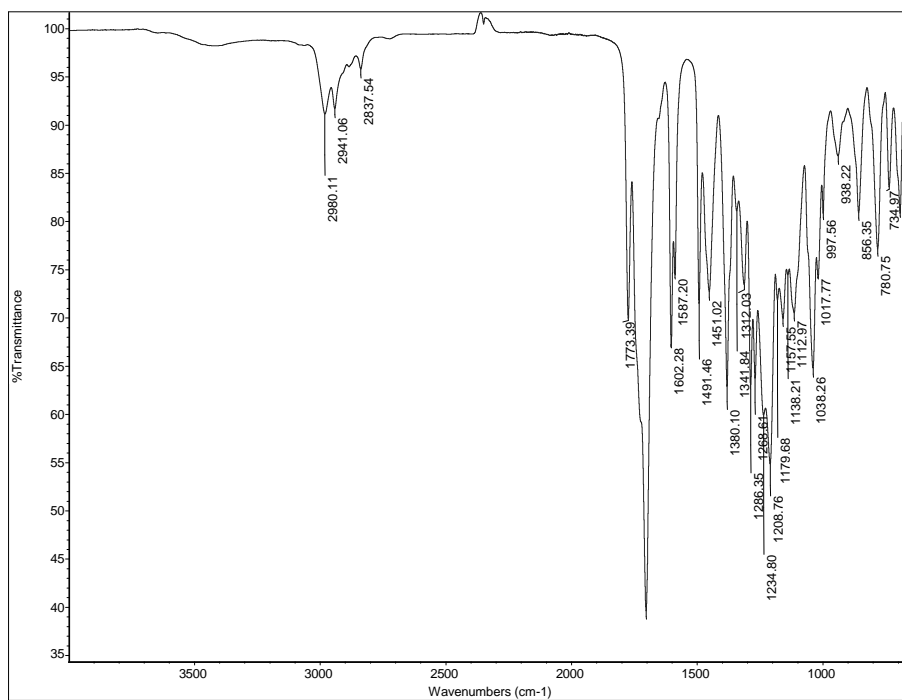
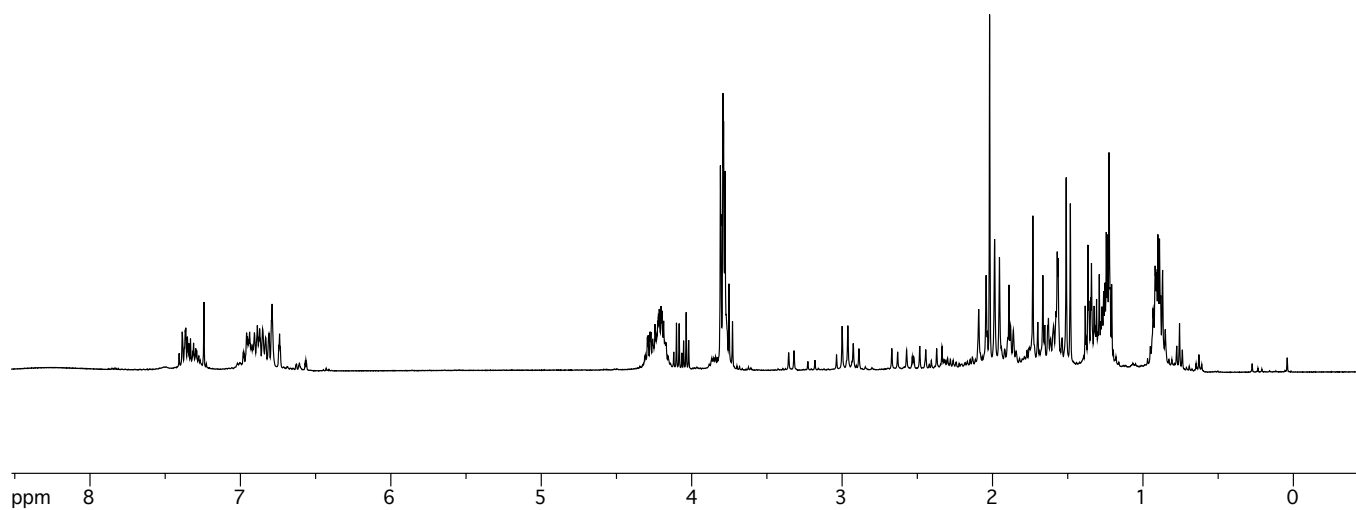
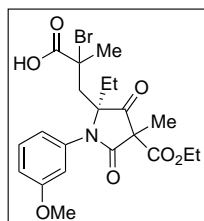
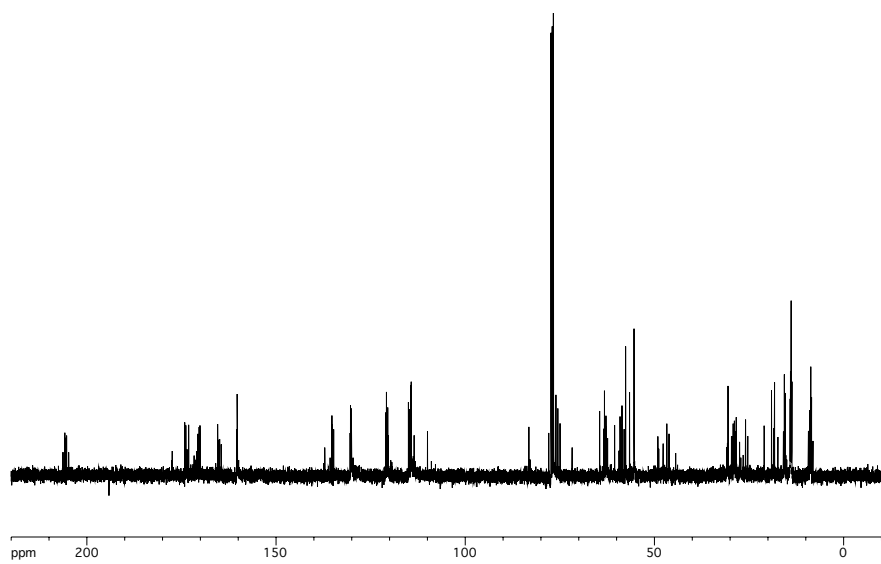


Figure A2.156. FTIR of aldehyde 342.



**Figure A2.157.**  $^1\text{H-NMR}$  of carboxylic acid **343**.



**Figure A2.158.**  $^{13}\text{C}$ -NMR of carboxylic acid **343**.

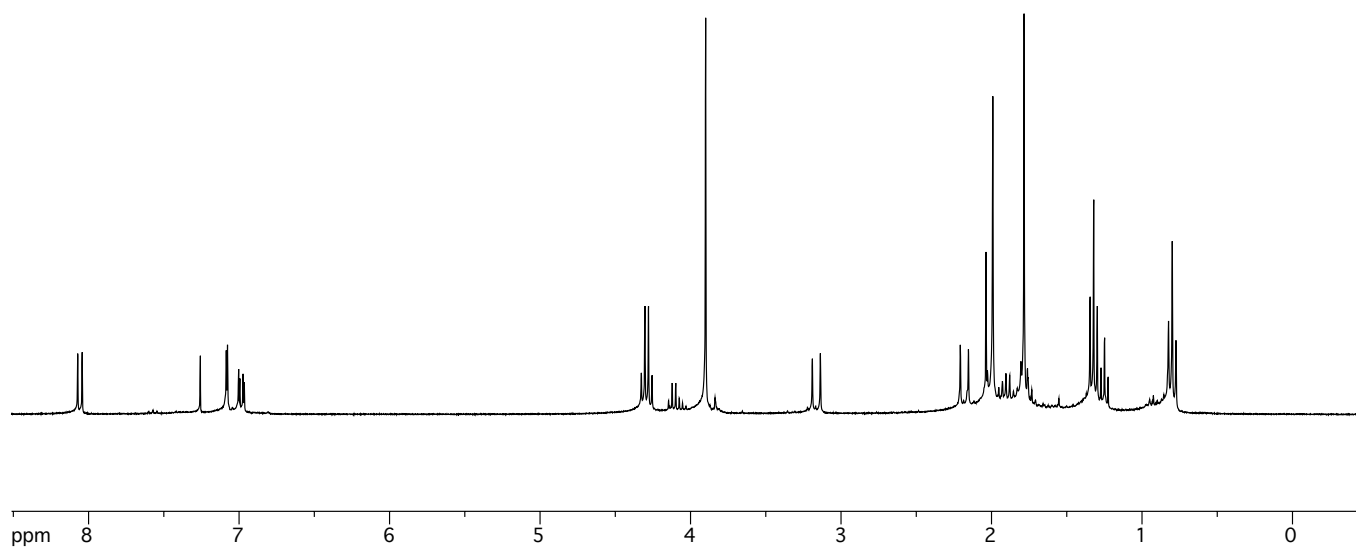
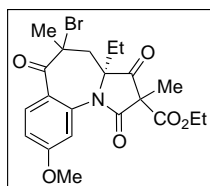


**Figure A2.159.** <sup>1</sup>H-NMR of ketone **344**.

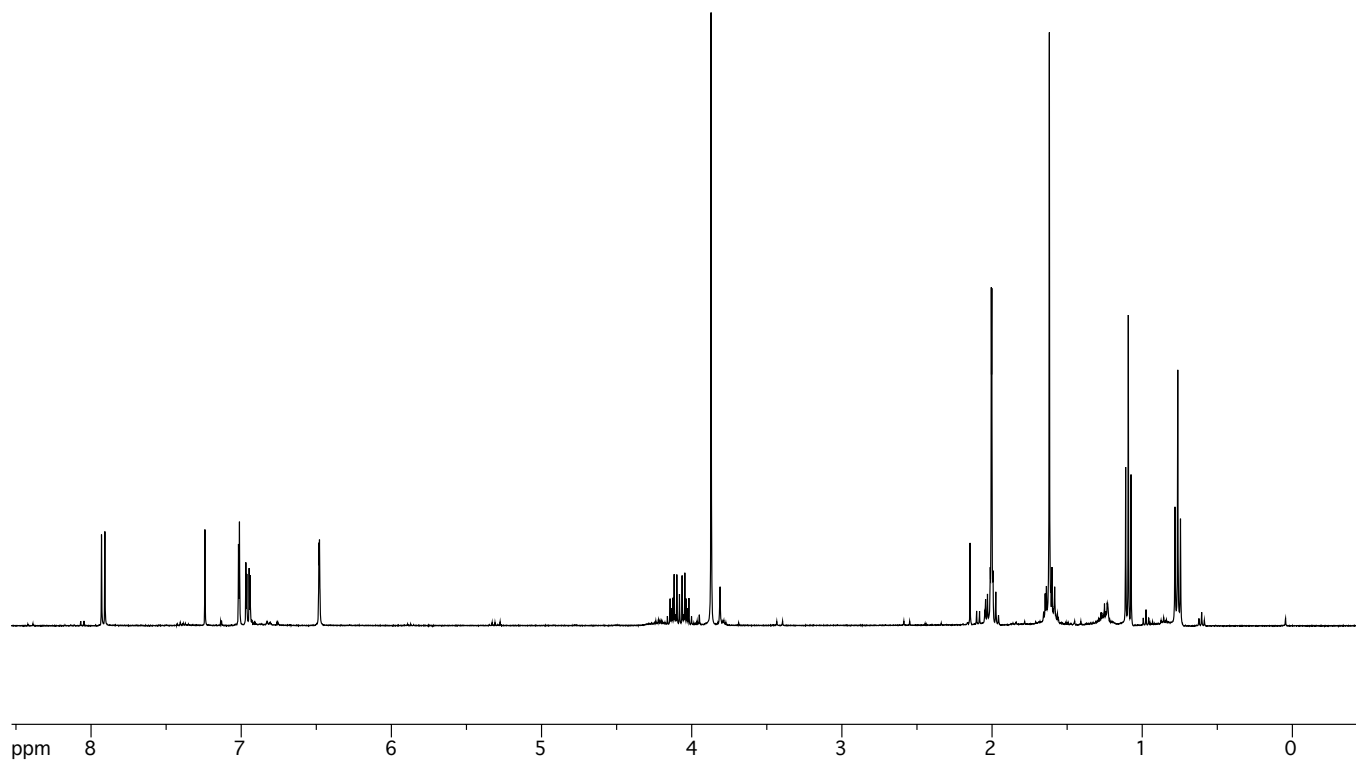
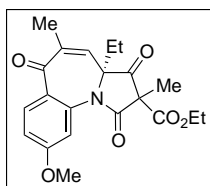


**Figure A2.160.**  $^1\text{H-NMR}$  of enone **345** (diastereomer A).

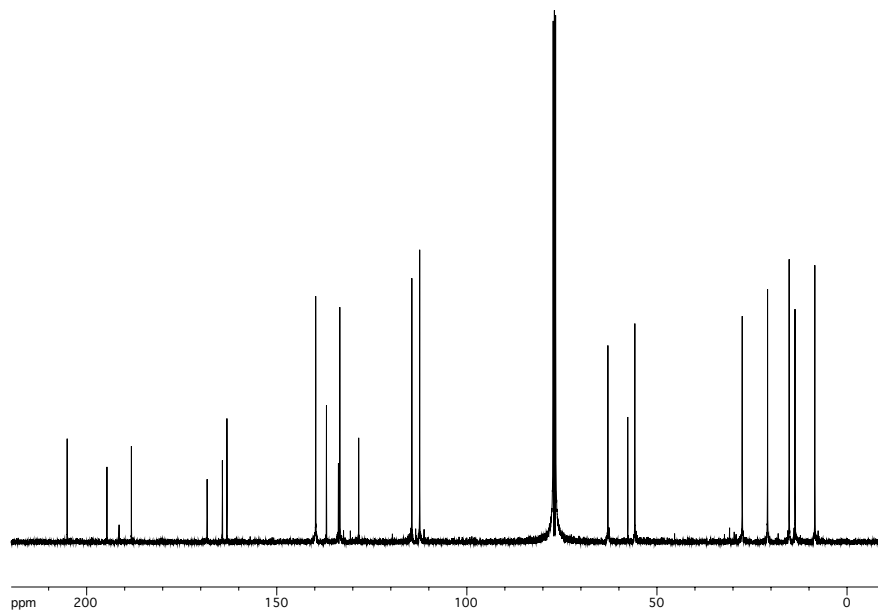


**Figure A2.161.**  $^{13}\text{C}$ -NMR of enone **345** (diastereomer A).

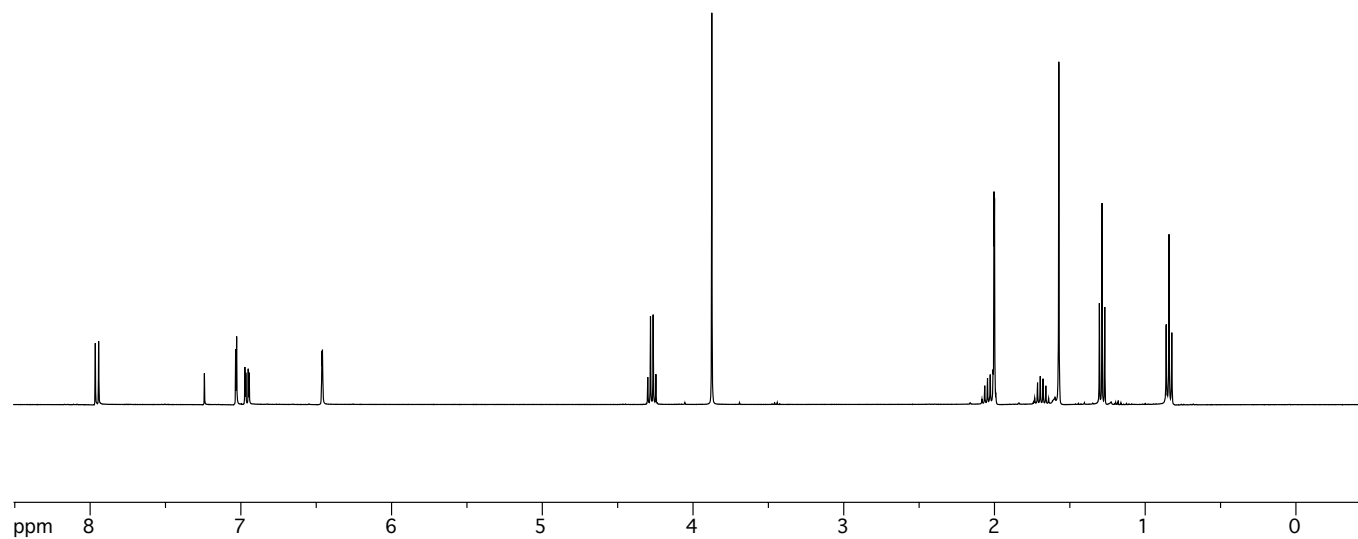
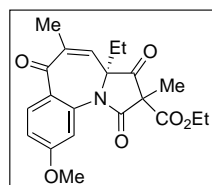


**Figure A2.162.** <sup>1</sup>H-NMR of enone **345** (diastereomer B).

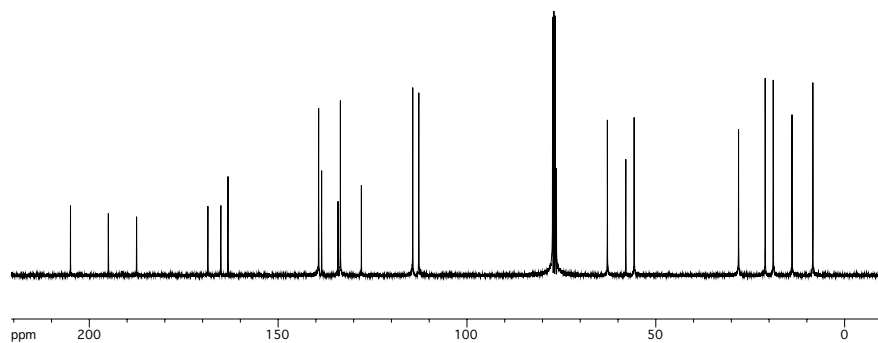


**Figure A2.163.**  $^{13}\text{C}$ -NMR of enone **345** (diastereomer B).

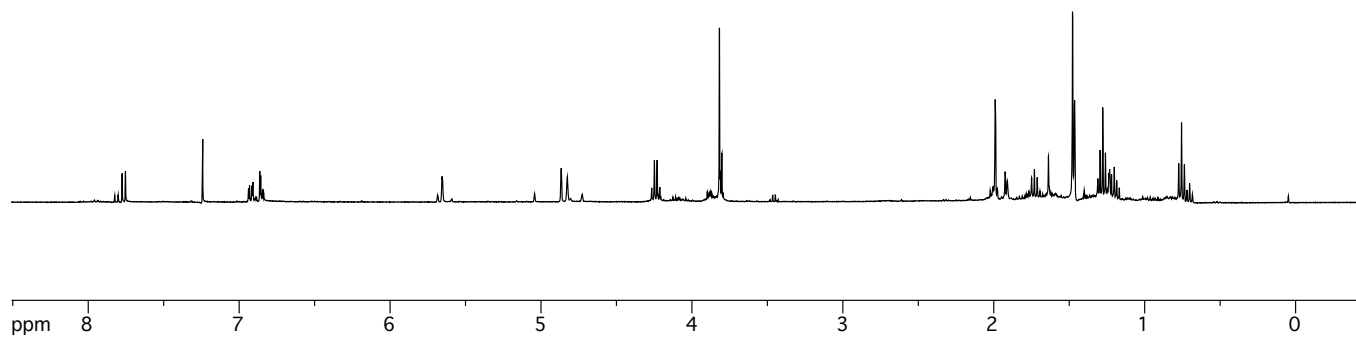
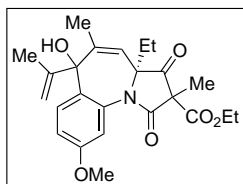


**Figure A2.164.** <sup>1</sup>H-NMR of alcohol **346**.

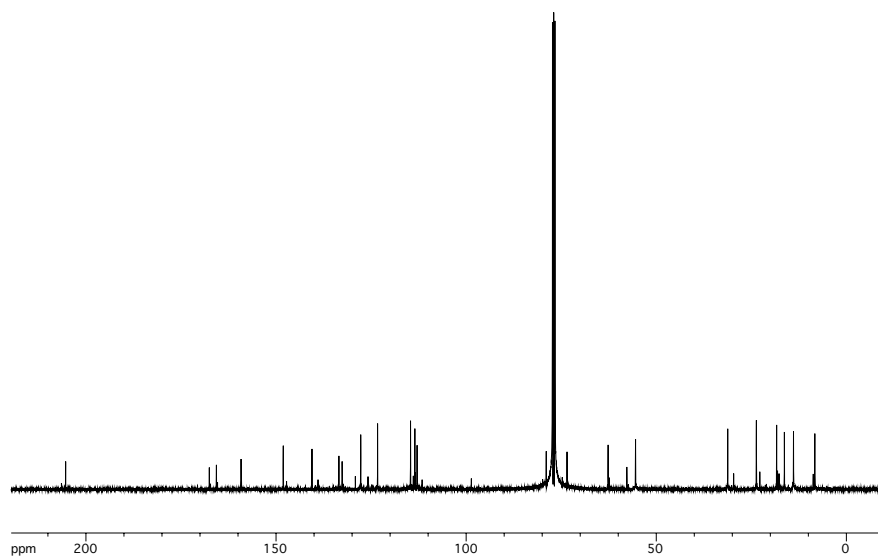


Figure A2.165.  $^{13}\text{C}$ -NMR of alcohol 346.

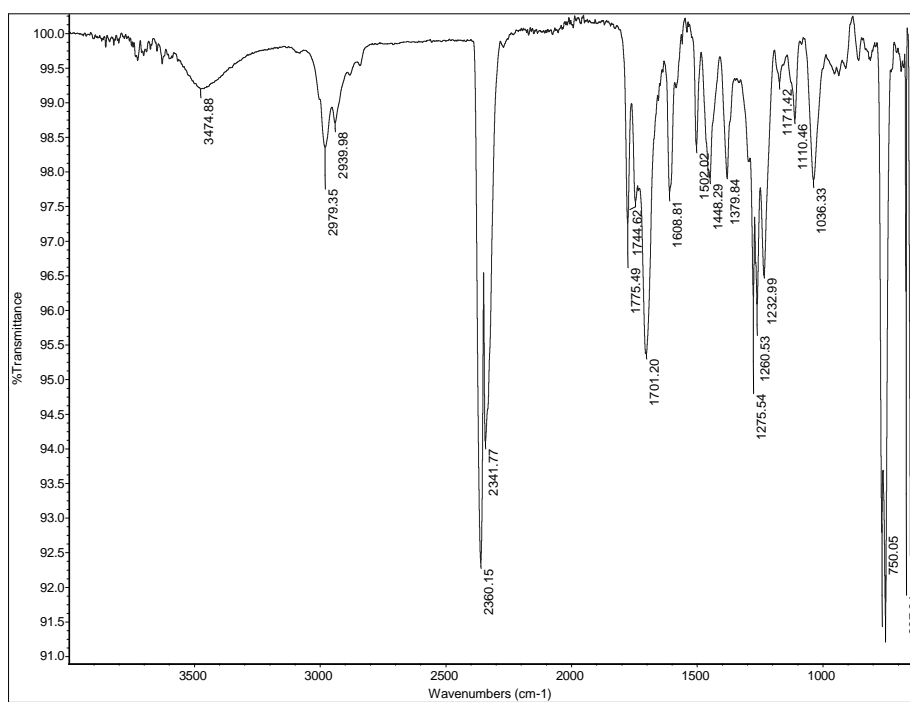
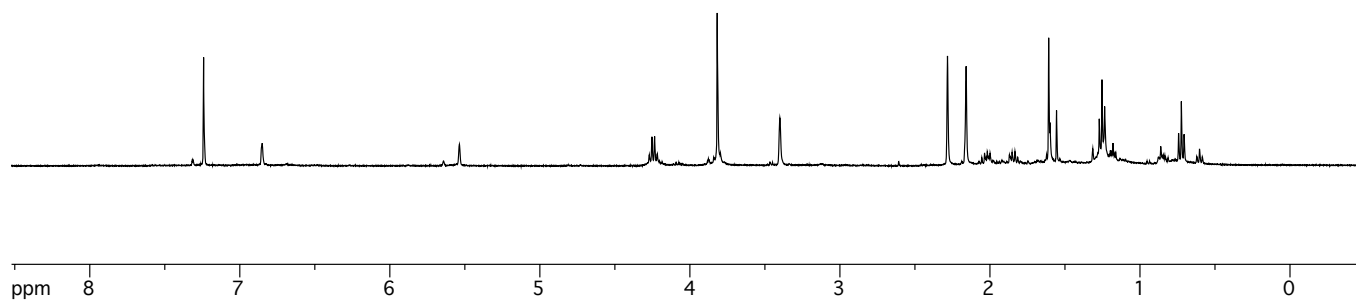
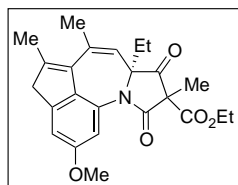


Figure A2.166. FTIR of alcohol 346.



**Figure A2.167.** <sup>1</sup>H-NMR of tetracycline **347**.

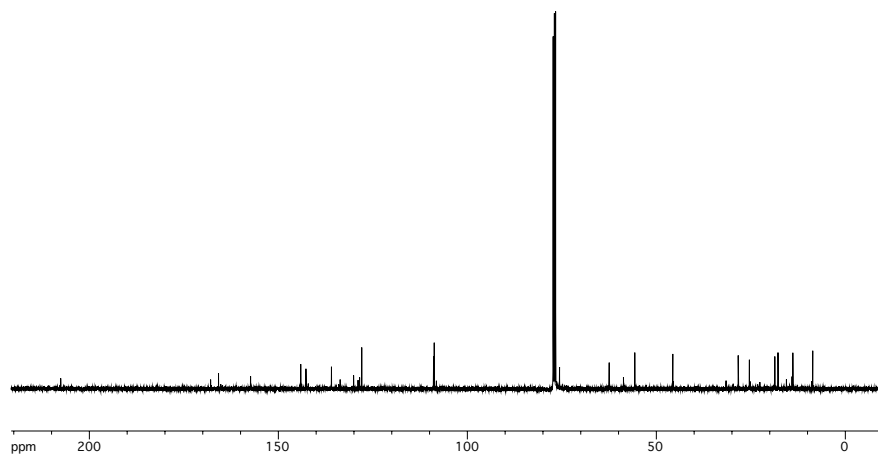


Figure A2.168.  $^{13}\text{C}$ -NMR of tetracycline 347.

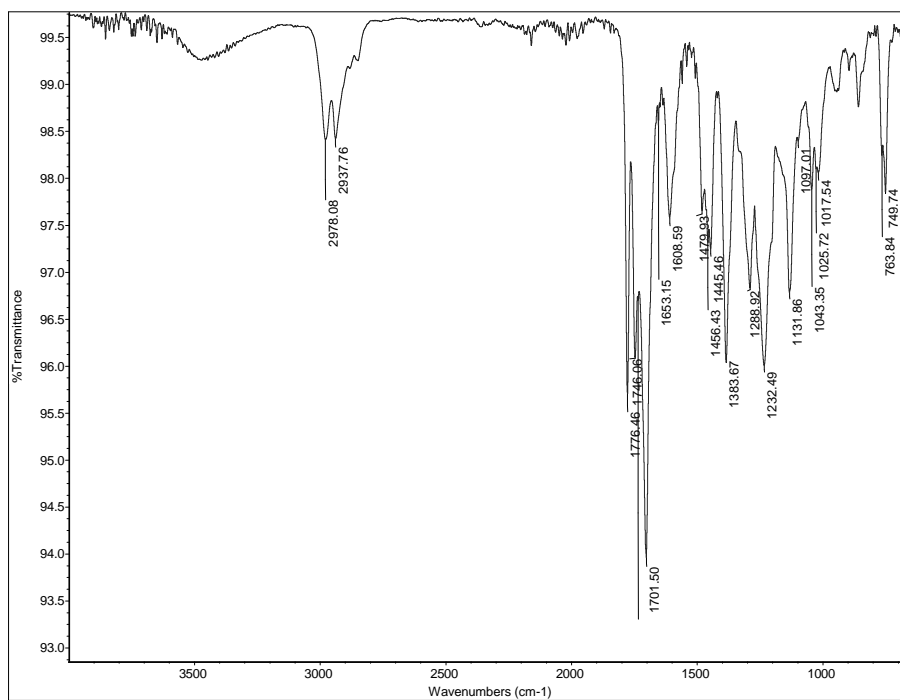
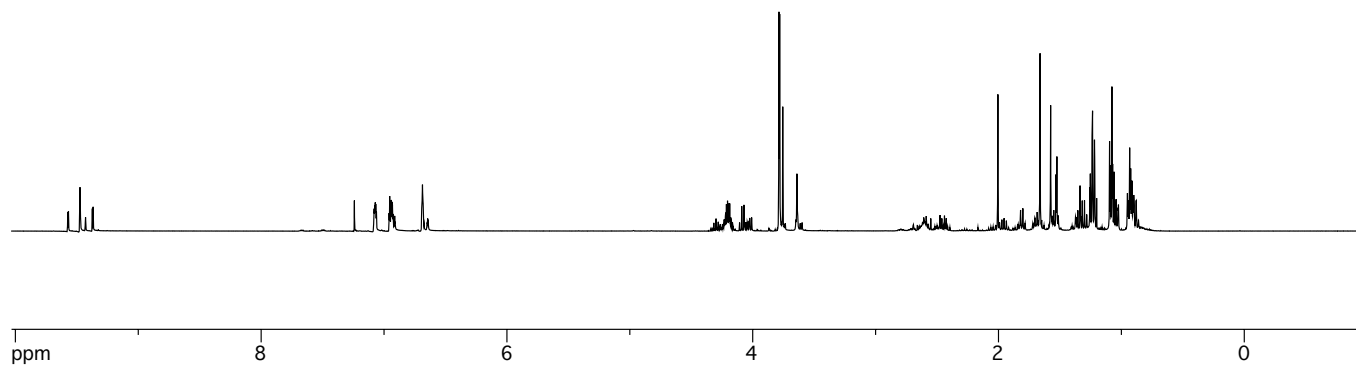
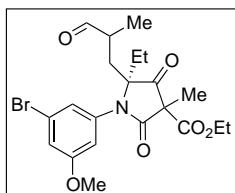


Figure A2.169. FTIR of tetracycline 347.



**Figure A2.170.** <sup>1</sup>H-NMR of aldehyde **355**.

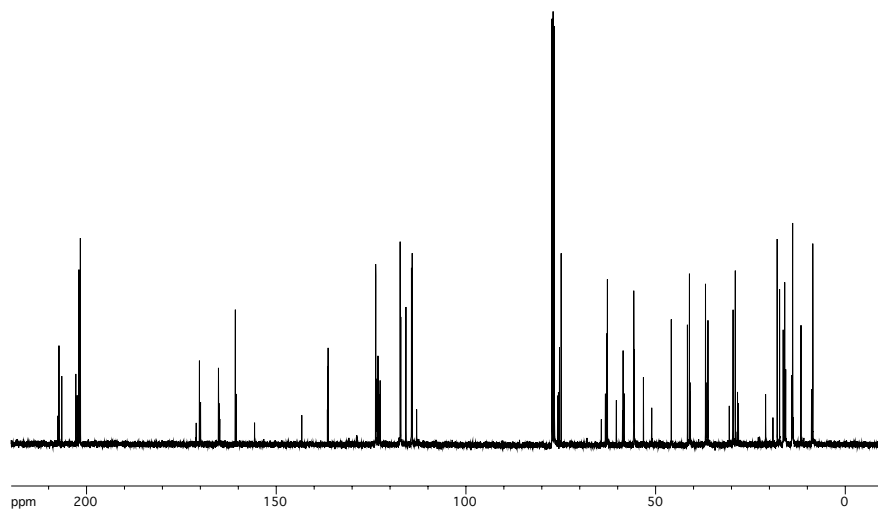


Figure A2.171.  $^{13}\text{C}$ -NMR of aldehyde 355.

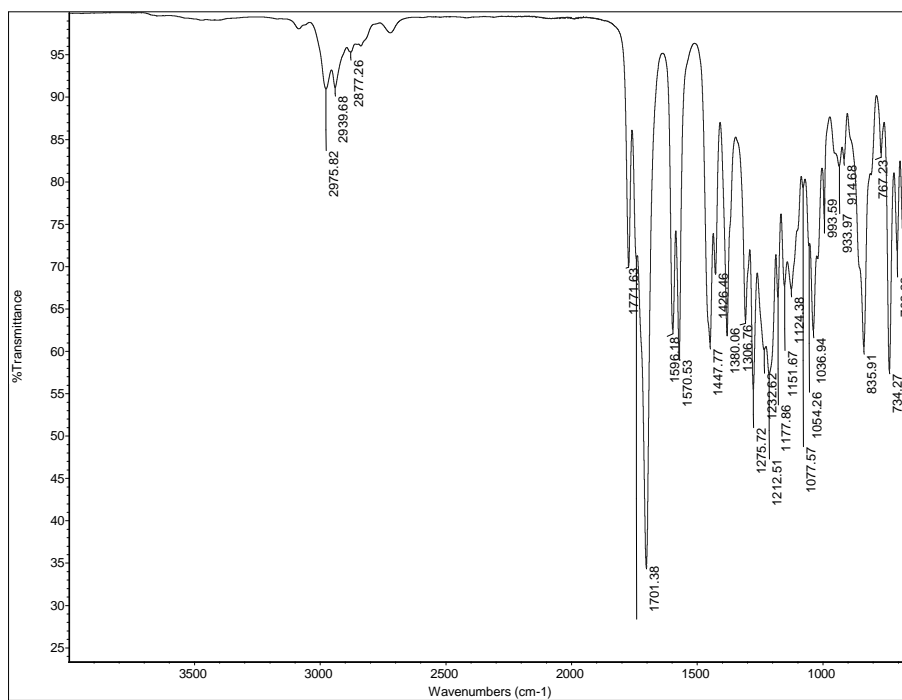
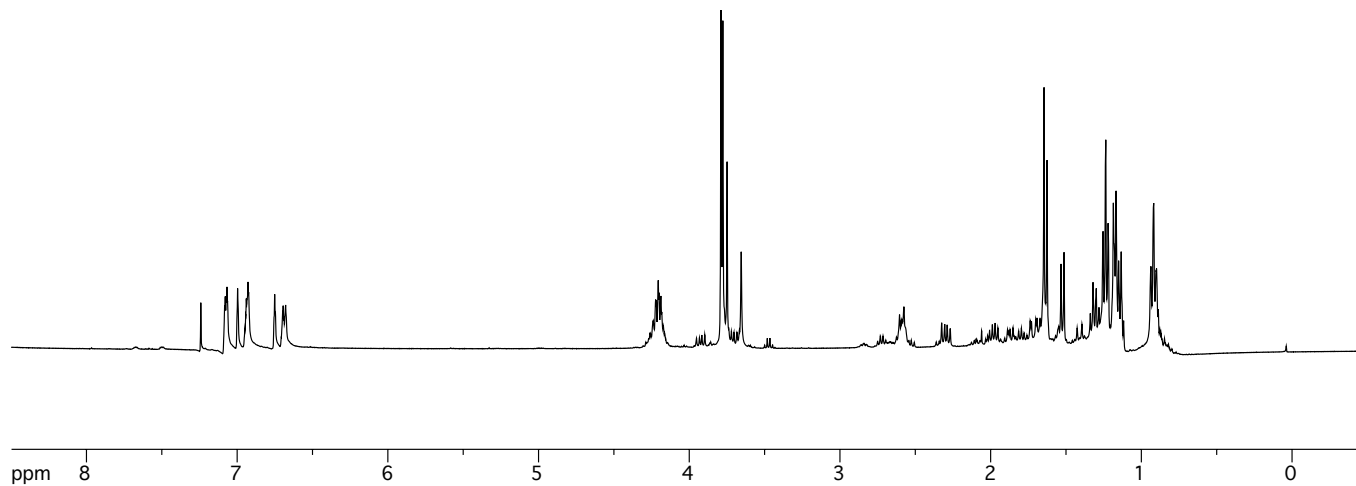
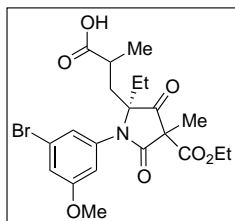


Figure A2.172. FTIR of aldehyde 355.



**Figure A2.173.**  $^1\text{H-NMR}$  of carboxylic acid **356**.

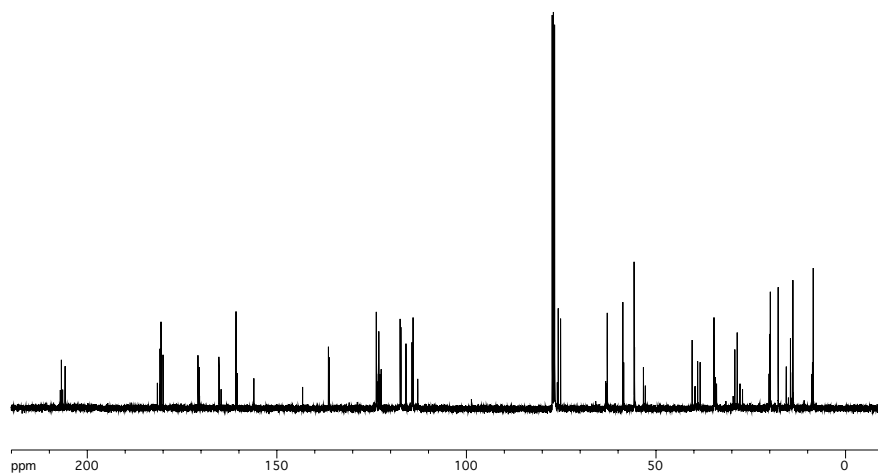


Figure A2.174.  $^{13}\text{C-NMR}$  of carboxylic acid **356**.

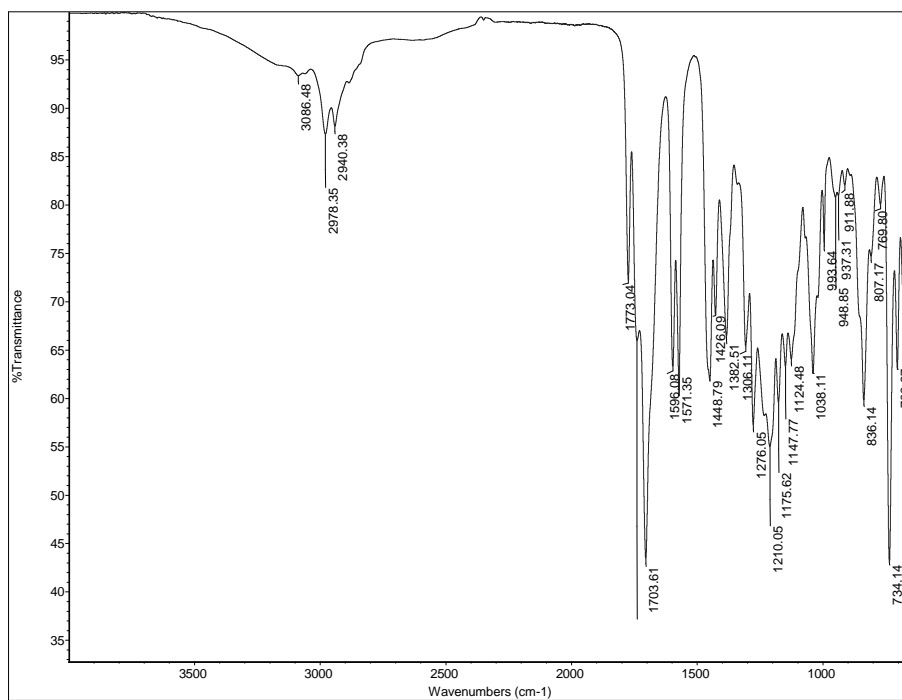
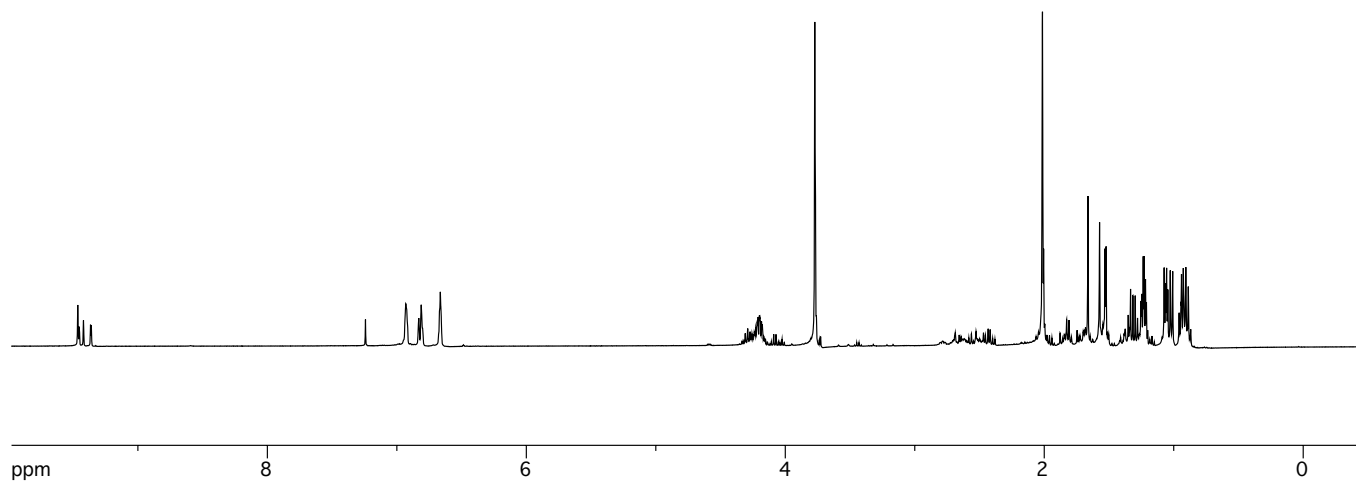
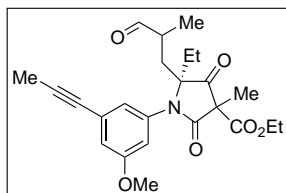


Figure A2.175. FTIR of carboxylic acid **356**.



**Figure A2.176.** <sup>1</sup>H-NMR of aldehyde **359**.

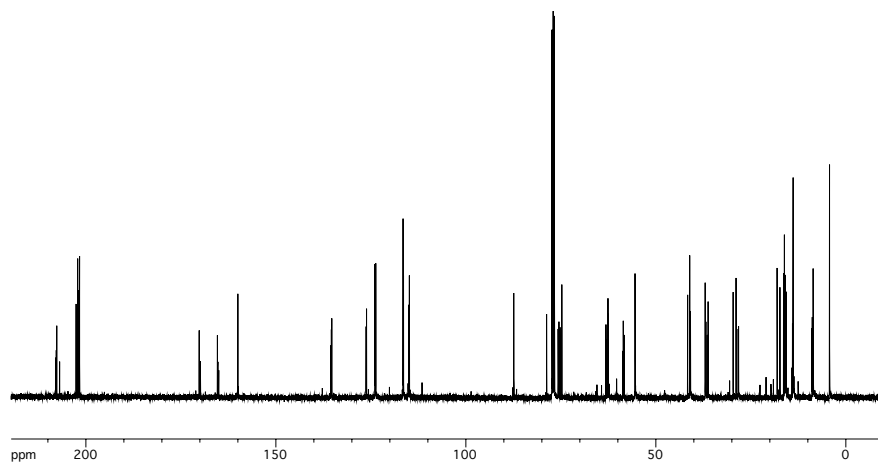


Figure A2.177.  $^{13}\text{C}$ -NMR of aldehyde 359.

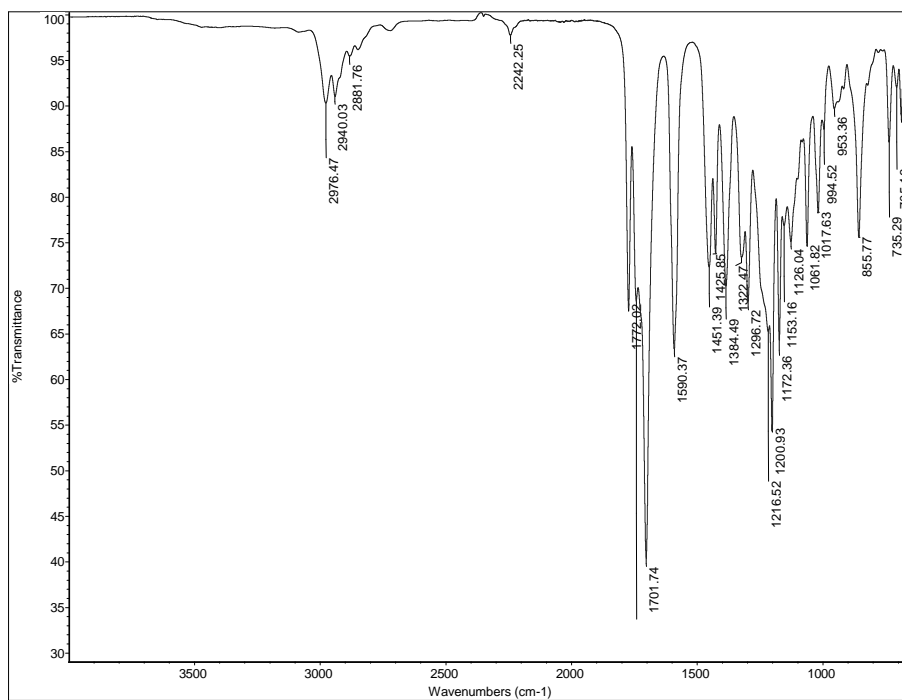
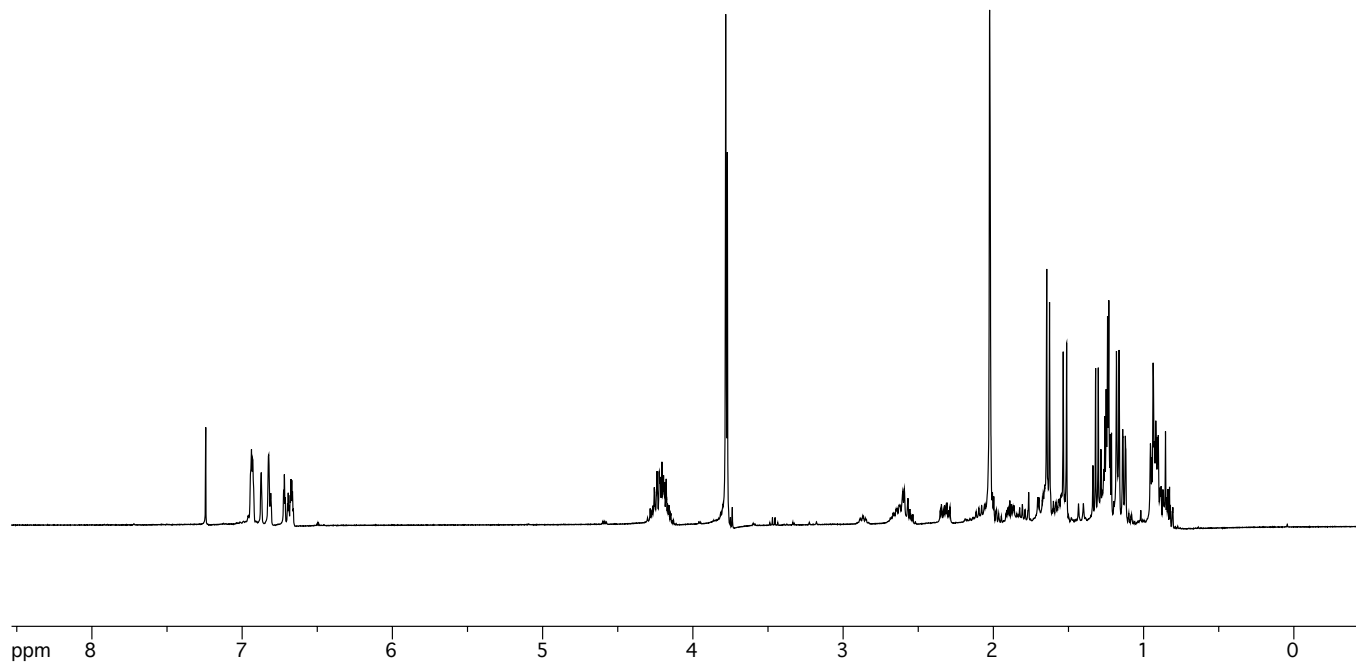
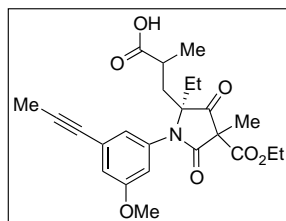


Figure A2.178. FTIR of aldehyde 359.



**Figure A2.179.**  $^1\text{H-NMR}$  of carboxylic acid **360**.

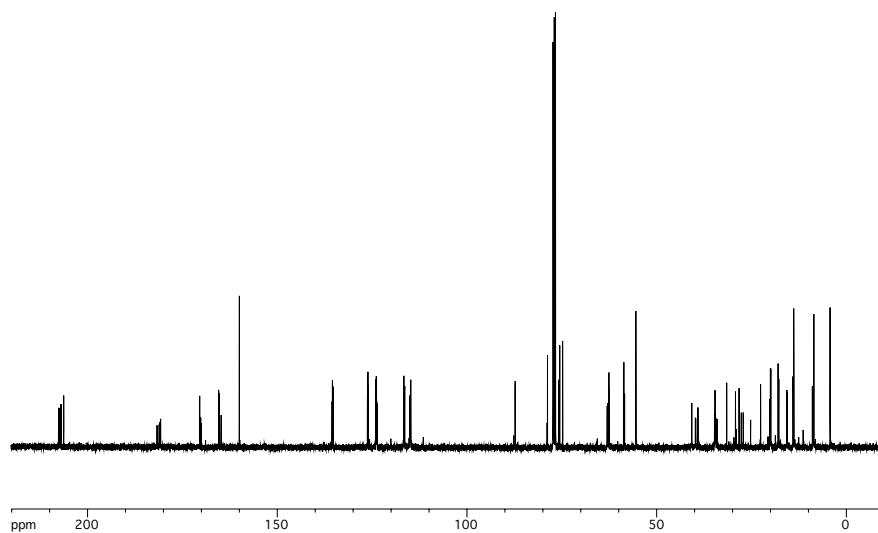


Figure A2.180.  $^{13}\text{C-NMR}$  of carboxylic acid **360**.

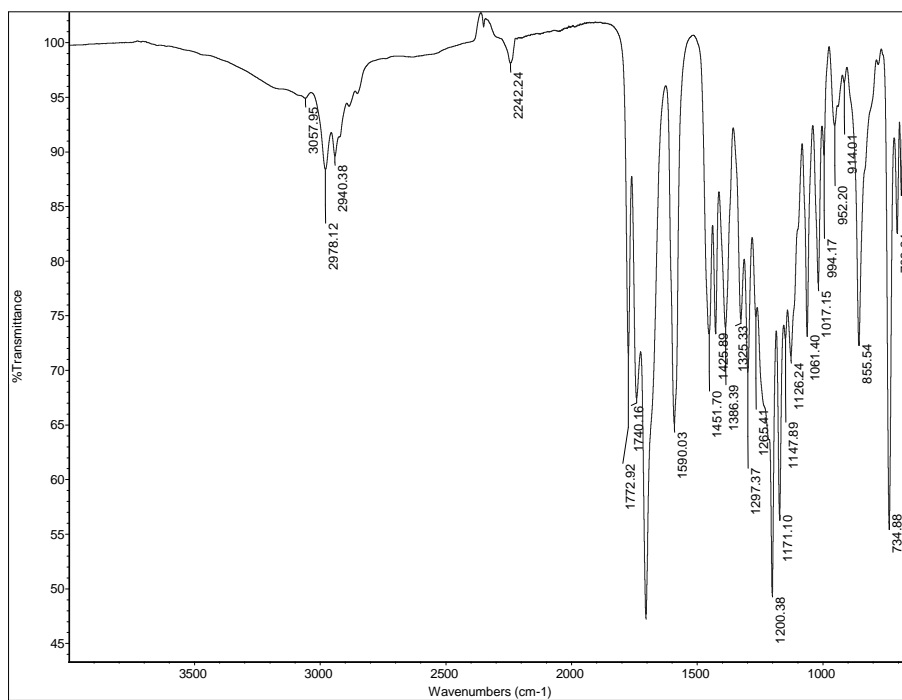
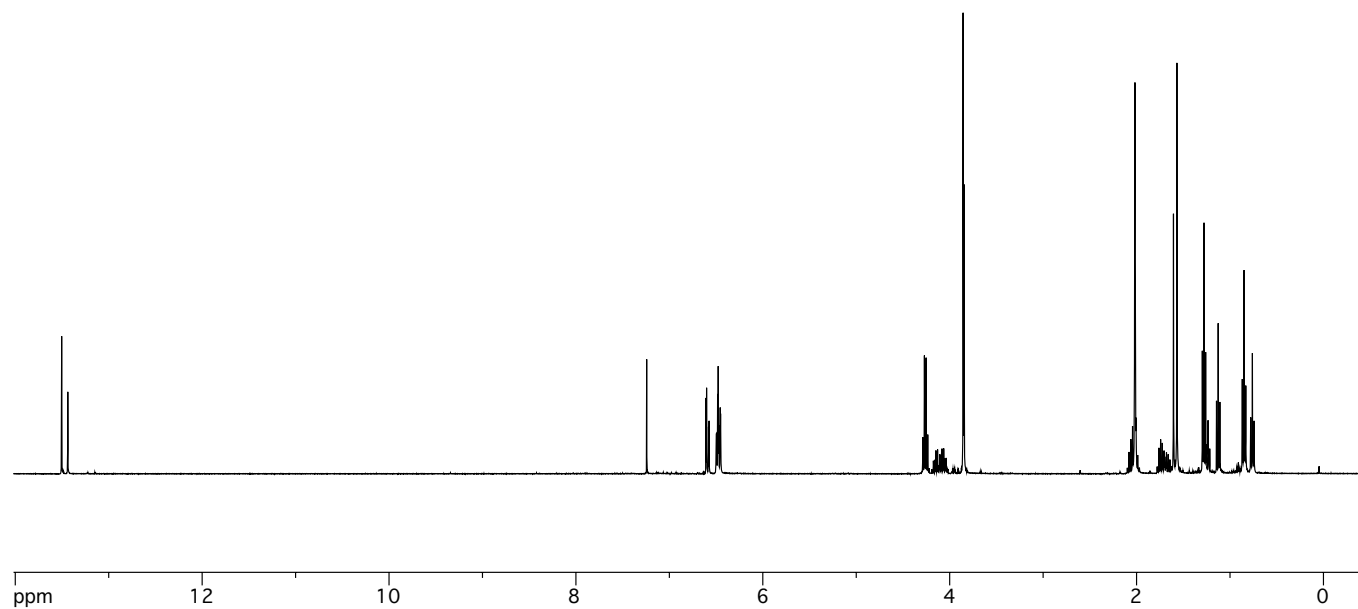
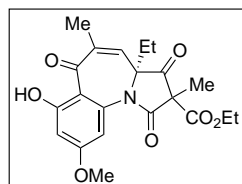


Figure A2.181. FTIR of carboxylic acid **360**.



**Figure A2.182.** <sup>1</sup>H-NMR of phenol **365**.

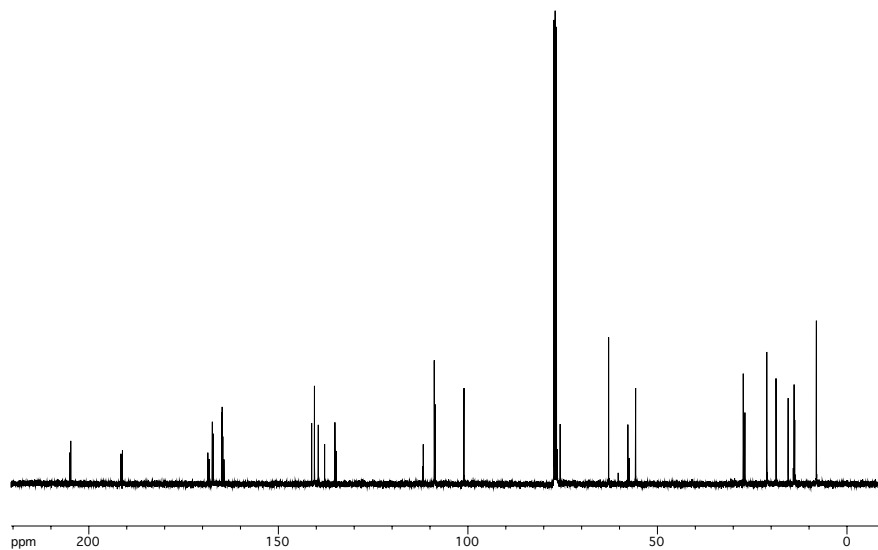


Figure A2.183.  $^{13}\text{C-NMR}$  of phenol 365.

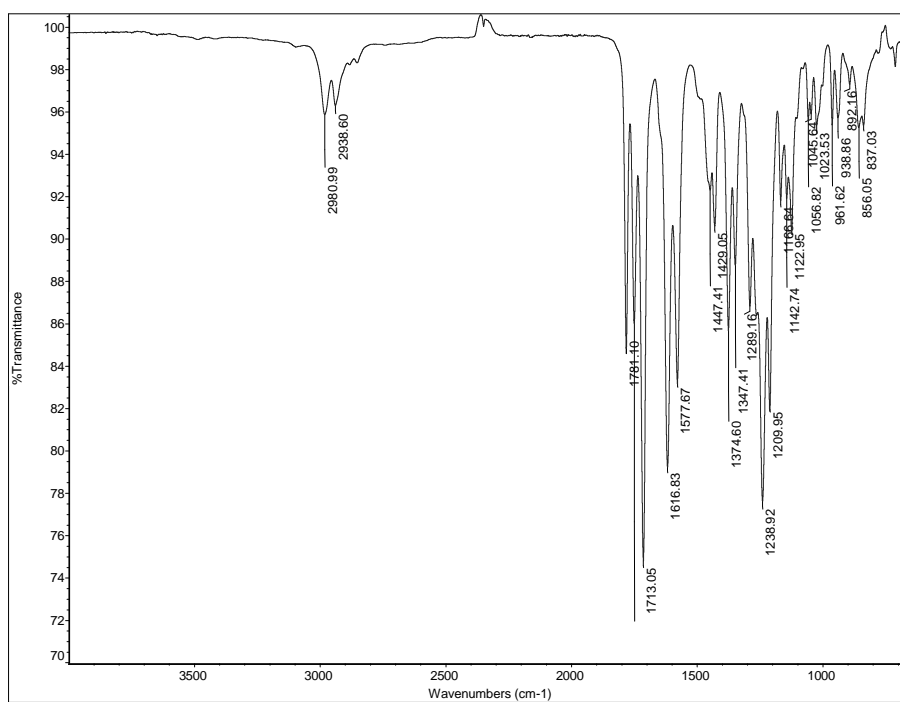
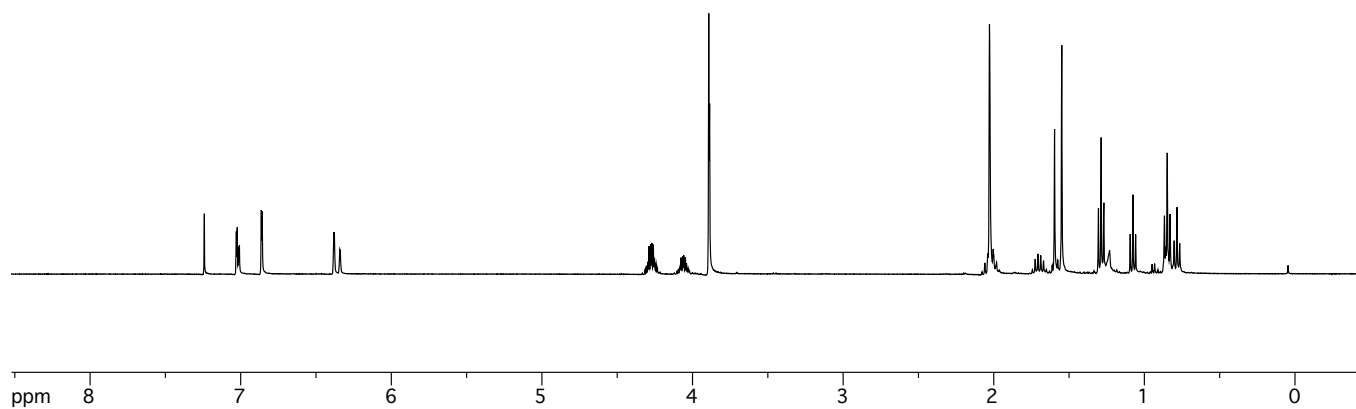
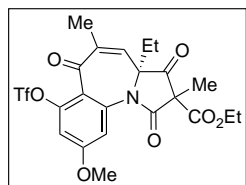
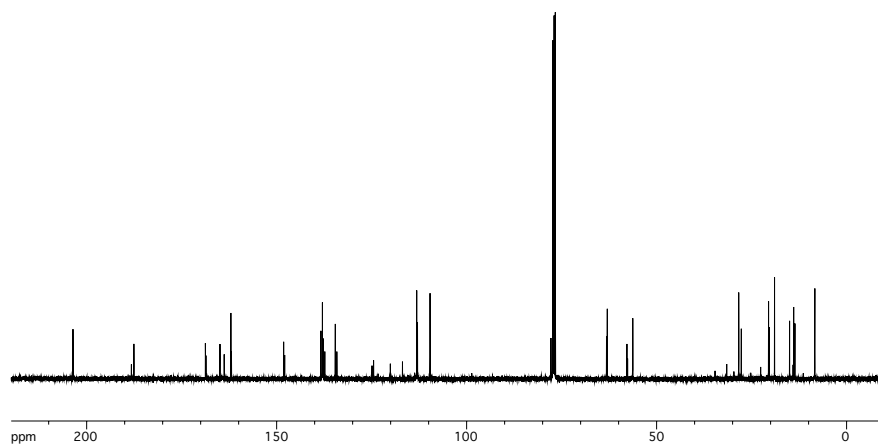


Figure A2.184. FTIR of phenol 365.



**Figure A2.185.** <sup>1</sup>H-NMR of triflate **366**.



**Figure A2.186.**  $^{13}\text{C}$ -NMR of triflate **366**.

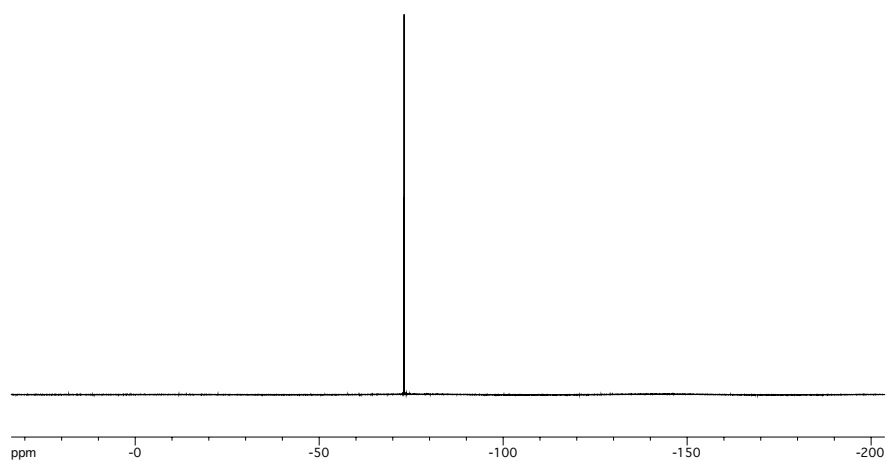


**Figure A2.187.**  $^{19}\text{F}$ -NMR of triflate **366**.

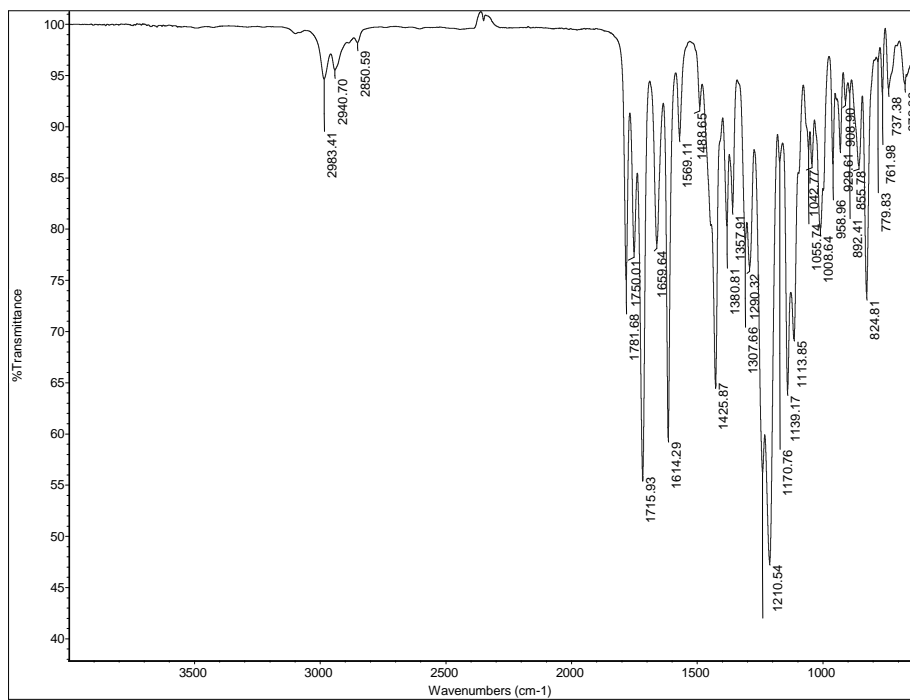


**Figure A2.188.** FTIR of triflate **366**.

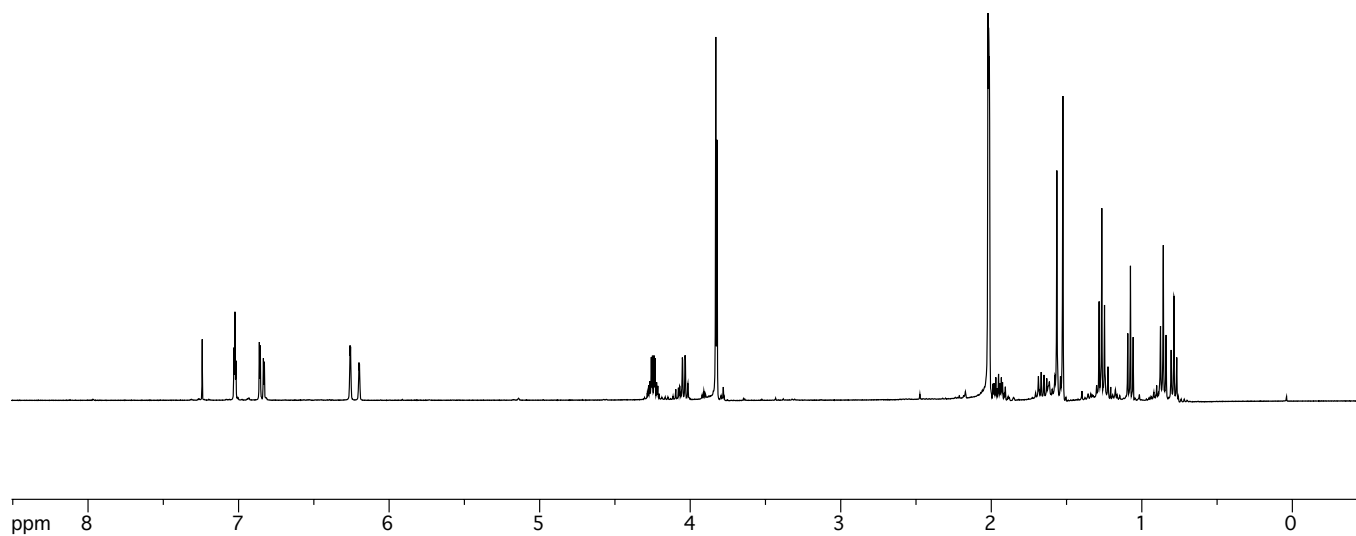
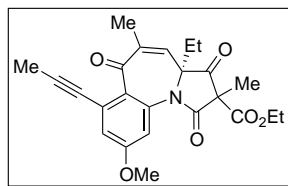


**Figure A2.189.** <sup>1</sup>H-NMR of alkyne 351.

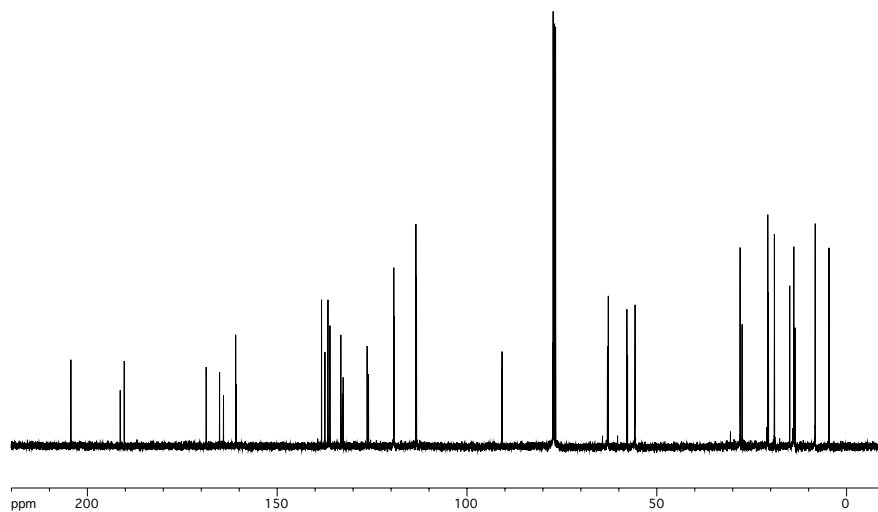


Figure A2.190.  $^{13}\text{C-NMR}$  of alkyne 351.

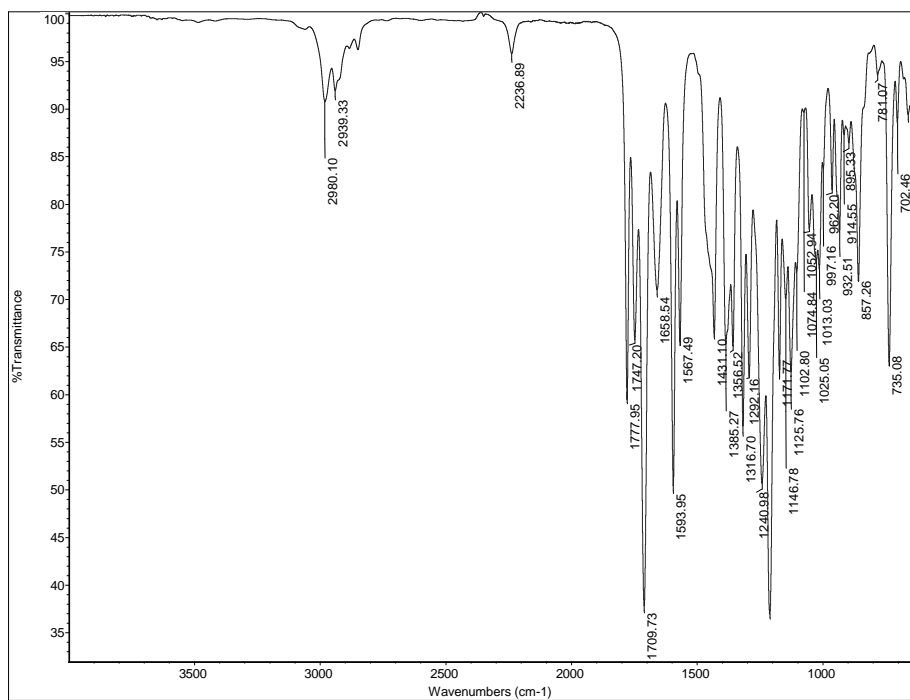
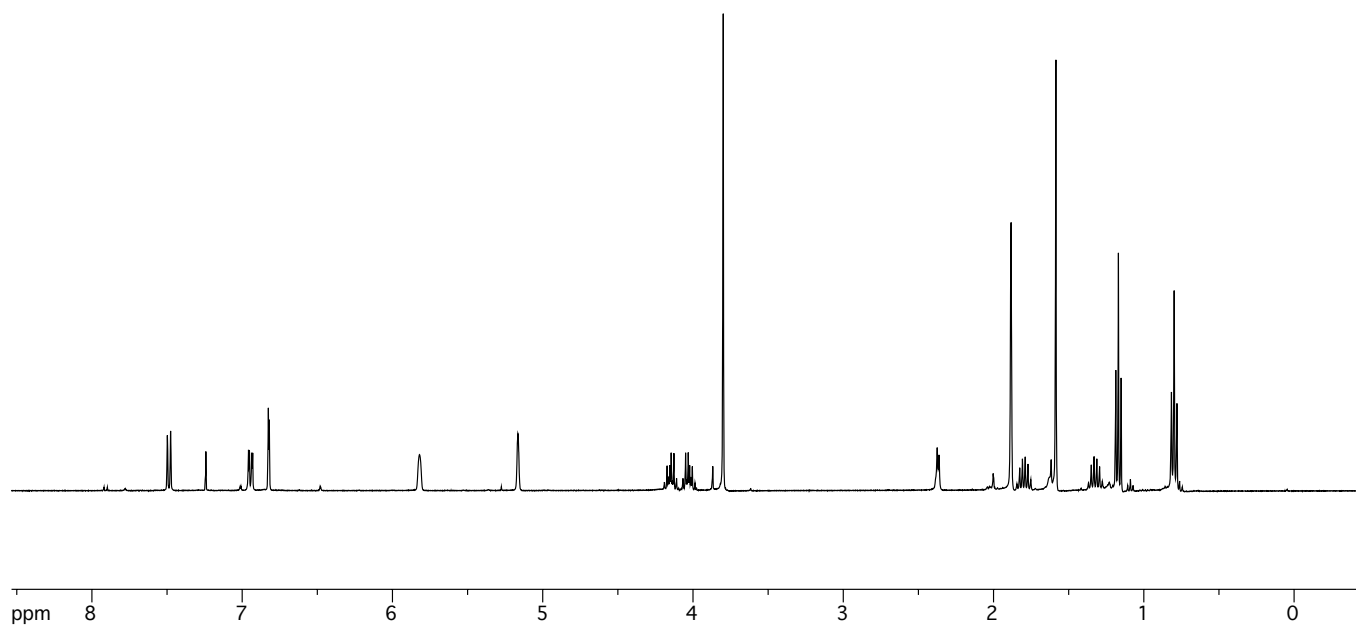
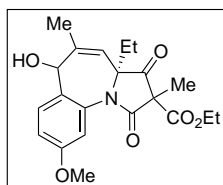
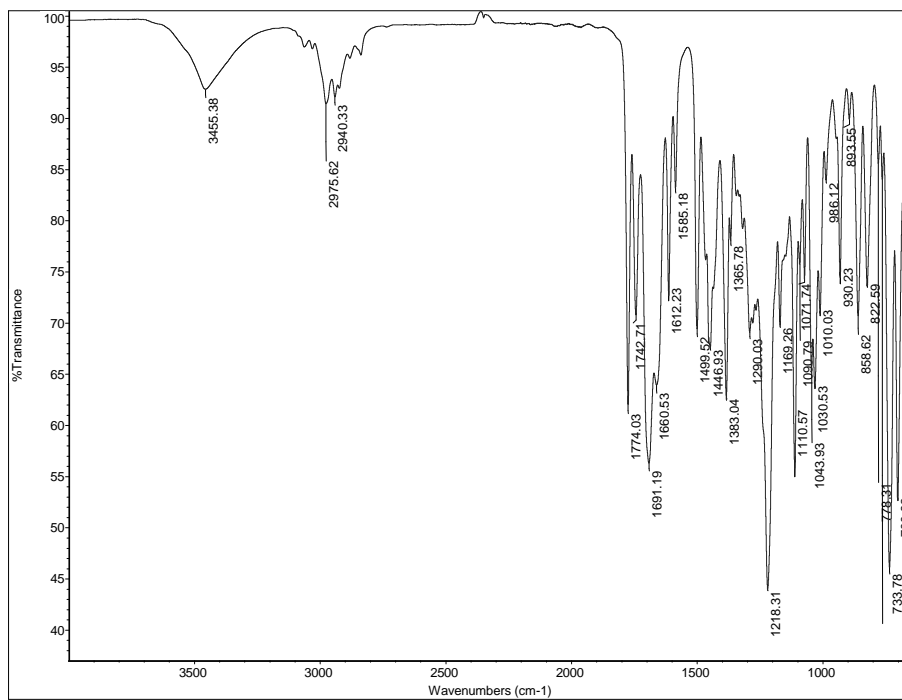


Figure A2.191. FTIR of alkyne 351.



**Figure A2.192.**  $^1\text{H-NMR}$  of allylic alcohol **367** (diastereomer A).



**Figure A2.193.** FTIR of allylic alcohol **367** (diastereomer A).

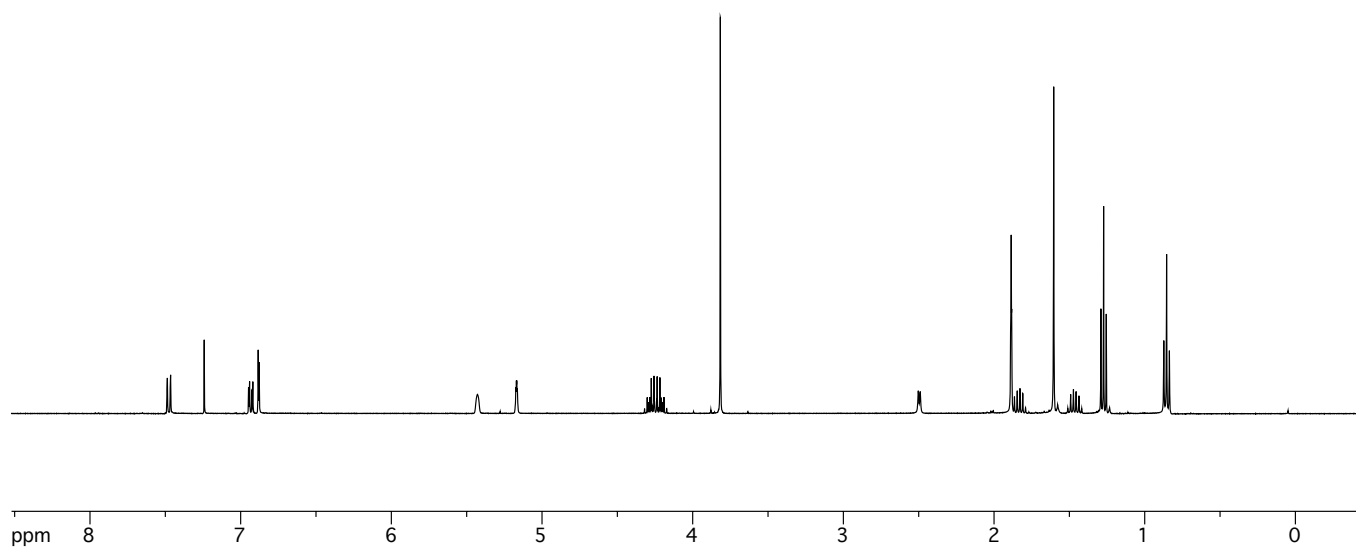
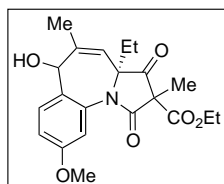


**Figure A2.194.**  $^1\text{H-NMR}$  of allylic alcohol **367** (diastereomer B).

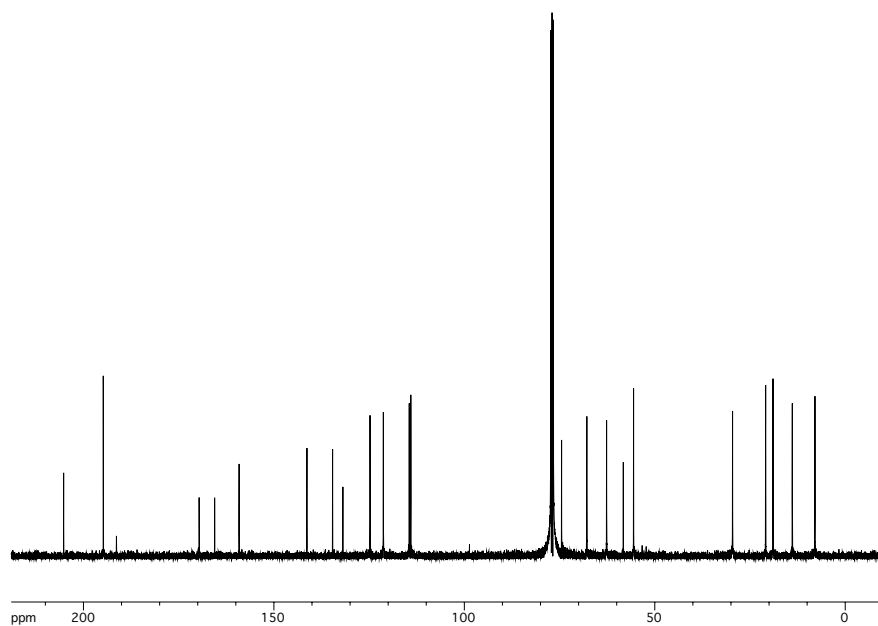


Figure A2.195. <sup>13</sup>C-NMR of allylic alcohol 367 (diastereomer B).

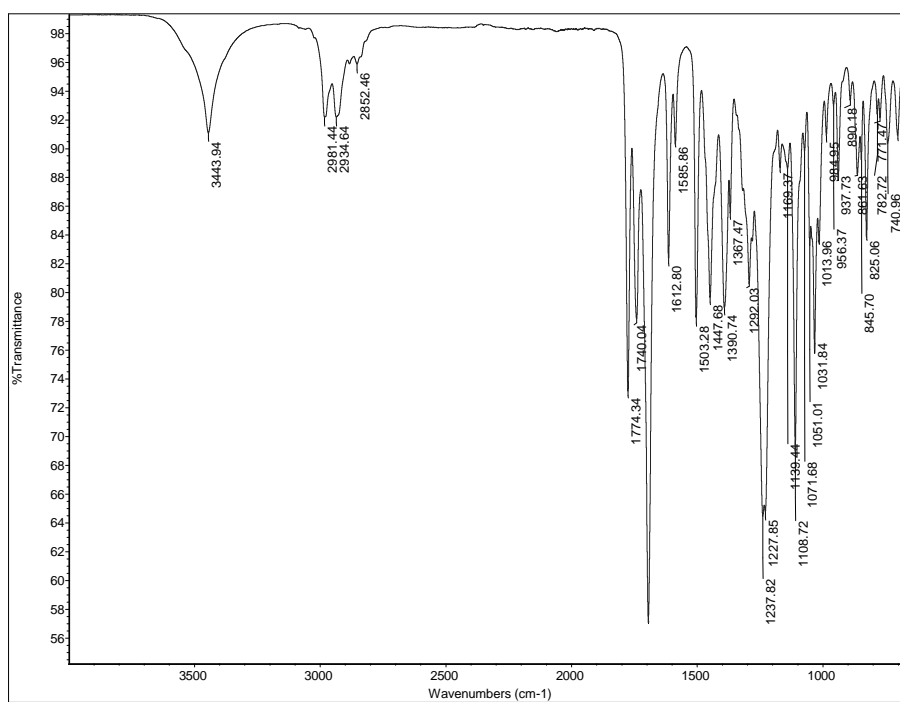
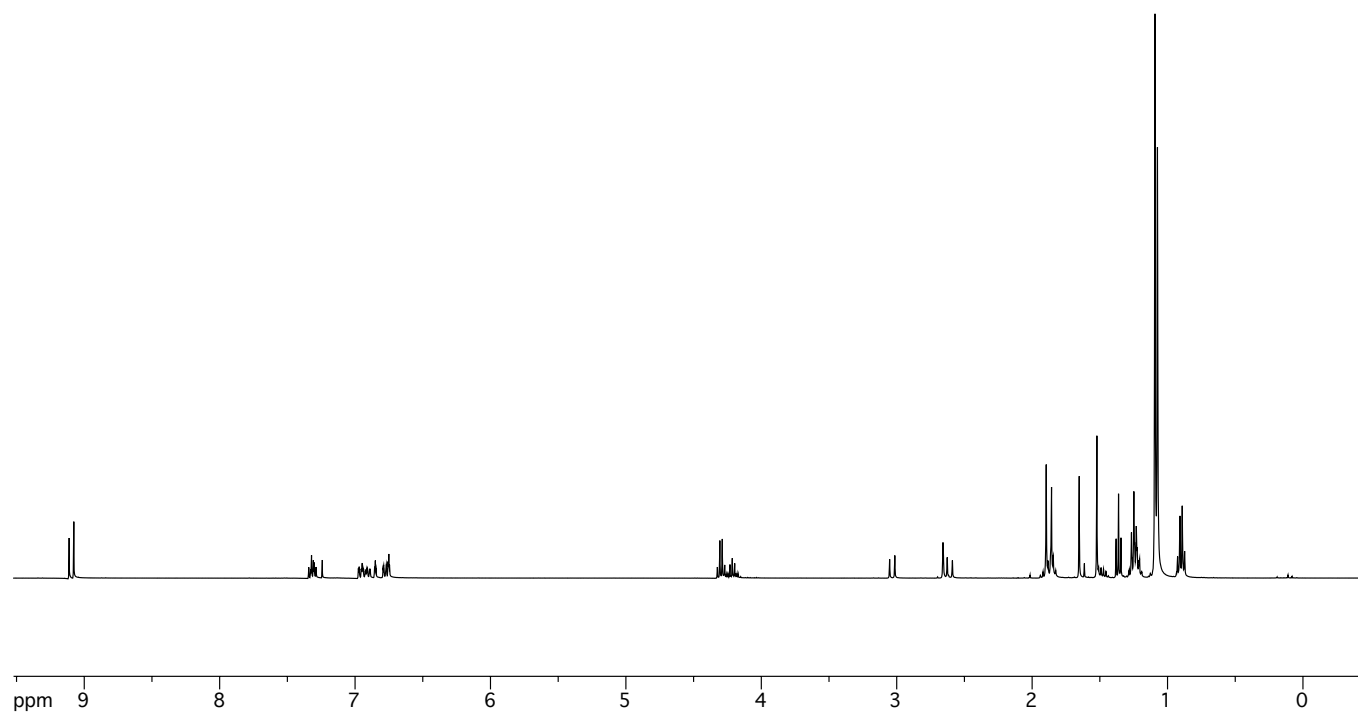
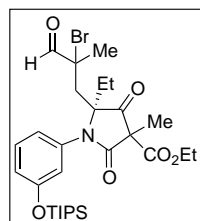


Figure A2.196. FTIR of allylic alcohol 367 (diastereomer B).



**Figure A2.197.** <sup>1</sup>H-NMR of aldehyde **370**.

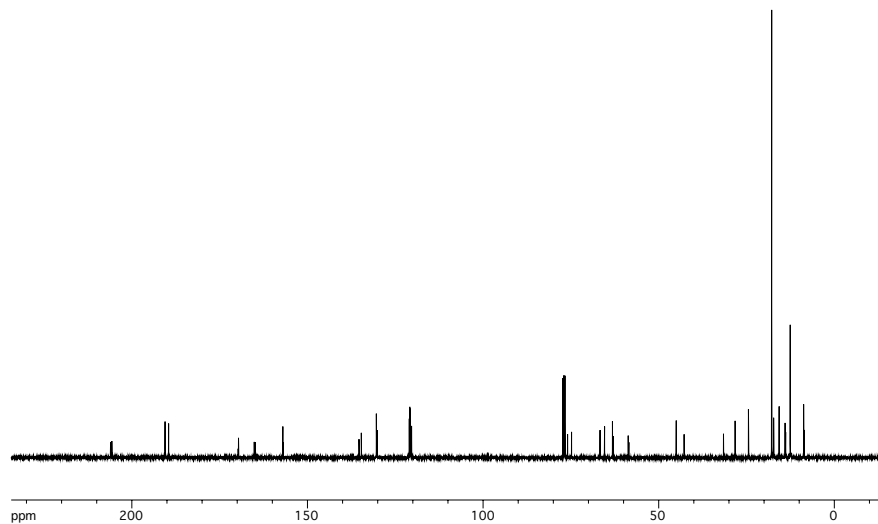


Figure A2.198.  $^{13}\text{C-NMR}$  of aldehyde 370.

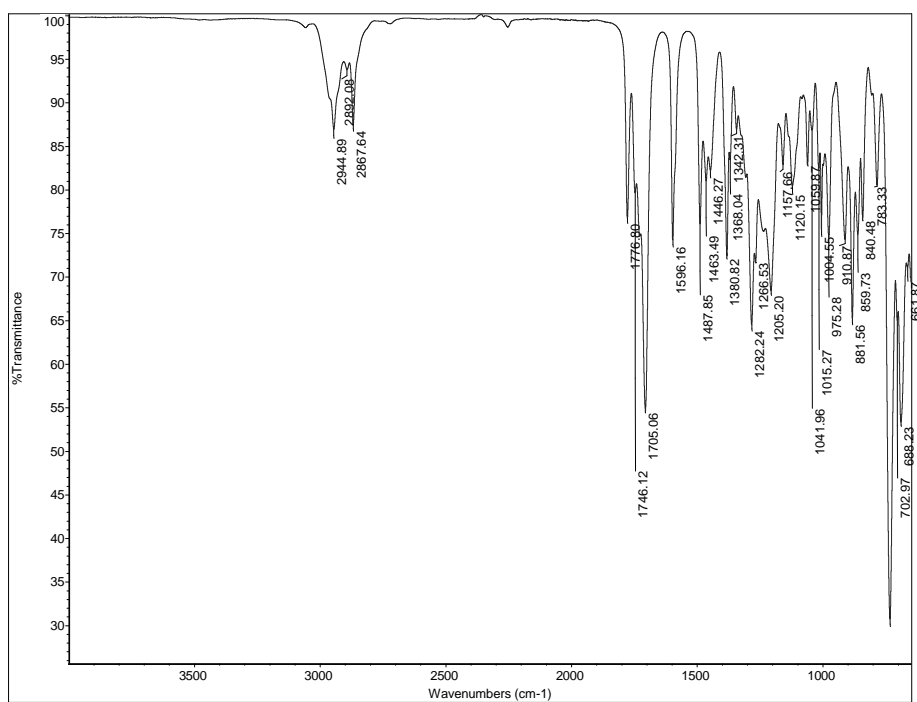
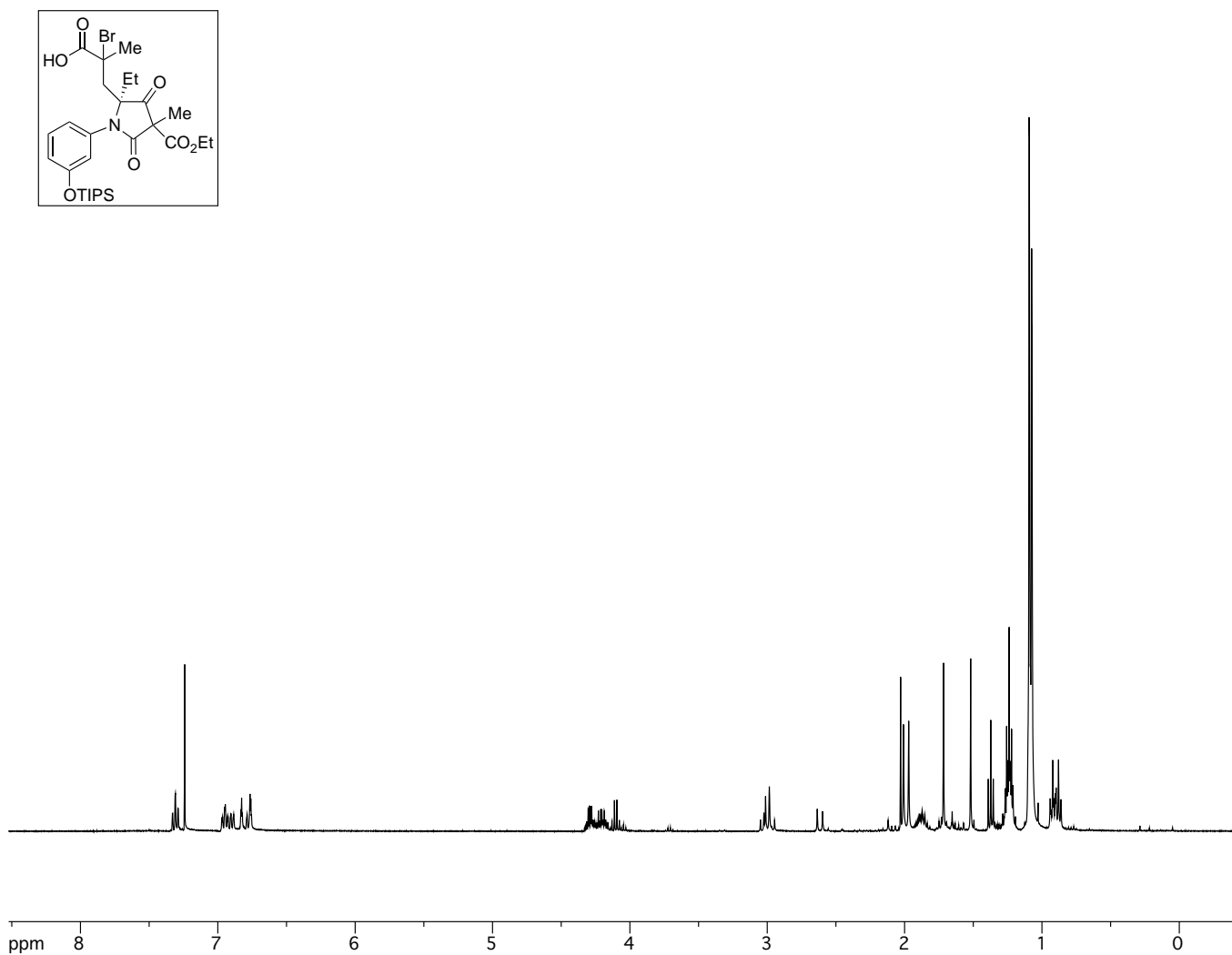


Figure A2.199. FTIR of aldehyde 370.



**Figure A2.200.** <sup>1</sup>H-NMR of carboxylic acid **371**.

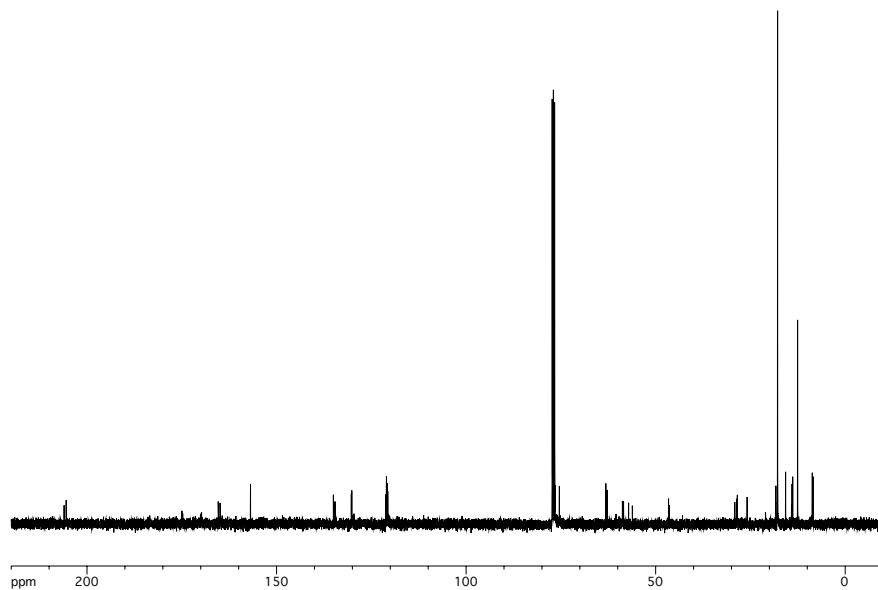


Figure A2.201.  $^{13}\text{C}$ -NMR of carboxylic acid **371**.

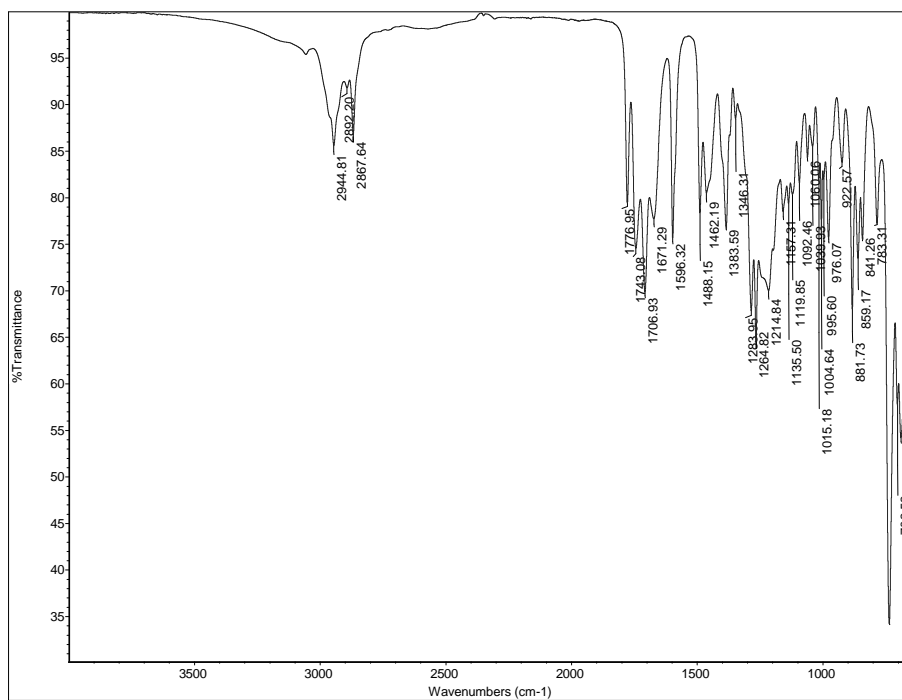
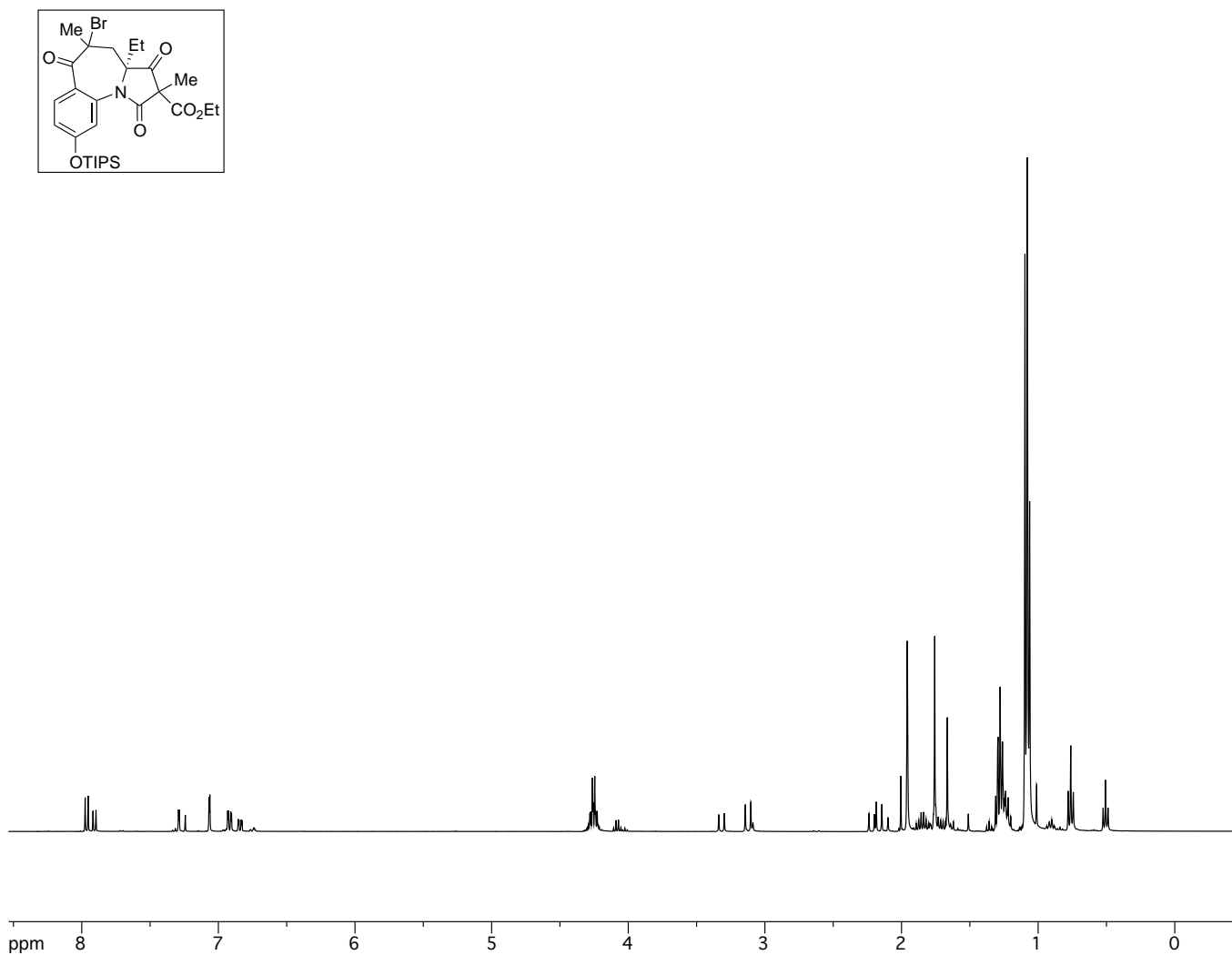


Figure A2.202. FTIR of carboxylic acid **371**.



**Figure A2.203.** <sup>1</sup>H-NMR of ketone **372**.

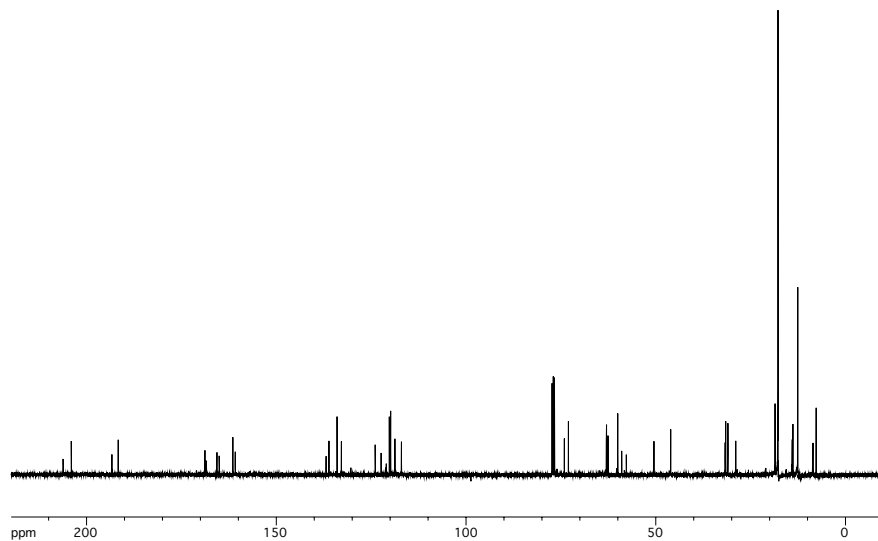


Figure A2.204.  $^{13}\text{C-NMR}$  of ketone 372.

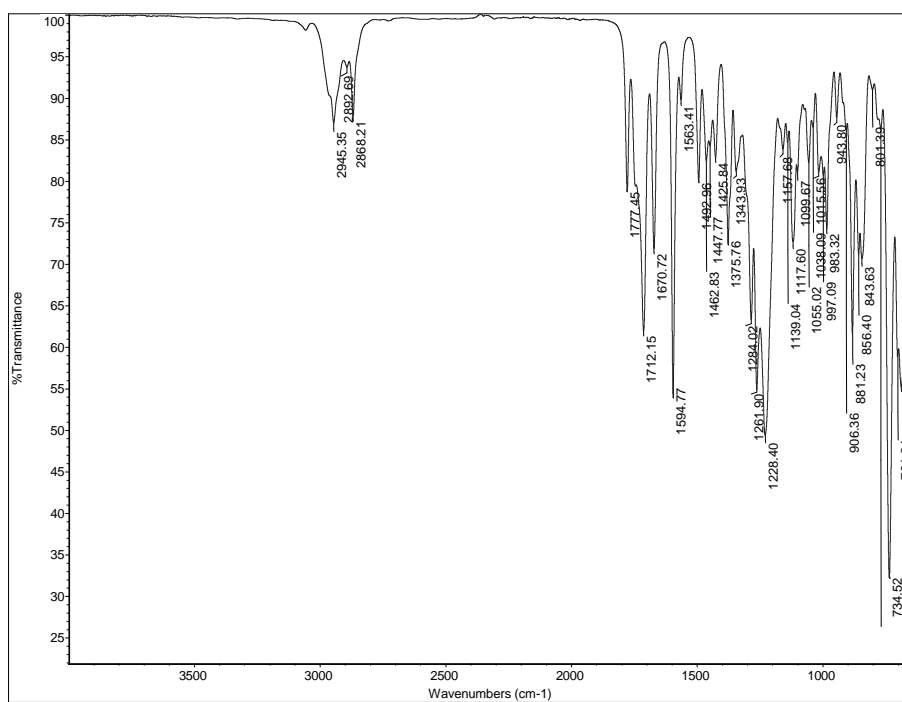
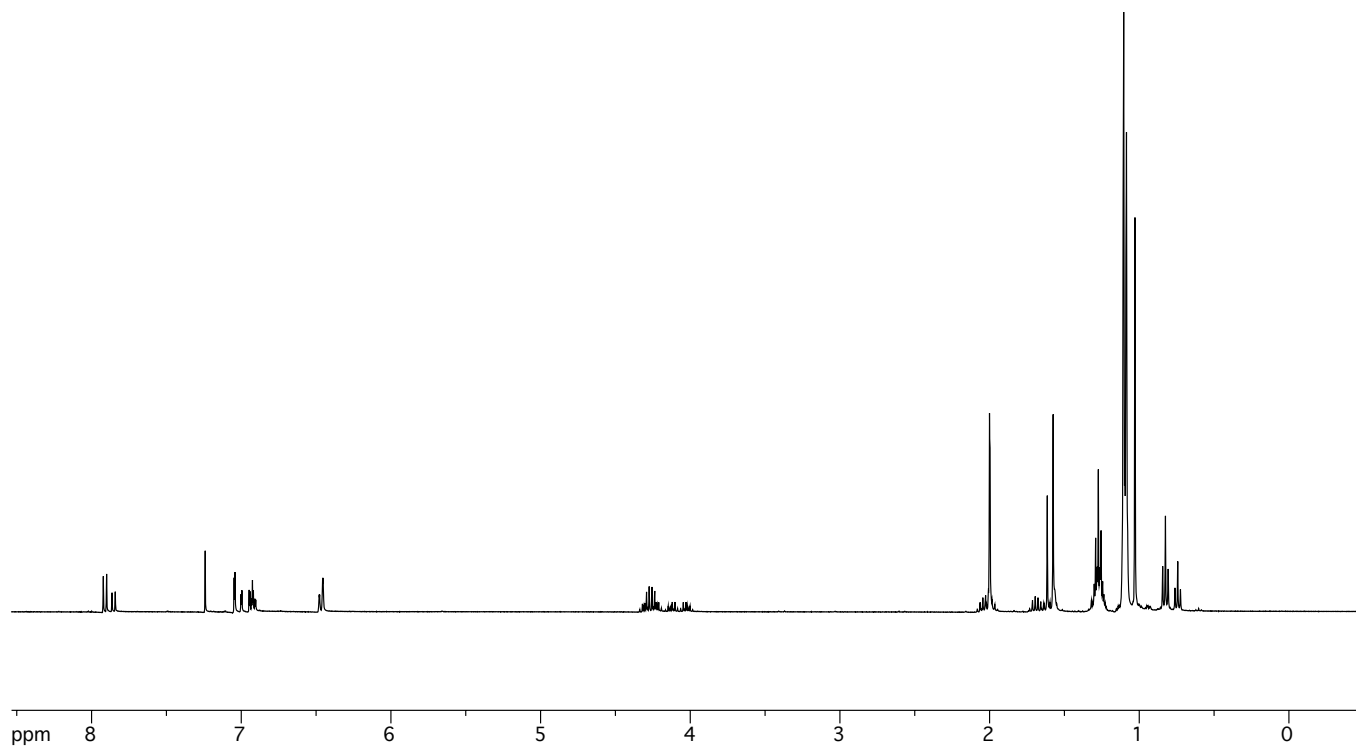
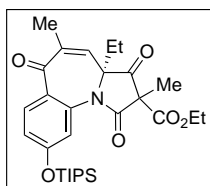


Figure A2.205. FTIR of ketone 372.



**Figure A2.206.** <sup>1</sup>H-NMR of enone **373**.

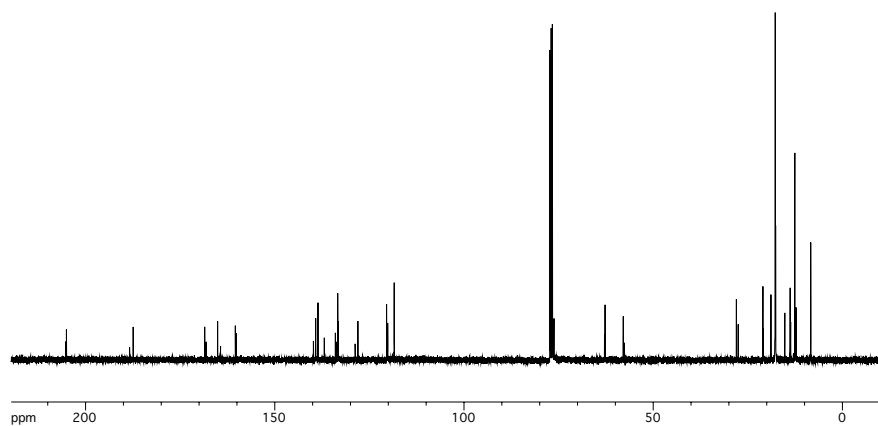


Figure A2.207.  $^{13}\text{C-NMR}$  of enone 373.

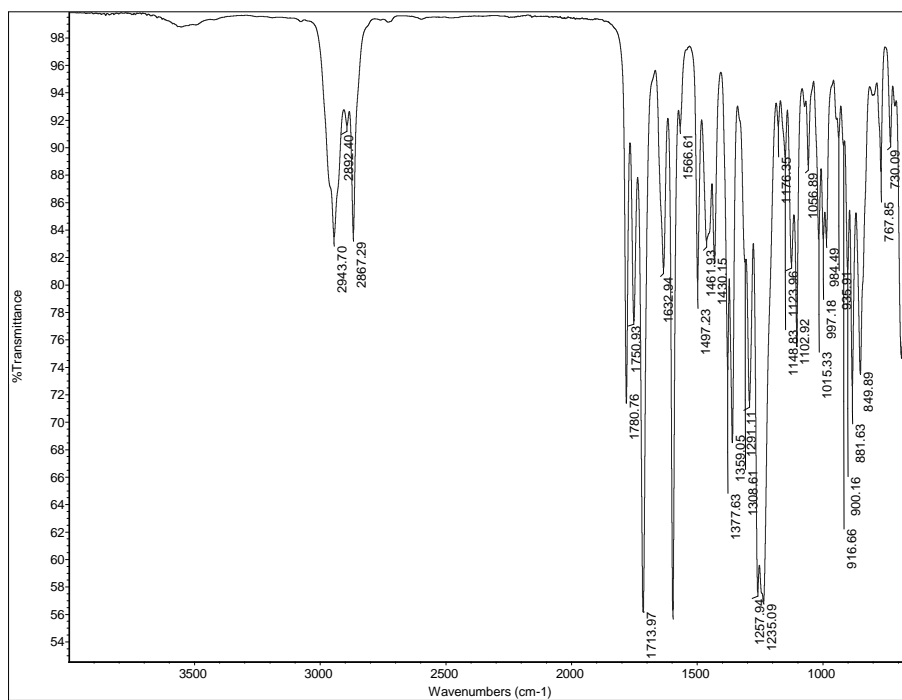


Figure A2.208. FTIR of enone 373.

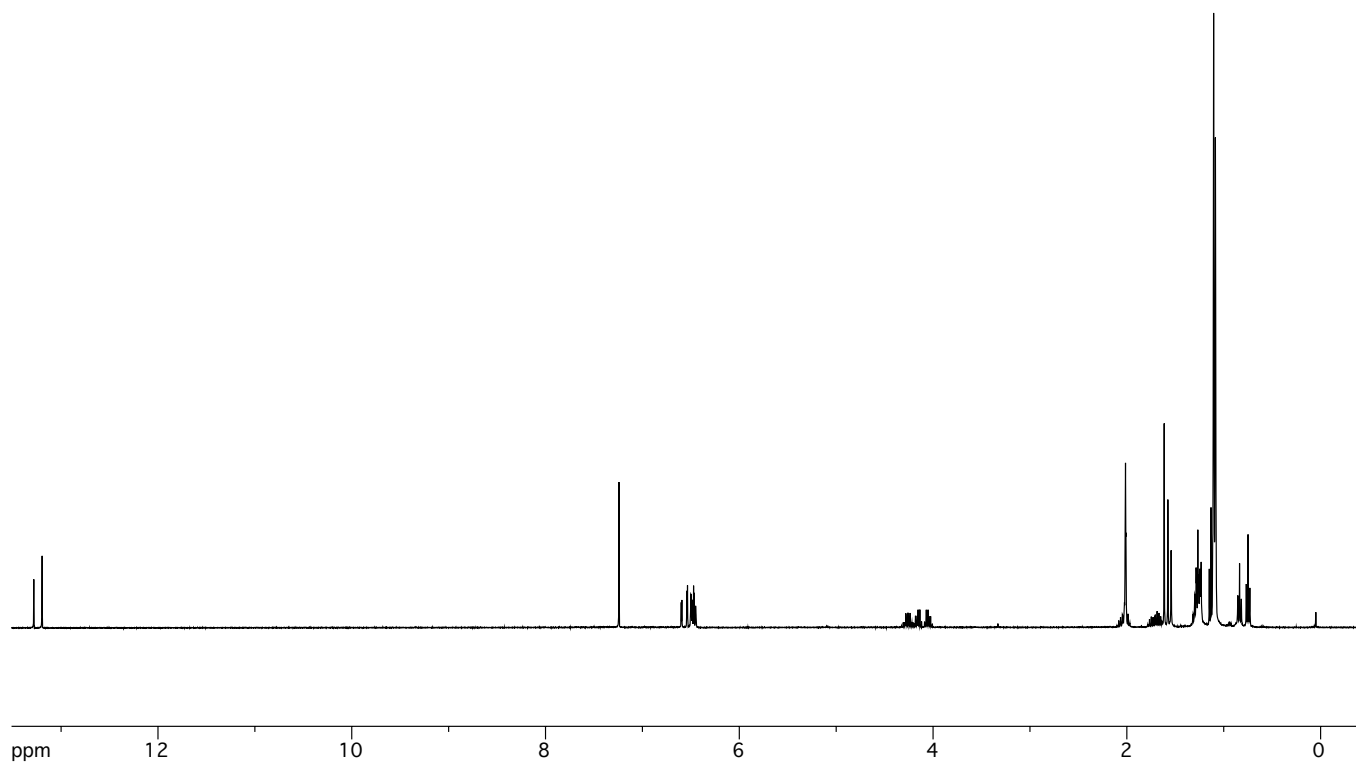
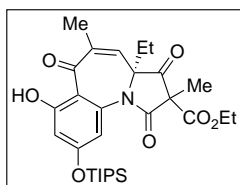


Figure A2.209. <sup>1</sup>H-NMR of phenol 374.

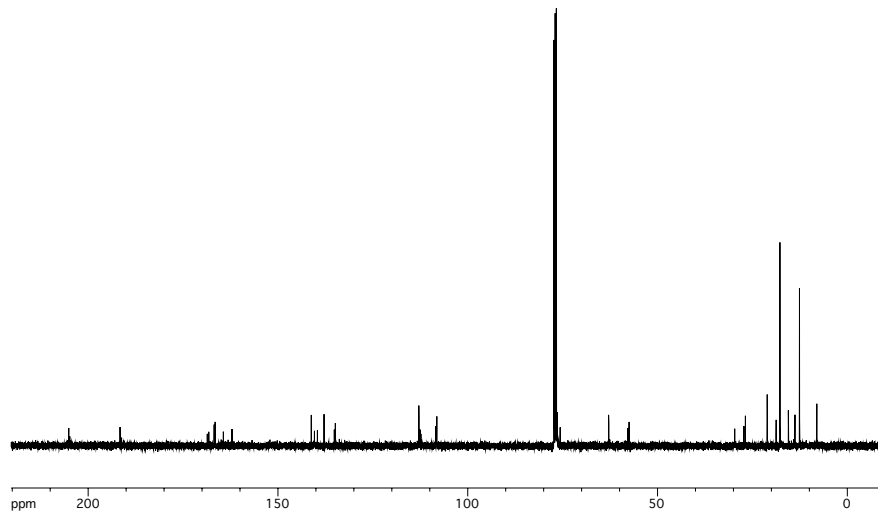


Figure A2.210. <sup>13</sup>C-NMR of phenol 374.

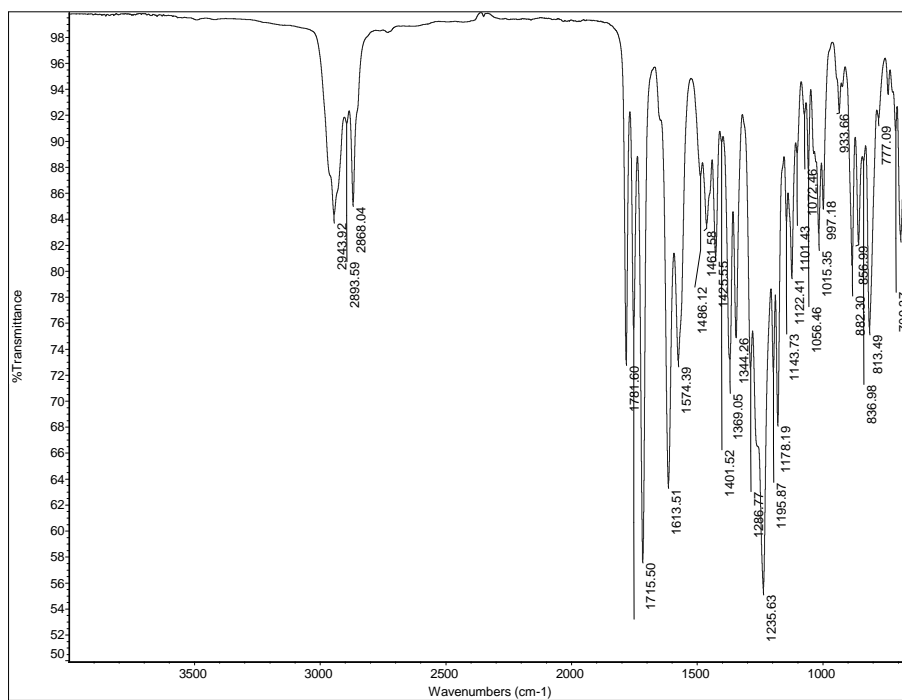
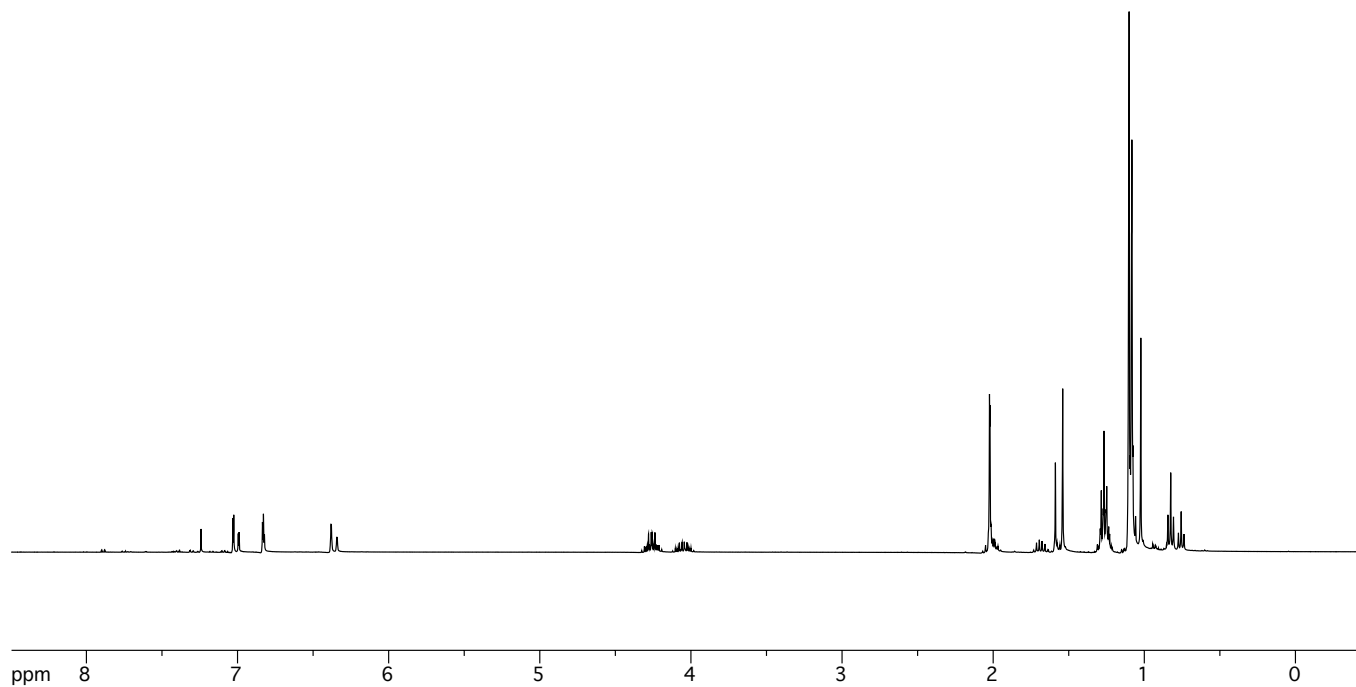
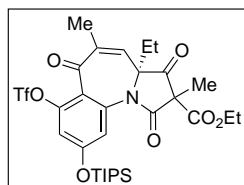
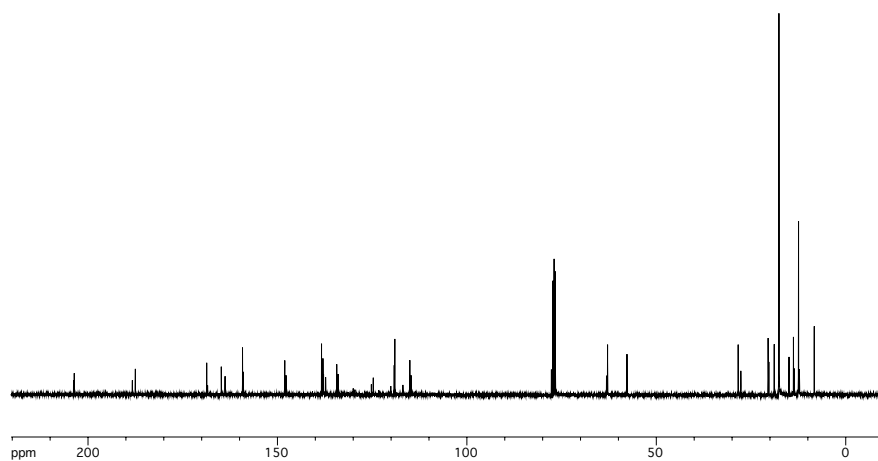


Figure A2.211. FTIR of phenol 374.



**Figure A2.212.** <sup>1</sup>H-NMR of triflate **375**.



**Figure A2.213.**  $^{13}\text{C}$ -NMR of triflate **375**.

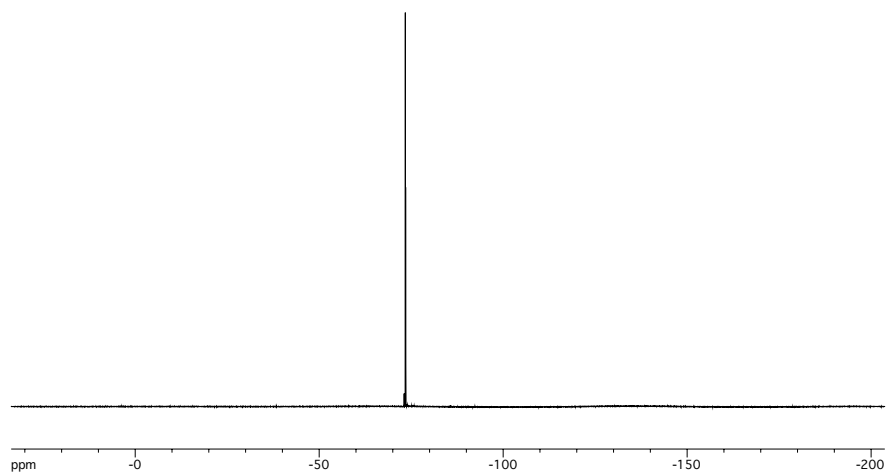


**Figure A2.214.**  $^{19}\text{F}$ -NMR of triflate **375**.

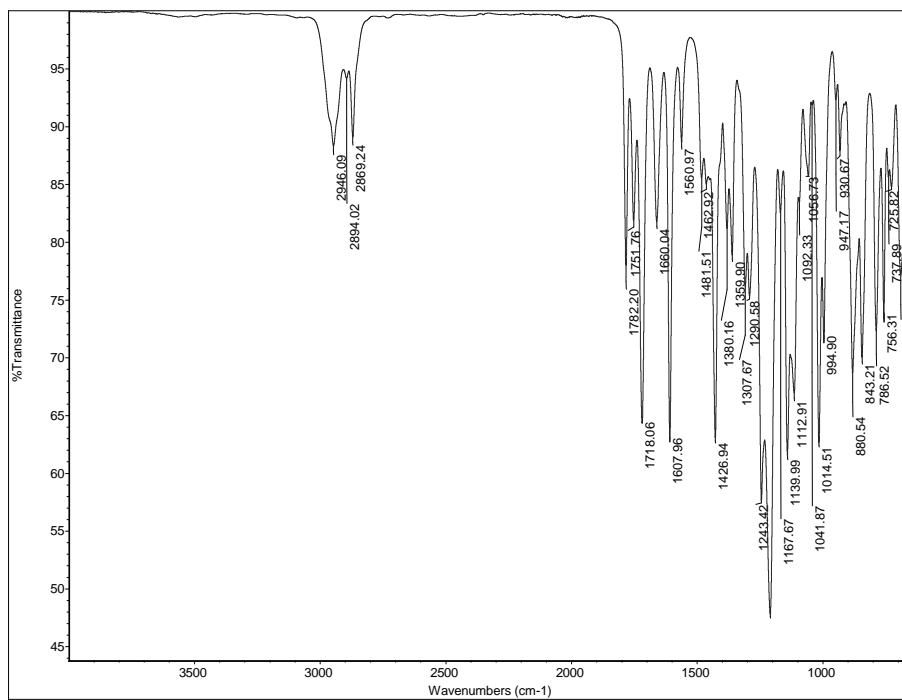


**Figure A2.215.** FTIR of triflate **375**.

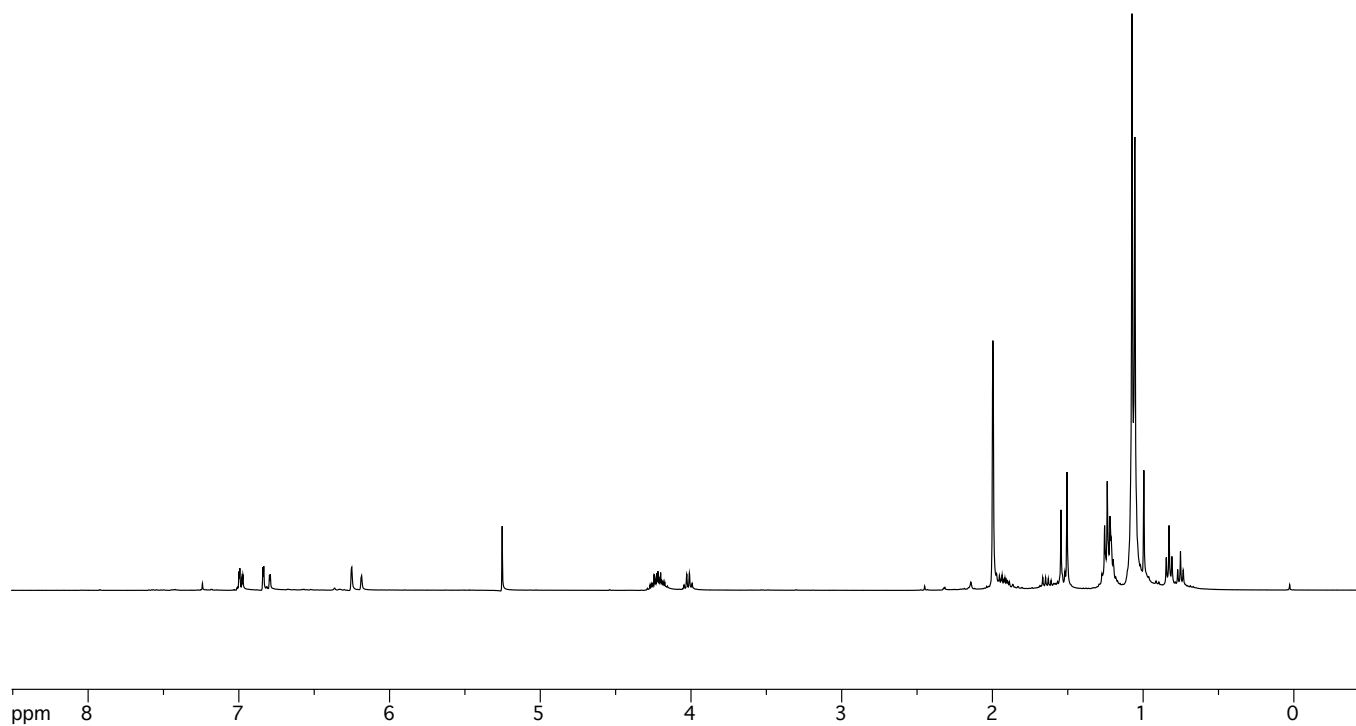
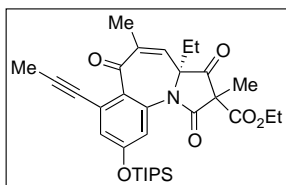


**Figure A2.216.** <sup>1</sup>H-NMR of alkyne **376**.

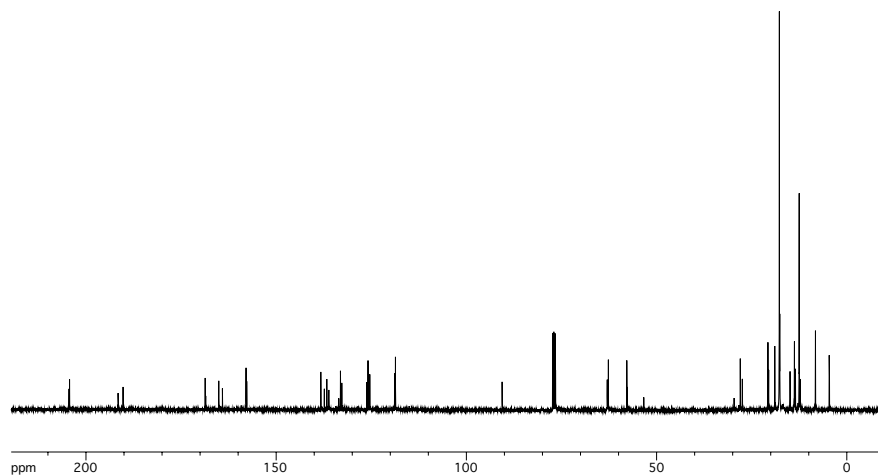


Figure A2.217.  $^{13}\text{C}$ -NMR of alkyne 376.

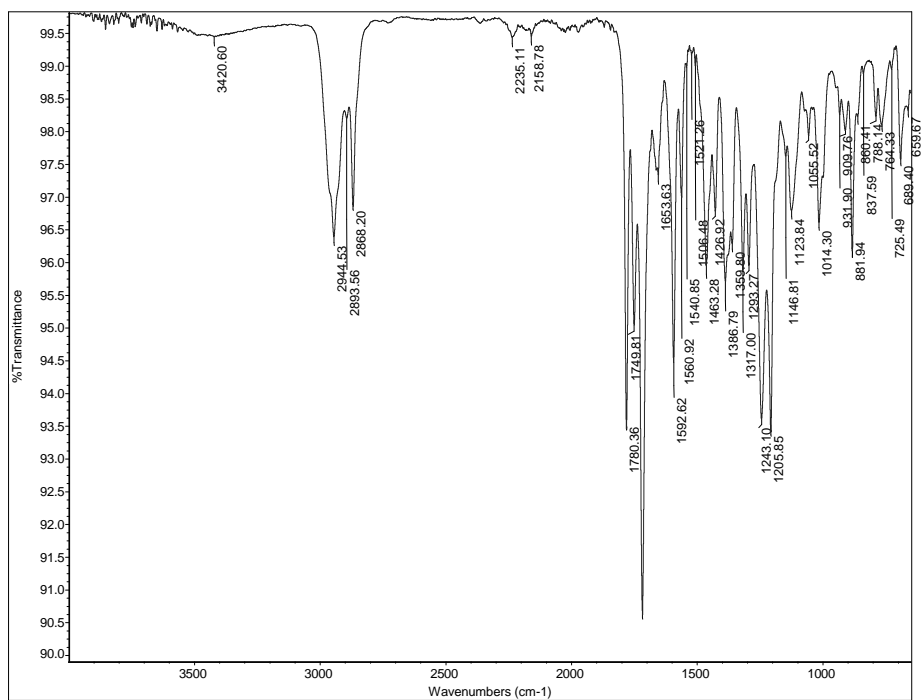
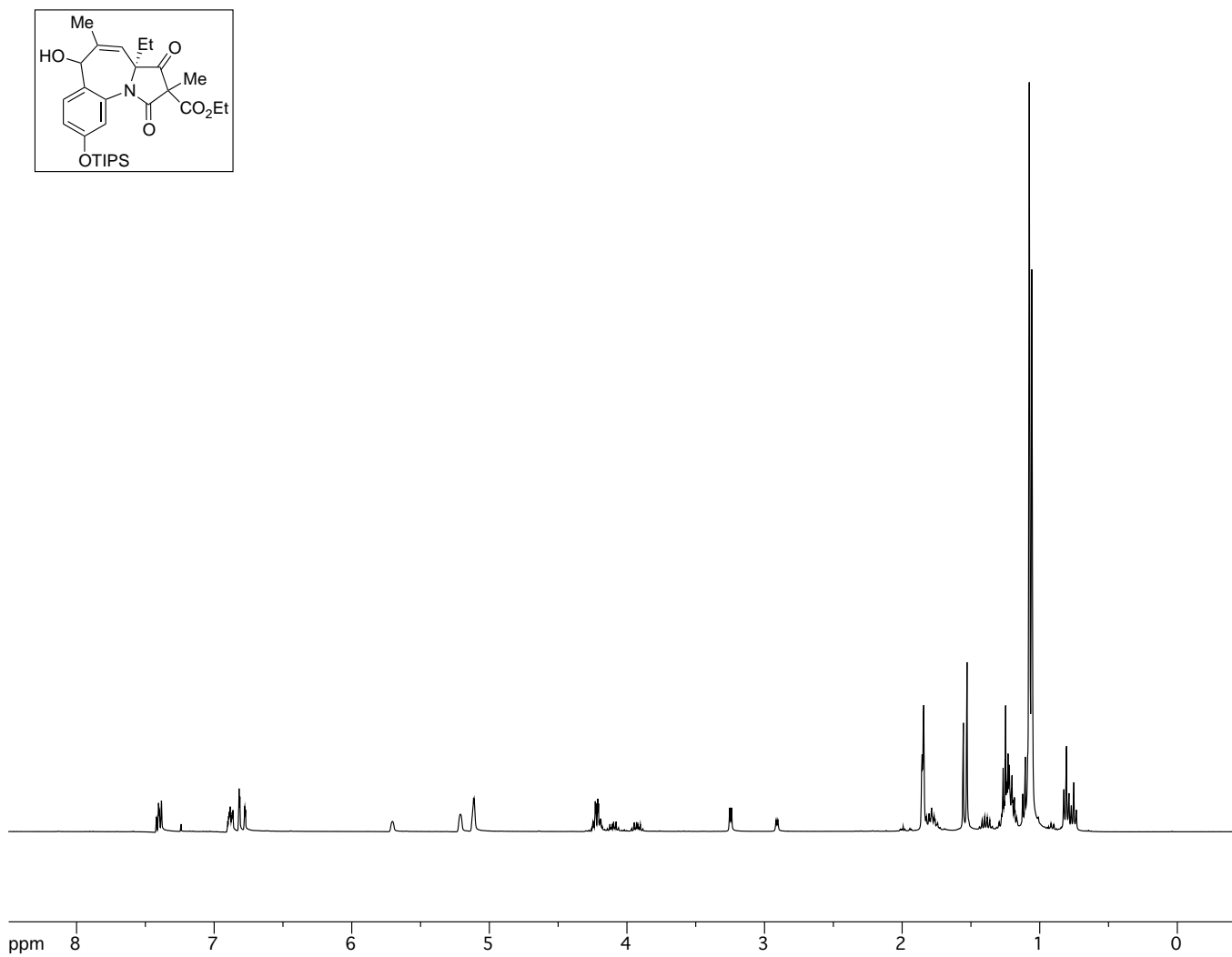


Figure A2.218. FTIR of alkyne 376.



**Figure A2.219.** <sup>1</sup>H-NMR of allylic alcohol **377**.

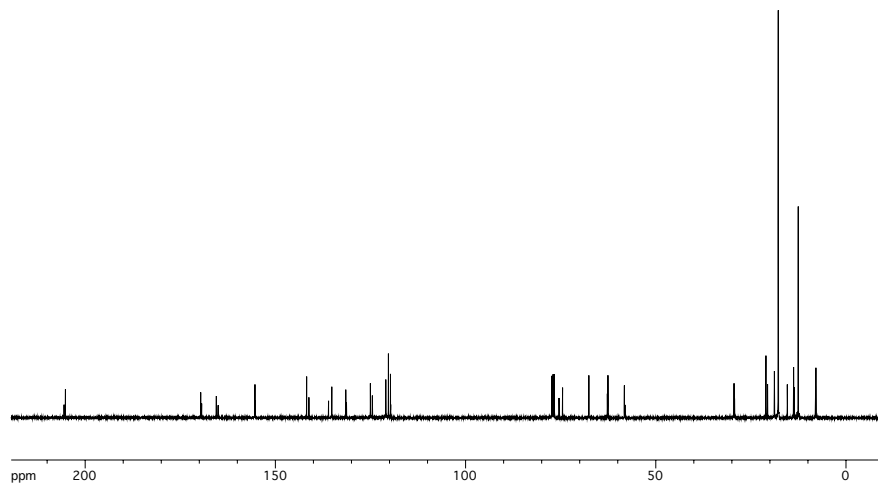


Figure A2.220.  $^{13}\text{C-NMR}$  of allylic alcohol 377.

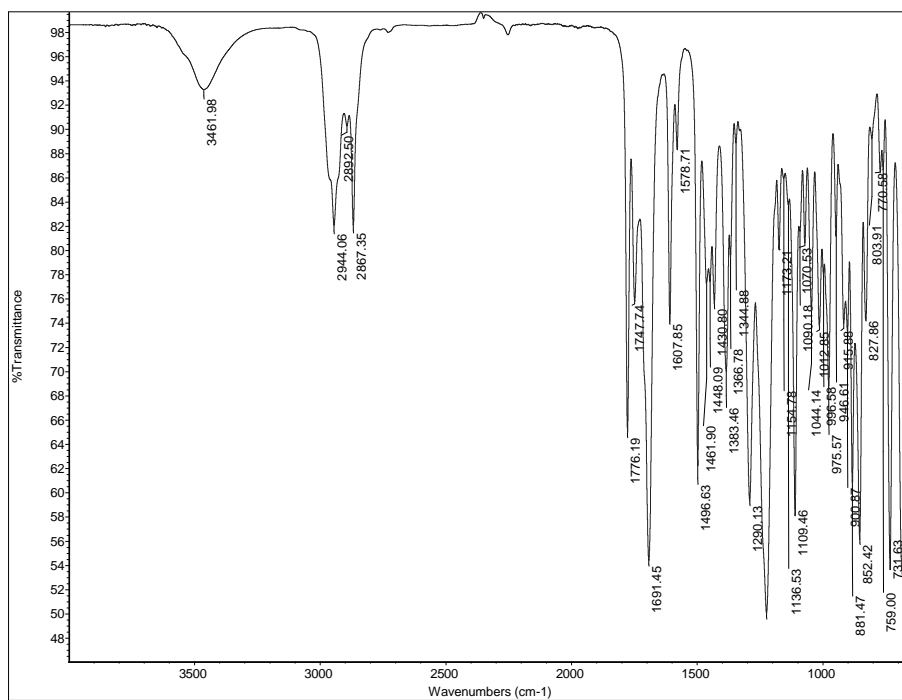
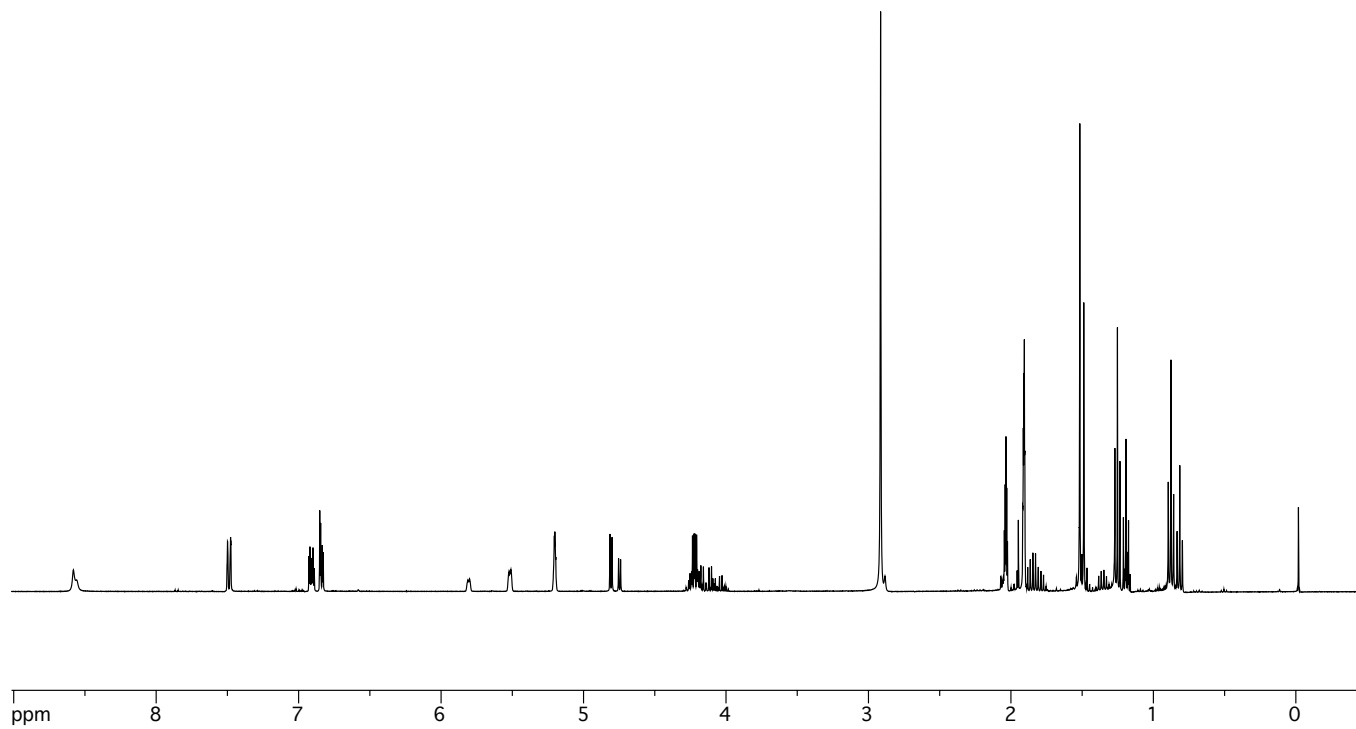
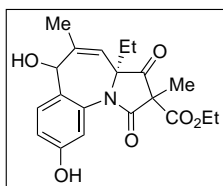
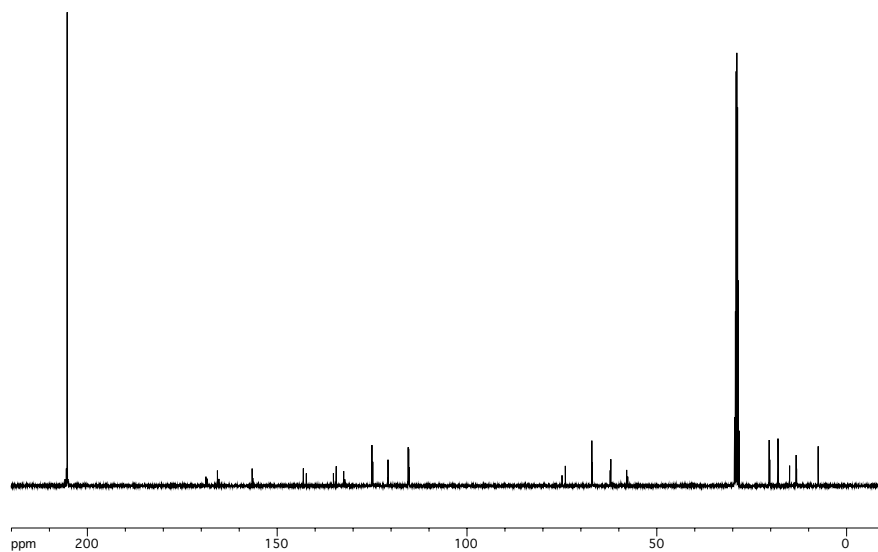


Figure A2.221. FTIR of allylic alcohol 377.



**Figure A2.222.** <sup>1</sup>H-NMR of phenol 368.



**Figure A2.223.**  $^{13}\text{C}$ -NMR of phenol **368**.

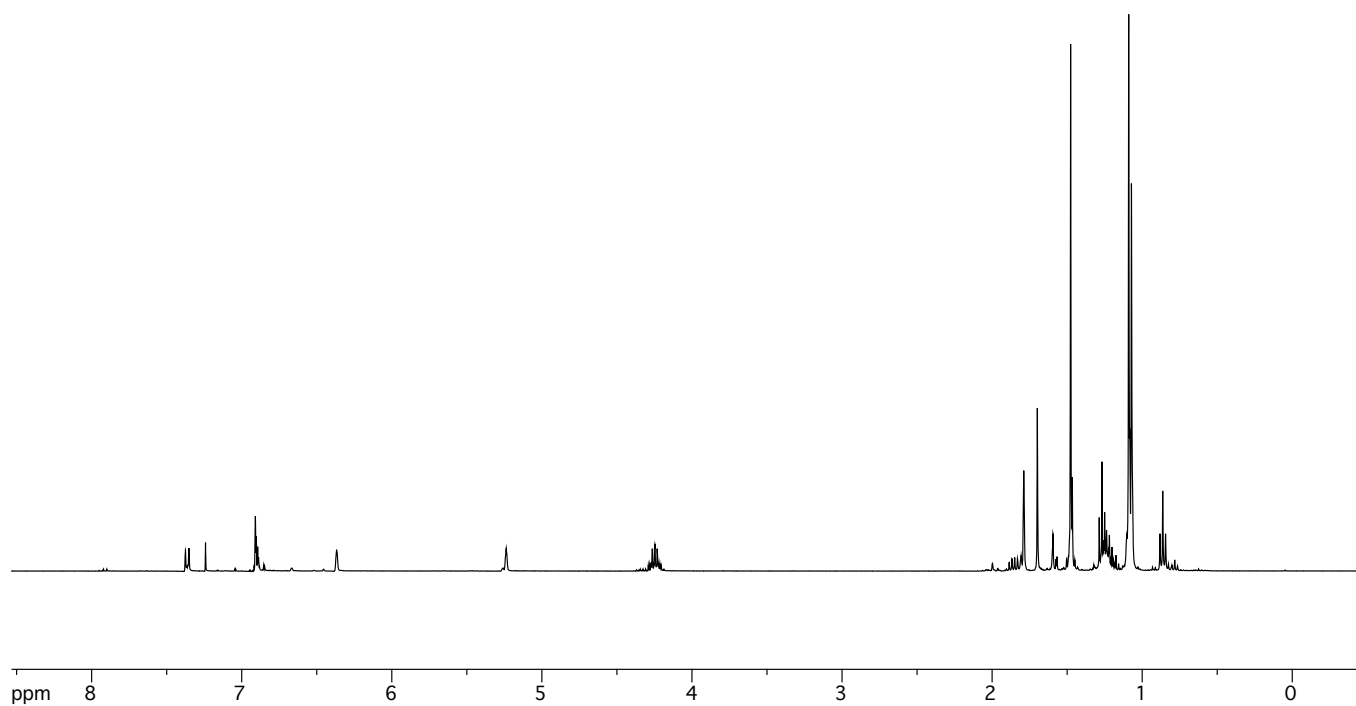
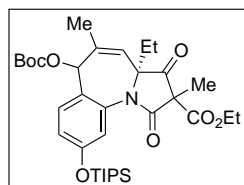


**Figure A2.224.** <sup>1</sup>H-NMR of carbonate **378**.

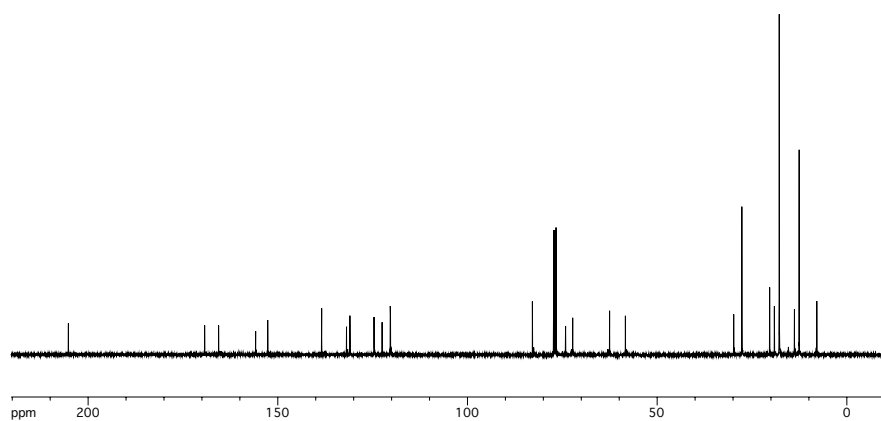


**Figure A2.225.**  $^{13}\text{C}$ -NMR of carbonate **378**.

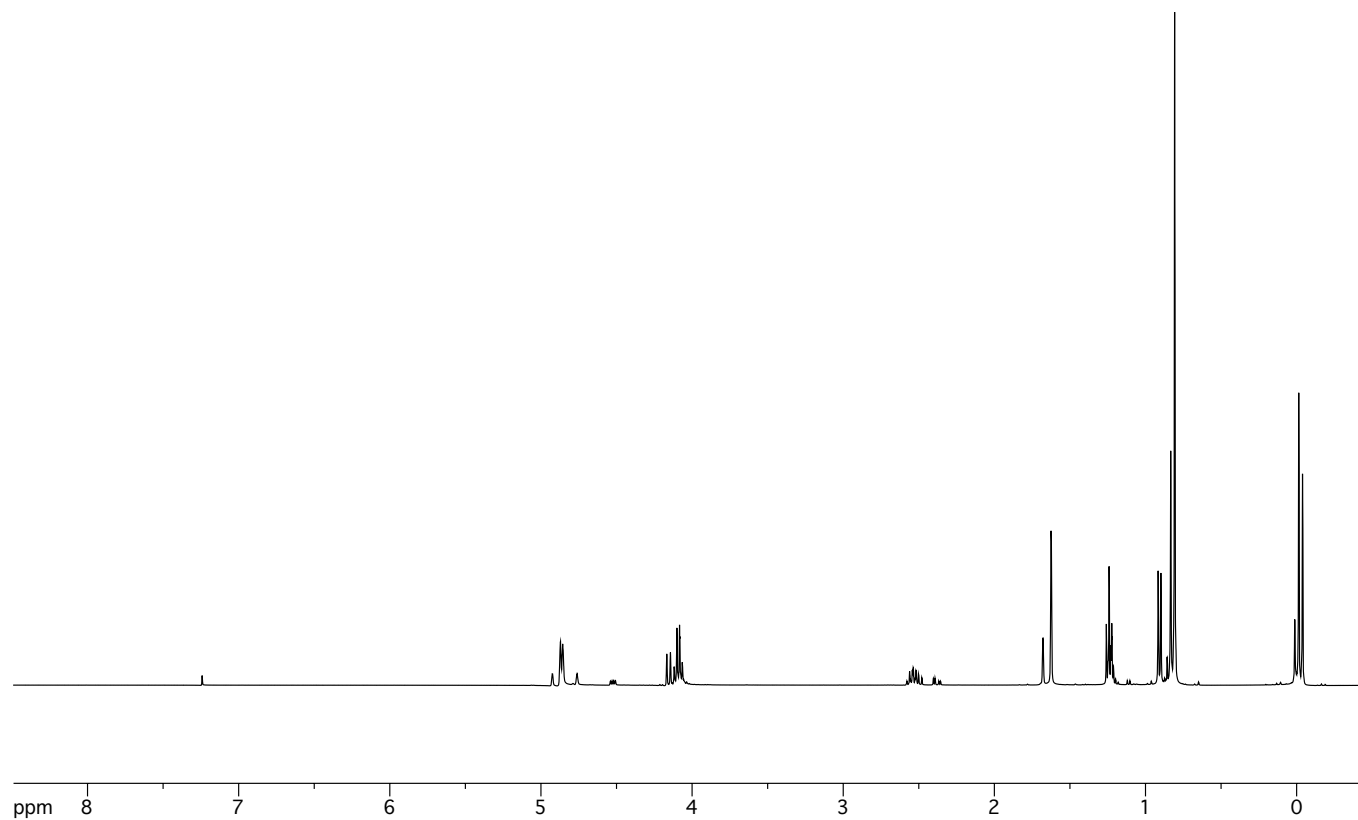
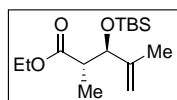


Figure A2.226. <sup>1</sup>H-NMR of silyl ether 465.

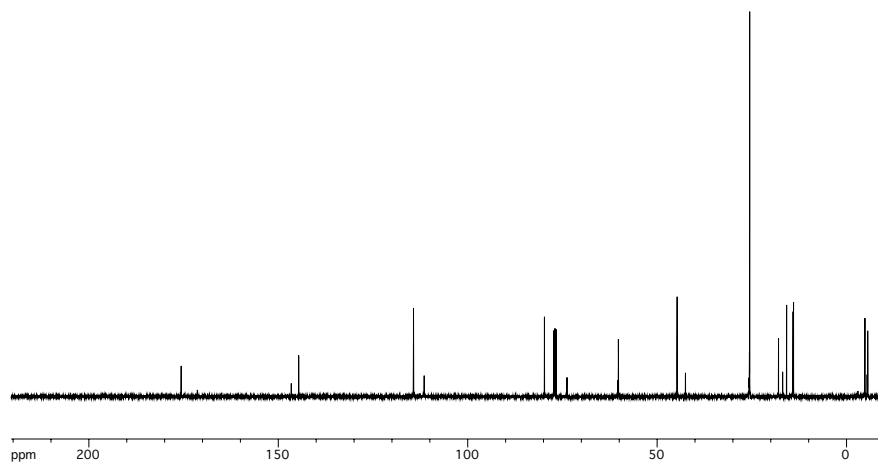


Figure A2.227.  $^{13}\text{C}$ -NMR of silyl ether **465**.

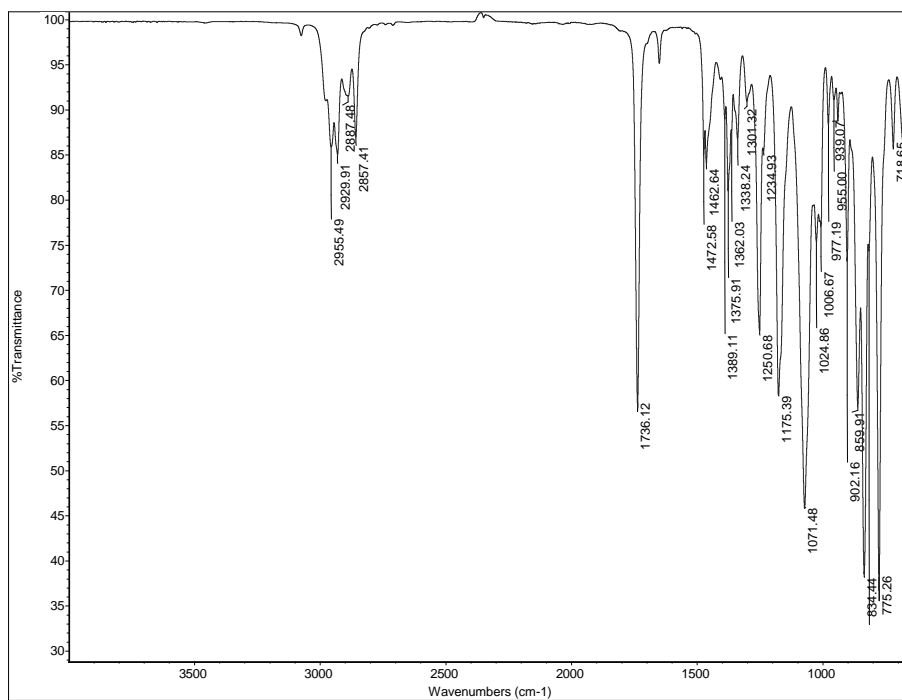


Figure A2.228. FTIR of silyl ether **465**.

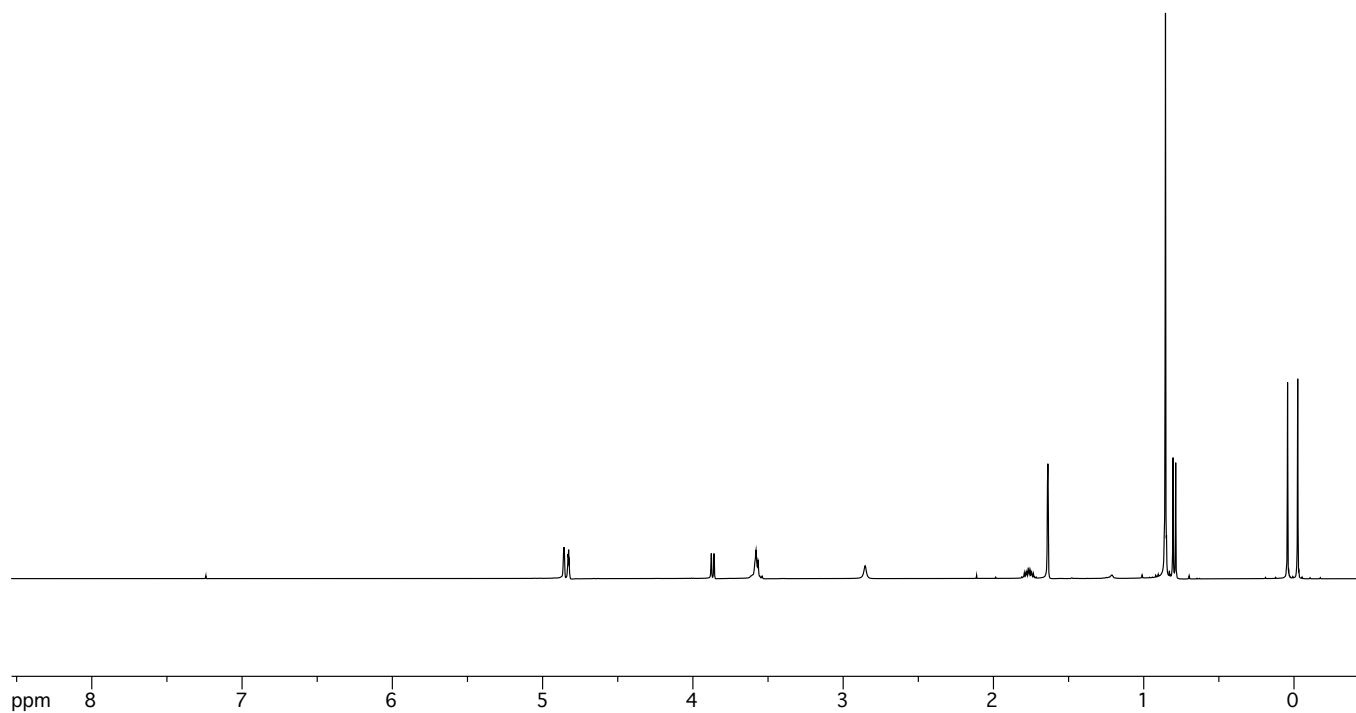
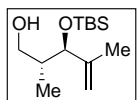


Figure A2.229.  $^1\text{H-NMR}$  of alcohol 466.

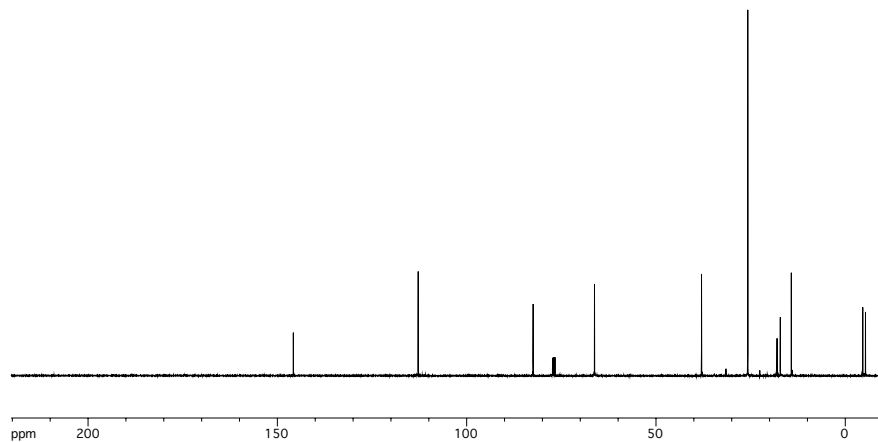


Figure A2.230.  $^{13}\text{C-NMR}$  of alcohol 466.

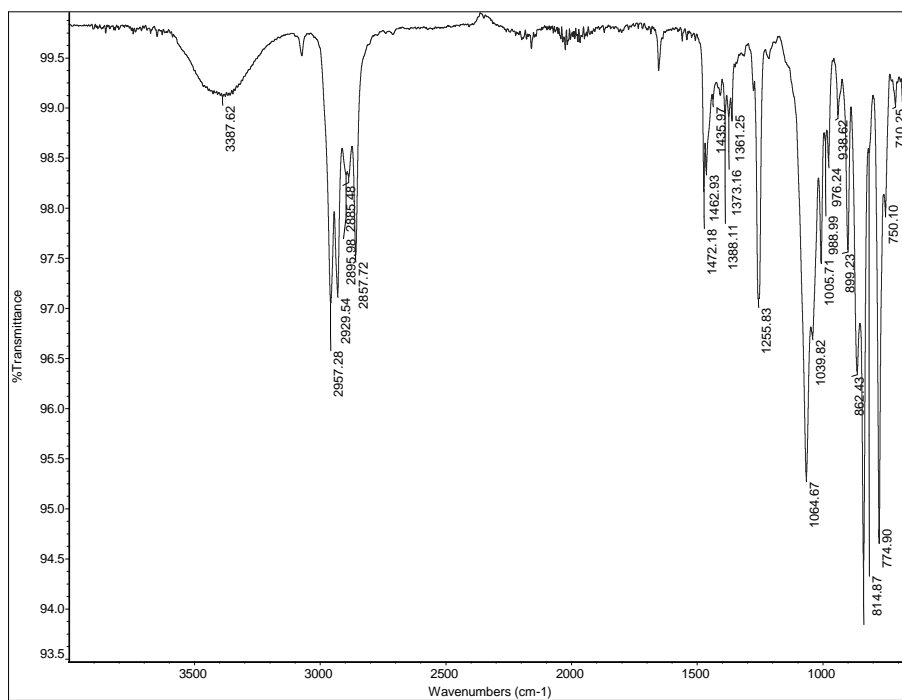


Figure A2.231. FTIR of alcohol 466.

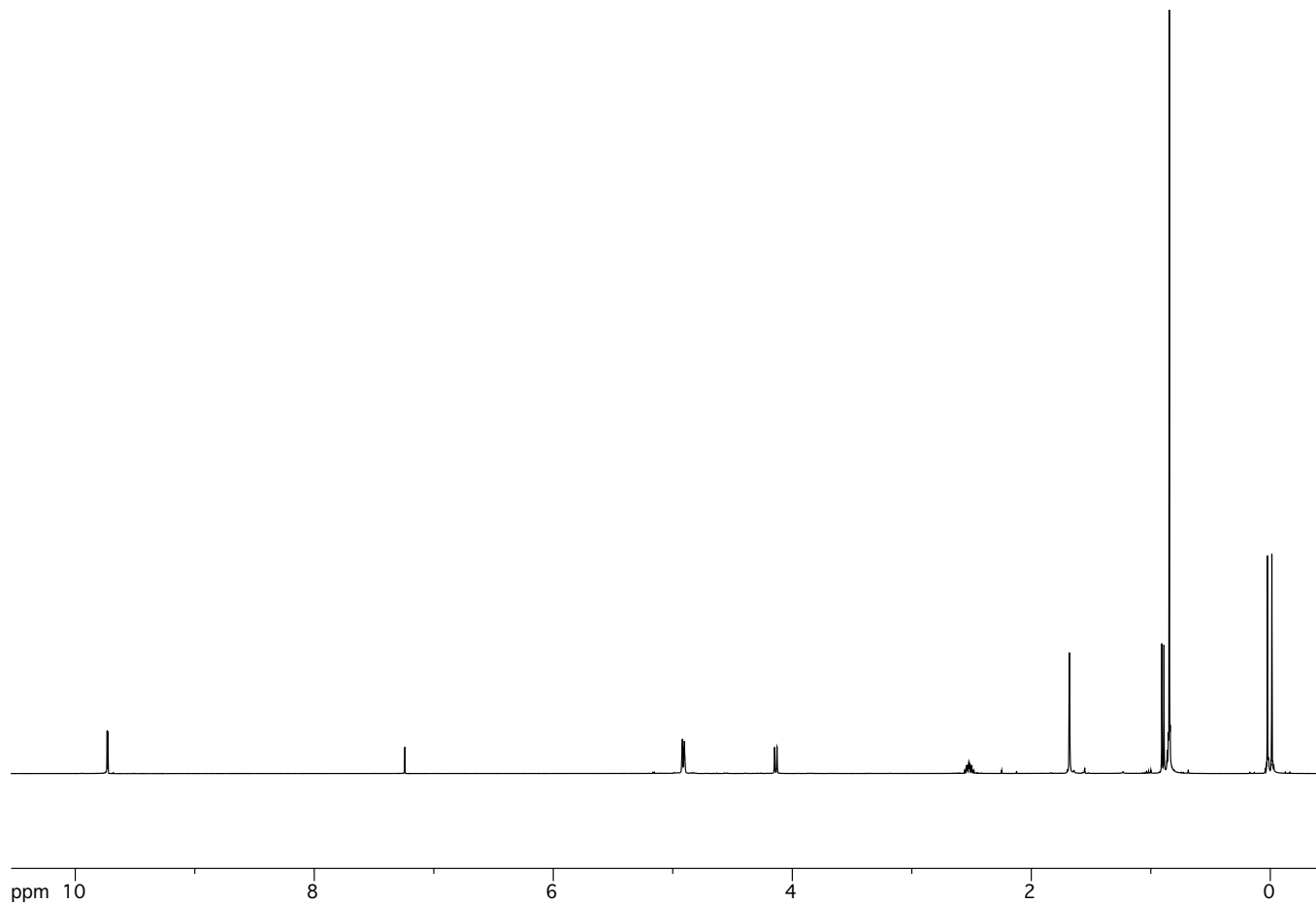
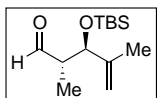


Figure A2.232.  $^1\text{H-NMR}$  of aldehyde 425.

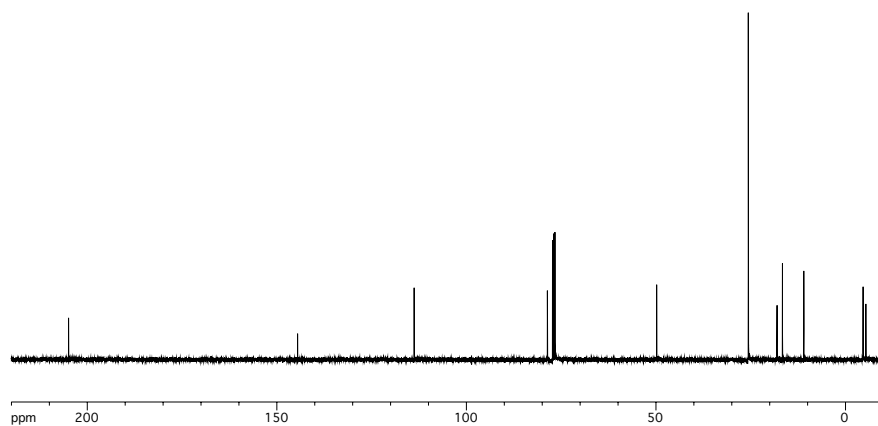


Figure A2.233.  $^{13}\text{C}$ -NMR of aldehyde 425.

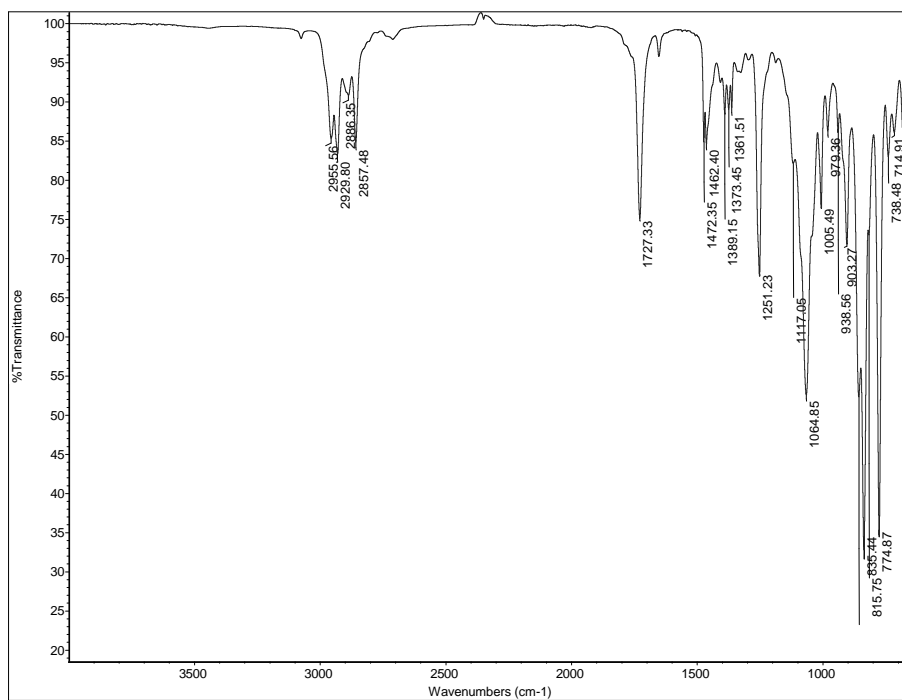
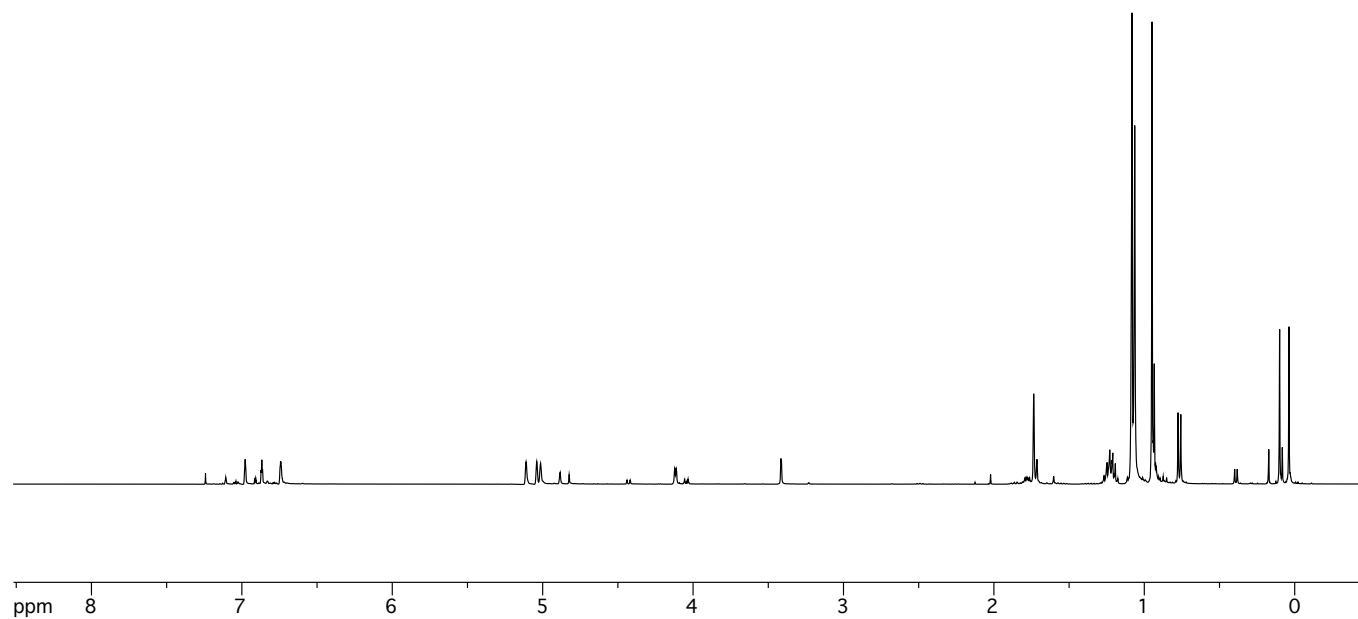
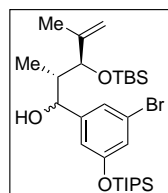


Figure A2.234. FTIR of aldehyde 425.



**Figure A2.235.** <sup>1</sup>H-NMR of alcohol **467**.

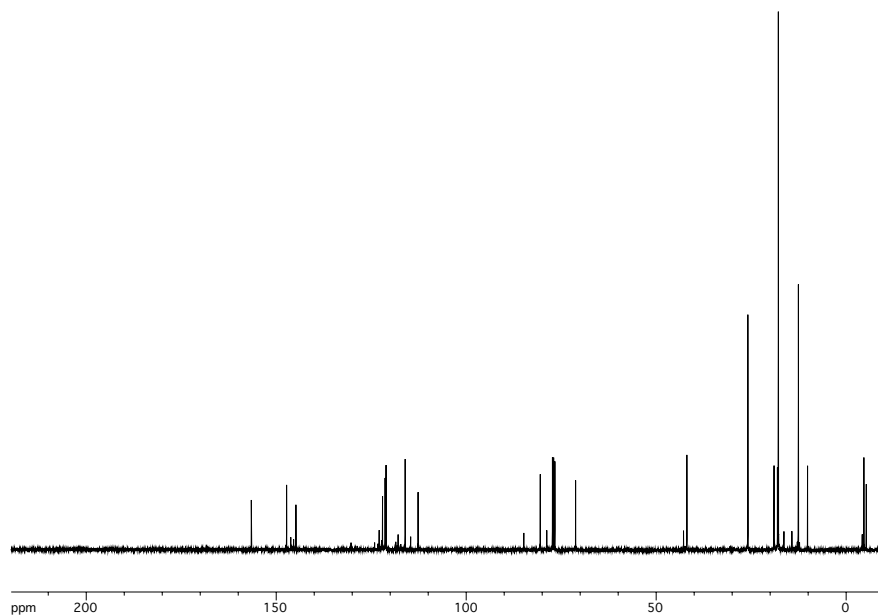


Figure A2.236. <sup>13</sup>C-NMR of alcohol 467.

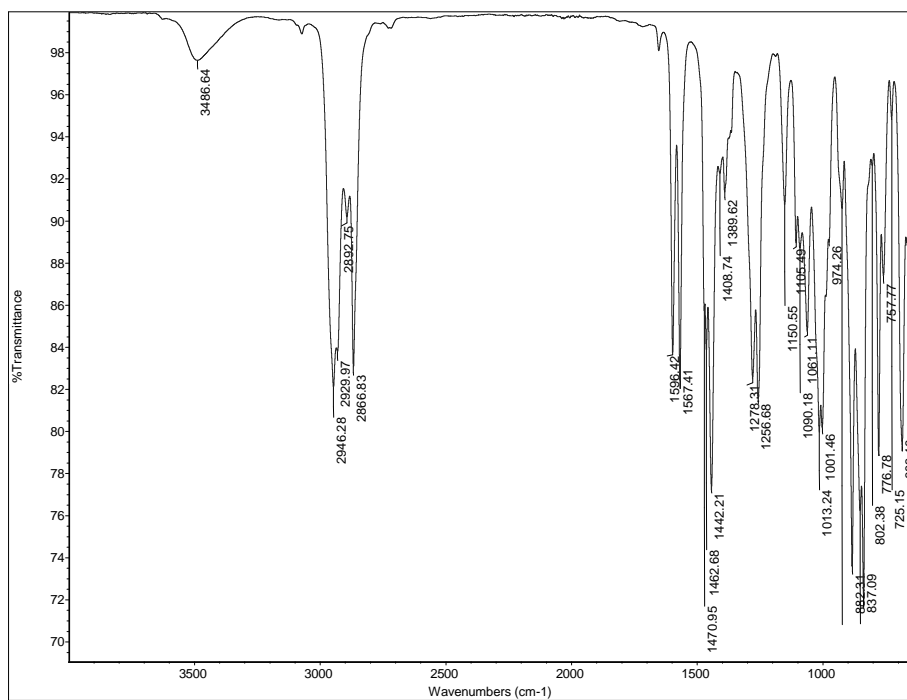
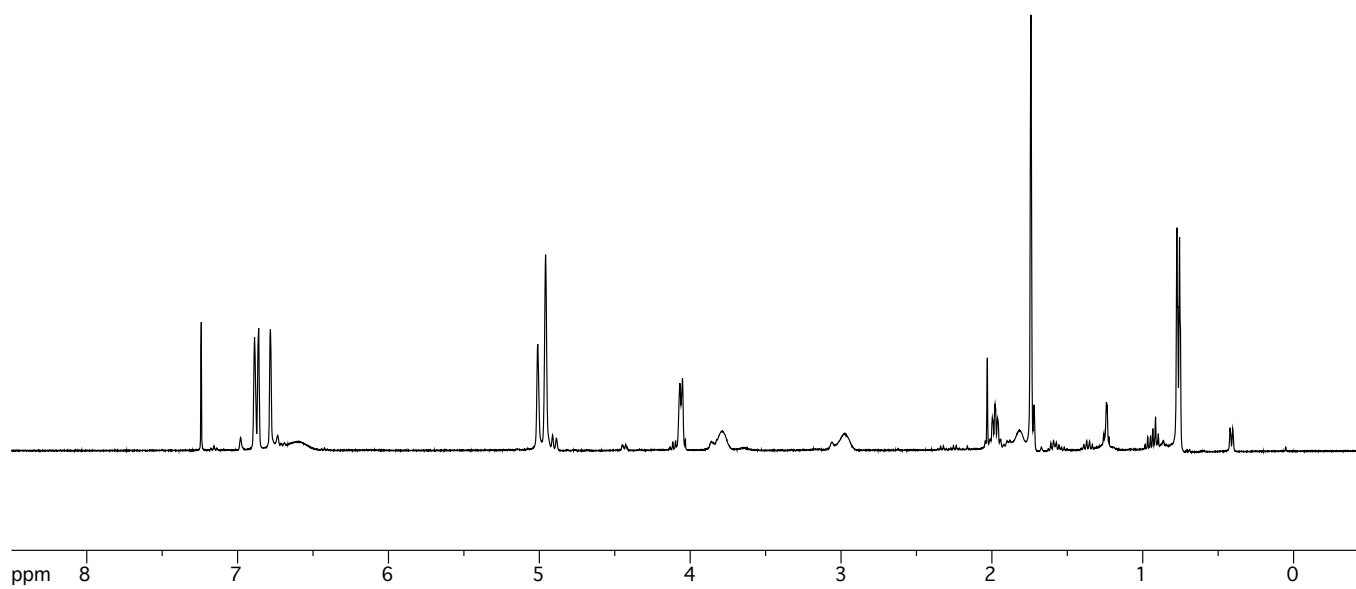
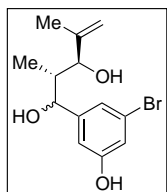
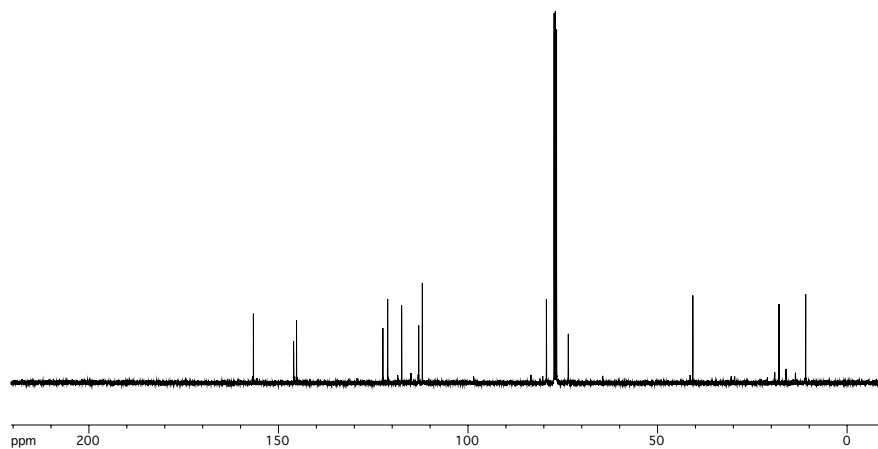


Figure A2.237. FTIR of alcohol 467.



**Figure A2.238.** <sup>1</sup>H-NMR of phenol 429.



**Figure A2.239.** <sup>13</sup>C-NMR of phenol 429.

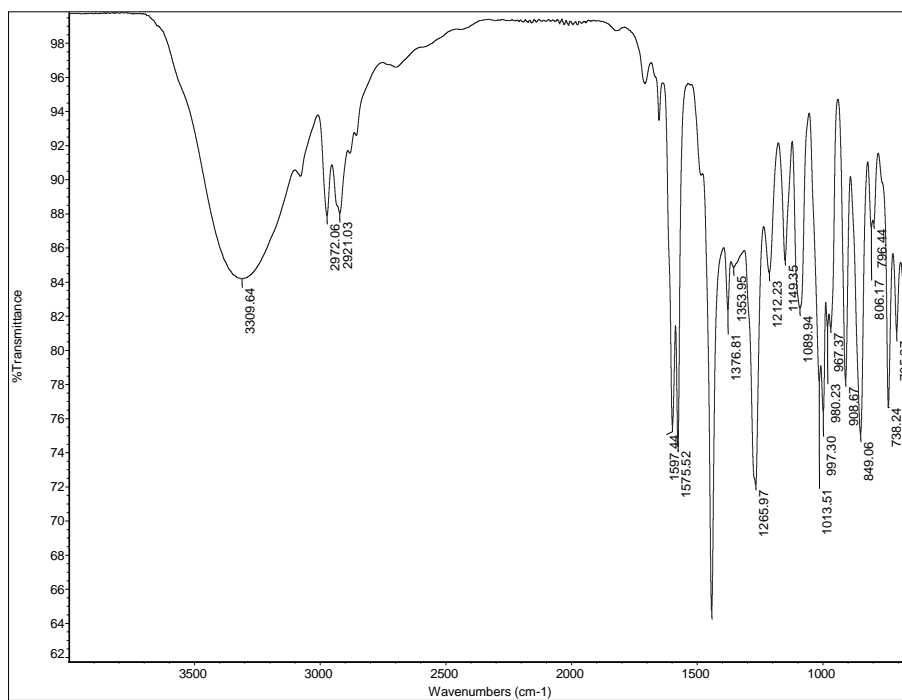


**Figure A2.240.** FTIR of phenol 429.

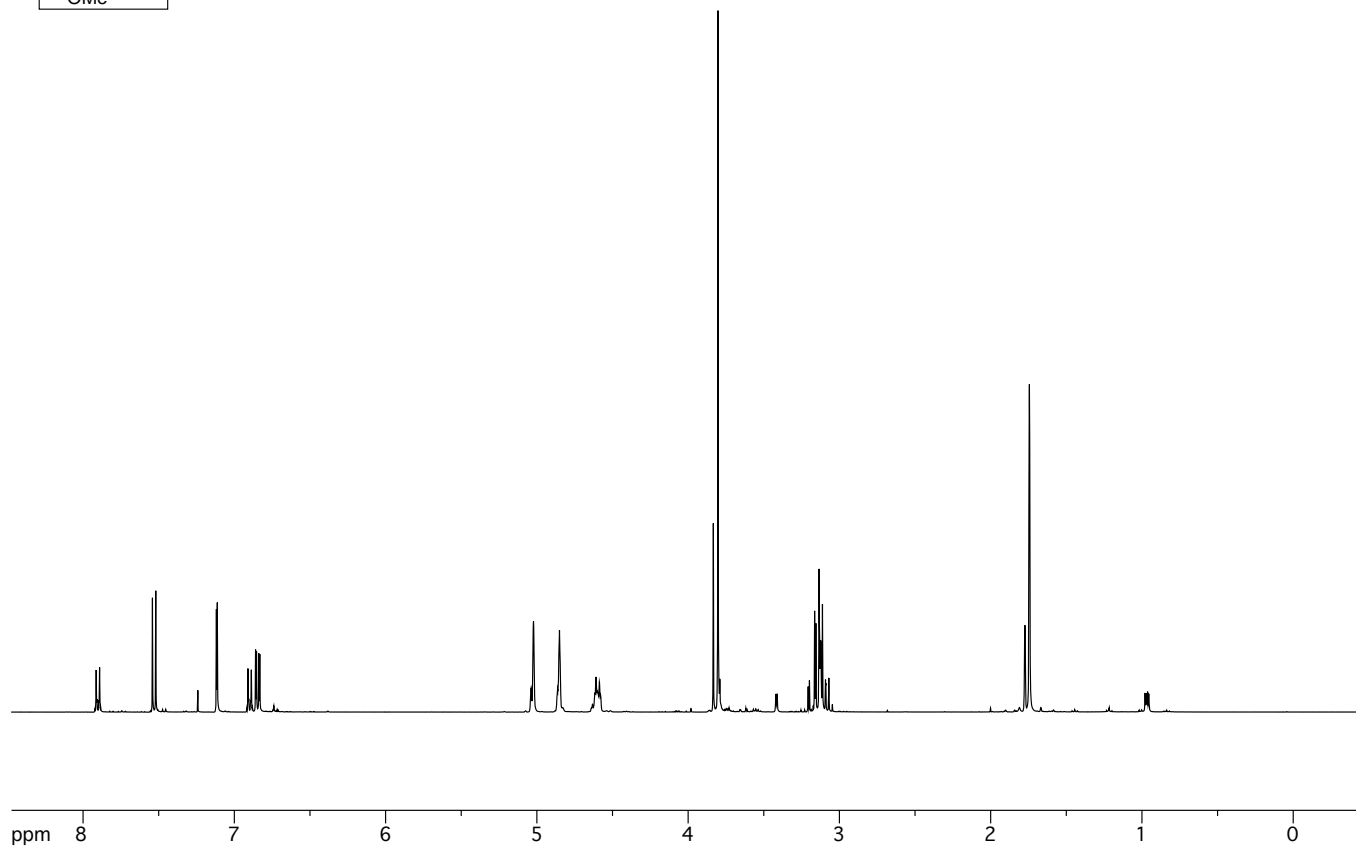
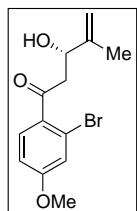


**Figure A2.241.**  $^1\text{H-NMR}$  of  $\beta$ -hydroxy ketone **437**.

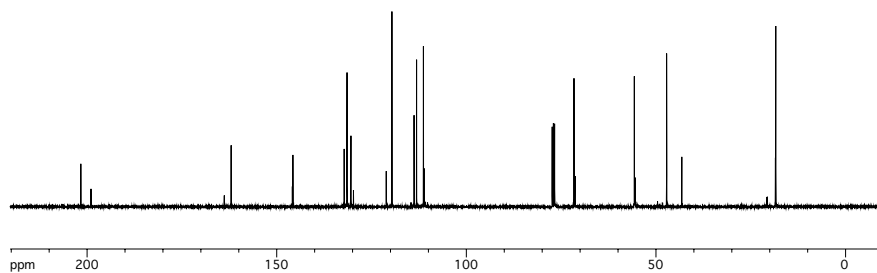


Figure A2.242.  $^{13}\text{C}$ -NMR of  $\beta$ -hydroxy ketone 437.

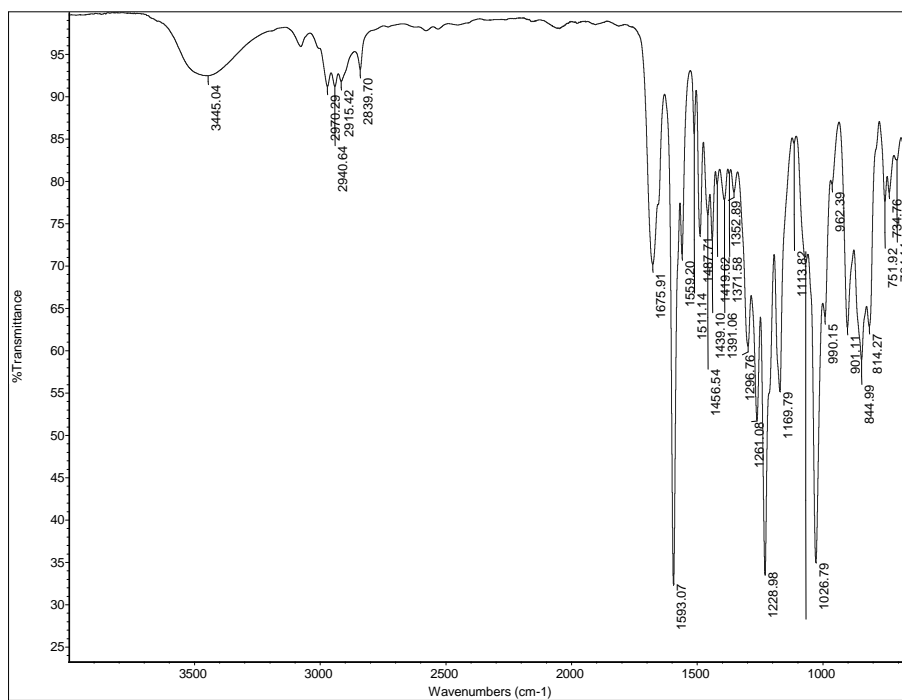
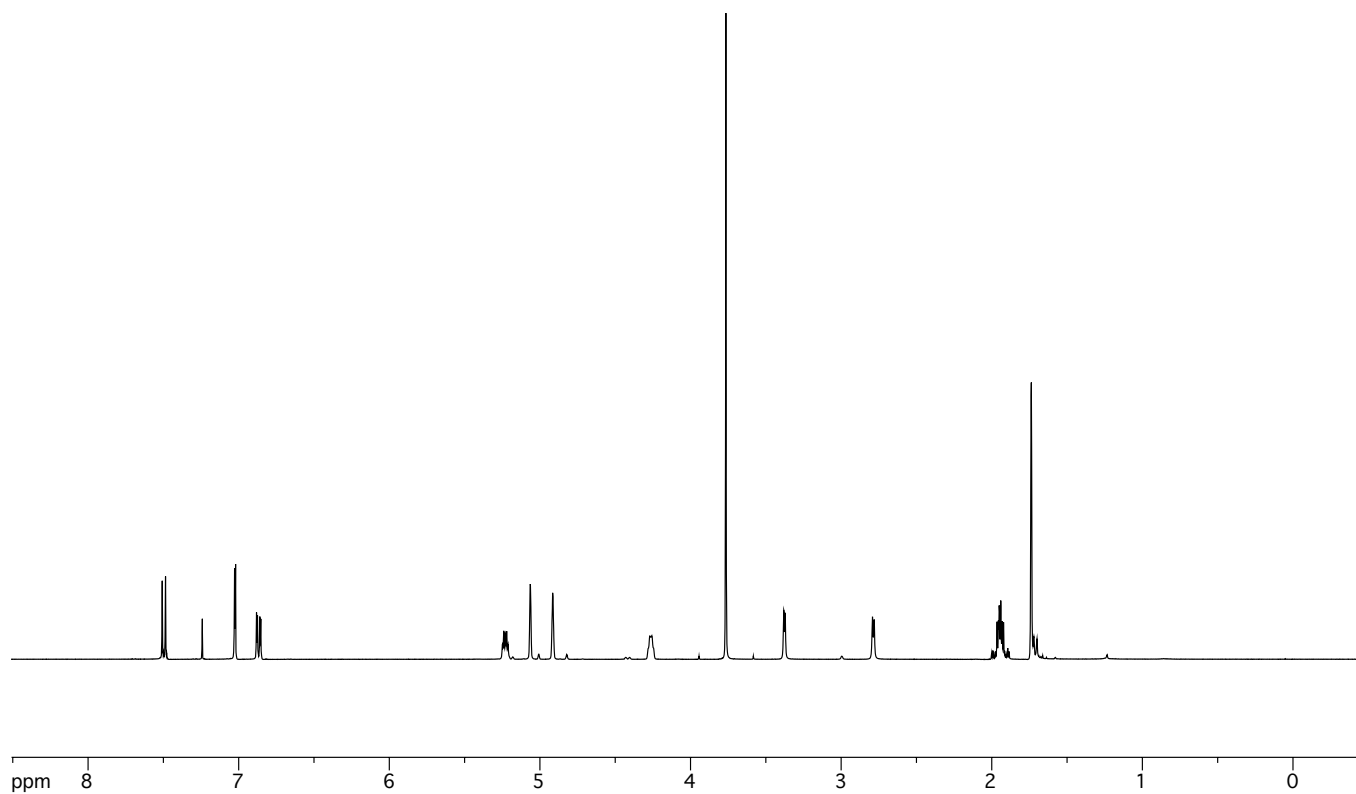
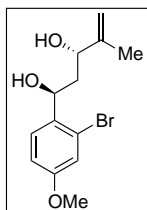


Figure A2.243. FTIR of  $\beta$ -hydroxy ketone 437.



**Figure A2.244.** <sup>1</sup>H-NMR of diol 438.

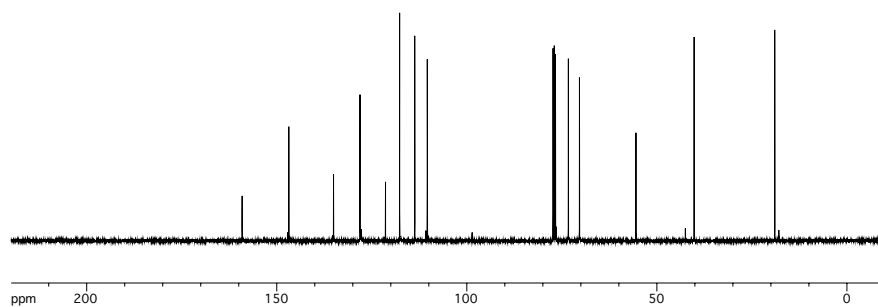


Figure A2.245. <sup>13</sup>C-NMR of diol 438.

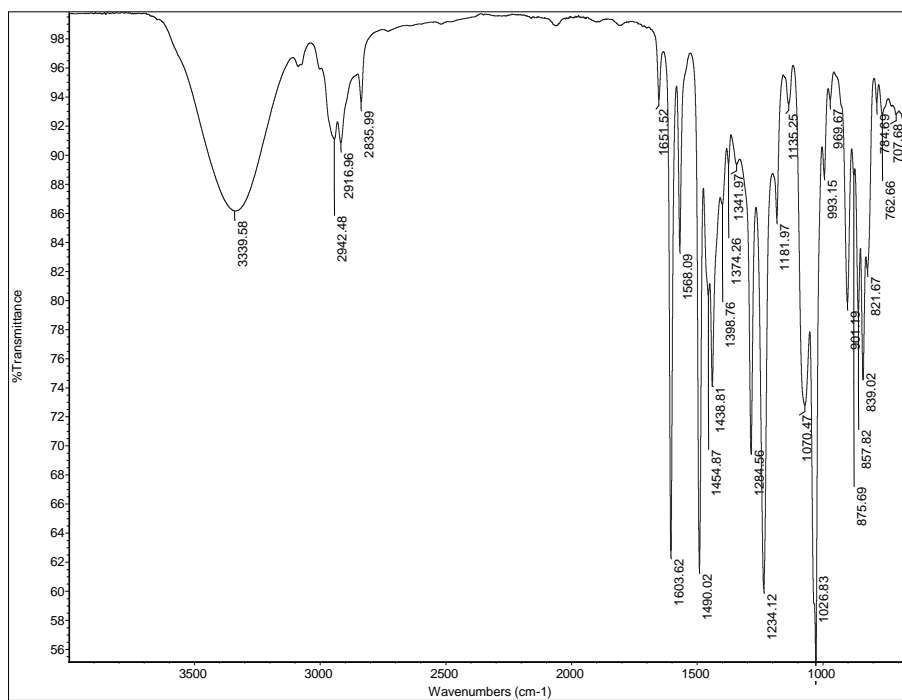
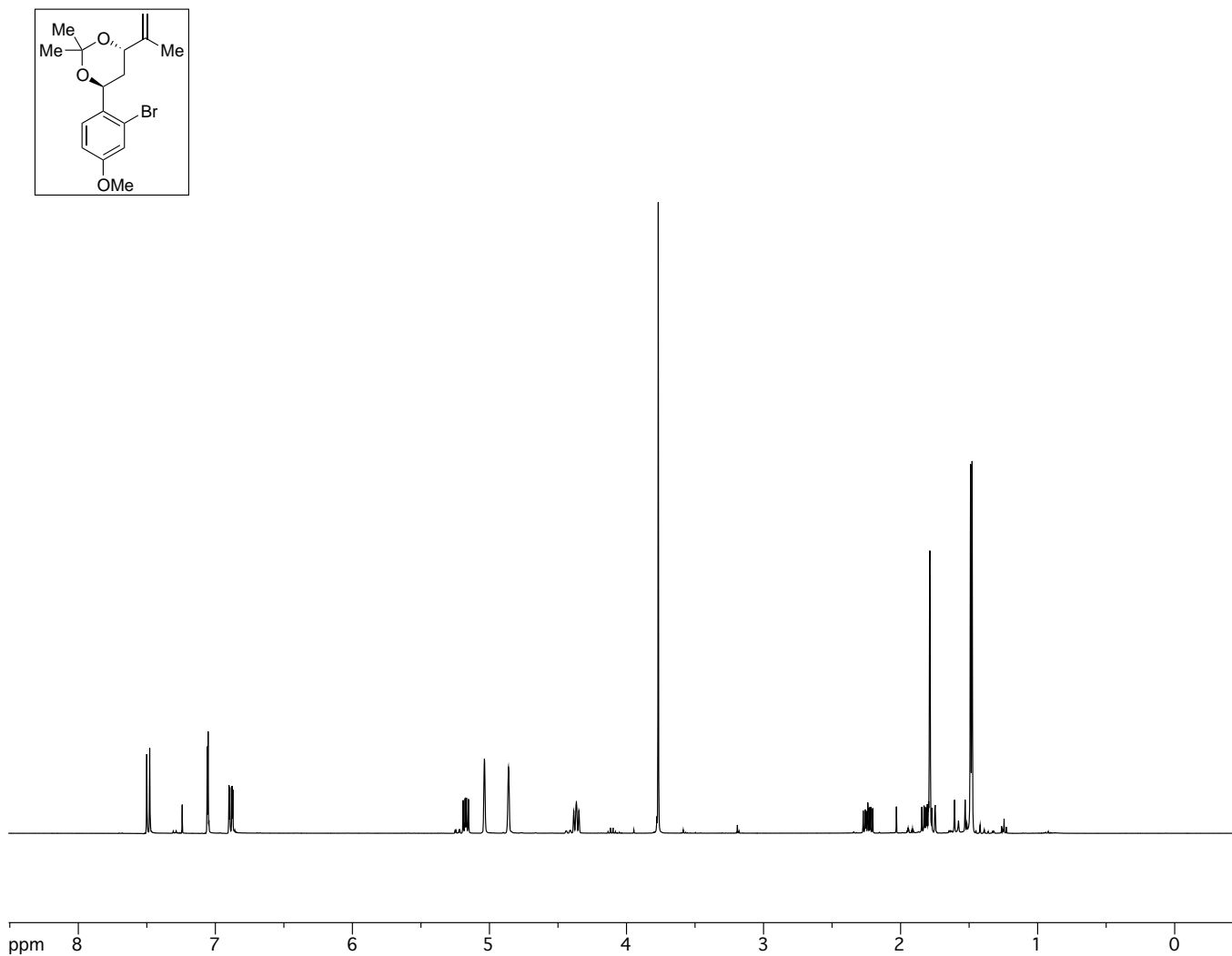


Figure A2.246. FTIR of diol 438.



**Figure A2.247.** <sup>1</sup>H-NMR of acetal **440**.

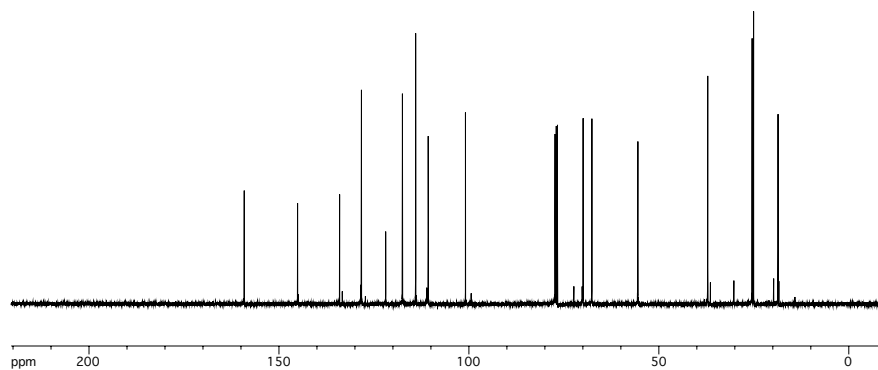


Figure A2.248.  $^{13}\text{C-NMR}$  of acetal 440.

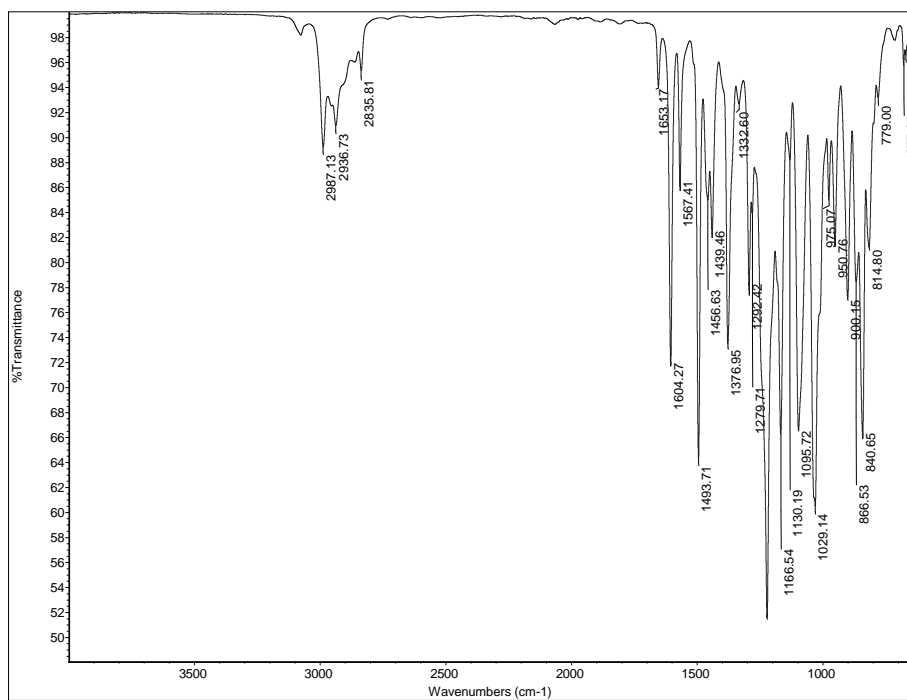


Figure A2.249. FTIR of acetal 440.

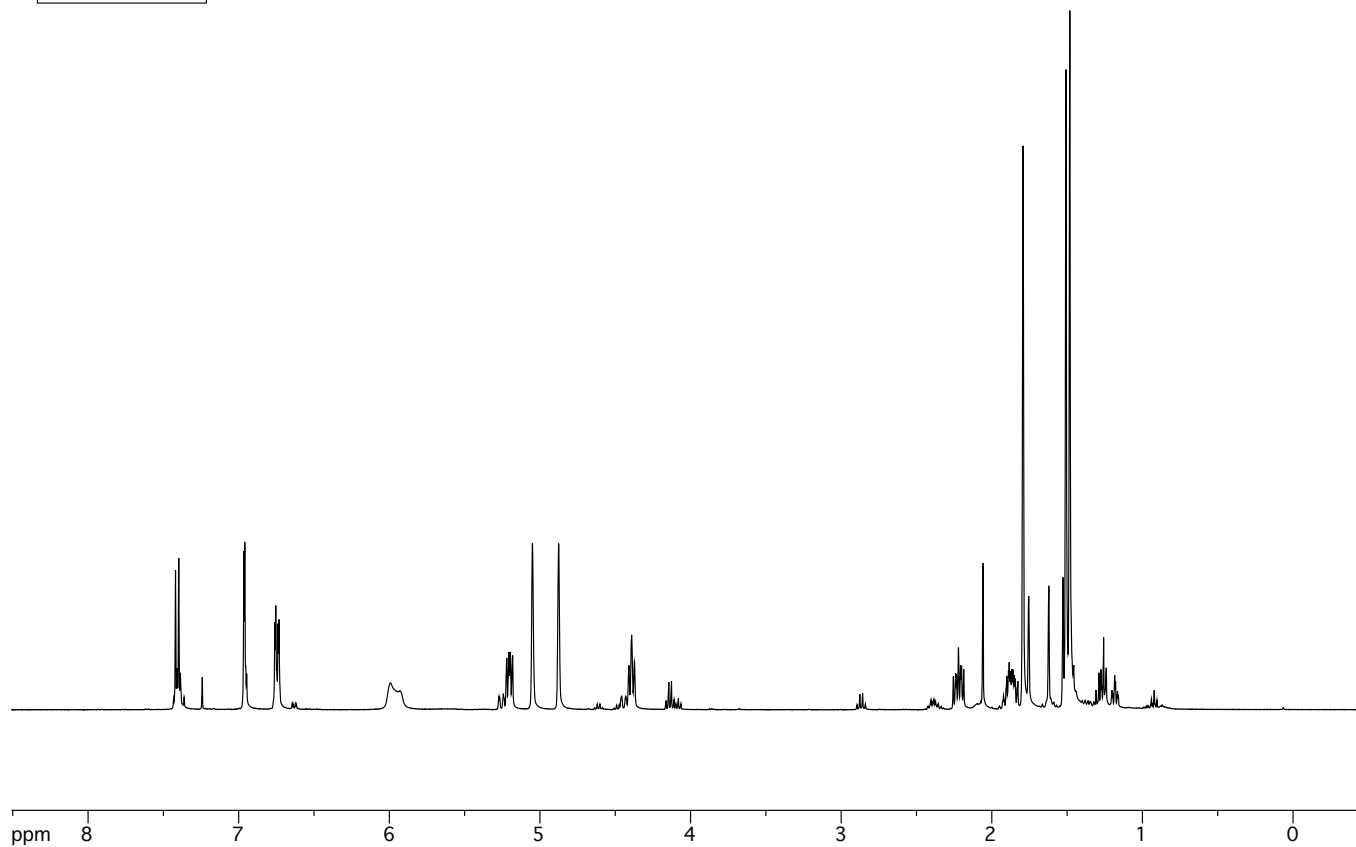
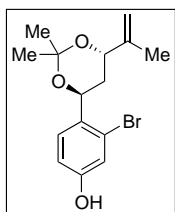


Figure A2.250. <sup>1</sup>H-NMR of phenol 468.

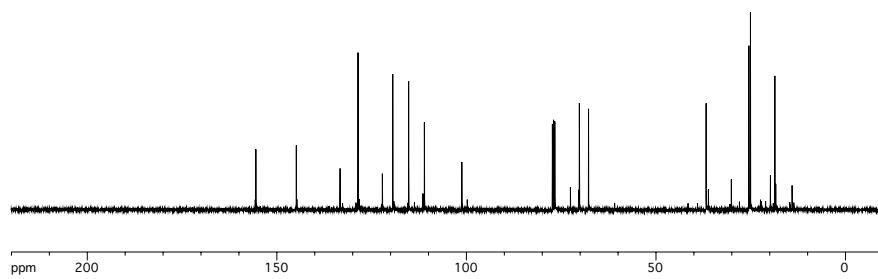


Figure A2.251. <sup>13</sup>C-NMR of phenol 468.

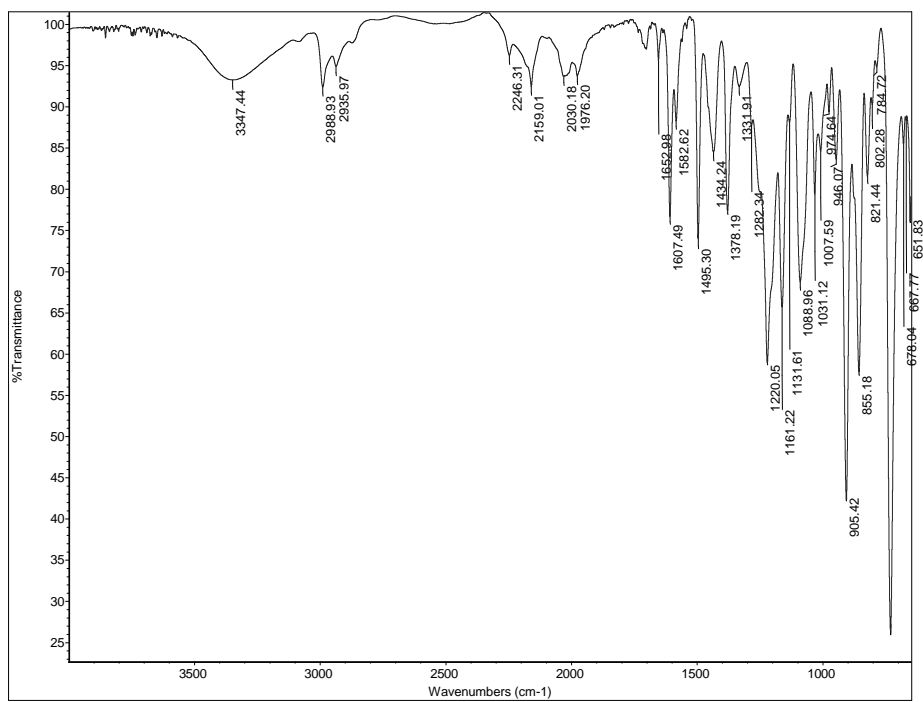
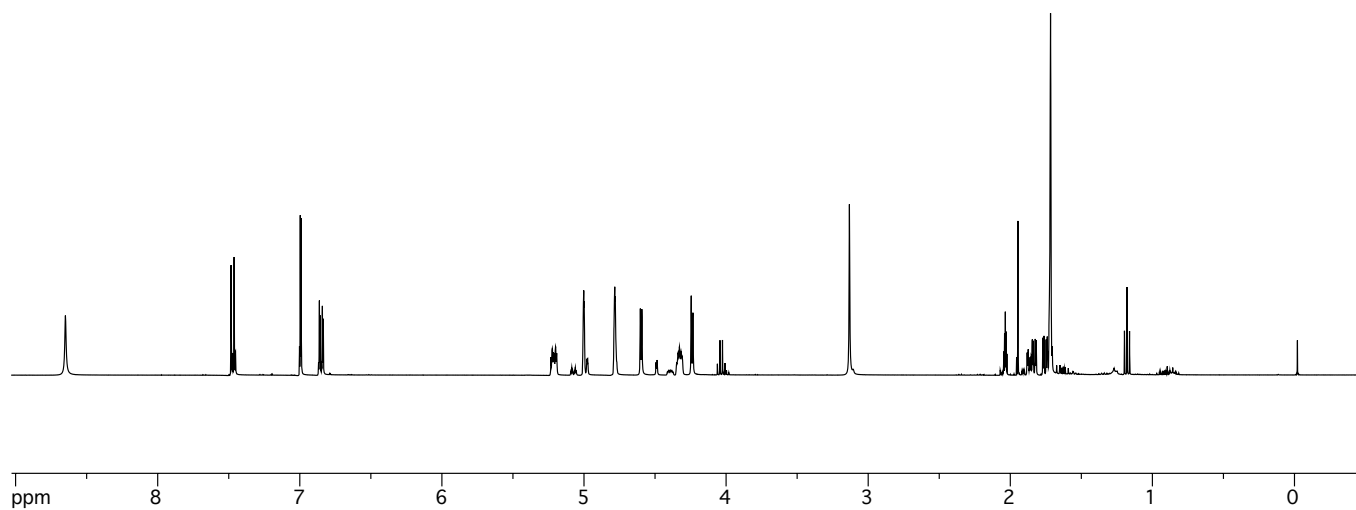
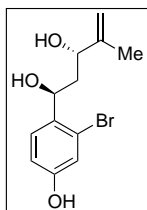
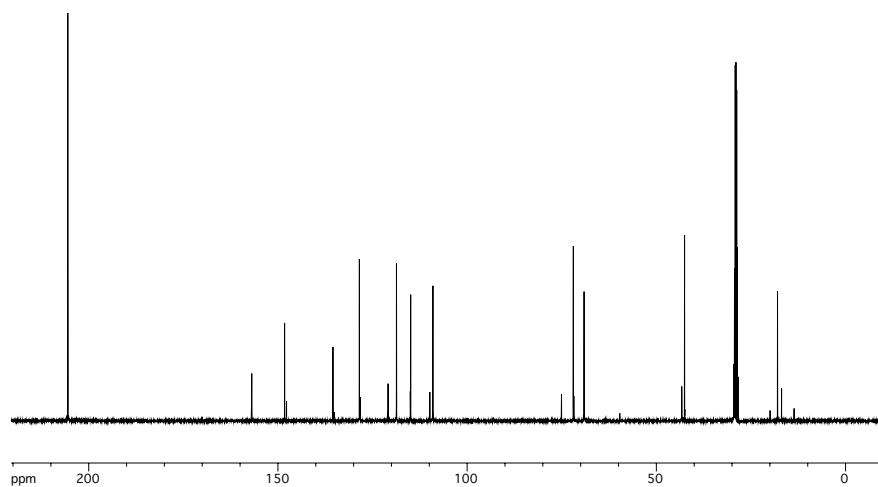


Figure A2.252. FTIR of phenol 468.



**Figure A2.253.** <sup>1</sup>H-NMR of phenol 441.



**Figure A2.254.**  $^{13}\text{C}$ -NMR of phenol 441.

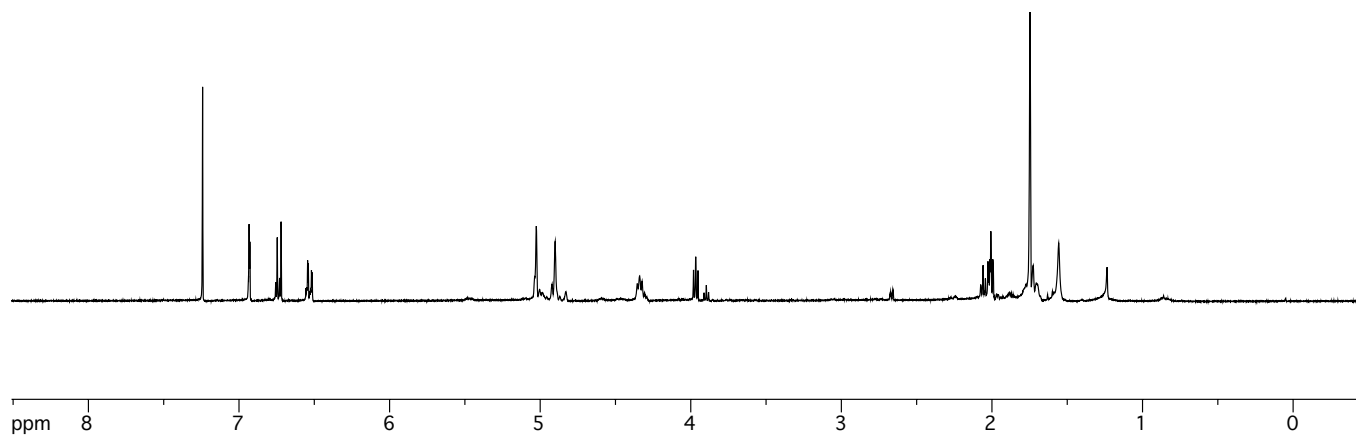
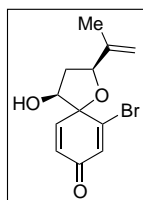


**Figure A2.255.**  $^1\text{H-NMR}$  of spiro[3.5]nonan-2-one derivative **443**.

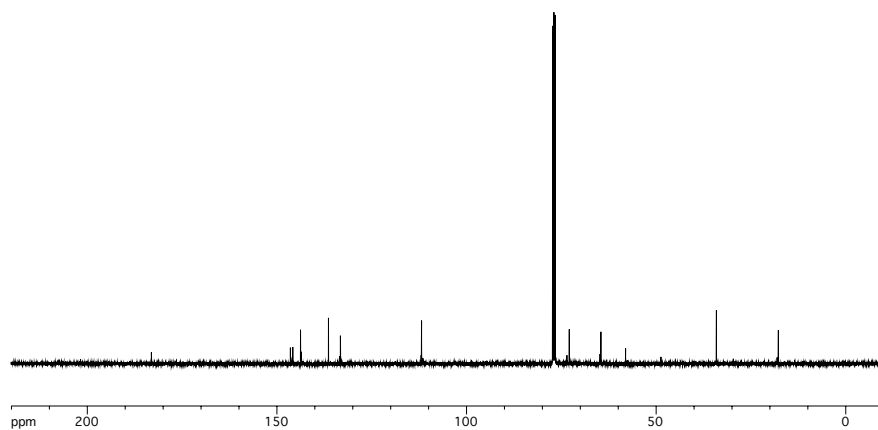


**Figure A2.256.**  $^{13}\text{C}$ -NMR of spirotetrahydrofuran **443**.

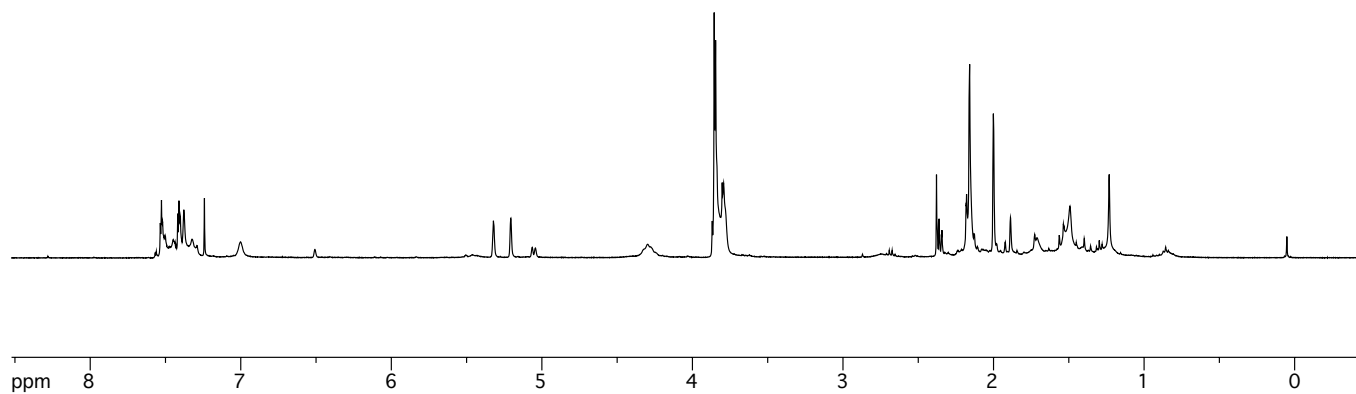
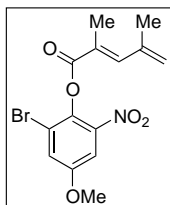


**Figure A2.257.** <sup>1</sup>H-NMR of ester 448.

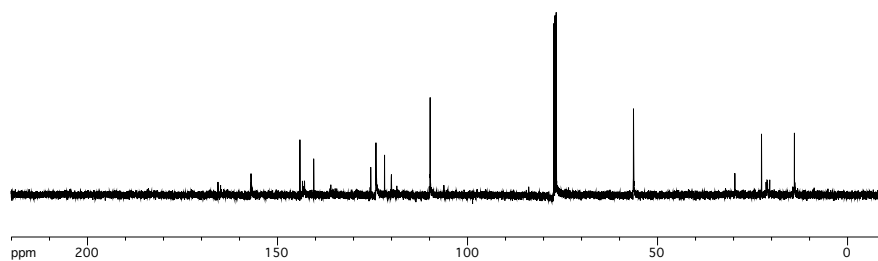


Figure A2.258.  $^{13}\text{C-NMR}$  of ester 448.

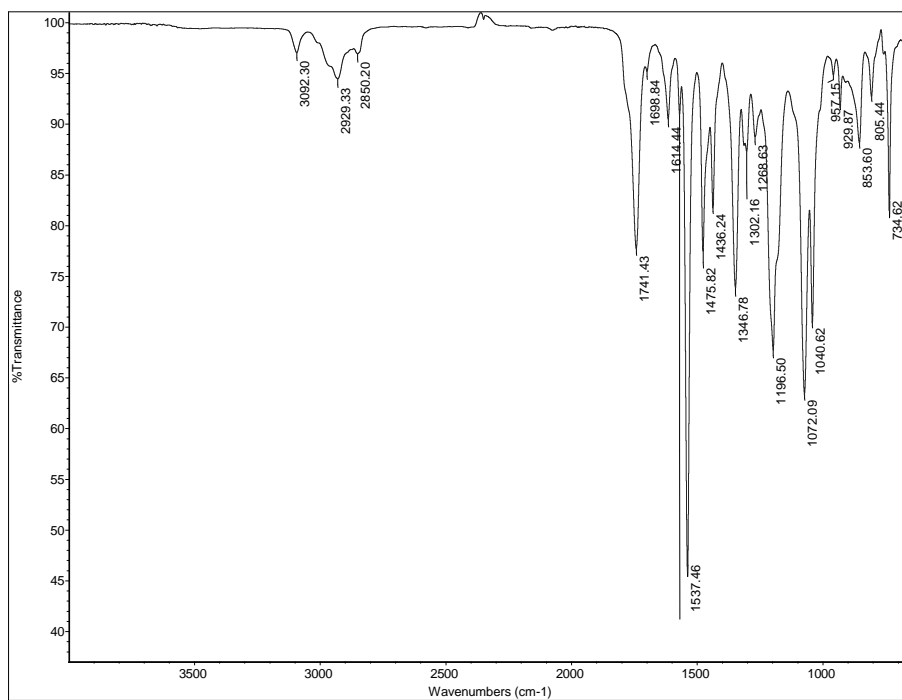


Figure A2.259. FTIR of ester 448.

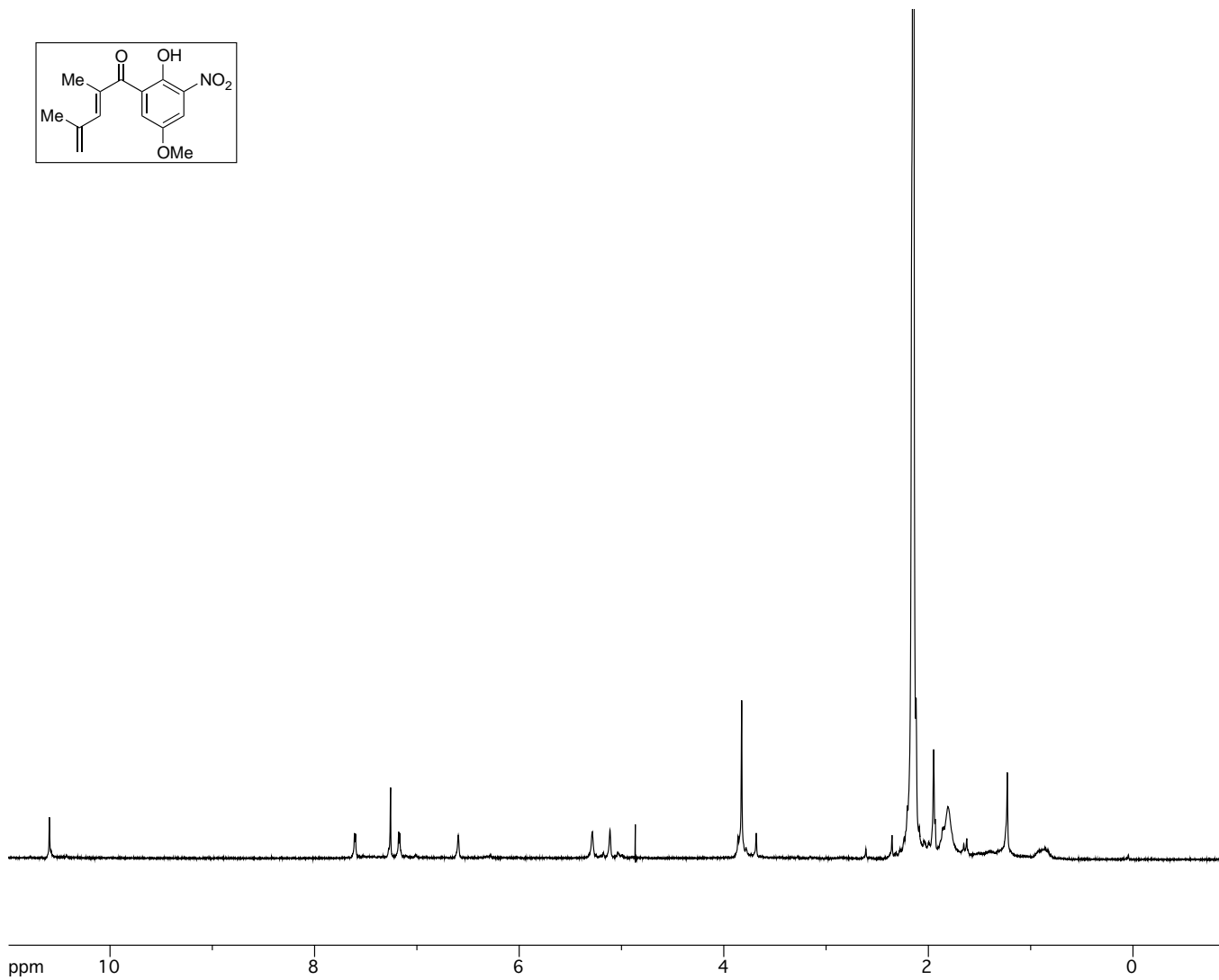
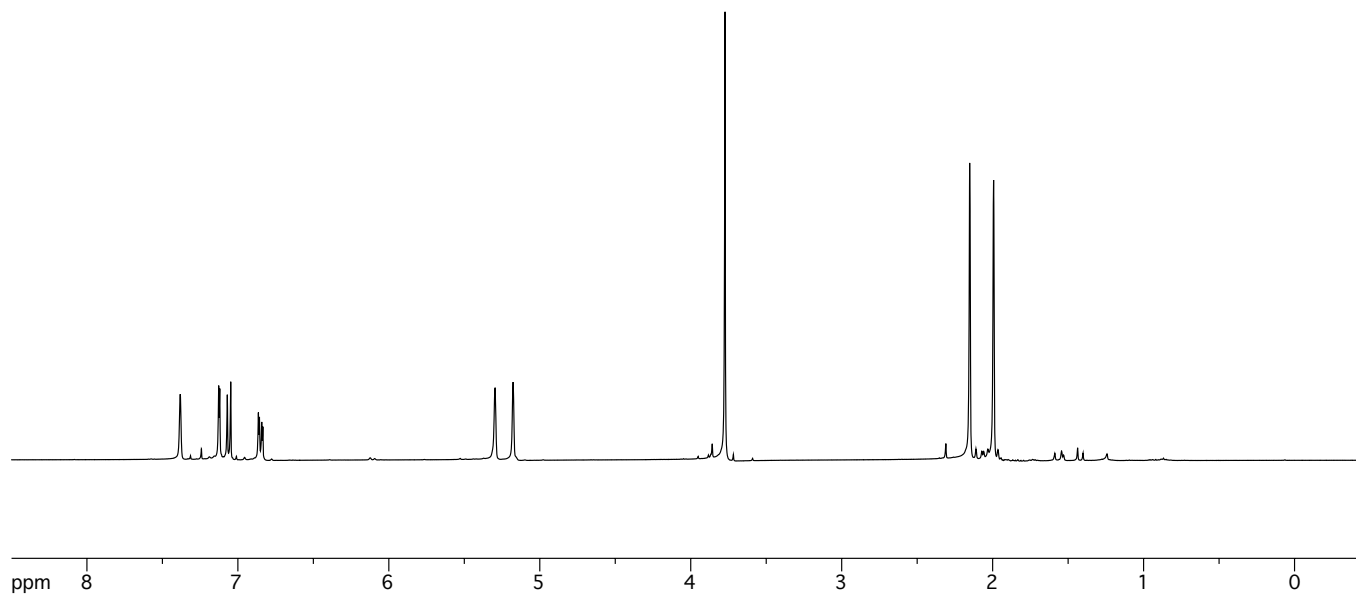
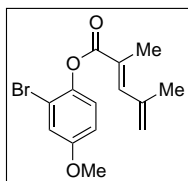


Figure A2.260. <sup>1</sup>H-NMR of enone 445.



**Figure A2.261.** <sup>1</sup>H-NMR of ester 451.

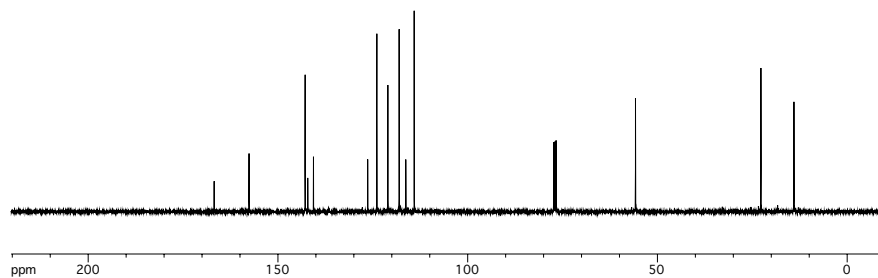


Figure A2.262.  $^{13}\text{C}$ -NMR of ester 451.

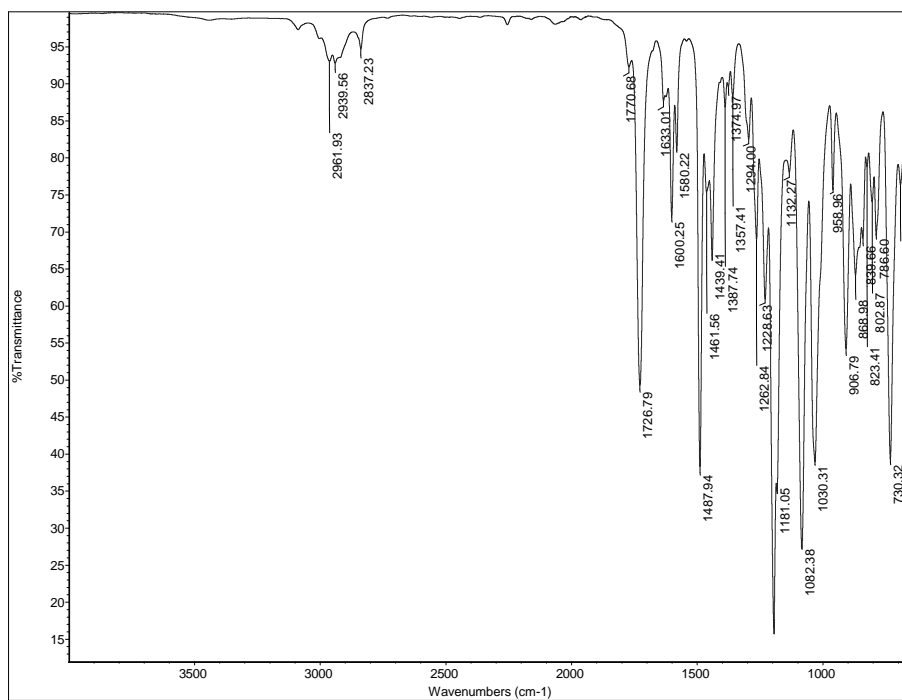
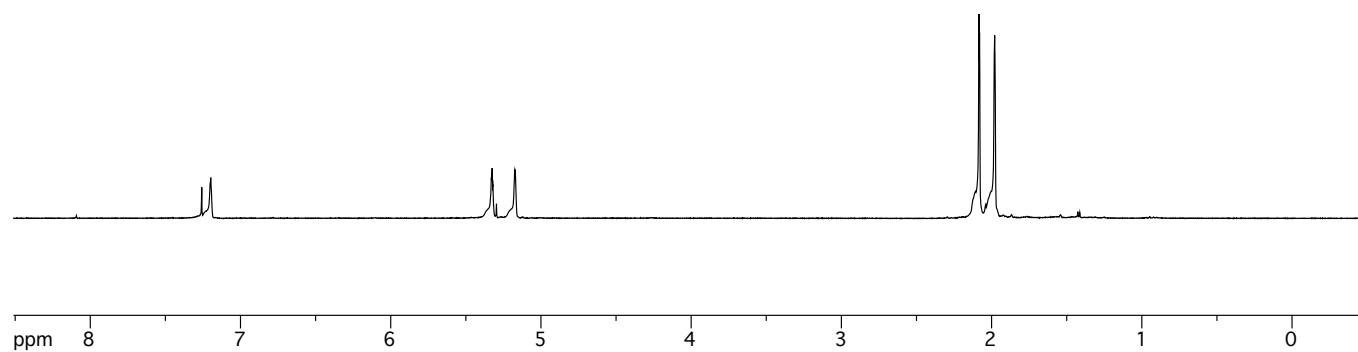
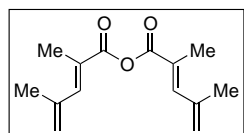


Figure A2.263. FTIR of ester 451.



**Figure A2.264.** <sup>1</sup>H-NMR of anhydride **452**.

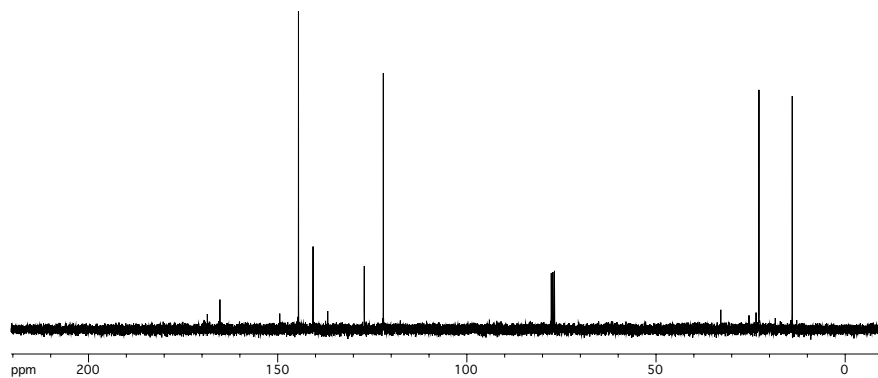


Figure A2.265.  $^{13}\text{C-NMR}$  of anhydride 452.

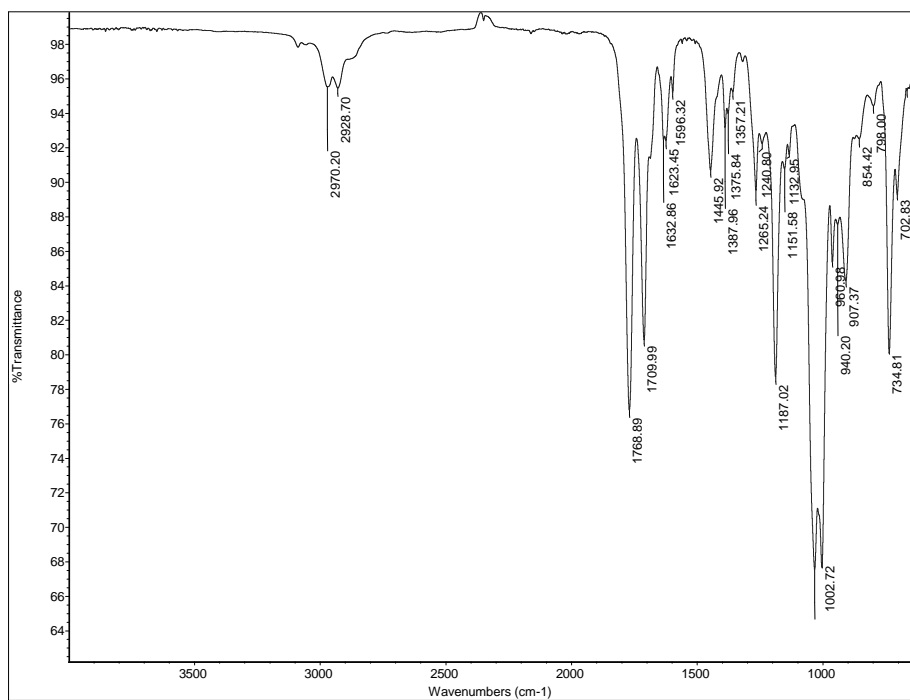
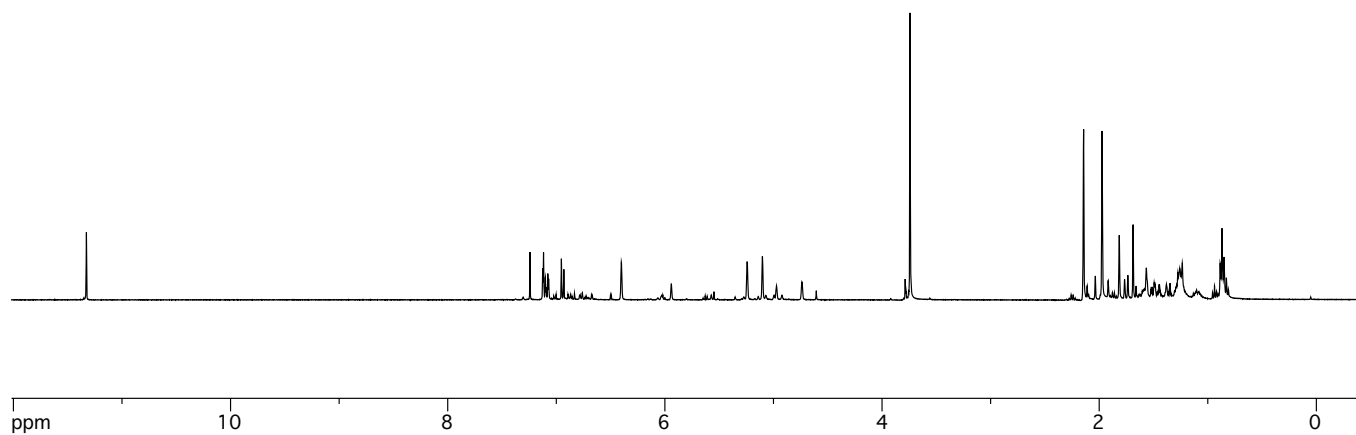
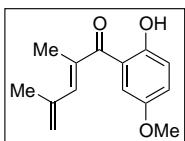


Figure A2.266. FTIR of anhydride 452.



**Figure A2.267.** <sup>1</sup>H-NMR of enone **449**.

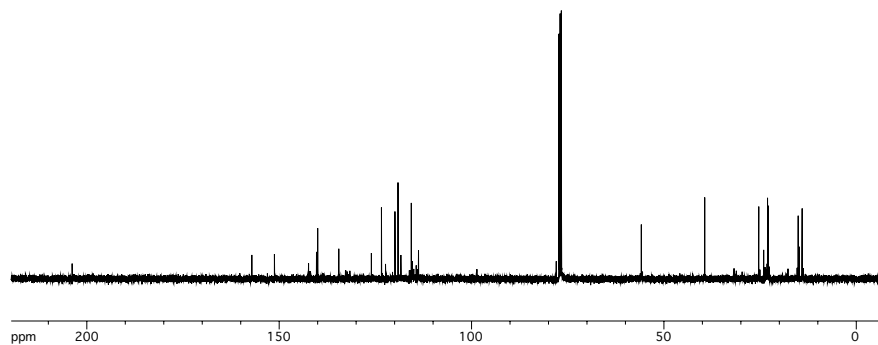


Figure A2.268.  $^{13}\text{C}$ -NMR of enone 449.

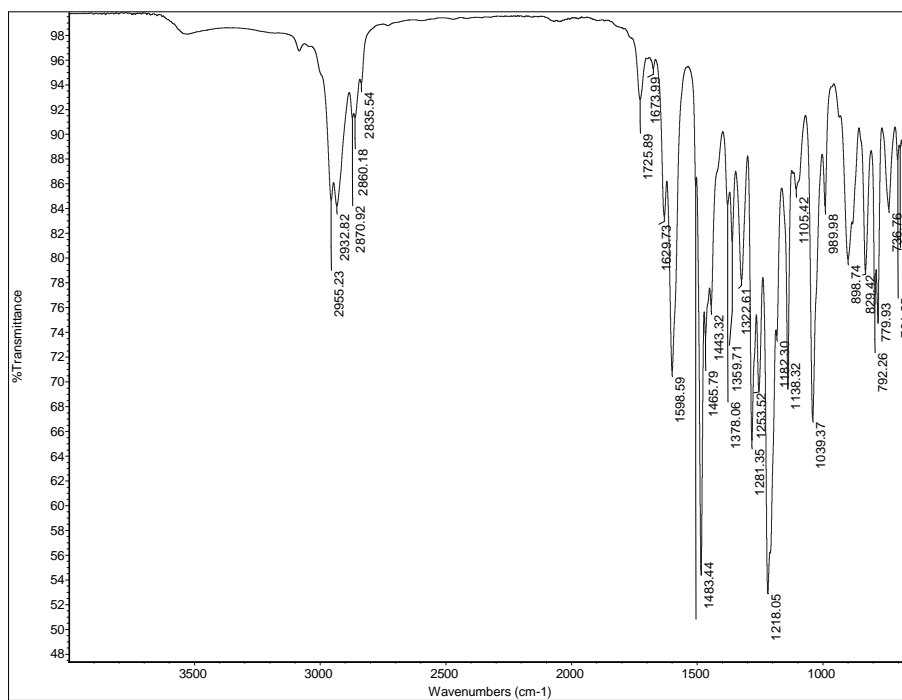
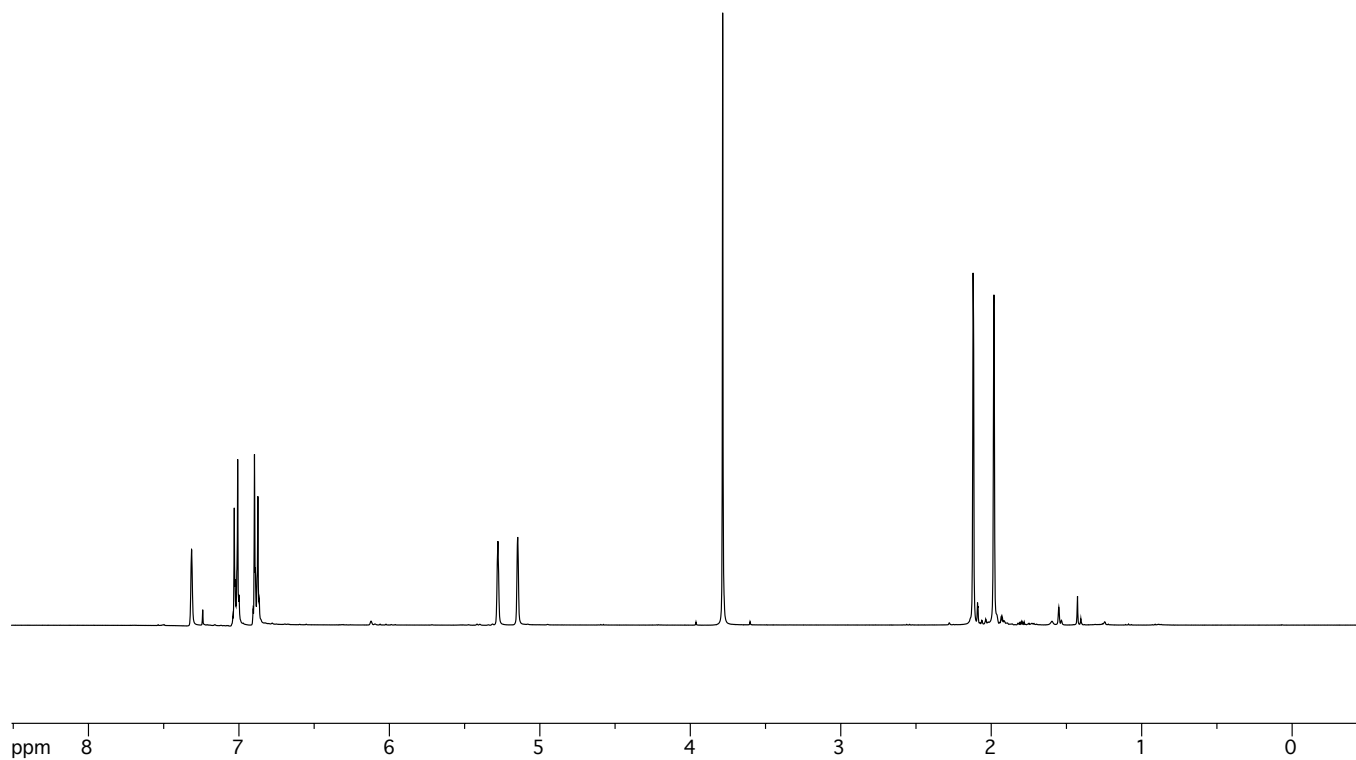
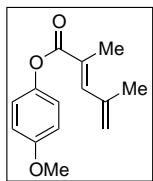


Figure A2.269. FTIR of enone 449.



**Figure A2.270.** <sup>1</sup>H-NMR of ester 453.

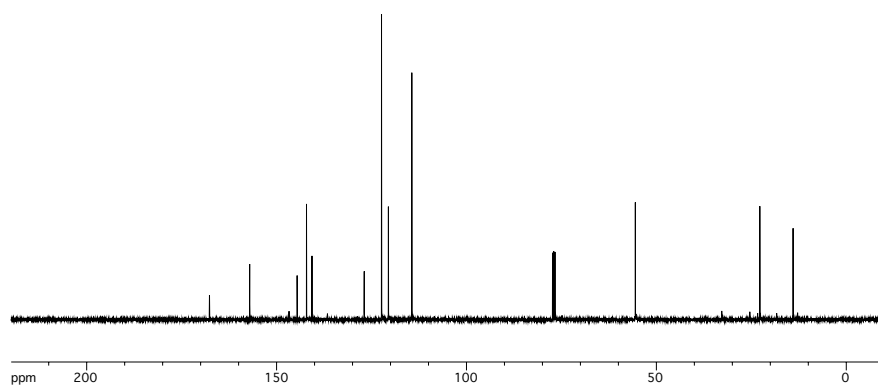


Figure A2.271.  $^{13}\text{C-NMR}$  of ester 453.

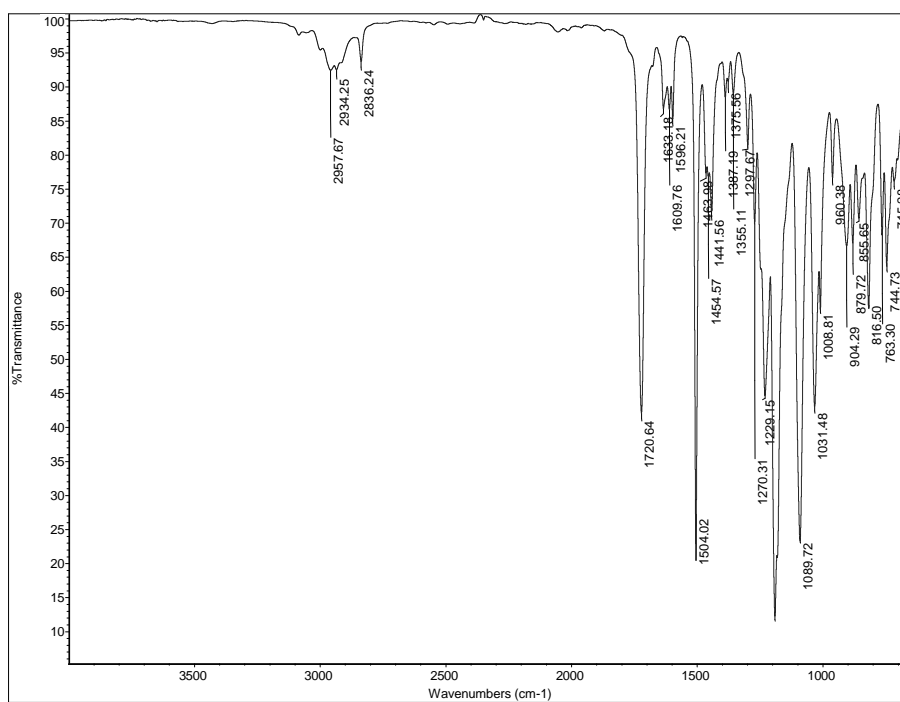
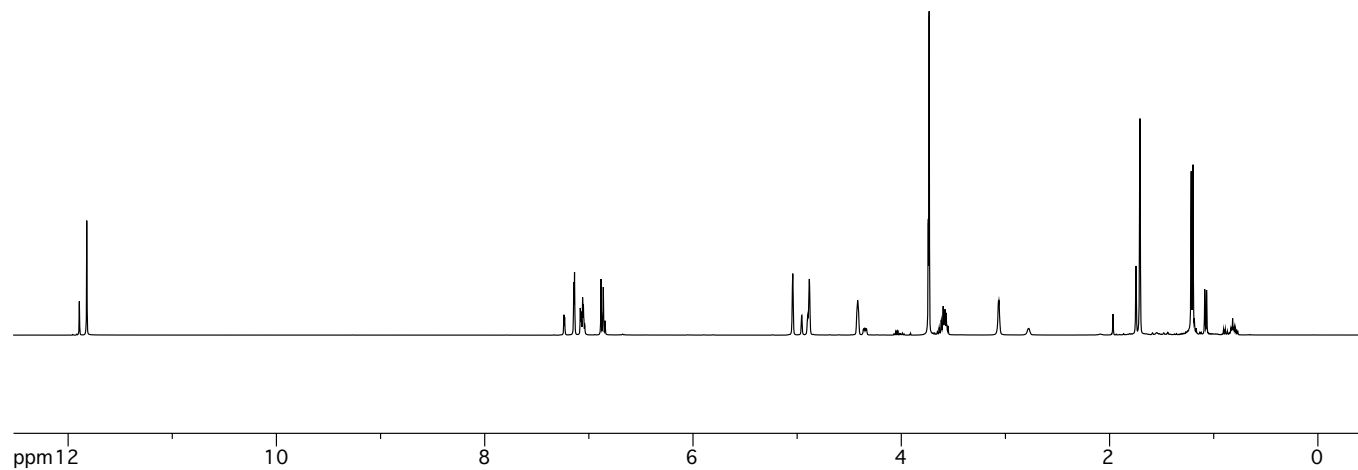
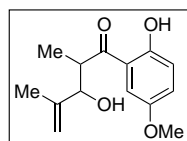
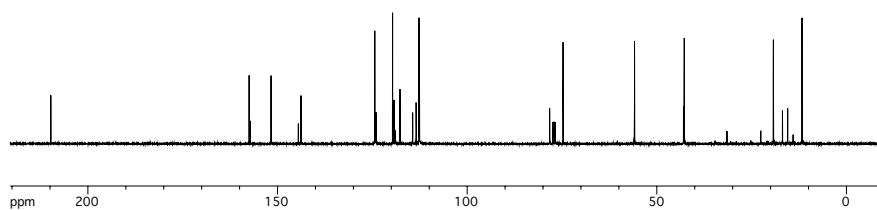


Figure A2.272. FTIR of ester 453.



**Figure A2.273.** <sup>1</sup>H-NMR of aldol product **456**.



**Figure A2.274.**  $^{13}\text{C-NMR}$  of aldol product **456**.

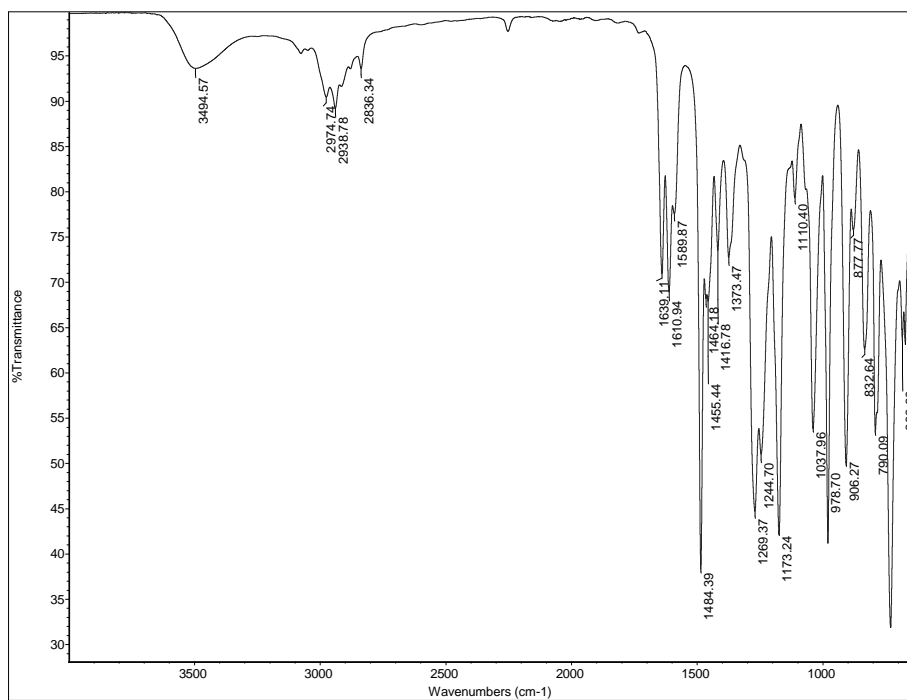


**Figure A2.275.** FTIR of aldol product **456**.

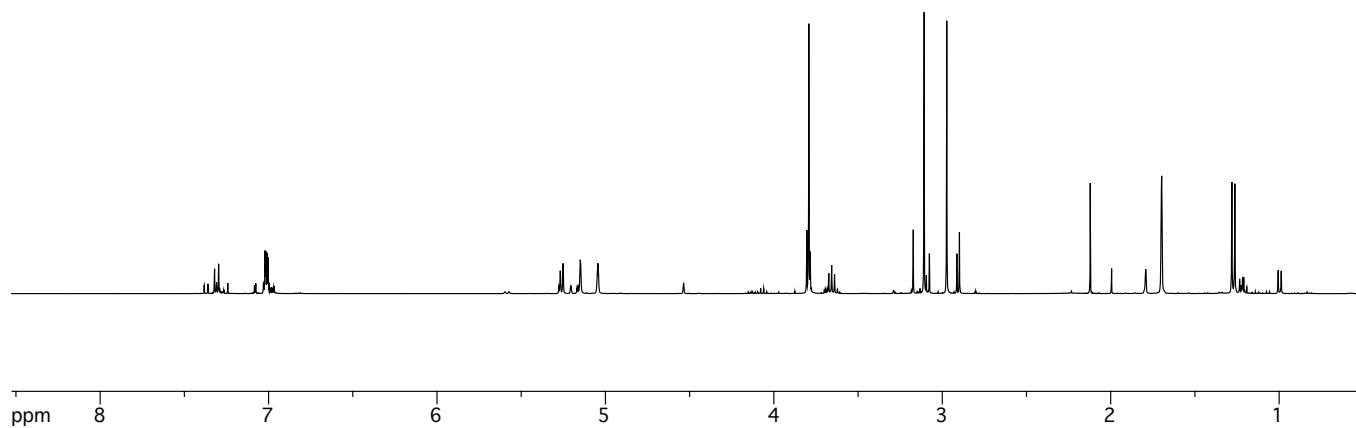
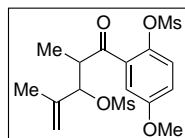


**Figure A2.276.** <sup>1</sup>H-NMR of bismesylate **457**.

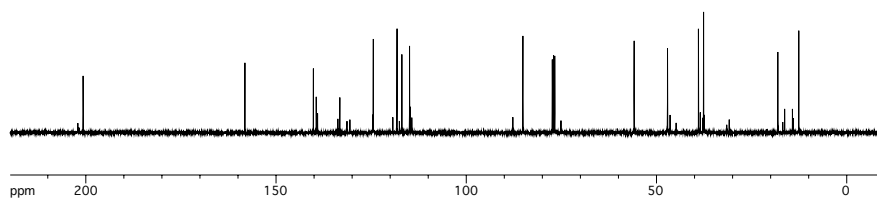


**Figure A2.277.** <sup>13</sup>C-NMR of bismesylate **457**.

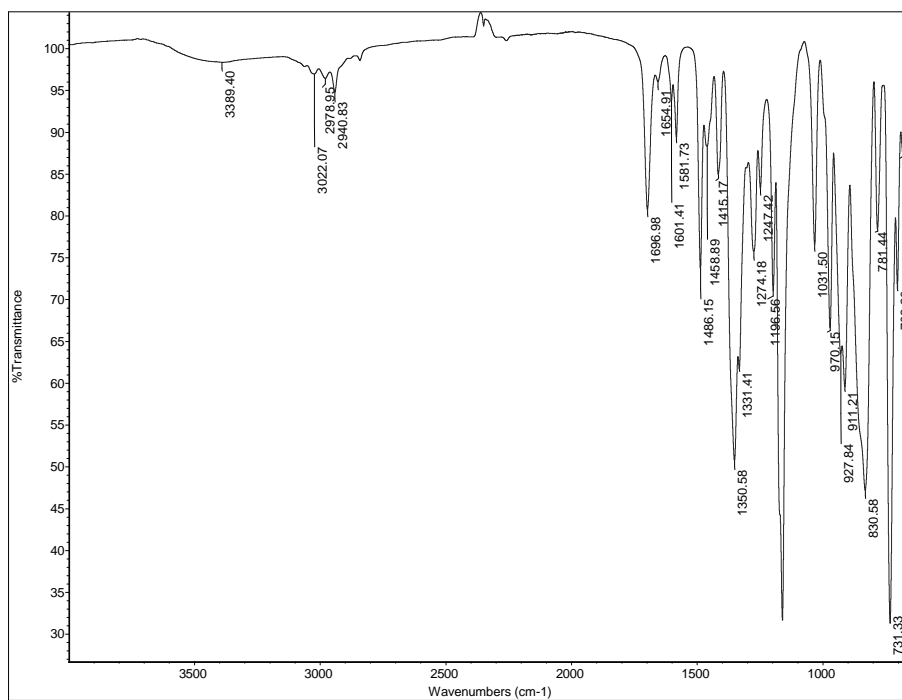


**Figure A2.278.** FTIR of bismesylate **457**.

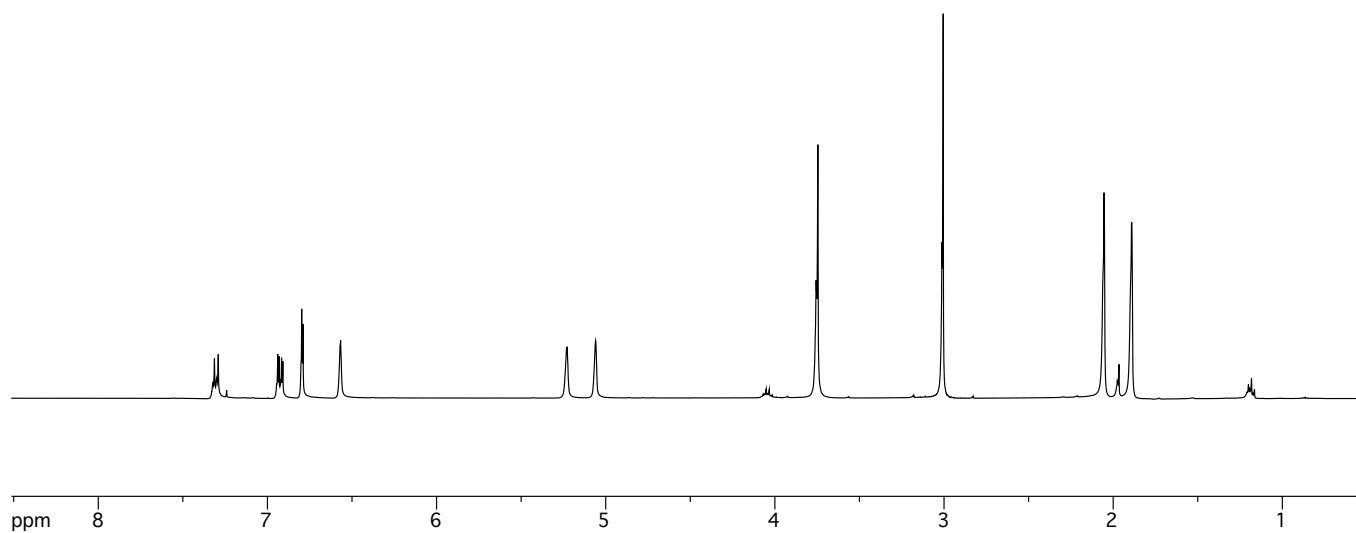
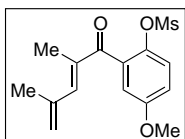


**Figure A2.279.** <sup>1</sup>H-NMR of enone **458**.

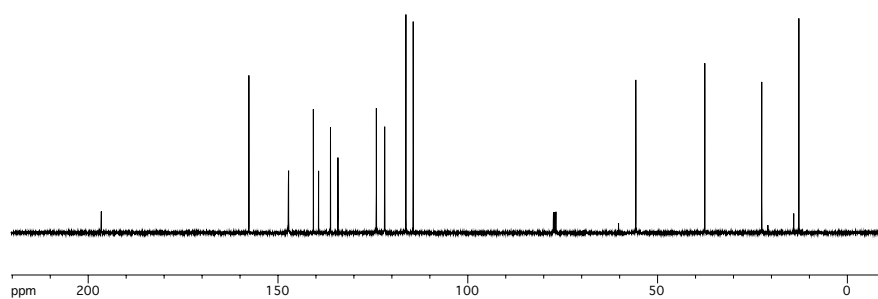


Figure A2.280.  $^{13}\text{C-NMR}$  of enone 458.

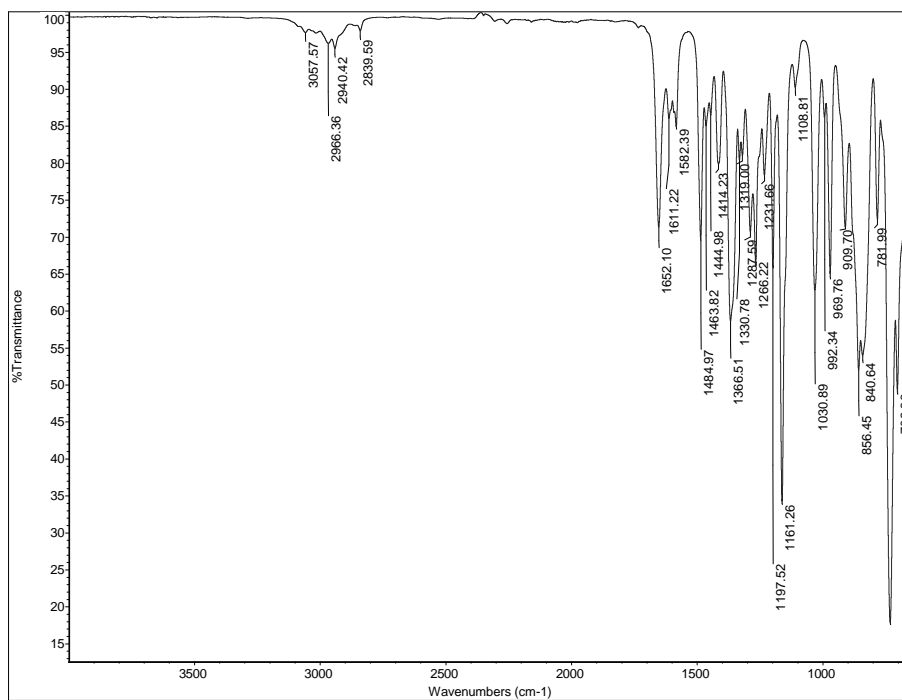


Figure A2.281. FTIR of enone 458.

## **Appendix Three**

### Crystallographic Data and Tables

## X-Ray Crystallography Report for Fused Tricycle 269

### A. Crystal data and structure refinement.

Identification code	wood22
Empirical formula	C <sub>32</sub> H <sub>47</sub> N O <sub>5</sub> Si
Formula weight	553.80
Temperature	120(2) K
Wavelength	0.71073 Å
Crystal system	Monoclinic
Space group	C2/c
Unit cell dimensions	a = 55.062(4) Å      α = 90°. b = 8.9017(7) Å      β = 100.454(4)°. c = 13.1258(10) Å    γ = 90°.
Volume	6326.8(8) Å <sup>3</sup>
Z	8
Density (calculated)	1.163 Mg/m <sup>3</sup>
Absorption coefficient	0.112 mm <sup>-1</sup>
F(000)	2400
Crystal size	0.15 x 0.15 x 0.03 mm <sup>3</sup>
Theta range for data collection	2.96 to 26.37°.
Index ranges	-68 ≤ h ≤ 63, -11 ≤ k ≤ 11, -15 ≤ l ≤ 16
Reflections collected	50816
Independent reflections	6457 [R(int) = 0.0471]
Completeness to theta = 26.37°	99.8 %
Absorption correction	None
Max. and min. transmission	0.9966 and 0.9833
Refinement method	Full-matrix least-squares on F <sup>2</sup>
Data / restraints / parameters	6457 / 0 / 352
Goodness-of-fit on F <sup>2</sup>	1.041
Final R indices [I > 2σ(I)]	R1 = 0.0435, wR2 = 0.1080
R indices (all data)	R1 = 0.0633, wR2 = 0.1193
Largest diff. peak and hole	0.305 and -0.304 e.Å <sup>-3</sup>

**B. Atomic coordinates (  $\times 10^4$ ) and equivalent isotropic displacement parameters ( $\text{\AA}^2 \times 10^3$ ).  $U(\text{eq})$  is defined as one third of the trace of the orthogonalized  $U^{ij}$  tensor.**

	x	y	z	$U(\text{eq})$
Si(1)	572(1)	7802(1)	1983(1)	29(1)
O(1)	697(1)	7541(2)	940(1)	29(1)
C(1)	1963(1)	7766(2)	3140(1)	16(1)
N(1)	1577(1)	8269(1)	2096(1)	17(1)
O(5)	2067(1)	6843(1)	4012(1)	18(1)
O(2)	1481(1)	10555(1)	2732(1)	20(1)
O(3)	1923(1)	9357(1)	5414(1)	30(1)
C(2)	2309(1)	6330(2)	3915(1)	20(1)
O(4)	1589(1)	8110(1)	4594(1)	23(1)
C(3)	2401(1)	7449(2)	3222(1)	19(1)
C(4)	2631(1)	7877(2)	3255(1)	28(1)
C(5)	2173(1)	8009(2)	2509(1)	18(1)
C(6)	2097(1)	7049(2)	1551(1)	19(1)
C(7)	2269(1)	6859(2)	804(1)	28(1)
C(8)	1870(1)	6513(2)	1486(1)	20(1)
C(9)	1749(1)	6979(2)	2379(1)	18(1)
C(10)	1607(1)	5691(2)	2781(1)	22(1)
C(11)	1752(1)	4245(2)	3080(1)	28(1)
C(12)	1612(1)	9442(2)	2764(1)	16(1)
C(13)	1851(1)	9204(2)	3545(1)	17(1)
C(14)	2013(1)	10608(2)	3598(2)	26(1)
C(15)	1796(1)	8910(2)	4627(1)	21(1)
C(16)	1528(1)	7711(2)	5592(1)	32(1)
C(17)	1276(1)	7083(4)	5411(2)	70(1)
C(18)	1365(1)	8167(2)	1276(1)	17(1)
C(19)	1395(1)	8238(2)	253(1)	21(1)
C(20)	1188(1)	8103(2)	-523(1)	25(1)
C(21)	958(1)	7879(2)	-280(1)	24(1)
C(22)	929(1)	7807(2)	749(1)	22(1)
C(23)	1135(1)	7970(2)	1533(1)	21(1)
C(24)	741(1)	6631(3)	3087(2)	50(1)

C(25)	845(1)	5161(3)	2755(2)	69(1)
C(26)	591(1)	6360(5)	3950(2)	90(1)
C(27)	596(1)	9848(3)	2350(2)	54(1)
C(28)	605(1)	10881(3)	1432(3)	85(1)
C(29)	393(1)	10342(4)	2944(3)	89(1)
C(30)	246(1)	7157(3)	1532(2)	40(1)
C(31)	225(1)	5463(3)	1330(2)	56(1)
C(32)	118(1)	8013(3)	584(2)	59(1)

---

**C. Bond lengths [Å] and angles [°].**

---

Si(1)-O(1)	1.6567(13)
Si(1)-C(30)	1.877(2)
Si(1)-C(27)	1.882(2)
Si(1)-C(24)	1.888(2)
O(1)-C(22)	1.364(2)
C(1)-O(5)	1.4394(18)
C(1)-C(5)	1.553(2)
C(1)-C(13)	1.556(2)
C(1)-C(9)	1.568(2)
N(1)-C(12)	1.354(2)
N(1)-C(18)	1.438(2)
N(1)-C(9)	1.491(2)
O(5)-C(2)	1.4354(19)
O(2)-C(12)	1.2211(18)
O(3)-C(15)	1.205(2)
C(2)-C(3)	1.497(2)
O(4)-C(15)	1.335(2)
O(4)-C(16)	1.456(2)
C(3)-C(4)	1.319(2)
C(3)-C(5)	1.506(2)
C(5)-C(6)	1.515(2)
C(6)-C(8)	1.326(2)
C(6)-C(7)	1.490(2)
C(8)-C(9)	1.510(2)
C(9)-C(10)	1.535(2)
C(10)-C(11)	1.528(2)
C(12)-C(13)	1.530(2)
C(13)-C(15)	1.528(2)
C(13)-C(14)	1.530(2)
C(16)-C(17)	1.475(3)
C(18)-C(23)	1.382(2)
C(18)-C(19)	1.383(2)
C(19)-C(20)	1.387(2)
C(20)-C(21)	1.379(2)

C(21)-C(22)	1.390(2)
C(22)-C(23)	1.395(2)
C(24)-C(25)	1.522(4)
C(24)-C(26)	1.536(3)
C(27)-C(28)	1.524(4)
C(27)-C(29)	1.539(3)
C(30)-C(32)	1.519(3)
C(30)-C(31)	1.532(3)

O(1)-Si(1)-C(30)	102.31(8)
O(1)-Si(1)-C(27)	109.13(10)
C(30)-Si(1)-C(27)	113.21(10)
O(1)-Si(1)-C(24)	109.65(9)
C(30)-Si(1)-C(24)	112.56(10)
C(27)-Si(1)-C(24)	109.68(12)
C(22)-O(1)-Si(1)	132.06(11)
O(5)-C(1)-C(5)	106.13(12)
O(5)-C(1)-C(13)	108.81(12)
C(5)-C(1)-C(13)	116.59(12)
O(5)-C(1)-C(9)	113.31(12)
C(5)-C(1)-C(9)	105.65(12)
C(13)-C(1)-C(9)	106.52(12)
C(12)-N(1)-C(18)	122.27(13)
C(12)-N(1)-C(9)	115.02(13)
C(18)-N(1)-C(9)	121.95(12)
C(2)-O(5)-C(1)	110.56(12)
O(5)-C(2)-C(3)	105.25(12)
C(15)-O(4)-C(16)	115.89(13)
C(4)-C(3)-C(2)	126.95(15)
C(4)-C(3)-C(5)	127.78(16)
C(2)-C(3)-C(5)	105.23(13)
C(3)-C(5)-C(6)	113.64(13)
C(3)-C(5)-C(1)	103.77(12)
C(6)-C(5)-C(1)	104.19(13)
C(8)-C(6)-C(7)	128.35(16)
C(8)-C(6)-C(5)	111.72(14)

C(7)-C(6)-C(5)	119.89(15)
C(6)-C(8)-C(9)	113.41(14)
N(1)-C(9)-C(8)	111.72(13)
N(1)-C(9)-C(10)	108.71(13)
C(8)-C(9)-C(10)	112.76(13)
N(1)-C(9)-C(1)	100.72(12)
C(8)-C(9)-C(1)	103.17(13)
C(10)-C(9)-C(1)	119.13(13)
C(11)-C(10)-C(9)	116.32(14)
O(2)-C(12)-N(1)	126.12(14)
O(2)-C(12)-C(13)	124.47(14)
N(1)-C(12)-C(13)	109.34(13)
C(15)-C(13)-C(14)	108.06(13)
C(15)-C(13)-C(12)	110.78(13)
C(14)-C(13)-C(12)	109.89(13)
C(15)-C(13)-C(1)	109.61(12)
C(14)-C(13)-C(1)	115.03(13)
C(12)-C(13)-C(1)	103.43(12)
O(3)-C(15)-O(4)	124.21(16)
O(3)-C(15)-C(13)	123.92(16)
O(4)-C(15)-C(13)	111.86(13)
O(4)-C(16)-C(17)	108.28(16)
C(23)-C(18)-C(19)	121.22(15)
C(23)-C(18)-N(1)	118.64(14)
C(19)-C(18)-N(1)	120.13(14)
C(18)-C(19)-C(20)	118.89(15)
C(21)-C(20)-C(19)	120.69(16)
C(20)-C(21)-C(22)	120.25(16)
O(1)-C(22)-C(21)	117.57(15)
O(1)-C(22)-C(23)	122.99(15)
C(21)-C(22)-C(23)	119.41(15)
C(18)-C(23)-C(22)	119.51(15)
C(25)-C(24)-C(26)	110.8(2)
C(25)-C(24)-Si(1)	114.38(17)
C(26)-C(24)-Si(1)	113.34(19)
C(28)-C(27)-C(29)	111.0(2)

C(28)-C(27)-Si(1)	113.11(19)
C(29)-C(27)-Si(1)	112.57(19)
C(32)-C(30)-C(31)	110.1(2)
C(32)-C(30)-Si(1)	112.35(16)
C(31)-C(30)-Si(1)	113.11(15)

---

**D. Anisotropic displacement parameters ( $\text{\AA}^2 \times 10^3$ ). The anisotropic displacement factor exponent takes the form:  $-2\pi^2 [ h^2 a^{*2} U^{11} + \dots + 2 h k a^* b^* U^{12} ]$**

	U <sup>11</sup>	U <sup>22</sup>	U <sup>33</sup>	U <sup>23</sup>	U <sup>13</sup>	U <sup>12</sup>
Si(1)	19(1)	41(1)	29(1)	-5(1)	8(1)	-4(1)
O(1)	14(1)	49(1)	24(1)	-2(1)	3(1)	-4(1)
C(1)	17(1)	16(1)	15(1)	1(1)	1(1)	2(1)
N(1)	14(1)	18(1)	18(1)	-1(1)	1(1)	2(1)
O(5)	18(1)	20(1)	17(1)	3(1)	3(1)	4(1)
O(2)	21(1)	20(1)	20(1)	1(1)	5(1)	6(1)
O(3)	30(1)	36(1)	20(1)	-9(1)	-4(1)	7(1)
C(2)	18(1)	21(1)	20(1)	0(1)	2(1)	5(1)
O(4)	28(1)	27(1)	15(1)	0(1)	6(1)	0(1)
C(3)	19(1)	23(1)	17(1)	-1(1)	2(1)	4(1)
C(4)	20(1)	40(1)	23(1)	5(1)	2(1)	2(1)
C(5)	16(1)	18(1)	18(1)	1(1)	3(1)	2(1)
C(6)	21(1)	20(1)	16(1)	3(1)	2(1)	7(1)
C(7)	25(1)	39(1)	19(1)	0(1)	5(1)	8(1)
C(8)	22(1)	19(1)	18(1)	-2(1)	1(1)	4(1)
C(9)	16(1)	17(1)	20(1)	0(1)	2(1)	3(1)
C(10)	22(1)	19(1)	23(1)	-2(1)	2(1)	-2(1)
C(11)	32(1)	19(1)	31(1)	2(1)	-1(1)	-4(1)
C(12)	17(1)	18(1)	15(1)	2(1)	6(1)	-1(1)
C(13)	16(1)	17(1)	19(1)	-3(1)	2(1)	2(1)
C(14)	20(1)	19(1)	36(1)	-5(1)	2(1)	-1(1)
C(15)	23(1)	19(1)	22(1)	-3(1)	1(1)	8(1)
C(16)	44(1)	35(1)	17(1)	4(1)	9(1)	5(1)
C(17)	55(2)	125(3)	32(1)	18(1)	15(1)	-27(2)
C(18)	16(1)	16(1)	19(1)	-1(1)	0(1)	-1(1)
C(19)	18(1)	25(1)	22(1)	2(1)	6(1)	-1(1)
C(20)	25(1)	34(1)	16(1)	1(1)	3(1)	-3(1)
C(21)	20(1)	30(1)	19(1)	0(1)	-2(1)	-2(1)
C(22)	15(1)	27(1)	24(1)	0(1)	4(1)	0(1)
C(23)	19(1)	28(1)	17(1)	-1(1)	4(1)	1(1)
C(24)	34(1)	84(2)	32(1)	14(1)	4(1)	-17(1)

C(25)	53(2)	56(2)	91(2)	38(2)	-1(2)	-4(1)
C(26)	62(2)	167(4)	42(2)	30(2)	12(1)	-36(2)
C(27)	28(1)	55(1)	79(2)	-28(1)	12(1)	-2(1)
C(28)	72(2)	38(1)	149(3)	1(2)	32(2)	7(1)
C(29)	44(2)	100(2)	124(3)	-73(2)	22(2)	0(2)
C(30)	21(1)	59(1)	41(1)	-7(1)	13(1)	-6(1)
C(31)	35(1)	63(2)	65(2)	-1(1)	2(1)	-21(1)
C(32)	23(1)	74(2)	74(2)	3(1)	-7(1)	0(1)

---

**E. Hydrogen coordinates ( x 10<sup>4</sup>) and isotropic displacement parameters (Å<sup>2</sup>x 10<sup>3</sup>).**

	x	y	z	U(eq)
H(2A)	2301	5334	3610	23
H(2B)	2417	6297	4586	23
H(4A)	2757	7471	3749	33
H(4B)	2668	8584	2785	33
H(5A)	2189	9070	2331	21
H(7A)	2194	6222	245	42
H(7B)	2420	6411	1152	42
H(7C)	2304	7823	535	42
H(8A)	1794	5908	944	24
H(10A)	1544	6048	3383	26
H(10B)	1465	5450	2252	26
H(11A)	1646	3517	3318	42
H(11B)	1890	4453	3621	42
H(11C)	1810	3855	2487	42
H(14A)	1930	11436	3855	38
H(14B)	2043	10843	2918	38
H(14C)	2167	10427	4054	38
H(16A)	1535	8594	6030	38
H(16B)	1644	6975	5937	38
H(17A)	1232	6813	6062	105
H(17B)	1270	6207	4981	105
H(17C)	1161	7820	5072	105
H(19A)	1551	8373	88	25
H(20A)	1206	8165	-1213	30
H(21A)	821	7775	-807	28
H(23A)	1117	7947	2225	26
H(24A)	885	7228	3404	60
H(25A)	929	4637	3356	103
H(25B)	958	5369	2299	103
H(25C)	712	4551	2402	103
H(26A)	687	5768	4489	135

H(26B)	441	5837	3670	135
H(26C)	552	7308	4229	135
H(27A)	753	9973	2827	64
H(28A)	615	11907	1662	127
H(28B)	458	10746	921	127
H(28C)	747	10642	1134	127
H(29A)	412	11389	3115	133
H(29B)	405	9764	3569	133
H(29C)	233	10182	2520	133
H(30A)	155	7374	2092	47
H(31A)	55	5197	1108	83
H(31B)	291	4931	1955	83
H(31C)	317	5200	800	83
H(32A)	-48	7650	383	88
H(32B)	206	7865	25	88
H(32C)	115	9064	744	88

---

## X-Ray Crystallography Report for Allylic Alcohol 367

### A. Crystal data and structure refinement.

Identification code	wood26	
Empirical formula	C <sub>21</sub> H <sub>25</sub> N O <sub>6</sub>	
Formula weight	387.42	
Temperature	120(2) K	
Wavelength	0.71073 Å	
Crystal system	Monoclinic	
Space group	P 21/c	
Unit cell dimensions	a = 8.9089(9) Å	α = 90°.
	b = 25.655(3) Å	β = 114.678(5)°.
	c = 9.3854(9) Å	γ = 90°.
Volume	1949.2(3) Å <sup>3</sup>	
Z	4	
Density (calculated)	1.320 Mg/m <sup>3</sup>	
Absorption coefficient	0.097 mm <sup>-1</sup>	
F(000)	824	
Crystal size	0.23 x 0.15 x 0.11 mm <sup>3</sup>	
Theta range for data collection	1.59 to 28.55°.	
Index ranges	-11 ≤ h ≤ 11, -34 ≤ k ≤ 34, -11 ≤ l ≤ 12	
Reflections collected	40478	
Independent reflections	4899 [R(int) = 0.0375]	
Completeness to theta = 28.55°	98.7 %	
Absorption correction	Semi-empirical from equivalents	
Max. and min. transmission	0.9895 and 0.9776	
Refinement method	Full-matrix least-squares on F <sup>2</sup>	
Data / restraints / parameters	4899 / 0 / 259	
Goodness-of-fit on F <sup>2</sup>	1.074	
Final R indices [I > 2σ(I)]	R1 = 0.0393, wR2 = 0.1014	
R indices (all data)	R1 = 0.0510, wR2 = 0.1146	
Largest diff. peak and hole	0.366 and -0.262 e.Å <sup>-3</sup>	

**B. Atomic coordinates ( x 10<sup>4</sup>) and equivalent isotropic displacement parameters (Å<sup>2</sup>x 10<sup>3</sup>). U(eq) is defined as one third of the trace of the orthogonalized U<sup>ij</sup> tensor.**

	x	y	z	U(eq)
O(1)	1855(1)	-566(1)	10109(1)	22(1)
O(2)	-3549(1)	306(1)	3717(1)	23(1)
O(3)	545(1)	2371(1)	6575(1)	18(1)
O(4)	3022(1)	767(1)	6421(1)	16(1)
O(5)	4478(1)	1807(1)	8281(1)	19(1)
O(6)	4288(1)	2198(1)	6068(1)	27(1)
N(1)	819(1)	1015(1)	6938(1)	12(1)
C(1)	922(1)	-249(1)	8896(1)	15(1)
C(2)	-670(2)	-427(1)	7969(1)	17(1)
C(3)	-1707(2)	-146(1)	6667(1)	16(1)
C(4)	-1185(1)	321(1)	6266(1)	14(1)
C(5)	361(1)	510(1)	7270(1)	13(1)
C(6)	1439(1)	229(1)	8569(1)	14(1)
C(7)	3543(2)	-425(1)	11000(2)	28(1)
C(8)	-2176(2)	603(1)	4727(1)	16(1)
C(9)	-2821(1)	1134(1)	4953(1)	15(1)
C(10)	-4625(2)	1240(1)	3960(2)	24(1)
C(11)	-1884(1)	1498(1)	5939(1)	15(1)
C(12)	-74(1)	1484(1)	7059(1)	13(1)
C(13)	113(2)	1578(1)	8749(1)	16(1)
C(14)	1889(2)	1609(1)	9988(1)	20(1)
C(15)	819(1)	1912(1)	6569(1)	13(1)
C(16)	2036(1)	1664(1)	6011(1)	13(1)
C(17)	2073(1)	1097(1)	6500(1)	12(1)
C(18)	1315(2)	1698(1)	4212(1)	19(1)
C(19)	3730(1)	1923(1)	6758(1)	16(1)
C(20)	6089(2)	2051(1)	9144(2)	27(1)
C(21)	6797(2)	1844(1)	10783(2)	33(1)

**C. Bond lengths [Å] and angles [°].**

---

O(1)-C(1)	1.3635(14)
O(1)-C(7)	1.4288(16)
O(2)-C(8)	1.4162(14)
O(3)-C(15)	1.2035(15)
O(4)-C(17)	1.2196(14)
O(5)-C(19)	1.3337(15)
O(5)-C(20)	1.4616(14)
O(6)-C(19)	1.1987(15)
N(1)-C(17)	1.3576(15)
N(1)-C(5)	1.4312(15)
N(1)-C(12)	1.4738(15)
C(1)-C(6)	1.3888(17)
C(1)-C(2)	1.3949(17)
C(2)-C(3)	1.3872(17)
C(3)-C(4)	1.3933(17)
C(4)-C(5)	1.3909(15)
C(4)-C(8)	1.5239(16)
C(5)-C(6)	1.3956(16)
C(8)-C(9)	1.5288(17)
C(9)-C(11)	1.3336(17)
C(9)-C(10)	1.5080(16)
C(11)-C(12)	1.5135(16)
C(12)-C(15)	1.5344(16)
C(12)-C(13)	1.5430(17)
C(13)-C(14)	1.5250(17)
C(15)-C(16)	1.5256(17)
C(16)-C(17)	1.5213(16)
C(16)-C(19)	1.5259(16)
C(16)-C(18)	1.5379(16)
C(20)-C(21)	1.496(2)
C(1)-O(1)-C(7)	117.66(10)
C(19)-O(5)-C(20)	115.73(10)
C(17)-N(1)-C(5)	123.48(10)

C(17)-N(1)-C(12)	115.81(9)
C(5)-N(1)-C(12)	120.72(9)
O(1)-C(1)-C(6)	124.61(11)
O(1)-C(1)-C(2)	115.58(11)
C(6)-C(1)-C(2)	119.79(11)
C(3)-C(2)-C(1)	120.58(11)
C(2)-C(3)-C(4)	120.66(11)
C(5)-C(4)-C(3)	117.65(10)
C(5)-C(4)-C(8)	119.69(10)
C(3)-C(4)-C(8)	122.47(10)
C(4)-C(5)-C(6)	122.58(11)
C(4)-C(5)-N(1)	117.30(10)
C(6)-C(5)-N(1)	120.12(10)
C(1)-C(6)-C(5)	118.48(10)
O(2)-C(8)-C(4)	112.14(10)
O(2)-C(8)-C(9)	107.60(9)
C(4)-C(8)-C(9)	113.21(10)
C(11)-C(9)-C(10)	120.01(11)
C(11)-C(9)-C(8)	123.89(10)
C(10)-C(9)-C(8)	116.09(10)
C(9)-C(11)-C(12)	129.92(11)
N(1)-C(12)-C(11)	114.78(9)
N(1)-C(12)-C(15)	101.34(9)
C(11)-C(12)-C(15)	108.08(9)
N(1)-C(12)-C(13)	112.10(9)
C(11)-C(12)-C(13)	109.68(10)
C(15)-C(12)-C(13)	110.49(9)
C(14)-C(13)-C(12)	115.10(10)
O(3)-C(15)-C(16)	125.78(11)
O(3)-C(15)-C(12)	124.49(11)
C(16)-C(15)-C(12)	109.67(9)
C(17)-C(16)-C(15)	102.93(9)
C(17)-C(16)-C(19)	112.67(9)
C(15)-C(16)-C(19)	111.65(9)
C(17)-C(16)-C(18)	109.40(9)
C(15)-C(16)-C(18)	108.78(9)

C(19)-C(16)-C(18)	111.06(10)
O(4)-C(17)-N(1)	126.15(11)
O(4)-C(17)-C(16)	124.88(10)
N(1)-C(17)-C(16)	108.84(10)
O(6)-C(19)-O(5)	125.19(11)
O(6)-C(19)-C(16)	124.23(11)
O(5)-C(19)-C(16)	110.57(10)
O(5)-C(20)-C(21)	108.22(12)

---

**D. Anisotropic displacement parameters ( $\text{\AA}^2 \times 10^3$ ). The anisotropic displacement factor exponent takes the form:  $-2\pi^2 [ h^2 a^{*2} U^{11} + \dots + 2 h k a^* b^* U^{12} ]$**

	U <sup>11</sup>	U <sup>22</sup>	U <sup>33</sup>	U <sup>23</sup>	U <sup>13</sup>	U <sup>12</sup>
O(1)	20(1)	15(1)	22(1)	7(1)	2(1)	0(1)
O(2)	20(1)	14(1)	23(1)	-4(1)	-2(1)	0(1)
O(3)	22(1)	9(1)	26(1)	0(1)	12(1)	1(1)
O(4)	15(1)	12(1)	22(1)	0(1)	8(1)	2(1)
O(5)	13(1)	22(1)	20(1)	-3(1)	5(1)	-5(1)
O(6)	27(1)	25(1)	33(1)	3(1)	16(1)	-9(1)
N(1)	13(1)	8(1)	17(1)	1(1)	7(1)	0(1)
C(1)	19(1)	12(1)	15(1)	1(1)	7(1)	2(1)
C(2)	22(1)	12(1)	18(1)	0(1)	9(1)	-4(1)
C(3)	17(1)	13(1)	17(1)	-2(1)	5(1)	-4(1)
C(4)	15(1)	11(1)	15(1)	-1(1)	5(1)	0(1)
C(5)	15(1)	9(1)	17(1)	0(1)	8(1)	0(1)
C(6)	13(1)	12(1)	16(1)	-1(1)	5(1)	0(1)
C(7)	18(1)	25(1)	31(1)	8(1)	1(1)	2(1)
C(8)	16(1)	13(1)	16(1)	-1(1)	3(1)	0(1)
C(9)	15(1)	14(1)	18(1)	2(1)	7(1)	0(1)
C(10)	14(1)	19(1)	32(1)	-2(1)	3(1)	1(1)
C(11)	12(1)	13(1)	20(1)	1(1)	7(1)	2(1)
C(12)	14(1)	8(1)	17(1)	-1(1)	6(1)	0(1)
C(13)	18(1)	14(1)	20(1)	-1(1)	10(1)	-1(1)
C(14)	22(1)	19(1)	17(1)	-2(1)	7(1)	0(1)
C(15)	13(1)	12(1)	13(1)	0(1)	4(1)	-1(1)
C(16)	14(1)	10(1)	14(1)	0(1)	6(1)	-1(1)
C(17)	11(1)	11(1)	10(1)	-1(1)	2(1)	-2(1)
C(18)	22(1)	19(1)	15(1)	3(1)	8(1)	1(1)
C(19)	15(1)	11(1)	22(1)	-2(1)	9(1)	0(1)
C(20)	14(1)	32(1)	31(1)	-9(1)	6(1)	-8(1)
C(21)	22(1)	30(1)	33(1)	-7(1)	-2(1)	2(1)

**E. Hydrogen coordinates ( $\times 10^4$ ) and isotropic displacement parameters ( $\text{\AA}^2 \times 10^{-3}$ ).**

---

	x	y	z	U(eq)
H(2)	-3231	8	3600	34
H(2A)	-1046	-744	8232	20
H(3)	-2785	-273	6042	19
H(6)	2503	362	9214	17
H(7A)	4111	-405	10304	41
H(7B)	4080	-688	11810	41
H(7C)	3597	-85	11497	41
H(8)	-1433	660	4185	20
H(10A)	-4885	1600	4121	36
H(10B)	-5300	1001	4261	36
H(10C)	-4862	1188	2852	36
H(11)	-2438	1815	5937	18
H(13A)	-457	1907	8770	19
H(13B)	-456	1292	9036	19
H(14A)	2458	1280	10007	29
H(14B)	1889	1670	11018	29
H(14C)	2461	1896	9734	29
H(18A)	2050	1517	3836	28
H(18B)	1213	2064	3893	28
H(18C)	223	1533	3762	28
H(20A)	5965	2435	9155	32
H(20B)	6834	1970	8633	32
H(21A)	6045	1923	11274	50
H(21B)	7870	2008	11387	50
H(21C)	6941	1466	10762	50

---

## List of Abbreviations

[O]	oxidation
°C	degrees Celsius
Å	angstrom
Ac	acetyl
acac	acetylacetone
ACS	American Chemical Society
AHBA	3-amino-5-hydroxybenzoic acid
AIBN	azoisobutyronitrile
aq.	aqueous
atm	atmosphere
B <sub>2</sub> Pin <sub>2</sub>	bis(pinacolato)diboron
Bn	benzyl
Boc	<i>tert</i> -butoxycarbonyl
BOM	benzyl methyl ether
BPin	pinacolborane
Bz	benzoyl
CHDA	cyclohexyldiamine
cm <sup>-1</sup>	inverse centimeters
cod	1,5-cyclooctadiene
COSY	correlation spectroscopy
Cy	cyclohexyl
d	doublet
d.r.	diastereomeric ratio
dba	dibenzylidene acetone
DBU	1,8-diazabicyclo[5.4.0]-undec-7-ene
DCC	dicyclohexylcarbodiimide
DCE	dichloroethane
DCM	dichloromethane
dd	doublet of doublets
ddd	doublet of doublet of doublets
DDQ	2,3-dichloro-5,6-dicyano benzoquinone
ddt	doublet of doublet of triplets
DEPT	distortionless enhancement by polarization transfer
DIBAL-H	diisobutylaluminum hydride
DIPHOS (dppe)	1,2-bis(diphenylphosphino)ethane
DKP	diketopiperazine
DMAP	<i>N,N</i> -dimethylamino pyridine
DMEDA	<i>N,N</i> -dimethylethylenediamine
DMF	<i>N,N</i> -dimethylformamide
DMS	dimethyl sulfide
DMSO	dimethyl sulfoxide
dt	doublet of triplets
dtbpy	4,4-di- <i>tert</i> -butyl bipyridine
DTT	dithiothreitol
E <sub>0</sub>	reduction potential at 25 °C
EDCI	<i>N</i> -Ethyl- <i>N'</i> -(3-dimethylaminopropyl)carbodiimide hydrochloride

ESeP	epidisenodiketopiperazine
ESI-APCI	electrospray ionization-atmospheric pressure chemical ionization
Et	ethyl
EtOH	ethanol
ETP	epidithiodiketopiperazine
FTIR	Fourier transform infrared spectroscopy
g	gram
HMBC	heteronuclear multiple bond correlation
HMPA	hexamethylphosphoramide
HMQC	heteronuclear multiple quantum correlation
HPLC	high performance liquid chromatography
HRMS	high-resolution mass spectroscopy
Hz	hertz
h $\nu$	light
<i>i</i> -Pr	isopropyl
IBX	2-iodoxybenzoic acid
IC <sub>50</sub>	half maximum inhibitory concentration
IMes•HCl	1,3-dimesitylimidazolium chloride
imid.	imidazole
INADEQUATE	incredible natural abundance double quantum transfer experiment
<i>J</i>	coupling constant
kg	kilogram
KHMDS	potassium hexamethyldisilazide
L	liter
LA	Lewis acid
LDA	lithium diisopropylamide
LHMDS	lithium hexamethyldisilazide
LTMP	lithium 2,2,6,6-tetramethylpiperidide
M	molar
<i>m</i>	multiplet
<i>m</i> -CPBA	<i>meta</i> -chloroperoxybenzoic acid
<i>m/z</i>	mass to charge ratio
Me	methyl
MeOH	methanol
mg	milligram
MHz	megahertz
MIC	minimum inhibitory concentration
mL	milliliter
mmol	millimole
mol	mole
MOM	methoxy methyl
Ms	mesyl
MTB	<i>Mycobacterium tuberculosis</i>
mV	millivolts
N	normal
<i>n</i> -Bu (Bu)	normal butyl
NaHMDS	sodium hexamethyldisilazide
NBS	<i>N</i> -bromosuccinimide
NCS	<i>N</i> -chlorosuccinimide
NHK	Nozaki-Hiyama-Kishi
nm	nanometer

nM	nanomolar
NMR	nuclear magnetic resonance
NOE	nuclear Overhauser effect
NOESY	nuclear Overhauser effect spectroscopy
NuH	nucleophile
OTFA	trifluoroacetate
Pg	protecting group
Ph	phenyl
PhH	benzene
PIDA	bisacetoxyiodo benzene
PIFA	[bis(trifluoroacetoxy)iodo]benzene
Piv	pivaloyl
PMB	<i>para</i> -methoxybenzyl
PMP	<i>para</i> -methoxyphenyl
PPA	polyphosphoric acid
<i>p</i> TSA	<i>para</i> -toluenesulfonic acid
pyr.	pyridine
q	quartet
R	generic carbon group or hydrogen
RCM	ring-closing metathesis
R <sub>f</sub>	retention factor
ROS	reactive oxygen species
s	singlet
sat.	saturated
SBL	soybean lipoxygenase
SEM	methyl 2-trimethylsilylethyl ether
t	triplet
<i>t</i> -Bu	<i>tert</i> -butyl
TASF	tris(dimethylamino)sulfonium difluorotrimethylsilicate
TB	tuberculosis
TBAF	tetrabutylammonium fluoride
TBAI	tetrabutylammonium iodide
TBAT	tetrabutylammonium difluorotriphenylsilicate
TBDPS	<i>tert</i> -butyldiphenyl silyl
TBHP	<i>tert</i> -butyl hydrogenperoxide
TBS	<i>tert</i> -butyldimethyl silyl
Tf	triflate
TFA	trifluoroacetic acid
THF	tetrahydrofuran
TIPS	triisopropyl silyl
TMS	trimethyl silyl
Ts	tosyl
tt	triplet of triplets
UV	ultraviolet
X	generic halogen
μg	microgram
μM	micromolar